Methods in Molecular Biology 2640

Springer Protocols

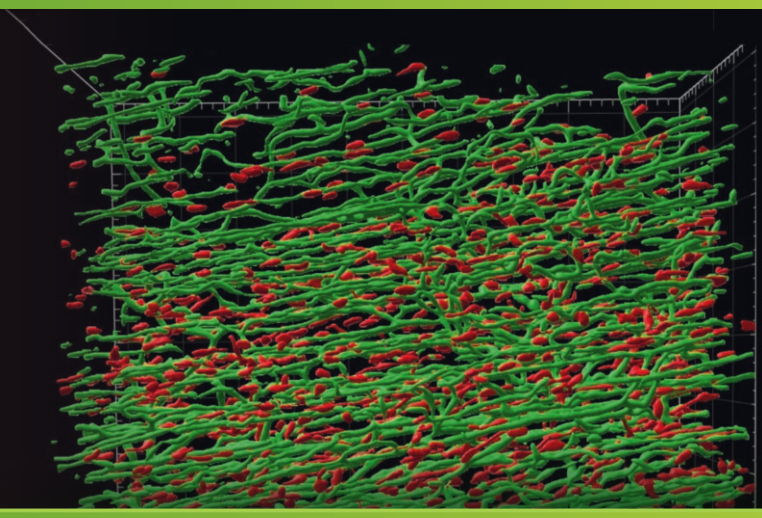

Atsushi Asakura
Editor

Skeletal Muscle Stem Cells

Methods and Protocols

MOREMEDIA

Humana Press

METHODS IN MOLECULAR BIOLOGY

Series Editor
John M. Walker
School of Life and Medical Sciences
University of Hertfordshire
Hatfield, Hertfordshire, UK

For further volumes:
http://www.springer.com/series/7651

For over 35 years, biological scientists have come to rely on the research protocols and methodologies in the critically acclaimed *Methods in Molecular Biology* series. The series was the first to introduce the step-by-step protocols approach that has become the standard in all biomedical protocol publishing. Each protocol is provided in readily-reproducible step-by-step fashion, opening with an introductory overview, a list of the materials and reagents needed to complete the experiment, and followed by a detailed procedure that is supported with a helpful notes section offering tips and tricks of the trade as well as troubleshooting advice. These hallmark features were introduced by series editor Dr. John Walker and constitute the key ingredient in each and every volume of the *Methods in Molecular Biology* series. Tested and trusted, comprehensive and reliable, all protocols from the series are indexed in PubMed.

Skeletal Muscle Stem Cells

Methods and Protocols

Edited by

Atsushi Asakura

Stem Cell Institute, University of Minnesota Medical School, Minneapolis, MN, USA

Humana Press

Editor
Atsushi Asakura
Stem Cell Institute
University of Minnesota Medical School
Minneapolis, MN, USA

ISSN 1064-3745 ISSN 1940-6029 (electronic)
Methods in Molecular Biology
ISBN 978-1-0716-3035-8 ISBN 978-1-0716-3036-5 (eBook)
https://doi.org/10.1007/978-1-0716-3036-5

Preface

Skeletal muscle is the most abundant tissue in the body, and its structures, gene expression, and protein expression are very conserved within the animal kingdom. Neonatal and adult skeletal muscle possesses extraordinary growth and regeneration capabilities. After muscle injury or intensive exercise, large numbers of new muscle fibers are rapidly formed within a week because of expansion and differentiation of muscle satellite cells, a stem cell population for postnatal myogenesis. However, our understanding of the mechanisms of skeletal muscle growth, degeneration, regeneration, and aging remains still limited. Over the past two decades, our understanding of skeletal muscle progenitor/stem cell development and cellular biology has rapidly advanced, and laboratory research on skeletal muscle regeneration and aging has surged. Most of these advances have been due to new technologies and methods combined with new genetic tools available in animal models that have reshaped the field. As the field has expanded with many new researchers focusing on several animal models, book chapters collecting these important protocols were needed. I would like to thank all my colleagues who contributed to these intensive book chapters. The methods are grouped into three general areas: Muscle Stem Cells and Progenitor Cells, Animal Models for Muscle Stem Cells and Regeneration, and Bioinformatics and Imaging Analysis for Muscle Stem Cells. We hope that this book will serve as a comprehensive resource for experimental research on skeletal muscle growth, repair, degeneration, aging, and regenerative medicine.

Minneapolis, MN, USA *Atsushi Asakura*

Contents

Part III Bioinformatics & Imaging Analysis for Muscle Stem Cells

Contributors

Takayuki Akimoto • *Laboratory of Muscle Biology, Faculty of Sport Sciences, Waseda University, Saitama, Japan*

Yoshitsugu Aoki • *Department of Molecular Therapy, National Institute of Neuroscience, National Center of Neurology and Psychiatry (NCNP), Tokyo, Japan*

Atsushi Asakura • *Stem Cell Institute, University of Minnesota Medical School, Minneapolis, MN, USA*

Yoko Asakura • *Stem Cell Institute, University of Minnesota Medical School, Minneapolis, MN, USA*

Carmen Birchmeier • *Max-Delbrück-Center for Molecular Medicine in the Helmholtz Association (MDC), Developmental Biology/Signal Transduction Group, Berlin, Germany; Neurowissenschaftliches Forschungzentrum, NeuroCure Cluster of Excellence, Charité-Universitätsmedizin Berlin, Berlin, Germany*

Thomas Braun • *Department of Cardiac Development and Remodeling, Max Planck Institute for Heart and Lung Research, Bad Nauheim, Germany; German Centre for Cardiovascular Research (DZHK), Partner site Rhein-Main, Frankfurt am Main, Germany*

Sunny S. K. Chan • *Department of Pediatrics, Lillehei Heart Institute and Paul and Sheila Wellstone Muscular Dystrophy Center, University of Minnesota, Minneapolis, MN, USA*

Bénédicte Chazaud • *Institut NeuroMyoGène, Unité Physiopathologie et Génétique du Neurone et du Muscle, CNRS, UMR5261, INSERM U1315, Université Claude Bernard Lyon 1, Lyon, France*

Xiyue Chen • *Department of Animal Sciences, Purdue University, West Lafayette, IN, USA*

Tom H. Cheung • *Division of Life Science, Center for Stem Cell Research, HKUST-Nan Fung Life Sciences Joint Laboratory, State Key Laboratory of Molecular Neuroscience, Molecular Neuroscience Center, Hong Kong University of Science and Technology, Kowloon, Hong Kong, China; Division of Life Science, Center for Stem Cell Research, HKUST-Nan Fung Life Sciences Joint Laboratory, State Key Laboratory of Molecular Neuroscience, Molecular Neuroscience Center, The Hong Kong University of Science and Technology, Hong Kong, SAR, China*

Filippo Conti • *Translational Cardiomyology Laboratory, Stem Cell and Developmental Biology Unit, Department of Development and Regeneration, KU Leuven, Leuven, Belgium*

Dong Ding • *Department of Cardiac Development and Remodeling, Max Planck Institute for Heart and Lung Research, Bad Nauheim, Germany*

Christina R. Ferreira • *Purdue Metabolite Profiling Facility, Purdue University, West Lafayette, IN, USA*

Shin Fujimaki • *Department of Muscle Development and Regeneration, Institute of Molecular Embryology and Genetics, Kumamoto University, Kumamoto, Japan*

Ryo Fujita • *Division of Regenerative Medicine, Transborder Medical Research Center (TMRC), University of Tsukuba, Ibaraki, Japan*

So-ichiro Fukada • *Laboratory of Stem Cell Regeneration and Adaptation, Graduate School of Pharmaceutical Sciences, Osaka University, Osaka, Japan*

Johanna Galvis • *Division of Life Science, Center for Stem Cell Research, HKUST-Nan Fung Life Sciences Joint Laboratory, State Key Laboratory of Molecular Neuroscience, Molecular Neuroscience Center, Hong Kong University of Science and Technology, Kowloon, Hong Kong, China*

Massimo Ganassi • *Randall Centre for Cell and Molecular Biophysics, King's College London, London, UK*

Nefele Giarratana • *Translational Cardiomyology Laboratory, Stem Cell and Developmental Biology Unit, Department of Development and Regeneration, KU Leuven, Leuven, Belgium*

Katsumasa Goto • *Department of Physiology, Graduate School of Health Sciences, Toyohashi SOZO University, Toyohashi, Aichi, Japan*

Stefan Guenther • *Department of Cardiac Development and Remodeling, Max Planck Institute for Heart and Lung Research, Bad Nauheim, Germany; German Centre for Cardiovascular Research (DZHK), Partner site Rhein-Main, Frankfurt am Main, Germany*

Stefan Günther • *Department of Cardiac Development and Remodelling, Max Planck Institute for Heart and Lung Research (W.G Kerckhoff-Institute), Bad Nauheim, Germany*

Gary J. He • *Division of Life Science, Center for Stem Cell Research, HKUST-Nan Fung Life Sciences Joint Laboratory, State Key Laboratory of Molecular Neuroscience, Molecular Neuroscience Center, Hong Kong University of Science and Technology, Kowloon, Hong Kong, China*

Liangqiang He • *Department of Chemical Pathology, Li Ka Shing Institute of Health Sciences, The Chinese University of Hong Kong, Hong Kong, China*

Merry He • *Department of Medical Genetics, Faculty of Medicine and Dentistry, University of Alberta, Edmonton, AB, Canada*

Zhiming He • *Department of Chemical Pathology, Li Ka Shing Institute of Health Sciences, The Chinese University of Hong Kong, Hong Kong, China*

Xiaotong Hong • *Spanish National Center on Cardiovascular Research (CNIC), Madrid, Spain; Altos Labs Inc, San Diego, CA, USA*

Simon M. Hughes • *Randall Centre for Cell and Molecular Biophysics, King's College London, London, UK; Randall Centre for Cell & Molecular Biophysics, King's College London, London, UK*

Madoka Ikemoto-Uezumi • *Muscle Aging and Regenerative Medicine, Tokyo Metropolitan Institute of Gerontology, Tokyo, Japan*

Michihiro Imamura • *Department of Molecular Therapy, National Institute of Neuroscience, National Center of Neurology and Psychiatry (NCNP), Tokyo, Japan*

Gaëtan Juban • *Institut NeuroMyoGène, Unité Physiopathologie et Génétique du Neurone et du Muscle, CNRS, UMR5261, INSERM U1315, Université Claude Bernard Lyon 1, Lyon, France*

Smrithi Karthikeyan • *Stem Cell Institute, University of Minnesota Medical School, Minneapolis, MN, USA*

Kyutae Kim • *Stem Cell Institute, University of Minnesota Medical School, Minneapolis, MN, USA*

Anita E. M. Kneppers • *Institut NeuroMyoGène, Unité Physiopathologie et Génétique du Neurone et du Muscle, CNRS, UMR5261, INSERM U1315, Université Claude Bernard Lyon 1, Lyon, France*

Robert D. Knight • *Centre for Craniofacial and Regenerative Biology, King's College London, London, UK*
Jana Koth • *Randall Centre for Cell & Molecular Biophysics, King's College London, London, UK; Weatherall Institute of Molecular Medicine, John Radcliffe Hospital, Oxford, UK*
Shihuan Kuang • *Department of Animal Sciences, Purdue University, West Lafayette, IN, USA; Center for Cancer Research, Purdue University, West Lafayette, IN, USA*
Manami Kubota • *Laboratory of Stem Cell Regeneration and Adaptation, Graduate School of Pharmaceutical Sciences, Osaka University, Osaka, Japan*
Tamaki Kurosawa • *Muscle Aging and Regenerative Medicine, Tokyo Metropolitan Institute of Gerontology, Tokyo, Japan*
Michael Kyba • *Department of Pediatrics, Lillehei Heart Institute, University of Minnesota, Minneapolis, MN, USA*
Ines Lahmann • *Max-Delbrück-Center for Molecular Medicine in the Helmholtz Association (MDC), Developmental Biology/Signal Transduction Group, Berlin, Germany; Neurowissenschaftliches Forschungzentrum, NeuroCure Cluster of Excellence, Charité-Universitätsmedizin Berlin, Berlin, Germany*
Justin Law • *Department of Cardiac Development and Remodelling, Max Planck Institute for Heart and Lung Research (W.G Kerckhoff-Institute), Bad Nauheim, Germany*
Fabien Le Grand • *Institut NeuroMyoGène, Université Claude Bernard Lyon 1, Lyon, France*
Yuying Li • *Department of Orthopaedics and Traumatology, Li Ka Shing Institute of Health Sciences, The Chinese University of Hong Kong, Hong Kong, China*
Ke Ma • *Department of Diabetes Complications & Metabolism, Beckman Research Institute of City of Hope, Duarte, CA, USA*
Keitaro Minato • *Muscle Aging and Regenerative Medicine, Tokyo Metropolitan Institute of Gerontology, Tokyo, Japan*
Katsura Minegishi • *Department of Molecular Therapy, National Institute of Neuroscience, National Center of Neurology and Psychiatry (NCNP), Tokyo, Japan*
Ricardo Mondragon-Gonzalez • *Lillehei Heart Institute, Department of Medicine, University of Minnesota, Minneapolis, MN, USA*
Norio Motohashi • *Department of Molecular Therapy, National Institute of Neuroscience, National Center of Neurology and Psychiatry (NCNP), Tokyo, Japan*
Rémi Mounier • *Institut NeuroMyoGène, Unité Physiopathologie et Génétique du Neurone et du Muscle, CNRS, UMR5261, INSERM U1315, Université Claude Bernard Lyon 1, Lyon, France*
Pura Muñoz-Cánoves • *Department of Experimental and Health Sciences, Pompeu Fabra University (UPF), CIBER on Neurodegenerative diseases (CIBERNED), Barcelona, Spain; Altos Labs Inc, San Diego, CA, USA*
Katsuyuki Nakamura • *Department of Veterinary Physiology, Graduate School of Agricultural and Life Sciences, The University of Tokyo, Tokyo, Japan*
Kazuya Ohashi • *Department of Physiology, Graduate School of Health Sciences, Toyohashi SOZO University, Toyohashi, Aichi, Japan*
Satoshi Oikawa • *Laboratory of Muscle Biology, Faculty of Sport Sciences, Waseda University, Saitama, Japan*
Yusuke Ono • *Department of Muscle Development and Regeneration, Institute of Molecular Embryology and Genetics, Kumamoto University, Kumamoto, Japan*

Georgiana Panci • *Institut NeuroMyoGène, Unité Physiopathologie et Génétique du Neurone et du Muscle, CNRS, UMR5261, INSERM U1315, Université Claude Bernard Lyon 1, Lyon, France*
Rita C. R. Perlingeiro • *Lillehei Heart Institute, Department of Medicine, University of Minnesota, Minneapolis, MN, USA; Stem Cell Institute, University of Minnesota, Minneapolis, MN, USA*
Tapan G. Pipalia • *Randall Centre for Cell & Molecular Biophysics, King's College London, London, UK*
Megan Reilly • *Department of Comparative Biosciences, The Stem Cell and Regenerative Medicine Center, University of Wisconsin, Madison, WI, USA*
Lorenza Rinvenuti • *Translational Cardiomyology Laboratory, Stem Cell and Developmental Biology Unit, Department of Development and Regeneration, KU Leuven, Leuven, Belgium*
Samantha Robertson • *Department of Comparative Biosciences, The Stem Cell and Regenerative Medicine Center, University of Wisconsin, Madison, WI, USA*
Flavio Ronzoni • *Translational Cardiomyology Laboratory, Stem Cell and Developmental Biology Unit, Department of Development and Regeneration, KU Leuven, Leuven, Belgium*
Hidetoshi Sakurai • *Department of Clinical Application, Center for iPS Cell Research and Application (CiRA), Kyoto University, Kyoto, Japan*
Maurilio Sampaolesi • *Translational Cardiomyology Laboratory, Stem Cell and Developmental Biology Unit, Department of Development and Regeneration, KU Leuven, Leuven, Belgium; Histology and Medical Embryology Unit, Department of Anatomy, Forensic Medicine and Orthopaedics, Sapienza University of Rome, Rome, Italy*
Masae Sato • *Department of Clinical Application, Center for iPS Cell Research and Application (CiRA), Kyoto University, Kyoto, Japan*
Takahiko Sato • *International Center for Cell & Gene Therapy, Fujita Health University, Toyoake, Japan; Department of Anatomy, Fujita Health University, Toyoake, Japan; Department of Ophthalmology, Kyoto Prefectural University of Medicine, Kyoto, Japan*
Sridhar Selvaraj • *Lillehei Heart Institute, Department of Medicine, University of Minnesota, Minneapolis, MN, USA*
Ahmed S. Shams • *Department of Pediatrics, Lillehei Heart Institute, University of Minnesota, Minneapolis, MN, USA*
Narin Sheri • *Department of Medical Genetics, Faculty of Medicine and Dentistry, University of Alberta, Edmonton, AB, Canada*
Chie Sotozono • *Department of Ophthalmology, Kyoto Prefectural University of Medicine, Kyoto, Japan*
Sami H. A. Sultan • *Centre for Craniofacial and Regenerative Biology, King's College London, London, UK*
Hao Sun • *Department of Chemical Pathology, Li Ka Shing Institute of Health Sciences, The Chinese University of Hong Kong, Hong Kong, China*
Masatoshi Suzuki • *Department of Comparative Biosciences, The Stem Cell and Regenerative Medicine Center, University of Wisconsin, Madison, WI, USA*
Kohei Takeda • *Faculty of Health and Sport Sciences, University of Tsukuba, Ibaraki, Japan; School of Political Science and Economics, Meiji University, Tokyo, Japan*
Tohru Takemasa • *Faculty of Health and Sport Sciences, University of Tsukuba, Ibaraki, Japan*
Takao Tanaka • *KAC Co., Limited, Bioscience Center, Shiga, Japan*

Morio Ueno • *Department of Ophthalmology, Kyoto Prefectural University of Medicine, Kyoto, Japan*
Akiyoshi Uezumi • *Muscle Aging and Regenerative Medicine, Tokyo Metropolitan Institute of Gerontology, Tokyo, Japan*
Mayank Verma • *Stem Cell Institute, University of Minnesota Medical School, Minneapolis, MN, USA*
Huating Wang • *Department of Orthopaedics and Traumatology, Li Ka Shing Institute of Health Sciences, The Chinese University of Hong Kong, Hong Kong, China*
Shuichi Watanabe • *Department of Cardiac Development and Remodelling, Max Planck Institute for Heart and Lung Research (W.G Kerckhoff-Institute), Bad Nauheim, Germany*
Ning Xie • *Department of Pediatrics, Lillehei Heart Institute and Paul and Sheila Wellstone Muscular Dystrophy Center, University of Minnesota, Minneapolis, MN, USA*
Xuekai Xiong • *Department of Diabetes Complications & Metabolism, Beckman Research Institute of City of Hope, Duarte, CA, USA*
Yukito Yamanaka • *Department of Ophthalmology, Kyoto Prefectural University of Medicine, Kyoto, Japan*
Keitaro Yamanouchi • *Department of Veterinary Physiology, Graduate School of Agricultural and Life Sciences, The University of Tokyo, Tokyo, Japan*
Michail Yekelchyk • *Department of Cardiac Development and Remodeling, Max Planck Institute for Heart and Lung Research, Bad Nauheim, Germany; German Centre for Cardiovascular Research (DZHK), Partner site Rhein-Main, Frankfurt am Main, Germany*
Toshifumi Yokota • *Department of Medical Genetics, Faculty of Medicine and Dentistry, University of Alberta, Edmonton, AB, Canada*
Lu Yue • *Division of Life Science, Center for Stem Cell Research, HKUST-Nan Fung Life Sciences Joint Laboratory, State Key Laboratory of Molecular Neuroscience, Molecular Neuroscience Center, The Hong Kong University of Science and Technology, Hong Kong, SAR, China*
Peter S. Zammit • *Randall Centre for Cell and Molecular Biophysics, King's College London, London, UK*
Lidan Zhang • *Laboratory of Stem Cell Regeneration and Adaptation, Graduate School of Pharmaceutical Sciences, Osaka University, Osaka, Japan*
Mingming Zhao • *Department of Clinical Application, Center for iPS Cell Research and Application (CiRA), Kyoto University, Kyoto, Japan*

Part I

Muscle Stem & Progenitor Cells

Chapter 1

Flow Cytometer Analyses, Isolation, and Staining of Murine Muscle Satellite Cells

Manami Kubota, Lidan Zhang, and So-ichiro Fukada

Abstract

Fluorescence-activated cell sorting (FACS) is a powerful and requisite tool for the analysis and purification of adult stem cells. However, it is difficult to separate adult stem cells from solid organs than from immune-related tissues/organs. This is because of the presence of large amounts of debris, which increases noise in the FACS profiles. In particular, it is extremely difficult for unfamiliar researchers to identify muscle stem cell (also known as muscle satellite cell: MuSC) fraction because all myofibers, which are mainly composed of skeletal muscle tissues, become debris during cell preparation. This chapter describes our FACS protocol, which we have used for more than a decade, to identify and purify MuSCs.

Key words Muscle satellite cells, Skeletal muscle, Collagenase, FACS profile, Sorting

1 Introduction

Muscle satellite cells (MuSCs) are characterized by their unique anatomical location [1] and expression of paired box protein 7 (Pax7) in skeletal muscles across species [2]. In intact muscles, MuSCs remain in a mitotically quiescent and undifferentiated state; however, when the muscle is injured, MuSCs escape from the quiescent state, proliferate, and fuse with each other to generate new myofibers. In addition, MuSCs are responsible for the increased number of myonuclei during muscle hypertrophy [3, 4].

Myogenic cell lines are widely used to investigate myogenic differentiation. In a pioneering study, myogenic-lineage cells from the regenerating muscles of C3H strain mice were cloned by David Yaffe [5] and were named C2 cells. Thereafter, Helen Blau established a subcloned C2 cell line (C2C12) [6], which is widely used as the myogenic cell line worldwide and has been used in many studies on myogenesis and regeneration. However, C2C12 as well as other cell lines have limitations for studying the physiological roles and regulations of MuSCs. Thus, primary cells from rat and mouse skeletal muscles are also widely used for the analyses of myogenesis

Atsushi Asakura (ed.), *Skeletal Muscle Stem Cells: Methods and Protocols*, Methods in Molecular Biology, vol. 2640,
https://doi.org/10.1007/978-1-0716-3036-5_1,

and regeneration. Further, gradient density and pre-plating techniques were developed to purify myogenic cells from crude primary cells [7]. However, although these techniques are useful for obtaining cultured satellite cells (myoblasts) at low cost and with high cell viability, cell purification requires constant human intervention. In addition, we cannot exclude the possibility that isolated cells are a biased population due to the heterogeneity of MuSCs.

Several researchers have identified many cell surface molecules expressed on MuSCs. Representative molecules expressed on MuSCs are M-cadherin, N-cadherin, Integrin α7β1, Syndecan-3/4, Tie2, Vcam-1, c-Met, Calcitonin receptor, Cxcr4, and Tenm4 [8–16]. In 2004, we developed and reported a novel monoclonal antibody (SM/C-2.6) by immunizing rats with C2/4, a subclone of C2C12 [17]. Our group first established and reported an isolation protocol for MuSCs from murine skeletal muscles using this antibody. Further, functionally important genes for MuSC maintenance have been identified using freshly isolated cells using this methodology [10, 18–21]. In addition, this methodology has been used to isolate myogenic cells from regenerating muscles [22]. In this chapter, we present our detailed protocol for the isolation and staining of MuSCs.

2 Materials

2.1 Preparation of Mononuclear Cells from Murine Skeletal Muscles

1. Mice: all inbred mice and genetically mutant mice. Our protocol can be applied for the analysis of mice expressing fluorescence proteins. However, attention is to be paid to fluorescence. For example, Fluorescein isothiocyanate (FITC)-labeled antibodies cannot be used for the analyses of mice expressing GPF or YFP proteins.
2. Two pairs of sterile scissors (for the skin and skeletal muscle) (Fine Science Tools Inc.)
3. Three pairs of sterile forceps (one for skin incision, one to remove muscles, and one to mince muscles) (Fine Science Tools Inc).
4. 0.2% Collagenase II digestion solution: Collagenase type II (Worthington, #: CLSS2) is dissolved in Dulbecco's Modified Eagle Medium (serum-free).
5. Sterile 40 μm cell strainers (FALCON, #352340).
6. Ammonium Chloride-Tris-buffer (ACT) solution: 0.17M Tris-HCl (pH.7.65) and 0.83% NH_4Cl/H_2O solution is mixed in the ratio of 1:9.
7. Washing buffer: 2% fetal calf serum (FCS) in Phosphate buffered saline (PBS) (*see* **Note 1**).

2.2 Staining of Mononuclear Cells and Isolation of Muscle Satellite Cells

1. Antibody: FITC-labeled rat anti-mouse CD31 (BD Biosciences, #558738).
2. Antibody: FITC-labeled rat anti-mouse CD45 (eBioscience, #11-0451-82).
3. Antibody: Phycoerythrin (PE)-labeled rat anti-mouse Sca-1 (BD Biosciences, #553336 or #553108).
4. Antibody: Biotinylated SM/C-2.6 antibody (non-labeled SM/C-2.6 antibody is commercially available from MABT857, Millipore) [17] (*see* **Note 2**).
5. Streptavidin (Sta)-allophycocyanin (APC) (BD Biosciences, #554067).
6. 5 mL round-bottom fluorescent-activated cell sorting (FACS) tubes (FALCON, #352054).
7. Propidium iodide (PI) solution (BD Biosciences, #556463).
8. Sterile 40 μm cell strainers (FALCON, #352340).
9. RNase-free 1.5 mL tubes.
10. TRIzol-LS (Invitrogen, #10296-010).

2.3 Staining of Isolated Muscle Satellite Cells

1. Cytospin (Thermo Fisher Science)
2. Cytospin-Funnel set: CytoSep Cytology Funnel (Thermo Fisher Science, #M964-1), caps (Thermo Fisher Science, #M965C), paper (Thermo Fisher Science, #M965FW), glass slide
3. Antibody: mouse anti-Pax7 antibody (Clone: Pax7, DSHB)
4. Antibody: Alexa 568 goat anti-mouse secondary antibody (Invitrogen, #A-11004)
5. Fixed solution: 0.4 g PFA is dissolved in 10 mL PBS
6. Washing buffer: 2% FCS in PBS
7. Wash-out solution: 0.1% Triton-X 100 in PBS
8. Blocking solution: 5% skim milk in PBS
9. Mounting medium: VECTASHIELD Mounting Medium with DAPI (Vector, #H1200)

3 Methods

3.1 Preparation of Mononuclear Cells from Murine Skeletal Muscles

1. Euthanize mice using a suitable procedure.
2. To protect against contamination, disinfect the mice's skin with 70% ethanol.
3. Make an incision around the foot and cut the skin from the incision to above the groin.
4. Pull the skin toward the groin to expose the muscles.

5. Cut the tendons of the tibialis anterior (TA) and extensor digitorum longus (EDL) muscles located at the dorsum pedis. Thereafter, carefully pull the tendon to the knee and remove the TA and EDL.
6. Insert scissors into the crevice of the hamstring and thereafter, open the scissors to visibly separate the hamstring and gastrocnemius.
7. Simultaneously, cut the tendons of the gastrocnemius, soleus, and plantaris at the heel and remove these muscles.
8. After cutting the quadriceps tendon at the knee, pull the tendon toward the groin and remove the quadriceps (*see* **Note 3**).
9. Weigh the muscles on the electronic balance (*see* **Note 4**).
10. Soak the muscles in PBS on ice.
11. Remove non-muscle tissues such as tendons, fat, fur, and vessels using forceps in a clean bench, while keeping the muscles in PBS.
12. After draining PBS, mince the muscles with scissors (*see* **Note 5**).
13. Add the minced muscles and pre-warmed 0.2% Collagenase II digestion solution (3 mL/1 g muscle) to a 10 mL beaker and stir for 60 min on the magnetic stirrer in the incubator maintained at 37 °C (*see* **Notes 3** and **6**).
14. Homogenize the suspension by passing it 10 times through the 18G needle attached to a 5 mL syringe. If a muscle piece does not pass through the needle, cut the muscle to a smaller size with scissors.
15. Stir the suspension for 30 min on the magnetic stirrer in the incubator maintained at 37 °C.
16. Homogenize the suspension by passing it 10 times through the same needle and syringe system (**step 14**).
17. Dilute the suspension with pre-warmed PBS (approximately 50 mL/1 g muscle) (*see* **Note 7**).
18. Homogenize the suspension by passing it 10 times through an 18G needle attached to a 10 mL syringe.
19. Transfer a small amount of the suspension (approximately 10 mL) to a beaker. After homogenizing the suspension by passing it 10 times through the 18G needle attached to a 10 mL syringe (**step 18**), the suspension is transferred to new 50 mL conical tubes by filtering through a 40 μm cell strainer.
20. Repeat **step 19** until the entire suspension is filtered.
21. Centrifuge at 500 *g* for 10 min and remove the supernatant.
22. Tap the bottom of the tube to suspend the cell pellet.

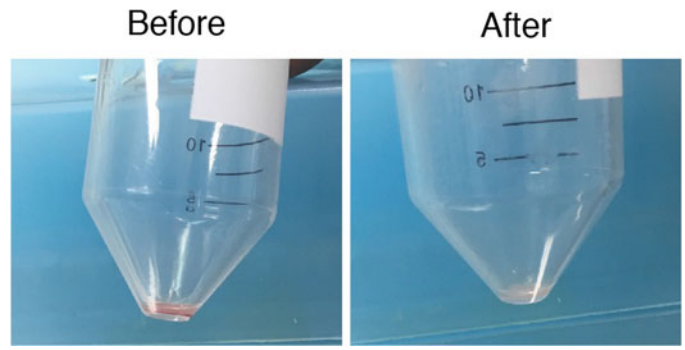

Fig. 1 ACT treatment. Before ACT treatment, the color of the aggregated cells is red. After ACT treatment, the color of the aggregated cells becomes pink. White color indicates excessive reaction-time of ACT

23. Incubate the suspended pellet with cooled ACT solution (1 mL/1 g muscle) for 1–2 min on ice to eliminate erythrocytes (*see* **Note 8**) (*see* Fig. 1).
24. Add 50 mL washing buffer and centrifuge at 500 *g* for 5 min. Remove the supernatant.

3.2 Staining of Mononuclear Cells and Isolation of Satellite Cells

1. Add 400 μL washing buffer and resuspend the pellet.
2. Incubate with SM/C-2.6-biotin antibody for 30 min on ice.
3. Add 30 mL washing buffer.
4. Centrifuge the tube at 500 *g* for 5 min and remove the supernatant.
5. Add 400 μL washing buffer and resuspend the pellet.
6. Incubate with anti-Sca1-PE, CD31-FITC, and CD45-FITC antibodies and Sta-APC for 30 min on ice.
7. Add 30 mL washing buffer.
8. Centrifuge the tube at 500 *g* for 5 min and remove the supernatant.
9. Tap the bottom of the tube to suspend the cell pellet.
10. Add 4 mL washing buffer.
11. Add 10 μL PI solution per 1 mL washing buffer and filter the suspension through a 40 μm nylon mesh.

3.3 FACS Analyses

1. Make the forward scatter (FSC)/side scatter (SSC) profile and analyze the FACS profile of mononuclear cells by gated 1 (R1) (*see* **Note 9**) (*see* Fig. 2a).
2. Make the PI/APC profile and analyze the FACS profile of living mononuclear cells by gated 2 (R2) (*see* Fig. 2b).
3. Make the FITC/PE profile and analyze the FACS profile of $CD31^{-}CD45^{-}$ cells by gated 3 (R3) (*see* Fig. 2c).

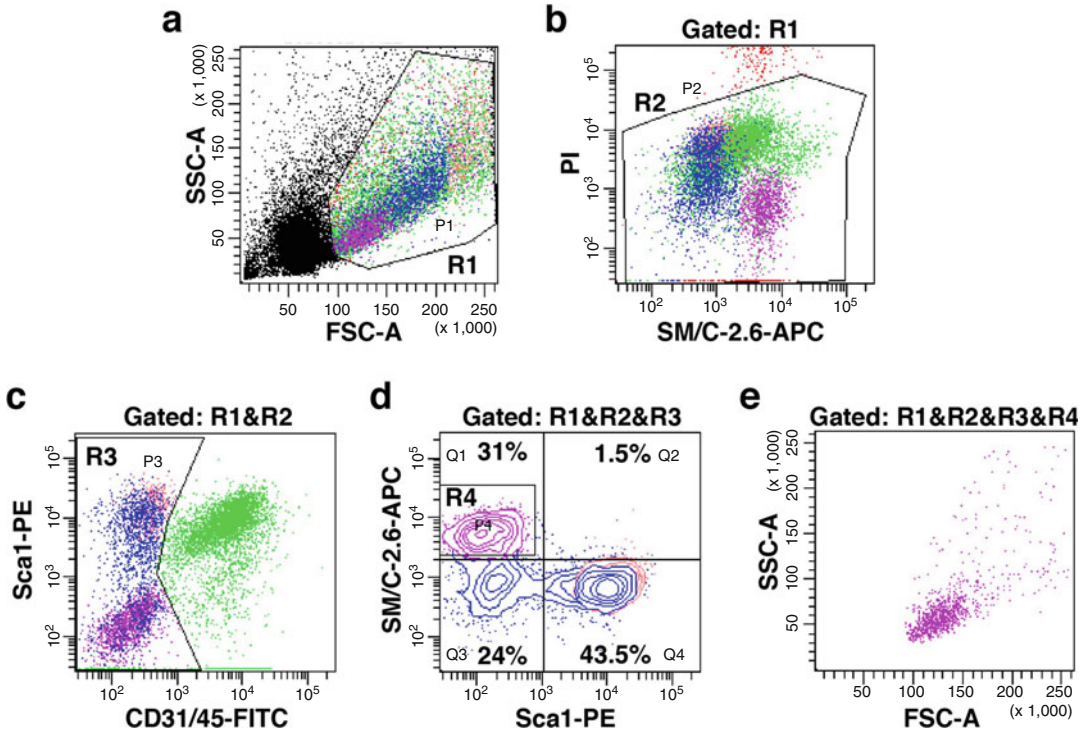

Fig. 2 FACS profile of mononuclear cells from intact skeletal muscles. The FSC/SSC gate (R1) excluded debris. PI-negative cells (R2) indicate living cells. CD31/45-negative cells (R3) include MuSCs. The SM/C-2.6-APC and Sca1-PE (R4) indicate the MuSC fraction (R4). The population of MuSCs is relatively small in the FSC/SSC profile. MuSC fractions are shown in purple color in all profiles

4. Make the PE/APC profile and analyze the FACS profile of MuSCs by gated 4 (R4) (*see* Fig. 2d).
5. To confirm the presence of MuSC fraction, analyze the FSC/SSC profile defined by R1–R4 gates (*see* Fig. 2e).
6. Add 1 mL TRIzol-LS to 1.5 mL RNase-free collection tubes (*see* **Note 10**).
7. Sort $CD31^{-}CD45^{-}Sca1^{-}SM/C\text{-}2.6^{+}$ cells (R4) as MuSCs into the collection tubes.
8. More than 1×10^5 MuSCs are obtained per mouse head.

3.4 Staining of Isolated MuSCs (See Fig. 3)

1. Suspend the sorted cells in the washing buffer ($1–2 \times 10^4$ cells/200 μL) (*see* **Note 11**).
2. Apply 100 μL cell suspension to the cytospin-funnel set.
3. Centrifuge at 800 rpm for 3 min by cytospin and take the glass slide.
4. Dry the cells on glass slide at room temperature for 10 min. When the glass slide is dried, the cells are surrounded by liquid blocker.

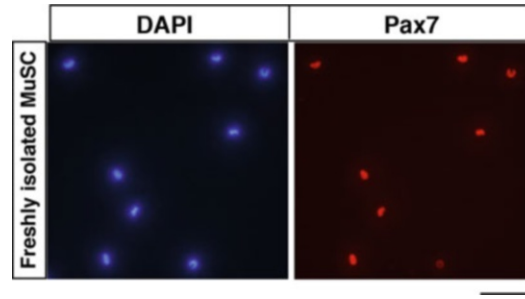

Fig. 3 Staining of freshly isolated MuSCs. The isolated MuSCs on glass slides were stained with anti-Pax7 (red) and DAPI (blue). Scale bar: 50 μm

5. Mount the cooled fixed solution on the cells for 10 min.
6. Put the glass slide into the coupling jar filled with the wash-out solution.
7. After 5 min, the wash-out solution is replaced with the new wash-out solution.
8. Repeat **step 7** twice.
9. After 5 min, the wash-out solution is replaced with PBS.
10. Take the glass slide and mount the blocking solution on the cells for 1 h.
11. After removing the blocking solution, incubate the cells with anti-Pax7 antibody overnight at 4 °C.
12. Put the glass slide into the coupling jar filled with wash-out solution.
13. After 5 min, the wash-out solution is replaced with the new wash-out solution.
14. Repeat **step 11** twice.
15. Shield the cells with the mounting medium.

4 Notes

1. To avoid contamination, make only the volume required for a day.
2. While non-labeled SM/C-2.6 antibody is commercially available, biotinylation is needed by itself.
3. To obtain the maximum amount of MuSCs, the gluteus maximus and triceps brachii muscles should be used. A 20 mL beaker is appropriate if two or three mice heads are used for obtaining MuSCs.
4. Avoid drying the muscles during preparation.
5. Non-muscle tissues may be removed in this process.

6. Avoid bubbles due to the stirring.
7. PBS should be warmed in a water bath at 37 °C. It is critical to dilute the cell suspension before filtration.
8. Pink color is the best. Do not repeat this procedure if many red cells are remaining.
9. All gates are in a hierarchical position.
10. If the isolated cells are cultured, collect 1×10^5 cells in a 1.5 mL tube containing 1 mL washing buffer.
11. If fluorescence proteins (GFP, YFP, etc.) are stained, MuSCs are fixed with the fixed solution, and then centrifuged. Continue from **step 5** after the cells are dried for 10 min and are surrounded by liquid blocker.

Acknowledgments

We acknowledge the funding support of the Japan Society for the Promotion of Science (a Grant-in-Aid for Scientific Research (B), 19H04000). M.K. received funding from the Fuji Seal Foundation.

References

1. Mauro A (1961) Satellite cell of skeletal muscle fibers. J Biophys Biochem Cytol 9:493–495
2. Seale P, Sabourin LA, Girgis-Gabardo A, Mansouri A et al (2000) Pax7 is required for the specification of myogenic satellite cells. Cell 102:777–786
3. McCarthy JJ, Mula J, Miyazaki M et al (2011) Effective fiber hypertrophy in satellite cell-depleted skeletal muscle. Development 138: 3657–3666
4. Fukada SI, Akimoto T, Sotiropoulos A (2020) Role of damage and management in muscle hypertrophy: different behaviors of muscle stem cells in regeneration and hypertrophy. Biochim Biophys Acta, Mol Cell Res 1867(9): 118742
5. Yaffe D, Saxel O (1977) Serial passaging and differentiation of myogenic cells isolated from dystrophic mouse muscle. Nature 270:725–727
6. Blau HM, Chiu CP, Webster C (1983) Cytoplasmic activation of human nuclear genes in stable heterocaryons. Cell 32:1171–1180
7. Qu-Petersen Z, Deasy B, Jankowski R et al (2002) Identification of a novel population of muscle stem cells in mice: potential for muscle regeneration. J Cell Biol 157:851–864
8. Irintchev A, Zeschnigk M, Starzinski-Powitz A et al (1994) Expression pattern of M-cadherin in normal, denervated, and regenerating mouse muscles. Dev Dyn 199:326–337
9. Goel AJ, Rieder MK, Arnold HH et al (2017) Niche Cadherins control the quiescence-to-activation transition in muscle stem cells. Cell Rep 21:2236–2250
10. Fukada S, Uezumi A, Ikemoto M et al (2007) Molecular signature of quiescent satellite cells in adult skeletal muscle. Stem Cells 25:2448–2459
11. Yamaguchi M, Ogawa R, Watanabe Y et al (2012) Calcitonin receptor and Odz4 are differently expressed in Pax7-positive cells during skeletal muscle regeneration. J Mol Histol 43: 581–587
12. Sherwood RI, Christensen JL, Conboy IM et al (2004) Isolation of adult mouse myogenic progenitors: functional heterogeneity of cells within and engrafting skeletal muscle. Cell 119:543–554
13. Cornelison DD, Filla MS, Stanley HM et al (2001) Syndecan-3 and syndecan-4 specifically mark skeletal muscle satellite cells and are implicated in satellite cell maintenance and muscle regeneration. Dev Biol 239:79–94
14. Rozo M, Li L, Fan CM (2016) Targeting beta1-integrin signaling enhances regeneration in aged and dystrophic muscle in mice. Nat Med 22:889–896

15. Tatsumi R, Anderson JE, Nevoret CJ et al (1998) HGF/SF is present in normal adult skeletal muscle and is capable of activating satellite cells. Dev Biol 194:114–128
16. Abou-Khalil R, Le Grand F, Pallafacchina G et al (2009) Autocrine and paracrine angiopoietin 1/Tie-2 signaling promotes muscle satellite cell self-renewal. Cell Stem Cell 5:298–309
17. Fukada S, Higuchi S, Segawa M et al (2004) Purification and cell-surface marker characterization of quiescent satellite cells from murine skeletal muscle by a novel monoclonal antibody. Exp Cell Res 296:245–255
18. Fukada S, Yamaguchi M, Kokubo H et al (2011) Hesr1 and Hesr3 are essential to generate undifferentiated quiescent satellite cells and to maintain satellite cell numbers. Development 138:4609–4619
19. Yamaguchi M, Watanabe Y, Ohtani T et al (2015) Calcitonin receptor signaling inhibits muscle stem cells from escaping the quiescent state and the niche. Cell Rep 13:302–314
20. Zhang L, Noguchi YT, Nakayama H et al (2019) The CalcR-PKA-Yap1 Axis is critical for maintaining quiescence in muscle stem cells. Cell Rep 29:2154-63 e5
21. Noguchi YT, Nakamura M, Hino N et al (2019) Cell-autonomous and redundant roles of Hey1 and HeyL in muscle stem cells: HeyL requires Hes1 to bind diverse DNA sites. Development 146:dev163618
22. Ogawa R, Ma Y, Yamaguchi M et al (2015) Doublecortin marks a new population of transiently amplifying muscle progenitor cells and is required for myofiber maturation during skeletal muscle regeneration. Development 142:51–61

Chapter 2

Extra Eyelid-Derived Muscle Stem Cells

Takahiko Sato, Yukito Yamanaka, Morio Ueno, and Chie Sotozono

Abstract

Skeletal muscle stem cells (MuSCs) have been proposed as suitable candidates for cell therapy to muscular disorders since they exhibit a good capacity for myogenic regeneration. However, for better therapeutic outcomes, it is necessary to isolate human MuSCs from a suitable tissue source that possess high myogenic differentiation. In this context, isolated CD56+CD82+ cells from extra eyelid tissues were tested in vitro myogenic differentiation potential. Primary human myogenic cells derived from extra eyelids including orbicularis oculi, might be good candidates for human muscle stem cell-based research.

Key words Skeletal muscle, Muscle stem cells, Blepharoplasty, Orbicularis ocular muscle, CD56, CD82, Pax7

1 Introduction

Skeletal muscle tissue has its own repair and maintenance system, which is based on adult skeletal muscle stem cells (MuSCs), including muscle satellite cells. Adult MuSCs normally exist as quiescent and are activated upon muscle damage, either by muscular injury or under pathological conditions such as Duchenne muscular dystrophy (DMD). They proliferate, differentiate to enter the regenerative myogenic program, fuse with damaged myofibers, and also generate a novel population of quiescent MuSCs [1]. In this section, we introduce the method of sampling human myogenic stem cells from extra eyelid tissues collected in the operation of blepharoplasty.

Blepharoplasty is one of the most performed surgical repairs where the eyelid skin, orbicularis oculi muscle, and orbital fat are excised (Fig. 1). As we age, eyelids gradually stretch and the thinning of the levator aponeurosis leads to ptosis of the upper eyelid [2]. Besides making you look older, severe ptosis can limit your peripheral vision, especially the upper parts of your field of vision. Blepharoplasty is done for both esthetic and functional indications. After this surgery, extra eyelids are normally removed and discarded

Atsushi Asakura (ed.), *Skeletal Muscle Stem Cells: Methods and Protocols*, Methods in Molecular Biology, vol. 2640, https://doi.org/10.1007/978-1-0716-3036-5_2,

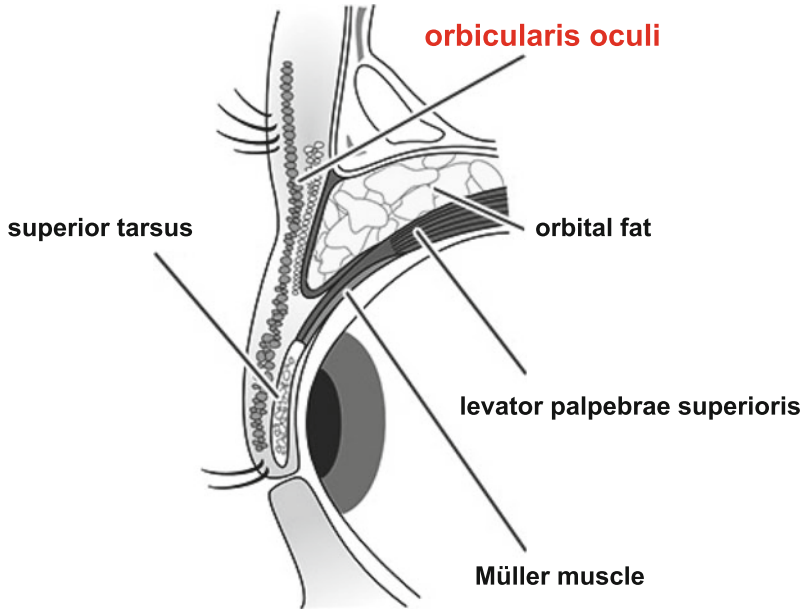

Fig. 1 The schematic representation of a sagittal cross-section of the upper lid, including orbicularis oculi muscle, highlighted in red

as medical waste, although orbicularis oculi or levator muscles might be attached to them [3] (Fig. 2a, b).

We speculated their potential as a source of myogenic stem cells able to generate high amounts of human myogenic CD56+CD82+ stem cells [4] from freshly isolated primary human ocular biopsy cultures. It has been known that CD56 is the marker that enables isolation of human myogenic cells [5], and CD82 is a novel marker for detecting human muscle stem cells [4, 5]. We demonstrated that human CD56+CD82+ myogenic cells derived from orbicularis oculi expressed high *PAX7* transcripts, which are a transcriptional marker of muscle satellite cells. These methods facilitate the primary isolation of human myogenic cells from human fresh muscle tissues to analyze intact skeletal muscle stem cells in vitro and in vivo.

2 Materials

Human biopsies of the extra eyelid, which include skeletal muscle tissues, were collected during ophthalmologic surgeries of healthy patients with proper permission (Fig. 2a) [6]. All methods relating to the human study were performed in accordance with the guidelines.

1. Coating culture dish: 0.05% of Geltrex Basement Membrane Matrix (GIBCO) or Matrigel (BD) on cell culture dishes.

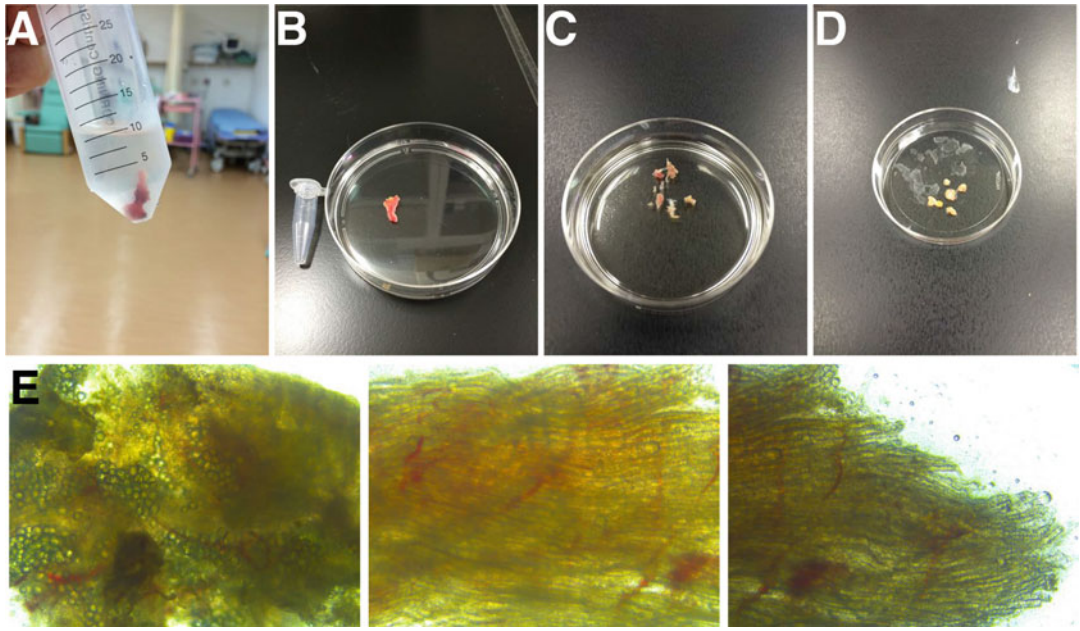

Fig. 2 Collecting human skeletal muscle cells obtained from extra tissues containing orbicularis oculi muscles at the time of ophthalmic surgery. (**a**) Surgically excised eyelid tissues soaked in cold PBS solution. (**b**) An example of the actual size of the extra eyelid tissue compared with a 1.5 mL microtube. (**c**) The obtained skeletal muscle tissue was finely selected with scissors and tweezers. (**d**) Shows morphological features of isolated tissues, the mass of lipids (left panel), blood capillaries (middle panel), and disconnected skeletal muscle fibers (right panel)

2. Dissociation stock solution: 2% collagenase type II (Worthington) in Phosphate buffered saline, pH 7.4 (PBS).
3. Basic FGF (bFGF) stock solution: 10 μg/mL of bFGF in PBS.
4. Human myogenic cell growth medium: 20% of Fetal bovine serum (FBS) in DMEM supplemented with 5 ng/mL of bFGF.
5. Human myogenic cell differentiation medium: 2% of horse serum (SIGMA) in DMEM.
6. FACS washing buffer: 1% of FBS in Hank's Balanced Salt Solution buffer (HBSS).
7. Fixation solution: 4% paraformaldehyde (PFA) in PBS.
8. Permeabilization buffer: 0.2% of Triton X-100 and 50 mM of NH_4Cl in PBS.
9. Washing buffer (PBS-T): 0.1% Tween 20 in PBS.
10. Antibody dilution buffer: 5% of Blocking One (Nacalai) in PBS-T.
11. Antibodies: anti-CD56-PE (diluted with 1/50, BioLegend), anti-CD82-PE-Alexa647 (diluted with 1/50, BioLegend), SYTOX Green (diluted in 1/500, Thermo Fisher Scientific),

anti-MyoD (diluted with 1/100, Santa Cruz Biotechnology), anti-myogenin (diluted with 1/100, DAKO), anti-troponin T (diluted with 1/250, Sigma), and anti-MyHC (MF20, diluted with 1/200, R&D), 4,6-diamidino-2-phenylindole (DAPI, diluted with 1/2000, Thermo Fisher Scientific).

3 Methods

Carry out all procedures at room temperature unless otherwise noted.

3.1 Preparation of Cells for Primary Culture

1. Prepare for Geltrex Basement Membrane Matrix-coated cell culture dishes at 37 °C (*see* **Note 1**).
2. To isolate myogenic cells from orbicularis oculi, blood and fats are carefully removed to avoid contamination with non-muscle cells present in the excised eyelid (Fig. 2c–e).
3. Obtained tissues are finely chopped by scissors (Fig. 3a, *see* **Note 2**).
4. Chopped samples are enzymatically dissociated with 0.2% of collagenase type II in DMEM at 37 °C for 60 min (Fig. 3b).
5. Dissociated cells are resuspended with FACS washing buffer and filtered with cell strainers (Fig. 3c, *see* **Note 3**).
6. Centrifuge and resuspend these cells in DMEM containing 20% of FBS and 5 ng/mL of bFGF (Fig. 3d).
7. Resuspended cells are plated on Geltrex-coated dishes.
8. Fresh media is added regularly until colonies with spindle-shaped cells are obtained (Fig. 4a).

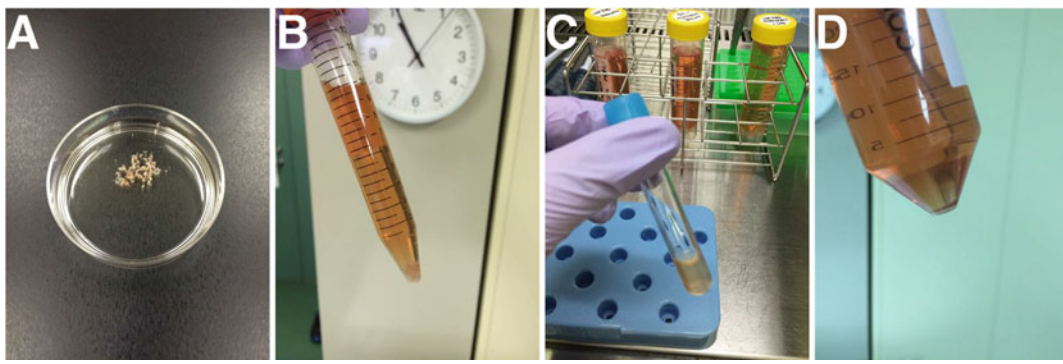

Fig. 3 Dissociation of single human myogenic cells. (**a**) The obtained tissue was finely chopped with scissors. (**b**) Chopped samples were enzymatically treated with collagenase type II, then filtrated (**c**) after enzymatic digestion, and centrifuged to collect single myogenic cells (**d**)

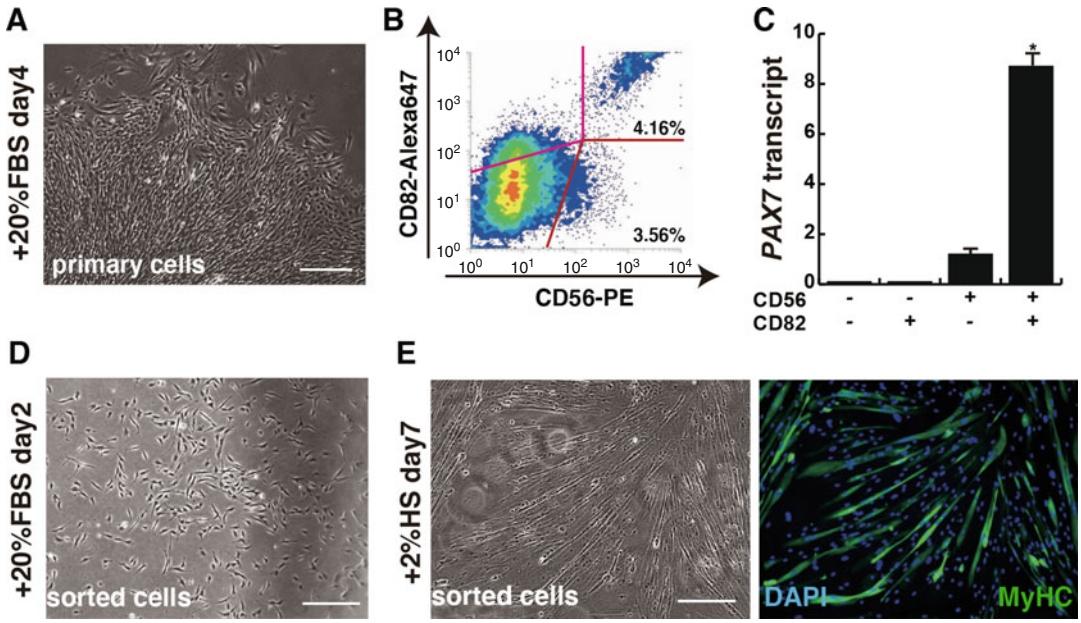

Fig. 4 CD56+CD82+ double-positive myogenic cells from primary cultured orbicularis oculi muscles. (**a**) Image of primary cultured cells digested from isolated eyelid tissue. (**b**) FACS profile of CD56- and CD82-double-positive cells from primary cultured orbicularis oculi muscles from extra eyelids. (**c**) PAX7 transcriptome analyses of CD56+CD82+ sorted cells shown in (**b**). (**d**) Morphological features of sorted cells of orbicularis oculi muscles, cultured for 2 days. (**e**) Myogenic differentiation with sorted cells in 2% of horse serum medium for 7 days. MyHC; green, DAPI; blue. $n = 3$ independent replicates, *P*-values are determined by t-test from a two-tailed distribution. $^*P < 0.01$. $n = 3$ independent replicates, *P*-values are determined by Dunnett's multiple-comparisons test. $^*P < 0.01$. All scale bars = 100 μm

3.2 Preparation of Cultured Myogenic Cells for Cell Sorting

1. For cell sorting, cultured cells are detached with Accutase from cell culture dishes.
2. Detached cells are resuspended with FACS washing buffer at 4 °C.
3. Incubate with the monoclonal anti-human antibodies anti-CD56-PE and anti-CD82-Alexa647 for 30 min at 4 °C (*see* **Note 4**).
4. Wash samples with FACS washing buffer for 3 times.
5. For live cell sorting, dissociated single cells are stained with SYTOX Green to exclude dead cells.
6. Human myoblasts, including muscle stem cells, defined as CD56+CD82+, are sorted by FACS (Fig. 4b, c).

3.3 Characterization of Isolated Cells Ex Vivo

1. Isolated CD56+CD82+ double positive cells were resuspended in the growth medium, DMEM containing 20% FBS and 5 ng/mL of bFGF.
2. Cells were cultured in 35 mm dishes coated with Geltrex at 5.0×10^3 cells per dish (Fig. 4d).

3. A few days later, the medium was changed to the differentiation medium, which consisted of DMEM with 2% horse serum (Fig. 4e).

3.4 Immuno-cytochemical Analysis

<Day1>

1. Cultured cells were fixed with 4% PFA in PBS at 4 for 15 min (*see* **Note 5**).
2. Wash it twice with PBS and permeabilize with 0.2% Triton, with 50 mM NH_4Cl in PBS.
3. Cells were incubated with 5% Blocking One for 30 min.
4. The following antibodies are used as primary antibodies: anti-MyoD (diluted with 1/100), anti-myogenin (diluted with 1/100), anti-troponin T (diluted with 1/250), and anti-MyHC (MF20, diluted with 1/200, Fig. 4e) in 5% Blocking One solution for overnight at 4 °C.

<Day2>

5. Wash them with PBS-T for 10 min 3 times.
6. Incubate with secondary antibodies coupled to fluorochromes Alexa 488, 594 or 647 in 5% Blocking One solution for 60 min. 4,6-Diamidino-2-phenylindole is used to counter-stain nuclei (*see* **Note 6**).
7. For quantification, at least 500 cells in culture are counted from randomly chosen fields for each stage.

4 Notes

1. You can use Matrigel-coating dishes instead of Geltrex.
2. The more you chop with scissors, the better single cells you can gain after enzymatic digestion.
3. You can directly isolate myogenic cells from eyelid tissues by FACS, however, the numbers of CD56+CD82+ would be quite low.
4. Isotype control antibodies, PE- and Alexa647-conjugated mouse IgG are used for FACS.
5. If it is not required for performing immunostaining, 0.05% of glutaraldehyde solution instead of 4% PFA may be added to the fixative solution.
6. All samples must be shielded from light using aluminum foil during the washing and incubating period to prevent the loss of immunofluorescence after the incubation with 2nd antibodies.

References

1. Keefe AC, Lawson JA, Flygare SD et al (2015) Muscle stem cells contribute to myofibres in sedentary adult mice. Nat Commun 6:7087. https://doi.org/10.1038/ncomms8087
2. Frueh BR (1980) The mechanistic classification of ptosis. Ophthalmology 87:1019–1021. https://doi.org/10.1016/s0161-6420(96)30744-6
3. Jones LT, Quickert MH, Wobig JL (1975) The cure of ptosis by aponeurotic repair. Arch Ophthalmol 93:629–634. https://doi.org/10.1001/archopht.1975.01010020601008
4. Alexander MS, Rozkalne A, Colletta A et al (2016) CD82 is a marker for prospective isolation of human muscle satellite cells and is linked to muscular dystrophies. Cell Stem Cell 19:800–807. https://doi.org/10.1016/j.stem.2016.08.006
5. Uezumi A, Nakatani M, Ikemoto-Uezumi M et al (2016) Cell-surface protein profiling identifies distinctive markers of progenitor cells in human skeletal muscle. Stem Cell Reports 7:263–278. https://doi.org/10.1016/j.stemcr.2016.07.004
6. Yamanaka Y, Takenaka N, Sakurai H et al (2019) Human skeletal muscle cells derived from the orbicularis oculi have regenerative capacity for duchenne muscular dystrophy. Int J Mol Sci 20:3456. https://doi.org/10.3390/ijms20143456

Chapter 3

Isolation, Culture, and Analysis of Zebrafish Myofibers and Associated Muscle Stem Cells to Explore Adult Skeletal Myogenesis

Massimo Ganassi, Peter S. Zammit, and Simon M. Hughes

Abstract

Adult skeletal musculature experiences continuous physical stress, and hence requires maintenance and repair to ensure its continued efficient functioning. The population of resident muscle stem cells (MuSCs), termed satellite cells, resides beneath the basal lamina of adult myofibers, contributing to both muscle hypertrophy and regeneration. Upon exposure to activating stimuli, MuSCs proliferate to generate new myoblasts that differentiate and fuse to regenerate or grow myofibers. Moreover, many teleost fish undergo continuous growth throughout life, requiring continual nuclear recruitment from MuSCs to initiate and grow new fibers, a process that contrasts with the determinate growth observed in most amniotes. In this chapter, we describe a method for the isolation, culture, and immunolabeling of adult zebrafish myofibers that permits examination of both myofiber characteristics ex vivo and the MuSC myogenic program in vitro. Morphometric analysis of isolated myofibers is suitable to assess differences among slow and fast muscles or to investigate cellular features such as sarcomeres and neuromuscular junctions. Immunostaining for Pax7, a canonical stemness marker, identifies MuSCs on isolated myofibers for study. Furthermore, the plating of viable myofibers allows MuSC activation and expansion and downstream analysis of their proliferative and differentiative dynamics, thus providing a suitable, parallel alternative to amniote models for the study of vertebrate myogenesis.

Key words Zebrafish, Myonucleus, Skeletal muscle, Pax7, MuSC, Stem cell, Myofiber, Adult

1 Introduction

Skeletal musculature produces the force that enables body support and movement. To respond efficiently to different workload demands, vertebrates have evolved two major types of muscle fibers, defined as slow or fast, arising from their specialized ability to support either endurance tasks or rapid powerful movements, respectively [1, 2]. Whereas in amniote vertebrates, such as humans, rodents, and birds, slow and fast myofibers can be found interspersed both within and between different muscle groups, in

Atsushi Asakura (ed.), *Skeletal Muscle Stem Cells: Methods and Protocols*, Methods in Molecular Biology, vol. 2640,
https://doi.org/10.1007/978-1-0716-3036-5_3,

the trunk muscle of teleost fish, for example, zebrafish, the two fiber types are spatially segregated throughout life [3–5]. Slow myofibers are localized exclusively near the lateral line on the lateral surface of the myotome and tend to have oxidative metabolism adapted to gentle persistent swimming, whereas a larger proportion of fast glycolytic myofibers make up the bulk of the myotome and generate more forceful contractions. Intermediate myofiber types also exist between these extremes [6, 7]. This spatial separation facilitates myofiber-type specific studies [8].

Despite divergence in structure and function, fast and slow muscles share the ability to adapt rapidly to external stimuli like increased functional demand or injury. To sustain such plasticity, myofibers are equipped with a specialized population of resident precursor cells, the muscle stem cells (MuSCs), which in normal conditions lie quiescent underneath the basal lamina of adult myofibers, and are usually termed satellite cells [9, 10]. When needed, MuSCs sustain both the growth and repair of myofibers [11, 12]. Upon activation, MuSCs leave their quiescent state, enter proliferation, and generate myoblasts that fuse either to existing myofibers or together for de novo myofiber formation. A fraction of newly-generated MuSCs subsequently withdraw from the cell cycle to re-enter quiescence, thereby renewing the MuSC reservoir [13–15].

The dynamics of MuSC multi-step progression through proliferation, fusion, and differentiation reiterate many aspects of muscle formation in developing embryos [16]. It is well established that embryonic development of skeletal muscle is broadly conserved between zebrafish and amniotes, occurring through several myogenic waves controlled by homologous molecular cascades [17–21]. Less is known about the mechanisms regulating zebrafish adult muscle homeostasis. Moreover, in contrast to rodents, the study of adult myogenesis in zebrafish is in its infancy due to lack of suitable methods, and has been limited to culture of progenitor cells derived from mechanical trituration of bulk muscle [22, 23]. Thus, MuSC biology in zebrafish is ripe for exploration.

In this chapter, we describe how to isolate intact, single, viable myofibers and their associated stem cells from the trunk musculature of adult zebrafish through enzymatic digestion and fine trituration, an approach adapted from the classical mouse protocol [24, 25], derived from methodologies using rodent muscles to explore myofiber characteristics such as morphology and innervation [26–28]. Isolation of myofibers from various murine models has quickly become an indispensable tool to investigate muscle stem cell biology, providing understanding of MuSC behavior and regulation in quiescence, activation, proliferation, self-renewal, and differentiation in health and disease over the last decades [25, 29–35]. However, despite its potential, the use of this method in fish has remained mostly limited to the study of physical or contractile

properties of muscle fibers [37–39] with only few reports implementing it to assess zebrafish MuSC biology [17, 40–42].

Understanding human adult myogenesis is of great clinical significance, not only for neuromuscular disorders, but also in aging-related muscle weakening, otherwise known as sarcopenia, that is a major cause of debility, with attendant individual, familial, and societal costs [43, 44]. Moreover, diseases such as cancer, rheumatoid arthritis, COPD, and AIDS all lead to muscle wasting. Treatments for these conditions require testing in model organisms. Just as with rodents, we show that viable zebrafish myofibers, once isolated, can be plated to allow associated MuSCs to activate and recapitulate skeletal myogenesis in vitro, thus providing an alternative and reliable tool to study vertebrate muscle biology. Moreover, in contrast to the mechanical dissociation of whole muscle, myofiber plating ensures maximum purity of the cell population, yielding nearly pure myogenic progenitors in culture [17]. We recently established the described protocol to explore Myogenin function in adult MuSC activation, proliferation, and differentiation [17, 42, 45], showing its ability to yield insight into adult muscle biology at multiple levels. The described method is simple, efficient, and cost-effective and permits study of (a) myofiber characteristics ex vivo, (b) mechanisms of adult muscle formation, development, and maintenance, and (c) the behavior of MuSC-derived myoblasts in vitro, thereby providing an appropriate toolbox for comparative analysis of adult myogenesis across vertebrates. Application of our techniques to adult zebrafish muscle has potential to contribute to understanding genetic and cellular mechanisms maintaining and adapting skeletal myogenesis in people.

2 Materials

2.1 Materials for Dissection and Dissociation of Adult Zebrafish Muscle

1. Tricaine methanesulfonate (MS-222) solution)
2. Tissue culture hood or lamina flow cabinet
3. Tissue culture incubator (humidified, 28.5 °C, 5% CO_2)
4. Dissection microscope with transmission illumination (we use Zeiss Stemi SV6 and Leica M50)
5. Cork dissection board (Ikea, #870.777.00)
6. Dissection metal pins
7. Fine forceps, one pair (Idealtek, No. 5A.s)
8. Sterile disposable scalpels No. 10. (Swann-Morton, #0501)
9. Deep Petri dishes (150 mm and 100 mm) sterile, cell culture grade
10. Glass Pasteur pipettes (22 cm), sterile (Volac, #D812)

11. Rubber pipette bulbs, 1.5 mL
12. 0.45 and 0.2 μm sterile syringe filters
13. Sterile syringe, 50 mL
14. Aluminum foil
15. Bijou tubes, 7 mL
16. Bunsen burner
17. Diamond pen

2.2 Materials Required for Myofiber Isolation and MuSC Culture

1. Ethanol solution (in deionized water), 70%
2. Virkon solution (in deionized water), 1%
3. Phosphate-buffered saline Ca^{2+} and Mg^{2+} free (PBS), sterile
4. 5% Bovine serum albumin (BSA)
5. Collagenase from *Clostridium histolyticum* (Sigma Aldrich, #C0130)
6. Penicillin and Streptomycin solution
7. Gentamicin
8. Dulbecco's modified Eagle's medium (DMEM), high glucose, GlutaMAX, Pyruvate (ThermoFisher, #31966)
9. Fetal bovine serum (FBS), heat inactivated
10. Horse serum (HS)
11. Matrigel (Corning, #354263)
12. 24-well plates cell culture grade
13. 5-ethynyl-2′-deoxyuridine (EdU) solution (From Click-iT EdU kit, ThermoFisher, #C10646)

2.3 Materials Required for Myofiber and MuSC-Derived Cells Immunostaining

1. Paraformaldehyde (PFA) solution, 4% in PBS
2. Cover glasses 50 mm × 22 mm
3. Glass Slides
4. Liquid blocker super pap pen (Pyramid Innovation)
5. Crystal-clear plastic microcentrifuge tubes, 2 mL (Starlab, #S-1620-2700)
6. Triton X-100 detergent solution
7. Primary antibodies (Table 1)
8. Fluorochrome-conjugated Alexa Fluor secondary antibodies (Table 1)
9. Hoechst 33342 solution
10. Fluorochrome-conjugated Alexa Fluor Phalloidin and α-Bungarotoxin (Table 1)
11. Normal goat serum (NGS)

Table 1
Primary and secondary antibodies and toxins

Description	Source	Reference	Working dilution	Clonality
Mouse anti-Pax3/Pax7 (DP312)	Nipam Patel, UC Berkeley, USA	DP312; Davis et al. (2001) Ref. (58)	1:50	Monoclonal
Chicken anti-GFP	Abcam	#13970; RRID:AB_300798	1:400	Polyclonal
Mouse anti-MyHC (A4.1025) supernatant	Hughes lab; Developmental Studies Hybridoma Bank (DSHB); Merck	DSHB #A4.1025; Merck #05-716; RRID:AB_309930	1:5	Monoclonal
Mouse anti-MyHC (MF20) concentrated	Developmental Studies Hybridoma Bank (DSHB)	#MF20; RRID:AB_2147781	1:300	Monoclonal
Goat anti-mouse IgG (H + L) Alexa Fluor® 594	Thermo Fisher Scientific	A11032; RRID:AB_2534091	1:1000	Polyclonal
Goat anti-chicken IgY (H + L) Alexa Fluor® 488	Thermo Fisher Scientific	A11039; RRID:AB_2534096	1:1000	Polyclonal
Phalloidin-Alexa Fluor® 488	Thermo Fisher Scientific	A12379; RRID:AB_2315147	1:80 working solution 0.15 μM	–
α-Bungarotoxin-Alexa Fluor® 555	Thermo Fisher Scientific	B35451; RRID:AB_2617152	1:1000 working solution 1 μg/mL	–

(*H* + *L*) Immunoglobulins heavy and light chains

12. Glycerol-based mounting medium
13. Transparent nail varnish

3 Method

3.1 Preparation

Where possible, all steps are performed under sterile conditions in a tissue culture hood or lamina flow cabinet.

1. Prepare 10% vol/vol Penicillin/Streptomycin solution in PBS (P/S-PBS) and aliquot 25 mL into a 100 mm plastic Petri dish.
2. Prepare 200 mL of complete DMEM (cDMEM) by adding Penicillin/Streptomycin solution at 1% vol/vol and gentamicin to 50 μg/mL to DMEM.
3. Prepare 100 mL 5% BSA solution in sterile PBS (BSA, PBS) and heat-inactivate at 60 °C for 60 min before filtering through a 0.45 μm syringe filter (*see* **Note 1**).
4. Rinse one 150 mm and two 100 mm sterile Petri dishes per fish with BSA,PBS solution to prevent myofiber adhesion to the dish. Remove excess BSA,PBS solution and add 25 mL and 10 mL of cDMEM to the 150 mm and 100 mm dishes, respectively. Place dishes in a 28.5 °C 5% CO_2 incubator for at least 30 min to allow the cDMEM to warm.
5. Immediately before dissection, prepare a 0.2% Collagenase solution in cDMEM.
6. In the tissue culture hood, filter-sterilize the Collagenase/cDMEM solution using a sterile syringe with a 0.2 μm filter. For each fish (two fillets), aliquot approximately 2 mL Collagenase/cDMEM solution into a 7 mL bijou tube (*see* **Note 2**).

3.2 Muscle Dissection

It is essential to wash and sterilize thoroughly to avoid microbial contamination.

1. Euthanize the fish (*see* **Note 20**) by immersion in ice-cold 0.3 mg/mL tricaine solution. To minimize distress, immerse fish in tricaine solution aliquoted into a 50 mL tube and keep in ice for the required amount of time (*see* **Note 3**).
2. Immerse fish carcass in 25 mL of 1% Virkon solution in a 100 mm dish and incubate for 5 min to kill bacteria and fungi (Fig. 1a).
3. Wash the carcass by transferring it with clean forceps to the 100 mm dish containing 25 mL P/S-PBS and incubate for 5 min (Fig. 1a′).
4. Transfer fish carcass into a new empty 100 mm Petri dish and remove scales using a disposable scalpel. For efficient removal, position the blade perpendicular to the antero-posterior axis

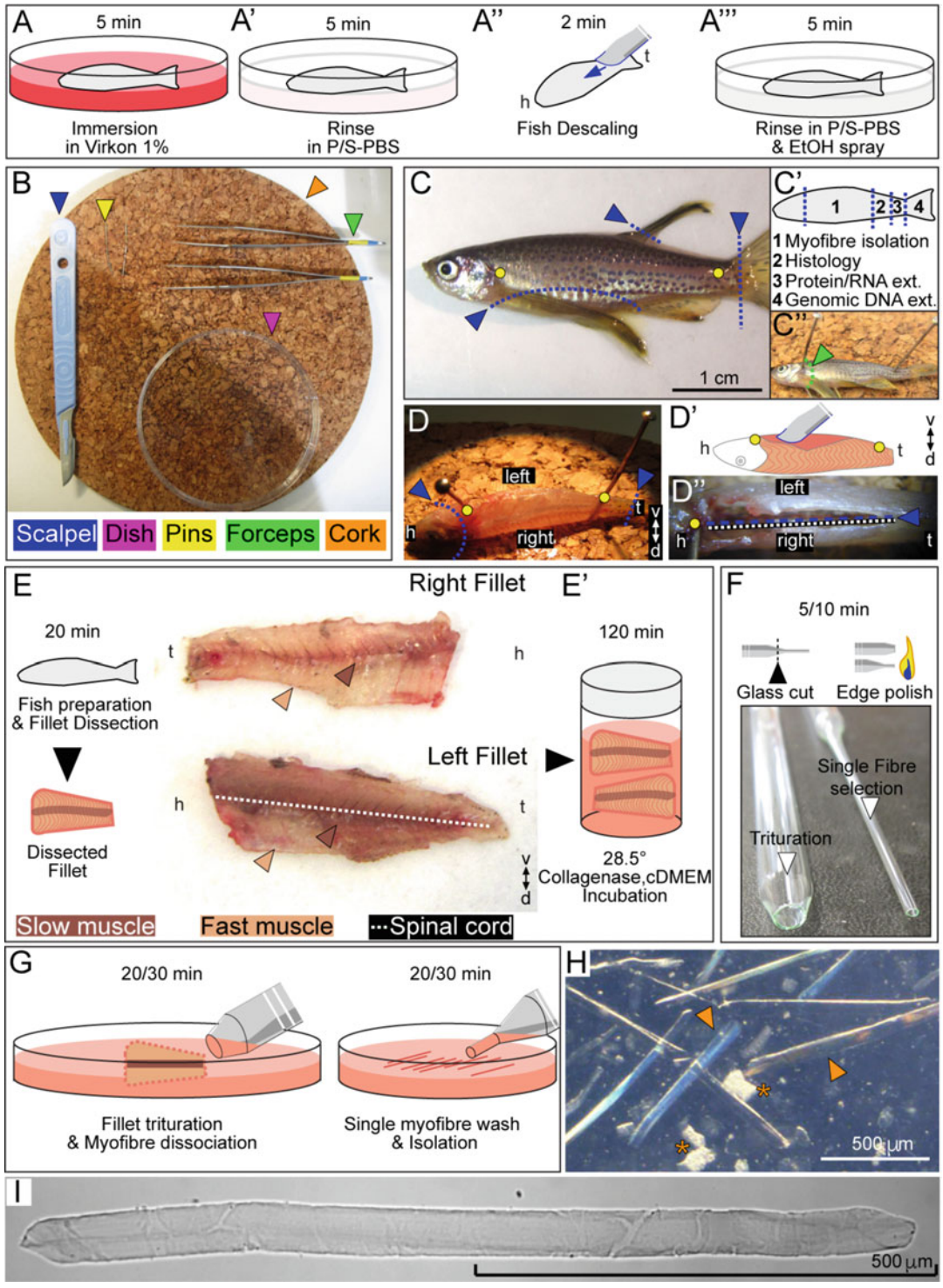

Fig. 1 Dissection and Isolation of Zebrafish Adult Myofibeers. (**a**–**a**‴). Schematics of fish body preparation prior to muscle dissection. Immersion in 1% Virkon solution (**a**), rinse in 10% Penicillin/Streptomycin in PBS (P/S-PBS) (**a**′), scale removal (**a**″), final rinse in P/S-PBS and 70% ethanol spray (**a**‴). Blue arrow in (**a**″) indicates head (h) -to-tail (t) direction of blade movement for optimal descaling. Estimated duration of each

of the body, and gently scrub fish surface from tail to head (Fig. 1a″).

5. Wash the descaled carcass by moving it into a new 100 mm dish containing 25 mL of fresh P/S-PBS and incubate for 5 min.
6. Carefully wipe dissection metal pins, corkboard, and fine forceps with 70% Ethanol solution (70% EtOH). Move the fish to an empty 100 mm dish, dry with cloth, and spray with 70% EtOH on both sides. Finally, move the fish carcass to the dissecting corkboard (Fig. 1b).
7. Pin the fish onto the corkboard, placing one pin passing through tissue just behind the gill operculum and a second posterior pin penetrating the tissue just anterior to the base of the caudal fin (Fig. 1c).
8. Using the scalpel, eliminate fins by cutting as close as possible to the fish body (Fig. 1c). Removing fish fins facilitates handling and reduces the risk of downstream microbial contamination.

Fig. 1 (continued) step is given. (**b**) Instruments and equipment required for dissecting fish and isolating myofibres. Arrowheads indicate specific items: disposable sterile scalpel N.10 (blue), metal dissection pins (yellow), fine metal forceps (green), dissecting corkboard (orange) and 100 mm sterile tissue culture grade plastic dish (magenta). (**c**–**c**″) Representative picture of an 8-month-old adult zebrafish. Pin positioning for the correct anchoring of the fish carcass to the corkboard is indicated (yellow dots). Blue dashed lines indicate cuts to remove fins and to perform ventral incision for evisceration (**c**). Upon dissection, different portions of the carcass can be used in multiple downstream analyses (**c**′). Green dashed and arrowhead indicate incision and pinch positions for fish skinning (**c**″). (**d**–**d**″) Representative picture of fish repositioning after initial skinning. Fish is rotated by 90° on its antero-posterior axis to expose the ventral incision upward and arrange the opening towards the operator. Dashed lines and arrowheads indicate positions of cuts (blue) and pins (yellow) respectively (**d**). Diagram of blade positioning for cutting fish fillets across the ventral incision (**d**′). Ventral view of the ventral incision showing the position of the cut along the spinal cord, as a guide for proper filleting (**d**″). Blue dashed lines and arrowheads indicate cut for the left fillet; a similar cut on the right can also be made to remove vertebral column and spinal cord, but is not essential. Yellow dots indicate pins. Antero-posterior and dorso-ventral orientations are indicated (*h* head, *t* tail, *v* ventral, *d* dorsal). Dashed white line indicates the spinal cord. (**e**–**e**′) Diagram of fish preparation and muscle fillet dissection with estimated duration (left panel). After dissection, slow (brown arrowhead) and fast (pink arrowhead) muscle compartments are visible in both right and left muscle fillets (right panel), which are ready for incubation in the bijou tube containing Collagenase/cDMEM solution for 120 min (**e**′). Dashed white line indicates the remaining vertebral column and spinal cord in the left fillet (*h* head, *t* tail). (**f**) Schematic and representative picture of glass Pasteur pipettes cut and heat-polished to obtain wide and small diameter apertures for muscle trituration and single myofiber handling, respectively. Black dashed line and arrowhead indicate cut position with diamond pen. Estimated time for glass cutting and polishing is reported. (**g**) Schematic of fillet trituration and single myofiber isolation and wash with estimated duration in minutes. (**h**) Representative picture of single myofibers during washes. Orange arrowheads denote intact viable myofibers whereas asterisks denote hypercontracted myofibers. (**i**) Representative picture of an intact viable single myofiber after isolation procedure, viewed under 40X magnification on an Axiophot microscope (Zeiss)

9. Use the blade to make a curved incision along the ventral side of the carcass to facilitate evisceration using fine forceps (Fig. 1c).
10. At this point, different portions of the carcass can be collected for required downstream analyses (*see* **Note 4**) (Fig. 1c′).
11. Using the scalpel, carefully make a light incision on the skin, avoiding touching the muscle beneath, just behind the gill operculum and perpendicular to the fish antero-posterior axis. Using the fine forceps, gently pinch and lift the skin along the incision edge. Carefully grab and pull the skin toward the fish tail to expose the muscle beneath. Continue to pull gently until reaching the pin positioned close to the tail (*see* **Note 5**). At this point, most of the trunk musculature should be exposed.
12. Unpin the fish, turn it over, re-pin it, and remove skin from contralateral side, following the same procedure.
13. When skinning is completed, unpin the fish and rotate it 90° onto its back, so that the ventral side (belly) points upward toward the operator (Fig. 1d).
14. Re-pin fish to the corkboard in its new position, using one pin passing through its lower jaw and head and the second at the base of the tail. Vertebral column should be visible and accessible through the opening in the belly (Fig. 1d′).
15. Angle the scalpel to cut along the right side of the vertebral column along the entire antero-posterior axis to create two muscle fillets, one bearing the associated vertebral column and spinal cord and the other without (Fig. 1d′, d″) (*see* **Note 6**).
16. Use scalpel to remove the fish head and fully release the two muscle fillets. The obtained fish fillets display slow and fast muscle compartments. Following **step 15**, the spinal cord should be visible in the left fillet (Fig. 1e).

3.3 Myofiber Dissociation and Isolation

1. Place the fillets in the bijou tube with Collagenase/cDMEM solution, apply cap loosely, and incubate at 28 °C in 5% CO_2 incubator for 120 min with occasional (3–4 times during the process) gentle swirling of the tube (Fig. 1e′) (*see* **Note 7**).
2. In parallel, use a diamond pen to score the glass pipettes and create openings with diameter of approximately 1 and 4 mm (Fig. 1f).
3. Use a Bunsen burner to melt the glass around the opening to heat-polish and smooth any sharp edges. Proper edge polishing can be tested by circling the edge on aluminum foil, no cut should be produced. Quickly flame the freshly prepared glass

pipettes to sterilize, wrap in aluminum foil, and store in the tissue culture hood until use.

4. When incubation is completed (*see* **Notes 7** and **8**), place the bijou tube in the tissue culture hood. Also, collect the 150 mm dish with warm cDMEM from incubator and place it in the culture hood.
5. Gently discard most of Collagenase/cDMEM solution from the bijou tube, until only the fillets, in a drop of liquid, are left. Invert the bijou tube to pour the muscle fillets in the 150 mm Petri dish containing cDMEM.
6. Return the Petri dish with fillets to the incubator for 20–30 min. This allows the muscle to rest and dilute the Collagenase, promoting inactivation of the enzyme.
7. Place the dissecting microscope in the culture hood, if possible, otherwise use a clean area away from doors, windows, and draughts, or other contamination sources. Collect the 150 mm dish with fillets and place it under the microscope.
8. Rinse the heat-polished glass pipettes with BSA,PBS solution to prevent myofiber adhesion.
9. Using the pipette with larger diameter, repeatedly blow a stream of cDMEM onto the fillets for at least 10 min. Tissue dissociation can be enhanced by carefully passing the fillets once or twice in and out of the glass pipette (Fig. 1f). Avoid continuous passage through glass pipette to limit damage to myofibers. As a result, visible hair-like structures (i.e. myofibers) will be released from the muscle bulk.
10. Continue the trituration process until most myofibers have been released. Together with intact viable myofibers, the procedure will also result in the release of debris, including fat droplets and hypercontracted myofibers (Fig. 1g), which will increase the turbidity of the medium (*see* **Note 9**).
11. Place the 150 mm plate back in the incubator for 10–15 min to allow released myofibers to rest and sink at the bottom.
12. Using the glass pipette with smaller diameter, carefully collect intact myofibers and transfer them onto a 100 mm dish with fresh cDMEM. If needed, the remaining muscle bulk can be further processed to enhance the release of residual myofibers.
13. Place the 100 mm dish containing cleaned myofibers back in the incubator for another 10–15 min to allow the myofibers to rest and sink at the bottom. As needed, selected myofibers can be transferred into a new cDMEM-containing 100 mm dish for further cleaning and selection.
14. At this point, cleaned myofibers should look intact and elongated and are ready for downstream use/analysis. Viable

myofibers appear translucent and with a clean surface (Fig. 1h, i). If significant debris is still present in the dish, repeat **steps 12** and **13**.

3.4 Morphometric Analysis of Isolated Myofibers

The isolation of intact myofibers allows analysis of multiple morphometric aspects of adult muscle. In this section, we describe how such a procedure can be used to assess differences in size, nucleation, and myonuclear domain between slow and fast muscle fibers in an 8-month-old adult *Tg(9.7kb smyhc1:GFP)*^{i104} transgenic fish [46]. In this transgenic fish line, the slow muscle is highlighted by GFP expression and thus, it is easily distinguishable under a fluorescent microscope, following removal of the skin, in its anatomical position along the fish horizontal myoseptum (Fig. 2a). The described method allows efficient dissociation of both slow (GFP-positive) and non-slow (GFP-negative, i.e. fast) myofiber types (Fig. 2b, b″). In line with this, counts of a sample of dissociated myofibers confirmed a higher proportion of fast compared to slow type (Fig. 2c), further validating the applicability of the procedure for efficient isolation of both muscle types. In the example shown, myofiber length, which is readily measurable upon observation of viable non-dead/non-hypercontracted myofibers under a fluorescent microscope, appeared significantly shorter for slow GFP-positive fibers compared to fast GFP-negative fibers (Fig. 2d). Moreover, counts of myofiber nuclei, after myofiber fixation and nuclear staining with Hoechst 33342, showed that slow myofibers have significantly fewer nuclei than fast myofibers (Fig. 2e, f). Measurement of diameter and subsequent calculation of myofiber volume (assuming a cylindrical cross-section) and the size of the myonuclear domain (i.e. the portion of myofiber volume notionally served by each nucleus) confirmed an overall size reduction in slow myofibers, which results in a reduced myonuclear domain, reflecting the increased density of nuclei per unit myofiber volume (Fig. 1e′, g). Thus, the analysis of isolated myofibers from adult zebrafish showed that slow myofibers have significantly smaller diameter, volume, and absolute nuclear count, leading to an approximately fourfold lower myonuclear domain size compared to fast myofibers (Fig. 2g). Congruently, slow myofibers have significantly more nuclei per unit length than fast myofibers (Fig. 2g).

1. Prepare and process fish fillets to isolate myofibers as described in Subheadings 3.2 and 3.3.
2. Isolated intact myofibers can be photographed under the epifluorescent microscope to allow retrospective measurement of whole myofiber length using publicly available software (e.g. Fiji; NIH, www.Fiji.sc) (Fig. 2b″, d). Analysis of length on viable myofibers allows exclusion of the ones that are hypercontracted or damaged from isolation process. Depending on the microscope used, damaged myofibers that are not yet fully

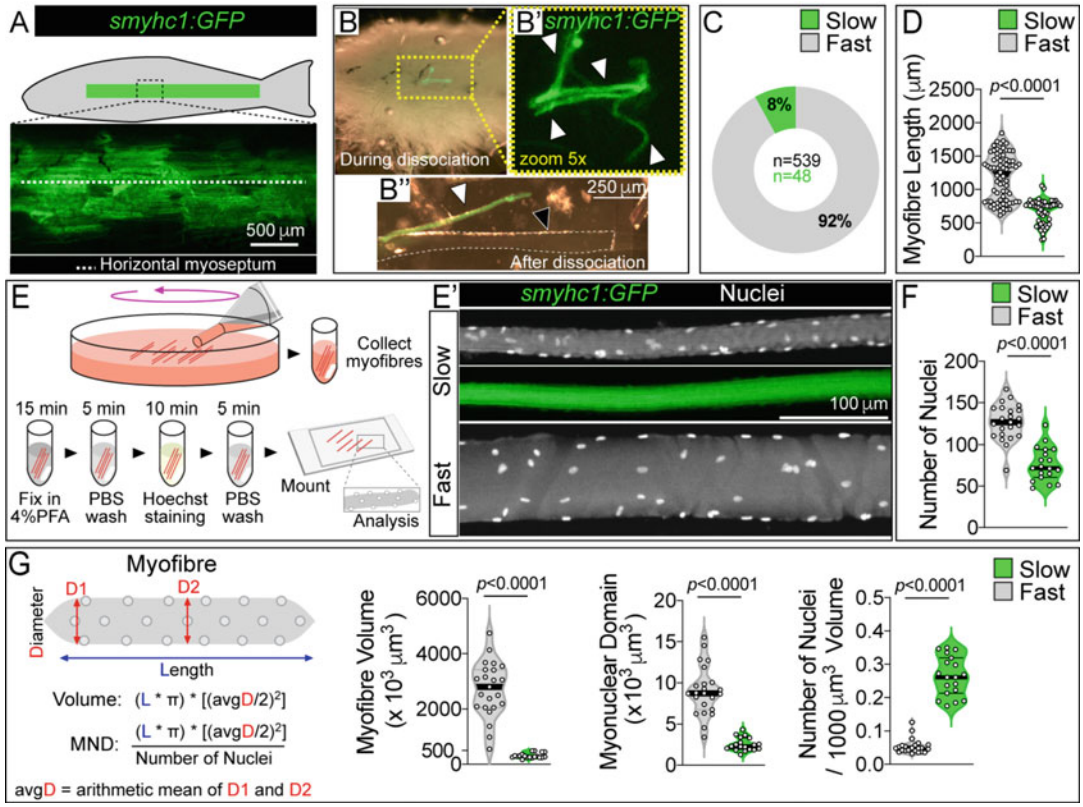

Fig. 2 Example of morphometric analysis on slow and fast myofibers. (**a**) Diagram of *Tg(9.7kb smyhc1:GFP)*^{i104} (*smyhc1:GFP*) transgenic fish indicating the position of the slow muscle domain (top panel, green line). Slow (GFP-positive) myofibers run parallel to the horizontal myoseptum (dashed white line) (bottom panel). (**b**) Representative images of GFP-positive (slow) and GFP-negative (fast) myofibers during muscle dissociation (**b**). Box highlights the magnified area displaying semi-detached slow GFP-positive myofibers (white arrowheads) above GFP-negative fast muscle (**b′**). After dissociation, both slow (white arrowhead) and fast (black arrowhead) myofibers are visible under an epifluorescent microscope (**b″**). (**c**) Live count on a sample of GFP-positive (slow) and GFP-negative (fast) myofibers immediately after dissociation and cleaning, from one fish, confirms that slow muscle represents the minor proportion of the trunk musculature. Number counted (*n*) and relative percentage (%) of each myofiber type is indicated. (**d**) Absolute length measurement of live myofiber revealing that slow myofibers ($n = 50$) are significantly shorter than fast ($n = 74$). (**e**–**e′**) Schematic of myofiber collection from plate after isolation, prior to fixation for nuclear staining with Hoechst 33342, mounting and analysis. Estimated duration of each passage is shown. Magenta arrow indicates the direction of swirling to gather myofibers at the center of the Petri dish and facilitate the collection. Representative images of fixed GFP-positive (slow) and GFP-negative (fast) myofibers (**e′**). (**f**) Absolute number of nuclei on GFP-positive (slow) and GFP-negative (fast) myofibers ($n = 31$ each type), from one fish, showing reduced nuclear number in slow muscle. (**g**) Combination of average diameter (myofiber width, D, red arrows) and unit length (blue arrow) revealing reduced myofiber volume and myonuclear domain but increased nuclear density per given myofiber volume (1000 μm^3) in GFP-positive (slow) myofibers ($n = 19$) compared to GFP-negative (fast) ($n = 23$) from one fish. Avg. indicates arithmetic mean of diameter measure (D1 and D2) across myofiber length. All graphs report mean (black line) ± SEM and unpaired, two-tailed t-test of analysis performed on myofibers isolated from one fish

hypercontracted appear shorter and opaque, with rough and irregular surface.

3. Nuclear counting and subsequent analyses require myofiber fixation. Under the microscope, use the glass pipette with smaller diameter (Fig. 2e) to collect isolated myofibers and place them in a 2 mL clear round-bottomed microcentrifuge tube that has also been rinsed with BSA,PBS to prevent myofiber adhesion. Gently swirl the dish to gather all myofibers at the center of the plate to reduce the volume of cDMEM medium collected with myofibers. No more than 30–40 myofibers should be collected in the same tube to avoid damage.
4. Allow the myofibers to sink to the bottom of the collection tube by leaving the tube standing upright for 5 min at room temperature.
5. Carefully remove the medium above myofibers and replenish the tube with 1 mL of 4% PFA in PBS solution (PFA, PBS) by gentle trickling. Incubate for 15 min (*see* **Note 10**).
6. Remove PFA,PBS solution and gently replenish with 1.5 mL of PBS to wash the myofibers. Incubate for 5 min and repeat the wash with fresh PBS. At this point, myofibers can be stored at 4 °C (*see* **Note 11**).
7. Remove PBS, wash, and replace with freshly prepared Hoechst 33342 dye solution diluted in PBS to stain myofiber nuclei. Incubate for 15 min and replace with fresh PBS (as in **step 6**). Myofibers are now ready to be mounted on glass slides for analysis.
8. Use a water-repellent pap pen to outline a rectangular area (size depending on the size of the coverslip to be used) on several glass slides. Under the microscope, use clean polished glass pipettes (smaller diameter, pre-rinsed with BSA,PBS) to collect myofibers from the 2 mL tube and transfer them onto a glass slide. Limiting the number of myofibers to 10/15 maximum per slide should facilitate downstream handling.
9. Remove as much PBS as possible from the glass slide to ease myofiber adhesion and reduce risk of damage/loss in later steps. A 200 μL micropipette tip wrapped in aluminum foil and pre-immersed in BSA,PBS can be used to carefully reposition myofibers after PBS removal.
10. Place two drops of glycerol-based mounting medium on the glass slide and gently lower a 50 mm × 22 mm coverslip onto the slide. Avoid trapping air bubbles, which may misposition or sweep away myofibers. Wait 5 min to allow the mounting medium to spread beneath the coverslip.
11. Seal the coverslip and secure it to the glass slide by brushing on a small amount of nail varnish.

12. Use an epifluorescence or confocal microscope to photograph mounted myofibers for downstream morphometric analysis. The fluorescence of GFP encoded by the *smyhc1:GFP* transgene resists 4% PFA fixation and is detectable without immunostaining, thus allowing differential analysis of slow and non-slow (i.e. fast) myofibers. Use the detection of Hoechst and GFP fluorescence to count absolute number of nuclei on GFP-positive (slow) and GFP-negative (fast) myofibers (Fig. 2f). Analysis of 25–40 myofibers should provide a reproducible evaluation of slow versus fast difference within one animal. Store slides at 4 °C in the dark; GFP fluorescence lasts up to 14 days.
13. Using imaging software, measure myofiber width in at least two different positions along the visible portion of each myofiber. Concomitantly, measure myofiber length and count the number of nuclei in the measured portion.
14. Use myofiber average width (avg. diameter) and length to calculate the volume of the myofiber following the formula: $(\text{Length} \times \pi) \times [(\text{average Diameter}/2)^2]$ (*see* **Note 12**), where 'average' is the arithmetic mean of diameter measure on different positions of myofiber length. Obtained values can be compared with chosen statistical analysis (e.g. unpaired two-tailed t-test) to assess difference among muscle types (Fig. 2g). Graphs were produced in Graphpad Prism 8 (https://www.graphpad.com/scientific-software/prism/).
15. Myofiber volume and number of nuclei can be combined to calculate the myonuclear domain using the following formula: $\{(\text{Length} \times \pi) \times [(\text{average Diameter}/2)^2] / \text{Number of myofiber nuclei}\}$ (*see* **Note 12**). Compare calculation across myofiber types with chosen statistical analysis (Fig. 2g).

3.5 Immunostaining of Isolated Myofibers

Unfixed or fixed myofibers from Subheading 3.4, **steps 3** or **7**, respectively, can be further processed for immunostaining to detect specific markers/proteins (Fig. 3a). Nuclei associated with isolated myofibers are either myonuclei or the nuclei of resident MuSCs. MuSCs are responsible for myofiber growth and regeneration upon injury and are identifiable through immunostaining for the transcription factor Pax7, a canonical marker of quiescent MuSC in their anatomical niche on isolated myofibers, that is conserved across several vertebrate species [6, 16, 18, 47–53]. In this section, we describe how to process zebrafish myofibers for Pax7 immunostaining, taking advantage of the transgenic fish *TgBAC(pax7a:GFP)*^{t32239Tg} (Nüsslein-Volhard C.; MPI Tübingen) [54], in which MuSCs are highlighted by GFP fluorescence and thus easily identifiable, permitting cross-validation of antibody labeling (Fig. 3b). In parallel, myofibers can be specifically stained to reveal cellular structures such as filamentous actin (F-actin) or

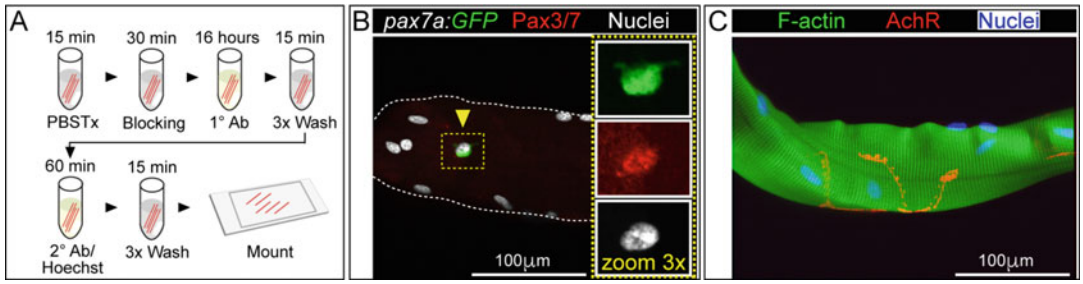

Fig. 3 Detection of MuSC and cellular structures on isolated myofibers. (**a**) Schematic of immunostaining protocol on isolated myofibers, from membrane permeabilization, blocking, washes, antibody incubations to mount on glass slides. Estimated duration of each passage is shown. (**b**) *TgBAC(pax7a:GFP)*^{t32239Tg} (*pax7a:GFP*) myofiber immunostained for GFP (green) and Pax3/Pax7 (red) reveals the position of a MuSC (yellow arrowhead) near the myofiber-end (outlined in white dashes), adjacent to a group of myofiber nuclei, counterstained with Hoechst 33342 (white). Dashed yellow rectangle highlights the magnified MuSC shown on the right panels. (**c**) Myofiber stained with Alexa Fluor 488 Phalloidin, Alexa Fluor 555 α-Bungarotoxin and Hoechst 33342 to reveal sarcomere structure (filamentous actin; F-actin, green), neuromuscular junctions (Acetylcholine Receptor; AchR, red) and myofiber nuclei (blue)

Acetylcholine receptor (AchR) to assess morphological characteristics such as sarcomere length or position/number of neuromuscular junctions, respectively, using fluorochrome-conjugated toxins such as Phalloidin or α-Bungarotoxin (Fig. 3c).

1. Remove the PBS from the fixed myofibers with the smaller-diameter glass pipette (Fig. 1e) and replace with 0.5% Triton-X100 detergent in PBS (PBSTx). Incubate for 15 min to permeabilize the cell membranes of both myofibers and associated MuSCs (*see* **Note 13**).
2. Remove PBSTx and gently add the 10% normal goat serum (NGS) in PBS blocking solution to block non-specific antibody binding. Incubate for at least 30 min, occasionally tilting the tube (*see* **Note 14**). Alternatively, 5% NGS,PBS solution can be used to incubate for 1 h.
3. Prepare antibody solution by diluting anti-Pax3/Pax7 (DP312 (Davis et al. 2001), *see* **Note 15**) and anti-GFP primary antibodies Table 1) into 0.1% Triton-X100 detergent PBS solution (PBSTx0.1) containing 2% NGS. Remove blocking solution from the tube and gently add the primary antibody solution. Incubate overnight (16 h) at 4 °C.
4. Remove the primary antibody solution and replace with fresh PBSTx0.1 to wash myofibers for 5 min. Incubated primary antibody solution can be stored at 4 °C and re-used reliably within 1 week (and perhaps longer if 0.002% sodium azide in PBS is added). Wash myofibers three times for 5 min each using PBSTx0.1 with occasional gentle tilting of the tube.

5. Dilute fluorochrome-conjugated Alexa Fluor secondary antibodies (Table 1) and Hoechst 33342 solution dye (10 μg/mL final) in PBSTx0.1 and incubate for at least 60 min at room temperature with occasional tube tilting. Secondary antibody solution can be stored at 4 °C and reused reliably within 1 week (and perhaps longer if 0.002% sodium azide in PBS is added).
6. Myofibers can be alternatively (or concomitantly) stained with fluorochrome-conjugated toxins to detect subcellular structures such as filamentous actin (F-actin) using Phalloidin or AchR using α-Bungarotoxin.
7. Carefully transfer myofibers onto a clean prepared glass slide as described in section as in Subheading 3.4, **step 8**. Process each glass slide as indicated in Subheading 3.4, **steps 9** and **10**.
8. Sealed glass slides with mounted (immuno)stained myofibers are ready for analysis using an epifluorescent or confocal microscope. Examples of a *pax7a:GFP* MuSC on a myofiber immunostained for Pax3/Pax7 or a wild-type myofiber showing F-actin and AchR are reported in Fig. 3b, c.

3.6 Myofiber-Derived MuSC Culture and Immunostaining

Freshly isolated viable myofibers can be plated to allow the associated MuSCs to activate and proliferate on a culture substrate such as Matrigel (Fig. 4a). 24 hours after plating, MuSCs begin to activate and migrate away from the myofiber (Fig. 4a′). Over the next 48 h, activated MuSCs proliferate and form visible colonies, most of which are near the original myofiber (Fig. 4a″). Here, we describe how to culture MuSC-derived myoblasts to explore either proliferation dynamics or myogenic differentiation (Fig. 4b, c). The proliferation rate of MuSC-derived myoblasts can be assessed by EdU incorporation assay, which is best performed no earlier than 2 days from myofiber plating (Fig. 4b), as shorter culture periods will result in poor myofiber adhesion to Matrigel and consequent loss of fibers, leading to unreliable assessment of myoblast proliferation. Proper progression of the myogenic program can be assessed by culturing zebrafish primary myoblasts in a low serum medium for 5 days prior to immunostaining for structural components such as myosins (Fig. 4c). We previously used this differentiation regime to explore myogenesis in primary myoblasts lacking myogenin function [17, 42].

1. Coat the desired number of wells of a 24-well plate by rinsing with Matrigel. Be sure to completely cover the surface of each well. Immediately pour off excess Matrigel and return it to 4 °C to avoid precocious solidification. Place the prepared plate in the 28.5 °C 5% CO_2 incubator for 45 min to allow Matrigel gelling.
2. Prepare the proliferation medium (PM) by supplementing DMEM with 1% Penicillin/Streptomycin, 10 μg/mL

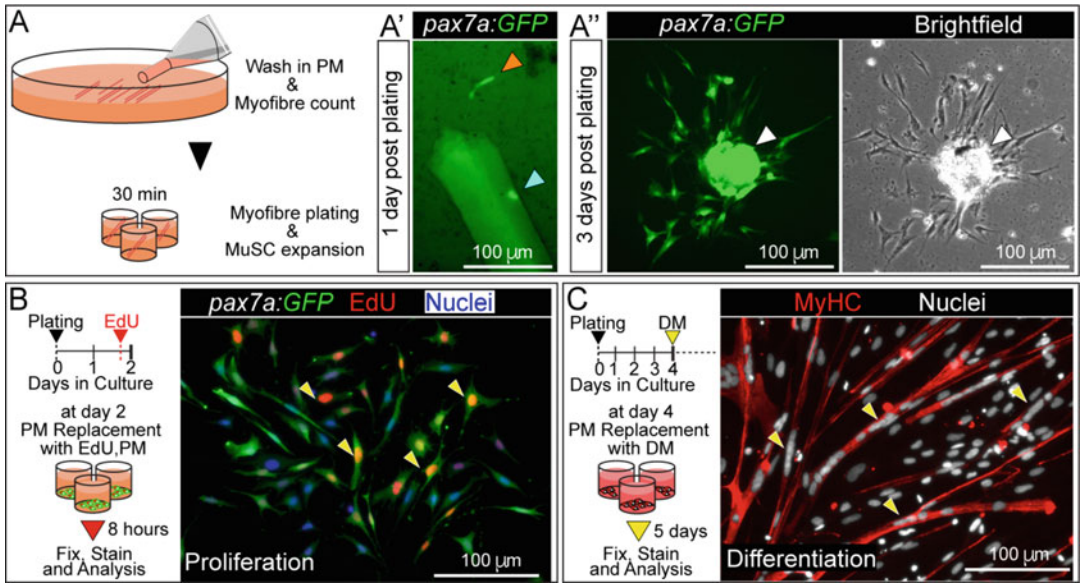

Fig. 4 Myofiber plating and immunostaining of MuSC-derived cells. (**a**–**a**″) Schematic of myofiber preparation prior to plating for MuSC culture. After washing in proliferation medium (PM) myofibers are counted and plated in 24-well plate(s). Estimated duration of this step is indicated (**a**). 1 day post plating, *pax7a:GFP* MuSCs are observed using an inverted fluorescence microscope, and may either retain association with myofiber (cyan arrowhead) or already migrate onto the culture substrate (orange arrowhead) (**a**′). In the following 2 days, activated *pax7a:GFP* MuSCs proliferate and form colonies. White arrowhead indicates a hypercontracted myofiber from which the surrounding MuSC-derived colony arose (**a**″). (**b**) Schematic and representative picture of *pax7a:GFP* MuSC-derived myoblasts (green) given an EdU pulse (red) (yellow arrowheads) 2 days after myofiber plating in proliferation medium (PM). Nuclei, counterstained with Hoechst 33342, are highlighted in blue. (**c**) Schematic and representative picture of differentiated multinucleated myotubes (yellow arrowheads) containing MyHC (red) after 5 days of culture in differentiation medium (DM). Nuclei were counterstained with Hoechst 33342 (white)

gentamicin and 20% FBS. Prewarm the PM to 28.5 °C in the incubator prior to aliquoting 200 µL per Matrigel-coated well.

3. The transfer of myofibers has often led to concomitant carry-over of nearly 200 µL of cDMEM from the original dish to the final culture well. Such a volume of cDMEM dilutes the serum concentration in PM contained in the final culture well, resulting in sub-optimal MuSC activation and proliferation. To avoid this, myofibers from final 100 mm cDMEM wash dish are transferred onto a new 100 mm dish containing 5 mL of 40% FBS,cDMEM solution. At the end of the transfer process, given the volume carried over with myofibers, the final 100 mm dish contains circa 10 mL of DMEM with approximately 20% FSB, thus preventing further dilution of PM in the final culture well.
4. Gently swirl the dish to gather myofibers at its center. Use a small diameter glass pipette pre-rinsed with BSA,PBS to

transfer approximately 90–100 freshly-isolated myofibers into each Matrigel-coated well. Ensure that the myofibers are evenly spaced across the well by moving the plate laterally in cross-like movements several times.

5. Place the 24-well plate(s) in the incubator and culture the myofibers undisturbed for at least 48 h. In the initial 24 h, myofibers can easily be dislodged, impacting on MuSC activation, proliferation, migration, and adhesion to the culture plate. Even opening/closing the door can cause enough vibration to dislodge myofibers.
6. After 24 h, a fraction of MuSCs get activated and start to migrate from the associated myofiber to adhere to the Matrigel coating. Migrating *pax7a:GFP* MuSCs can be observed live using an inverted epifluorescence microscope (Fig. 4a′). An additional 48 h of culture results in the formation of MuSC colonies, occasionally around the hypercontracted parent myofiber (Fig. 4a″), which often becomes detached from Matrigel. If myofibers/MuSCs are to be cultured for longer periods, replace half of the medium with a fresh one every 48 h.
7. Generally, after 48 h of culture, MuSCs are ready for downstream analysis. To explore the dynamics of MuSC proliferation, dilute 5-ethynyl-2′-deoxyuridine (EdU) at a final concentration of 10 μM in fresh pre-warmed PM. In parallel, cells can be collected at desired time point(s) for RNA extraction and gene expression analysis by RT-qPCR (*see* **Note 16**).
8. For proliferation analysis by an EdU pulse, remove PM from culture well and rinse vigorously with freshly prepared PM twice to remove plated myofibers. At this time point, most myofibers should be either floating or loosely adhering to Matrigel, and thus, easily removed by the rinses.
9. Remove PM and quickly rinse twice with PBS. Replace PBS with EdU,PM solution and place for 2–8 h in 28.5 °C 5% CO_2 incubator (*see* **Note 17**). Duration of incubation can be changed according to experimental design.
10. At the end of incubation, remove EdU,PM solution, wash vigorously twice with PBS and fix with PFA,PBS for 15 min.
11. The process for immunostaining plated cells is the same used for myofibers (see Subheading 3.4, **steps 6**, **7**, **8** and **9**).
12. After the final wash in PBSTx0.1, perform click chemistry to reveal EdU incorporation following supplier's instructions (Click-iT EdU Imaging Kits, Invitrogen).
13. Wash twice with fresh PBS, then replenish each well with 300 μL PBS. The cells are now ready to be visualized using an inverted epifluorescence microscope (*see* **Note 11**). EdU incorporation analysis can be coupled with GFP

immunostaining and Hoechst counterstain to explore *pax7a:GFP* MuSC-derived myoblast proliferation (Fig. 4b).

14. Alternatively, plated MuSC-derived myoblasts can be prompted to differentiate to evaluate the progression of the myogenic program. Prepare the differentiation medium (DM) by supplementing DMEM with 1% Penicillin/Streptomycin, 10 μg/mL gentamicin, and 2% horse serum. Pre-warm the DM medium to 28.5° in the incubator.
15. After 96 h of initial plating, remove PM and wash twice with sterile PBS to eliminate serum residues. Remove PBS and add 500 μL of DM to each well. Replace DM every 48 h. Myoblasts usually differentiate and form visible multinucleated myotubes after 5 days of culture in DM (*see* **Note 18**).
16. Myotubes can be immunostained for myosin heavy chain (MyHC) using MF20 and/or A4.1025 [3] (Table 1) and counterstained with Hoechst 33342 to assess the extent of differentiation and cell fusion (Fig. 4c) (*see* **Note 19**). Immunostaining protocol is the same as that used for myoblast culture (*see* Subheading 3.4, **steps 6**, 7, **8** and **9**).

4 Notes

1. BSA,PBS blocking solution can be prepared in stock and stored at 4 °C for a few days, or at −20 °C for a longer term.
2. Depending on the experimental design, single fish fillets can be processed separately in two different bijou tubes with no modification of Collagenase/cDMEM volume per fillet.
3. Duration of Tricaine incubation depends on fish age and size and is defined as described in [55, 56].
4. The described procedure allows collection of samples for various parallel downstream analyses from each animal. As indicated in Fig. 1c′: (1) whereas most of the trunk musculature is used for myofiber isolation, (2) an adjacent 5 mm section of muscle can be cryopreserved for histological analysis, (3) a further muscle region, which is usually damaged by the dissecting pin, can be used for whole muscle RNA/Protein analysis. Finally, (4) dissected fins can be used for retrospective genomic DNA isolation and genotyping. Note that muscle character may vary along the body axis [57].
5. Slow muscle is strongly attached to the overlying skin. Pull very gently to avoid damaging the slow myofibers.
6. Tilt the scalpel tip towards the dorsal midline so that the tip of blade penetrates the anteriormost muscle tissue close to the vertebral column. Draw the blade posteriorly until the tail pin is

reached, leaving the ribs in the fillet. Stopping or hesitating whilst cutting along the column can lead to varying fillet thickness and damage the medialmost muscle. It is important to batch-test replacement reagents, such as Collagenase, against existing, optimized components. There are variable amounts of proteases in batches of Collagenase, but Collagenase with neutral protease around 53 U and clostripain at approximately 0.6 U is ideal, as described [25].

7. Adult (8–15 months old) zebrafish trunk muscle is usually digested after 2 h. Although longer incubations (3+ h) have little or no effect on myofiber viability, shorter incubation may reduce digestion efficiency and therefore, reduce myofiber recovery after trituration. However, digestion of a 4-week-old juvenile fillet requires only 1 h of incubation. The precise time depends upon both the age and the size of the fish and the activity of the batch of Collagenase used and should be determined empirically.
8. A well-digested muscle looks slightly swollen and, under the microscope, hair-like myofibers appear dislodged around the edge of the muscle mass.
9. When muscle requires prolonged trituration time, allow a further 5 min incubation at 28.5 °C, 5% CO_2 to re-equilibrate the temperature and pH of the medium. If medium reaches temperatures below physiological (22–29 °C) for an extended time, myofibers will hypercontract and die.
10. During each incubation period, myofibers tend to sink to the bottom of the tube. To avoid this, gently tilt the tube occasionally to ensure efficient treatment.
11. For prolonged storage at 4 °C (2–4 weeks), replace PBS with PBS containing 0.002% sodium azide to prevent microbial growth.
12. Myofiber average width (avg. diameter) and length can be used to calculate the surface area (SA) of the myofiber, following the formula: Length × π × avg. Diameter. The Surface Area Domain Size (SADS), the notional SA occupied by each myofiber nucleus, is calculated using the formula: SADS = SA/number of myofiber nuclei.
13. Solutions containing Triton X-100 can be prepared in advance. For long-term storage, use PBS containing 0.002% sodium azide instead of PBS and wrap the tube/bottle in aluminum foil to protect it from light.
14. The normal serum used for blocking should derive from the species in which the secondary antibody was raised.
15. The anti-PAX7 antibody from DSHB (Developmental Studies Hybridoma Bank, deposited by Kawakami, A., AB_528428)

can alternatively be used at 1:10 dilution, if using the supernatant version.

16. To collect cells for gene expression analysis, remove medium and wash twice with PBS. Incubate with appropriate volume (e.g. 200 μL for a 24-well plate well) of Accutase® reagent to detach the cells from Matrigel for 10 min (or until complete detachment of all cells; check under a microscope, but this should not be longer than 15 min) at 28.5 °C, 5% CO_2. Collect cells in a 1.5 mL clear tube, pellet by centrifugation at 200 × *g* at 4 °C, and wash once in PBS. Pelleted cells are now ready for RNA extraction and downstream analysis.
17. The duration of the EdU pulse can be varied according to the experimental hypothesis and design.
18. Differentiation regime can be varied according to experimental hypothesis and design. Visible myotubes are usually formed after 96–120 h of culture in DM.
19. Alternatively, differentiated cells can be collected (*see* **Note 16**) for RNA extraction and subsequent RT-qPCR analysis for selected target genes.
20. All lines used were reared at King's College London on a 14/10 h light/dark cycle at 28.5 °C, with staging and husbandry as described [56]. All procedures were performed on adult zebrafish in accordance with licenses held under the UK Animals (Scientific Procedures) Act 1986 and later modifications, conforming to all relevant guidelines and regulations.

Acknowledgments

We thank all members of the Hughes lab and Nicolas Figeac for advice. We are grateful to Huascar Pedro Ortuste Quiroga for initial help in establishing the method and to Bruno Correia da Silva and his staff for fish care. This work is supported by grants from the Medical Research Council to S.M.H. (MRC Programme Grants G1001029 and MR/N021231/1) and P.S.Z. (MR/P023215/1 and MR/S002472/1) to P.S.Z.

References

1. Schiaffino S, Reggiani C (2011) Fiber types in mammalian skeletal muscles. Physiol Rev 91: 1447–1531
2. Talbot J, Maves L (2016) Skeletal muscle fiber type: using insights from muscle developmental biology to dissect targets for susceptibility and resistance to muscle disease. Wiley Interdiscip Rev Dev Biol 5:518–534
3. Blagden CS, Currie PD, Ingham PW et al (1997) Notochord induction of zebrafish slow muscle mediated by Sonic hedgehog. Genes Dev 11:2163–2175
4. Hromowyk KJ, Talbot JC, Martin BL et al (2020) Cell fusion is differentially regulated in zebrafish post-embryonic slow and fast muscle. Dev Biol 462:85–100

5. van Raamsdonk W, Pool CW, te Kronnie G (1978) Differentiation of muscle fibre types in the teleost Brachydanio rerio. Anat Embryol (Berl) 153:137–155
6. Pipalia TG, Koth J, Roy SD et al (2016) Cellular dynamics of regeneration reveals role of two distinct Pax7 stem cell populations in larval zebrafish muscle repair. Dis Model Mech 9: 671–684
7. Rowlerson A, Scapolo PA, Mascarello F et al (1985) Comparative study of myosins present in the lateral muscle of some fish: species variations in myosin isoforms and their distribution in red, pink and white muscle. J Muscle Res Cell Motil 6:601–640
8. Johnston IA, Bower NI, Macqueen DJ (2011) Growth and the regulation of myotomal muscle mass in teleost fish. J Exp Biol 214:1617–1628
9. Katz B (1961) The termination of the afferent nerve fibre in the muscle spindle of the frog. Philos Trans R Soc Lond Ser B Biol Sci 243: 221–240
10. Mauro A (1961) Satellite cell of skeletal muscle fibers. J Biophys Biochem Cytol 9:493–495
11. Purohit G, Dhawan J (2019) Adult muscle stem cells: exploring the links between systemic and cellular metabolism. Front Cell Dev Biol 7: 312
12. Relaix F, Zammit PS (2012) Satellite cells are essential for skeletal muscle regeneration: the cell on the edge returns centre stage. Development 139:2845–2856
13. Collins CA, Olsen I, Zammit PS et al (2005) Stem cell function, self-renewal, and behavioral heterogeneity of cells from the adult muscle satellite cell niche. Cell 122:289–301
14. Halevy O, Piestun Y, Allouh MZ et al (2004) Pattern of Pax7 expression during myogenesis in the posthatch chicken establishes a model for satellite cell differentiation and renewal. Dev Dyn 231:489–502
15. Zammit PS, Golding JP, Nagata Y et al (2004) Muscle satellite cells adopt divergent fates: a mechanism for self-renewal? J Cell Biol 166: 347–357
16. Buckingham M, Relaix F (2015) PAX3 and PAX7 as upstream regulators of myogenesis. Semin Cell Dev Biol 44:115–125
17. Ganassi M, Badodi S, Ortuste Quiroga HP et al (2018) Myogenin promotes myocyte fusion to balance fibre number and size. Nat Commun 9: 4232
18. Hammond CL, Hinits Y, Osborn DP et al (2007) Signals and myogenic regulatory factors restrict pax3 and pax7 expression to dermomyotome-like tissue in zebrafish. Dev Biol 302:504–521
19. Hinits Y, Osborn DP, Hughes SM (2009) Differential requirements for myogenic regulatory factors distinguish medial and lateral somitic, cranial and fin muscle fibre populations. Development 136:403–414
20. Hinits Y, Williams VC, Sweetman D et al (2011) Defective cranial skeletal development, larval lethality and haploinsufficiency in Myod mutant zebrafish. Dev Biol 358:102–112
21. Osborn DPS, Li K, Cutty SJ et al (2020) Fgf-driven Tbx protein activities directly induce myf5 and myod to initiate zebrafish myogenesis. Development 147:dev184689
22. Alexander MS, Kawahara G, Kho AT et al (2011) Isolation and transcriptome analysis of adult zebrafish cells enriched for skeletal muscle progenitors. Muscle Nerve 43:741–750
23. Froehlich JM, Seiliez I, Gabillard JC et al (2014) Preparation of primary myogenic precursor cell/myoblast cultures from basal vertebrate lineages. J Vis Exp 86:51354
24. Moyle LA, Zammit PS (2014) Isolation, culture and immunostaining of skeletal muscle fibres to study myogenic progression in satellite cells. Methods Mol Biol 1210:63–78
25. Rosenblatt JD, Lunt AI, Parry DJ et al (1995) Culturing satellite cells from living single muscle fiber explants. In Vitro Cell Dev Biol Anim 31:773–779
26. Bischoff R (1975) Regeneration of single skeletal muscle fibers in vitro. Anat Rec 182:215–235
27. Cardasis CA, Cooper GW (1975a) An analysis of nuclear numbers in individual muscle fibers during differentiation and growth: a satellite cell-muscle fiber growth unit. J Exp Zool 191:347–358
28. Cardasis CA, Cooper GW (1975b) A method for the chemical isolation of individual muscle fibers and its application to a study of the effect of denervation on the number of nuclei per muscle fiber. J Exp Zool 191:333–346
29. Baruffaldi F, Montarras D, Basile V et al (2017) Dynamic phosphorylation of the myocyte enhancer factor 2Calpha1 splice variant promotes skeletal muscle regeneration and hypertrophy. Stem Cells 35:725–738
30. Beauchamp JR, Heslop L, Yu DS et al (2000) Expression of CD34 and myf5 defines the majority of quiescent adult skeletal muscle satellite cells. J Cell Biol 151:1221–1234
31. Bischoff R (1986) Proliferation of muscle satellite cells on intact myofibers in culture. Dev Biol 115:129–139
32. Brack AS, Bildsoe H, Hughes SM (2005) Evidence that satellite cell decrement contributes to preferential decline in nuclear number from

large fibres during murine age-related muscle atrophy. J Cell Sci 118:4813–4821
33. Kuang S, Kuroda K, Le Grand F et al (2007) Asymmetric self-renewal and commitment of satellite stem cells in muscle. Cell 129:999–1010
34. Lukjanenko L, Karaz S, Stuelsatz P et al (2019) Aging disrupts muscle stem cell function by impairing matricellular WISP1 secretion from fibro-adipogenic progenitors. Cell Stem Cell 24:433–446 e437
35. Yablonka-Reuveni Z, Rivera AJ (1994) Temporal expression of regulatory and structural muscle proteins during myogenesis of satellite cells on isolated adult rat fibers. Dev Biol 164:588–603
36. Zammit PS, Relaix F, Nagata Y et al (2006) Pax7 and myogenic progression in skeletal muscle satellite cells. J Cell Sci 119:1824–1832
37. Davies MLF, Johnston IA, van de Wal JW (1995) Muscle fibers in rostral and caudal myotomes of the Atlantic Cod (*Gadus morhua* L.) have different mechanical properties. Physiol Zool 68:673–697
38. Johnston I, Altringham J (1988) Muscle contraction in polar fishes: experiments with demembranated muscle fibres. Comp Biochem Physiol 90B:547–555
39. Johnston IA, Abercromby M, Vieira VL et al (2004) Rapid evolution of muscle fibre number in post-glacial populations of Arctic charr Salvelinus alpinus. J Exp Biol 207:4343–4360
40. Anderson JE, Wozniak AC et al (2012) Single muscle-fiber isolation and culture for cellular, molecular, pharmacological, and evolutionary studies. Methods Mol Biol 798:85–102
41. Zhang H, Anderson JE (2014) Satellite cell activation and populations on single muscle-fiber cultures from adult zebrafish (Danio rerio). J Exp Biol 217:1910–1917
42. Ganassi M, Badodi S, Wanders K et al (2020) Myogenin is an essential regulator of adult myofibre growth and muscle stem cell homeostasis. elife 9:e60445
43. Ganassi M, Muntoni F, Zammit PS (2022) Defining and identifying satellite cellopathies within muscular dystrophies and myopathies. Exp Cell Res 411:112906. https://doi.org/10.1016/j.yexcr.2021.112906
44. Ganassi M, Zammit PS (2022) Involvement of muscle satellite cell dysfunction in neuromuscular disorders: Expanding the portfolio of satellite cell-opathies. Eur J Transl Myol 32. https://doi.org/10.4081/ejtm.2022.10064
45. Ganassi M, Zammit PS, Hughes SM (2021) Isolation of myofibres and culture of muscle stem cells from adult zebrafish. Bio Protoc 11:e4149. https://doi.org/10.21769/BioProtoc.4149
46. Elworthy S, Hargrave M, Knight R et al (2008) Expression of multiple slow myosin heavy chain genes reveals a diversity of zebrafish slow twitch muscle fibres with differing requirements for Hedgehog and Prdm1 activity. Development 135:2115–2126
47. Berberoglu MA, Gallagher TL, Morrow ZT et al (2017) Satellite-like cells contribute to pax7-dependent skeletal muscle repair in adult zebrafish. Dev Biol 424:162–180
48. Chen Y, Lin G, Slack JM (2006) Control of muscle regeneration in the Xenopus tadpole tail by Pax7. Development 133:2303–2313
49. Hollway GE, Bryson-Richardson RJ, Berger S et al (2007) Whole-somite rotation generates muscle progenitor cell compartments in the developing zebrafish embryo. Dev Cell 12:207–219
50. Kawakami A, Kimura-Kawakami M, Nomura T et al (1997) Distributions of PAX6 and PAX7 proteins suggest their involvement in both early and late phases of chick brain development. Mech Dev 66:119–130
51. Olguin HC, Olwin BB (2004) Pax-7 up-regulation inhibits myogenesis and cell cycle progression in satellite cells: a potential mechanism for self-renewal. Dev Biol 275:375–388
52. Seale P, Sabourin LA, Girgis-Gabardo A et al (2000) Pax7 is required for the specification of myogenic satellite cells. Cell 102:777–786
53. Seger C, Hargrave M, Wang X et al (2011) Analysis of Pax7 expressing myogenic cells in zebrafish muscle development, injury, and models of disease. Dev Dyn 240:2440–2451
54. Mahalwar P, Walderich B, Singh AP et al (2014) Local reorganization of xanthophores fine-tunes and colors the striped pattern of zebrafish. Science 345:1362–1364
55. Harper C, Lawrence C (2011) The laboratory zebrafish. CRC Press, Boca Raton
56. Westerfield M (2000) The zebrafish book – a guide for the laboratory use of zebrafish (Danio rerio). University of Oregon Press
57. Nord H, Burguiere AC, Muck J et al (2014) Differential regulation of myosin heavy chains defines new muscle domains in zebrafish. Mol Biol Cell 25:1384–1395
58. Davis GK, Jaramillo CA, Patel NH (2001) Pax group III genes and the evolution of insect pair-rule patterning. Development 128:3445–3458

Chapter 4

The Satellite Cell Colony Forming Cell Assay as a Tool to Measure Self-Renewal and Differentiation Potential

Ahmed S. Shams and Michael Kyba

Abstract

The muscle satellite cell population is responsible for homeostatic maintenance of muscle fibers in response to muscle injury and normal wear and tear. This population is heterogeneous, and its capacity for self-renewal and differentiation can be altered either by mutation of genes that regulate these processes or with natural processes such as aging. The satellite cell colony assay is a facile way to extract information about the proliferation and differentiation potential of individual cells. Here, we provide a detailed protocol for the isolation, single cell plating, culture, and evaluation of colonies derived from single satellite cells. The variables of cell survival (cloning efficiency), proliferative potential (nuclei per colony), and differentiation propensity (ratio of nuclei within myosin heavy chain-positive cytoplasm to total nuclei) can thus be obtained.

Key words Satellite cells, Skeletal muscle, Colony, Self-renewal, Differentiation

1 Introduction

Skeletal muscle growth and regeneration are mediated by satellite cells, a cell population residing beneath the basal lamina of and adjacent to the myofiber [1]. Transplantation studies have shown that when a muscle is injured, satellite cells give rise to new muscle fibers in addition to contributing to the satellite cell pool of the recipient muscle [2–4]. On the other hand, when cultured in vitro, their proliferating progeny rapidly lose muscle engraftment capability [4]. This is considered a major obstacle in the development of satellite cells for cell therapy modality of muscle disease.

The ex vivo culture of SCs, usually performed on plastic substrates, decreases their regenerative ability significantly because the SCs immediately lose the signals that keep them in their quiescent stem cell state [5]. Notably, the in vitro culture of SCs results in their inevitable commitment to myoblasts and progressive transition from quiescent *Pax7*$^{+}$/MyoD^{-} cells to differentiated *Pax7*$^{-}$/MyoD^{+} cells [6]. Pax7 is essential for the maintenance of muscle

Atsushi Asakura (ed.), *Skeletal Muscle Stem Cells: Methods and Protocols*, Methods in Molecular Biology, vol. 2640, https://doi.org/10.1007/978-1-0716-3036-5_4,

stem cells [7] and the loss of Pax7 during in vitro cell culture is an indicator of the loss of the upstream stem-like state as SCs become activated myoblasts, thereby losing their cell therapeutic potential [8]. Understanding the physiological regulation of muscle growth and regeneration is an important goal of the field. Likewise, understanding how cells respond to ex vivo culture and developing optimized conditions for expansion of myogenic progenitors could have a significant impact on the attempts to use myogenic cell transplantation for muscle disease [9, 10].

The Colony Forming Cell (CFC) assay is an in vitro assay testing the ability of a single undifferentiated cell to grow into a colony of many, usually differentiated, cells. While it was first deployed to evaluate progenitor cells of the hematopoietic system [11], it has also been applied to other lineage-specific progenitor cells [12]. The assay essentially tests how many cell divisions the founder cell can undergo. The colony-forming cell assay has led to the discovery of many hematopoietic regulatory factors [13–15]. Clonal assays have similarly been useful in the study of skeletal muscle progenitors by allowing the identification of surface markers [16] as well as identifying growth factor requirements [17]. In the context of satellite cells, the progeny of the proliferating satellite cells is a mixture of mononuclear cells and multinuclear myotubes, the product of myoblast fusion. Therefore, gathering information about the state of the cell or its response to the culture condition requires analysis of the cellular composition of the colony, for example, determining how many total cells the colony has (a measure of proliferative potential of the CFC), and the ratio of terminally differentiated cells to undifferentiated cells (a measure of propensity to differentiate) [18]. We present a protocol that allows the elucidation of these parameters from satellite cells by FACS sorting single satellite cells into 96-well dishes, culturing in a medium that allows proliferation and differentiation, and analyzing for nuclear number and differentiation rate by staining to visualize DNA and sarcomeric myosin, respectively.

2 Materials

2.1 Harvest of Satellite Cells for FACS Sorting

1. Mice carrying the *Pax7-ZsGreen* reporter gene [19] (*see* **Note 1**)
2. Digestion Solution 1: 500 mL DMEM High Glucose plus 4500 mg/L Glucose without L-Glutamine and Sodium Pyruvate supplemented with 1% Penicillin/Streptomycin and 1 gram collagenase type II
3. Rinsing Solution: Ham's/F-10 medium plus 1.00 mM L-Glutamine supplemented with 10% Horse Serum, 1% 1 M HEPES Buffer Solution, and 1% Penicillin/Streptomycin

4. Digestion Solution 2: 7 mL Rinsing Solution supplemented with 500 μL of Digestion Solution 1 and 1.25 mL of 0.4% Dispase in Rinsing Solution per sample
5. Sorvall LEGEND RT Centrifuge (Thermo Electron Corporation)
6. 100 X 15 mm Petri dishes
7. Razor blades
8. Serological pipettes
9. 50 mL conical tubes (sterile)
10. Pasteur pipettes
11. Small pipette bulbs
12. 10 mL syringes
13. 18-gauge needles
14. 16-gauge needles
15. 40 micron cell strainers
16. 96-well cell culture plate
17. 10% gelatin, dissolved in PBS
18. Culture Medium (myogenic medium): DMEM/F12 medium without L-glutamine containing 20% FBS, 10% horse serum, 50 ng/μL human basic fibroblast growth factor (Peprotech, Rocky Hill, NJ; 100-18), 1% penicillin/streptomycin, 1% Glutamax (Gibco, 35050-061), and 0.5% chick embryonic extract (US Biological, Swampscott, MA; C3999)

2.2 FACS Staining

1. Phosphate-Buffered Saline (PBS)
2. FACS Staining Medium: PBS without calcium and magnesium supplemented with 2% Fetal Bovine Serum
3. FACS Staining Medium with Propidium Iodide: as above, supplemented with 1 μg/mL Propidium Iodide
4. Antibody Mixture: (1 μL CD31-PE-Cy7, 1 μL CD45-PE-Cy7, 1 μL VCAM-Biotin,1 μL Streptavidin-PE, 2 μL α7-integrin-647) in a total volume of 100 μL FACS Staining Medium with PI (*see* **step 3**).
5. CD31-PECy7 Clone 390 (BD Biosciences – 561410)
6. CD45-PE-Cy7 Clone 30-F11 (BD Biosciences – 552848)
7. VCAM-Biotin Clone 429(MVCAM.A) (BD Biosciences – 553331)
8. Streptavidin-PE (BD Biosciences – 554061)
9. α7-integrin Clone R2F2 (AbLab – 67-0010-05)

2.3 Antibody Staining of Colonies

1. 4% paraformaldehyde (PFA) in PBS
2. 0.3% triton-X 100 in PBS
3. 3% bovine serum albumin (BSA) in PBS
4. MF 20, a monoclonal antibody against sarcomeric myosin (obtained from the Developmental Studies Hybridoma Bank, University of Iowa), at a dilution of 1:20 in 3% BSA/PBS
5. Alexa Fluor 555 goat anti-mouse secondary antibody solution 1:1000 in 3% BSA/PBS
6. 4′,6-diamidino- 2-phenylindole (DAPI) 1:1000 dilution in PBS

3 Methods

3.1 Preparing the Cell Culture Plates

1. Place the 96-well plate in the tissue culture hood.
2. Coat the wells in the plate by adding 50 μL of 10% gelatin to cover the bottom of the wells.
3. Leave the plates to be gelatinized for 30 min at room temperature.
4. Aspirate the gelatin using a Pasteur pipette.
5. Add 100 μL of the culture medium to every well of the plate.

3.2 Harvest of Satellite Cells

1. Carefully dissect both hind limbs, triceps, and psoas muscles.
2. Chop the muscle parallel to the muscle fiber direction into approximately 2 mm thick pieces (use the razor blade as a straight edge and pull along the straight edge with a curved forceps) (for images of this procedure, see Ref. 20).
3. Place the sample into a 50 mL tube containing 15 mL of digestion solution 1.
4. Keep the samples on ice until all samples have been harvested.
5. Incubate and shake for 75 min at 37 °C.
6. Invert the tubes five times, then let the sample gravity settle for approximately 5 min.
7. Aspirate the supernatant to the 10 mL mark of the 50 mL conical tube. Add 6 mL rinsing solution, invert the tubes five times, then let the samples settle for 5 min.
8. Repeat **step 7**.
9. Aspirate the supernatant again, leaving behind 10 mL.
10. Add 2 mL rinsing solution and pour muscle solution into an inclined 100 × 15 cm petri dish.
11. Scrape the muscle solution against the bottom of the inclined Petri dish and squeeze into and out of a sheared Pasteur pipette

(with small bulb). This will mechanically disrupt the muscle fibers.

12. Add 2 mL rinsing solution to wash the Petri dish, transferring the solution back to the 50 mL conical tube. Repeat this rinse to collect as much residue as possible.
13. Centrifuge the samples at 300 × *g* for 5 min on a benchtop centrifuge.
14. Aspirate the supernatant, leaving behind 5 mL.
15. Add 10 mL rinsing solution and resuspend the pellet.
16. Centrifuge the samples at 300 × *g* for 5 min.
17. Aspirate the supernatant to the 5 mL mark of the tube.
18. Add 8.5 mL digestion solution 2 and resuspend the pellet.
19. Vortex for 30 s.
20. Incubate shaking for 30 min at 37 °C.
21. Vortex for 30 s.
22. Place a 40 μm cell strainer on a new 50 mL conical tube and wet with 2 mL rinsing solution.
23. Draw the sample into and out of a 10 mL syringe with a 16-G needle four times.
24. Draw into and out of a 10 mL syringe with an 18-G needle four times.
25. Apply the sample through the 40 μm cell strainer, collecting it into the new 50 mL conical tube.
26. Collect any residue in the original 50 mL tube by adding 10 mL rinsing solution and pouring it through the cell strainer into the new 50 mL tube.
27. Centrifuge the samples at 300 × *g* for 5 min.
28. Place a 40 μm cell strainer onto a new 50 mL conical tube and wet with 2 mL rinsing solution.
29. Again, draw the sample into and out of a 10 mL syringe with an 18-G needle four times.
30. Strain the sample through the 40 μm cell strainer, collecting it in the new 50 mL conical tube.
31. Collect any residue by adding 10 mL rinsing solution to the new 50 mL tube through the strainer.
32. Centrifuge the samples at 300 × *g* for 5 min.
33. Carefully aspirate until there is only approximately 100 μL volume left above the cell pellet.
34. Add 2 mL of staining medium to the sample, resuspend the cells, and transfer to a new 15 mL conical tube for FACS sorting.

3.3 Antibody Staining (Optional)

In the case where mice lacking the Pax7-ZsGreen reporter need to be analyzed, antibody staining followed by FACS can be used to isolate the satellite cells. The cell samples are stained for CD31 and CD45 (Lineage-negative markers) as well as the satellite cell markers VCAM1 and α7-integrin [21–25]. Cloning efficiency is typically lower with this approach (one-half to two-thirds that of Pax7-ZsGreen+ cells).

1. Prepare Antibody Mixture. Subheading 2.2, **step 4** provides the recipe per TA. Multiply these volumes by the number of TAs to be analyzed and add 4 uL of PBS to ensure that the last sample is not treated with a smaller volume than the others.
2. Add 6 μL of the antibody mixture to each TA sample (this is enough to stain approximately 2 million cells).
3. Incubate on ice for 20 min (*see* **Note 2**).
4. Add 5 mL Staining Medium to each sample.
5. Centrifuge at 300 × *g* for 5 min.
6. Aspirate the Staining Medium until only approximately 50 μL remains in the conical tube.
7. Tap the tubes to resuspend the cells.
8. Add 250 μL of staining medium with propidium iodide to resuspend the cells for analysis on the FACS machine.

3.4 FACS Gating Strategy and Single Cell Sorting

Cells can be analyzed/sorted on a variety of instruments, using the same strategies. The examples provided below pertain to our instrument of choice, a BD FACS Aria II, equipped with red (641 nm), blue (488 nm), and yellow-green (561 nm) lasers. The cells are analyzed sequentially through a series of gates. Below are the gates utilized to isolate the satellite cells for both approaches (isolating based on the Pax7-ZsGreen reporter or on the basis of immunostaining for Lin– VCAM+ α7-integrin+).

1. The Forward Scatter Threshold eliminates the signal from debris. Setting this threshold appropriately is important to ensure speed and efficiency of sorting (*see* **Note 3**).
2. Side Scatter Area × Forward Scatter Area is a plot of event complexity versus size of events. This plot allows for exclusion of debris and inclusion of mononuclear cells (Fig. 1a).
3. Forward Scatter Height × Forward Scatter Width plots exclude doublets (Fig. 1b).
4. Side Scatter Height × Side Scatter Width plots exclude doublets (Fig. 1c).
5. Live cells are identified by their ability to exclude propidium iodide (Fig. 1d). We plot PI against PE because of the strong spectral overlap of these two channels, using a triangular gate to

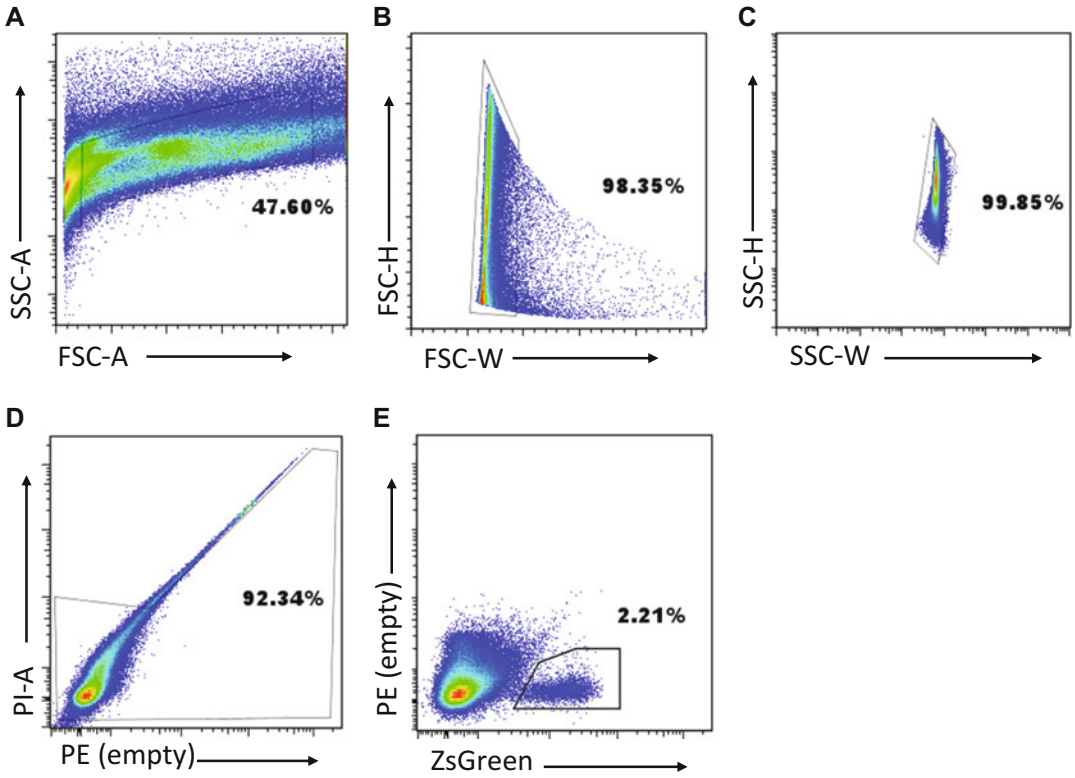

Fig. 1 Gating strategy for FACS sorting of ZsGreen satellite cells from bulk hind limb. (**a**) FACS plot showing threshold and first gate set on forward scatter area (FSC-A) X side scatter area (SSC-A). (**b**) Second gate on forward scatter height (FSC-H) X forward scatter width (FSC-W). (**c**) Third gate on side scatter height (SSC-H) X side scatter width (SSC-W). (**d**) Fourth gate on propidium iodide (PI) X phycoerythrin (PE) channel. (**e**) Sorting gate on plot of green channel (ZsGreen) X PE

include all PI− cells, including those with a strong PE signal that bleeds into the PI channel, but to exclude true PI+ cells.

6. The Pax7-ZsGreen satellite cells are identified using the green channel vs. the PE channel (Fig. 1e).
7. When using mice lacking the Pax7-ZsGreen reporter, we use the same **steps** from **1** to **5**, then gate on the negative fraction as satellite cells do not express the lineage surface markers CD31 and CD45 (PE-Cy7 or lineage negative cells) (Fig. 2e).
8. Lineage negative cells are examined for the expression of VCAM and α7-integrin and a gate is placed on the well-separated double-positive population representing the satellite cells (Fig. 2f).
9. Single satellite cells are sorted using the 96-well plate adaptor and single cell precision in the BD FACS Aria II sorting layout (*see* **Note 4**).

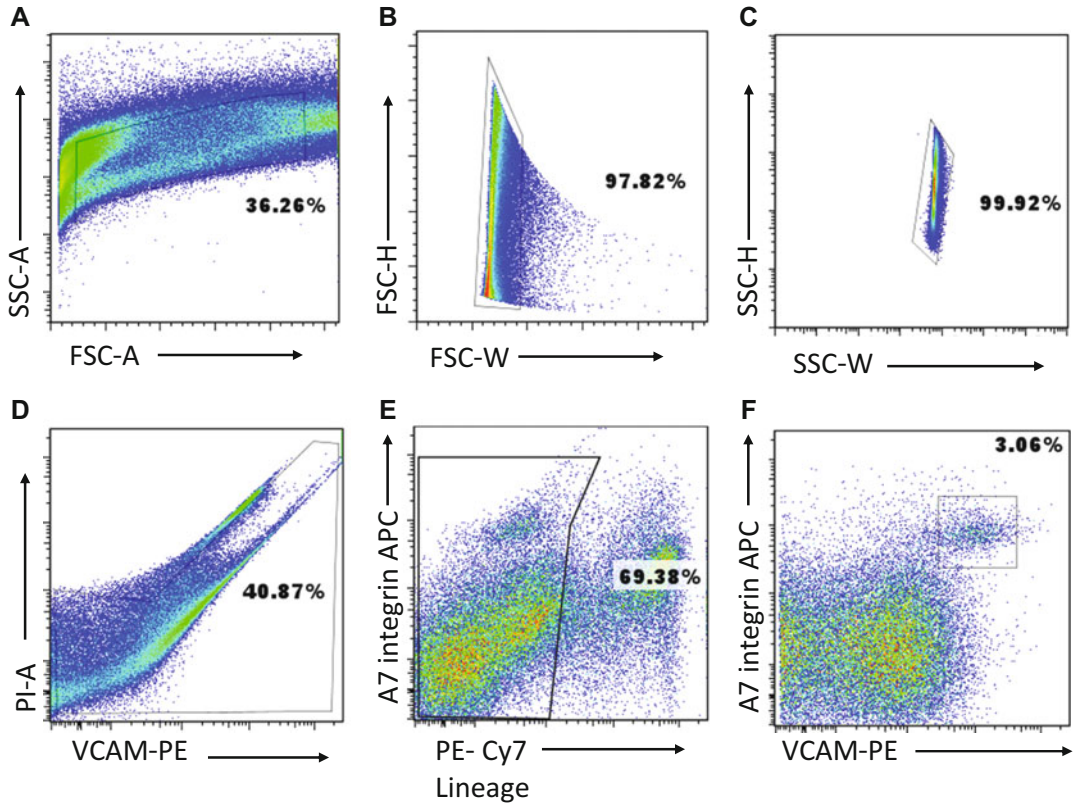

Fig. 2 Gating strategy for FACS sorting of Lin– α7+ VCAM+ satellite cells from bulk hind limb. (**a**) Forward scatter threshold, and first gate set on FSC-A X SSC-A. (**b**) Second gate on FSC-H X FSC-W. (**c**) Third gate on SSC-H X SSC-W. (**d**) Fourth gate on PE (VCAM) X PI. (**e**) Fifth gate PE-Cy7 (Lineage)-negative X APC (α7-integrin). (**f**) Sorting gate on plot of PE (VCAM) X APC (α7-integrin)

3.5 Cell Culture, Staining, and Imaging

Plates are grown at 37 °C under reduced oxygen conditions (5% O_2, 5% CO_2) using a 3 gas incubator, or glass chamber filled with a custom gas mixture (5% O_2, 5% CO_2, 90% N_2) which is then sealed and maintained for 8 days at 37 °C. We use reduced oxygen as primary mouse cells are particularly sensitive to oxidative stress [26]. The plates are then processed as follows:

1. On day 8, remove plates from their respective incubators and identify colonies by circling the well with a sharpie.
2. Fix the positive wells with 4% paraformaldehyde for 20 min at room temperature.
3. Permeabilize the colonies with 0.3% triton-X for 20 min at room temperature.
4. Wash once with PBS for 5 min.
5. Block with 3% bovine serum albumin (BSA) in PBS for 1 h at room temperature.

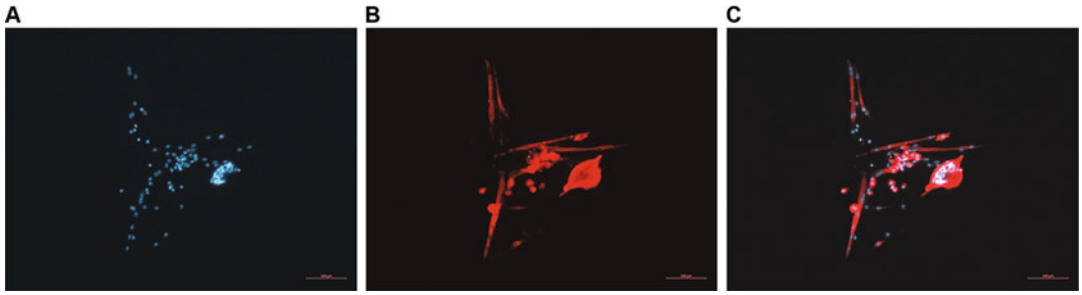

Fig. 3 Immunofluorescence staining of a typical satellite cell colony. (**a**) Channel for DAPI, showing nuclei. (**b**) Red channel, showing myosin heavy chain (AF 555). (**c**) Merged images

6. Stain the colonies at 4 °C with MF 20, a monoclonal antibody, against sarcomeric myosin overnight at 4 °C.
7. The following day, wash the plates three times with PBS, 5 min each.
8. Incubate the colonies with Alexa Fluor 555 goat anti-mouse secondary antibody solution for 1 h and 30 min at room temperature.
9. Wash three times with PBS for 5 min.
10. Counterstain the colonies with 4′,6-diamidino-2-phenylindole (DAPI).
11. The stained cells are covered with PBS and imaged on a Zeiss AxioObserver Z1 inverted microscope with an AxioCamMR3 camera (Thornwood, NY) (Fig. 3).
12. Cloning efficiency is determined as the percentage of single cells with a visible colony.
13. Number of nuclei per colony can be counted by ImageJ software using Integrated Intensity. Briefly, change the type of image to "32-bit" using the menu Image/Type/32-bit. Then add "Integrated intensity," "Mean" to "Analyze/Set Measurements." Then, subtract background by finding an empty region, draw a rectangle, and press 'M', then call Process/Math/Subtract with the value in the results table that appears, under "Mean." Then, draw a rectangle around an isolated nucleus and press "M." Intensity of single nucleus (Tn) in the results table will be under "Raw integrated intensity." Then deselect everything in the image and press 'M' to measure the total intensity of the whole image (Ti). Divide the value of Ti by Tn. This is the estimated total number of nuclei. These steps can be recorded in the Macro and then batched on all the images (Fig. 4).
14. Fraction of nuclei in myosin-heavy chain-positive cytoplasm serves as an indicator of differentiation. This can be determined by manual counting or by using an algorithm such as G-tool [18].

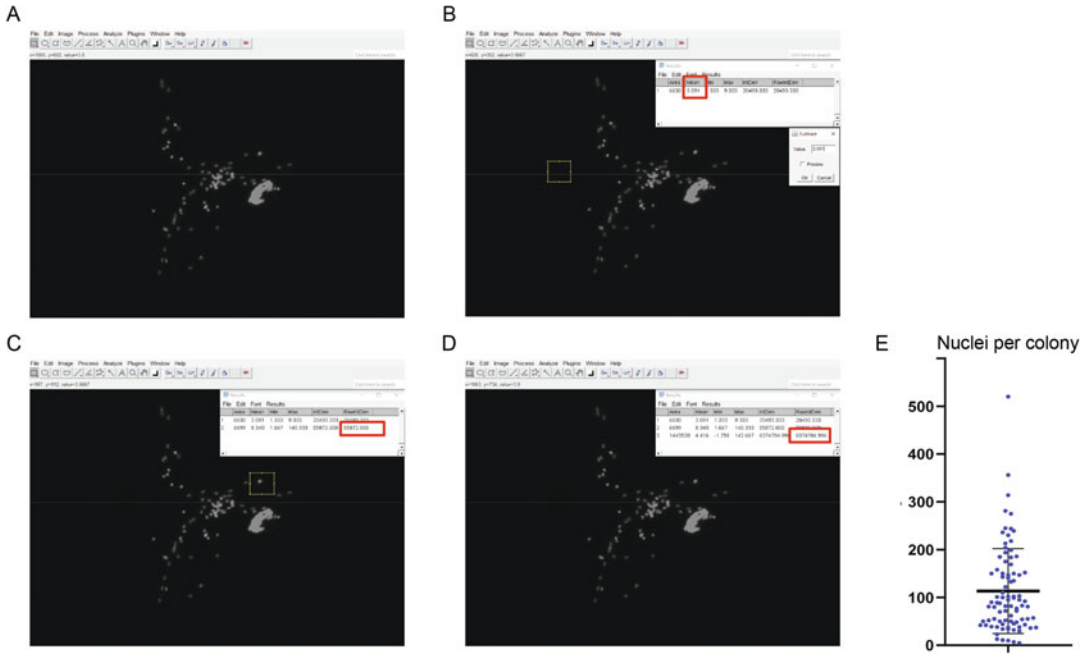

Fig. 4 Image analysis using Fiji ImageJ. Image converted to 32-bit. (**a**) Image with background subtracted. Process> Math> Subtract was performed, Red box indicates the mean value used. (**b**) Intensity of Single Nucleus (Tn) in the red box under Raw Intensity Density. (**c**) Intensity of Single Nucleus (Ti) in the red box under Raw Intensity Density, Colony Size = Tn/Ti. (**d**) Data presentation for colonies from Pax7-ZsGreen+ cells of a wild-type adult C57BL/6 mouse (Mean and SD)

4 Notes

1. The Pax7-ZsGreen transgene should always be maintained in the heterozygous state. We maintain this stock by breeding either males or females to wild-type C57BL/6 mice and selecting ZsGreen+ progeny by PCR genotyping. We have found that the ZsGreen transgene can undergo generational silencing in the homozygous state. Therefore, carrier mice must never be allowed to breed with each other.
2. 20 min is the minimum time. Incubation with antibodies on ice may be extended to 40 min.
3. On the BD FACS Aria II, we set the Forward Scatter Threshold to 5000.
4. Sorting 1000 cells into the first well "A1" in the 96 wells plate serves as a control for finding the focal plane, because sometimes the single cell colonies are small and difficult to find without being in the correct focal plane.

References

1. Mauro A (1961) Satellite cell of skeletal muscle fibers. J Biophys Biochem Cytol 9(2):493
2. Collins CA, Olsen I, Zammit PS, Heslop L, Petrie A, Partridge TA et al (2005) Stem cell function, self-renewal, and behavioral heterogeneity of cells from the adult muscle satellite cell niche. Cell 122(2):289–301
3. Sacco A, Doyonnas R, Kraft P, Vitorovic S, Blau HM (2008) Self-renewal and expansion of single transplanted muscle stem cells. Nature 456(7221):502–506
4. Montarras D, Morgan J, Collins C, Relaix F, Zaffran S, Cumano A et al (2005) Direct isolation of satellite cells for skeletal muscle regeneration. Science 309(5743):2064–2067
5. Aziz A, Sebastian S, Dilworth FJ (2012) The origin and fate of muscle satellite cells. Stem Cell Rev Rep 8(2):609–622
6. Cornelison D, Wold BJ (1997) Single-cell analysis of regulatory gene expression in quiescent and activated mouse skeletal muscle satellite cells. Dev Biol 191(2):270–283
7. Seale P, Sabourin LA, Girgis-Gabardo A, Mansouri A, Gruss P, Rudnicki MA (2000) Pax7 is required for the specification of myogenic satellite cells. Cell 102(6):777–786
8. Tedesco FS, Cossu G (2012) Stem cell therapies for muscle disorders. Curr Opin Neurol 25(5):597–603
9. Mendell JR, Kissel JT, Amato AA, King W, Signore L, Prior TW et al (1995) Myoblast transfer in the treatment of Duchenne's muscular dystrophy. N Engl J Med 333(13): 832–838
10. Vilquin J (2005) Myoblast transplantation: clinical trials and perspectives. Mini-review. Acta Myol 24(2):119–127
11. Bradley T, Metcalf D (1966) The growth of mouse bone marrow cells in vitro. Aust J Exp Biol Med Sci 44(3):287–300
12. Franken NA, Rodermond HM, Stap J, Haveman J, Van Bree C (2006) Clonogenic assay of cells in vitro. Nat Protoc 1(5):2315
13. Burgess AW, Camakaris J, Metcalf D (1977) Purification and properties of colony-stimulating factor from mouse lung-conditioned medium. J Biol Chem 252(6): 1998–2003
14. Kaushansky K, Lok S, Holly RD, Broudy VC, Lin N, Bailey MC et al (1994) Promotion of megakaryocyte progenitor expansion and differentiation by the c-Mpl ligand thrombopoietin. Nature 369(6481):568–571
15. Wendling F, Maraskovsky E, Debili N, Florindo C, Teepe M, Titeux M et al (1994) c-Mpl ligand is a humoral regulator of megakaryocytopoiesis. Nature 369(6481):571–574
16. Sherwood RI, Christensen JL, Conboy IM, Conboy MJ, Rando TA, Weissman IL et al (2004) Isolation of adult mouse myogenic progenitors: functional heterogeneity of cells within and engrafting skeletal muscle. Cell 119(4):543–554
17. Mezzogiorno A, Coletta M, Zani B, Cossu G, Molinaro M (1993) Paracrine stimulation of senescent satellite cell proliferation by factors released by muscle or myotubes from young mice. Mech Ageing Dev 70(1–2):35–44
18. Ippolito J, Arpke RW, Haider KT, Zhang J, Kyba M (2012) Satellite cell heterogeneity revealed by G-Tool, an open algorithm to quantify myogenesis through colony-forming assays. Skelet Muscle 2(1):13
19. Bosnakovski D, Xu Z, Li W, Thet S, Cleaver O, Perlingeiro RC et al (2008) Prospective isolation of skeletal muscle stem cells with a Pax7 reporter. Stem Cells 26(12):3194–3204
20. Arpke RW, Kyba M (2016) Flow cytometry and transplantation-based quantitative assays for satellite cell self-renewal and differentiation. In: Skeletal muscle regeneration in the mouse. Springer, pp 163–179
21. Chan SS, Shi X, Toyama A, Arpke RW, Dandapat A, Iacovino M et al (2013) Mesp1 patterns mesoderm into cardiac, hematopoietic, or skeletal myogenic progenitors in a context-dependent manner. Cell Stem Cell 12(5):587–601
22. Blanco-Bose WE, Yao CC, Kramer RH, Blau HM (2001) Purification of mouse primary myoblasts based on alpha 7 integrin expression. Exp Cell Res 265(2):212–220
23. Fukada S, Uezumi A, Ikemoto M, Masuda S, Segawa M, Tanimura N et al (2007) Molecular signature of quiescent satellite cells in adult skeletal muscle. Stem Cells 25(10):2448–2459
24. Jesse TL, LaChance R, Iademarco MF, Dean DC (1998) Interferon regulatory factor-2 is a transcriptional activator in muscle where it regulates expression of vascular cell adhesion molecule-1. J Cell Biol 140(5):1265–1276
25. Seale P, Ishibashi J, Holterman C, Rudnicki MA (2004) Muscle satellite cell-specific genes identified by genetic profiling of MyoD-deficient myogenic cell. Dev Biol 275(2): 287–300
26. Parrinello S, Samper E, Krtolica A, Goldstein J, Melov S, Campisi J (2003) Oxygen sensitivity severely limits the replicative lifespan of murine fibroblasts. Nat Cell Biol 5(8):741–747

Chapter 5

Co-cultures of Macrophages with Muscle Stem Cells with Fibroadipogenic Precursor Cells from Regenerating Skeletal Muscle

Georgiana Panci, Anita E. M. Kneppers, Rémi Mounier, Bénédicte Chazaud, and Gaëtan Juban

Abstract

Adult muscle stem cells rebuild myofibers after damage. Although they are highly powerful to implement the adult myogenic program, they need environmental cues provided by surrounding cells for efficient and complete regeneration. Muscle stem cell environment includes fibroadipogenic precursors, vascular cells, and macrophages. A way to decipher the complexity of the interactions muscle stem cells establish with their neighborhood is to co-culture cells freshly isolated from the muscle and assess the impact of one cell type on the behavior/fate of the other cell type. Here, we present a protocol allowing the isolation of primary muscle stem cells, macrophages, and fibroadipogenic precursors by Fluorescence Activated Cell Sorting (FACS) or Magnetic Cell Separation (MACS), together with co-culture methods using a specific setup for a short time window to keep as much as possible the *in vivo* properties of the isolated cells.

Key words Skeletal muscle, Cell isolation, Co-culture, Muscle stem cells, Macrophages, Fibroadipogenic precursors, MACS, FACS

1 Introduction

Skeletal muscle is composed of various cell types, including multinucleated myofibers, myogenic stem cells or satellite cells (MuSCs), endothelial cells, and mesenchymal progenitors called fibroadipogenic precursors (FAPs). After an injury, MuSCs rapidly activate and implement the adult myogenic program to form new myofibers. Injury triggers an inflammatory response that lasts the whole muscle regeneration process. Neutrophils, macrophages, and Tregs, which are present in small numbers in steady state muscle, invade the regenerating muscle. All these cell types cooperate during the regeneration process to recover muscle function [1].

After injury, blood monocytes rapidly infiltrate the damaged tissue and differentiate into pro-inflammatory macrophages (MPs)

Atsushi Asakura (ed.), *Skeletal Muscle Stem Cells: Methods and Protocols*, Methods in Molecular Biology, vol. 2640, https://doi.org/10.1007/978-1-0716-3036-5_5,

expressing the surface marker Ly6C [2]. Pro-inflammatory MPs phagocyte muscle debris, stimulate MuSC proliferation, and trigger FAP apoptosis [2–5]. Upon phagocytosis, pro-inflammatory MPs shift their profile towards a restorative phenotype that supports MuSC differentiation, fusion, and myofiber growth [2, 3]. Restorative MPs also contribute to the extracellular matrix remodeling as they stimulate collagen production by FAPs [4, 5]. Alteration of the regulating properties of MP subsets triggers regeneration defect [6–8] or is responsible for the development of fibrosis in degenerative myopathies [5].

Therefore, the interplay between MPs and other cell types during normal or pathological skeletal muscle regeneration is of interest, notably to identify molecular pathways involved in the regulation of the biological processes at work. A way to study these cell interactions is to isolate the cells of interest and to co-culture them in a controlled environment. Here, we present a protocol allowing the isolation of primary MuSCs, MPs, and FAPs by FACS or MACS (magnetic cell sorting), sorting together with co-culture methods using specific set-up for a short time window to keep as much as possible in the *in vivo* properties of the isolated cells. Cellular parameters (*e.g.*, proliferation, differentiation…) are analyzed in FAPs and MuSCs by immunofluorescence.

2 Materials

2.1 Cell Sorting and Culture

- Material for mouse dissection (thin forceps, thin scissors, thin sharp scissors).
- 0.22 μm filters.
- Parafilm.
- 5 ml BD Falcon FACS tubes.
- 30 ml Sterilin Polystyrene tube (Sterilin #080005).
- 50 ml Polypropylene conical tubes.
- 30 μm cell strainers (Miltenyi Biotec #130-098-458).
- 70 μm cell strainers (Miltenyi Biotec #130-098-462).
- 100 μm cell strainers (Miltenyi Biotec #130-098-463).
- MS Columns (Miltenyi Biotec #130-042-201) or LS Columns (Miltenyi Biotec # 130-042-401).
- Miltenyi magnetic stand and magnets for columns (QuadroMACS™ Separator, Miltenyi Biotec #130-090-976).
- Needle (20G).
- Syringe (30 ml).
- Cell culture plastic supports (*e.g.*, 24 well plates, 96 well plates, 8 chamber slides, etc.).

- Culture inserts pore size 0.4 μm (NUNC #056408) and 24 well plates.
- Collagenase II (Gibco LifeTechnologies #17101-105).
- Collagenase B (Roche #11 088 831 001).
- Dispase (Gibco LifeTechnologies #17105-041).
- Dispase II (Roche #04 942 078 001).
- DMEM/F12 medium.
- DMEM-high: DMEM high glucose with pyruvate.
- Ham's F-10.
- Fetal Bovine Serum (FBS) Heat-inactivated (56 °C for 30 min).
- Horse Serum (HS).
- Penicillin/Streptomycin (P/S).
- PBS 1X.
- MACS buffer: PBS pH 7.4, containing 0.5% Bovine Serum Albumin (BSA) (Roche #10735 078001), 2 mM EDTA filtrated through 0.22 μm (filtration is required to degas the buffer, store at −20 °C).
- ACK Lysing Buffer (Lonza #10-548E).
- FcR-blocking reagent (Miltenyi Biotec #130-059-901).
- Anti-CD45-Beads (Miltenyi Biotec #130-052-301).
- Anti-CD64-AF647 antibody (Biolegend #139322).
- Anti-Cy5/Anti-Alexa Fluor 647 Microbeads (Miltenyi Biotec #130-091-395).
- Satellite Cell Isolation Kit (Miltenyi Biotec, #130-104-268).
- Antibodies for FACS and isotypic controls: see Table 1.
- DAPI.
- Matrigel High Growth Factor (BD Biosciences #354234).
- Ultroser G (Pall #15950-017).
- Digestion medium (2.4 U/ml Collagenase B and 2.4 U/ml Dispase II in DMEM/F12 medium). Filtrate through 0.22 μm and heat the medium at 37 °C.

2.2 Immunostaining

- Paraformaldehyde (PFA).
- Triton X-100.
- Bovine Serum Albumin (BSA).
- Antibodies: see Table 2.
- Hoechst.
- Fluoromount mounting medium.

Table 1
List of antibodies and isotypes used for FACS sorting

Antibodies	Isotypes	Quantity[a]
Rat monoclonal anti-CD45, PE-Cy7 (eBioscience #25-0451-82)	Rat IgG2b kappa isotype control, PE-Cy7 (eBioscience #25-4031-82)	0.1 μg
Rat monoclonal anti-CD31, PE (eBioscience #12-0311-82)	Rat IgG2a kappa isotype control, PE (eBioscience #12-4321-80)	0.1 μg
Rat monoclonal anti-Sca-1, PerCP-Cy5.5 (eBioscience #45-5981-82)	Rat IgG2a kappa isotype control, PerCP-Cy5.5 (eBioscience #45-4321-80)	0.1 μg
Rat monoclonal anti-α7-integrin, AF647 (AbLab #AB0000951)	Rat IgG2b kappa isotype control, AF647 (Biolegend #400626)	2.5 μg
Rat monoclonal anti-CD34, FITC (eBioscience #11-0341-82)	Rat IgG2a kappa isotype control, FITC (Biolegend #11-4321-80)	1.25 μg
Mouse monoclonal anti-CD64, AF647 (BD Biosciences #558539)	Mouse IgG1 kappa isotype control, AF647 (BD Biosciences #557732)	0.4 μg
Rat monoclonal anti-Ly6C, PE (eBioscience #12-5932-82)	Rat IgG2b kappa isotype control, PE (BD Biosciences #553989)	0.1 μg

[a]Given for 2 Tibialis Anterior muscles, or up to 5.10^6 cells

Table 2
List of primary and secondary antibodies used for immunostaining

Cell type	Parameter assessed	Primary antibodies (dilution)	Secondary antibodies (1/200 dilution)
MuSCs FAPs	Proliferation	Rabbit anti-Ki67 (1/50) (Abcam, #ab15580)	Cy3 or FITC anti-rabbit IgGs (Jackson Immuno Research #711-165-152 and #711-095-152)
FAPs	Apoptosis	Rabbit anti-active Caspase 3 (1/500) (Abcam, #ab13847)	
MuSCs	Myogenic differentiation	Rabbit anti-Desmin (1/200) (Abcam, #Ab 32362)	
FAPs	Fibrogenic differentiation	Mouse anti-alpha-SMA (1/250) (Sigma-Aldrich #A5228)	FITC anti-mouse IgGs (Jackson Immuno Research #715-095-150)
FAPs	Fibrogenic differentiation	Goat anti-Collagen1 (1/400) (Southern Biotech #1310-01)	Cy3 anti-goat IgGs (Jackson Immuno Research, #705-165-147)
FAPs	Adipogenic differentiation	Rabbit anti-Perilipin1 (1/200) (Abcam, #Ab3526)	FITC anti-rabbit IgGs (Jackson Immuno Research, #711-095-152)

3 Methods

3.1 Digestion

Two digestion protocols are presented here. Depending on the cell type and the yield of cells that is required, one or the other can be used. For instance, cells are quite easily retrieved from regenerating muscle (so single digestion is enough), while higher yield of MuSCs is obtained from resting muscle using the double digestion protocol.

3.1.1 Single Digestion

1. Dissect the muscles. Roughly discard visible fat, tendons, and fascia (*see* **Note 1**).
2. Place the harvested muscles in a cold 30 ml Sterilin polystyrene tube and mince with thin sharp scissors to obtain a pulp.
3. Add the digestion medium (*see* **Note 2**) (10 ml for 2 whole limbs; 1 ml for 1 muscle, *e.g.* Tibialis Anterior or Gastrocnemius).
4. Seal the tube with Parafilm and incubate in the water bath at 37 °C with gentle shaking (60–70 rpm) for 60–90 min (*see* **Note 3**).
5. Stop the digestion by adding FBS (1:4 FBS:digestion medium), homogenize by pipetting and place the tube on ice. From now on, keep the samples at 4 °C.
6. Add 2 ml of DMEM/F12 medium and filtrate the digested muscle through a 70 μm cell strainer. Rinse the tube and the cell strainer with 2 ml of DMEM/F12 medium.
7. Centrifuge at 400 g for 10 min at 4 °C.
8. Discard the supernatant and lyse red blood cells with 0.5 ml of ACK Lysing Buffer. Vortex until the solution gets a pink/red color (3 to 5 sec) and stops the lysis with 5 ml of PBS containing 2% FBS (*see* **Note 4**).
9. Centrifuge at 400 g for 10 min at 4 °C.
10. Remove the supernatant and resuspend the pellet into 5 ml of PBS containing 2% FBS (for FACS isolation) or MACS buffer (for MACS isolation).
11. Count the cells and evaluate their viability (*e.g.*, with Trypan blue dye).

3.1.2 Double Digestion (from [9])

1. Before dissection, prepare the digestion medium 1 (800 U/ml Collagenase II, 10% HS) in Ham's F-10 medium. Filtrate through 0.22 μm and heat the medium at 37 °C.
2. Dissect the muscles required for the experiment. Roughly discard visible fat, tendons, and fascia (*see* **Note 1**).
3. Place the harvested muscles in a cold 30 ml Sterilin Polystyrene and mince with thin sharp scissors to obtain a pulp.

4. Add the digestion medium (*see* **Note 2**) (10 ml for digesting 2 whole limbs; 1 ml for 1 muscle, *e.g.,* Tibialis Anterior or Gastrocnemius).
5. Seal the tube with Parafilm and incubate in the water bath at 37 °C with gentle shaking for 45–60 min (*see* **Note 3**).
6. Triturate 5–10 times with a pipette and add Ham's F-10, 10% HS, 1% P/S up to 50 ml, and gently invert a few times to mix.
7. Centrifuge at 400 g for 10 min at 4 °C.
8. Aspirate the supernatant down to 20 ml (*see* **Note 5**) and add 1 ml 3000 U/ml Collagenase II and 1 ml 33 U/ml Dispase.
9. Resuspend the pellet with a 10 ml serological pipette, triturate 10–15 times, and add Ham's F-10, 10% HS, 1% P/S up to 30 ml.
10. Seal the tube with Parafilm and incubate in the water bath at 37 °C with gentle shaking for 30 min.
11. Using a 30 ml syringe with a 20-gauge needle, go back and forth 10 times to triturate the muscle suspension. Filter the cell suspension through a cell strainer (70 μm).
12. Rinse the cell strainer with another 10 ml of Ham's F-10, 10% HS, 1% P/S.
13. Centrifuge at 400 g for 10 min at 4 °C.
14. Discard the supernatant and lyse red blood cells with 0.5 ml of ACK Lysing Buffer. Vortex until the solution gets a pink/red color (3–5 sec) and stops the lysis with 5 ml of PBS containing 2% FBS (*see* **Note 4**).
15. Centrifuge at 400 g for 10 min at 4 °C.
16. Remove the supernatant and resuspend the pellet into 5 ml of PBS containing 2% FBS (for FACS isolation) or MACS buffer (for MAC isolation).
17. Count the cells and evaluate their viability (*e.g.*, with Trypan blue dye).

3.2 MACS Cell Sorting

MACS cell sorting allows to isolate FAPs and MPs from the same muscle sample or MuSCs and FAPs from the same muscle sample. However, co-culture experiments using MPs require isolation from different mice than the ones used for MuSC and FAP isolation. Indeed, FAPs and MuSCs need to be cultured for a few hours/days (particularly if a high number of cells are needed). Adhesion, a procedure completed in 4–6 h, is performed in a high serum-medium. Waiting for the other cell type to be ready for co-culture or being in high serum condition would alter the inflammatory status of MPs.

3.2.1 MPs: CD64^{pos} MACS Cell Sorting (see Note 6)

1. From **step 11** of Subheading 3.1.1. or **step 18** of Subheading 3.1.2, centrifuge the cells for 10 min at 400 g.
2. Remove the supernatant, but leave about 100 µl in the tube (*see* **Note 7**).
3. Resuspend the pellet with a 100–200 µl tip and add 2 µl of anti-CD64-AF647 antibody.
4. Mix with a 100–200 µl tip and incubate for 20 min at 4 °C.
5. Add 5 ml of MACS buffer, centrifuge for 10 min at 400 g, and homogenize the pellet in 90 µl of MACS buffer.
6. Add 10 µl of AntiCy5/anti-AF647 microbeads.
7. Mix with a 100–200 µl tip and incubate for 15 min at 4 °C.
8. Add 5 ml of MACS buffer, centrifuge for 10 min at 400 g, and homogenize the pellet in 1 ml of MACS buffer.
9. Install an MS Miltenyi column on the magnetic stand with a 30 µm cell strainer on top and rinse the column with 1 ml of MACS buffer (*see* **Note 8**). From this step, the column must always stay moisturized. Let the MACS buffer go through the column into a bin tube.
10. Pour the cell suspension onto the cell strainer on top of the column. CD64^{pos} cells are retained in the column while CD64^{neg} cells pass through into a "CD64^{neg} collection tube".
11. Rinse the tube containing the cells with 0.5 ml of MACS buffer 3 times and transfer onto the column. For each wash, let the MACS buffer go completely through the column.
12. Take off the column from the magnet and put it on top of a new collection tube. Add 1 ml of MACS buffer and gently flush with the piston to recover the CD64^{pos} cells.
13. Count the cells and check the viability (with trypan blue) in both CD64^{neg} and CD64^{pos} cell suspensions.
14. At this point, CD64^{neg} cells can be centrifuged for 10 min at 400 g. Resuspend them in 10 ml of DMEM-high, 10% FBS, 1% P/S for the FAP sorting (i.e. preplating), according to the procedure Subheading 3.2.3 below from **step 6**.
15. CD64^{pos} cells are MPs and can be directly seeded for experiments (see Subheading 3.4 co-culture section below).

3.2.2 MuSCs: MACS Negative Sorting

1. From **step 11** of Subheading 3.1.1. or **step 18** of Subheading 3.1.2, centrifuge the cells for 10 min at 400 g.
2. Remove the supernatant and resuspend the cell pellet in 80 µl of MACS buffer.
3. Add 20 µl of satellite cell isolation kit.
4. Mix with a 100–200 µl tip and incubate for 15–30 min at 4 °C.

5. Adjust the volume to 500 µl by adding 400 µl of MACS buffer.
6. Install an MS Miltenyi column on the magnetic stand with a 30 µm cell strainer on top and rinse the column with 1 ml of MACS buffer (*see* **Note 8**). From this step, the column must always stay moisturized. Let the MACS buffer go through the column into a bin tube.
7. Pour the cell suspension onto the cell strainer on top of the column. Rinse the tube containing the cells with 0.5 ml of MACS buffer 3 times and transfer onto the column. For each wash, let the MACS buffer go completely through the column.
8. Collect the flow-through cell suspension that contains MuSCs and centrifuge at 400 g for 10 min at 4 °C.
9. Remove supernatant and resuspend the pellet in 10 ml of DMEM F-12, 20% FBS, 2% Ultroser G, 1% P/S, and seed the cells for culture experiments (see Subheading 3.4 co-culture section below).
10. To sort FAPS, take off the column from the magnet and put it on top of a new collection tube. Add 1 ml of MACS buffer and gently flush with the piston to recover the non-MuSCs.
11. Centrifuge for 10 min at 400 g and resuspend with 10 ml of in DMEM-high, 10% FBS, 1% P/S for the FAP sorting (*i.e.*, preplating) according to the procedure Subheading 3.2.3 below from **step 6**.

3.2.3 FAPs: Isolation via Preplating

FAPs can be isolated from $CD64^{neg}$ or non-MuSC cell fraction after MACS sorting of MPs and MuSCs, respectively, and can also be directly isolated from muscle.

1. From Subheading 3.1.1 **step 4** (digestion), stop the digestion by adding DMEM-high, 10% FBS, 1% P/S, 1.5-fold the digestion volume.
2. Centrifuge 150 g for 5 min at RT.
3. Filter the supernatant containing the cells with a 100 µm cell strainer in a 50 ml falcon and discard the pellet.
4. Centrifuge the filtered supernatant at 400 g for 10 min at RT.
5. Discard the supernatant and resuspend the pellet in 10 ml of DMEM-high, 10% FBS, 1% P/S.
6. Put the cell suspension in 75 cm^2 flask and incubate the cells at 37 °C, 5% CO_2 for 3 h. The fibroblasts attach to the flask.
7. Discard the medium and replace it with DMEM-high, 10% FBS, 1% P/S medium.
8. Renew the medium after 3 days. After approximately 5–6 days, FAPs can reach up to 1×10^6 cells.

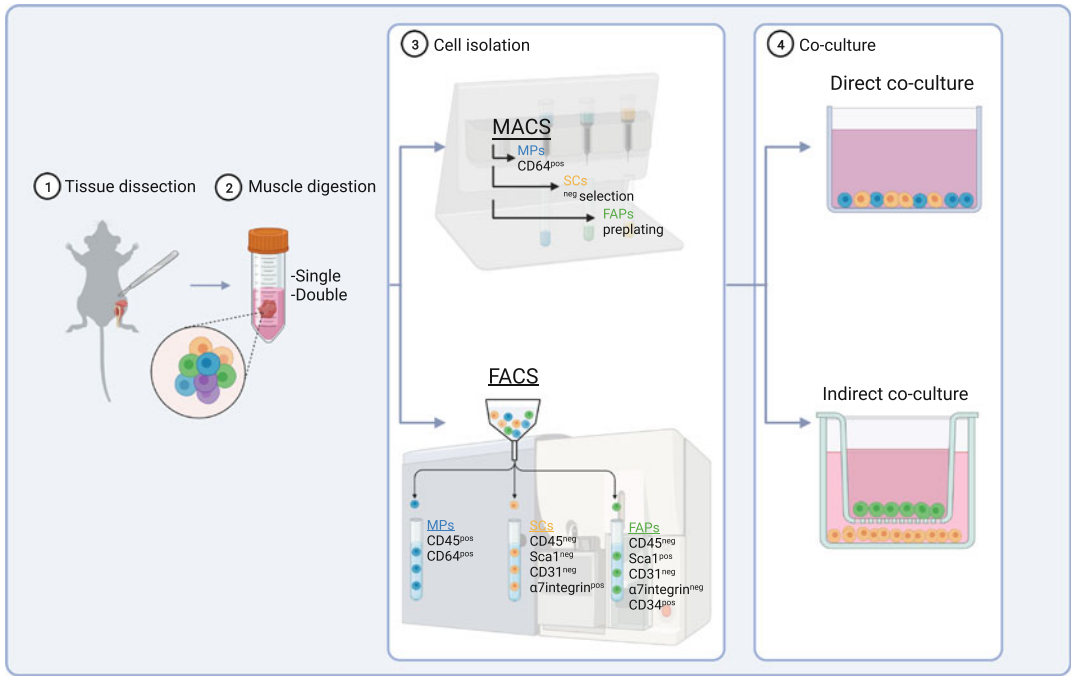

Fig. 1 Workflow for isolation and co-culture of MPs with MuSCs or FAPs. **1.** Cells are isolated from the hindlimb muscles. **2.** The tissue is digested either with a single or a double round of enzymatic digestion, depending on the purpose of the experiment. **3.** Cells are sorted using either MACS or FACS. **4.** Once isolated, cell interactions are analyzed using either direct co-cultures or indirect (inserts) co-cultures

3.3 FACS Isolation (Fig. 1)

Depending on the number of collecting tubes available at the FACS, a MACS isolation step may be required for $CD45^{pos}$ cells. Moreover, this improves the quality of the sorting of the other cell types when high numbers of immune cells are present.

1. From **step 11** of Subheading 3.1.1. or **step 18** of Subheading 3.1.2, centrifuge the cells at 400 g for 10 min.
2. Follow procedure described in Subheading 3.2.1 using anti-CD45-beads instead of the anti-CD64 antibodies.
3. From **step 12**, centrifuge the $CD45^{pos}$ cell fraction at 400 g for 10 min, discard the supernatant, and resuspend the cells in 100 µl of PBS containing 2% FBS.
4. From **step 12**, centrifuge the $CD45^{neg}$ cell fraction at 400 g for 10 min, discard the supernatant, and resuspend the cells in 100 µl of PBS containing 2% FBS.
5. For each fraction, add 2 µl of FcR Blocking Reagent for up to 1.10^6 cells and incubate for 20 min at 4 °C.
6. Add antibodies (*see* **Note 9**). For the $CD45^{pos}$ fraction, add anti-CD64-AF647 and anti-Ly6C-PE (Table 1). For the

CD45^{neg} fraction, add anti-CD45-PE-Cy7, anti-Sca1-PerCP-Cy5.5, anti-CD31-PE, anti-α7 integrin-AF647 and anti-CD34-FITC (Table 1).

7. Mix by gentle pipetting with a 100–200 µl tip and incubate for 30 min at 4 °C protected from light.
8. Add 2 ml of PBS containing 2% FBS.
9. Centrifuge at 400 g for 10 min at 4 °C.
10. Remove the supernatant and homogenize the pellet with 300 µl of PBS containing 2% FBS.
11. Filter through a 30 µm strainer into a FACS tube.
12. Immediately before sorting, add 1 µg/ml DAPI for viability staining.
13. MuSCs are isolated as CD45^{neg}Sca1^{neg}CD31^{neg}α7integrin^{pos} cells (*see* **Note 10**). FAPs are isolated as CD45^{neg}Sca1^{pos} CD31^{neg} α7-integrin^{neg} CD34^{pos}, MPs as CD45^{pos}CD64^{pos}Ly6C^{pos} or Ly6C^{neg} cells (Fig. 2).
14. Collect MuSCs in DMEM-F12, 10% FBS, 2% Ultroser G, 1% P/S, FAPs in DMEM-high, 10% FBS, 1% P/S and MPs in DMEM containing 2% FBS (*see* **Note 11**).

3.4 Co-cultures (Fig. 1)

Depending on the number of cells that are recovered (*see* **Note 12**) and the number of cells needed for the experiments, an amplification step of MuSCs and FAPs may be required. MuSCs and FAPs are cultured in the medium used for their collection.

3.4.1 Direct Co-cultures

Co-culture of MPs with MuSCs

1. Coat the cell culture support with Matrigel (*see* **Note 13**) diluted at 1/10 in cold DMEM and incubate for 30 min at 37 °C, 5% CO_2. Aspirate the excess liquid and rinse once carefully with PBS.
2. Seed MuSCs in DMEM-F12, 10% FBS, 2% Ultroser G, 1% P/S. Cell density is:
   - 10,000 cells/cm^2 for proliferation/apoptosis assay (*see* **Note 14**).
   - 30,000 cells/cm^2 for myogenesis assay (*see* **Note 14**).
3. Let MuSCs adhere to the culture support for about 6 h at 37 °C, 5% CO_2.
4. MPs may be isolated (see sections above) during the adhesion time.
5. For MuSC proliferation assay, resuspend MPs in DMEM-F12, 2.5% FBS, 1% P/S (*see* **Note 15**). For MuSC differentiation assay, resuspend MPs in DMEM- F12, 2% HS, 1% P/S (*see* **Note 16**). Calculate the cell concentration to obtain a ratio of 3:1 MPs:MuSCs in the adequate volume of medium (for instance 100 µl in a 96-well or 250 µl in an 8-chamber slide).

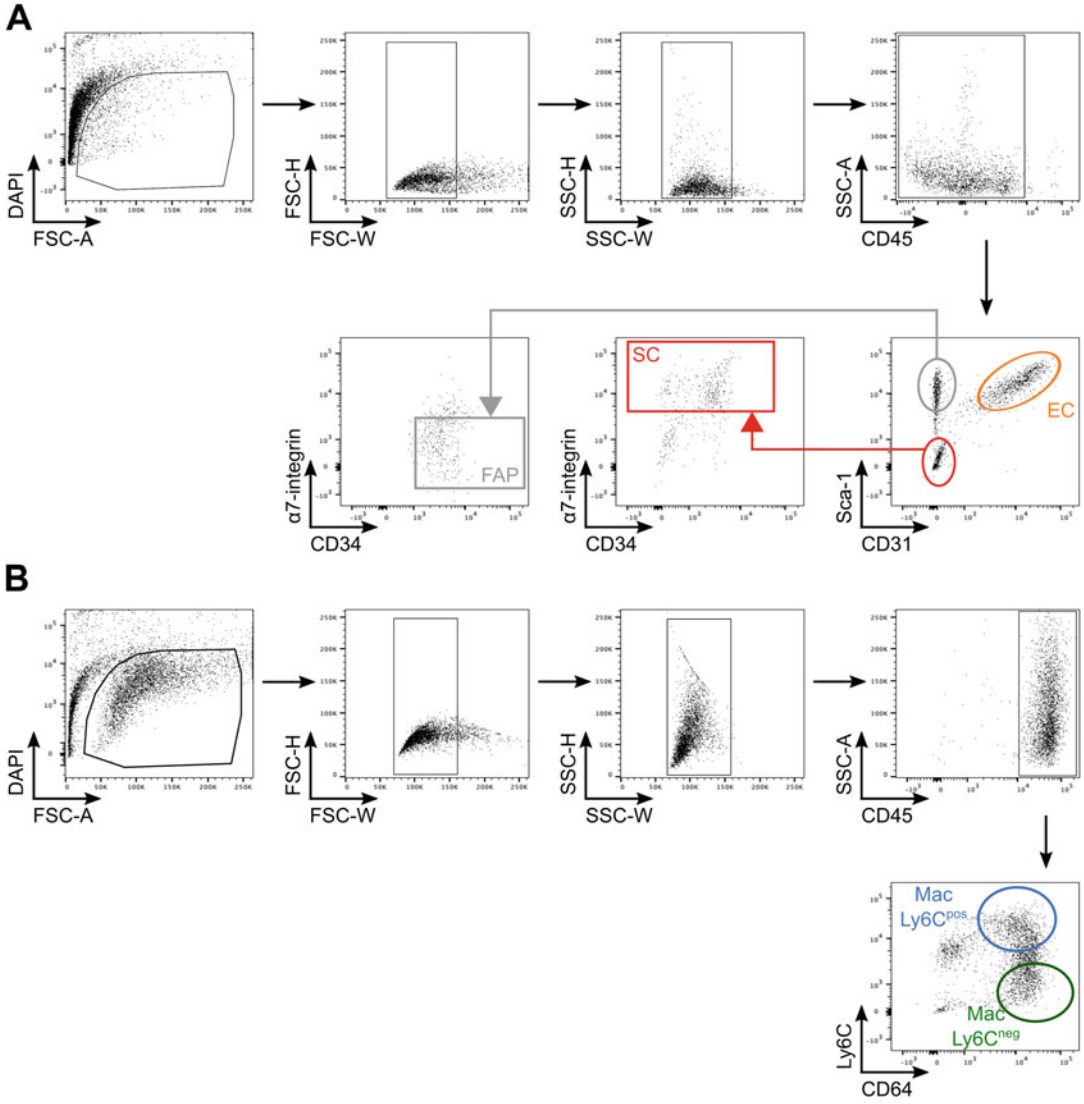

Fig. 2 Gating strategy to isolate cell populations from skeletal muscle. Example of FACS plots observed on *Tibialis Anterior* muscle 2 days after a cardiotoxin injury. Muscles were digested with Collagenase B and Dispase II enzymes and cells were separated based on their CD45 expression using magnetic beads. (**a**) $CD45^{neg}$ fraction was labeled with CD45, CD31, Sca-1, α7-integrin and CD34 antibodies to purify MuSCs ($CD45^{neg}CD31^{neg}Sca\text{-}1^{neg}$ $\alpha7\text{-integrin}^{pos}$) and FAPs ($CD45^{neg}$ $CD31^{neg}$ $Sca\text{-}1^{pos}\alpha7\text{-integrin}^{neg}CD34^{pos}$). Endothelial cells (EC) are also shown ($CD45^{neg}CD31^{neg}Sca\text{-}1^{pos}$). (**b**) $CD45^{pos}$ fraction was labeled with CD45, CD64 and Ly6C antibodies to isolate inflammatory (Mac $Ly6C^{pos}$; $CD45^{pos}$ $CD64^{pos}$ $Ly6C^{pos}$) and restorative (Mac $Ly6C^{neg}$; $CD45^{pos}$ $CD64^{pos}$ $Ly6C^{neg}$) MP subsets

6. Carefully remove the medium in the MuSC cultures and gently rinse once with PBS (*see* **Note 17**) and add MPs onto MuSCs.
7. Incubate the cells at 37 °C for 24 h for proliferation assay and 48 h for differentiation assays, and proceed to immunostaining.

Co-culture of MPs with FAPs

1. Seed FAPs in DMEM-high, 10% FBS, 1%P/S, at 10,000 cells/cm^2 (for instance in 48 well plate).
2. Let FAPs adhere to the culture support for about 4–6 h 37 °C, 5% CO_2.
3. MPs may be isolated (see sections above) during the adhesion time.
4. Resuspend MPs in DMEM-high, 2.5% FBS, 1% PS (*see* **Note 15**). Calculate the cell concentration to obtain a ratio of 3:1 MPs:FAPs in the adequate volume of medium (for instance, seed 200 µl in a 48-well).
5. Carefully remove the medium in the FAP cultures and gently rinse once with PBS (*see* **Note 17**) and add MPs onto FAPs.
6. Incubate cells at 37 °C, 5% CO_2 for 24 h (for proliferation or apoptosis assays), or 5 days (for the differentiation assay) and proceed for immunostaining.

3.4.2 Indirect Co-culture (with inserts)

1. FAPs are seeded in DMEM-high 10% FBS, 1%P/S, in inserts of 0.4 µm for 24 well plate for 24 h. Keep a 3:1 ratio FAPs:MuSCs for the seeding density.

Co-culture of FAPs with MuSCs

2. Seed MuSCs in DMEM-F12, 10% FBS, 2% UltroserG, 1% P/S. Cell density is:
   - 10,000 cells/cm^2 for proliferation/apoptosis assay (*see* **Note 14**).
   - 30,000 cells/cm^2 for myogenesis assay (*see* **Note 14**).
3. Let MuSCs adhere to the culture support for about 6 h at 37 °C, 5% CO_2, then remove the medium from both wells and inserts, and wash once with PBS.
4. Place the inserts containing the FAPs into the wells with the MuSCs using clean forceps.
5. Add 300 µl low serum medium (DMEM, 2.5% FBS, 1% PS) in the insert and 500 µl in the well.
6. Incubate the cells at 37 °C for 24 h for proliferation assay and 48 h for differentiation assays, and proceed to immunostaining.

Co-culture of FAPs with MPs

1. FAPs are seeded in DMEM-high 10% FBS, 1%P/S, in inserts of 0.4 µm for 24 well plate for 24 h.
2. MPs are isolated (see sections above) during the adhesion time.
3. Resuspend MPs in DMEM-high, 2.5% FBS, 1% P/S.
4. Seed MPs in inserts of 0.4 µm for 24 well plates. Calculate the cell concentration to obtain a ratio of 3:1 MPs:FAPs.
5. Carefully remove the medium in the FAP cultures and gently rinse once with PBS (*see* **Note 17**) and add the inserts with the MPs onto FAPs using clean forceps.

6. Add 300 µl low serum medium (DMEM, 2.5% FBS, 1% PS) in the insert.
7. Incubate the cells at 37 °C for 24 h for proliferation/apoptosis assay and 5 days for differentiation assays, and proceed to immunostaining.

3.5 Immunostainings

1. Wash once with PBS. Washes should be performed very carefully to avoid detaching of the cells, even after fixation (*see* **Note 17**). The cell preparation should never dry.
2. Fix the cells with 4% PFA for 10 min at room temperature (RT).
3. Wash with PBS (3 × 5 min).
4. Permeabilize the cells with 0.5% Triton X-100 in PBS for 10 min at RT.
5. Wash with PBS (3 × 5 min).
6. Block non-specific binding sites with 4% BSA in PBS for 1 h at RT.
7. Wash with PBS (3 × 5 min).
8. Incubate with primary antibodies diluted in PBS (Table 2) overnight at +4 °C in a humid chamber.
9. Wash with PBS (3 × 5 min).
10. Incubate with secondary antibodies diluted in PBS (Table 2) for 1 h at 37 °C in a humid chamber.
11. Wash with PBS (3 × 5 min).
12. Incubate for 10–20 sec with 2 µM of Hoechst in PBS.
13. Wash once with PBS (1 × 5 min).
14. Add Fluoromount medium.
15. Store at +4 °C until imaging.

4 Notes

1. Rapid dissection is an important parameter to obtain a good yield. Dissection must be performed on ice and it should last less than 5 min, otherwise the number of viable cells (especially MuSCs) may strongly decrease.
2. Depending on the purpose of the experiment and the type of muscle, several mice may be used and the cells pooled to get enough material. For instance, steady state muscle contains very low amounts of macrophages while cardiotoxin-injured muscle contains millions of macrophages at day 2 and 4 after injury.

3. Digestion duration has to be adjusted depending on the type of muscle. Regenerating muscle is easier to digest than dystrophic or fibrotic muscle. Monitor the digestion process: The muscle fragments should appear as loose, filamentous structures.
4. Carefully monitor the time the cells are exposed to ACK Lysing Buffer to avoid prolonged incubation that would damage the other cells.
5. The pellet being big and loose, only a part of the supernatant is retrieved before the second round of digestion.
6. Alternatively, to $CD64^{pos}$ cell enrichment, $CD45^{pos}$ cell enrichment can be performed, although it is less specific. Also, $CD45^{pos}$ cell enrichment can be useful to enrich the MP population when a low number of MPs is expected (*e.g.,* from a resting normal muscle), or on the contrary, to deplete the muscle from MPs to reduce the time and contamination level of cell sorting of the other cell types (*e.g.,* in a muscle that contains high numbers of MPs 1 to 4 days after cardiotoxin injury).
7. In cases of dystrophic or fibrotic muscle, an additional washing step is required to remove matrix components that may saturate the column.
8. MS columns are used for up to 2×10^8 total cells (up to 1×10^7 magnetically labeled cells). For higher numbers of cells, samples can be separated using LS columns. Volumes are given for an MS column.
9. Before adding the antibodies for labeling, it is important to keep some cells to perform 3 controls for FACS: isotype controls, single antibody controls, and Fluorescence Minus One (FMO) controls (about 10–20,000 cells per tube).
10. Quiescent or activated MuSCs can be separated based on CD34 expression. CD34 is expressed by quiescent MuSCs and is downregulated upon activation.
11. If MuSCs or FAPs are cultured for expansion, they should be seeded as soon as possible after sorting. Usually, MuSCs form clusters due to their high proliferating rate. Therefore, cells must be trypsinized regularly during the expansion phase to avoid the formation of myotubes in the clusters. FAPs are cultured at a density of 5000–7000 cells/cm^2. Usually, cells are expanded for 3–4 days before co-culture.
12. The yield of recovered cells is highly variable, depending on the muscle condition (steady state, regenerating, myopathy, etc.). For instance, about 30–45,000 MuSCs, 300–1100 MPs, and 300–1500 FAPs are recovered from 2 uninjured *Tibialis Anterior* muscles. These numbers may increase to hundreds of thousands in cases of regenerating muscle.

13. Mouse MuSCs hardly adhere to plastic. Coating with diluted Matrigel (strictly following the instructions of Matrigel use) allows homogenous adhesion of MuSCs on the culture support.
14. MuSC proliferation assay is easily performed in 96-well plates while MuSC differentiation assay should not because of edge effects of the wells, inducing artifact in cell fusion and heterogeneity of fusion events in the well. Prefer larger supports, such as 8-well chamber slides.
15. Since Ultroser G stimulates MuSC proliferation, it is absent in the co-culture medium. In the same way, the concentration of FBS is reduced to 2.5%.
16. Under low-serum conditions, MuSCs rapidly differentiate into myocytes and fuse.
17. Washing small wells has the risk of detaching some cells. To avoid this, use a needle and a syringe to carefully aspirate and pour. The beveled edge of the needle should be against the wall of the well to reduce the flow pressure.

References

1. Wosczyna MN, Rando TA (2018) A muscle stem cell support group: coordinated cellular responses in muscle regeneration. Dev Cell 46(2):135–143
2. Arnold L, Henry A, Poron F et al (2007) Inflammatory monocytes recruited after skeletal muscle injury switch into antiinflammatory macrophages to support myogenesis. J Exp Med 204:1071–1081
3. Saclier M, Yacoub-Youssef H, Mackey AL et al (2013) Differentially activated macrophages orchestrate myogenic precursor cell fate during human skeletal muscle regeneration. Stem Cells 31:384–396
4. Lemos DR, Babaeijandaghi F, Low M et al (2015) Nilotinib reduces muscle fibrosis in chronic muscle injury by promoting TNF-mediated apoptosis of fibro/adipogenic progenitors. Nat Med 21:786–794
5. Juban G, Saclier M, Yacoub-Youssef H et al (2013) AMPK activation regulates LTBP4-dependent TGF-beta1 secretion by pro-inflammatory macrophages and controls fibrosis in duchenne muscular dystrophy. Cell Rep 25:2163–2176
6. Mounier R, Theret M, Arnold L et al (2013) AMPKalpha1 regulates macrophage skewing at the time of resolution of inflammation during skeletal muscle regeneration. Cell Metab 18: 251–264
7. Perdiguero E, Sousa-Victor P, Ruiz-Bonilla V et al (2011) p38/MKP-1-regulated AKT coordinates macrophage transitions and resolution of inflammation during tissue repair. J Cell Biol 195:307–322
8. Tonkin J, Temmerman L, Sampson RD et al (2015) Monocyte/macrophage-derived IGF-1 orchestrates murine skeletal muscle regeneration and modulates autocrine polarization. Mol Ther 23:1189–1200
9. Liu L, Cheung TH, Charville GW et al (2015) Isolation of skeletal muscle stem cells by fluorescence-activated cell sorting. Nat Protoc 10:1612–1624

Chapter 6

Measuring Oxygen Consumption Rate (OCR) and Extracellular Acidification Rate (ECAR) in Muscle Stem Cells Using a Seahorse Analyzer: Applicability for Aging Studies

Xiaotong Hong and Pura Muñoz-Cánoves

Abstract

In recent years, evidence showing metabolism as a fundamental regulator of stem cell functions has emerged. In skeletal muscle, its stem cells (satellite cells) sustain muscle regeneration, although they lose their regenerative potential with aging, and this has been attributed, at least in part, to changes in their metabolism. In this chapter, we describe a protocol to analyze the metabolism of satellite cells using the Seahorse technology, which can be applied to aging mice.

Key words Stem cells, Satellite cell, Skeletal muscle, Tissue regeneration, Aging, Seahorse Technology, Metabolism, Oxygen consumption rate, Extracellular Acidification rate

1 Introduction

Satellite cells are the *bona fide* stem cells of the skeletal muscle tissue. Under homeostasis, satellite cells are in quiescence (a reversible G_0 arrest state) characterized by low transcriptional and metabolic activities [1–6]. In response to stress or injury, these cells exit the G_0 quiescent state and activate, and subsequently undergo rapid proliferation and differentiation to repair the injured myofibers, or self-renew to replenish the quiescent stem cell pool (reviewed in the studies conducted by [7–9]). With aging, satellite cell functions decline, and this has been attributed to age-associated changes in both intrinsic and extrinsic (local and systemic) mechanisms. In particular, changes in metabolism have been associated with the loss of regenerative capacity of distinct types of stem cells with aging (revised in [10, 11]).

Cells obtain energy through metabolism, which comprises two categories of processes: anabolism, the building up of cell components such as proteins and nucleic acids, and catabolism, the

Atsushi Asakura (ed.), *Skeletal Muscle Stem Cells: Methods and Protocols*, Methods in Molecular Biology, vol. 2640, https://doi.org/10.1007/978-1-0716-3036-5_6,

breaking down of intracellular components (releasing energy for anabolism). A balance of anabolic and catabolic processes is essential for the homeostasis of the cell. Adenosine triphosphate (ATP), the key energy-transporting molecule, is generated mainly via oxidative-phosphorylation (OXPHOS) or glycolysis. As one of the most important energy sources, glucose can be processed to pyruvate via glycolysis and yields small amounts of ATP molecules. Pyruvate derived from glycolysis can either be converted into acetyl-CoA in the mitochondria, which then enters the tricarboxylic acid (TCA cycle, also called Krebs cycle and citric acid cycle), or it can be converted to lactate in the cytoplasm when oxygen is limited (a process termed anaerobic glycolysis). In fact, ATP generation by mitochondria via OXPHOS is much more efficient than that by glycolysis: Mitochondria can produce up to 36 ATP molecules from one molecule of glucose, whereas glycolysis produces only 2 molecules of ATP [12]. However, glycolysis is advantageous for fast proliferating cells (such as cancer cells) due to its ability to rapidly generate ATP as well as glycolytic intermediates for the biosynthesis of essential biomolecules [13–15]. Further, mitochondria can also use intermediates from the metabolism of other energy sources. For instance, the metabolism of fatty acids involves a series of oxidation steps (termed fatty acid oxidation, FAO) that generates acetyl-CoA, which enters the TCA cycle and glutaminolysis, a process that converts glutamine into glutamate; this can also be coupled to TCA cycle upon conversion of glutamate to α-ketoglutarate (α-KG) (Fig. 1).

The mitochondrial ETC located on the inner mitochondrial membrane (IMM) is composed of 5 complexes: NADH:ubiquinone oxidoreductase (complex I, CI), succinate dehydrogenase (complex II, CII), Coenzyme Q-cytochrome c reductase (complex III, CIII), cytochrome c oxidase (complex IV, CIV), and the F1F0 ATP synthase (complex V, CV) [16] (Fig. 2). Electrons derived from NADH or FADH2 are transported through complex I/III/IV or complex II/III/IV in an exergonic process that drives the protons pumping from the mitochondrial complex into the intermembrane space. The accumulated proton gradient then drives the synthesis of ATP via complex V, or it can be consumed by uncoupling.

Growing evidence points to the importance of metabolism in stem cell functions [10, 17–22]. Satellite cells are exposed to distinct micro-environment and energy demands in their different myogenic states, and therefore, exhibit distinct metabolic profiles [3, 17, 18]. Quiescent satellite cells possess very small mitochondrial content and low metabolic activity. Adult satellite cells, however, exhibit a progressive increase in mitochondrial content from quiescence to activation/proliferation states in vivo [3, 5, 17] or in culture [18]. In addition, proliferating fetal and perinatal satellite cells also show significantly higher mitochondrial content

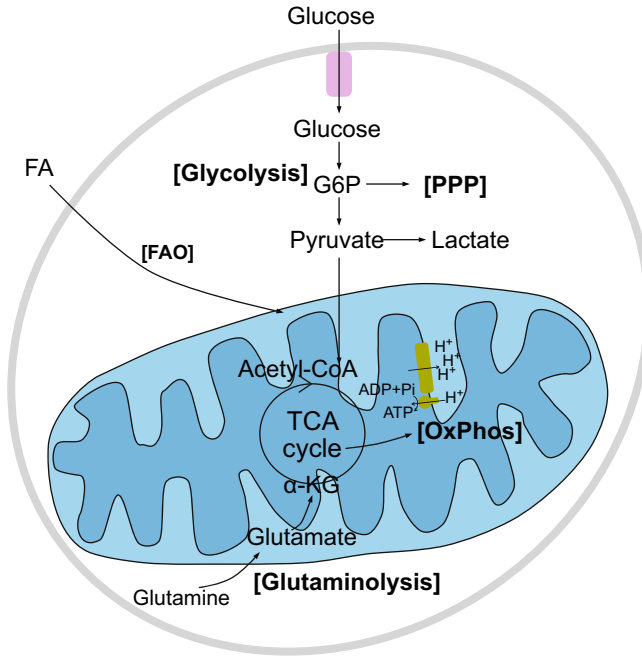

Fig. 1 Scheme of the major cellular energy metabolism pathways. After transportation into the cell, glucose is converted to glucose-6-phosphate (G6P) by hexokinase. G6P can be converted to pyruvate through a series of enzymatic reactions known as the glycolysis pathway. On the other hand, G6P can also undergo pentose phosphate pathway (PPP), which is essential for purine and pyrimidine metabolism. Pyruvate from glycolysis reactions can then enter mitochondria, where it is converted to acetyl-CoA and enters the tricarboxylic acid (TCA) cycle. Fatty acids (FAs) can also be converted into acetyl-CoA through a series of oxidation steps (fatty acid oxidation, FAO)

compared to adult quiescent satellite cells [3]. Interestingly, despite the increase in mitochondrial content, satellite cells undergo a metabolic switch from FAO to glycolysis upon activation *in vitro* and rely mainly on glycolysis during proliferation [18]. Similarly, proliferating fetal myogenic cells have been shown to rely mainly on glycolysis [3]. However, compared to quiescent satellite cells, proliferating satellite cells in response to muscle injury experience a dramatic increase in OXPHOS, glycolysis activity, and FAO, as indicated by the oxygen consumption rate (OCR), extracellular acidification rate (ECAR) and the content of L-carnitine [3], respectively. Furthermore, compared to young satellite cells, their aged counterparts show defects in OXPHOS metabolism and shift their energy dependence toward glycolysis [3, 17].

Therefore, a deeper knowledge of satellite cell metabolism is needed. In this chapter, we describe a protocol using Seahorse technology to measure OCR and ECAR of freshly isolated satellite cells.

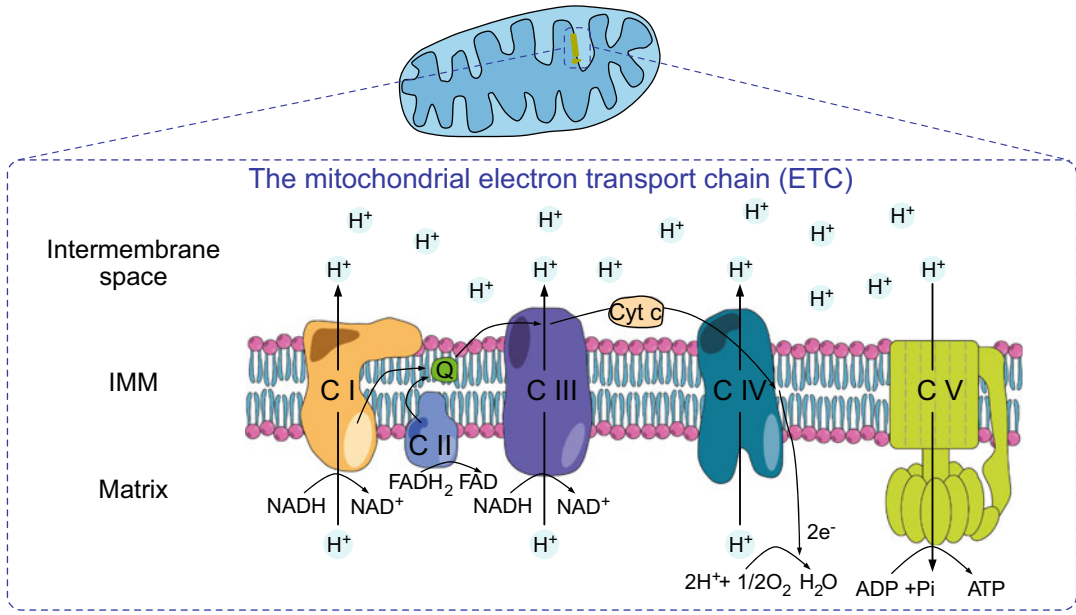

Fig. 2 Scheme of the mitochondrial electron transport chain (ETC). The ETC is located at the mitochondrial inner membrane (IMM) and is composed of 4 complexes (complex I to IV). The oxidation of NADH takes place on complex I, giving 2 electrons to ubiquinone (Q), a lipid-soluble carrier. The transfer of the first electron results in the semiquinone form of Q while the transfer of the second electron reduces the semiquinone form to the ubiquinol form (QH_2). In the meantime, 4 protons (H+) are pumped across the IMM to the intermembrane space, creating a proton gradient. In complex II, $FADH_2$ is oxidized to FAD and more electrons are transferred to the quinone pool. In complex III, QH_2 are converted back to Q and 2 electrons are transferred to cytochrome c (Cyt c), a water-soluble electron carrier in the intermembrane space. The reaction is coupled with the pumping of H^+s. Finally, in complex IV, 2 electrons are removed from 2 molecules of Cyt c and transferred to produce one molecule of H_2O from oxygen. The accumulated proton gradient works as a driving force for the ATP synthase, also called complex V, to generate ATP via oxidative phosphorylation. The coupling of the ETC and phosphorylation is essential for the production of ATP

The Seahorse analyzer uses a sensor cartridge system that enables real-time measurement of mitochondrial respiration (indicated by OCR) and glycolysis (indicated by ECAR). We describe the classic mitochondrial stress measurement protocol using mitochondria perturbing agents: oligomycin, Carbonyl cyanide 4-(trifluoromethoxy) phenylhydrazone (FCCP), rotenone/antimycin A (R + A) and 2-Deoxy-d-glucose (2-DG). Oligomycin inhibits ATP synthase by blocking its proton channel (F0 subunit) and the difference between basal respiration and oligomycin-treated respiration gives the respiration for ATP production. FCCP is a mitochondrial uncoupler that blocks proton transport across the IMM. The addition of FCCP causes the cells to respire at the maximal level. Furthermore, R + A causes complete inhibition of the mitochondrial ETC; the OCR rate after this treatment indicates non-mitochondrial respiration, and finally, the addition of 2-DG completely inhibits glycolysis, which reveals the level of non-glycolytic acidification (Fig. 3). The

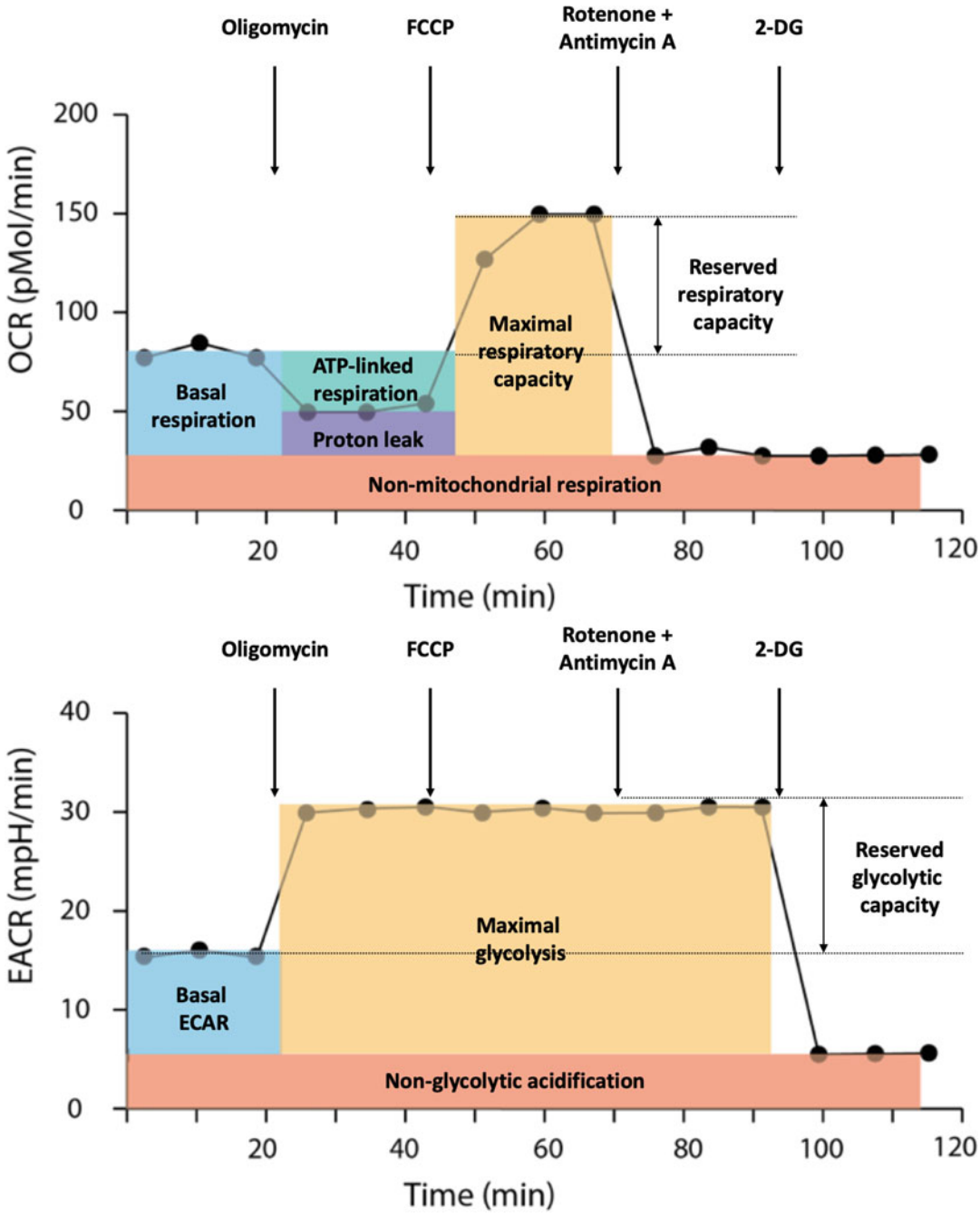

Fig. 3 Scheme of the OCR and ECAR graph. In the OCR graph (upper panel), the OCR level after R + A treatment (red) reveals the non-mitochondrial respiration. The initial OCR subtracted by the non-mitochondrial respiration gives rise to the basal respiration (blue). After oligomycin treatment, the reduction of OCR indicates the ATP-linked respiration while the post-oligomycin respiration minus the non-mitochondrial respiration (purple) gives rise to the proton leak level. The post-FCCP OCR minus the non-mitochondrial respiration reveals the maximal respiratory capacity of the cells (orange) and the difference of this rate to the basal respiration indicates the reserved (spared) respiratory capacity. For ECAR (lower panel), the ECAR level after 2-DG treatment (red) indicates the non-glycolytic acidification. Similarly, the initial ECAR subtracted by the non-glycolytic acidification gives rise to the basal ECAR. After oligomycin treatment, the maximal glycolysis rate (orange) and the reserved glycolytic capacity can be obtained

procedure that we describe here can be used on satellite cells from both young/adult and aging mice.

2 Materials

2.1 Isolation of Satellite Cells by Fluorescence-Activated Cell Sorting (FACS)

Reagents and buffers:

- DMEM with Penicillin/Streptomycin (P/S).
- Ham's F10.
- Cardiotoxin (Latoxan L8102) diluted in ddH_2O (10 μM). Store aliquots in −20 °C.
- 1× RBC Lysis Buffer (eBioscience, 00-4333-57)
- FACS Buffer: PBS 1×, 5% Goat Serum.
- Digestion medium (100 ml):
  - Liberase, 0.1 mg/g muscle weight, (Roche, 5401127001, stock solution 5 mg/ml).
  - Dispase, 0.3% final concentration (Sigma-Aldrich, D4693-1G).
  - DMEM, 1%P/S
- Collection medium (growth medium):
  - Ham's F10: DMEM = 1:1, 1% P/S, 1% glutamine (Lonza, 17-605E), 20% Fetal Bovine Serum (FBS), recombinant bFGF (PEPROTECH, 100-18B, 0.0025 μg ml^{-1}).

Antibodies and dyes for FACS:

- PE/Cy7 anti-mouse Ly-6A/E (Sca-1) (Biolegend, 108114).
- PE/Cy7 anti-mouse CD45 (Biolegend, 103114).
- PE/Cy7 anti-mouse CD31 (Biolegend, 102418).
- α-7 integrin R-Phycoerythrin (AbLab, 53-0010-05),
- Alexa Fluor 647 Rat anti-mouse CD34 (BD Pharmingen, 560230).
- DAPI (Invitrogen, D1306, stock solution 1 mg/ml).

Disposable material:

- Filters 100, 70, and 40 μm (SPL Lifescience, 93100/93070/93040).
- M tube (Miltenyi Biotec, GentleMACS™).
- Falcon tube 50 ml.
- Falcon tube 15 ml.

Equipment:

- Tissue dissociator (Miltenyi Biotec, gentleMACS™ Octo Dissociator).

- Centrifuge (Eppendorf, 5810 R).
- Hypoxic incubator (RUSKINN Sci-tive-u, 3% O_2, 5% CO_2).

2.2 Seahorse Plate Preparation

Reagents and buffers:

- Cell-Tak (Corning®, 354240).
- Neutral buffer solution: 0.1 M sodium bicarbonate (stock concentration 7.5%), pH = 8.

2.3 Seahorse Experiment Preparation

Disposable material:

- Seahorse XFe96 Flux Pack (Agilent, 102416-100): Seahorse 96-well culture plate, cartridge and XF calibration medium are included.

2.4 Seahorse Analysis

Reagents and buffers:

- 1× DMEM: Dissolved in ddH_2O
- Seahorse assay media: 25 ml of 1× DMEM supplied with 700 μL glucose (stock 1 M, in-house prepared), 250 μL L-glutamine and 250 μL sodium pyruvate.
- Drug solution media: 20 ml of 1× DMEM supplied with 500 μL sodium pyruvate.
- KOH 1 M for adjusting pH.
- HCL 1 M for adjusting pH.
- Oligomycin: Aliquot as 2.5 mM stock solution (in 100% ethanol), stock in −20 °C.
- Carbonyl cyanide 4-(trifluoromethoxy) phenylhydrazone (FCCP): Aliquot as 2.5 mM stock solution (in DMSO), stock in −20 °C.
- Rotenone: Aliquot as 2.5 mM stock solution (in DMSO), stock in −20 °C.
- Antimycin A: Aliquot as 2.5 mM stock solution (in DMSO), stock in −20 °C.
- 2-deoxy-glucose (2-DG): Dilute to 1 M in Seahorse assay media before use.

Equipment:

- pH meter (CRISON, basic 20).
- Seahorse XF96 Extracellular Flux Analyzer.

2.5 Normalization

Reagents and buffers:

- CyQUANT™ NF Cell Proliferation Assay Kit (Invitrogen™ C35006).

Equipment:

- Microplate fluorometer (Thermo Labsystems, Fluoroskan™ Ascent).

2.6 Data Analysis

Software:

– Seahorse Wave program.

3 Methods

Carry out all procedures at room temperature unless otherwise specified.

3.1 Satellite Cells' Isolation by FACS

1. Quiescent satellite cells are isolated from the resting muscles of mice. Euthanize mice according to institute regulations. The following steps should be performed in a tissue culture hood in order to limit contamination (*see* **Notes 1–3**). To isolate satellite cells from regenerating muscles, mouse muscles are previously injected with cardiotoxin (CTX) (40 μL, 50 μL, 50 μL for each tibialis anterior (TA), quadriceps and gastrocnemius muscle, respectively *see* **Note 4**) to induce damage and regeneration. Activated or proliferating satellite cells are usually isolated 1 or 3 days post injury (DPI), respectively.
2. Collect muscles from fore and hind limbs in cold DMEM 1% P/S into 50 ml falcon tubes. In the case of regenerating muscles, only muscles injected with CTX are collected.
3. Discard the medium and remove visible connective tissue and fat.
4. Mince muscles with scissors.
5. Collect minced muscles into an M tube and add digestion medium (4 ml for hind limb muscles, 8 ml for fore + hind limb muscles).
6. Place the tubes onto the Miltenyi tissue dissociator and start the dissociation program 37C_mr_SMDK_1 (*see* **Note 5**).
7. At the end of the program, leave the tube for 5 min on ice to let the sample sediment.
8. Add 5 ml FBS to each M tube to block the digestion buffer and transfer the muscle homogenate into a 50 ml Falcon tube.
9. Rinse the M tube 1–2 times with 10 ml cold DMEM and collect the medium into the same Falcon tube.
10. Add cold DMEM 1% P/S up to 40 ml.
11. Filter the supernatant with 100 μm filter, wash the Falcon tube, and filter with 5 ml cold DMEM.

12. Filter the supernatant with 70 μm filter, wash the Falcon tube, and filter with 5 ml cold DMEM.
13. Centrifuge the supernatant for 10 min at 50 × *g* and at 4 °C.
14. Collect the supernatant and discard the pellet (optional: the pellet can be washed and the supernatant can be collected and pooled with the previous supernatants).
15. Centrifuge at 600 × *g* for 10 min at 4 °C.
16. Discard the supernatant and resuspend the cells with 1 ml (quiescent limb muscles) or 2 ml (post-injury limb muscles) 1× RBC lysis buffer. Incubate on ice for 10 min (protect from light).
17. Add 30 ml of cold FACS buffer to stop the lysis process and pass through a 40 μm filter. (For reporter cells, skip the following steps and go to **step 24**.
18. Centrifuge at 600 × *g* for 10 min at 4 °C, and discard the supernatant.
19. Resuspend the pellet in 1 ml of cold FACS buffer and count the number of cells for each sample.
20. Antibody mixture preparation:
    (a) Negative selection: Sca1-PECy7, CD31-PECy7, CD45-PECy7 (0.5/100 μL FACS buffer).
    (b) Positive selection: α-7 integrin-PE (1/100 μL FACS buffer) and CD34-APC (3/100 μL FACS Buffer) (*see* **Note 6**).
    (c) Controls: Single staining and FMO controls are required to set up the gates.
21. Centrifuge at 600 × *g* for 10 min at 4 °C and resuspend the pellet at 1×10^4cells/μL (1×10^6 cells in 100 μL) in antibody mixture.
22. Incubate the cells with antibodies for 1 h at 4 °C (protect from light).
23. At the end of incubation, add 30 ml FACS buffer to the cell-antibody mixture.
24. Centrifuge at 600 × *g* for 10 min at 4 °C and resuspend the cells in 300 μL FACS buffer for sample sorting.
25. Add DAPI (final concentration 1 μg/ml) 5 min prior to FACS to detect and exclude dead cells.
26. Collect Sca1-/CD31-/CD45-/CD34+/α7-integrin+ satellite cells or reporter satellite cells in Eppendorf tubes with 50 μL of collection medium (growth medium) at 4 °C (*see* **Note 7**).

3.2 Seahorse Plate Preparation and Seeding

The Seahorse plate preparation is carried out in a tissue culture hood.

1. Prepare neutral buffer solution by diluting the stock sodium bicarbonate to 0.1 M in ddH_2O, adjust pH to 8.
2. Calculate the surface area to coat with Cell-Tak (example *see* **Note 8**), including the experimental wells and at least 4 wells as blank.
3. Prepare the solution by diluting the μl Cell-Tak stock into 300 μL neutral buffer and distribute immediately to the designated wells (22 μL/well).
4. Incubate the Seahorse plate with Cell-Tak coating at 37 °C for 20 min (*see* **Note 9**).
5. After incubation, aspirate the coating solution and rinse the wells twice with ddH_2O.
6. Air-dry the plate in the tissue culture hood.
7. If it is to be used the same day, maintain the plate with lid in RT, otherwise seal the plate with parafilm and store at 4 °C for up to 2 weeks.
8. After FACS isolation, carefully load the desired amount of freshly-sorted satellite cells from the wall of the well onto the Cell-Tak coated culture plate (no more than 200 μL/well). For quiescent cells, a density of 50,000–100,000 satellite cells/well is required while for proliferating cells (3 DPI), 30,000–50,000 satellite cells/well is sufficient. At the end of the Seahorse analysis, a normalization step is essential. (*see* **Note 10**).
9. Rest the plate for 10 min in RT and centrifuge the plate at 50 × *g* for 8 min.
10. Carefully remove around 80% of the medium from the top (*see* **Note 11**).
11. Carefully replace it with 150 μL warm growth medium from the wall.
12. Incubate the cells for 6 h in a hypoxic chamber (3% O_2, 5% CO_2, 37 °C) before the Seahorse analysis (*see* **Note 12**).

3.3 Seahorse Experiment Preparation

The preparation must be done one day prior to the seahorse experiment.

1. In a new cartridge set, remove the drug loading plate.
2. In a tissue culture hood, remove the cartridge and lid carefully, and place on a surface with the cartridge sensors facing up.
3. Load ddH_2O into all the wells of the plate (200 μL/well).
4. Put the cartridge and lid back carefully.

5. In a clean 50 ml Falcon tube, load around 35 ml Seahorse calibration medium.
6. Place the cartridge set and the calibration medium in the 37 °C CO_2-free Seahorse incubation chamber overnight.

3.4 Seahorse Analysis

1. Turn on the Seahorse and computer.
2. In a clean 50 ml Falcon tube, load around 50 ml of Seahorse medium.
3. Adjust the pH to 7.4 using KOH and HCL (*see* **Note 13**) and keep at 37 °C.
4. Prepare Seahorse analysis medium as described in session 2. Keep at 37 °C.
5. Prepare drug solution medium as described in session 2.
6. Once the analysis medium from **step 4** is warm, take the satellite cell culture plate from the hypoxia chamber, replace the medium with Seahorse analysis medium, and incubate it in the Seahorse incubator for at least 45 min before the analysis starts (*see* **Note 14**).
7. With respect to the cartridge, after overnight hydration, remove the water from the plate and replace each well with 175 μL calibration medium. Return to the Seahorse incubator.
8. Pipette 3 ml drug solution medium from **step 5** into a separate 15 ml Falcon, repeat 4 times (labeled as A, B, C, and D).
9. Prepare the drug solution to reach the final analytic concentration of (*see* **Note 15**):
   - A: oligomycin 1 μM
   - B: FCCP 1 μM
   - C: rotenone 1 μM + antimycin A 1 μM
   - D: 2-DG 100 mM
10. In the cartridge, load 25 μL of A, B, C, and D drug mixture into each well of port A, B, C, and D. Return the cartridge back to the Seahorse incubator until use.
11. Turn on the Seahorse program (MitoStress). In the assay wizard, introduce requested information: cell type, plating, replicates, culture medium, drug injection protocol, etc. (*see* **Note 16**).
12. Run Seahorse program (*see* **Note 17**)
    1. Calibrate probes
    2. Equilibrate
    3. (1) Mix for 5 Min. 0 sec.
    4. (1) Measure for 3 Min. 0 sec.
    5. (2) Mix for 4 Min. 0 sec.

6. (2) Measure for 3 Min. 0 sec.
7. (3) Mix for 4 Min. 0 sec.
8. (3) Measure for 3 Min. 0 sec.
9. Inject Port A.
10. (4) Mix for 5 Min. 0 sec.
11. (4) Measure for 3 Min. 0 sec.
12. (5) Mix for 4 Min. 0 sec.
13. (5) Measure for 3 Min. 0 sec.
14. (6) Mix for 4 Min. 0 sec.
15. (6) Measure for 3 Min. 0 sec.
16. Inject Port B
17. (7) Mix for 5 Min. 0 sec.
18. (7) Measure for 3 Min. 0 sec.
19. (8) Mix for 4 Min. 0 sec.
20. (8) Measure for 3 Min. 0 sec.
21. (9) Mix for 4 Min. 0 sec.
22. (9) Measure for 3 Min. 0 sec.
23. Inject Port C
24. (10) Mix for 5 Min. 0 sec.
25. (10) Measure for 3 Min. 0 sec.
26. (11) Mix for 4 Min. 0 sec.
27. (11) Measure for 3 Min. 0 sec.
28. (12) Mix for 4 Min. 0 sec.
29. (12) Measure for 3 Min. 0 sec.
30. Inject Port D
31. (13) Mix for 5 Min. 0 sec.
32. (13) Measure for 3 Min. 0 sec.
33. (14) Mix for 4 Min. 0 sec.
34. (14) Measure for 3 Min. 0 sec.
35. (15) Mix for 4 Min. 0 sec.
36. (15) Measure for 3 Min. 0 sec.

Program End

3.5 Normalization

1. After the Seahorse program finishes, retrieve the analysis plate and discard the cartridge.
2. Prepare in dark the CyQUANT normalization medium: 4 ml ddH_2O, 1 ml 5x CyQUANT buffer and 10 μL CyQUANT dye.

3. Carefully remove the Seahorse medium in each well of the plate and replace with 50 μL CyQUANT normalization medium per well.
4. Cover the plate with aluminum foil and incubate in a normal 37 °C incubator for 30 min.
5. After incubation, place the plate in a fluorometer and measure the emission (filters: excitation 485 nm, emission 538 nm, *see* **Note 18**).

3.6 Data Analysis

1. In the Wave program, open the experiment (.xfd) and verify the plating information. Analyze the OCR of the experiment from selected wells.
2. In the normalization tab, introduce the emission data from the fluorometer, then the normalized results will be updated by the Wave program. The normalization unit is a.u.
3. Results can be exported as Prism files and various XF reports can be generated.

4 Notes

1. Euthanize mice using approved protocols in your institution. Prior to muscle collection, spray the skin of the mouse with 70% ethanol. Cut and remove the skin and expose the fore-limb and hind-limb muscles.
2. Classification of mice according to age: young (2–3 months old), adult (6–8 months old), old (18–24 months old), geriatric (older than 28 months of age) [4].
3. For aging studies, as mouse mortality starts to increase around 18 months of age, increasing the number of mice cohorts to study old and geriatric age is highly recommended.
4. Anesthetize mice using approved protocols in your institution. Shave the hair of the hind limb and spray the skin with 70% ethanol prior to CTX injection. Detailed CTX protocol is described in [19].
5. Alternatively, muscles can be digested using 50 mL Falcon tubes incubated in a conventional water bath (37 °C, 60 u/min, 2 h) with the same amount of digestion buffer.
6. For the isolation of quiescent satellite cells, the lineage (PE-Cy7) negative, α-7 integrin (PE) and CD34 (APC) positive population are collected. For the isolation of proliferating satellite cells at 3 DPI, the lineage (PE-Cy7) negative, α-7 integrin (PE) positive and CD34 (APC) negative population is collected to enrich the proliferating cell population, as

proliferating satellite cells lose the expression of CD34 characteristic of the quiescent state [20].

7. The Eppendorf tubes must be fully-rinsed with serum-containing medium prior to collection.
8. Example for coating 10 wells from a 96-well Seahorse microplate:

   Surface area: 0.106 cm2 (each well) × 10 = 1.06 cm^2.

   Coating concentration: 3 to 3.5 μg/cm^2.

   μl of Cell-Tak stock needed = (3.5 μg/cm^2 × 1.06 cm^2)/(M mg/ml).

   The amount of Cell-Tak stock needed is batch-dependent, please check on the datasheet or bottle label the molecular weight M.

   Volume for distribution: 25 μL/well × 10 = 250 μL.
9. The coating solution must be prepared right before coating and used immediately. Do not add too much volume/well to avoid cell adhesion on the walls.
10. Within this range, the higher density assures lower standard deviation among the replicates.
11. While removing the media, it is essential to leave around 20–30 μL of media at the bottom of the well. At this time, the cells are not yet completely settled, so the removal of all liquid will cause loss of cells.
12. The sorting procedure causes stress to the cells. Therefore, freshly-sorted cells do not respond well to the treatments from the Seahorse analysis.
13. NaOH should not be used.
14. The culture medium must be fully removed before adding the Seahorse assay medium.
15. For the drug preparation, it must be taken into consideration that after each injection, an additional volume of 25 μL is added to the total volume.
16. The experimental information can be modified in the Wave program during data analysis. But it is recommended to note as much information as possible when starting the program.
17. This protocol allows for the stable measurement of OCR after each drug injection in our case. However, other timing could be applied. Especially when a permeabilization protocol is applied or when measuring OCR from isolated mitochondria, a shorter mixing and measuring time should be applied. Please follow the instruction from the Seahorse program. Numbers in parenthesis correspond to those appearing in the Seahorse program. For calibration, place the cartridge with the

calibration medium onto the Seahorse loading platform. The lid of the plate must be removed. After the calibration step (usually takes around 30 min), follow the instruction of the Seahorse program, remove the plate with calibration medium, and place the cell culture plate. Again, the lid must be removed. Be aware of the plate's position.

18. The wavelength of the filers can differ from machine to machine, please check the compatibility of the fluorometer and the CyQUANT kit manual.

Acknowledgments

Work in the authors' laboratory has been supported by MINECO-Spain (RTI2018-096068), ERC-2016-AdG-741966, LaCaixa-HEALTH-HR17-00040, MDA, UPGRADE-H2020-825825, Milky Way Research Foundation (MWRF), AFM and DPP-Spain, as well as María-de-Maeztu-Program for Units of Excellence to UPF (MDM-2014-0370), Severo-Ochoa-Program for Centers of Excellence to CNIC (SEV-2015-0505). X.H is recipient of a Severo-Ochoa Pre-doctoral Fellowship.

References

1. Brack AS, Rando TA (2012) Tissue-specific stem cells: lessons from the skeletal muscle satellite cell. Cell Stem Cell 10:504–514. https://doi.org/10.1016/j.stem.2012.04.001
2. García-Prat L, Perdiguero E, Alonso-Martín S et al (2020) FoxO maintains a genuine muscle stem-cell quiescent state until geriatric age. Nat Cell Biol 22:1307–1318. https://doi.org/10.1038/s41556-020-00593-7
3. Pala F, di Girolamo D, Mella S et al (2018) Distinct metabolic states govern skeletal muscle stem cell fates during prenatal and postnatal myogenesis. J Cell Sci 131. https://doi.org/10.1242/jcs.212977
4. Rocheteau P, Gayraud-Morel B, Siegl-Cachedenier I et al (2012) A subpopulation of adult skeletal muscle stem cells retains all template DNA strands after cell division. Cell 148:112–125. https://doi.org/10.1016/j.cell.2011.11.049
5. Rodgers JT, King KY, Brett JO et al (2014) mTORC1 controls the adaptive transition of quiescent stem cells from G0 to GAlert. Nature 510:393–396. https://doi.org/10.1038/nature13255
6. Schultz E, Gibson MC, Champion T (1978) Satellite cells are mitotically quiescent in mature mouse muscle: an EM and radioautographic study. J Exp Zool 206:451–456. https://doi.org/10.1002/jez.1402060314
7. Evano B, Tajbakhsh S (2018) Skeletal muscle stem cells in comfort and stress. NPJ Regen Med 3:24. https://doi.org/10.1038/s41536-018-0062-3
8. Galliot B, Crescenzi M, Jacinto A, Tajbakhsh S (2017) Trends in tissue repair and regeneration. Development 144:357–364. https://doi.org/10.1242/dev.144279
9. Sousa-Victor P, Neves J, Muñoz-Cánoves P (2020) Muscle stem cell aging: identifying ways to induce tissue rejuvenation. Mech Ageing Dev 188:111246. https://doi.org/10.1016/j.mad.2020.111246
10. García-Prat L, Sousa-Victor P, Muñoz-Cánoves P (2017) Proteostatic and metabolic control of stemness. Cell Stem Cell 20:593–608. https://doi.org/10.1016/j.stem.2017.04.011
11. Hong X, Campanario S, Ramírez-Pardo I et al (2022) Stem cell aging in the skeletal muscle: the importance of communication. Ageing Res Rev 73:101528. https://doi.org/10.1016/j.arr.2021.101528
12. Mookerjee SA, Brand MD (2015) Measurement and analysis of extracellular acid

production to determine glycolytic rate. J Vis Exp. https://doi.org/10.3791/53464

13. Lunt SY, vander Heiden MG (2011) Aerobic glycolysis: meeting the metabolic requirements of cell proliferation. Annu Rev Cell Dev Biol 27:441–464. https://doi.org/10.1146/annurev-cellbio-092910-154237
14. Ryall JG (2013) Metabolic reprogramming as a novel regulator of skeletal muscle development and regeneration. FEBS J 280:4004–4013. https://doi.org/10.1111/febs.12189
15. Warburg O (1956) On respiratory impairment in cancer cells. Science 124:269–270
16. Mitchell P (1961) Coupling of phosphorylation to electron and hydrogen transfer by a chemi-osmotic type of mechanism. Nature 191:144–148. https://doi.org/10.1038/191144a0
17. Hong X, Isern J, Campanario S et al (2022) Mitochondrial dynamics maintain muscle stem cell regenerative competence throughout adult life by regulating metabolism and mitophagy. Cell Stem Cell 29:1298–1314.e10. https://doi.org/10.1016/j.stem.2022.07.009
18. Ryall JG, Dell'Orso S, Derfoul A et al (2015) The NAD+-dependent SIRT1 deacetylase translates a metabolic switch into regulatory epigenetics in skeletal muscle stem cells. Cell Stem Cell 16:171–183. https://doi.org/10.1016/j.stem.2014.12.004
19. Chandel NS, Jasper H, Ho TT, Passegué E (2016) Metabolic regulation of stem cell function in tissue homeostasis and organismal ageing. Nat Cell Biol 18:823–832. https://doi.org/10.1038/ncb3385
20. Yucel N, Wang YX, Mai T et al (2019) Glucose metabolism drives histone acetylation landscape transitions that dictate muscle stem cell function. Cell Rep 27:3939–3955.e6. https://doi.org/10.1016/j.celrep.2019.05.092
21. Maryanovich M, Zaltsman Y, Ruggiero A et al (2015) An MTCH2 pathway repressing mitochondria metabolism regulates haematopoietic stem cell fate. Nat Commun 6:7901. https://doi.org/10.1038/ncomms8901
22. Chen F, Zhou J, Li Y et al (2019) YY1 regulates skeletal muscle regeneration through controlling metabolic reprogramming of satellite cells. EMBO J 38(10):e99727. https://doi.org/10.15252/embj.201899727

Chapter 7

High Throughput Screening of Mitochondrial Bioenergetics in Myoblasts and Differentiated Myotubes

Kohei Takeda, Tohru Takemasa, and Ryo Fujita

Abstract

Skeletal muscles contain stem cells called satellite cells, which are essential for muscle regeneration. The population of satellite cells declines with aging and the incidence of pathological conditions such as muscular dystrophy. There is increasing evidence that metabolic switches and mitochondrial function are critical regulators of cell fate decision (quiescence, activation, differentiation, and self-renewal) during myogenesis. Thus, monitoring and identifying the metabolic profile in live cells using the Seahorse XF Bioanalyzer could provide new insights on the molecular mechanisms governing stem cell dynamics during regeneration and tissue maintenance. Here we described a method to assess mitochondrial respiration (oxygen consumption rate) and glycolysis (ECAR) in primary murine satellite cells, multinucleated myotubes, and C2C12 myoblasts.

Key words Skeletal muscle, Satellite cell, Myotube, Metabolism, Mitochondria, Oxygen consumption rate, Seahorse XF Analyzer

1 Introduction

Skeletal muscle is made up of numerous multinucleated myofibers that utilize contractile machinery (myosin and actin) to generate force. In addition, skeletal muscle plays a major role in determining basal energy expenditure. It is known that skeletal muscles are responsible for 70–85% of the insulin-mediated glucose uptake and metabolic dysfunctions in skeletal muscles often contribute to the etiology and development of metabolic diseases, such as type II diabetes. Mitochondria are well-known as the essential energy-producing organelles in our cells. Previous reports from our lab [1, 2] and others [3–5] have suggested that mitochondrial abnormalities and dysfunctions in skeletal muscles result in decreased muscle mass, decline in whole-body glucose intolerance, and insulin sensitivity, as well as the pathogenic progression of myopathy. In humans, a strong association of mitochondrial dysfunction with insulin resistance has been reported in the elderly and mutations

Atsushi Asakura (ed.), *Skeletal Muscle Stem Cells: Methods and Protocols*, Methods in Molecular Biology, vol. 2640, https://doi.org/10.1007/978-1-0716-3036-5_7,

of the mitofusin 2 (a pro-fusion protein on the mitochondrial outer membrane) or OPA1 (a pro-fusion protein on the mitochondrial inner membrane) has been shown to lead to the late-onset of myopathy [6–8].

Skeletal muscles contain a population of resident stem cells, called satellite cells, localized underneath the basal lamina of muscle fibers [9]. Satellite cells are mitotically quiescent but can immediately be activated to re-enter the cell cycle and produce myogenic progenitors that fuse together to form new myotubes or myofibers during regeneration [10, 11], wherein a small subpopulation of satellite cells returns to quiescence, the so-called self-renewal, to repopulate the stem cell pool for the next round of injury [12]. Quiescent satellite cells have a low metabolic rate with few mitochondria [13, 14] and maintain low rates of protein synthesis, mediated in part by the phosphorylation of eukaryotic translation initiation factor 2a (eIF2a) [15–17]. The exit of satellite cells from quiescence into activation is marked by a major metabolic shift associated with increased biosynthesis of proteins. In order to meet the high energetic demands of the activation and stem cell differentiation processes, both the mitochondrial biogenesis and respiration pathways are dramatically upregulated [18–22].

Understanding the mitochondrial dynamics and function in satellite cells and differentiated myotubes/myofibers is critical for delineating the mechanisms behind the pathogenic progression of various chronic health conditions associated with the failure of skeletal muscle adaptation. The Seahorse XF Bioanalyzer is a powerful tool to measure the extracellular rate of changes in oxygen partial pressure and pH, allowing researchers to simultaneously assess the oxygen consumption rate (OCR) and extracellular acidification rate (ECAR, glycolysis) in a high-throughput format in live cells and in real-time. Such analyses could provide a deeper insight into the contribution of mitochondria to both physiologic and pathophysiologic conditions in human health. Here, we described a method that allows for the real-time assessment of metabolism in primary satellite cells and differentiated myotubes, as well as in C2C12 myoblasts.

2 Materials

2.1 Isolation and Culture of Primary Satellite Cells (Myotubes) and C2C12 Myoblasts

1. Collagenase D stock: 500 mg of collagenase D (Roche Applied Science) powder dissolved in 50 ml Ham's F12 medium, 1% penicillin, and streptomycin. The stock solution was sterilized by getting filtered through a 0.2 μm filter and stored at −20 °C.
2. Ultracer G(PALL Life Science): Ultracer G lyophilized powder dissolved in 20 ml of Ham's F12 medium with 1% penicillin

and streptomycin. The reconstituted solution was sterilized by filtering through a 0.2 μm filter and stored at −20 °C.

3. Growth medium (GM) for C2C12 myoblasts: DMEM high glucose, 10% FBS, 1% penicillin, and streptomycin (*see* **Note 1**).
4. Growth medium (GM) for satellite cells: DMEM high glucose, 20% FBS, 1% chick embryonic extract (CEE) or 2% Ultracer G and 1% penicillin and streptomycin for satellite cells (*see* **Note 1**).
5. Differentiation medium (DM) for the differentiation of satellite cells: DMEM high glucose, 5% horse serum, 1% penicillin, and streptomycin.
6. Matrigel: Matrigel diluted with ice-cold DMEM to a concentration of 1 mg/ml before use.

2.2 Extracellular Flux Assay

1. XF DMEM assay medium: Agilent Seahorse XF Base medium (#102353-100; Seahorse Bioscience), 1 mM sodium pyruvate, 11 mm glucose, 2 mm GlutaMAX, and 1% penicillin, and streptomycin.
2. Calibration buffer (#100840-000; Seahorse Bioscience).
3. Seahorse Mito Stress Test kit (#103015-100): oligomycin 63 nmol, FCCP 72 nmol, and 27nml of both rotenone and antimycin.
4. Flux Pak (#102416-100): Seahorse XFe96 well plate, sensor cartridge, and calibration plate.
5. Seahorse XFe96 analyzer.

3 Methods

Satellite cells or C2C12 myoblasts were seeded at a given density in Seahorse cell culture plates. We first measured the basal oxygen consumption rate (OCR) and the extracellular acidification rate (ECAR) as indicators of oxidative phosphorylation and glycolysis, respectively; the cells were then successively treated with 3 different compounds to change their metabolic profile. For successful measurement of the bioenergetic profile in satellite cells or myotubes, it is important to isolate a pure population of satellite cells from skeletal muscles without contamination by non-myogenic cells, such as adipocytes and fibroblasts, which might confound results. Here, we described a method to measure OCR and ECAR using the Seahorse XF Bioanalyzer in a pure myogenic population isolated by the single fiber method.

3.1 Isolation of Satellite Cells Using the Single Fiber Method

1. Both proximal and distal tendons should be kept intact during dissection to ensure the intact state and avoid any damage to the extensor digitorum longus (EDL) muscle.
2. Place the muscle in 2 ml of 0.2% collagenase D and incubate at 37 °C in a CO_2 incubator for approximately 1 h.
3. During the digestion of the muscle, coat a dish with FBS, pour 10% FBS/DMEM in the dish, and incubate at 37 °C with 5% CO_2 until the completion of digestion of the EDL muscle.
4. Place the digested EDL muscle into the dish containing the warmed-up medium.
5. Gently pipette the EDL muscle up and down using a large-bore glass pipette until the release of the myofibers. Clean up the debris and contracted fibers (Fig. 1a, b).
6. Pick up the live myofibers (300–400 live myofibers/mouse, approximately 50–60 live myofibers/well of a 6 well plate) and transfer them to a Matrigel-coated dish (*see* **Notes 2** and **3**) containing GM for satellite cells. Alternatively, 2% Ultracer G can also be used instead of 1% CEE.

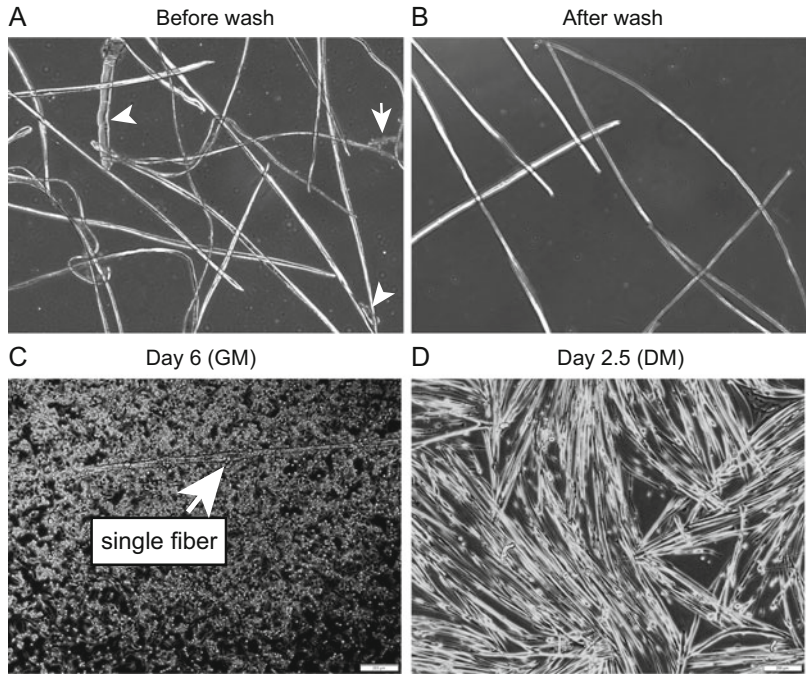

Fig. 1 Representative images of the isolation and culture of single myofibers. (**a**) Bright field image of single EDL myofibers before the wash step. Hypercontracted myofibers and debris are indicated by white arrowheads and white arrow, respectively. (**b**) Bright field image of single EDL myofibers after several wash steps. Image shows long intact myofibers. (**c**) Representative result of a plated single myofiber with its associated satellite cells. Single fiber-associated satellite cells are migrated onto a Matrigel-coated dish and rapidly expanded in high serum medium for 6 d. (**d**) Representative result of myotubes differentiated for 2.5 d in differentiation medium

	1	2	3	4	5	6	7	8	9	10	11	12
A	Background	N	N	N	N	N	N	N	N	N	N	Background
B	N	Exp. 1	Exp. 1	Exp. 1	Exp. 1	Exp. 1	Exp. 4	Exp. 4	Exp. 4	Exp. 4	Exp. 4	N
C	N	Exp. 1	Exp. 1	Exp. 1	Exp. 1	Exp. 1	Exp. 4	Exp. 4	Exp. 4	Exp. 4	Exp. 4	N
D	N	Exp. 2	Exp. 2	Exp. 2	Exp. 2	Exp. 2	Exp. 5	Exp. 5	Exp. 5	Exp. 5	Exp. 5	N
E	N	Exp. 2	Exp. 2	Exp. 2	Exp. 2	Exp. 2	Exp. 5	Exp. 5	Exp. 5	Exp. 5	Exp. 5	N
F	N	Exp. 3	Exp. 3	Exp. 3	Exp. 3	Exp. 3	Exp. 6	Exp. 6	Exp. 6	Exp. 6	Exp. 6	N
G	N	Exp. 3	Exp. 3	Exp. 3	Exp. 3	Exp. 3	Exp. 6	Exp. 6	Exp. 6	Exp. 6	Exp. 6	N
H	Background	N	N	N	N	N	N	N	N	N	N	Background

Fig. 2 The 96-well grid layout and an example of group assignments. The corner of the plate is used as blank (A1, A12, H1, and H12). Avoid adding cells at the wells in the corners of the plate; however, add an equivalent volume of assay medium

7. Culture for 3 days without changing the medium and then change the medium every day after that. Satellite cells will migrate from the fibers to the Matrigel-coated dish and expand, as shown in Fig. 1c.
8. At day 6 or 7, trypsinize satellite cells and seed them in an XF96 cell culture plate coated with Matrigel at an equivalent number.

3.2 Preparation of Extracellular Flux Assay (the Day Before Assay)

1. A day before the assay, turn on the Agilent Seahorse XFe/XF machine, and let it warm up overnight.
2. Hydrate a sensor cartridge in the Seahorse XF calibrant at 37 °C in a non-CO_2 incubator overnight (*see* **Note 5**).
3. If you use satellite cells or C2C12 myoblasts in growing condition, we recommend that cells are seeded in an XF96 cell culture plate coated with Matrigel at a density of 2×10^4 cells/well for satellite cells and 1×10^4 cells/well in 100 μL of GM a day before the assay. (Fig. 2).
4. If you use primary myotubes, place the cells in an XF96 cell culture plate at a density of 2×10^4 cells/well. The next day, replace the medium with a differentiation medium and let them differentiate for 2–3 d (Fig. 1d) (*see* **Note 4**).

3.3 Preparation of Extracellular Flux Assay (Day of the Assay)

1. Examine the health of the cells and confirm that they have reached 70–80% confluency, under a microscope. Regarding myotubes, confirm that cells are fused together and multinucleated, as shown in Fig. 1d.
2. Aspirate the cell culture medium (GM or DM) from the XF96 cell culture plate and add 175 μl of warmed XF DMEM assay medium per well.
3. Incubate cells at 37 °C in a non-CO_2 incubator for 1 h prior to the assay.

3.4 Preparation of Compounds, Loading of Compounds to Each Port, and Analysis

1. For the mitochondrial stress test, first prepare stock solutions of each compound (oligomycin, FCCP, and rotenone/antimycin A). As shown in Table 1, add XF DMEM assay medium to vials containing each compound to make stock solutions. Pipette up and down to solubilize the compounds.

Table 1
Preparation of stock solution of each compound

Compound	Volume of XF assay medium	Concentration
Oligomycin	630 μL	100 μM
FCCP	720 μL	100 μM
Rotenone/antimycin A	540 μL	50 μM

Table 2
Preparation of working solution of each compound for loading to the XFe96 sensor cartridge

Compound	Final concentration	Stock solution (μL)	XF assay medium (μL)	Working solution concentration	Volume added to port (μL)	Volume of medium (175 μL)
Port A Oligomycin	1.0 μM	240	2760	8.0 μM	25	200
Port B FCCP	0.5 μM	135	2865	4.5 μM	25	225
Port C Rotenone/antimycin A	0.5 μM	300	2700	5.0 μM	25	250

Note that in this assay, the starting volume of the medium per well of the cell plate is 175 μL, but will change following the successive addition of each compound (from port A, B, and C) (*see* **Note 6**)

2. Next, use each stock solution to make compound working solutions that will be used for loading into the injection ports on the sensor cartridges. The optimal final concentration of each compound will vary according to the cell type. For primary myoblasts/myotubes and C2C12 myoblasts, we recommend the following concentrations: oligomycin, 1 μM; FCCP, 0.5 μM; and rotenone/antimycin A, 0.5 μM. Prepare 3 mL working solutions for each compound in the assay medium, as shown in Table 2 (Also *see* **Note 6**).
3. Load 25 μL of each compound into the appropriate injector ports (oligomycin-Port A, FCCP-Port B, rotenone/antimycin A-Port C) on the sensor cartridge, as shown in Fig. 3. Warm compounds up to 37 °C prior to their loading on the sensor cartridge.
4. Place the calibration plate with the loaded sensor cartridge on the instrument tray. Start the calibration; it takes approximately 30 min.

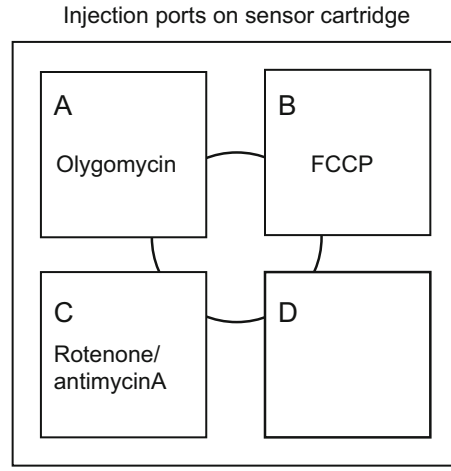

Fig. 3 Location of injection ports on the sensor cartridge

Table 3
Protocol commands for the Mito Stress Test

Step	Loop
Calibration	
Equilibrate	
Baseline readings (Loop X3)	Mix 3 min, wait 2 min, measure 3 min
Inject Port A (oligomycin)	
Measure (Loop X3)	Mix 3 min, wait 2 min, measure 3 min
Inject Port B (FCCP)	
Measure (Loop X3)	Mix 3 min, wait 2 min, measure 3 min
Inject Port C (rotenone/ antimycin A)	
Measure (Loop X3)	Mix 3 min, wait 2 min, measure 3 min
End program	

5. Replace the calibration plate with the XF96 cell culture plate.
6. Set up the program for Extracellular Flux Assay Protocol (Table 3) and then click start.
7. Use the Wave software and Report generator for analysis (Fig. 4a) (*see* **Notes 7**, **8**, and **9**).
8. Representative results are shown in Figs. 4b, c.

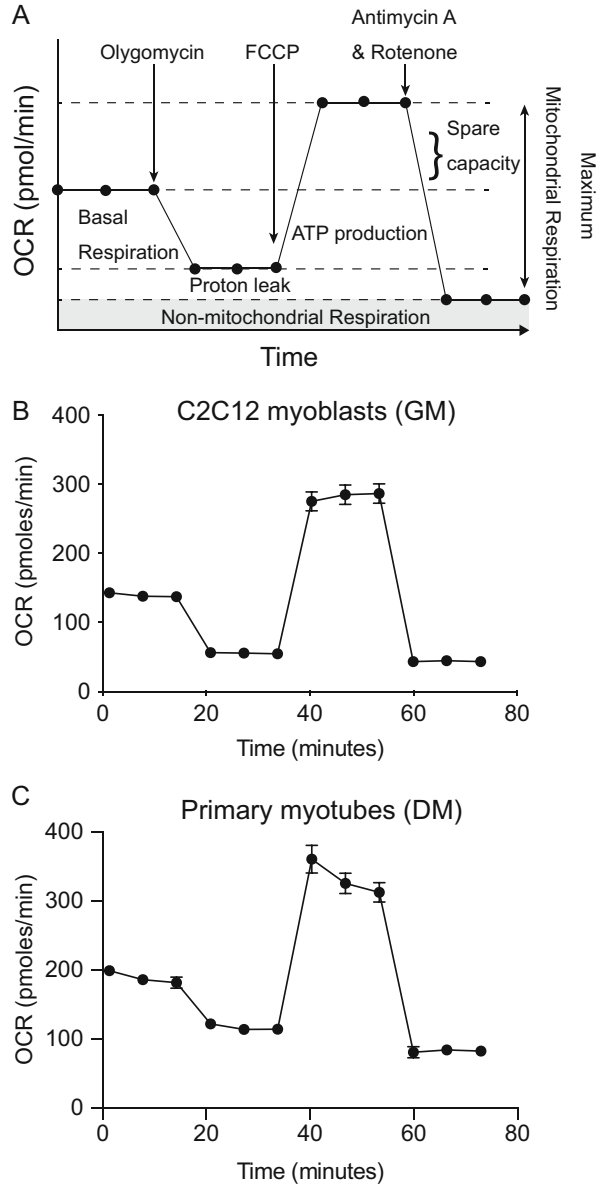

Fig. 4 Representative result of a Mito Stress test in primary myotubes and C2C12 myoblasts. (**a**) Illustration of the graph of the oxygen consumption rate. (**b**) Representative result of OCR in C2C12 myoblasts. (**c**) Representative result of OCR in primary differentiated myotubes

4 Notes

1. FBS might vary considerably between lots, even from the same company. It is important to validate whether FBS works on the expansion of satellite cells before the experiments.

2. Keep Matrigel at 4 °C at all times and coat dishes with enough volume to cover the surface of the well. After 1 min, remove the Matrigel and let them dry at 37 °C for 1 h.
3. Aliquots of diluted Matrigel can be reused multiple times if stored at 4 °C.
4. A longer differentiation time might result in cells detaching from the plate during the assay. Researchers should optimize the differentiation time points on their own by changing the initial seeding density, and so on.
5. Wrap the sensor cartridge to avoid the evaporation of the calibration buffer during hydration. Do not incubate for longer than 72 h.
6. To achieve the required final concentration, it is important to consider the amount of medium before injecting each compound, because each time a compound is added to the medium, the total volume changes.
7. After finishing the program, you can normalize the results according to protein concentration or cell number per well. Add 50–100 μL RIPA buffer/well to fully lyse cells and measure the protein concentration using the BCA assay following the manufacturer's protocol.
8. It is recommended to not use the outer wells of the plate (A, H, and 1, 12) to avoid the edge effect; however, these wells should be filled with an equivalent amount of assay medium for background correction.
9. Sometimes we found outliers in our data set. To eliminate these outliers, it is suggested to create multiple wells in one group in order to determine potential outlier in the obtained data set (*see* Fig. 2). You could also assess the quality of the data by checking the changes in the levels of O_2 and pH after injection of the compounds.

Acknowledgments

The authors thank Dr. Kazuo Yamamoto (Nagasaki University, School of Medicine, Nagasaki, Japan) and Dr. Yusuke Ono (Institute of Molecular Embryology and Genetics, Kumamoto University) for technical support. This work was supported by a MEXT Leading Initiative for Excellent Young Researchers.

References

1. Fujita R, Yoshioka K, Seko D et al (2018) Zmynd17 controls muscle mitochondrial quality and whole-body metabolism. FASEB J 32: 5012–5025
2. Yoshioka K, Fujita R, Seko D et al (2019) Distinct roles of Zmynd17 and PGC1α in mitochondrial quality control and biogenesis in skeletal muscle. Front Cell Dev Biol 7:330
3. Chen H, Vermulst M, Wang YE et al (2010) Mitochondrial fusion is required for mtDNA stability in skeletal muscle and tolerance of mtDNA mutations. Cell 141:280–289
4. Koves TR, Ussher JR, Noland RC et al (2008) Mitochondrial overload and incomplete fatty acid oxidation contribute to skeletal muscle insulin resistance. Cell Metab 7:45–56
5. Mootha VK, Lindgren CM, Eriksson K-F et al (2003) PGC-1α-responsive genes involved in oxidative phosphorylation are coordinately downregulated in human diabetes. Nat Genet 34:267–273
6. Petersen KF (2003) Mitochondrial dysfunction in the elderly: possible role in insulin resistance. Science 300:1140–1142
7. Petersen KF, Dufour S, Befroy D et al (2004) Impaired mitochondrial activity in the insulin-resistant offspring of patients with type 2 diabetes. N Engl J Med 350:664–671
8. Amati-Bonneau P, Valentino ML, Reynier P et al (2008) OPA1 mutations induce mitochondrial DNA instability and optic atrophy "plus" phenotypes. Brain 131:338–351
9. Mauro A (1961) Satellite cell of skeletal muscle fibers. J Biophys Biochem Cytol 9:493–495
10. Yin H, Price F, Rudnicki MA (2013) Satellite cells and the muscle stem cell niche. Physiol Rev 93:23–67
11. Brack AS, Rando TA (2012) Tissue-specific stem cells: lessons from the skeletal muscle satellite cell. Cell Stem Cell 10:504–514
12. Dumont NA, Wang YX, Rudnicki MA (2015) Intrinsic and extrinsic mechanisms regulating satellite cell function. Dev Camb Engl 142: 1572–1581
13. Rodgers JT, King KY, Brett JO et al (2014) mTORC1 controls the adaptive transition of quiescent stem cells from G0 to GAlert. Nature 510:393–396
14. Tang AH, Rando TA (2014) Induction of autophagy supports the bioenergetic demands of quiescent muscle stem cell activation. EMBO J 33:2782–2797
15. Zismanov V, Chichkov V, Colangelo V et al (2016) Phosphorylation of eIF2α is a translational control mechanism regulating muscle stem cell quiescence and self-renewal. Cell Stem Cell 18:79–90
16. Fujita R, Crist C (2018) Translational control of the myogenic program in developing, regenerating, and diseased skeletal muscle. In: Current topics in developmental biology. Elsevier, pp 67–98
17. Crist CG, Montarras D, Buckingham M (2012) Muscle satellite cells are primed for myogenesis but maintain quiescence with sequestration of Myf5 mRNA targeted by microRNA-31 in mRNP granules. Cell Stem Cell 11:118–126
18. Ryall JG, Dell'Orso S, Derfoul A et al (2015) The NAD+-dependent SIRT1 deacetylase translates a metabolic switch into regulatory epigenetics in skeletal muscle stem cells. Cell Stem Cell 16:171–183
19. Ryall JG, Cliff T, Dalton S et al (2015) Metabolic reprogramming of stem cell epigenetics. Cell Stem Cell 17:651–662
20. Sala D, Cunningham TJ, Stec MJ et al (2019) The Stat3-Fam3a axis promotes muscle stem cell myogenic lineage progression by inducing mitochondrial respiration. Nat Commun 10: 1796
21. Sin J, Andres AM, Taylor DJR et al (2016) Mitophagy is required for mitochondrial biogenesis and myogenic differentiation of C2C12 myoblasts. Autophagy 12:369–380
22. Khacho M, Clark A, Svoboda DS et al (2016) Mitochondrial dynamics impacts stem cell identity and fate decisions by regulating a nuclear transcriptional program. Cell Stem Cell 19:232–247

Chapter 8

State of the Art Procedures for the Isolation and Characterization of Mesoangioblasts

Nefele Giarratana, Filippo Conti, Lorenza Rinvenuti, Flavio Ronzoni, and Maurilio Sampaolesi

Abstract

Adult skeletal muscle is a dynamic tissue able to regenerate quite efficiently, thanks to the presence of stem cell machinery. Besides the quiescent satellite cells that are activated upon injury or paracrine factors, other stem cells are described to be directly or indirectly involved in adult myogenesis. Mesoangioblasts (MABs) are vessel-associated stem cells originally isolated from embryonic dorsal aorta and, at later stages, from the adult muscle interstitium expressing pericyte markers. Adult MABs entered clinical trials for the treatment of Duchenne muscular dystrophy and the transcriptome of human fetal MABs has been described. In addition, single cell RNA-seq analyses provide novel information on adult murine MABs and more in general in interstitial muscle stem cells. This chapter provides state-of-the-art techniques to isolate and characterize murine MABs, fetal and adult human MABs.

Key words Human adult and fetal stem cells, Mesoangioblasts, Skeletal muscle regeneration, Stem cell culture, FACS, Single cell RNA-seq, Transcriptome

1 Introduction

The scientific community is still debating on the intrinsic regeneration ability of skeletal muscles and there is a large consensus that besides satellite cells, known as skeletal muscle quiescent progenitors [1, 2], other adult stem cell populations contribute to adult myogenesis [3]. In injured skeletal muscles, several chemokines, growth factors and eventually recombinant proteins [4, 5], play a crucial role in the stem cell machinery. Although satellite cells are the main players in skeletal muscle development and repair, other local progenitors, including mesoangioblasts (MABs) have been showed to directly contribute to muscle repair [6–12]. MABs were originally isolated from murine dorsal aorta and subsequently identified in murine and human adult skeletal muscles associated with small interstitial vessels. MABs still retain the ability to differentiate in mesodermal cell lineages [13], including osteogenic,

Atsushi Asakura (ed.), *Skeletal Muscle Stem Cells: Methods and Protocols*, Methods in Molecular Biology, vol. 2640, https://doi.org/10.1007/978-1-0716-3036-5_8,

Table 1
MAB marker profile during proliferation evaluated by FACS and scRNA-seq

Sample	Positive (35–95%)	Negative (<5%)
Murine skMABs	*SCA1+++, CD44+++, CD140b++, CD140a++, NG2+* Single-cell RNA-seq analysis: Acta2, Anx5, Desmin, Pdgfr2	*CD45, CD31, Itga7, Ter119* Single-cell RNA-seq analysis: Pdgfra, Fmod, Tnmd
Human skMABs		
Adult	*AP+++, CD44+++, CD140b++, CD140a+, CD146+, CD13+++, CD90+, CD149+++*	*CD45, CD31, CD56*
Fetal	*AP+++, CD146+, NG2++, CD90+++, CD13+++*	*CD45, CD31, CD56*

+ between 35% and 45% positive cells, ++ between 45% and 80% positive cells, +++ between 80% and 97% positive cells. Molecular MAB marker profile by scRNA-seq was directly performed on freshly isolated skeletal muscle cells

adipogenic and chondrogenic cell types, and they can extensively be expanded in vitro since they express the clonogenic marker CD146 (see Table 1). In muscle degenerative disease animal models, several studies have shown the intrinsic capacity of MABs to contribute to muscle regeneration [14–18]. Recently, it has been demonstrated that MABs derived from fetal tissues show high plasticity and elevate differentiation capabilities [19]. In particular, transcriptional profiles of MABs derived from aorta, atrial, ventricular, and skeletal muscles of fetuses revealed that each subset of MABs displayed a set of differentially expressed genes, which seem to reflect their distinct tissue derivations. The differential transcription profiles of MABs also correlated with the inherent myogenic differentiation properties of each tissue type. Moreover, while differentially expressed gene profiles demonstrated a global opposite set of upregulated and downregulated genes between skeletal and cardiac muscle MABs, the aorta MABs displayed an intermediate profile. Moreover, both fetal and adult MABs can be easily transduced with lentiviruses [20].

In this chapter, we illustrate the current protocols for isolation, expansion, characterization, and freezing procedures of MABs from adult murine skeletal muscles and from human adult and fetal muscle biopsies [21, 22]. Fluorescence-activated cell sorter (FACS) techniques are not only crucial for the isolation and characterization of fetal and adult MABs, but also for the more innovative single-cell OMICS analyses, including single cell RNA sequencing (scRNA-seq) as reported. A full protocol complete with procedures for collagen-based coating of tissue culture surfaces for MABs is also provided. Since MABs have been recently tested in clinical trials [15], we also provide a method to test their cell fusion potential by means of C2C12 cell co-culture experiments. Indeed, C2C12 cells are considered as the gold standard for myogenic cell lines since activated satellite cells tend to

differentiate quickly and it is not possible to keep them in culture in undifferentiated state. We also describe various cell differentiation methods, including spontaneous myogenic differentiation, induction of smooth muscle cells, osteocytes, adipocytes and chondrocytes. It is important to note that basic animal handling, dissection, and tissue culture skills are mandatory for successful attempts in order to obtain and expand MABs in vitro. It is also necessary to have basic knowledge in histochemistry, biochemistry, and molecular biology for the successful characterization of MABs. Importantly, sterile conditions in both Class II biohazard flow hoods are recommended for human materials and approvals from local Institutional Ethics Committee and patient-informed consent are needed.

Finally, note-taking is a crucial point of the troubleshooting process. Thus, we provide a list of notes to keep the process of troubleshooting as easy as possible, especially for beginners.

2 Materials

2.1 Basic Materials

- Skeletal muscle biopsies from murine or human samples (see Methods).
- C2C12 myogenic cell line (ATCC # CRL-1772).
- Sterile rounded-edge disposable scalpels.
- Sterile curved forceps.
- Sterile sharp-edged straight forceps.
- 3.5-, 6-, 10 cm, Petri dishes
- Calf skin collagen.
- Suitable polypropylene tubes, with and without cell filter.
- Culture-grade water.
- Sterile Phosphate-buffered saline (PBS) Ca^{2+}/ Mg^{2+}-free.
- Sterile TrypLE Express Trypsin.
- Glacial acetic acid.
- Cell incubator set at 5% CO_2, 5% O_2, 90% N_2.
- Phycoerythrin-conjugated monoclonal anti-human/mouse AP, clone B4–78 (R&D, USA).
- 7-ADD dead or alive markers
- Cryobox.
- 96 well plates (4titude, #4ti-0960)
- Triton X-100.
- Biotinylated Oligo-dT (10 mM).
- dNTPs (10 mM),

- RNase inhibitor (0.5 U/μl).
- KAPA HIFI Hot Start ReadyMix (Roche #07958919001).
- Magnetic beads (CleanNA #CPCR).
- Qubit fluorometer (Thermo Scientific).
- Agilent 2100 BioAnalyzer (Agilent).
- Nextera XT library prep and index kit (Illumina #FC-131-1096 and #FC-131-2001).
- Dual-index primers (i7 and i5, Illumina, 14 cycles).
- Echo 555 (Labcyte).
- Hiseq2500 or HiSeq4000 (Illumina).
- C57Bl6 mice.

2.2 Media

- Collagen solution (100 ml): Dissolve by stirring 0.005 mg/ml of calf skin collagen in glacial acetic acid (i.e. 100 mg/20 ml) overnight at room temperature. Carefully mix and add 20% of the acid collagen solution to culture-grade water (i.e. 80 ml). Filter through a 0.22 μm membrane to ensure sterility. Store at 4 °C.
- Growth medium for murine MABs (DMEM20 medium; 250 ml): DMEM high glucose, supplemented with 20% sterile heat-inactivated Fetal Bovine Serum (FBS), 1% penicillin/streptomycin solution (100 units), 2 mM glutamine, 1 mM sodium pyruvate, and 1% non-essential amino acid solution. Filter through a 0.22 μm membrane to ensure sterility. Store at 4 °C for up to 3 weeks.
- Growth medium for human MABs (IMDM15 medium; 250 ml): IMDM, supplemented with 15% sterile heat-inactivated FBS, 1% penicillin/streptomycin solution (100 units), 2 mM glutamine, 1% non-essential amino acid solution, 0.1 mM 2-mercaptoethanol, 1% of 100X Insulin-Transferrin-Selenium, and 1.25 μg human bFGF. Filter through a 0.22 μm membrane to ensure sterility. When supplemented with bFGF, store at 4 °C for up to 1 week, else store for longer and add bFGF freshly upon using (second option is recommended).
- Growth medium for human fetal MABs (MegaCell DMEM medium; 250 ml): MegaCell DMEM supplemented with 5% fetal bovine serum (FBS,), 5 ng/mL of human bFGF freshly added, 2 mM L-glutamine, 0.1 mM β-mercaptoethanol, 1% non-essential amino acid solution, and 1% penicillin/streptomycin. Filter through a 0.22 μm membrane to ensure sterility.
- C2C12 myoblast cell growth medium (DMEM10 medium; 250 ml): DMEM high glucose supplemented with 10% sterile

heat-inactivated FBS, 1% penicillin/streptomycin solution, 1 mM sodium pyruvate. Filter through a 0.22 μm membrane to ensure sterility. Store at 4 °C for up to 2 weeks.

- Freezing medium (FM; 50 ml): heat-inactivated FBS supplemented with 10% Hybri-MAX® DMSO (Sigma-Aldrich, USA). Filter through a 0.22 μm membrane to ensure sterility. Store at 4 °C for up to 4 weeks. Keep cold until use.
- Spontaneous differentiation medium (DM; 250 ml): DMEM high glucose supplemented with 2% sterile heat-inactivated Horse Serum (HS), 1% penicillin/streptomycin solution, 2 mM glutamine, and 1 mM sodium pyruvate. Filter through a 0.22 μm membrane to ensure sterility. Store at 4 °C for up to 4 weeks.
- Smooth muscle differentiation medium (SMM medium; 250 ml): DMEM high glucose supplemented with 2% sterile heat-inactivated HS, 1% penicillin/streptomycin solution, 2 mM glutamine, 1 mM sodium pyruvate, and 1.25 μg TGFβ. Filter through a 0.22 μm membrane to ensure sterility. When supplemented with TGFβ, store at 4° for up to 1 week, else store for longer and add TGFβ freshly upon using (second option strongly recommended).
- Osteogenic differentiation medium (OM; 250 ml): αMEM basal medium supplemented with 10% sterile heat-inactivated FBS, 0.1 μM dexamethasone, 2 mM glutamine, 50 μM ascorbic acid, 10 μM 2-glycerophosphate, 1% penicillin/streptomycin. Filter through a 0.22 μm membrane to ensure sterility. Store at 4 °C in the dark for 4 weeks.
- Adipogenic differentiation medium (AD medium): We recommend the use of StemPro Adipogenesis differentiation kit (Invitrogen).
- Chondrogenic differentiation medium (CD medium): We suggest StemPro Chondrogenesis differentiation kit (Thermofisher).

2.3 Antibodies (See Table 1)

- PE-Cy7-conjugated anti-alkaline phosphatase (AP) (R&D Systems)
- APC-conjugated anti-CD13 (e-Bioscience)
- FITC-conjugated anti-CD90 (BD-Pharmingen)
- PE-Cy7-conjugated anti-CD146 (BD-Pharmingen)
- AlexaFluor647-conjugated anti-NG2
  AlexaFluor488 anti-CD56 (BD-Pharmingen)

3 Methods

3.1 Adult MAB Isolation

1. Murine and human MABs can be isolated from hindlimb skeletal muscles of adult animals (*see* **Note 1**) and from small muscle biopsies respectively.
2. Adult muscle fragments can be stored in DMEM20 medium for up to one day at 4 °C before proceeding further.
3. Positive cells for CD140a, CD140b, and Alkaline Phosphatase and lineage negative (lin^-) for endothelial and hematopoietic markers ($CD31^-$, $CD45^-$ and $Ter119^-$) can be sorted out from the murine bulk cell population (see Table 1). Similarly, lin^- cells positive for CD140a, CD140b, and Alkaline Phosphatase and can be sorted out from the human bulk cell population. In order to avoid satellite cell contamination, anti-CD56 and/or anti-alpha-7 integrin (Itga7) can be included in the list of lin^- Abs.

3.2 Human Fetal MAB Isolation

1. Fetal tissue samples can be obtained from aborted material of gestational age, normally between 9.5–13 weeks, donated to research under informed consent.
2. Human fetal MABs (hfMABs) can be isolated from aorta, cardiac, and skeletal muscle fragments as previously described [23]. Rinse skeletal muscle fragments in phosphate-buffered saline (PBS) (w/o Ca2+ Mg 2+), cut into small pieces (1–2 mm diameter), and transfer to Petri dishes previously coated with type I collagen (*see* **Notes 2**, **3**).
3. Culture skeletal muscle fragments approximately for 7–10 days in growth medium for hfMABs, and after the initial outgrowth of fibroblast-like cells, round-shaped and reflective cells can be observed on top of them (*see* **Note 4**).
4. Seed hfMAB cultures at 5×10^3 cells per cm^2 in a 5.5% CO_2 humidified incubator in hypoxic conditions (5% O_2) and split cells every 2–3 days.

3.3 Murine Adult MAB Isolation by Fluorescence-Activated Cell Sorter (FACS)

1. As the second incubation starts, monitor the fragments daily: add 500 ml of fresh DMEM20 and check the extent to which the cells spread from the biopsies. If the medium acidifies, gently remove it and change it with fresh DMEM20. Once the cell layer spreads for approximately 1 cm from each fragment (see Fig. 3), immediately proceed to the next step (*see* **Note 4**).
2. Firstly, place the muscles from each mouse in a 10 cm dish and rinse them with 5 ml PBS to wash away the blood. Using separate dishes for each muscle is recommended for separate isolation from different muscles.

3. Move the muscles onto a clean 10 cm dish. After checking for and removing any fibrous or fat tissue that may be left, use a sterile, round-shaped scalpel to dissect the muscle into fragments measuring about 2 mm^2.
4. With the help of sterile, curved forceps, transfer the fragments obtained from each muscle onto a 3.5 cm, collagen-coated dish (*see* **Note 2**). The distance between the samples must be kept constant (to ensure optimal results, 10 fragments should be placed on each dish, at 8–9 mm from one another).
5. Delicately put 100 ml of pre-warmed DMEM20 on top of every muscle fragment, then start an 18–24 h incubation in a humidified incubator (37 °C, 5% CO_2/5% O_2) (*see* **Note 3**).
6. After the incubation, use 1.5 ml of DMEM20 for each dish to cover the fragments. To avoid detachment of the samples, slowly add the medium against the side of the dish. Clean the dishes from any fragment that did not attach by using a sterile, curved forceps. Incubate again, for at least 72 h (37 °C, 5% CO_2/5% O_2).
7. As the second incubation starts, monitor the fragments daily: add 500 ml of fresh DMEM20 and check the extent to which cells spread from the biopsies. If the medium acidifies, gently remove it and replace it with fresh DMEM20. Once the cell layer spreads for approximately 1 cm from each fragment (see Fig. 3), immediately proceed to the next step (*see* **Note 4**).
8. Using sterile, sharp-edged forceps, gently remove the fragments from the dish, collect the medium in a 15 or 50 ml tube, then wash with PBS. Do not discard the medium since some cells might still be present in suspension.
9. To detach the cells, add 600 μl of pre-warmed trypsin to the dish and let it act for 2–3 min at 37 °C, gently tapping on the sides of the dish to facilitate detachment. Once the cells are suspended, add 1 ml of DMEM20 to the dish and carefully collect all the cells into a 15 or 50 ml tube (the same tube used to collect the medium) (rinsing the dish by gently pipetting the suspension is recommended to avoid losing cells). Form cells pellets by centrifuging the samples for 5 minutes (500 g, room temperature).
10. Add a suitable volume of DMEM20 to the tube and homogeneously resuspend the cell pellet (no clumps should be present), then proceed to count the cells.
11. At this point, it is generally better to immediately proceed to the next step, avoiding re-plating the cells. However, if the number of cells is limited ($<5 \times 10^5$), re-plate them onto collagen-coated 6-multiwell-plates and wait until the confluence reaches 85–90% before proceeding to the next step.

12. Prepare sterile, FACS-suitable, capped polystyrene tubes and add:
    - 10^5 cells for the blank sample
    - The remaining cells for the sorting sample ($>1 \times 10^6$ is suggested)
13. Centrifuge the samples for 5 min at 500 g at room temperature, discard the supernatant, and re-suspend the cells pellets either by gently vortexing or by pipetting. For the blank sample, use 200 μl of PBS, but for the sorting sample, use 48 μl of PBS together with 2 μl (1:25) of the suitable Alkaline-Phosphatase (AP) FACS antibody (*see* also **Note 5**).
14. Incubate for 30 minutes, keeping the samples covered from the light and on ice.
15. After incubation, centrifuge for 5 minutes at 500 g at room temperature, discard the supernatant, add 200 μl of PBS, and vortex gently to homogenously wash the cells.
16. Repeat this last wash step once.
17. Move the samples in a 5 ml polystyrene tube while filtering the cells (place a filter on top of the tube or use a filter top tip), then proceed to sort the cells: MABs will stain positive for AP (see Fig. 3). Additionally, it is suggested to stain the cells with 7-AAD dead or alive markers (1:25) just before sorting.
18. Collect the sorted MABs in sterile, FACS-suitable polypropylene tubes, previously filled with 500 μl of DMEM20. Supplement the medium with penicillin (1:20) and streptomycin (100 units) to prevent contamination (*see* **Note 6**).
19. Centrifuge the sorted cells for 5 minutes at 500 g at room temperature, discard the supernatant, carefully resuspend them in an appropriate volume of DMEM20, and finally plate them onto a suitable surface (*see* **Note 7**).
20. Culture and expand the obtained MABs on collagen-coated, multi-well plates, using DMEM20 and keeping them in a humidified incubator (37 °C, 5% CO_2/5% O_2).
21. Passaging cells is recommended with a confluence of 85–90%, at a ratio of 1:5. MABs can maintain their proliferation/differentiation capacity for 20–25 passages. In later passages, MABs generally undergo senescence, or anyway a loss of potency can be observed.

3.4 Human Adult MAB (hMAB) Isolation by FACS

1. To harvest the cells, follow the same protocol as for murine MABs (see above, Paragraph 3.3). Replace DMEM20 with IMDM15 medium (*see* **Note 8**).

2. Culture and expand adult human MABs on collagen-coated, multi-well plates, using IMDM15 and keeping them in a humidified incubator (37 °C, 5% CO_2/5% O_2).
3. Passaging cells is recommended with a confluence of 80%, at a 1:3 ratio (*see* **Note 9**). Human adult MABs can maintain their proliferation/differentiation capacity for about 20 passages. In later passages, adult human MABs generally start showing signs of senescence and apoptosis.

3.5 Human Fetal MAB (hfMAB) Isolation by FACS

1. Detach the cells with 0.05% trypsin-EDTA and rinse with PBS containing 3% FBS.
2. Incubate around 2–3 × 10^6 cells for 20 min at 4 °C in the dark with specific conjugated mouse anti-human antibodies or isotype controls (1 μg/ml) (see Table 1).

3.6 MAB Batches Long-Term Storage

1. After expansion, remove medium, wash with PBS, and cover the cell layer with a proper amount of trypsin.
2. Incubate for 5 min at 37 °C in a 5% CO_2/ 5% O_2 humidified incubator. Add the same amount of growing medium to block trypsin reaction, and carefully collect the cells in a 15 ml tube. Count the viable cells and spin down 5 min at 400 g at room temperature.
3. Resuspend in a suitable amount of FM medium (1 ml/ 2 × 10^6 cells) and pipette 1 ml of cell suspension per cryovial.
4. Incubate the cryovials in isopropanol-containing cryobox overnight at −80 °C. After 24 h, transfer the vials into −150 °C freezers or liquid N_2 tanks for long-term storage.

3.7 Murine Adult MAB Isolation by FACS for Single Cell RNA Sequencing (scRNA-seq)

1. Single-cell sort LIN- muscle cells by FACS in 96 well plates. Each well contained 0.4% Triton X-100 in RNase-free water supplemented with 10 mM biotinylated Oligo-dT, 10 mM dNTPs, and 0.5 U/μl RNase inhibitor for a total volume of 4 μl lysis buffer.
2. cDNA libraries were generated based on the Smart-seq2 protocol [24–26].
3. Briefly, incubate lysed cells at 72 °C for 3 min and amplify cDNA via a 22-cycle PCR. Amplification is done with KAPA HIFI Hot Start ReadyMix and purification by magnetic beads.
4. Assess quantity and quality of cDNA with a Qubit fluorometer and Agilent 2100 BioAnalyzer with a high-sensitivity chip, respectively.
5. Make library preparation with the Nextera XT library prep and index kit. Tagmented 100 pg of cDNA by transposase Tn5 and amplify it with dual-index primers (i7 and i5, 14 cycles). Mix the reagents together by the Echo 555 and purify the pooled Nextera XT libraries. Pool together the single-cell libraries

(384 in this experiment) and sequence single-end 50 bp on a single lane of a Hiseq2500 or HiSeq4000.

6. All results related to scRNA-seq (Figs. 1 and 2) are based on freshly isolated muscle cells from C57Bl6 mice, and experiments were performed on the same day.

3.8 scRNA-seq Analysis

1. Analysis of SmartSeq2 scRNA-seq data can be performed with the Seurat [27] R package (version 3.0.1).
2. For importing data into Seurat, make the raw counts previously gathered [24] compatible by transforming ENSEMBL# to gene Symbol.
3. Filter cells containing a high content of mitochondrial genes and a high content of ERCC's (Seurat QC).
4. Further analyze the remaining cells for their expression value scaling and normalization.
5. PCA and UMAP dimensionality reductions and clustering were performed. The expression values were renormalized, rescaled, and re-clustered, and cells were manually annotated based on their differentially expressed genes (Fig. 1a–c).
6. Identification and analysis of differentially expressed gene markers representative for each cluster are shown by violin plots. Marker gene median is represented and every dot within the violin indicates one single cell (Fig. 2a).

3.9 Collagen Coating

1. Add collagen solution until the bottom is homogeneously covered. Incubate for 5 min at room temperature, remove the collagen solution, and dry the dish out. Incubate the dish at 37 °C overnight in a sterile oven.
2. After 24 h, wash the surface at least 3 times with PBS. Before seeding cells, ensure the correct pH by covering the bottom with a Red Phenol-containing medium. If the medium turns yellow, wash again with PBS.

3.10 Cell Fusion Potential: MABs and C2C12 Cell Cocultures

1. Expand murine C2C12 myoblasts in DMEM10 medium at 37 °C in a 5% CO_2/ 5% O_2 humidified incubator, splitting 1: 6 upon 70% confluence. Change DMEM10 medium daily and avoid myotube formation.
2. At day 0 of differentiation, start the co-cultures seeding C2C12 myoblasts and murine or rat MABs together with the ratio of 1: 1 so that after 24 h, cells will be 80–85% confluent (2×10^4 in each well of collagen-coated 12 mw). Incubate at 37 °C with DMEM20 medium. After 24 h, remove medium, wash with PBS, add myogenic differentiation medium, and incubate.
3. Refresh DM medium every 2–3 days until appearance of myotubes (usually after approximately 5–7 days) and proceed to analyses (*see* **Note 10**).

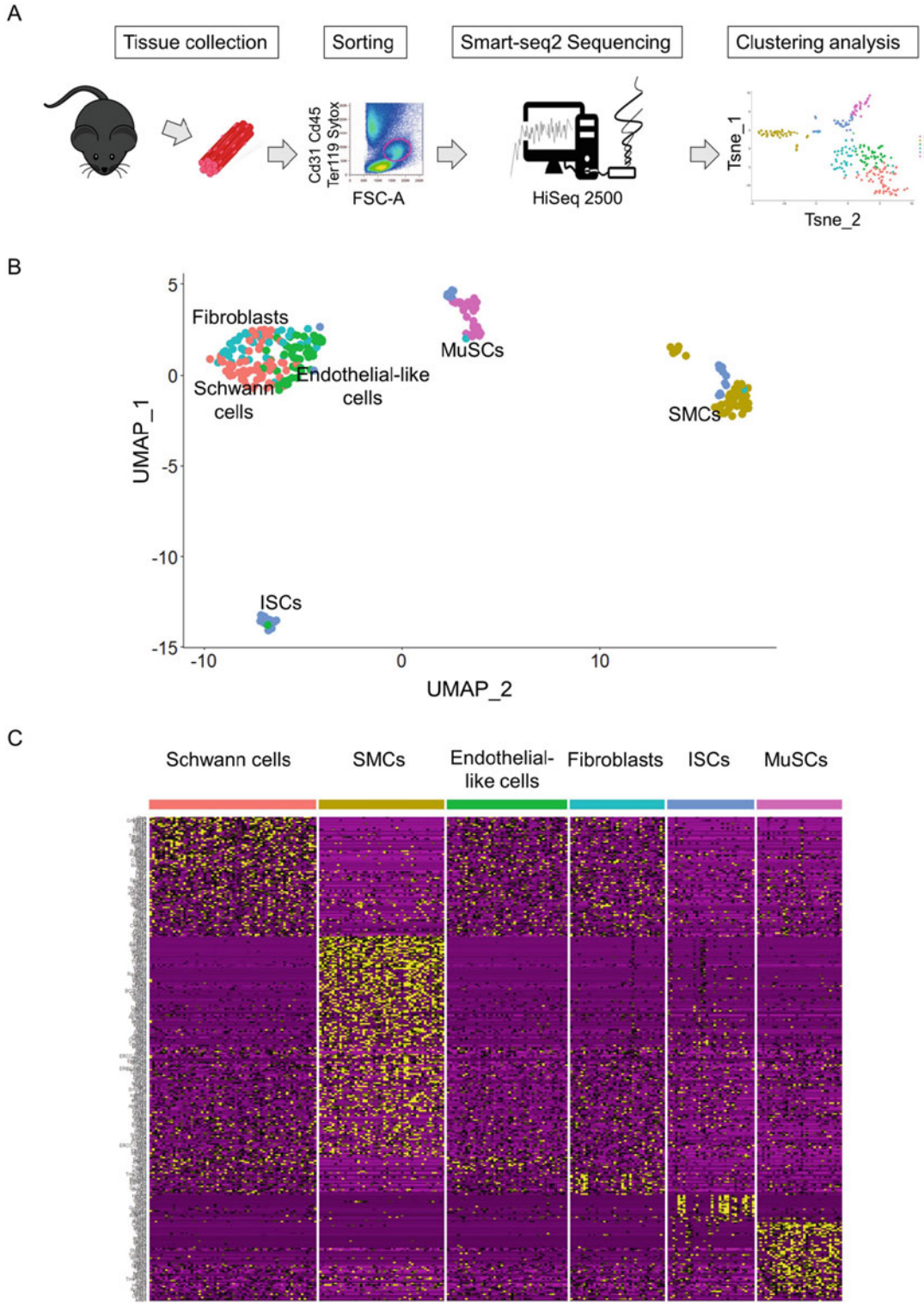

Fig. 1 scRNA-seq analysis of mononucleated lin$^-$ cells freshly isolated from murine muscles. (**a**) Schematic diagram showing the isolation of single cells from the hindlimbs of healthy mice with SMART-seq2. (**b**) UMAP plot and k-means clustering of cells from murine skeletal muscle identifying 6 clusters: Schwann cells, Smooth muscle cells (SMCs), Endothelial-like cells, Fibroblasts, Interstitial Stromal Cells (ISCs as reported in [24]) and activated Satellite Cells (MuSCs); each point represents one cell. (**c**) Heatmap of k-means clusters of differentially expressed marker genes (representative genes for each cluster are listed)

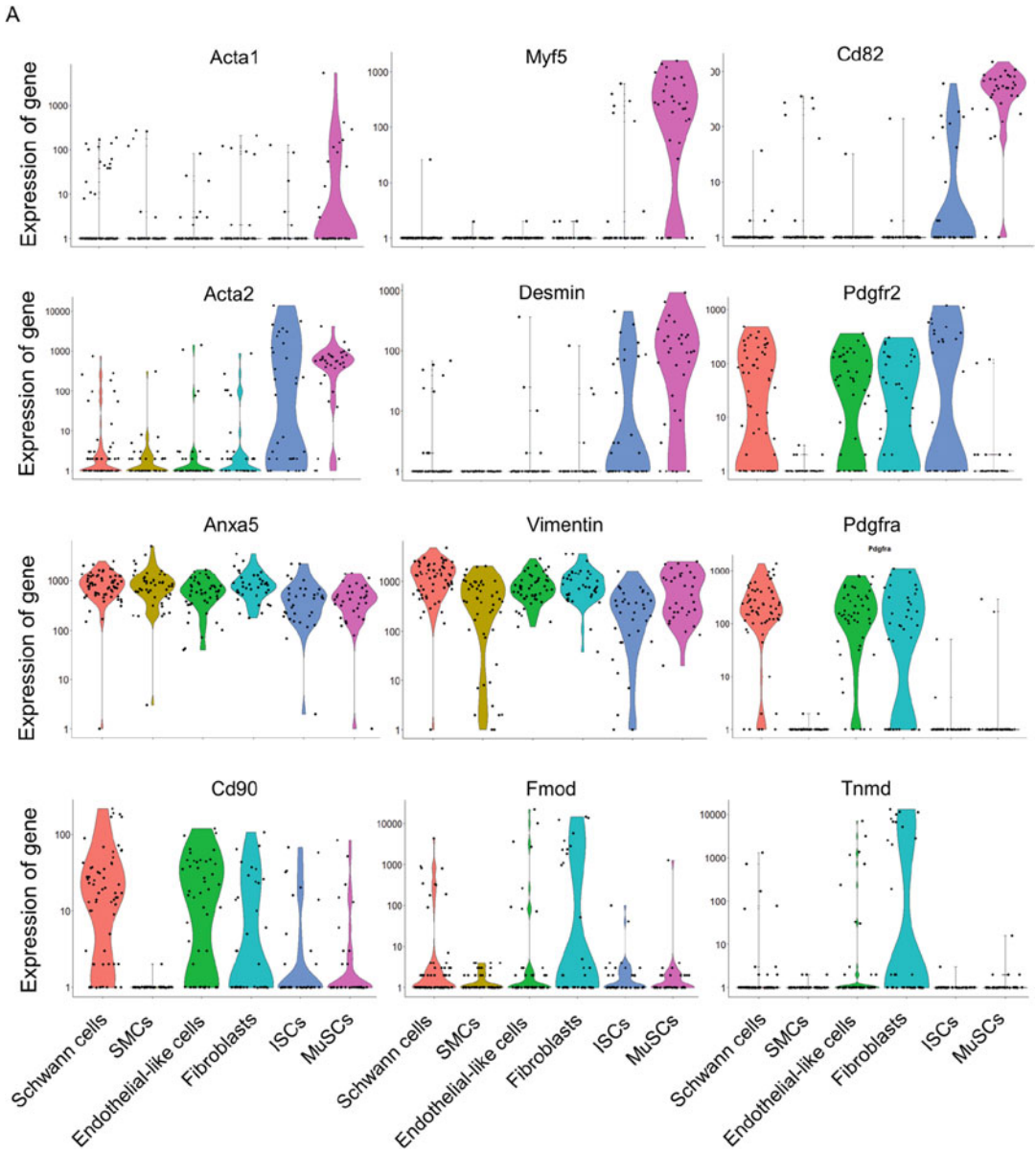

Fig. 2 Representative marker genes from single-cell analysis on fresh muscle. (**a**) Violin plot with median visualizing marker genes (*Acta1*, *Myf5*, *Cd82*, *Acta2*, *Desmin*, *Pdgfr2* known as *Pdgfrb*, *Anxa5* known as *Annexin V*, *Vimentin*, *Pdgfra*, *Cd90*, *Fmod* and *Tnmd*) for the identified clusters. All markers have been compared to literature [24, 28]

3.11 MAB Smooth Muscle Induction

1. Expand MABs, either with IMDM15 or with DMEM20 medium for human and murine adult cells respectively and MegaCell DMEM medium for hfMABs, at 37 °C in a 5% CO_2/ 5% O_2 humidified incubator.

2. To induce smooth muscle differentiation, plate either ~5.10^3 cells/ cm^2 for murine MABs, or ~1×10^4 cells/cm^2 for human MABs in collagen-coated plates, incubated at 37 °C with either murine or human growth medium. Day 1 of differentiation.
3. After 24 h, remove the medium, wash with PBS, add SMM medium, and incubate for 7–8 days, changing the medium every 2 days. Proceed to analyses (*see* **Note 11**).

3.12 MAB Osteogenic Induction

1. Expand MABs, either with IMDM15 or with DMEM20 medium for human and murine adult cells respectively and MegaCell DMEM medium for hfMABs, at 37 °C in a 5% CO_2/ 5% O_2 humidified incubator.
2. Upon 100% confluence, remove the medium, wash with PBS, add OM medium, and incubate.
3. Change OM medium every 4 days for 2–3 weeks and proceed to analyses (*see* **Note 12** and Fig. 3).

3.13 MAB Adipogenic Induction

1. Expand MABs, either with IMDM15 or with DMEM20 medium for human and murine adult cells respectively and MegaCell DMEM medium for hfMABs, at 37 °C in a 5% CO_2/ 5% O_2 humidified incubator.
2. Upon 100% confluence, remove the medium, wash with PBS, add AD medium, and incubate.
3. Refresh medium every 2–3 days until the appearance of adipocytes (approximately 10–14 days).
4. Proceed to analyses (*see* **Note 13** and Fig. 3).

3.14 MAB Chondrogenic Induction

1. Expand hfMABs with MegaCell DMEM medium at 37 °C in a 5% CO_2/ 5% O_2 humidified incubator.
2. Upon 100% confluence, remove the medium, wash with PBS, add CD medium, and incubate.
3. Refresh medium every 2–3 days until the appearance of adipocytes (approximately 10–14 days).
4. Proceed to analyses (*see* **Note 14** and Fig. 3).

4 Notes

1. Murine adult MABs can be isolated from 7-day-old mice until 4-week-old onwards. However, MAB proliferation and differentiation ability reduce with age.
2. Keep a thin layer of collagen coating onto the plates or dishes for 5 min at room temperature and before proceeding to culture cells, wash abundantly with PBS to remove any acidic traces of collagen solution.

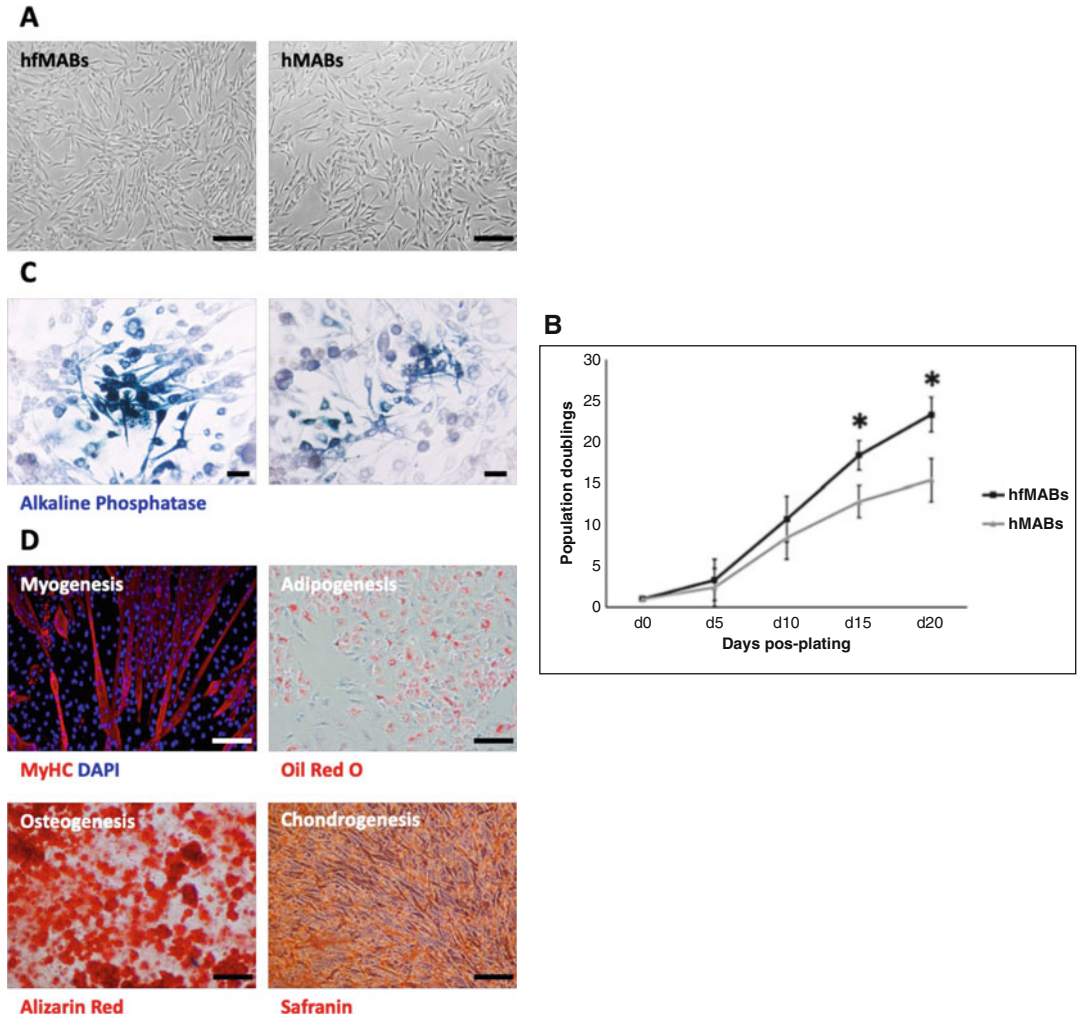

Fig. 3 Proliferation and differentiation of fetal MABs. (**a**) Proliferating hfMABs show a star-shaped morphology comparable to human adult MABs. Scale bar = 100 mm. (**b**) Growth curves showing hfMABs and hMABs population doublings (*$p < 0.01$). (**c**) Both hfMABs and hMABs are positive for AP staining. Scale bar = 10 mm. (**d**) Representative images of hfMAB differentiation capacity are shown by IF analysis (Myogenesis: MyHC in red) and specific staining protocols (Adipogenesis: Oil Red O, Osteogenesis: Alizarin Red, Chondrogenesis: Safranin). Scale bar = 100 mm

3. Let the dish bottom dry out to encourage tissue fragment adhesion. Then, incubate the fragment-containing 3.5 cm dishes in a sterile, covered humid chamber containing a PBS lid-free dish, in order to avoid medium drop evaporation. Given that the isolation may take up to 10 days, check the PBS level regularly and eventually rinse it.
4. Erythrocytes start to sprout out in the first 48 h, and then after 72 h, fibroblast-like cells containing hMABs should appear.

hMABs look small, round-shaped, and very bright. Once attached to the collagen layer, they start appearing as spindle-shaped cells.

5. In the case of testing different Ab combinations, antibody quantities must be titrated according to the manufacturer's datasheet.
6. If cells are plated directly into DMEM20 supplemented with extra antibiotics (0,5% gentamicin, 5% streptomycin, 5% penicillin), remove the medium 24 h after plating, wash with PBS, and rinse with 2 ml fresh DMEM20.
7. Murine adult MABs should be plated around 30–40% confluence. For instance, $<5 \times 10^3$ cells should be plated in 1 well of 96 multi-well plates and between 5 to 10×10^5 in one well of 6 multi-well plates.
8. Human MABs generally need a longer incubation time (up to 14 days) to sprout out and be ready for sorting.
9. We recommend passing hMABS when 80% confluent at the latest to prevent spontaneous cell fusions. Murine MABs are easily transduced to express fluorescent markers that can reveal C2C12 chimeric myotubes to assess their cell fusion potential. Myogenic differentiation potential should be confirmed by qRT-PCR, western blot, and immunofluorescence analyses to detect late myogenic markers, such as myosin heavy chain or sarcomeric actin.
10. Human MABs have the ability to produce myotubes upon serum starvation, conversely to rodent MABs that need to be co-cultivated with muscle progenitor cells.
11. In smooth muscle cell induction, MABs should be kept at 60% confluence. Thus, it might be necessary to pass the cells during the differentiation process. Calponin and alpha-smooth muscle actin should be detected by qRT-PCR, western blot, immunofluorescence, and flow cytometry analyses in order to quantify the smooth muscle differentiation rate.
12. Alizarin Red staining should be performed in order to reveal calcium deposits in MABs subjected to osteogenic induction, since proliferating MABs are already alkaline phosphatase positive.
13. Although we suggest Oil Red O for lipid-containing vacuole staining [29] in MAB adipogenic induction protocol, Nile red staining or Peroxisome proliferator-activated receptor gamma detection can be also performed.
14. Safranin staining could be carried out for proteoglycans and glycosaminoglycans detection, revealing chondrogenic differentiation of MABs, as reported in Fig. 3.

Acknowledgments

Work in the authors' laboratory is supported by The Research Foundation Flanders (FWO) (#G066821N), INTERREG – Euregio Meuse-Rhine (GYM, Generate your muscle 2020-EMR116), and Italian Ministry of Health, Ricerca Finalizzata (RF-2019-12369703). MS is recipient of Hercules Foundation grant (AKUL/19/34) for the financing provided to purchase the high throughput calcium imaging system.

References

1. Kuang S, Kuroda K, Le Grand F et al (2007) Asymmetric self-renewal and commitment of satellite stem cells in muscle. Cell 129:999–1010
2. Cossu G, Biressi S (2005) In seminars in cell & developmental biology. (Elsevier) 16:623–631
3. Cassano M, Quattrocelli M, Crippa S et al (2009) Cellular mechanisms and local progenitor activation to regulate skeletal muscle mass. J Muscle Res Cell Motil 30(7–8):243–253
4. Agosti E, De Feudis M, Angelino E et al (2020) Both ghrelin deletion and unacylated ghrelin overexpression preserve muscles in aging mice. Aging (Albany NY) 12(14): 13939–13957
5. Ronzoni F, Ceccarelli G, Perini I et al (2017) Met-activating genetically improved chimeric factor-1 promotes angiogenesis and hypertrophy in adult Myogenesis. Curr Pharm Biotechnol 18(4):309–317
6. Dellavalle A, Sampaolesi M, Tonlorenzi R et al (2007) Pericytes of human skeletal muscle are myogenic precursors distinct from satellite cells. Nat Cell Biol 9(3):255–267
7. Dellavalle A, Maroli G, Covarello D et al (2011) Pericytes resident in postnatal skeletal muscle differentiate into muscle fibres and generate satellite cells. Nat Commun 2:499
8. Quattrocelli M, Costamagna D, Giacomazzi G et al (2014) Notch signaling regulates myogenic regenerative capacity of murine and human mesoangioblasts. Cell Death Dis 5(10):e1448
9. Costamagna D, Quattrocelli M, van Tienen F et al (2016) Smad1/5/8 are myogenic regulators of murine and human mesoangioblasts. J Mol Cell Biol 8(1):73–87
10. Bonfanti C, Rossi G, Tedesco FS et al (2015) PW1/Peg3 expression regulates key properties that determine mesoangioblast stem cell competence. Nat Commun 6:6364
11. Breuls N, Giacomazzi G, Sampaolesi M (2019) (Epi)genetic modifications in myogenic stem cells: from novel insights to therapeutic perspectives. Cells 8(5):429
12. Pozzo E, Chai YC, Sampaolesi M. (2020) Comprehensive overview of non-coding RNAs in cardiac development. Adv Exp Med Biol 1229:197–211
13. Giarratana N, Conti F, La Rovere R et al (2020) MICAL2 is essential for myogenic lineage commitment. Cell Death Dis 11(8):654
14. Sampaolesi M, Torrente Y, Innocenzi A et al (2003) Cell therapy of α-sarcoglycan null dystrophic mice through intra-arterial delivery of mesoangioblasts. Science 301(5632):487–492
15. Sampaolesi M, Blot S, D'Antona G et al (2006) Mesoangioblast stem cells ameliorate muscle function in dystrophic dogs. Nature 444(7119):574–579
16. Quattrocelli M, Swinnen M, Giacomazzi G et al (2015) Mesodermal iPSC–derived progenitor cells functionally regenerate cardiac and skeletal muscle. J Clin Invest 125(12): 4463–4482
17. Cossu G, Previtali SC, Napolitano S et al (2015) Intra-arterial transplantation of HLA-matched donor mesoangioblasts in Duchenne muscular dystrophy. EMBO Mol Med 7(12):1513–1528
18. Crisan M, Yap S, Casteilla L et al (2008) A perivascular origin for mesenchymal stem cells in multiple human organs. Cell Stem Cell 3: 301–313
19. Ronzoni FL, Lemeille S, Kuzyakiv R et al (2020) Human fetal mesoangioblasts reveal tissue-dependent transcriptional signatures. Stem Cells Transl Med 9:575–589
20. Santoni de Sio FR, Gritti A, Cascio P et al (2008) Lentiviral vector gene transfer is limited by the proteasome at postentry steps in various types of stem cells. Stem Cells 26:2142–2152

21. Quattrocelli M, Giacomazzi G, Broeckx SY et al (2016) Equine-induced pluripotent stem cells retain lineage commitment toward myogenic and chondrogenic fates. Stem Cell Rep 6:55–63
22. Tonlorenzi R, Dellavalle A, Schnapp E et al (2007) Isolation and characterization of mesoangioblasts from mouse, dog, and human tissues. Curr Protoc Stem Cell Biol Chapter 2:Unit 2B.1
23. Barbuti A, Galvez BG, Crespi A et al (2010) Mesoangioblasts from ventricular vessels can differentiate in vitro into cardiac myocytes with sinoatrial-like properties. J Mol Cell Cardiol 48:415–423
24. Camps J, Breuls N, Sifrim A et al (2020) Interstitial cell remodeling promotes aberrant adipogenesis in dystrophic muscles. Cell Rep 31: 107597
25. Picelli S, Faridani OR, Björklund AK et al (2014) Full-length RNA-seq from single cells using Smart-seq2. Nat Protoc 9:171–181
26. Breuls N, Giarratana N, Yedigaryan L et al (2021) Valproic acid stimulates myogenesis in pluripotent stem cell-derived mesodermal progenitors in a NOTCH-dependent manner. Cell Death Dis. 12(7): 677. https://doi.org/10.1038/s41419-021-03936-w. PMID: 34226515; PMCID: PMC8257578.
27. Butler A, Hoffman P, Smibert P et al (2018) Integrating single-cell transcriptomic data across different conditions, technologies, and species. Nat Biotechnol 36:411–420
28. Ronzoni FL, Giarratana N, Crippa S et al (2021) Guide Cells Support Muscle Regeneration and Affect Neuro-Muscular Junction Organization. Int J Mol Sci. 22(4):1939. https://doi.org/10.3390/ijms22041939. PMID: 33669272; PMCID: PMC7920023
29. Marini V, Marino F, Aliberti F et al (2022) Long-term culture of patient-derived cardiac organoids recapitulated Duchenne muscular dystrophy cardiomyopathy and disease progression. Front Cell Dev Biol. 10:878311. https://doi.org/10.3389/fcell.2022.878311. PMID: 36035984; PMCID: PMC9403515

Chapter 9

Analyses of Mesenchymal Progenitors in Skeletal Muscle by Fluorescence-Activated Cell Sorting and Tissue Clearing

Madoka Ikemoto-Uezumi, Tamaki Kurosawa, Keitaro Minato, and Akiyoshi Uezumi

Abstract

Mesenchymal progenitors, which are resident progenitor populations residing in skeletal muscle interstitial space, contribute to pathogeneses such as fat infiltration, fibrosis, and heterotopic ossification. In addition to their pathological roles, mesenchymal progenitors have also been shown to play important roles for successful muscle regeneration and homeostatic muscle maintenance. Therefore, detailed and accurate analyses of these progenitors are essential for the research on muscle diseases and health. Here, we describe a method for purification of mesenchymal progenitors based on the expression of PDGFRα, which is a specific and well-established marker for mesenchymal progenitors, using fluorescence-activated cell sorting (FACS). Purified cells can be used in several downstream experiments including cell culture, cell transplantation, and gene expression analysis. We also describe the method for whole-mount 3-dimensional imaging of mesenchymal progenitors by utilizing tissue clearing. The methods described herein provide a powerful platform for studying mesenchymal progenitors in skeletal muscle.

Key words Skeletal muscle, Mesenchymal progenitors, Cell isolation, FACS, Tissue clearing

1 Introduction

Skeletal muscle possesses a remarkable regenerative potential that depends on tissue-specific stem cells called satellite cells. Satellite cells reside beneath the basal lamina of myofibers. Satellite cells are essential for adult muscle regeneration, which cannot be compensated by other cell types [1–3]. In contrast to satellite cells, mesenchymal progenitors reside in the muscle interstitial space, and therefore, represent a distinct cell population from satellite cells [4]. These cells are non-myogenic in nature but have differentiation potentials toward adipogenic, fibrogenic, and chondro/osteogenic lineages [4–7]. In pathological conditions, mesenchymal progenitors have been proven to contribute to ectopic fat cell formation, fibrosis, and heterotopic ossification [4–7]. In contrast, these cells have also been shown to exert positive effects by stimulating

Atsushi Asakura (ed.), *Skeletal Muscle Stem Cells: Methods and Protocols*, Methods in Molecular Biology, vol. 2640, https://doi.org/10.1007/978-1-0716-3036-5_9,

satellite cell-dependent myogenesis during muscle regeneration [1, 8]. Furthermore, a recent study demonstrated the essential roles for mesenchymal progenitors in steady-state maintenance of skeletal muscle [8]. Therefore, mesenchymal progenitors have a considerable impact on skeletal muscle health. To study mesenchymal progenitors, it is important to accurately identify and purify these cells because skeletal muscle contains many different types of cells. For accurate identification of mesenchymal progenitors, PDGFRα is considered the best marker because it is highly specific and conserved in both mice and humans [9, 10].

Previously, we described a method for the purification of mesenchymal progenitors using PDGFRα as a positive marker by fluorescence-activated cell sorting (FACS) [11]. In the following sections, we updated the method to improve its accuracy. This method enables simultaneous isolation of both mesenchymal progenitors and satellite cells, and therefore, it is also useful for the study of satellite cells. We also describe whole-mount 3-dimensional imaging of mesenchymal progenitors by utilizing tissue clearing for the analyses of their localization and distribution in skeletal muscle tissue.

2 Materials

2.1 Dissociating Cells from Skeletal Muscle

1. Mice: 8- to 12-wk-old female mice (*see* **Note 1**).
2. Forceps and scissors. For trimming and mincing muscle tissues, fine-tipped forceps and curved scissors are recommended.
3. Sterile 60 mm dishes.
4. Sterile 5, 10, and 25 ml pipettes.
5. PBS without Ca^{2+} and Mg^{2+} (sterile).
6. Dissection microscope.
7. Hank's balanced saline solution (HBSS) (sterile).
8. Collagenase Type II (Worthington, CLSS2).
9. Sterile 10 ml syringe.
10. Sterile 0.22 μm PVDF membrane syringe-driven filter unit.
11. A 20 ml beaker.
12. Magnetic stirrer and stir bar.
13. Tissue culture incubator (humidified, 5% CO_2, ambient O_2, 37 °C).
14. An 18-gauge needle.
15. Sterile 100 μm cell strainers.
16. Sterile 40 μm cell strainers.
17. Sterile 15 and 50 ml conical tubes.

18. Benchtop centrifuge.
19. Hypotonic solution: prepare 0.83% NH_4Cl and 0.17 M Tris-HCl (pH 7.65) separately, and autoclave them separately. Mix at the ratio of 9:1.
20. Sterile 200 and 1000 μl pipette tips.
21. Hemocytometer.
22. Washing buffer: PBS supplemented with 2.5% fetal bovine serum (FBS).

2.2 Purification of Mesenchymal Progenitors and Satellite Cells by FACS

1. Washing buffer, as above.
2. Sterile 1.5 ml microcentrifuge tubes.
3. Benchtop centrifuge.
4. Sterile 10, 200, and 1000 μl pipette tips.
5. Antibodies and secondary reagent: PE/Cy7-conjugated rat anti-mouse CD31 (BioLegend, clone: 390), APC-eFluor 780-conjugated rat anti-mouse CD45 (eBioscience, clone: 30-F11), PE-conjugated goat polyclonal anti-mouse PDGFRα (R&D, cat#:FAB1062P), biotinylated rat anti-mouse satellite cells ([12], clone: SM/C-2.6), streptavidin-PE-CF594 (BD Horizon), PE/Cy7-conjugated rat IgG2a κ isotype control (BioLegend), APC-eFluor 780-conjugated rat IgG2b κ isotype control (eBioscience), and PE-conjugated goat IgG isotype control (R&D).
6. Sterile 40 μm cell strainers.
7. Sterile 50 ml conical tubes.
8. 5 ml round-bottom FACS tubes.
9. Sytox™ red dead cell stain (Invitrogen).
10. Hoechst 33342 (Invitrogen): Dissolve in distilled water at the concentration of 1 mg/mL and sterilize through 0.22 μm PVDF membrane syringe-driven filter unit. Freeze the aliquots for storage.
11. Cell sorter.

2.3 Whole-Mount Immunofluorescent Imaging of Mesenchymal Progenitors

1. Mice.
2. Forceps and scissors. For preparing a whole-mount muscle sample, fine-tipped forceps are recommended.
3. 4% paraformaldehyde (PFA) in PBS.
4. Intradermal needles (Seirin, NS type).
5. Silicone rubber base material (ShinEtsu silicon, KE-103).
6. Silicone rubber curing agent (ShinEtsu silicon, CAT-103).
7. A 100 mL beaker.
8. A 10 cm petri dish (Greiner).

9. 2,2'-Thiodiethanol (TDE) (Sigma-Aldrich).
10. PBS without Ca^{2+} and Mg^{2+} (sterile).
11. Blocking solution (1% Triton X-100, 4% bovine serum albumin in PBS).
12. Antibodies and secondary reagents: goat polyclonal anti-mouse PDGFRα (R&D, cat#: AF1062), Alexa Fluor 647-conjugated isolectin GS-IB_4 (Invitrogen), and Cy3-conjugated donkey anti-goat IgG (Jackson laboratory).
13. Silicone rubber sheet, 0.5 mm thick (Wako).
14. NEO glass cover, thickness No. 1 (Matsunami).
15. Confocal laser scanning microscope.

3 Methods

3.1 Dissociating Cells from Skeletal Muscle

1. Before processing muscle tissue, autoclave forceps and scissors. Place a stir bar in a 20 ml beaker, cover the beaker with aluminum foil, and then autoclave them.
2. Weigh a 60 mm dish containing PBS.
3. Excise hind limb muscles of the mouse. Transfer the excised muscles to the 60 mm dish containing PBS and then weigh the dish.
4. Calculate tissue weight by subtracting weight in **Step 2** from weight in **Step 3**.
5. Carefully remove remaining nerves, blood vessels, tendons, and fat using fine-tipped forceps under a dissection microscope.

   The following steps should be performed in a sterile laminar flow hood.
6. Transfer trimmed muscles into a new 60 mm tissue dish and mince them thoroughly using the curved scissors.
7. Dissolve collagenase type II in HBSS to make 0.2% collagenase solution. Four ml collagenase solution per g of tissue is required for digestion (*see* **Note 2**). Sterilize collagenase solution by forcing it through a 0.22 μm syringe-driven filter unit into the autoclaved beaker.
8. Transfer minced muscles into the beaker containing collagenase solution with the stir bar. Cover the beaker with aluminum foil.
9. Place the beaker and magnetic stirrer in tissue culture incubator, and then digest muscles for 60 min at 37 °C while stirring it with the magnetic stirrer (*see* **Note 3**).
10. Pass digested muscles through the 18 gauge needle 5–7 times using a sterile syringe.

11. Continue digestion for 30 min at 37 °C while stirring it with the magnetic stirrer (*see* **Note 3**).
12. Add 10 ml PBS to the digested slurry and mix thoroughly using a 10 ml pipette.
13. Filter the digested slurry through a 100 μm cell strainer over a 50 ml conical tube. Dilute the digested slurry by washing the cell strainer with PBS and adjust the total volume to 25 ml/g of tissue (*see* **Note 4**).
14. Filter the slurry filtered in **step 13** through a 40 μm cell strainer on a new 50 ml conical tube. Dilute the slurry by washing the cell strainer with PBS and adjust the total volume to 50 ml/g of tissue (*see* **Note 4**).
15. Centrifuge cells for 5 min at 800 × *g*.
16. Resuspend the pellet in a hypotonic solution. Use 2 ml hypotonic solution per gram of tissue. Transfer cells to a 15 ml conical tube and incubate for 1 min at room temperature to eliminate erythrocytes. Add at least 1 volume of PBS. Count cells using a hemocytometer.
17. Centrifuge cells for 5 min at 800 × *g*.
18. Resuspend the pellet in washing buffer and adjust cell concentration to 1×10^7 cells/ml. Proceed to Subheading 3.2.

3.2 Purification of Mesenchymal Progenitors and Satellite Cells by FACS

3.2.1 Antibody Staining for FACS

1. Divide cells resuspended in washing buffer (**step 18** in Subheading 3.1) into eight sterile 1.5 ml microcentrifuge tubes. Label these tubes as "A" to "H": tube A for isotype control, tube B for PE-Cy7 single-stained control, tube C for APC-eFluor 780 single-stained control, tube D for PE single-stained control, tube E for PE-CF594 single-stained control, tube F for Sytox™ red Dead Cell Stain single-stained control, tube G for Hoechst 33342 single-stained control, and tube H for all-stained samples. Isotype control or single-stained controls are used for compensation settings (*see* **Note 5**).
2. Add Hoechst 33342 solution prepared in **step 10** in Subheading 2.2 (1:200) to tube G and H. The final concentration should be 5 μg/ml.
3. Incubate samples at 37 °C for 15 min in the dark.
4. Fill the tubes with washing buffer, and centrifuge cells for 5 min at 800 × g.
5. Resuspend the pellet in washing buffer and adjust cell concentration to 1×10^7 cells/ml.
6. Add the same amount of isotype control antibodies as used in the following staining to tube A. Add PE/Cy7-conjugated rat anti-mouse CD31 (1:300) to tube B; add APC-eFluor 780-conjugated rat anti-mouse CD45 (1:300) to tube C; add

PE-conjugated goat polyclonal anti-mouse PDGFRα (15 μl/test) to tube D; add biotinylated rat SM/C-2.6 (1:300) to tube E; and add PE/Cy7-conjugated rat anti-mouse CD31, APC-eFluor 780-conjugated rat anti-mouse CD45, PE-conjugated goat polyclonal anti-mouse PDGFRα, and biotinylated rat SM/C-2.6 to tube H.

7. Incubate samples at 4 °C for 30 min in the dark.
8. Fill the tubes with washing buffer, and centrifuge cells for 5 min at 800 × g.
9. Resuspend the pellet in washing buffer and adjust cell concentration to 1×10^7 cells/ml.
10. Add PE-CF594 streptavidin (1:300) to tube A, E, and H.
11. Incubate samples at 4 °C for 30 min in the dark.
12. Fill the tubes with washing buffer and centrifuge cells for 5 min at 800 × g.
13. Resuspend the pellet in washing buffer and adjust the volume to 1 ml/tube.
14. Filter control and stained samples through 40 μm cell strainers placed on 50 ml conical tubes. Transfer filtered control and stained samples to 5 ml FACS round-bottom tubes.
15. Add Sytox™ red dead cell stain (1:1000) to tube F and H, and incubate them on ice for a minimum of 15 min in the dark.

3.2.2 Cell Sorting of Mesenchymal Progenitors and Satellite Cells

Here, we describe procedures specific to the purification of mesenchymal progenitors and satellite cells from mouse skeletal muscle briefly. The general settings of the cell sorter should follow the manufacturer's instructions.

1. Exclude debris on a forward scatter (FSC) vs. side scatter (SSC) graph (*see* Fig. 1a).
2. Exclude doublets on an FSC-area vs. FSC-height graph (*see* Fig. 1b).
3. Adjust detector voltage and compensation to optimal levels to clearly visualize negative and positive populations by analyzing isotype or single-stained controls (tubes A–G in Subheading 3.2.1).
4. Exclude dead cells (Sytox™ red-positive cells) on a Sytox™ red vs. SSC graph (*see* Fig. 1c).
5. On a Hoechst 33342 vs. SSC graph, gate for Hoechst-positive mononucleated population (*see* Fig. 1d).
6. Analyze all-stained samples (tube H in Subheading 3.2.1). Display a CD31-PE/Cy7 vs. CD45-APC-eFluor 780 graph and gate for $CD31^-CD45^-$ cells (*see* Fig. 1e).

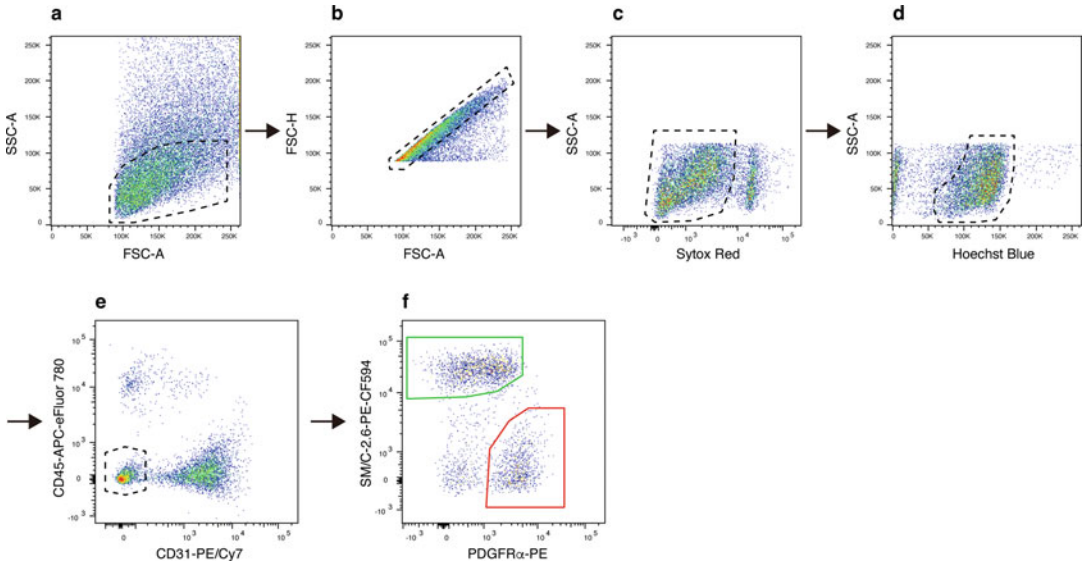

Fig. 1 Purification of mesenchymal progenitors and satellite cells by FACS. (**a**) FACS dot plots showing FSC (x-axis) and SSC (y-axis) profiles. The gate was set to exclude debris. (**b**) FACS dot plots showing FSC-area (x-axis) and FSC-height (y-axis) profiles. The gate was set to exclude doublets. (**c**) FACS dot plots showing Sytox red fluorescence (x-axis) and SSC profile (y-axis). The gate was set to exclude Sytox red-positive dead cells. (**d**) FACS dot plots showing Hoechst 33342 fluorescence (x-axis) and SSC profile (y-axis). The gate was set to analyze Hoechst 33342-positive mononucleated cells. (**e**) FACS dot plots showing the expression of CD31 (x-axis) and CD45 (y-axis). The gate was set to analyze CD31-CD45$^-$ cells. (**f**) FACS dot plots showing the expression of PDGFRα (x-axis) and SM/C-2.6 (y-axis) in CD31-CD45$^-$ cells. Red and green gates indicate mesenchymal progenitors and satellite cells, respectively

7. Display data of CD31$^-$CD45$^-$ cells on a PDGFR-α-PE vs. SM/C-2.6-PE-CF594 graph. Gate for PDGFRα$^+$SM/C-2.6$^-$ cells (red gate) and PDGFRα$^-$SM/C-2.6$^+$ cells (green gate) as shown in Fig. 1f.
8. Prepare collection tubes by adding 1 ml washing buffer to sterile 1.5 ml microcentrifuge tubes.
9. Sort CD31$^-$CD45$^-$PDGFRα$^+$SM/C-2.6$^-$ cells as mesenchymal progenitors and CD31$^-$CD45$^-$PDGFRα$^-$SM/C-2.6$^+$ cells as satellite cells (*see* **Note 6**).

3.3 Whole-Mount Immunofluorescent Imaging of Mesenchymal Progenitors

Here, we focus on procedures specific to the preparation of immunofluorescently stained muscle samples for whole-mount imaging of mesenchymal progenitors and skip the details for microscopy. The general settings of the confocal laser scanning microscope should follow the manufacturer's instructions.

3.3.1 Making Silicone Rubber Plate for Tissue Fixation

1. Mix 25 g of silicone rubber base material and 1.25 g of silicone rubber curing agent while stirring it by the magnetic stirrer in a 100 ml beaker for 5 min.

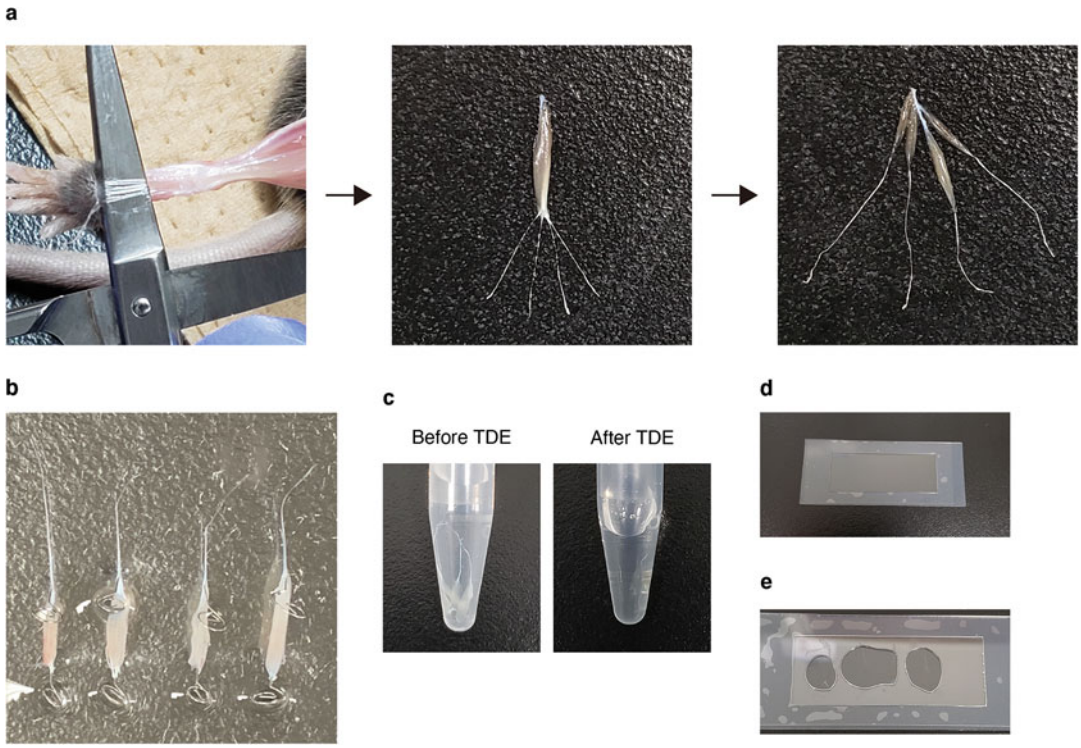

Fig. 2 Preparation of immunofluorescently stained muscle for whole-mount 3-dimensional imaging. (**a**) Mouse EDL muscle was excised with four distal tendons and split into four muscle heads. (**b**) Pinned each muscle head on a silicone rubber plate in 4% PFA. (**c**) EDL muscle with or without tissue clearing by 60% TDE. (**d**) Placed silicone rubber sheet on cover glass. (**e**) Cleared muscle mounted on the cover glass with 60% TDE

2. Pour the mixed reagent into a 10 cm petri dish and place it on the benchtop at room temperature for 2 days until curing is completed.

3.3.2 Whole-Mount Immunofluorescent Staining of Mouse Skeletal Muscle

For whole-mount imaging, smaller muscle is easier to handle. Thus, here we describe procedures for whole-mount imaging of mouse extensor digitorum longus (EDL) muscle. EDL is a multi-tendon muscle with distal insertions on digits II to V of the foot, and therefore, it can be split into four muscle heads that are suitable for whole-mount imaging.

1. Excise EDL muscle with four distal tendons (*see* Fig. 2a).
2. Split EDL muscle into four muscle heads (*see* Fig. 2a).
3. Pin each muscle head on the silicone rubber plate prepared in Subheading 3.3.1 using intradermal needles and fix them in 4% PFA for 30 min on ice (*see* Fig. 2b and **Note 7**).
4. Wash samples in PBS for 30 min three times.
5. Incubate samples in blocking solution (**step 11** in Subheading 2.3) at 4 °C overnight.

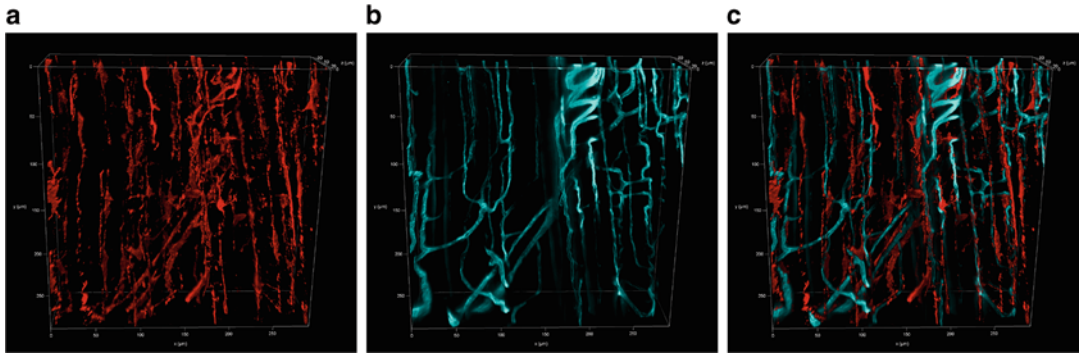

Fig. 3 Whole-mount 3-dimensional image of mesenchymal progenitors. Whole-mount immunofluorescent imaging of cleared EDL muscle for PDGFRα (**a**) and isolectin GS-IB_4 (**b**). The merged image was shown in (**c**). Fluorescently-labeled isolectin was used to visualize vasculature

6. Incubate samples with goat polyclonal anti-mouse PDGFRα (1:400) diluted in blocking solution at 4 °C overnight.
7. Wash samples in PBS for 30 min three times.
8. Incubate samples with Alexa Fluor 647-conjugated isolectin GS-IB_4 (1:100) and Cy3-conjugated donkey anti-goat IgG (1:1000) diluted in blocking solution at 4 °C overnight in the dark.
9. Wash samples in PBS for 30 min three times.
10. Incubate samples in 60% TDE (diluted with PBS) for 30 min (*see* Fig. 2c and **Note 8**).
11. Place silicone rubber sheet on cover glass (*see* Fig. 2d). Mount the samples using 60% TDE and cover with another cover glass (*see* Fig. 2e and **Note 9**).
12. Observe samples using a confocal laser scanning microscope. Capture Z-stack images and reconstruct 3-dimensional images (*see* Fig. 3).

4 Notes

1. Muscles of young female mice are digested more easily than those of male or older mice. We usually use C57BL/6, but we have confirmed that other strains such as BALB/c or ICR can be used as well.
2. Use at least 4 ml collagenase solution for efficient stirring, even when tissue weight is less than 1 g.
3. Digestion time depends on sample condition. If a male mouse or older mice are used, longer digestion should be performed.
4. Use one 50 ml conical tube with a 100 μm cell strainer and one 50 ml conical tube with a 40 μm cell strainer per gram of tissue

(e.g., if starting tissue weight is 3 g, use three sets of conical tubes with cell strainers). If starting tissue weight is less than 1 g, use one conical tube with cell strainer and dilute the digested slurry, adjusting the final volume to 50 ml.

5. At least 5×10^5 cells should be used for the compensation setting (tubes A–G). All the remaining cells are used for the all-stained sample (tube H).
6. If the cell concentration is too high to analyze by FACS, dilute the sample with washing buffer as appropriate. It is important to use bright fluorophores for clear identification of each cell population. Cell yields by these methods are about $1–1.5 \times 10^5$ cells/young female mouse for mesenchymal progenitors and satellite cells.
7. Pinning the muscle is required to preserve the shape of the muscle. Unpinned muscle tends to bend during PFA fixation.
8. Tissue clearing with 60% TDE is compatible with immunostaining of PDGFRα. We also tested other clearing methods including CUBIC, Sca*l*e, and SeeDB2, but these were not compatible with immunostaining of PDGFRα.
9. Refractive index of 60% TDE is 1.45 [13]. Use appropriate immersion reagent and microscope setting, taking this refractive index into account.

Acknowledgments

This work was supported by JSPS KAKENHI Grant Number JP19K09614 (to M.I-U.) and JSPS KAKENHI Grant Number JP19H04063 (to A.U.).

References

1. Murphy MM, Lawson JA, Mathew SJ et al (2011) Satellite cells, connective tissue fibroblasts and their interactions are crucial for muscle regeneration. Development 138(17): 3625–3637. https://doi.org/10.1242/dev.064162
2. Sambasivan R, Yao R, Kissenpfennig A et al (2011) Pax7-expressing satellite cells are indispensable for adult skeletal muscle regeneration. Development 138(17):3647–3656. https://doi.org/10.1242/dev.067587
3. Lepper C, Partridge TA, Fan CM (2011) An absolute requirement for Pax7-positive satellite cells in acute injury-induced skeletal muscle regeneration. Development 138(17): 3639–3646. https://doi.org/10.1242/dev.067595
4. Uezumi A, Fukada S, Yamamoto N et al (2010) Mesenchymal progenitors distinct from satellite cells contribute to ectopic fat cell formation in skeletal muscle. Nat Cell Biol 12(2):143–152. https://doi.org/10.1038/ncb2014
5. Uezumi A, Ito T, Morikawa D et al (2011) Fibrosis and adipogenesis originate from a common mesenchymal progenitor in skeletal muscle. J Cell Sci 124(Pt 21):3654–3664. https://doi.org/10.1242/jcs.086629
6. Wosczyna MN, Biswas AA, Cogswell CA et al (2012) Multipotent progenitors resident in the skeletal muscle interstitium exhibit robust BMP-dependent osteogenic activity and mediate heterotopic ossification. J Bone Miner Res

27(5):1004–1017. https://doi.org/10.1002/jbmr.1562

7. Lees-Shepard JB, Yamamoto M, Biswas AA et al (2018) Activin-dependent signaling in fibro/adipogenic progenitors causes fibrodysplasia ossificans progressiva. Nat Commun 9(1):471. https://doi.org/10.1038/s41467-018-02872-2
8. Wosczyna MN, Konishi CT, Perez Carbajal EE et al (2019) Mesenchymal stromal cells are required for regeneration and homeostatic maintenance of skeletal muscle. Cell Rep 27(7):2029–2035.e2025. https://doi.org/10.1016/j.celrep.2019.04.074
9. Uezumi A, Ikemoto-Uezumi M, Tsuchida K (2014) Roles of nonmyogenic mesenchymal progenitors in pathogenesis and regeneration of skeletal muscle. Front Physiol 5:68. https://doi.org/10.3389/fphys.2014.00068
10. Uezumi A, Fukada S, Yamamoto N et al (2014) Identification and characterization of PDGFRα+ mesenchymal progenitors in human skeletal muscle. Cell Death Dis 5(4):e1186. https://doi.org/10.1038/cddis.2014.161
11. Uezumi A, Kasai T, Tsuchida K (2016) Identification, isolation, and characterization of mesenchymal progenitors in mouse and human skeletal muscle. Methods Mol Biol 1460:241–253. https://doi.org/10.1007/978-1-4939-3810-0_17
12. Fukada S, Higuchi S, Segawa M et al (2004) Purification and cell-surface marker characterization of quiescent satellite cells from murine skeletal muscle by a novel monoclonal antibody. Exp Cell Res 296(2):245–255
13. Aoyagi Y, Kawakami R, Osanai H et al (2015) A rapid optical clearing protocol using 2,2′--thiodiethanol for microscopic observation of fixed mouse brain. PLoS One 10(1):e0116280. https://doi.org/10.1371/journal.pone.0116280

Chapter 10

In Vitro Maturation of Human Pluripotent Stem Cell-Derived Myotubes

Ricardo Mondragon-Gonzalez, Sridhar Selvaraj, and Rita C. R. Perlingeiro

Abstract

Pluripotent stem cells have a multitude of potential applications in the areas of disease modeling, drug screening, and cell-based therapies for genetic diseases, including muscular dystrophies. The advent of induced pluripotent stem cell technology allows for the facile derivation of disease-specific pluripotent stem cells for any given patient. Targeted in vitro differentiation of pluripotent stem cells into the muscle lineage is a key step to enable all these applications. Transgene-based differentiation using conditional expression of the transcription factor PAX7 leads to the efficient derivation of an expandable and homogeneous population of myogenic progenitors suitable for both in vitro and in vivo applications. Here, we describe an optimized protocol for the derivation and expansion of myogenic progenitors from pluripotent stem cells using conditional expression of PAX7. Importantly, we further describe an optimized procedure for the terminal differentiation of myogenic progenitors into more mature myotubes, which are better suited for in vitro disease modeling and drug screening studies.

Key words Induced pluripotent stem (iPS) cells, Myogenic differentiation, PAX7, Small molecules, Myotubes

1 Introduction

Muscular dystrophies (MD) denote a group of more than 40 different genetically heterogeneous diseases that result in the degeneration and weakening of various muscles of the body [1]. Duchenne Muscular Dystrophy (DMD) is one of the most common and serious forms of MD, which affects various skeletal muscles and the cardiac muscle. Patients typically die between 20 and 30 years of age due to cardiorespiratory failure. Current treatments for muscular dystrophies are palliative and there is no cure for any form of MD. Animal models have been pivotal for the understanding of pathogenesis and for testing therapeutics for muscular dystrophies. However, for most forms of muscular dystrophies, animal models

Ricardo Mondragon-Gonzalez and Sridhar Selvaraj contributed equally to this work.

Atsushi Asakura (ed.), *Skeletal Muscle Stem Cells: Methods and Protocols*, Methods in Molecular Biology, vol. 2640, https://doi.org/10.1007/978-1-0716-3036-5_10,

do not recapitulate the severity and all features of the human disease, in part due to differences in genome complexity between species [2]. The derivation of primary muscle tissue from MD patients without damaging the muscle is difficult due to the invasive nature of the procedure. Thus, the use of myogenic cells derived from patient-specific pluripotent stem cells (PSC) is an attractive and valuable option to develop human models of MD due to the ease of their derivation and unlimited proliferative capacity. Human PSCs include embryonic stem cells (ESC) [3] and induced pluripotent stem cells (iPSC). The latter result from the reprogramming of somatic cells into the pluripotent stage by the ectopic expression of the four pluripotency transcription factors Oct4, Klf4, cMyc, and Sox2 [4, 5]. The breakthrough of iPSC technology paved the way for the feasible derivation of disease-specific pluripotent stem cells from any given patient, including those with MD [6–10]. Differentiation of pluripotent stem cells into the muscle lineage is a key step for enabling disease modeling and drug screening applications in MD. Several protocols using either transgene- or chemical-based methods have been reported for the differentiation of hPSC into myogenic progenitors in the past decade [9, 11–17]. We have shown that the transgene-based protocol based on the conditional expression of the transcription factor PAX7 (iPAX7) leads to the efficient derivation of myogenic progenitors that give rise to myotubes in vitro and contribute to muscle regeneration in vivo. Transplantation of iPAX7 myogenic progenitors into several mouse models of MD results in myofiber and satellite cell engraftment as well as improved muscle function [6, 12, 18].

Along the different stages of muscle development, specific forms of myosin heavy-chain *(*MyHC*)* are expressed: *MYH3* for embryonic, *MYH8* for neonatal, and *MYH1*, *MYH2*, and *MYH7* for adult muscle [19]. This profile represents a useful readout for assessing the maturation status of in vitro-generated myotubes. This is important since one caveat associated with PSC-based disease modeling is the typically embryonic nature of in vitro-generated PSC-derivatives [20–23]. Most forms of MD are adult-onset diseases, and some MD-associated proteins are not expressed at the embryonic stage. For instance, limb girdle muscular dystrophy type 2A (LGMD2A) occurs due to mutations in Calpain 3, which is not expressed in embryonic muscle [6]. To circumvent this issue, we have performed a small molecule screening in search of compounds that induce maturation of hPSC-derived myotubes. From this screening, we identified a cocktail of small molecules that can promote the maturation of PSC-derived myotubes, as shown by gene expression and functional studies [24]. In this chapter, we describe in detail the optimized protocol for the iPAX7-based differentiation of hPSC into myogenic progenitors and their subsequent differentiation into mature myotubes for in vitro studies.

2 Materials

2.1 Pluripotent Stem Cell Culture

1. mTeSR™1 maintenance medium for human ES and iPS cells (STEMCELL Technologies, 85850).
2. Nunc cell culture treated T25 flasks pre-coated with Matrigel® hESC-Qualified Matrix (Corning, 354277). Matrigel aliquots are prepared based on the protein concentration specified for each lot (following manufacturer's instructions). Each aliquot of Matrigel is diluted in 12 mL of cold DMEM/F12 medium (Corning, 15-090-CV) and 3 mL of the mixture is added to each T25 flask. Flasks are incubated for 1 h at room temperature and the mixture is removed before plating the cells.
3. Accumax cell dissociation solution (Innovative Cell Technologies, AM105).
4. Y-27632 dihydrochloride, ROCK inhibitor (Tocris, 1254) – resuspended in sterile water to make 10 mM stock.
5. Dulbecco's Phosphate-Buffered Saline (PBS) without calcium and magnesium.

2.2 Lentivirus Production and Transduction of PS Cells

1. 293T cells (ATCC, CRL-3216) for lentivirus production.
2. 293T culture medium : high glucose DMEM supplemented with 10% fetal bovine serum (FBS) and 1% penicillin-streptomycin.
3. Trypsin-EDTA (0.25%) cell dissociation reagent.
4. Falcon 60 mm tissue culture treated dishes.
5. Opti-MEM™ I reduced serum medium (Thermo Fisher Scientific, 11058021).
6. Lipofectamine™ LTX Reagent with PLUS™ Reagent (Thermo Fisher Scientific, 15338100).
7. Lentiviral transfer plasmids: pSAM2-iPAX7-IRES-GFP and FUGW-rtTA (Perlingeiro lab).
8. Lentiviral packaging plasmids: Δ8.9 and VSVG (Perlingeiro lab).
9. Nunc cell-culture treated 6-well plates.
10. 10 ml Luer-Lok Syringe.
11. 0.45 μm Cellulose acetate syringe filters.

2.3 Myogenic Differentiation of PS Cells

1. Myogenic medium: Iscove's Modified Dulbecco's Medium (IMDM) supplemented with 15% FBS, 10 % horse serum, 1% penicillin-streptomycin, 1% glutaMAX (Thermo Fisher Scientific, 35050061), 1% KnockOut Serum Replacement (KOSR) (Thermo Fisher Scientific, A3181502), 50 mg/ml ascorbic

acid and 4.5 mM monothioglycerol (MP Biomedicals, 02155723-CF).

2. Small molecules: CHIR99021 (Cayman Chemical, 13122), SB431542 (Cayman Chemical, 13031), and LDN193189 (Cayman Chemical, 19396). All small molecules are resuspended in DMSO to make working stocks.
3. Falcon 60 mm non-tissue culture treated dishes.
4. Doxycycline hydrochloride (Dox) (Sigma-Aldrich, D3447) resuspended in sterile water to make stock solution at 1 mg/ml (1000X).
5. Recombinant human FGF-basic (bFGF) (Peprotech, 100-18B) resuspended in sterile water to make a stock solution at 10 μg/ml.
6. Gelatin is resuspended in water to make 0.1% solution and autoclave sterilized for coating cell culture dishes.
7. Nunc cell culture treated T75 flasks.
8. Trypsin-EDTA (0.25%) cell dissociation reagent.
9. IKA260 orbital shaker (Diagger scientific, EF5361B).
10. FACS sorting buffer: PBS without calcium and magnesium supplemented with 10% FBS and 1% penicillin-streptomycin.
11. Falcon 5 mL round bottom polystyrene test tube, with cell strainer snap cap (Corning, 352235).
12. Freezing medium composition: 90% FBS and 10% dimethyl sulfoxide.

2.4 Differentiation of Myogenic Progenitors into Myotubes

1. Differentiation medium (DM) composition: KnockOut DMEM (Thermo Fisher Scientific, 10829018) supplemented with 20% KOSR (Thermo Fisher Scientific, A3181502), 1% penicillin-streptomycin, 1% MEM non-essential amino acids and 1% GlutaMAX (Thermo Fisher Scientific, 35050061).
2. Small molecules: SB431542 (Cayman Chemical, 13031), DAPT (Selleckchem, S2215), Dexamethasone (Cayman Chemical, 11015), and Forskolin (Cayman Chemical, 11018). All small molecules must be resuspended in DMSO to make 10 mM (1000X) stock solutions.
3. Pan-Myosin Heavy-Chain (MHC) antibody (Developmental Studies Hybridoma Bank, MF20-s).
4. Myosin Heavy-Chain – neonatal (MYH8) antibody (Leica, MHCN).
5. 4% Paraformaldehyde solution.
6. Triton X-100 diluted to 0.3% in DPBS.
7. Bovine serum albumin resuspended in DPBS to make 3% solution.

8. Alexa Fluor 555 goat anti-mouse secondary antibody (Thermo Fisher Scientific, A21424).
9. TRIzol reagent (Thermo Fisher Scientific, 15596026).
10. Purelink RNA mini kit (Thermo Fisher Scientific, 12183020).
11. SuperScript VILO cDNA synthesis kit (Thermo Fisher Scientific, 11754050).
12. Premix Ex Taq Master Mix for qPCR (Takara, RR39WR).
13. Taqman probes (Thermo Fisher Scientific): *MYH1* (Hs00428600_m1), *MYH2* (Hs00430042_m1), *MYH3* (Hs01074230_m1), *MYH7* (Hs01110632_m1), *MYH8* (Hs00267293_m1), *MYOG* (Hs01072232_m1), *CAPN3* (Hs01115989_m1), *ATP2A1* (Hs01092295_m1), *CKM* (Hs00176490_m1), *ENO3* (Hs01093275_m1), *MYF6* (Hs00231165_m1), *TNNT3* (Hs00952980_m1).

3 Methods

3.1 Generation of iPAX7-hPS Cells

1. Maintain hPS cells under standard stem cell culture conditions at low passages ($p < 20$) (*see* **Notes 1, 2** and **3**).
2. Day 0: Plate 1.2×10^6 293T cells on two 60 mm tissue culture-treated Petri dishes. Use 5 ml of 293T culture media per dish.
3. Day 1: Replace both dishes with fresh 293T media, typically 1 h before transfection. Transfect 293T cells with the iPAX7 lentiviral transfer and packaging plasmids [12] as follows: On dish 1, transfect the plasmids VSVG (2 μg), Δ8.9 (4 μg) and pSAM2-iPAX7-IRES-GFP (4 μg) and on dish 2, transfect the plasmids VSVG (2 μg), Δ8.9 (4 μg) and FUGW-rtTA (4 μg) (*see* **Note 4**). For each dish, prepare a mixture of 200 μl of OptiMEM medium, plasmid DNA (as indicated above), 8 μl of Plus reagent and then incubate at room temperature for 5 min. Following this incubation, add 8 μl of Lipofectamine LTX reagent to the mixture, mix well by pipetting up and down, and incubate at room temperature for 30 min. After the incubation, add the transfection mixture drop by drop to the 293T cells. Swirl the plate to evenly distribute the transfection mixture and incubate the plate at 37 °C.
4. Day 2: Successful 293T cells transfection can be assessed after 24 h by observing green fluorescent 293T cells on dish 1 using a fluorescence microscope. Replace with fresh 293T cell media. This will be used to collect viral particles. Important: Make sure to follow proper biosafety protocols when handling transfected 293T cells as viral particles are produced and secreted in the culture media. Dissociate hPS cells at 80–90% confluency using Accumax. Count and plate 2×10^5 hPS cells to be transduced

on a Matrigel-coated well of a 6 well plate using hPS cell media supplemented with 10 μM ROCK inhibitor, Y-27632.

5. Day 3: Using a 10 ml syringe (no needle attached to it), collect the virus-loaded supernatant from dishes 1 and 2 so that the supernatants mix with each other. Attach a 0.45 μm filter to the end of the syringe and filter the collected supernatant onto a 50 ml tube. Replenish dish 1 and 2 with fresh 293T cell media for repeating transduction. Aspirate off the media from the hPS cells and add 5 ml of filtered viral supernatant to the well. Spinfect (centrifuge) the plate at 2500 rpm, 30 °C, for 1.5 h. Carefully aspirate off the media and replace with fresh hPS cell media (non-viral). Place transduced cells back in the incubator.
6. Day 4: Repeat the steps in 3.1.5 to further enhance the transduction efficiency.
7. When transduced cells reach 80–90% confluency, expand the cells on the preferred dish size following hPS cell standard culture practices and freeze aliquots to establish a stock of transduced cells (hereafter referred as iPAX7-hPS cells. Furthermore, plate an aliquot of transduced cells onto each of the two Matrigel-coated wells of a 12- or 24-well plate. These cells will be used to assess the efficiency of transduction.
8. The next day, supplement the culture media of one of the wells with 1 μg/ml doxycycline (Dox) and the other well with the vehicle. Incubate cells overnight.
9. The following day, collect the cells treated with Dox or vehicle, and by flow cytometry, analyze the percentage of cells expressing GFP, which shows the efficiency of the transduction procedure (*see* **Note 5**). Use vehicle-treated cells to properly set the gates for GFP signal.

3.2 Myogenic Differentiation of iPAX7-hPS Cells

1. The steps in the differentiation protocol are summarized in Fig. 1. Day 0: Dissociate iPAX7-hPS cells using Accumax (*see* **Note 3**), count and plate 1×10^6 cells on a 60 mm petri dish (*see* **Notes 6** and **7**) using 5 ml of mTeSR1 media supplemented with 10 μM Y-27632. Incubate for 2 days on an orbital shaker at 60 rpm at 37 °C.
2. Day 2: Verify the formation of well-rounded embryoid bodies (EBs) using a standard bright field microscope. Swirl the dish to gather the EBs toward the center of the dish and carefully remove the culture media by aspirating from the periphery of the dish without disturbing the EBs. Add 5 ml of myogenic media supplemented with 10 μM GSK3β inhibitor, CHIR99021. Place the EBs back on the shaker and incubate for 2 days.
3. Day 4: Remove the culture media and wash EBs with 5 ml of PBS, following the technique described above (*see* **Note 8**).

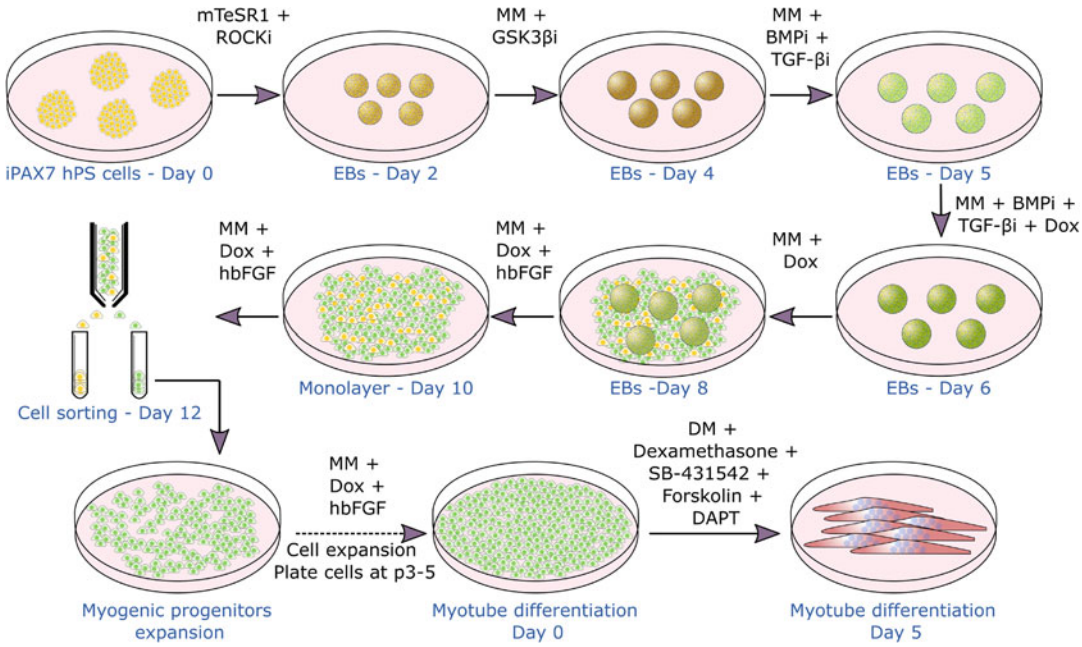

Fig. 1 Myogenic differentiation of human pluripotent stem cells through conditional PAX7 expression. This scheme shows the steps involved in the derivation of myogenic progenitors from human pluripotent stem (PS) cells. PS cells are cultured in non-adherent conditions in agitation to promote the formation of EBs. From day 0 to day 6, small molecules are used to promote the transition towards a paraxial mesoderm-like state at Day 4 (resulting in expression of *MSGN1* and *TBX6*) and a somite-like state at Day 6 (resulting in expression of *MEOX1* and *PAX3*). PAX7 expression induction starts at Day 5 with the addition of Dox and remains throughout the protocol. At Day 12, cells expressing PAX7, as evidenced by co-expression of GFP or surface markers, are sorted and expanded as myogenic progenitors. To induce terminal differentiation, myogenic progenitors are grown to 100% confluency and switched to a low-nutrient differentiation medium supplemented with small molecules and incubated for 5 days to generate myotubes

Add 5 ml of myogenic media supplemented with 200 nM BMP inhibitor, LDN193189, and 10 μM TGFβ inhibitor, SB431542. Place the EBs back on the shaker and incubate on agitation.

4. Day 5: Without replacing the culture media, simply add 5 μl of 1 μg/μl Dox (final concentration of 1 μg/ml) to the EBs. Keep the plate on agitation.
5. Day 6: Remove the culture media and wash the EBs with 5 ml of PBS, following the technique described above (*see* **Note 9**). Add 5 ml of myogenic media supplemented with 1 μg/ml Dox (withdraw LDN193189 and SB431542 treatment). Return the EBs to incubation in agitation for 2 days.
6. Day 8: The EBs will now be plated for expansion in monolayer. Collect the EBs by gently swirling the dish and pipetting them up from the middle of the plate using a serological pipette. Transfer the EBs to a 15 ml conical tube and wait until the EBs settle at the bottom of the tube. Aspirate off the supernatant

and add 4 ml of fresh myogenic media supplemented with 1 μg/ml Dox and 5 ng/ml human basic fibroblast growth factor (hbFGF). After gently resuspending EBs with the supplemented myogenic media, transfer 0.5 ml of the EBs' suspension (approximately 1/8 of the EB volume) onto a gelatin-coated T75 flask (*see* **Note 10**) and add 14.5 ml of Dox/hbFGF supplemented media so that the total media volume in the flask is 15 ml. From this step on, cells are cultured without agitation. Right before placing the flask in the incubator, be sure to properly swirl the flask so that the EBs are evenly and sparsely distributed. Incubate cells at 37 °C for 2 days.

7. Day 10: Verify that cells started expanding in monolayer from the periphery of the attached EBs. Replace culture media with fresh Dox/hbFGF supplemented myogenic media. Incubate cells for 2 days.
8. Day 12: Aspirate off culture media and wash the cells with PBS. Add 5 ml of 0.25% trypsin-EDTA and incubate cells for 5 min at 37 °C. Tap the side of the flask until the clumps of cells are visibly detached from the flask. Gently, pipette the cells up and down a few times with a 5 ml pipette to promote dissociation and collect the cells by adding 10 ml of fresh myogenic media, and then transfer the whole cell suspension into a 15 ml conical tube. Centrifuge the cells at 300 g for 5 min and carefully aspirate off the supernatant, resuspending the cells with 10 ml of PBS. Filter the cells through a sterile 35 μm cell strainer to remove the remaining clumps and count the cells in the filtrate. Centrifuge the filtrate at 300 g for 5 min and resuspend with an adequate volume of sorting buffer (*see* **Note 11** and **12**). Transfer the suspension of cells to a test tube with cell strainer snap cap by filtering the volume through the cap and place the cells on ice. Perform cell sorting of PAX7+ living cells based on GFP expression or cell surface markers staining [25], and collect the sorted cells in a tube containing 5 ml of fresh myogenic media supplemented with 10 μM ROCK inhibitor, 5 ng/ml hbFGF and 1 μg/ml Dox. Centrifuge the collected cells at 300 g for 5 min, resuspend them with fresh supplemented myogenic media (ROCK inhibitor, hbFGF, and Dox), and plate the cells onto a flask or plate pre-coated with 0.1% gelatin. The volume of supplemented myogenic media used for resuspension and the size of the culture vessel used for subsequent plating depend on the number of PAX7+ sorted cells (*see* **Note 13**). From this step on, we refer to the PAX7+ sorted cells as myogenic progenitors (*see* **Note 14**).
9. Day 13: Replace the culture media with fresh myogenic media supplemented with 5 ng/ml hbFGF and 1 μg/ml Dox. Repeat this step every other day and sub-culture the cells once they have reached a 90% confluency (usually every 3 to 4 days, *see* **Notes 15** and **16**).

3.3 Optimized Protocol for Enhanced Myotube Differentiation/ Maturation

1. Start with a 90% confluent myogenic progenitors' culture (*see* **Note 17**). Sub-culture the cells following the procedure described above and count the harvested cells. Plate myogenic progenitors on gelatin-pre-coated wells (*see* **Note 18**) at a density of 4×10^4 cells per cm^2 of the surface area using myogenic media supplemented with 5 ng/ml hbFGF and 1 μg/ml Dox and place the cells in the incubator.
2. Once cells have reached 100% confluency (usually 3 days after plating), aspirate off the media and wash the cells with PBS. Induce myotube differentiation by switching to a low nutrient differentiation media (DM) supplemented with a cocktail of small molecules (SB-431542, S; DAPT, D; Dexamethasone, D; Forskolin, F; 10 μM each; *see* **Note 19**). Place the cells in the incubator for 5 days.
3. On day 5, verify the presence of differentiated myotubes under a light microscope and use the cells for downstream analysis (*see* **Note 20**). If desired, myotubes might be left for more than 5 days in culture; however, depending on the density of differentiated myotubes and whether they show spontaneous contraction, it is possible that the myotubes are more prone to detachment after day 5. This can be ameliorated if wells are coated with Matrigel instead of gelatin. If myotubes are left in culture for more than 5 days, replenish with fresh DM without small molecule supplement every 3 days after day 7. Importantly, to remove liquids from the myotubes culture (e.g. cell media or PBS), aspirate off the volume slowly and gently to avoid myotube detachment.
4. For immunostaining analysis, remove the media and wash the myotubes with PBS very gently to avoid detaching the myotubes. Fix the myotubes with 4% PFA in PBS and incubate for 15 min at RT. Gently, remove the PFA, wash with PBS, and permeabilize the myotubes by adding 0.3% Triton X-100 in PBS and incubating for 15 min at RT. Remove the permeabilization solution, wash with PBS, and add a blocking solution made of 3% BSA in PBS. Incubate for 30 min at RT. Add a primary antibody against pan-MyHC in PBS at proper dilution (we suggest starting at a 1:50 dilution). Incubate the myotubes overnight at 4 °C. The following day, remove the primary antibody solution gently and wash the cells 3X by incubating with PBS for 5 min in no agitation at RT. Add secondary antibody labeled with a fluorochrome of choice, specific against the host species of the primary antibody and diluted in PBS as appropriate (we suggest starting at a 1:500 dilution). Incubate the cells in dark for 1 h at RT. Repeat the PBS washes as done for the primary antibody. Counterstain the nuclei by adding the reagent of choice (e.g. DAPI). Visualize the cells in a fluorescence microscope. Myotubes are positively stained for pan-MyHC and display an elongated shape. In addition, to verify the maturation status of resulting myotubes, we suggest

staining with an antibody against the neonatal isoform of MyHC (MYH8) using the protocol described above. Myotubes derived with small molecule treatment should uniformly express neonatal MyHC protein.

5. For RT-qPCR analysis, we recommend cell lysis and total RNA isolation using TRIzol reagent (use 1 ml volume per 10 cm^2 surface area of cell culture dish). After cell lysis, extract total RNA using purelink RNA mini kit following manufacturer's instructions. Perform reverse transcription of the total RNA using SuperScript VILO cDNA synthesis kit. For this, use 100–250 ng of total RNA, 1 μl of 5X reaction mix, 0.5 μl of 10X enzyme mix, and make up the total volume to 5 μl with nuclease-free water. Incubate the reaction at 25 °C for 10 min, followed by 42 °C for 60 min, and terminate the reaction at 85 °C for 5 min. For qPCR analysis, we recommend using Taqman gene expression assays. For each qPCR reaction, use RT sample volume corresponding to 10 ng of total RNA, 0.5 μl of Taqman probe, 5 μl of 2X qPCR master mix, and make up the total volume to 10 μl with nuclease-free water. Perform qPCR analysis in the equipment of choice, determine the C_t values for the gene of interest (GOI) and for housekeeping gene (HKG). Normalize the C_t value of GOI with that of HKG (2^ -(C_t GOI- C_t HKG)).

4 Notes

1. While we have successfully differentiated several patient-specific hiPS cells from various muscular dystrophies [24], it is important to consider that the pathology itself might influence the efficiency of myogenic differentiation if the disease phenotype is present either at the pluripotent state or during the course of the differentiation procedure.
2. It is important to first verify the chromosomal stability (karyotype) and pluripotency (germ layers-derivation) of the PS cell line to be used. Note that poor hPS cell culture practices (e.g. inadequate culture confluency maintenance) might lead to spontaneous differentiation, which compromises the myogenic differentiation efficiency.
3. The optimal reagents used for PS cell culture (including cell media, dish-coating, and dissociation reagents) might vary among cell lines. For instance, hiPS cells may be more compatible with the culture conditions used during cell reprogramming. In this protocol, we use mTeSR1 medium, Matrigel-coated dishes, and Accumax (for single cell-like dissociation) as the standard reagents for cell culture.

4. We recommend the use of Lipofectamine LTX with Plus reagent for an efficient 293 T transfection.
5. Although the efficiency of transduction can be assessed by fluorescence microscopy on cells incubated with Dox compared to vehicle, we strongly suggest doing flow cytometry analysis instead. Optimal transduction efficiency will be at least 30–40% GFP^+ cells.
6. The medium volume used in this protocol was calculated based on a starting 60 mm petri dish. If a different petri dish size is used, the volume must be adjusted accordingly. Make sure to use non-treated non-coated Petri dishes as EBs might attach to the plastic otherwise.
7. An additional culture with non-induced PAX7 cells can be used to properly set the GFP gates when performing cell sorting of myogenic progenitors.
8. The efficiency of mesoderm-like fate induction at day 4 can be assessed, if desired, by analyzing a sample of EBs for *MSGN1*, *TBX6,* and *T* transcripts by quantitative RT-PCR. If desired, include a sample of non-treated EBs as control.
9. The efficiency of somite-like fate induction at day 6 can be assessed, if desired, by analyzing a sample of EBs for *FOXC2, MEOX1, PAX3,* and *TCF15* transcripts by quantitative RT-PCR. If desired, include a sample of non-treated EBs as control.
10. To pre-coat the flasks or dishes with gelatin, simply add a sterile solution of 0.1% gelatin in water to the desired vessel in a volume similar to the one used for culture media. Incubate the flask at 37 °C for 20 min. Remove the gelatin solution right before plating the cells in the flask.
11. We recommend resuspending the cells with 250 μl of sorting buffer per 1×10^6 cells counted.
12. PAX7+ cells are sorted based on their GFP expression. In addition, in order to assess cell viability during sorting, we strongly recommend the addition of propidium iodide (PI) to the sorting buffer.
13. Use 15 ml of supplemented myogenic medium for 2×10^6 sorted cells to be plated onto a T-75 flask. Scale the medium volume and the vessel size accordingly. We have observed that when cells are plated at a low-density, the efficiency of myotube differentiation decreases.
14. Myogenic progenitors display a triangular shape homogeneously throughout the culture. From our experience, when the cells display a fibroblastic-like elongated shape or a prominent rounded shape, it is possible that the terminal differentiation efficiency has decreased. This can happen due to

instability of the pluripotent cell line used, low-density seeding of viable sorted myogenic progenitors, or technical mistakes along the protocol.

15. Myogenic progenitors are highly proliferative; therefore, cells can be expanded, and aliquots can be frozen at each passage to generate myogenic progenitor stocks. We recommend freezing aliquots of at least 5×10^5 cells at each passage for the first 3 passages.
16. Myogenic progenitors are cultured using myogenic media supplemented with 5 ng/ml hbFGF and 1 μg/ml Dox. We strongly suggest adding the supplements fresh when using the media rather than storing the supplemented media. Cell dissociation is performed by incubating cells with trypsin for 5 min at 37 °C. When splitting the cells, we recommend a ratio of 1:5 to 1:10 from a 90% confluent culture.
17. Myotube differentiation is optimal when myogenic progenitors are at passages 3 to 5 (post-cell sorting). Earlier or later passages might lead to inconsistent or decreased differentiation efficiency.
18. Instead of gelatin, other substrates might be used to promote myotube attachment to the surface (e.g. Matrigel).
19. During terminal differentiation, the cells remain untouched in the incubator for 5 days. Therefore, we suggest adding an extra 20% of the supplemented-DM volume. Although non-supplemented DM is itself useful to induce myotube differentiation, we have recently reported that adding the cocktail of SDDF small molecules significantly improves the efficiency of differentiation and enhances the subsequent maturation of myotubes [24]. Furthermore, we have found that this protocol is useful in enhancing the differentiation of patient-specific iPS cell lines displaying low myotube differentiation efficiency in the presence of standard culture conditions (non-supplemented differentiation medium). This cocktail has been proven to work in transgene-free protocols as well [24].
20. To assess myotube differentiation, we recommend immunostaining for pan-myosin heavy chain (pan-MyHC) in myotubes. To further verify the maturation status of the myotubes, we recommend analyzing the levels of MYH1, MYH2, MYH3, MYH7, MYH8, MYOG, CAPN3, ATP2A1, CKM, ENO3, MYF6 and TNNT3 genes at the mRNA level through RT-qPCR analysis. With small-molecule treatment, the listed genes should be expressed at higher levels at the mRNA level than otherwise in the myotubes. Only some of these genes might be significantly expressed at the protein level in the myotubes.

Acknowledgments

This work was supported by NIH grants R01 AR071439 and AR055299 (R.C.R.P.). We thank James Kiley for helpful commentaries on this protocol.

References

1. Mercuri E, Bonnemann CG, Muntoni F (2019) Muscular dystrophies. Lancet 394(10213):2025–2038
2. Ng R, Banks GB, Hall JK et al (2012) Animal models of muscular dystrophy. Prog Mol Biol Transl Sci 105:83–111
3. Thomson JA, Itskovitz-Eldor J, Shapiro SS et al (1998) Embryonic stem cell lines derived from human blastocysts. Science 282(5391): 1145–1147
4. Takahashi K, Yamanaka S (2006) Induction of pluripotent stem cells from mouse embryonic and adult fibroblast cultures by defined factors. Cell 126(4):663–676
5. Takahashi K, Tanabe K, Ohnuki M et al (2007) Induction of pluripotent stem cells from adult human fibroblasts by defined factors. Cell 131(5):861–872
6. Selvaraj S, Dhoke NR, Kiley J et al (2019) Gene correction of LGMD2A patient-specific iPSCs for the development of targeted autologous cell therapy. Mol Ther 27(12):2147–2157
7. Young CS, Hicks MR, Ermolova NV et al (2016) A single CRISPR-Cas9 deletion strategy that targets the majority of DMD patients restores Dystrophin function in hiPSC-derived muscle cells. Cell Stem Cell 18(4):533–540
8. Turan S, Farruggio AP, Srifa W et al (2016) Precise correction of disease mutations in induced pluripotent stem cells derived from patients with limb girdle muscular dystrophy. Mol Ther 24(4):685–696
9. Choi IY, Lim H, Estrellas K et al (2016) Concordant but varied phenotypes among Duchenne muscular dystrophy patient-specific myoblasts derived using a human iPSC-based model. Cell Rep 15(10):2301–2312
10. Wang Y, Hao L, Wang H et al (2018) Therapeutic genome editing for myotonic dystrophy type 1 using CRISPR/Cas9. Mol Ther 26(11): 2617–2630
11. Goudenege S, Lebel C, Huot NB et al (2012) Myoblasts derived from normal hESCs and dystrophic hiPSCs efficiently fuse with existing muscle fibers following transplantation. Mol Ther 20(11):2153–2167
12. Darabi R, Arpke RW, Irion S et al (2012) Human ES- and iPS-derived myogenic progenitors restore DYSTROPHIN and improve contractility upon transplantation in dystrophic mice. Cell Stem Cell 10(5):610–619
13. Tedesco FS, Gerli MF, Perani L et al (2012) Transplantation of genetically corrected human iPSC-derived progenitors in mice with limb-girdle muscular dystrophy. Sci Transl Med 4(140):140ra89
14. Shelton M, Metz J, Liu J et al (2014) Derivation and expansion of PAX7-positive muscle progenitors from human and mouse embryonic stem cells. Stem Cell Reports 3(3): 516–529
15. Chal J, Oginuma M, Al Tanoury Z et al (2015) Differentiation of pluripotent stem cells to muscle fiber to model Duchenne muscular dystrophy. Nat Biotechnol 33(9):962–969
16. Hicks MR, Hiserodt J, Paras K et al (2018) ERBB3 and NGFR mark a distinct skeletal muscle progenitor cell in human development and hPSCs. Nat Cell Biol 20(1):46–57
17. Wu J, Matthias N, Lo J et al (2018) A myogenic double-reporter human pluripotent stem cell line allows prospective isolation of skeletal muscle progenitors. Cell Rep 25(7): 1966–81 e4
18. Azzag K, Ortiz-Cordero C, Oliveira NAJ et al (2020) Efficient engraftment of pluripotent stem cell-derived myogenic progenitors in a novel immunodeficient mouse model of limb girdle muscular dystrophy 2I. Skelet Muscle 10(1):10
19. Schiaffino S, Rossi AC, Smerdu V (2015) Developmental myosins: expression patterns and functional significance. Skelet Muscle 5:22
20. Abdelalim EM, Emara MM (2015) Advances and challenges in the differentiation of pluripotent stem cells into pancreatic beta cells. World J Stem Cells 7(1):174–181
21. Aigha I (2016) Raynaud C (2016) maturation of pluripotent stem cell derived cardiomyocytes: the new challenge. Glob Cardiol Sci Pract 1:e201606
22. Chen C, Soto-Gutierrez A, Baptista PM et al (2018) Biotechnology challenges to in vitro

maturation of hepatic stem cells. Gastroenterology 154(5):1258–1272

23. Jiwlawat N, Lynch E, Jeffrey J et al (2018) Current Progress and challenges for skeletal muscle differentiation from human pluripotent stem cells using transgene-free approaches. Stem Cells Int 2018:6241681
24. Selvaraj S, Mondragon-Gonzalez R, Xu B et al (2019) Screening identifies small molecules that enhance the maturation of human pluripotent stem cell-derived myotubes. elife 8
25. Magli A, Incitti T, Kiley J et al (2017) PAX7 targets, CD54, integrin alpha9beta1, and SDC2, allow isolation of human ESC/iPSC-derived myogenic progenitors. Cell Rep 19(13):2867–2877

Chapter 11

Differentiation of Human Fetal Muscle Stem Cells from Induced Pluripotent Stem Cells

Masae Sato, Mingming Zhao, and Hidetoshi Sakurai

Abstract

Most muscular dystrophies are the result of genetic disorders. There is currently no effective treatment for these progressive diseases except palliative therapy. Muscle stem cells with potent self-renewal and regenerative potential are considered a target for treating muscular dystrophy. Human induced pluripotent stem cells have been expected as a source of MuSCs because of their infinite proliferation potential and less immunogenicity. However, the generation of engraftable MuSCs from hiPSCs is relatively difficult and encounters low efficiency and reproducibility. Here, we introduce a transgene-free protocol of hiPSCs differentiating into fetal MuSCs by identifying them as MYF5-positive cells. Flow cytometry analysis detected around 10% of MYF5-positive cells after 12 weeks of differentiation. Approximately 50 ~ 60% of MYF5-positive cells were positively identified using Pax7 immunostaining. This differentiation protocol is expected to be useful for not only the establishment of cell therapy but also the future drug discovery using patient-derived hiPSCs.

Key words Muscle stem cells, Skeletal muscle cell, Human iPSC, Myogenic differentiation, MYF5

1 Introduction

Most of the inherited muscular diseases such as Duchenne muscular dystrophy (DMD) [1] have been encountering difficulty in the development of curative therapy [2]. Even though several therapeutic options have been studied, cell therapy using human muscle stem cells (MuSCs) with self-renewal and regenerative potential is considered a potent therapy for these intractable muscle diseases. However, their clinical utility has been restricted by the limited cell numbers, insufficient engraftment after transplantation, and a high risk of immune rejection accompanying treatments with allogeneic cells. Human induced pluripotent stem cells (hiPSCs) have been expected as a source of MuSCs because of their infinite proliferation potential and less immunogenicity [3].

Atsushi Asakura (ed.), *Skeletal Muscle Stem Cells: Methods and Protocols*, Methods in Molecular Biology, vol. 2640, https://doi.org/10.1007/978-1-0716-3036-5_11,

Previous reports showed a therapeutic effect of myogenic progenitors derived from hiPSCs toward DMD model mouse [4] and α-Sarcoglycan deficient mouse [5]. However, both studies used the lentiviral transduction system to induce myogenic progenitors from hiPSCs, which has the potential risk of tumorigenicity.

Recently, several reports have demonstrated transgene-free protocols for myogenic progenitor differentiation recapitulating developmental stages from hiPSCs [6, 7]. These protocols induced engraftable myogenic progenitors from hiPSCs without genetic modification, which seem to be safer than previous transgene-dependent protocols. Nevertheless, hiPSC-derived myogenic progenitors generated by these published differentiation protocols demonstrated a low transplantation efficiency in vivo [8]. Instead of these myogenic progenitors from the early embryonic development stage, MuSCs from the fetal stage were expected to be suitable cells for cell therapy because the higher transplantation efficiency and the greater expansion with stemness have been reported in fetal MuSCs than in adult MuSCs [9]. We have recently reported a new protocol for transgene-free differentiation of hiPSCs into fetal MuSCs, which were identified as MYF5-tdTomato positive cells [10]. Fetal MuSCs induced by this protocol showed 50% Pax7+ cells and a high transplantation efficiency in the DMD-null/NSG DMD model mouse [10].

Here, we describe the precise protocol of hiPSCs differentiating into fetal MuSCs. This protocol provides details of the passage method at the initial stage of mesodermal differentiation, the typical cell morphologies, and the stepwise medium exchange toward the myotubes maturation and the induction of fetal MuSCs. We also demonstrate the method of fetal MuSCs validation by the myogenic marker expression assessed by flow cytometry and immunocytochemistry.

2 Materials

2.1 HiPSC Lines and Maintenance of Feeder-Free Culture

1. HiPSC line (201B7) was provided by Dr. Shinya Yamanaka [3]. To identify the fetal MuSCs, we generated a MYF5-tdTomato reporter cell line using the 201B7 cell line [10]. This differentiation protocol should be applicable generally to other hiPSC lines. Please feel free to contact us if you would like to use the 201B7-MYF5-tdTomato hiPSC clone.
2. StemFit (AJINOMOTO, Stemfit AK02N medium).
3. iMatrix-511 (Nippi, 892001/892002).
4. Y-27632 (Nacalai Tesque, 18188-04).
5. Accutase (Nacalai Tesque, 12679-54).

6. Penicillin-Streptomycin Mixed Solution.
7. Dulbecco's Phosphate Buffered Saline (D-PBS).
8. Trypan Blue Solution, 0.4%.

2.2 Differentiation of Fetal Skeletal Muscle Stem Cells

1. Matrigel Growth Factor Reduced Basement Membrane Matrix (Matrigel) (Corning, 356231).
2. Y-27632 (Nacalai Tesque, 18188-04).
3. Accutase (Nacalai Tesque, 12679-54).
4. Dulbecco's Phosphate Buffered Saline (D-PBS).
5. Trypan Blue Solution, 0.4%.
6. CDMi basal medium (expiry date is 1 month from manufacture date).

   To prepare 500 mL of CDMi basal medium, mix 250 mL of 1× Iscove's Modified Dulbecco's Medium (IMDM), 250 mL of 1× F-12 Nutrient Mixture (Ham's) with L-Glutamine, 5 g of bovine serum albumin (BSA) (Sigma-Aldrich, A9418-100G), 5 mL Penicillin-Streptomycin Mixed, 5 mL of Chemically Defined Lipid Concentrate (Gibco, 11905-031), 5 mL of Insulin-Transferrin-Selenium Supplement (Gibco, 41400-045), and 19.7 μL of 1-Thioglycerol (Sigma-Aldrich, M6145-25ML) and then filter the mixture by 0.22 μm filter.
7. SF-O3 basal medium (expiry date is 3 months from manufacture date).

   To prepare 1000 mL SF-O3 basal medium, make 1000 mL of S-Clone SF-O3 (SEKISUI CHEMICAL CO., LTD. 521652) with 5 mL Penicillin-Streptomycin Mixed, add 2 g of BSA (Sigma-Aldrich, A9418-100G) according to the manufacturer's instructions, and then filter the mixture by 0.22 μm filter.
8. Dulbecco's Modified Eagle Medium-high glucose (DMEM) basal medium (expiry date is 4 weeks from manufacture date).

   To prepare DMEM basal medium, mix 500 mL of DMEM, 2.5 mL of Penicillin-Streptomycin Mixed Solution, and 5 mL of 200 mM-L-glutamine.
9. Add the appropriate supplements to prepare a differentiation-inducing medium (*see* Table 1). Store the supplemented media at 4 °C in a dark chamber.
10. SB431542.
11. CHIR99021.
12. Recombinant Human IGF-I.
13. Recombinant Human HGF.
14. Recombinant Human Fibroblast Growth Factor 2 (bFGF).
15. 2-Mercaptoethanol.
16. Horse Serum, Heat inactivated.

Table 1
Protocol for medium preparation used for recapitulating the developmental stages to generate Fetal MuSCs from iPSCs

Medium A	CDMi basal medium	–
	CHIR	10 uM
	SB	5 uM
Medium B-1	SF-O3 basal medium	–
	IGF-1	10 ng/mL
	HGF	10 ng/mL
	bFGF	10 ng/mL
	2-ME	0.1 mM
Medium B-2	SF-O3 basal medium	–
	IGF-1	10 ng/mL
	2-ME	0.1 mM
Medium B-3	SF-O3 basal medium	–
	IGF-1	10 ng/mL
	HGF	10 ng/mL
	2-ME	0.1 mM
Medium C	DMEM basal medium	–
	SB	10 uM
	IGF-1	10 ng/mL
	House serum	2%
	L-glutamine	–
	2-ME	0.1 mM

2.3 Cell Preparation for FACS Analysis and Sorting

1. Detachment buffer: To prepare 10 mL detachment buffer, mix 9 mL of Dulbecco's Modified Eagle Medium-high glucose (DMEM), 50 μL of Collagenase G (Meiji Seika Pharma Co., Ltd., COLGS), 5 μL of Collagenase H (Meiji Seika Pharma Co., Ltd., COLHS), and 1 mL of 3 mg/mL Dispase I (Godo Shusei, 386-02281).
2. HBSS buffer: To prepare 1000 mL HBSS buffer, mix 900 mL of MILLIQ water, 100 mL of ×10 Hanks' Balanced Salt Solution (HBSS), and 10 g of bovine serum albumin (BSA).
3. Hoechst 33342.
4. FACS Aria (BD Biosciences) and FlowJo_v10.6.1.

2.4 Immunocytochemistry

1. Primary Antibody: PAX7: mouse monoclonal antibody (1:100, Developmental Studies Hybridoma Bank, AB 528428); MYOD1: rabbit monoclonal antibody (1:500, Abcam, ab133627).
2. Secondary Antibody: Alexa Fluor 488 conjugated goat-anti-mouse IgG1 (1:500, Invitrogen, A21121); Alexa Fluor 568 conjugated goat-anti-Rabbit IgG (1:500, Invitrogen, A11036).

3. 4%-Paraformaldehyde Phosphate Buffer Solution (PFA).
4. Smear Gel (Geno Staff, SG-01).
5. Washing buffer: to prepare 500 mL of washing buffer, mix 500 mL of Dulbecco's Phosphate Buffered Saline (D-PBS) and add 1 mL of Triton X- 100.
6. Blocking One (Nacalai Tesque, 03953-95).
7. 4′,6-Diamidino-2-Phenylindole, Dihydrochloride (DAPI).
8. BZ-X700 microscope (Keyence) and BZ-X analyzer software (Keyence).

3 Methods

3.1 Feeder-Free Culture for hiPSCs

Although we have many methods to maintain hiPSCs, a feeder-free culture system is an easy and reproducible way to culture hiPSCs with high quality for the following research and clinical application. For routine maintenance, passage the cells every 7 days using single-cell dissociation and seed at a density of 1.0×10^4 cells/well (6-well plate) (*see* **Note 1**). Culture cells in StemFit supplement with 10 μM Y-27632 (abbreviated as StemFit + Y) until 48 h after passage. Change the medium to 1.5 mL/well (6-well plate) of fresh StemFit every 2 days for the former 4 days, and every day for the latter 3 days (*see* **Note 1**). Details of the feeder-free culture method have been previously reported [11]. When the hiPSCs (6-well plate; 9.4 cm^2) reach 70 ~ 80% confluence, cells should be passaged.

1. To prepare the laminin-coated 6-well plates, add 1.5 mL of D-PBS and 10 μL (5 μg) of iMatrix511 (coating: 0.5 μg/cm^2) to each well. Mix well immediately and incubate at 37 °C in 5% CO_2 for at least 60 min.
2. Aspirate iMatrix511 suspension from the laminin-coated dish, then add 1.5 mL of StemFit + Y to the wells, and incubate at 37 °C in 5% CO_2 until cell seeding.
3. Aspirate the medium from the well of the hiPSCs, which need to be passaged, and gently wash the cell surface with 1 mL of D-PBS.
4. Aspirate D-PBS, then add 0.5 mL of Accutase to the well, and spread it evenly across the cell surface. Incubate the plate at 37 °C in 5% CO_2 for 5 min.
5. Gently detach the cells from the wells using a P1000 pipette while breaking up cell clusters. Add 2.5 mL of StemFit + Y to the well and gently mix by P1000 pipetting.
6. Collect the cell suspension in a 15 mL sterile tube.
7. Centrifuge the cell suspension at 160 × *g* at 4 °C for 5 min.

8. Discard the supernatant, resuspend the cell pellet in StemFit + Y, and count the cells with Trypan Blue staining.
9. Plate 1.0×10^4 living cells (1.1×10^3 cells/cm^2) in one well, then rock the plate gently to ensure even distribution immediately.
10. Incubate the plate at 37 °C, 5% CO_2 for 2 days.
11. After 2 days of incubation (day 2), change the medium to 1.5 ml of StemFit without Y-27632. Thereafter, change the medium with fresh StemFit on day 4, day 5, and day 6.

3.2 Differentiation of hiPSCs into Fetal MuSCs

For fetal MuSCs induction from hiPSCs, differentiation steps are divided into four steps: 1. cell plating step, 2. mesodermal differentiation step, 3. myogenic differentiation step, and 4. muscle maturation step (*see* Fig. 1). In the first step "cell plating," hiPSCs are seeded onto Matrigel-coated plate in Stemfit. Then the cells proliferate for 3 days. In the second step "mesodermal differentiation," treatment of Wnt agonist and TGFβ inhibitor induces paraxial mesoderm differentiation followed by dermomyotome differentiation. During the second step, cells are passaged twice on day 7 and day 14, since cells become fully confluent in this step. In the third step "myogenic differentiation," myogenic differentiation is initiated by the withdrawal of Wnt agonist and TGFβ inhibitor. Then, SF-O3 basal medium supplemented with bFGF, HGF, and IGF-1 induces myogenic differentiation from dermomyotome-like cells for 3 weeks. A number of embryonic myocytes can be

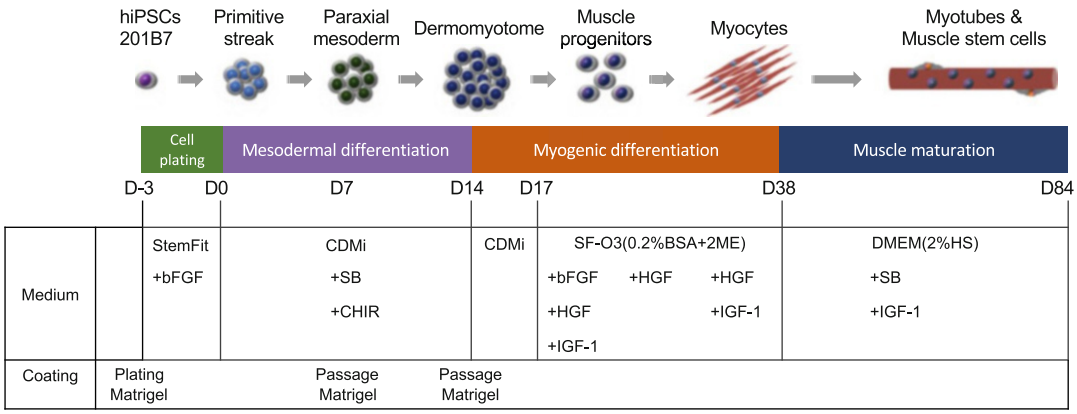

Fig. 1 Timeline of the differentiation protocol. The schematic diagram shows the state of cells at each differentiation stage and the composition of the medium and the coating material. Induce dermomyotome lineage by CDMi medium supplemented with SB431542 (SB) and CHR99021(CHIR) between days 0 and 14. Cells are cultured in CDMi medium from day 14 to day 17. Replace the medium with SF-03 medium containing bFGF, HGF, and IGF-1 to promote myogenic differentiation from dermomyotome from day 17. Then continue to replace the appropriate medium indicated in Table 1 up to day 38. After day 38 when infant myotubes are formed, change the medium to DMEM containing horse serum, SB, and IGF-1 which promotes myotube maturation

observed in this step. We previously reported that MYF5 is expressed in the early (4 weeks) and late stages (12 weeks) of differentiation induction [10]. In the early stages of development, MYF5-positive cells are round cells and considered to be skeletal muscle progenitor cells rather than fetal MuSCs. MYF5-tdTomato positive cells are confirmed around days 21–28 when the induction of skeletal muscle differentiation is proceeding normally (*see* Fig. 3).

In the final step "muscle maturation," embryonic myocytes become mature in a conventional muscle differentiation medium composed of low-concentration horse serum. Multinucleated myotubes can be observed after day 50 of differentiation, and MYF5-positive fetal MuSCs can be detected after day 70 of differentiation [10].

3.2.1 Day −3: Cell Plating

1. Prepare hiPSCs at approximately 70 ~ 80% confluency on a 6-well plate.
2. To prepare a Matrigel-coated 6-well plate, dilute Matrigel in StemFit (1:50 ratio), then add 1 mL of this 1:50 Matrigel solution to one well. Incubate at 37 °C, 5% CO_2 for at least 2 h.
3. After 2 h, remove the 1:50 Matrigel solution from the Matrigel-coated wells, then add 1.5 mL of StemFit + Y. Incubate the plate at 37 °C, 5% CO_2 until cell seeding.
4. Aspirate the medium from the 70 ~ 80% confluency hiPSCs culture dish and gently wash the well with 1 mL of D-PBS.
5. Aspirate D-PBS, then add 0.5 mL of Accutase to the hiPSCs culture dish, and spread it evenly across the cell surface. Incubate at 37 °C, 5% CO_2 for 5 min.
6. Gently detach the cells from the well using a P1000 pipette while breaking up cell clusters. Add 2.5 mL of StemFit and mix gently by using a P1000 pipette.
7. Collect the cell suspension to a 15 mL sterile tube.
8. Centrifuge the cell suspension at 160 × *g* at 4 °C for 5 min.
9. Discard the supernatant, resuspend the cell pellet in StemFit + Y, and count the cells with Trypan Blue staining.
10. Plate 2.0×10^4 living cells (2.1×10^3 cells/cm^2) in a well (*see* **Note 2**), then rock the plate gently to ensure even distribution immediately.
11. Incubate the plate at 37 °C, 5% CO_2 for 2 days.
12. After 2 days, change the medium to 1.5 mL of StemFit without Y-27632.

3.2.2 Day 0: Initiate Mesodermal Differentiation

1. Prepare Medium A as Table 1. Warm-up Medium A at room temperature for 20–30 min.
2. Aspirate StemFit from each well, then add 2 mL of Medium A to each well.

Table 2
The typical schedule of differentiation culture

	Mon	Tue	Wed	Thu	Fri	Sat	Sun
0W		−D3 Plating StemFit		−D1 M.C. StemFit	D0 M.C. Medium A		
1W	M.C. Medium A		M.C. Medium A		D7 Passage Medium A		
2W	M.C. Medium A		M.C. Medium A		D14 Passage CDMi basal medium		
3W	M.C. Medium B-1				M.C. Medium B-2		
4W	M.C. Medium B-3				M.C. Medium B-3		
5W	M.C. Medium B-3				M.C. Medium B-3		
6–12W	M.C. Medium C		M.C. Medium C				

M.C. indicates medium change

3. Incubate the plate at 37 °C, 5% CO_2 for 2–3 days.
4. Change medium with fresh Medium A every 2–3 days until day 7 (*see* Table 2).

3.2.3 Day 7: Passage for the Dermomyotome-Like Cells Differentiation

1. Confirm representative cell morphology at day 7 (*see* Fig. 2a) before performing subsequent steps.
2. To prepare a Matrigel-coated 6-well plate, dilute Matrigel in CDMi basal medium in a 1:50 ratio, then add 1 mL of this 1:50 Martigel solution to each well. Incubate at 37 °C, 5% CO_2 for at least 2 h.
3. After 2 h, aspirate the 1:50 Matrigel solution from Matrigel-coated wells, then add 2 mL of Medium A supplemented with 10 μM Y-27632 (abbreviated as Medium A + Y) to each well. Incubate the plate with the medium at 37 °C, 5% CO_2 until cell seeding.
4. Aspirate the medium from the well with 7 days cultured cells, then gently wash the well with 1 mL of D-PBS.
5. Aspirate D-PBS, add 0.5 mL of Accutase to each well, and then spread it evenly across the cell surface. Incubate at 37 °C, 5% CO_2 for 5 min.

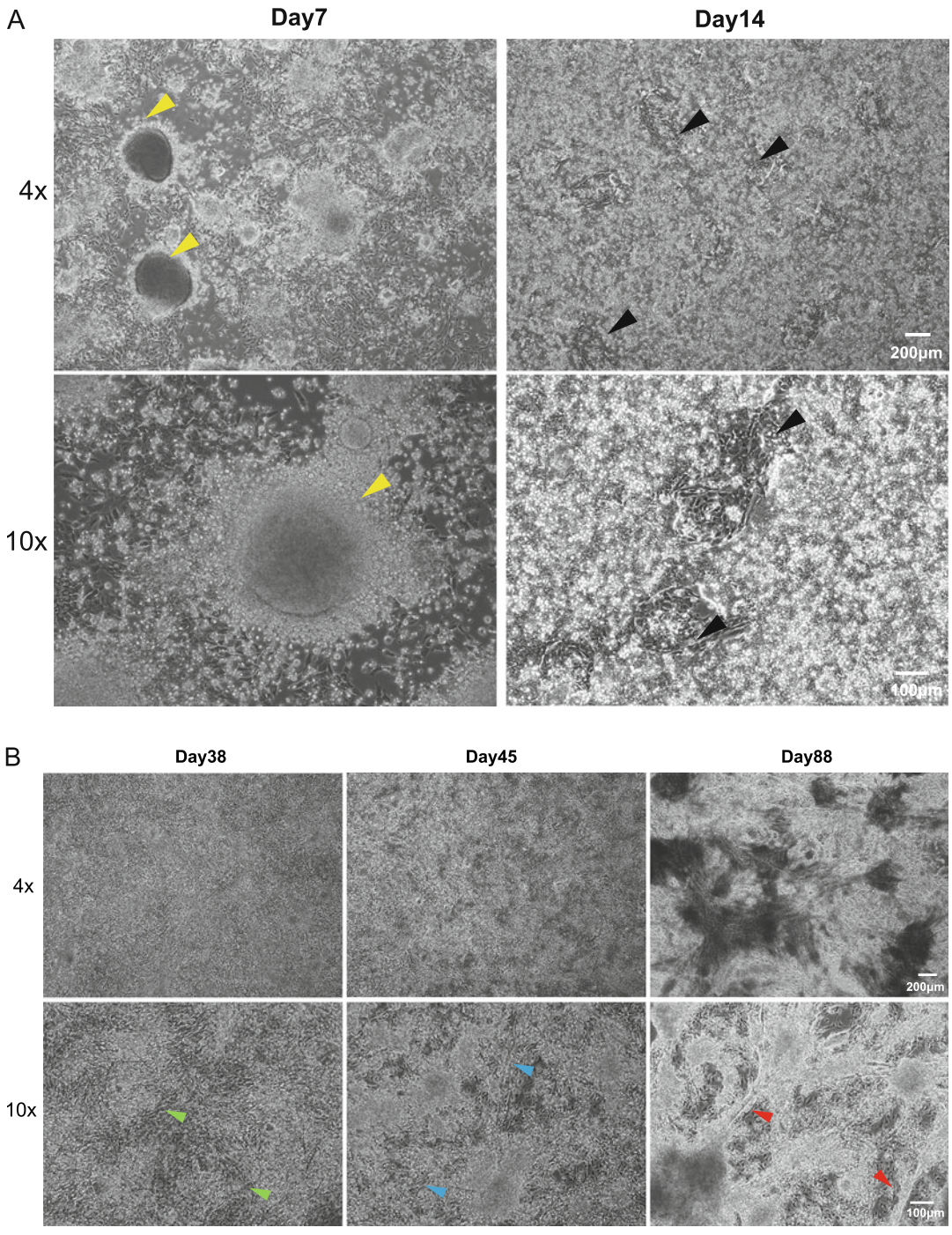

Fig. 2 Representative images of cell morphology at day 7 and day 14 of differentiation. (**a**) Spheroid-like cell clusters shown by yellow arrows are observed at day 7 of differentiation. Perform cell culture at a high density from day 9 to day 14, and the monolayer cells shown in black arrows are faintly observed. Cells are cultivated in a very dense state in areas other than the monolayer cells shown by black arrows. (**b**) Myotubes begin to appear on day 38 (green arrow), and a relatively clear myotube structure begins to appear on day 48 (blue arrow). The mature myotube structure appears at approximately day 70 ~ 80 (red arrow). The cell image in the upper row is a cell image taken at ×40, and the cell image in the lower row is a cell image taken at ×100

6. Gently detach the cells from the well using a P1000 pipette while breaking up cell clusters, and then add 2.5 mL of Medium A to the wells.
7. Collect the cell suspension in a 15 mL sterile tube.
8. Centrifuge the cell suspension at 160 × *g* at 4 °C for 5 min.
9. Aspirate the supernatant, resuspend the cell pellet in Medium A + Y, and count the cell with Trypan Blue staining.
10. Plate 4.5×10^5 cells (4.8×10^4 cells/cm^2) in a Matrigel-coated well. Prepare two wells for the final 6-well plate induction of fetal MuSCs. After seeding the cells, rock the plate gently to ensure even distribution immediately.
11. Incubate the plate at 37 °C, 5% CO_2.
12. Change medium with fresh Medium A on day 10 and day 12 (*see* Table 2).

3.2.4 Day 14: Passage for Myogenic Differentiation

1. Confirm representative cell morphology at day 14 (*see* Fig. 2a), before performing subsequent steps.
2. To prepare a Matrigel-coated 6-well plate, dilute Matrigel in CDMi basal medium (1:50 ratio), then add 1 mL of the 1:50 Matrigel solution to each well. Incubate at 37 °C, 5% CO_2 for at least 2 h.
3. After 2 h, aspirate the 1:50 Matrigel solution from the coated wells and then add 1 mL of CDMi basal medium supplemented with 10 μM Y-27632 (abbreviated as CDMi basal medium + Y) to the wells before cell seeding.
4. Aspirate the medium from the well of 14 days cultured cells, then gently wash the cell surface with 1 mL of D-PBS.
5. Aspirate D-PBS, add 0.5 mL of Accutase to each well, then incubate the plate at 37 °C, 5% CO_2 for 5 min.
6. Gently detach the cells from the dish using a P1000 pipette while breaking up cell clusters, then add 2.5 mL of CDMi basal medium to each well.
7. Collect the cell suspension in a 15 mL sterile tube.
8. Centrifuge the cell suspension at 160 × *g* at 4 °C for 5 min.
9. Aspirate the supernatant, resuspend the cell pellet in CDMi basal medium + Y, and count the cells with Trypan Blue staining.
10. Prepare a suspension of 8.0×10^5 cells/mL in CDMi basal medium + Y, then add 1 mL of the cell suspension to the Matrigel-coated well (0.4×10^5 cells/cm^2), and rock the plate gently to ensure even distribution immediately.
11. Incubate the plate at 37 °C, 5% CO_2 for 3 days.

3.2.5 Day 17: Promote Myogenic Differentiation

1. Refer to Table 1 to prepare Medium B-1 (also *see* **Note 3**). Warm the appropriate Medium at room temperate for 20–30 min.
2. Aspirate the CDMi basal medium + Y from each well after 3 days of culture, then add 2 mL of Medium B-1 to the wells.
3. Incubate the plate at 37 °C, 5% CO_2 for 4 days (*see* **Note 4**).
4. Replace the culture medium with Medium B-2 at day 21 and culture the cells for 3 days. Then, replace the culture medium with Medium B-3 on day 24.
5. Change medium with Medium B-3 every 3 or 4 days until day 35 (*see* Table 2).

3.2.6 Day 38: Initiate Muscle Maturation

1. Refer to Table 1 to prepare Medium C. Warm Medium C at room temperate for 20–30 min.
2. Aspirate the Medium B-3 from each well, then add 2 mL of Medium C.
3. Incubate the culture at 37 °C, 5% CO_2 for 2 ~ 3 days.
4. Change medium with Medium C every 2 ~ 3 days until 12 weeks (*see* Table 2 and also **Note 4**).

3.3 Cell Preparation for FACS Analysis and Sorting

For validation of fetal MuSCs induction efficiency, the flowcytometric analysis should be done. We usually analyze the population of the MYF5-tdTomato positive cells by FACS and sort the MYF5-tdTomato positive cells for further evaluation (*see* **Note 5**). Instead of using the MYF5-tdTomato reporter line, it is also applicable to use the surface marker antibody to detect fetal MuSCs. We have confirmed that ERBB3 [12] and CD82 [13] can be used for the detection of a part of fetal MuSCs.

1. Aspirate the medium from the cell culture wells, then gently wash the cell surface with 1 mL of D-PBS.
2. Add 1 mL of detachment buffer to each well and keep the plate at 37 °C, 5% CO_2 for 30–60 min. Add 2 mL of DMEM containing 2% House Serum (DMEM +2% HS) and mix gently by pipetting. Collect the cell suspension in a 50 mL sterile tube, add 4 ml of DMEM +2% HS to the 50 mL tube and mix gently.
3. Centrifuge the cell suspension at 190 × *g* at 4 °C for 10 min.
4. After removing the supernatant, loosen the cell pellet by tapping. Then, treat the cells with 0.5 ml of Accutase and incubate them at 37 °C, 5% CO_2 for 5 min.
5. After 5 min, add 2.5 mL of DMEM +2% HS and mix well by pipetting for dissociating the cells into single cells.
6. Centrifuge the cell suspension at 190 × *g* at 4 °C for 10 min.

7. After removing the supernatant, resuspend the cell pellet in 10 mL of HBSS buffer. Count the cell with Trypan Blue staining.
8. Centrifuge the cell suspension at 440 × *g* at 4 °C for 10 min.
9. After removal of the supernatant, resuspend the cell pellet in 2.0×10^6 cell/mL HBSS buffer containing 5 μg/ml Hoechst dye at the concentration of 2.0×10^6 cell/mL and filter the cell suspension using a 40 μm mesh.
10. Analyze and sort MYF5-tdTomato positive cells by FACS (BD, Aria II) (*see* Fig. 4a).

3.4 Immunocytochemistry of the Sorted Cells

To validate the characteristics of fetal MuSCs, the expression of Pax7 and MyoD should be assessed. Instead of immunocytochemistry, quantitative RT-PCR is also applicable [10].

1. Seed sorted cells onto glass slides using Smear Gel and fix with 2% PFA in PBS for 10 min at 4 °C.
2. Wash cells immobilized on glass slides twice with PBS and block them using Blocking One for 30 min at 4 °C.
3. Probe the cells with appropriate primary antibodies diluted in 10% Blocking One in PBS for 16 h at 4 °C.
4. Wash the cells three times with washing buffer and probe with appropriate secondary antibodies for 1 h at room temperature. Incubate the cells with 1:5000 DAPI in PBS for 5 min before observation.
5. The samples were observed and analyzed by a BZ-X700 microscope (*see* Fig. 4b, c).

4 Notes

1. Cell density for maintenance culture should be optimized in each hiPSC clone. Since 1.0×10^4 cells/6-well plate is a standard cell density for the 201B7 cell line, it is necessary to adjust cell density from 5.0×10^3 to 2.0×10^4 cells/well for getting 70 ~ 80% confluent after 7 days of maintenance culture for each cell line. When we want to arrange the timing of the medium change according to holidays, we usually passage the cells on Tuesday and change the medium on day 2, day 3 with 3 ml of medium, and day 6.
2. The seeding density at day −3 of differentiation is particularly important for the induction of dermomyotome-like cells. It is necessary to optimize the seeding density at day −3 when using a different cell line. Additionally, confirmation of cell

morphology is of high importance on day 7 and day 14 (*see* Fig. 2). Since 1.0×10^4 cells/6-well plate is a standard cell density for the 201B7 cell line, it is necessary to adjust cell density from 5.0×10^{43} to 6.0×10^4 cells/well in a 6-well plate for obtaining equivalent morphology and cell density at day 7 (*see* Fig. 2a). If necessary, optimize the differentiation protocol by analyzing the expression of paraxial mesoderm marker *TBX6* at day 6, and dermomyotome marker *SIX1* and *DMRT2* at day 14 using quantitative PCR [10].

3. During the myogenic differentiation step, we have used three different culture media B-1, B-2, and B-3 based on our previous report [14]. However, we have recently found that using Medium B-1 throughout the myogenic differentiation step (day 17 ~ 38) does not affect myogenic induction efficiency. It is no problem to use only Medium B-1 to avoid any mistake of adding growth factor supplementation.
4. Typical cell morphologies and fluorescence images are indicated in the figures.

   Days 21–28: MYF5-tdTomato positive cells can be seen under a microscope (*see* Fig. 3).

   Days 38–45: Myotubes would be observed in the culture (*see* Fig. 2b).

   Days 80–90: More mature structures can be observed from the middle stages of the culture (*see* Fig. 2b). Approximately 10% MYF5-tdTomato positive cells can be observed (*see* Fig. 4a).
5. The hiPSC-derived fetal MuSCs are emerging after day 70 and getting peak around day 84. After that, the efficiency is gradually decreasing. However, the characteristics of the fetal MuSCs are not so changed at least until day 140.

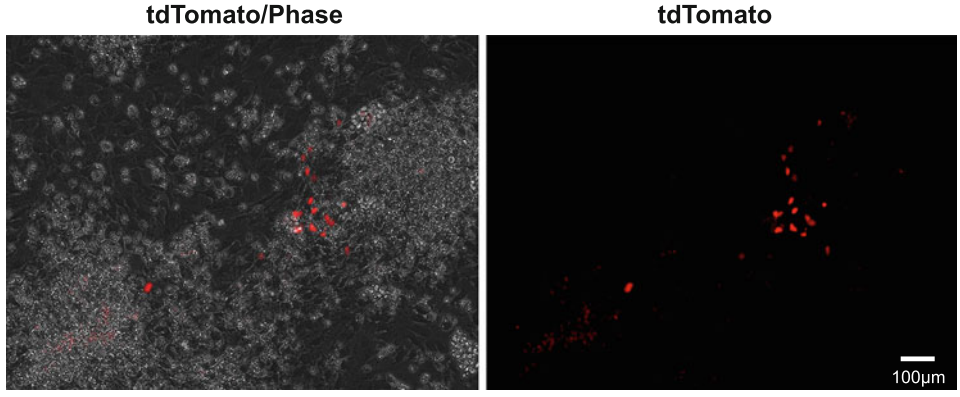

Fig. 3 Representative images of MYF5-tdTomato positive cells at day 28 of differentiation. Representative bright-field (Phase, Ph), left, and tdTomato, right, images of MYF5-tdTomato positive cells at 28 days. MYF5-tdTomato positive cells are confirmed around days 21–28

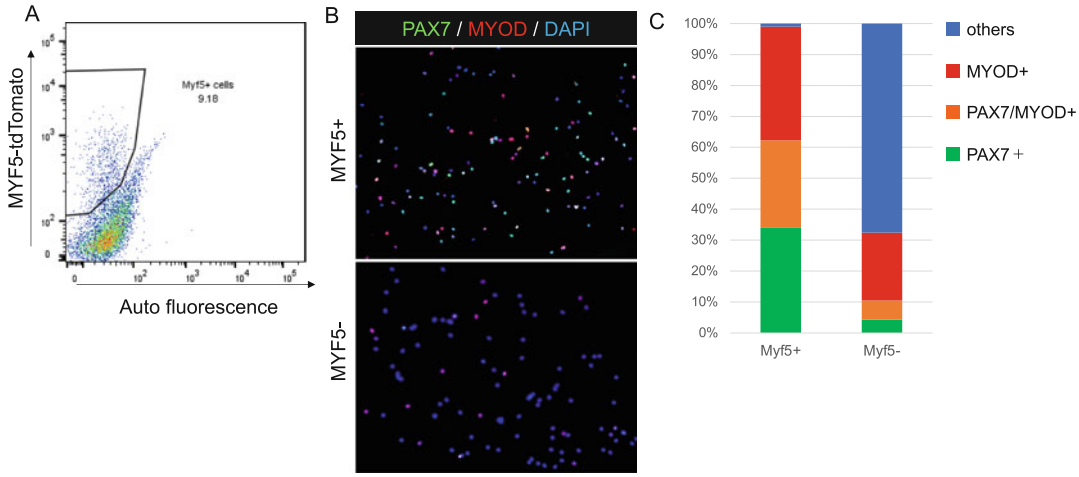

Fig. 4 Preparative flow cytometry plot of fetal MuSCs and population analysis of sorted fetal MuSCs. (**a**) FACS analysis for the isolation of fetal MuSCs. MYF5-tdTomato positive cells present within the gated population are hiPSCs-derived fetal MuSCs, and approximately 10% are MYF5-tdTomato positive cells in the total population. (**b**) Immunostaining of the MYF5 positive and negative cells for checking the expression of PAX7 and MYOD. (**c**) Based on the results of immunostaining (*see* Fig. 4b), the percentages of PAX7 positive cells, MYOD positive cells, PAX7 and MYOD positive cells, and other cells were plotted

References

1. Hoffman EP, Brown RH Jr, Kunkel LM (1987) Dystrophin: the protein product of the Duchenne muscular dystrophy locus. Cell 51:919–928. https://doi.org/10.1016/0092-8674(87)90579-4
2. Fairclough RJ, Wood MJ, Davies KE (2013) Therapy for Duchenne muscular dystrophy: renewed optimism from genetic approaches. Nat Rev Genet 14:373–378. https://doi.org/10.1038/nrg3460
3. Takahashi K, Tanabe K, Ohnuki M et al (2007) Induction of pluripotent stem cells from adult human fibroblasts by defined factors. Cell 131:861–872
4. Darabi R, Arpke RW, Irion S et al (2012) Human ES- and iPS-derived myogenic progenitors restore DYSTROPHIN and improve contractility upon transplantation in dystrophic mice. Cell Stem Cell 10:610–619. https://doi.org/10.1016/j.stem.2012.02.015
5. Tedesco FS, Gerli MFM, Perani L et al (2012) Transplantation of genetically corrected human iPSC-derived progenitors in mice with limb-girdle muscular dystrophy. Sci Transl Med 4:140ra189. https://doi.org/10.1126/scitranslmed.3003541
6. Shelton M, Metz J, Jun L et al (2014) Derivation and expansion of PAX7-positive muscle progenitors from human and mouse embryonic stem cells. Stem Cell Rep 3:516–529. https://doi.org/10.1016/j.stemcr.2014.07.001
7. Chal J, Oginuma M, Al Tanoury Z et al (2015) Differentiation of pluripotent stem cells to muscle fiber to model Duchenne muscular dystrophy. Nat Biotechnol 33:962–969. https://doi.org/10.1038/nbt.3297
8. Kim J, Magli A, Chan SSK et al (2017) Expansion and purification are critical for the therapeutic application of pluripotent stem cell-derived myogenic progenitors. Stem Cell Rep 9:12–22. https://doi.org/10.1016/j.stemcr.2017.04.022
9. Tierney MT, Gromova A, Sesillo FB et al (2016) Autonomous extracellular matrix remodeling controls a progressive adaptation in muscle stem cell regenerative capacity during development. Cell Rep 14:1940–1952. https://doi.org/10.1016/j.celrep.2016.01.072
10. Zhao M, Tazumi A, Takatyama S et al (2020) Induced fetal human muscle stem cells with high therapeutic potential in a mouse muscular dystrophy model. Stem Cell Rep 15:80–94. https://doi.org/10.1016/j.stemcr.2020.06.004
11. Nakagawa M, Taniguchi Y, Senda S et al (2014) A novel efficient feeder-free culture system for the derivation of human induced

pluripotent stem cells. Sci Rep 4:3594. https://doi.org/10.1038/srep03594

12. Hicks MR, Hiserodt J, Paras K et al (2018) ERBB3 and NGFR mark a distinct skeletal muscle progenitor cell in human development and hPSCs. Nat Cell Biol 20:46–57. https://doi.org/10.1038/s41556-017-0010-2
13. Uezumi A, Nakatani M, Ikemoto-Uezumi M et al (2016) Cell-surface protein profiling identifies distinctive markers of progenitor cells in human skeletal muscle. Stem Cell Rep 7:263–278. https://doi.org/10.1016/j.stemcr.2016.07.004
14. Sakurai H, Inami Y, Tamamura Y et al (2009) Bidirectional induction toward paraxial mesodermal derivatives from mouse ES cells in chemically defined medium. Stem Cell Res 3:157–169. https://doi.org/10.1016/j.scr.2009.08.002

Chapter 12

Sphere-Based Expansion of Myogenic Progenitors from Human Pluripotent Stem Cells

Megan Reilly, Samantha Robertson, and Masatoshi Suzuki

Abstract

The protocol presented here is to derive, maintain, and differentiate human pluripotent stem cells into skeletal muscle progenitor/stem cells (myogenic progenitors) using a sphere-based culture approach. This sphere-based culture is an attractive method for maintaining progenitor cells due to their longevity and the presence of cell-cell interactions and molecules. Large numbers of cells can be expanded in culture using this method, which represents a valuable source for cell-based tissue modeling and regenerative medicine.

Key words Human pluripotent stem cells, Human embryonic stem cells, Human induced pluripotent stem cells, EZ spheres, Skeletal muscle, Myogenic progenitors, Skeletal myotubes

1 Introduction

Human pluripotent stem cells (PSCs), including embryonic stem cells (ESCs) and induced pluripotent stem cells (iPSCs), are an attractive study model because of their potential for in vitro modeling and cell-based therapies [1, 2]. Specifically, human iPSCs have been utilized for the study of normal muscle tissue development and disease mechanisms due to their ability to form myogenic cells in culture [1–3]. Here, we introduce the culture protocol originally developed in our laboratory to derive skeletal muscle progenitor cells (also known as myogenic progenitors) from human PSCs (Fig. 1). Human PSC colonies are lifted and formed as free-floating spherical cell aggregates termed "EZ spheres." Sphere-based culture has been used for various cell types because of its ability to expand undifferentiated cells to a large scale for long periods [4–10]. We are using an adapted tissue chopping method for passaging EZ spheres, which can maintain cell-cell interactions and the expression of cell-surface molecules such as extracellular matrix proteins [6, 7]. By using the culture protocol with EZ spheres, a significant number of myogenic progenitor cells can be prepared from human PSCs [4, 5, 11–13]. These myogenic progenitors can

Atsushi Asakura (ed.), *Skeletal Muscle Stem Cells: Methods and Protocols*, Methods in Molecular Biology, vol. 2640, https://doi.org/10.1007/978-1-0716-3036-5_12,

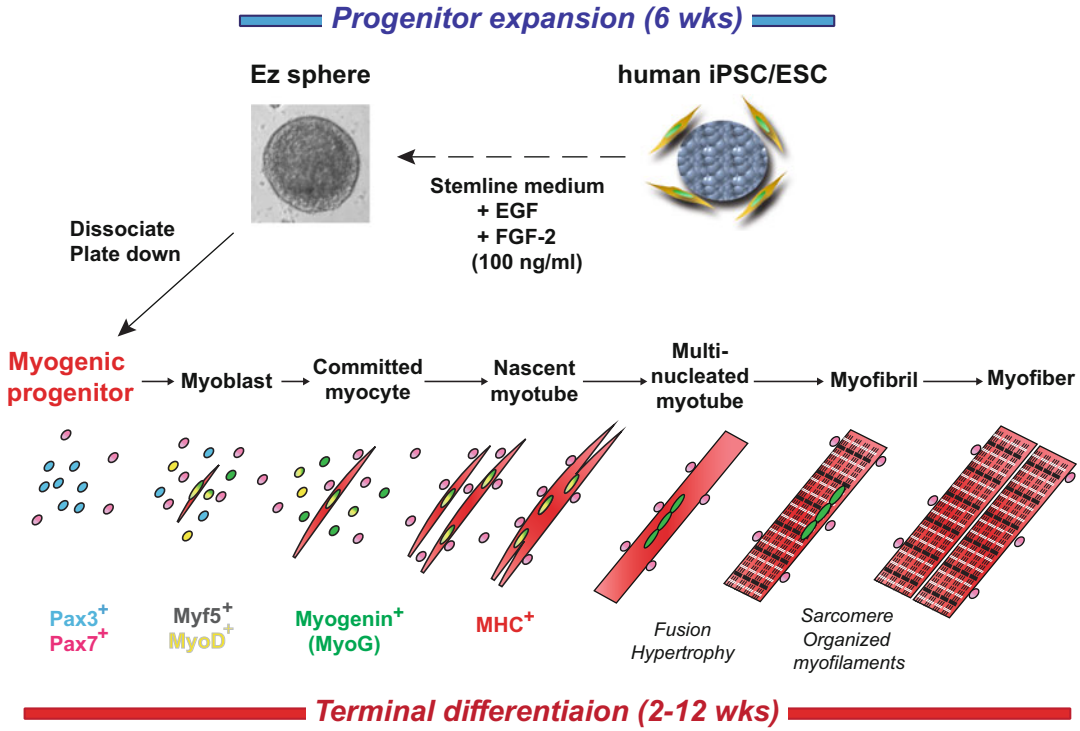

Fig. 1 Myogenic differentiation from human pluripotent stem cells using sphere-based culture. Human embryonic stem cells (ESC) and induced pluripotent stem cell (iPSC) are maintained as spherical aggregates (termed EZ spheres) in progenitor expansion medium (Stemline™ medium) containing high concentrations (100 ng/mL) of fibroblast growth factor-2 (FGF-2) and epidermal growth factor (EGF). EZ spheres are passaged weekly by mechanical chopping for 6 weeks. Myogenic progenitors in EZ spheres are plated on coverslips and terminally differentiated for 2–12 weeks. The stage of muscle cells can be determined by the expression of Pax 3, Pax7, myogenic differentiation 1 (MyoD), myogenic factor 5 (Myf5), Myogenin (MyoG), and myosin heavy chain (MHC). The illustration was prepared from the figures in Refs [4, 13]

be terminally differentiated into mature myotubes with sarcomere structures (Fig. 1). Human PSC-derived myotubes can be used for modeling normal muscle development and cellular pathology in neuromuscular disorders in vitro [4, 11, 12].

2 Materials

2.1 EZ Sphere Preparation and Passaging

1. Human PSC lines: Use well-grown human ESC or iPSC colonies that were cultured using methods previously described (*see* **Note 1**) [14–16].
2. Poly(2-hydroxyethyl methacrylate) (poly-HEMA) coated culture flasks: T12.5-, T25-, T75-, or T175-culture flasks coated with poly-HEMA (*see* **Note 2**).
3. Dulbecco's Phosphate-Buffered Saline (DPBS).

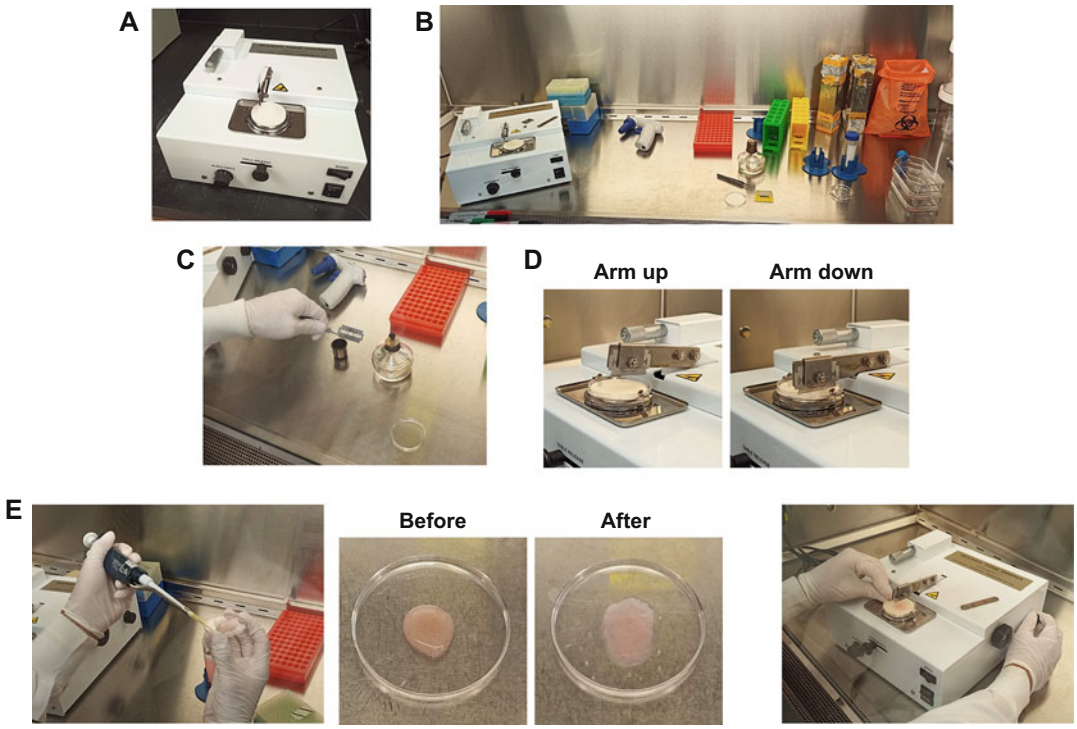

Fig. 2 Mechanical chopping of EZ spheres using a tissue chopper. (**a**) McIlwain tissue chopper with a blade arm and platform. (**b**) Prepared items in a biosafety cabinet for sphere chopping. There is a tissue chopper, a pipette controller, fine forceps, a razor blade, an alcohol burner, tube stands, poly-HEMA coated flasks, and Pasteur glass pipettes in containers. (**c**) Flame a blade by passing over the fire on the alcohol burner. Make sure to have the end of the fine forceps with the razor blade angled downwards away from your hand. (**d**) Set up the razor blade onto the arm of the tissue chopper, place the arm cover, and lightly tighten the screw over the cover and blade. At the arm down position, test out the level of the razor blade on the petri dish lid by running the chopper arm several times. Make sure that the blade is leaving nice parallel lines on the dish lid. (**e**) Pipette spheres onto the petri dish lid in a small droplet (before). Then use a P200 micropipette to carefully remove some excess media from the droplet without taking any spheres with it (after). (**f**) Chop all the way through the spheres (from right to left on the platform)

4. Protease solution: Use either 0.1% collagenase solution or 2 mg/mL dispase solution (*see* **Note 3**).
5. Expansion medium: Stemline® Neuronal Stem Cell Expansion Medium (MilliporeSigma, S3194), Antibiotic-Antimycotic (penicillin/streptomycin/amphotericin B, PSA; 1% vol/vol), 100 ng/mL human recombinant fibroblast growth factor-2 (FGF-2), 100 ng/mL epidermal growth factor (EGF), 5 ng/mL heparin sodium.
6. McIlwain tissue chopper (Mickle Laboratory Engineering, Surrey UK) (Fig. 2a).
7. Sterilized razor blades: In the biosafety cabinet, the blade is soaked with 100% ethanol and flamed with an alcohol burner (*see* **Note 4**) (Fig. 2c).

8. 50 × 9 mm plastic dishes: This specific type of the plate is suitable for the tissue chopper.
9. 15 mL or 50 mL conical tubes.
10. Cell scrapers.
11. A P1000 micropipette and its disposal tips.
12. Disposable and autoclaved cotton-plugged glass Pasteur pipettes.
13. A rubber bulb for small pipets.
14. A biosafety cabinet.
15. A CO_2 incubator.
16. An inverted microscope.
17. A centrifuge for conical tubes: Our model is Thermo IEC Centra CL2 Centrifuge with Rotor 236 4-Place Aerocarrier Horizontal Swing-out rotor (15 cm radius).

2.2 EZ Sphere Dissociation and Coverslip Plating for Terminal Differentiation

1. Sterile coverslips (*see* **Note 5**).
2. 100 μg/mL Poly-L-Lysine (PLL, MilliporeSigma, P5899) solution (*see* **Note 6**).
3. 50 μg/mL Laminin Solution (MilliporeSigma, L2020) (*see* **Note 7**).
4. 24-well flat-bottom cell culture plates.
5. Sterile distilled water (dH_2O).
6. Gibco™ TrypLE Select (1×) reagent (12604021).
7. Gibco™ defined Trypsin inhibitor (R007100).
8. Hemocytometer.
9. 0.4% trypan blue solution.
10. Dulbecco's Modified Eagle Medium (DMEM) with high glucose, pyruvate, GlutaMAX (ThermoFisher Scientific, 10566-016).
11. Terminal differentiation medium: DMEM, 1% PSA, 2% Gibco™ B-27 serum-free supplement (17504001).

2.3 Immunocytochemistry

1. Fine forceps.
2. A small moisture box (*see* **Note 8**).
3. Phosphate-Buffered Saline (PBS, pH 7.4).
4. 4% Paraformaldehyde in PBS (PFA-PBS): Dilute 32% PFA aqueous solution with PBS up to 4%.
5. Ice-cold methanol.
6. Blocking solution: PBS supplemented with 5% normal donkey serum (NDS) or normal goat serum (NGS) (*see* **Note 9**).

7. Primary antibody solution: PBS supplemented with 5% NDS or NGS, and 0.2% Triton X-100.
8. Primary antibodies for the markers of myogenic progenitors, satellite cells, and mature myocytes (Table 1).
9. Secondary antibodies conjugated with fluorophores (Table 1).
10. Hoechst solution: Dilute Hoechst 33258 fluorescence dye (0.5 μg/mL final concentration, MilliporeSigma, B1155) in PBS (*see* **Note 10**).
11. Coverslip mounting medium (Fluoromount-G Slide Mounting Medium, Southern Biotech, 0100-01).
12. Slide glasses.
13. Kimwipe.

3 Methods

Carry out all procedures at room temperature unless otherwise noted. All manipulation of human cell culture should be performed in a biosafety cabinet.

3.1 EZ Sphere Preparation from Human PSC Colonies

1. Rehydrate the culture surface of poly-HEMA-coated flasks using a proper amount of DPBS for each flask size (*see* **Note 11**). Remove the DPBS right before use.
2. Remove the medium from the wells where human PSCs were plated and rinse the wells with DPBS (2 mL per well).
3. Protease reaction: Add 1 mL collagenase solution to each well and incubate at room temperature for 60 min. Alternatively, use 1 mL dispase solution for each well and incubate at 37 °C for 7 min (*see* **Note 12**).
4. Scrape the cells using a cell scraper, gently pipette up and down using a P1000 micropipette to dislodge the colonies from the plate, and transfer the colonies and solution to a 15 mL or 50 mL conical tube.
5. Add 1 mL DPBS to a well, rinse with a P1000 micropipette by repeated pipetting, and add the DPBS to the same conical tube.
6. Centrifuge the tubes for 1.5 min at 1000 rpm (168 × g) and then remove the supernatant (*see* **Note 13**).
7. Resuspend the colonies in a 10 mL expansion medium. First mix the colonies in 1 mL medium using a P1000 micropipette and then add the rest of the medium.
8. Transfer the colony suspension to conical tubes and centrifuge the tubes for 1.5 min at 1000 rpm (168 × g) (*see* **Note 13**).

Table 1
Primary and secondary antibodies used for immunocytochemistry

Primary antibodies					
Protein	**Catalog no.**	**Vendor**	**Host species**	**Dilution**	**Clone**
Pax7	PAX7	Developmental Studies Hybridoma Bank (DSHB)	Mouse	1:40	
MyoD	554130	BD Biosciences	Mouse	1:40	
Myogenin (MyoG)	F5D	DSHB	Mouse	1:40	F5D
Myosin heavy chain (MHC)	MF-20-c	DSHB	Mouse	1:40	MF-20
MHC conjugated with Alexa Fluor 488	53-6503-80	eBioscience	Mouse	1:500	MF-20
Titin	9 D10-c	DSHB	Mouse	1:40	
MYH3 (embryonic MHC)	F1.652-c	DSHB	Mouse	1:40	F1.652
MYH8 (fetal/perinatal MHC)	N3.36-c	DSHB	Mouse	1:40	N3.36
MYH2 (adult MHC)	A4.74-c	DSHB	Mouse	1:40	A4.74
Secondary antibodies					
Name	**Catalog no.**	**Vendor**	**Host species**	**Dilution**	
Anti-mouse IgG conjugated with Alexa Fluor 488	A21202	Thermo Fisher	Donkey	1:1000	
Anti-mouse IgG conjugated with Cy3	715-165-150	Jackson ImmunoResearch	Donkey	1:1000	
Anti-rat IgG conjugated with Cy3	712-165-153	Jackson ImmunoResearch	Donkey	1:1000	
Anti-rabbit IgG conjugated with Cy3	711-165-152	Jackson ImmunoResearch	Donkey	1:1000	

9. Remove the supernatant, resuspend the colonies in a 10 mL expansion medium, and transfer the colony suspension to a poly-HEMA-coated flask (*see* **Note 14**). Store the flask in a CO_2 incubator.
10. On the next day, feed flasks by settling cells in a flask, removing half of the medium and replacing it with fresh medium. Tilt the flask and rest it on a tube rack, which allows the spheres to settle in the bottom corner of the flask.
11. Maintain the culture until the sphere size reaches an approximate 400–500 μm diameter. Feed flasks every 3 or 4 days by settling cells in a flask, removing half of the medium and replacing it with fresh medium. Usually it takes a few weeks until the spheres are fully grown up to the size described above.

3.2 Passaging EZ Spheres by Mechanical Chopping

1. Label new poly-HEMA coated flasks and add enough DPBS to rehydrate their bottom surface. Remove the DPBS right before use.
2. Place one of each 15 mL or 50 mL conical tubes on the tube stand. Add the fresh expansion medium to the 50 mL conical tube (*see* **Note 14**).
3. Clean the tissue chopper by spraying with 70% ethanol and place it in a biosafety cabinet.
4. Set up the flame-sterilized razor blade onto the arm of the tissue chopper, place the arm cover, and lightly tighten the screw over the cover and blade.
5. Place the petri dish lid on the turn table of the tissue chopper. Test out the level of the razor blade on the petri dish lid by running the chopper arm several times (Fig. 2d). Make sure that the blade is leaving nice parallel lines on the dish lid. Then use the wrench to tighten the screw over the arm cover and razor blade.
6. Allow spheres to settle down at one edge of the flask bottom, collect most of the conditioned medium, and transfer the required amount of the conditioned medium into each poly-HEMA coated flask (*see* **Note 14**).
7. Gently suspend spheres in a small remaining amount of the medium and then transfer them to a 15 mL conical tube.
8. Once spheres are settled at the bottom of the tube, remove the extra medium using an autoclaved cotton-plugged glass Pasteur pipette.
9. Use the same pipette to pick up what's left of the media along with the cells at the bottom of the conical tube. Allow the spheres to settle at the bottom of the pipette and then pipette them out onto the smaller half of the petri dish lid in a small droplet (*see* **Note 15**).

10. Use a P200 micropipette to carefully remove some excess media from the droplet without taking any spheres with it (*see* **Note 16**) (Fig. 2e).
11. Place the dish lid onto the chopping platform of the tissue chopper. Make sure the lid is secure. Use the front knob to adjust the stage so that the blade is to the most right of the spheres. Make sure the knob clicks into place.
12. Use the back knob to start the chopping. Adjust speed to where you are comfortable. Chop all the way through the spheres (from right to left on the platform) (Fig. 2f) and then stop the tissue chopper.
13. Turn the dish lid 90 ° and chop again (*see* **Note 17**).
14. Remove the dish from the chopper and apply a small amount of the medium to the chopped spheres using a fresh Pasteur pipette. Suck up the chopped spheres and transfer them to the fresh expansion medium in the 50 mL conical tube. Repeat as necessary until you have gotten most of the spheres off the dish lid.
15. Gently pipette the expansion medium and spheres in the tube four to five times. Split them into poly-HEMA coated flasks (*see* **Note 14**).
16. Maintain the culture until the sphere size reaches an approximate 400–500 μm diameter. Feed flasks every 3 or 4 days by settling cells in a flask, removing half of the medium and replacing it with fresh medium. We usually chop the spheres once every week.

3.3 EZ Sphere Dissociation and Terminal Differentiation of Myogenic Progenitors

1. PLL coating for coverslips: Place a sterile coverslip in each well of a 24-well plate. Add 45 μL of PLL solution to the center of each coverslip. Incubate at room temperature for 30 min in a biosafety cabinet.
2. Remove the PLL solution (*see* **Note 18**) and rinse each coverslip three times with 45 μL of dH_2O. Remove the last wash and allow the coverslip to dry overnight in a biosafety cabinet. PLL-coated coverslips can be stored at room temperature for several weeks.
3. Laminin coating: On the day for cell plating, add 45 μL of laminin solution to the center of each coverslip and incubate in a CO_2 incubator at 37 °C for 30 min. Remove the laminin solution (*see* **Note 18**) and rinse each coverslip three times with 45 μL of DMEM. Leave DMEM on the coverslips after the last wash and keep them in a CO_2 incubator at 37 °C. Prevent complete drying out of the coverslip surface. Remove DMEM right before plating cells.

4. Sphere dissociation: Allow spheres to settle down at one edge of the flask bottom and remove most of the conditioned medium. Let spheres flow a small remaining amount of the medium by pipetting with a serological pipette and transfer the spheres to a 15 mL conical tube.
5. Once spheres are settled at the bottom of the tube, remove the extra medium using an autoclaved cotton-plugged glass Pasteur pipette. Remove the medium as much as possible.
6. Add 2 mL of TrypLE and incubate in a water bath at 37 °C for 4 min. Gently agitate spheres every minute.
7. Add 2 mL of defined trypsin inhibitor in a biosafety cabinet and centrifuge the tube at 1500 rpm (387 × g) for 3 min.
8. Remove the supernatant, add 10 mL of pre-warmed DMEM for a wash, and centrifuge the tube at 1500 rpm (378 × g) for 5 min.
9. Remove the supernatant as much as possible and suspend spheres/cells in a small amount of terminal differentiation medium. We usually use between 200 μL and 1 mL of terminal differentiation medium, depending on the sphere pellet volume.
10. Using a P1000 micropipette, repeat pipetting 30–40 times until spheres seem mostly dissociated into single cells. Avoid forming air bubbles.
11. Using a P200 micropipette, repeat pipetting 30–40 times until spheres seem mostly dissociated into single cells. Avoid forming air bubbles.
12. Count cells in a 10 μL aliquot using a hemocytometer and assess cell viability using 0.4% trypan blue (*see* **Note 19**).
13. Adjust cell concentration to 4000 cells/μL using terminal differentiation medium. Remove DMEM from the coverslip and apply 50 μL of the final cell solution to each coverslip. This results in plating 200,000 cells per well.
14. Incubate coverslips at 37 °C in a CO_2 incubator for at least 2–4 h to allow cell attachment. If pre-matured progenitor cells are required for analysis, cells can be fixed with ice-cold methanol or 4% PFA-PBS at this moment. If the cells need to be further differentiated into skeletal myocytes and myotubes, add 500 μL of terminal differentiation medium to each well. Incubate cells at 37 °C in a CO_2 incubator for 2–16 weeks. Feed cells every 2 or 3 days by replacing half of terminal differentiation medium.

3.4 Immunocytochemistry to Confirm Myocytes and Myotubes

1. Remove medium and wash with 500 μL of PBS once.
2. Fix cells with 300 μL/well of ice-cold methanol for 10 min or 4% PFA-PBS for 20 min (*see* **Note 20**).
3. Remove the fixative and wash cells with 500 μL of PBS three times. When fixed with ice-cold methanol, cells should be rehydrated in PBS at least 15 min prior to the initiation of immunostaining. If necessary, fixed cells can be stored in PBS at 4 °C for several weeks.
4. Prepare a moisture box (*see* **Note 8**). Pick up the coverslip gently from the plate well using fine forceps and place the coverslip in the moisture box. Keep the side with plated cells up.
5. Rinse the coverslip with a small amount of PBS (approximately 200–300 μL) and aspirate PBS.
6. Blocking: Apply 100–200 μL of blocking solution on the coverslip. Make sure to cover the entire coverslip with the blocking solution. Incubate at room temperature for 1 h.
7. Wash the coverslip once with PBS. Add a small amount of PBS (approximately 200–300 μL), incubate at room temperature for 5 min, and then remove PBS.
8. Dilute the primary antibody in the primary antibody solution as instructed by the supplier (Table 1). Apply 100 μL of primary antibody solution on the coverslip. Make sure to cover the entire coverslip with the solution. Incubate at 4 °C overnight. Alternatively, a short incubation (at least for 1–2 h) at room temperature is acceptable.
9. After completing the incubation, wash the coverslip three times with PBS.
10. Dilute the secondary antibody in the blocking solution as instructed by the supplier (Table 1). Apply 200 μL of secondary antibody solution on the coverslip. Make sure to cover the entire coverslip with the solution. Incubate at room temperature for 1–2 h.
11. Wash the coverslip three times with PBS.
12. Apply 200 μL of Hoechst solution on the coverslip and incubate at room temperature for 10 min.
13. Wash the coverslip three times with PBS.
14. Put a drop of the mounting medium on a slide glass. Remove extra fluid on the coverslip, pick it up using fine forceps, and place it on the drop of the mounting medium. Make sure the cell side is on the bottom (i.e., the cells are laying against the slide glass). Remove the extra mounting medium using the edge of a Kimwipe. Protect the completed staining from light.
15. After the mounting medium has dried, check the staining using a fluorescence microscope (Figs. 3 and 4).

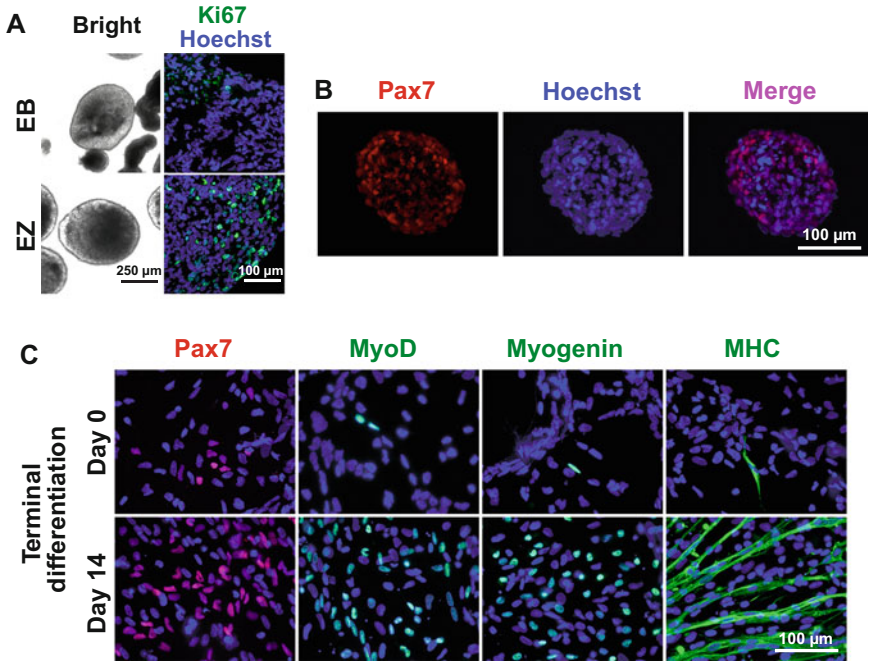

Fig. 3 Human PSC-derived EZ spheres can efficiently differentiate into skeletal muscle cells. (**a**) (Right) Representative brightfield images of ESC-derived embryoid bodies (EB) and EZ spheres (EZ). (Left) Immunostaining for a proliferation marker Ki67 indicates that the cells in ESC-derived EZ spheres actively proliferate and embryoid bodies have few proliferating cells. (**b**) Pax7-positive myogenic progenitors were detected in iPSC-derived EZ spheres following 6 weeks of spherical culture, as can be seen in a cryosection of EZ spheres (prior to dissociation, plating, and terminal differentiation). (**c**) Representative images of immunocytochemistry labeling for skeletal muscle cell markers in ESC-derived EZ sphere protocol for 6 weeks, then either acutely plated (day 0, no terminal differentiation step) or terminally differentiated for 2 weeks into myoblasts/myotubes (day 14). (Reproduced from Ref. [4] with permission from John Wiley and Sons)

4 Notes

1. We use human ESCs (WA09 and WA01; WiCell), wild-type iPSCs (IMR-90, WiCell), and patient-specific iPSC lines with neuromuscular disease background such as amyotrophic lateral sclerosis (ALS, familial and sporadic) [4, 17], Becker's muscular dystrophy [4], glycogen storage disease type II (Pompe disease) [18], and spinal muscular atrophy [4]. These PSC colonies were maintained as described previously by using either feeder-dependent [16] or independent protocols [14, 15].
2. The culture flask was precoated with Poly(2-hydroxyethyl methacrylate) (referred to as poly-HEMA) to prevent attachment of the cells to the surface. Poly-HEMA solution is created by mixing 8 g of Poly-HEMA into 20 mL of dH_2O, bringing up to 400 mL total with 100% ethanol, and then dissolving on

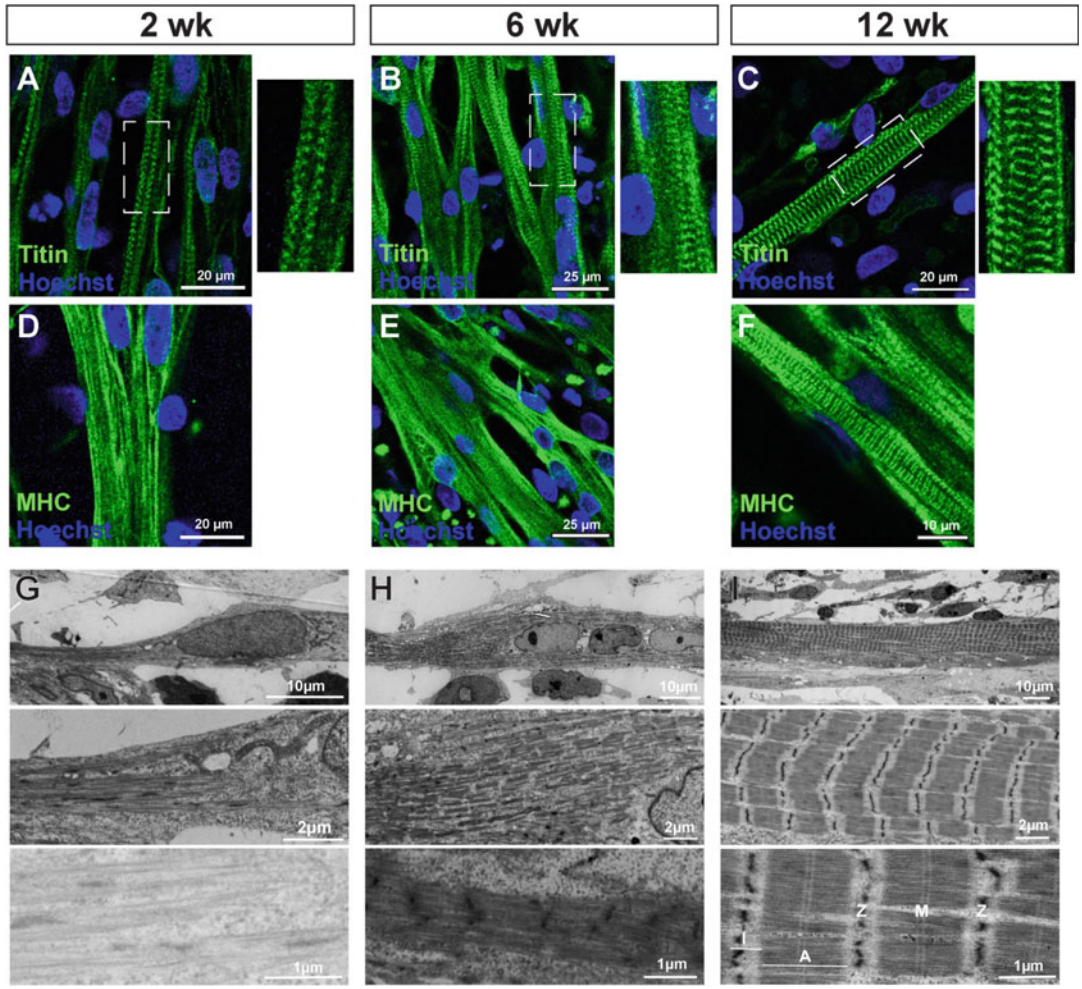

Fig. 4 Maturation and sarcomere formation in iPSC-derived myotubes. (**a**–**c**) Immunolabeling with sarcomeric filament titin. Titin staining revealed that striated patterns were already identified at 2 weeks of terminal differentiation (**a**). These patterns were clearly visible in the myotubes at 6 (**b**) and 12 weeks (**c**). (**d**–**f**) MHC staining in the same cell preparations used for titin labeling. (**g**–**i**) Ultrastructures of iPSC-derived myofibrils. After 2 weeks of differentiation, spindle-shaped myotubes contained undefined filaments with no sarcomere structure (**g**). After 6 weeks of differentiation, thick filaments assembled with a nascent Z line but no M-line (**h**). After 12 weeks of differentiation, mature sarcomeres were observed assembled into myofibrils (**i**). Morphological hallmarks, including I-band of actin filaments and A-band with distinct M-line across myosin filaments, were clearly visible. Sarcomere Z lines appeared to be reasonably aligned and gave rise to a striated pattern. (Reproduced from Ref. [13] with permission from Elsevier)

a stir plate with a magnetic stir bar overnight. Afterward, the prepared Poly-HEMA solution is used to coat the culture flasks with 7 mL per T175 flask, 5 mL per T75 flask, 2 mL per T25 flask, or 1.5 mL per T12.5 flask. The poly-HEMA flasks are manipulated to coat all sides of the flask (except the top side) twice and allowed to sit in the biosafety cabinet with the vent open and caps very loose overnight. After sitting overnight, the

flasks are moved to the benchtop and their caps slightly tightened. The flasks are manipulated again to ensure the bottom is evenly coated, after which the flask is allowed to dry for approximately 1 week.

3. To prepare collagenase solution, dissolve 1–1.5 mg collagenase (ThermoFisher Scientific, 17104-019) per well, when human PSCs are cultured in a 6-well plate. For dispase solution, prepare the solution at 2 mg/mL in DMEM/F12 medium (ThermoFisher Scientific, 11330-032). Freshly prepare solution as needed. Put and warm up in a water bath for a few minutes to dissolve if necessary.
4. Light an alcohol burner outside of the hood and transfer to inside the biosafety cabinet. Soak a razor blade with 100% ethanol in a small beaker. Flame the soaked blade by passing over the fire on the alcohol burner (Fig. 2c). Make sure to have the end of the fine forceps with the razor blade angled downwards away from your hand so that none of the flaming alcohol drips down onto your hand. Pass the blade quickly above the fire and then cool it down. The use of fire in the biosafety cabinet must be followed by the biosafety guidance at each research institute.
5. Sterile coverslips are prepared by layering coverslips in a glass petri dish on rounds of autoclave safe paper. The coverslips are laid out so that they are not overlapping and in a single layer. After one layer is complete, another paper is added, and the process repeated until the petri dish is full. After it is full, it is sealed shut with autoclave tape and sterilized in the autoclave, taking care not to tip or tilt the container.
6. To prepare the working solution, 5 mg of Poly-L-Lysine (PLL) is dissolved in 50 mL of ultrapure water, aliquoted, and stored at −20 °C.
7. 1 mL of 1 mg/mL Laminin is added to 19 mL of DPBS. The solution is aliquoted and stored at −20 °C.
8. Use a flat-bottomed container with a lid. Cut a small piece of filter paper and parafilm to fit the size of the container. Place the filter paper in the container, soak it lightly with dH_2O, and remove extra water. Layer the parafilm on the wet filter paper.
9. The serum in the blocking and antibody solutions should be used from the same host species as the secondary antibodies. Please note that the blocking solution is also used for the step of secondary antibody incubation.
10. Using bisBenzimid H 33258, 10,000 × stock solution (5 mg/mL in PBS) is prepared and stored at 4 °C with light protection.

11. Use 2–3 mL DPBS for T12.5 and T25, 3–5 mL for T75, and 5–7 mL for T175.
12. The time for enzyme incubation may need to be optimized. In our experience, the efficiency of sphere formation is varied in human PSC lines when using collagenase and dispase. The reaction with collagenase or dispase should be done until the edges of the colonies peel up a bit.
13. The time for centrifuge may need to be optimized, as a shorter time seems better for sphere formation.
14. We use 5 mL culture medium for T12.5, 10 mL for T25, 20 mL for T75, and 40 mL for T175 as a total volume for each flask type. When passaging the spheres, an equal amount of conditioned medium and fresh expansion medium is used. Depending on the flask number and size, the amount of the medium should be calculated as needed when adding the fresh medium into a 50 mL conical tube (Subheading 3.2, **step 2**) and the conditioned medium per poly-HEMA coated flask (Subheading 3.2, **step 5**).
15. Because of the relationship between the edge height of the petri dish and the available width of the razor blade at the tissue chopper arm, the lid of the petri dish is used instead of the dish.
16. Once enough media is removed that you can't get any more media without taking spheres up as well, use the pipette tip to spread the spheres around in a large circle on the dish. Then push all the spheres to one side and tilt the dish lid downwards so that any excess media drips down without the spheres. Use a P200 pipette to suck up this media. If spheres keep slipping down the dish with the media, expand the circle first and then try again. Once you have removed as much of the media as you can (Fig. 2e), push all spheres to the center of the dish and arrange in a monolayer as much as possible.
17. Optionally after this step, turn the stage at 45 ° and repeat the chopping if you want a larger quantity of small spheres.
18. PLL and Laminin solutions can be reused up to three times. The used solution is returned to a tube and stored at −20 °C.
19. Add 10 μL of cell suspension to 90 μL of the medium and mix well. Add 50 μL of this 10× dilution to 50 μL of 0.4% trypan blue solution and apply the hemocytometer with 10 μL of the mixed solution. The final samples dilution is 20×. Count four or five squares on the hemocytometer and determine the average number of live cells. Multiply the value by the dilution factor and then by 10,000 to give number of cell/mL.
20. While PFA-PBS is mainly acceptable for immunocytochemistry, methanol is preferable specifically for myosin heavy chain staining.

Acknowledgments

This work was supported by grants from Amyotrophic Lateral Sclerosis Association (15-IIP-201), National Institutes of Health (R01NS091540 and R01AR077191), Good Food Institute, University of Wisconsin Foundation, and UW Stem Cell & Regenerative Medicine Center to M.S.

References

1. Hosoyama T, Van Dyke J, Suzuki M (2012) Applications of skeletal muscle progenitor cells for neuromuscular diseases. Am J Stem Cells 1(3):253–263
2. Jiwlawat N, Lynch E, Jeffrey J et al (2018) Current progress and challenges for skeletal muscle differentiation from human pluripotent stem cells using transgene-free approaches. Stem Cells Int 2018:624168. https://doi.org/10.1155/2018/6241681
3. Tey SR, Robertson S, Lynch E et al (2019) Coding cell identity of human skeletal muscle progenitor cells using cell surface markers: current status and remaining challenges for characterization and isolation. Front Cell Dev Biol 7:284. https://doi.org/10.3389/fcell.2019.00284
4. Hosoyama T, McGivern JV, Van Dyke JM et al (2014) Derivation of myogenic progenitors directly from human pluripotent stem cells using a sphere-based culture. Stem Cells Transl Med 3(5):564–574. https://doi.org/10.5966/sctm.2013-0143
5. Hosoyama T, Meyer MG, Krakora D et al (2013) Isolation and in vitro propagation of human skeletal muscle progenitor cells from fetal muscle. Cell Biol Int 37(2):191–196. https://doi.org/10.1002/cbin.10026
6. Svendsen CN, Caldwell MA, Ostenfeld T (1999) Human neural stem cells: isolation, expansion and transplantation. Brain Pathol 9(3):499–513
7. Svendsen CN, Caldwell MA, Shen J et al (1997) Long-term survival of human central nervous system progenitor cells transplanted into a rat model of Parkinson's disease. Exp Neurol 148(1):135–146
8. Ebert AD, Shelley BC, Hurley AM et al (2013) EZ spheres: a stable and expandable culture system for the generation of pre-rosette multipotent stem cells from human ESCs and iPSCs. Stem Cell Res 10(3):417–427. https://doi.org/10.1016/j.scr.2013.01.009
9. Ebert AD, McMillan EL, Svendsen CN (2008) Isolating, expanding, and infecting human and rodent fetal neural progenitor cells. Curr Protoc stem cell biol chapter 2:unit 2D 2. https://doi.org/10.1002/9780470151808.sc02d02s6
10. Suzuki M, Wright LS, Marwah P et al (2004) Mitotic and neurogenic effects of dehydroepiandrosterone (DHEA) on human neural stem cell cultures derived from the fetal cortex. Proc Natl Acad Sci USA 101(9):3202–3207
11. Sakai-Takemura F, Nogami K, Elhussieny A et al (2020) Prostaglandin EP2 receptor downstream of Notch signaling inhibits differentiation of human skeletal muscle progenitors in differentiation conditions. Commun Biol 3(1):182. https://doi.org/10.1038/s42003-020-0904-6
12. Sakai-Takemura F, Narita A et al (2018) Premyogenic progenitors derived from human pluripotent stem cells expand in floating culture and differentiate into transplantable myogenic progenitors. Sci Rep 8(1):6555. https://doi.org/10.1038/s41598-018-24959-y
13. Jiwlawat S, Lynch E, Glaser J et al (2017) Differentiation and sarcomere formation in skeletal myocytes directly prepared from human induced pluripotent stem cells using a sphere-based culture. Differentiation 96:70–81. https://doi.org/10.1016/j.diff.2017.07.004
14. Ludwig TE, Bergendahl V, Levenstein ME et al (2006) Feeder-independent culture of human embryonic stem cells. Nat Methods 3(8):637–646. https://doi.org/10.1038/nmeth902
15. Ludwig TE, Levenstein ME, Jones JM et al (2006) Derivation of human embryonic stem cells in defined conditions. Nat Biotechnol 24(2):185–187. https://doi.org/10.1038/nbt1177
16. Thomson JA, Itskovitz-Eldor J et al (1998) Embryonic stem cell lines derived from human blastocysts. Science 282(5391):1145–1147
17. Lynch E, Semrad T, Belsito VS (2019) C9ORF72-related cellular pathology in

skeletal myocytes derived from ALS-patient induced pluripotent stem cells. Dis Model Mech 12(8). https://doi.org/10.1242/dmm.039552

18. Jiwlawat N, Lynch EM, Napiwocki BN et al (2019) Micropatterned substrates with physiological stiffness promote cell maturation and Pompe disease phenotype in human induced pluripotent stem cell-derived skeletal myocytes. Biotechnol Bioeng 116(9): 2377–2392. https://doi.org/10.1002/bit.27075

Chapter 13

Producing Engraftable Skeletal Myogenic Progenitors from Pluripotent Stem Cells via Teratoma Formation

Ning Xie and Sunny S. K. Chan

Abstract

Generating engraftable skeletal muscle progenitor cells is a promising cell therapy approach to treating degenerating muscle diseases. Pluripotent stem cell (PSC) is an ideal cell source for cell therapy because of its unlimited proliferative capability and potential to differentiate into multiple lineages. Approaches such as ectopic overexpression of myogenic transcription factors and growth factors–directed monolayer differentiation, while able to differentiate PSCs into the skeletal myogenic lineage in vitro, are limited in producing muscle cells that reliably engraft upon transplantation. Here we present a novel method to differentiate mouse PSCs into skeletal myogenic progenitors without genetic modification or monolayer culture. We make use of forming a teratoma, in which skeletal myogenic progenitors can be routinely obtained. We first inject mouse PSCs into the limb muscle of an immuno-compromised mouse. Within 3–4 weeks, α7-integrin+ VCAM-1+ skeletal myogenic progenitors are purified by fluorescent-activated cell sorting. We further transplant these teratoma-derived skeletal myogenic progenitors into dystrophin-deficient mice to assess engraftment efficiency. This teratoma formation strategy is capable of generating skeletal myogenic progenitors with high regenerative potency from PSCs without genetic modifications or growth factors supplementation.

Key words Pluripotent stem cell, Muscle stem cell, Skeletal myogenic progenitor, Teratoma, Cell transplantation, Cell therapy

1 Introduction

Stem cell therapy is an attractive strategy to treat muscular dystrophies by replacing diseased muscles with new healthy muscles in patients [1]. Endogenous muscle stem cells (MuSCs), also known as satellite cells, normally reside adjacent to muscle fibers under the basal lamina and are indispensable for postnatal muscle growth, maintenance, and repair [2]. Freshly isolated MuSCs retain robust engraftment capability when transplanted into recipient muscles [3, 4]. However, endogenous MuSCs are rare, representing only 1–2% of mononuclear cells in skeletal muscle, and thus MuSCs obtained from a small muscle biopsy are inadequate to provide a meaningful quantity for therapeutics [5]. Moreover, ex vivo

Atsushi Asakura (ed.), *Skeletal Muscle Stem Cells: Methods and Protocols*, Methods in Molecular Biology, vol. 2640, https://doi.org/10.1007/978-1-0716-3036-5_13,

expansion of MuSCs is challenging, as MuSCs quickly activate and differentiate into myoblasts in cultures, abruptly diminishing their engraftment capability [6].

Pluripotent stem cells (PSCs), such as embryonic stem cells (ESCs) and induced pluripotent stem cells (iPSCs), represent a plentiful cell source for targeting degenerating muscles [7]. PSCs have unlimited proliferative power and can differentiate into many specific cell lineages including skeletal muscles. In the last few decades, our increased knowledge in skeletal myogenesis during embryo development has inspired several in vitro protocols to generate skeletal muscle cells from PSCs [8–10]. During early embryogenesis, the skeletal myogenic lineage originates from the somites, which are formed from paraxial mesoderm segmentation in response to signals from the neural tube, surface ectoderm, and notochord [7]. The developing somite subdivides into two compartments, dermomyotome and sclerotome. Cells in the dermomyotome express the skeletal myogenic transcription factor Pax3 or Pax7, and differentiate and elongate to form the myotome. The epaxial region of the myotome gives rise to trunk and back muscles, whereas the hypaxial myotome develops into limb muscles [7, 11]. This skeletal myogenesis process is spatially and temporally controlled by a number of signaling pathways including Wnt, sonic hedgehog and bone morphogenetic protein pathways, and transcription factors including Pax3, Pax7, myogenic regulatory factors (MyoD, Myf5, myogenin, and MRF4) [9, 12].

Currently, genetic modification and monolayer differentiation are two common approaches to derive skeletal myogenic cells from PSCs. Ectopic overexpression of skeletal myogenic transcription factors, such as Pax3 and Pax7, in PSC-derived mesoderm, can effectively produce the skeletal myogenic lineage [13, 14]. However, these genetically modified cells may not truly represent endogenous skeletal myogenic progenitors [15]. On the other hand, non-transgenic methods involve the modulation of various signaling pathways (e.g., by growth factors and small molecules) under defined culture conditions. Several studies have successfully induced monolayer PSCs to form mesoderm first, then Pax7-expressing skeletal muscle progenitors and mature skeletal myocytes, by sequential addition of small molecule or growth factor cocktails [16–19]. However, these monolayer differentiation methods require complex procedures and expensive reagents with a relatively low skeletal myogenic differentiation efficiency, all of which limit their application. Most importantly, the skeletal myogenic cells derived from many of these methods do not reliably engraft in transplantation assays, let alone offer functional improvement in diseased muscles.

Here we describe an innovative method to generate skeletal myogenic progenitors from PSCs via teratoma formation [20–22]. This method is simple, robust, does not require genetic modifications nor complex cell cultures, and can produce engraftable skeletal myogenic progenitors with exceptional regenerative potency. We provide in detail instructions on (1) induction of teratomas, (2) isolation of teratoma cells, (3) purification of teratoma-derived skeletal myogenic progenitors, and (4) transplantation of these purified progenitors.

2 Materials

2.1 Cell Culture and Maintenance

1. Mouse embryonic fibroblast (MEFs) medium: DMEM high glucose, supplemented with 10% FBS, 1% penicillin-streptomycin (Pen/Strep).
2. Mouse embryonic stem cell (mESC) medium: Knock-out™ DMEM, supplemented with 15% ES-qualified FBS, 2 mM GlutaMAX, 0.1 mM nonessential amino acids, 0.1 mM β-mercaptoethanol, 1000 U/ ml LIF, 1% Pen/Strep.
3. Mouse embryonic fibroblasts (MEFs), irradiated.
4. Mouse embryonic stem cells (mESCs).
5. 0.1% Gelatin from porcine skin (w/v) in H_2O, sterilized.
6. Phosphate Buffer Saline (PBS).
7. 0.25% Trypsin-EDTA.
8. T25 culture flasks.
9. Hemacytometer.
10. Inverted microscope.
11. 37 °C Water bath.
12. Centrifuge.
13. Incubator for cell culture (37 °C, 5% CO_2).
14. Laminar flow cell culture cabinet.

2.2 Irradiation, Injury, and Transplantation

1. NSG-mdx^{4Cv} mice. This mouse strain was generated by crossing NOD.Cg-Prkdc^{scid}Il2rg^{tm1Wjl}/SzJ (NSG, JAX #005557) mice and B6Ros.Cg-Dmd$^{mdx-4Cv}$/J (mdx^{4Cv}, JAX #002378) mice, as previously reported [4]. Note that NSG mice will also be suitable as recipients for teratoma formation and cell transplantation purposes, but in this case the donor cells will require a label (e.g., GFP) for donor-derived fibers identification.
2. Ketamine (150 mg/kg) + xylazine (10 mg/kg).
3. Cardiotoxin (10 μM) from *Naja pallida* (e.g., Latoxan L8102).
4. 70% eEhanol.

5. Insulin syringe.
6. Lead shields.
7. X-Ray irradiator (e.g., Rad Source RS-2000).
8. Electronic shaver.
9. Surgical extra-fine scissors.
10. Forceps with a curved tip.
11. Hamilton syringe with a 26-G needle.
12. Needle holder.
13. 6-0 Nylon suture.
14. Heating pad.

2.3 Cell Isolation

1. Digestion solution: DMEM high glucose, supplemented with 0.2% (w/v) collagenase type II and 1% Pen/Strep.
2. Rinsing solution: Ham's/F-10 medium, supplemented with 10% horse serum, 1% HEPES buffer solution, and 1% Pen/Strep.
3. Incubator shaker (e.g., New Brunswick Innova 44 Shaker).
4. Petri dish.
5. Dumont #7 forceps.
6. Razor blades.
7. 50 mL Conical tubes.
8. 40 μm Cell strainers.
9. 10 mL Syringes.
10. 18-G Needles.

2.4 Fluorescence-Activated Cell Sorting (FACS)

1. FACS staining medium: PBS with 2% FBS.
2. Propidium iodide (PI, 1 μg/mL final concentration).
3. Antibodies for FACS staining (Table 1).

Table 1
Antibodies for fluorescence-activated cell sorting (FACS)

Antibodies	Source	Identifier	Volume per million cells
PE-Cy7 CD31	BD biosciences	Cat#561410	0.5 μL
PE-Cy7 CD45	BD biosciences	Cat#552848	0.5 μL
APC α7-integrin	AbLab	Cat#67–0010-05	1 μL
Biotin VCAM-1	BD biosciences	Cat#553331	0.5 μL
Streptavidin-PE	BD biosciences	Cat#554061	0.5 μL

Table 2
Antibodies for immunostaining

Description	Source	Identifier	Dilution
Primary antibody			
Rabbit anti-DYSTROPHIN	Abcam	Cat#ab15277	1:200
Secondary antibody			
Goat anti-rabbit IgG(H + L) Alexa Fluor 555	Thermo fisher scientific	Cat#A27039	1:1000

4. Myogenic medium: Ham's/F-10 medium, supplemented with 20% FBS, 1% GlutaMAX, 10 ng/mL human bFGF, 114.4 μM β-mercaptoethanol (4 μL in 500 mL), and 1% Pen/Strep.
5. FACS machine (e.g., BD FACSAria II).

2.5 Sectioning and Immunohistochemistry

1. Surgical scissors and Dumont #5 forceps.
2. Peel-A-Way embedding mold square S22.
3. Optimal cutting temperature (OCT) mounting medium.
4. Liquid nitrogen in a Styrofoam box.
5. 2-Methylbutane in a beaker.
6. Cryostat.
7. Hydrophilic SUPER PAP PEN.
8. Microscope slides.
9. Blocking buffer: 3% bovine serum albumin (BSA) in PBS.
10. Primary and secondary antibodies (Table 2).
11. DAPI.
12. Immuno-mount medium and coverslips.
13. Fluorescence microscope.

3 Methods

3.1 Mouse Embryonic Stem Cells Preparation

1. Coat a T25 flask with 4 mL of 0.1% gelatin and incubate it for a minimum of 20 min at 37 °C.
2. Thaw 1 vial of mouse embryonic fibroblasts (MEFs) (1×10^6 cells per vial) by swirling in a 37 °C water bath. Transfer the cells into a 15 mL sterile tube with 5 mL of warm MEF medium. Centrifuge the cells at 1200 rpm for 3 min at room temperature. Aspirate the supernatant and resuspend the cell pellet with 5 mL MEF medium. Aspirate the gelatin from the gelatin-coated T25 flask and seed the cell suspension. Incubate the cells in a cell culture incubator (37 °C, 5% CO_2) overnight before using them as a feeder layer.

3. Thaw 1 vial of mouse embryonic stem cells (mESCs) in a 37 °C water bath. Transfer the cells into a 15 mL sterile tube with 5 mL of pre-warmed mESC medium. Centrifuge the cells at 1200 rpm for 3 min and resuspend the cell pellet in 5 mL mESC medium. Aspirate the MEF medium from the T25 flask containing the feeder cells and seed the mESC suspension. Put the flask into a cell culture incubator.
4. The next day, replace the spent medium with 5 mL of fresh mESC medium. For optimal mESCs growth, the medium should be changed daily. A good mESC culture should have round colonies with well-defined edges (*see* **Note 1**).
5. On day 2, aspirate the medium and wash the cells twice with sterile PBS. Add 2 mL of 0.25% trypsin-EDTA and incubate the cells at 37 °C for 5 min or until the cells begin to detach. Pipette up and down three to five times to dissociate the cells into singlets (*see* **Note 2**). Add 4 mL of mESC medium to neutralize trypsin and transfer the cells into a 15 mL tube. Centrifuge the cells at 1200 rpm for 3 min.
6. Aspirate the supernatant and resuspend the cell pellet in 5 mL mESC medium. Transfer the cells into a T25 flask and put it in a cell culture incubator. After 40 min of incubation, gently transfer only the cell suspension into a 15 mL tube (*see* **Note 3**). Take a small aliquot of cells for cell count.
7. Centrifuge the cell suspension at 1200 rpm for 3 min. Resuspend the cell pellet in 5 mL PBS and pellet the cells again by centrifuging at 1200 rpm for 3 min.
8. Resuspend the mESCs in PBS at a concentration of 250,000–500,000 cells per 10 μL. Place the cells on ice for usage as described in Subheading 3.2.3.

3.2 Teratoma Induction

3.2.1 Hind Limb Irradiation (Day 2)

1. Anesthetize the recipient NSG-mdx^{4Cv} mice (3- to 4-month-old, 25–30 g bodyweight) by an intraperitoneal injection of ketamine/xylazine (*see* **Note 4**).
2. Place the fully anesthetized mice in a supine position on an irradiator platform. Cover each mouse with a lead shield with the hind limbs exposed, permitting irradiation exposure only to the hind limbs. Adjust the hind limbs to be naturally straightened with the tibialis anterior (TA) muscles facing upwards. Tape the feet to fix the position.
3. Give a dose of 1200 cGy X-ray irradiation (*see* **Note 5**).
4. After irradiation, remove the lead shield and the tape, and transfer the mice back to their cages on a heating pad until they are fully recovered.

3.2.2 Cardiotoxin Injury (Day 1)

1. Autoclave the surgical scissors, forceps, and Hamilton syringe before use.
2. Twenty-four hours post-irradiation, anesthetize the irradiated mice by an intraperitoneal injection of ketamine/xylazine.
3. Shave around the TA muscle and swab with 70% ethanol. Cut an incision of the shaved skin to expose the TA muscle (Fig. 1c, d).
4. Using a Hamilton syringe with a 26-G needle, inject 15 μL cardiotoxin intra-muscularly into the irradiated TA muscle. Maintain a consistent needle depth of 4 mm with an angle of 30° (Fig. 1e). Slowly retract the needle to minimize leakage.
5. Stitch the wound with a 6-0 suture needle. Transfer the mice back to their cages on a heating pad until they are fully recovered.

3.2.3 Cell Transplantation (Day 0)

1. Autoclave the surgical scissors, forceps, and Hamilton syringe before use.
2. Prepare the cells at a concentration of 250,000–500,000 mESCs in 10 μL sterile PBS, as described in Subheading 3.1. Place the resuspended cells in a microcentrifuge tube on ice.

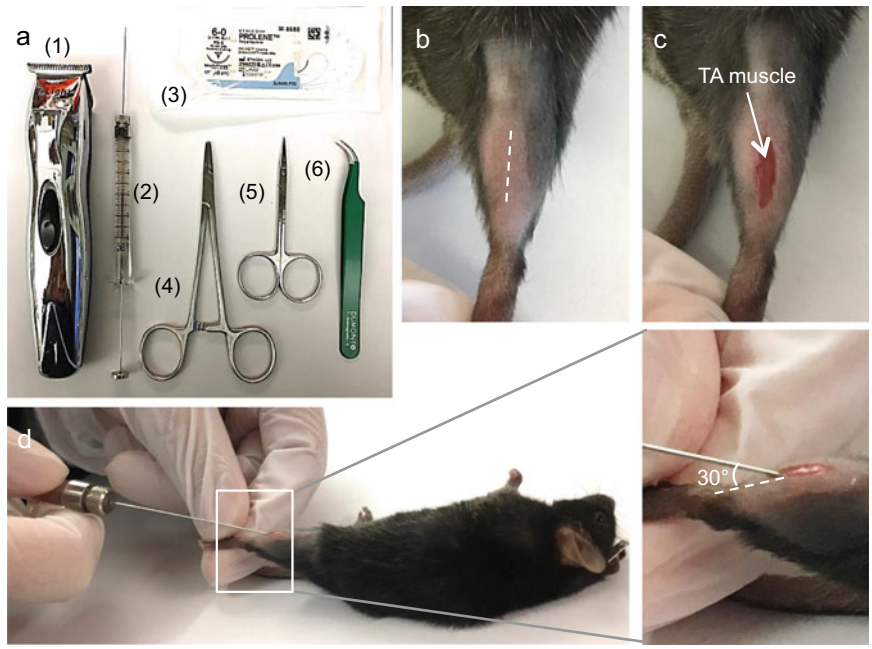

Fig. 1 Intra-muscular injection into the tibialis anterior (TA) muscle. (**a**) Equipment required for injection: (1) an electric shaver, (2) a 25 μL Hamilton syringe with a 26-G needle, (3) a 6–0 suture with needle, (4) a needle holder, (5) extra-fine scissors, and (6) forceps with curved tip. (**b**) A mouse hind limb is shaved to expose the skin on top of the TA muscle. (**c**) The TA muscle is exposed by a 7–10 mm skin incision. (**d**) Syringe positioning for injection: one hand holding the mouse foot and the other hand injecting from the Hamilton syringe into the TA muscle, maintaining an angle of 30°

3. Twenty-four hours post-injury, anesthetize the irradiated, cardiotoxin-injured mice by an intraperitoneal injection of ketamine/xylazine. Cut off the suture and open the incision to expose the TA muscle.
4. Draw 10 μL of cells into a Hamilton syringe with a 26-G needle. Slowly inject the cells intra-muscularly into the TA muscle. Maintain a consistent needle depth of 4 mm and angle of 30° (Fig. 1e). Wait 30 s before removing the needle to minimize leakage.
5. Stitch the wound with a 6-0 suture needle. Transfer the mice back to their cages on a heating pad until they are fully recovered.
6. Monitor the wound's healing status for several days. Monitor the mice to ensure institutional regulations of animal experiments are observed. Harvest the teratoma at 3–4 weeks; see the steps below.

3.3 Teratoma Cells Isolation

1. Autoclave the surgical scissors, forceps, and razor blades before tissue processing. Euthanize the mice with teratoma by CO_2 or other methods (*see* **Note 4**).
2. Spray the hind limb with 70% ethanol. Remove the skin from the knee to the heel to expose the teratoma and the entire hind limb. Use the surgical scissors to carefully dissect the teratoma from the TA muscle. Transfer the teratoma into a petri dish (Fig. 2). Subsequent steps should be performed under sterile conditions.

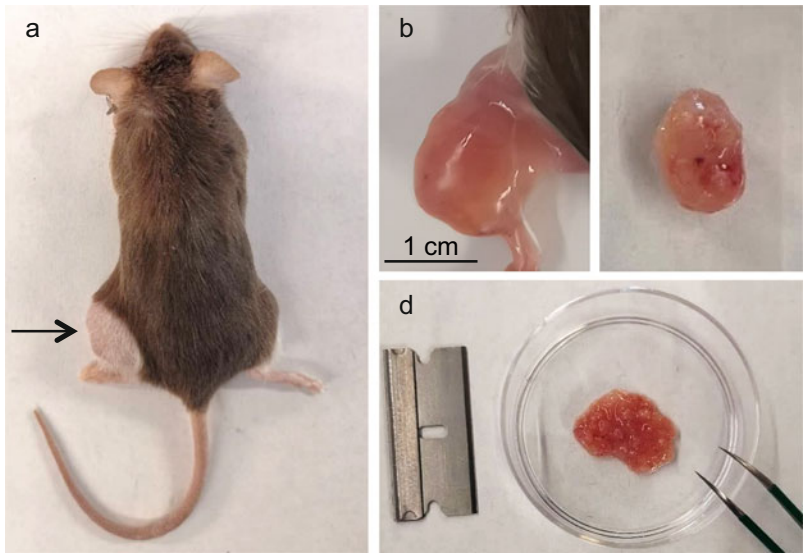

Fig. 2 Teratoma cell isolation. (**a**) Mouse with a teratoma grown at left hindlimb (arrow). (**b**) Skin is removed to expose the teratoma. (**c**) Excised teratoma. (**d**) Minced teratoma pieces

3. Measure the weight of the teratoma and calculate the volume of Digestion Solution at 15 mL per g of teratoma (*see* **Note 6**). The volumes described below correspond to 1 g of teratoma tissue, and the desired volumes for other weights can be calculated accordingly.
4. Cut the teratoma tissue into pieces approximately 2 mm thick, using a razor blade as a straight edge and pull along the edge with curved Dumont #7 forceps. Transfer the teratoma pieces into a 50 mL sterile conical tube containing 15 mL Digestion Solution.
5. Vortex for 3–5 s to ensure all tissues are submerged in the Digestion Solution. Incubate the tube in a shaker at 37 °C and 250 rpm for 30 min.
6. Remove the digested tissue from the shaker and vortex for 30 s. Filter the digested slurry through a 40 μm cell strainer to a new 50 mL conical tube:
   (a) For the flowthrough, add 15 mL Rinsing Solution for neutralization. Then centrifuge the cells at 1500 rpm, 4 °C for 10 min. Aspirate the supernatant, and put the cell pellet on ice (first-pass).
   (b) For tissues that are trapped by the cell strainer, transfer them back to the tube and add 7.5 mL of Digestion Solution. Vortex for 30 s and place the tube in a shaker at 37 °C and 250 rpm for 30 min. Remove the tube from the shaker and vortex for 30 sec. Pass the digested tissue through an 18-G needle four times using a 10 mL sterile syringe. Filter the digested slurry through a 40 μm cell strainer and collect the flowthrough into a new 50 mL conical tube. Wash the cell strainer with 15 mL of Rinsing Solution and collect the flowthrough into the same tube. Then centrifuge the cells at 1500 rpm, 4 °C for 10 min. Aspirate the supernatant, and put the cell pellet on ice (second-pass).
7. Combine first-pass and second-pass cells. Add 10 mL of Rinsing Solution to wash the cell pellet. Take a 10 μL aliquot for cell count (*see* **Note 7**). Centrifuge the rest of the cells at 1500 rpm, 4 °C for 5 min.
8. Carefully aspirate the supernatant. Resuspend the cells in FACS Staining Medium by pipetting up and down five to ten times. Cells are ready for subsequent steps.

3.4 Purification of Teratoma-Derived Skeletal Myogenic Progenitors

1. Prepare antibodies for single staining control (*see* **Note 8**) and staining mixture, as listed in Table 1. CD31 (endothelial marker) and CD45 (hematopoietic marker) serve as lineage-negative markers. α7-integrin and VCAM-1 are markers for skeletal myogenic progenitors.

2. Aliquot cells into 15 mL tubes (*see* **Note 9**) and add the antibodies. Mix by gentle tapping. Incubate the antibody-cell mixture on ice for 25 min in the dark.
3. Wash the cells with 5 mL of FACS Staining Medium and centrifuge at 1500 rpm, 4 °C for 5 min. Repeat once.
4. Aspirate the supernatant. Resuspend the cells in FACS Staining Medium with PI. Adjust the cell concentration to 10^6 cells per 100 μL approximately. PI is used to differentiate between live (PI–) and dead (PI+) cells. Put the stained cells on ice in the dark before FACS.
5. Filter the cells through a 40 μm cell strainer right before FACS to prevent clogging.
6. Set up the FACSAria II with a 100 μm nozzle, or other FACS machine with a similar setup (*see* Ref. [23]) with the following gating strategies (Fig. 3):
   (a) SSC-A vs. FSC-A to determine all cells.
   (b) FSC-W vs. FSC-H to determine singlets.
   (c) SSC-W vs. SSC-H to determine singlets.

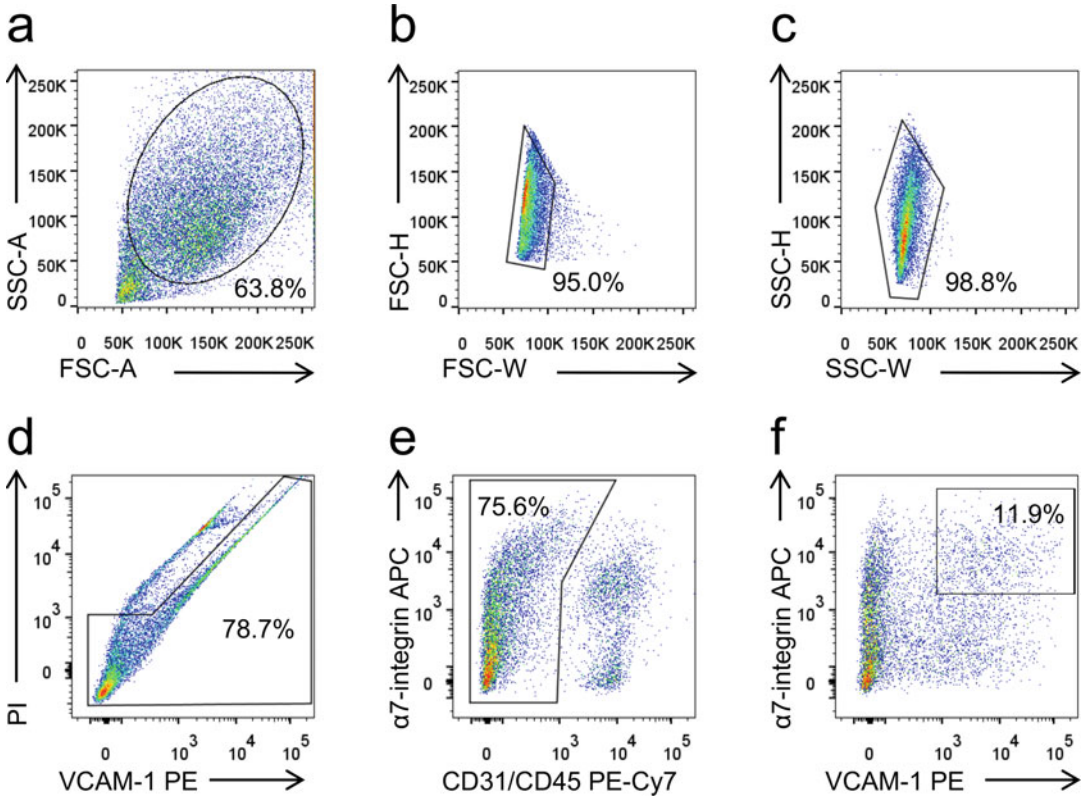

Fig. 3 Gating strategy for FACS analysis of teratoma-derived skeletal myogenic progenitors. (**a**–**c**) Forward and side scatter gates to determine cell singlets. (**d**) Live cell (PI–) gate. (**e**–**f**) Gating for the Lin– (CD31– CD45–) α7-integrin+ VCAM-1+ skeletal myogenic population

(d) PE vs. PI to determine live (PI−) cells.

(e) APC vs. PE-Cy7 to determine the Lin− (CD31− CD45−) population.

(f) APC vs. PE to determine the α7-integrin+ VCAM-1+ (α7+ VCAM+) population.

7. Run the single stain controls.
8. Sort α7+ VCAM+ cells, which are defined as skeletal myogenic progenitors. Cells are collected in a 15 mL tube containing 5 mL of Myogenic Medium at 4 °C (*see* **Note 10**).
9. Analyze the sorted cells to evaluate the sorting purity.

3.5 Transplantation of Teratoma-Derived Skeletal Myogenic Progenitors

1. Centrifuge the sorted α7+ VCAM+ cells at 1500 rpm, 4 °C for 5 min. Wash the cells with 5 mL of PBS and spin down. Aspirate the PBS and resuspend the pellet at a concentration of 40,000 cells per 10 μL PBS (*see* **Note 11**). Put the cells on ice for transplantation.
2. Refer to Subheading 3.2 for intra-muscular transplantation. Briefly, inject 10 μL of cell suspension into the TA muscle of an irradiated, cardiotoxin-injured recipient mouse. Harvest the TA muscles 4 weeks after transplantation for engraftment analysis.

3.6 Engraft Analysis

3.6.1 TA Muscle Harvest

1. Euthanize the recipient mouse and remove the skin of the mouse's hind limb. Gently remove the fascia that overlays the TA muscle and the surrounding hind limb muscles (Fig. 4a).

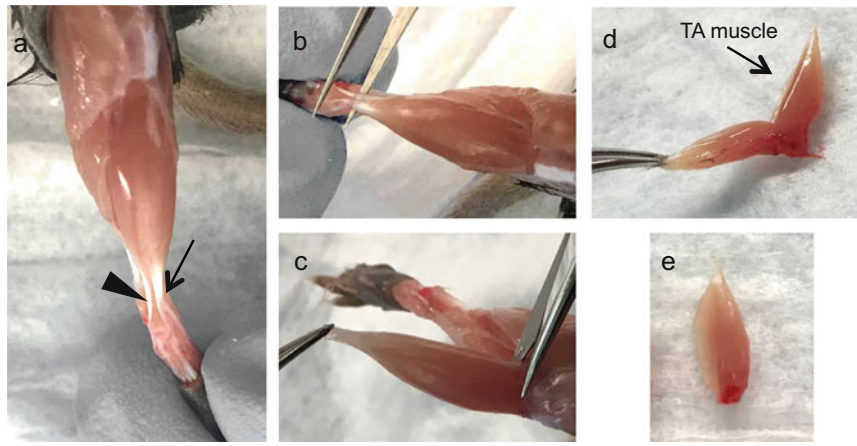

Fig. 4 Isolation of transplanted TA muscle. (**a**) The mouse hind limb musculature is exposed after skin removal. The arrow indicates the tendons of TA and extensor digitorum longus (EDL) muscle; the arrowhead indicates the tendons of peroneus brevis (PB) and peroneus longus (PL) muscle. (**b**) Forceps were inserted underneath of the tendons of TA, EDL, PB, and PL muscles, and the tendons at the ankle joint was cut. (**c**) Muscles are cut off together at the knee joint. (**d**, **e**) The TA muscle is separated by pulling it away from the other muscles

2. Removal of the skin and fascia exposes the four tendons on the anterior and lateral side of the ankle joint. These tendons respectively connect to, from the center to lateral, TA muscle, extensor digitorum longus (EDL) muscle, peroneus brevis (PB) muscle, and peroneus longus (PL) muscle. Insert the Dumont #5 forceps underneath these four tendons. Slide the forceps up to the knee to isolate the four muscles altogether. Keeping the Dumont #5 forceps underneath the muscles, use the Bonn scissors to cut the tendons at the ankle joints (Fig. 4b).
3. Grasp the distal part of the muscles by the tendons with the Dumont #5 forceps. Use the Bonn scissors to cut off the muscles at the knee joint (Fig. 4c). Be careful not to cut into the TA muscles.
4. Using two Dumont #5 forceps, one pair grasping the TA tendon, the other pair grasping the EDL, PB, and PL tendons, gently separate the two by pulling them apart (Fig. 4d, e; *see* **Note 12**).
5. Label a cryomold and fill in the OCT mounting medium to half. Submerge the isolated TA muscles into the OCT (*see* **Note 13**).
6. Prepare a 1000 mL beaker with 100 mL 2-methylbutane. Chill the beaker with liquid nitrogen until a frozen white layer of 2-methylbutane is formed. Put the embedded muscle in OCT on frozen 2-methybutane for 2 min for freezing. Store the frozen OCT-mounted muscles at −80 °C until sectioning.
7. Cut the OCT-mounted muscles into 10 μm sections using a cryostat. Collect sections onto microscope slides (*see* **Note 14**).
8. Air dry the slides at room temperature overnight, then store them in a slide case at −80 °C until analysis.

3.6.2 Engraftment Quantification

1. Warm up the slides from −80 °C at room temperature for 30 min.
2. Circle the sections on slides with the hydrophilic SUPER PAP PEN and let them air dry.
3. Rehydrate the sections in PBS twice for 5 min.
4. Incubate the sections with Blocking Buffer for 1 h at room temperature.
5. Incubate the sections with the primary antibody DYSTROPHIN (Table 2) in Blocking Buffer. Place sections in a humidified chamber overnight at 4 °C. Wash the sections three times with PBS, 5 min each.

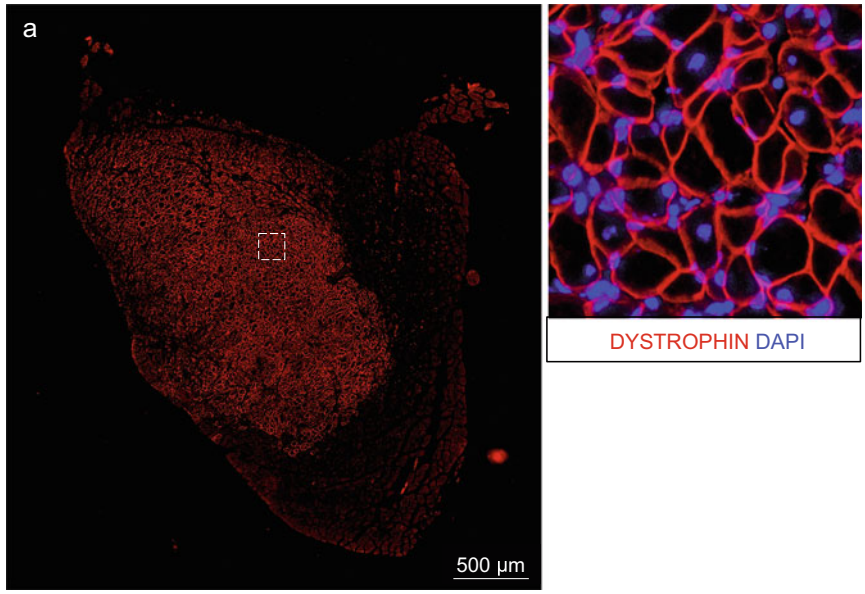

Fig. 5 Immunostaining of transplanted muscle cross-sections. (**a**) DYSTROPHIN+ fibers in the whole TA muscle. (**b**) A magnified image from the area indicated by the dotted square in (**a**)

6. Incubate the sections with secondary antibody (Table 2) in Blocking Buffer for 1 h, at room temperature in the dark. Wash the sections three times with PBS in the dark, 5 min each.
7. Incubate the sections with a 1:1000 dilution of DAPI in PBS. Incubate at room temperature for 10 min in the dark. Wash twice with PBS for 5 min each.
8. Mount the slide with Immuno-mount. Cover the slide with a coverslip and dry the slide for a few hours at room temperature. Store the stained slides in the dark at 4 °C.
9. View the slides and acquire images with an inverted fluorescence microscope. DYSTROPHIN+ fibers represent the engraftment of donor-derived α7+ VCAM+ myogenic progenitors (Fig. 5).

4 Notes

1. If more than 10% of mESC colonies look flattened (differentiated), passaging them at least once at 1:5–1:10 may help to restore their normal morphology.
2. Check cells under a microscope. If many cell clumps are present, pipette up and down several more times. A single ESC suspension is important to determine the cell number.
3. This step is essential to remove the MEF feeder cells. MEFs adhere to the T25 faster than mESCs, leaving the suspended

cells mainly mESCs. Incubation time can be increased to 60 min if some MEFs remain unattached.

4. Experiments using mice must be performed in accordance with the relevant institutional and governmental regulations.
5. Check the dose of the X-ray irradiator and calculate the desired irradiation time. For example, for a Rad Source RS-2000 X-Ray irradiator, the dose rate at shelf Level 3 is 200 cGy/min, therefore 1200 cGy corresponds to an irradiation time of 6 min.
6. The Digestion Solution should be freshly prepared to achieve a consistent enzyme activity.
7. Count the cells with a hemocytometer and use Trypan blue to exclude dead cells. One g of teratoma typically yields $2–3 \times 10^7$ cells.
8. Single staining control tubes, each containing a single specific antibody, are used to determine the fluorophore compensation matrix.
9. Adjust the volume of cell suspension between 200 μL and 500 μL for efficient staining.
10. Sorting speed should be determined empirically according to the FACS machine manual.
11. Avoid creating air bubbles.
12. There will be very little resistance when the fascia is completely removed. At this point, an intact TA muscle is separated.
13. Avoid creating bubbles. If necessary, use pipet tips to remove bubbles in the OCT, especially those near the muscle.
14. Collect one section every 200 μm apart such that 10 sections along the length of the transplanted TA muscle are collected in one single slide.

Acknowledgments

This work is supported by Regenerative Medicine Minnesota and the University of Minnesota start-up fund.

References

1. Blau HM, Daley GQ (2019) Stem cells in the treatment of disease. N Engl J Med 380(18): 1748–1760. https://doi.org/10.1056/NEJMra1716145
2. Charge SB, Rudnicki MA (2004) Cellular and molecular regulation of muscle regeneration. Physiol Rev 84(1):209–238. https://doi.org/10.1152/physrev.00019.2003
3. Montarras D, Morgan J, Collins C et al (2005) Direct isolation of satellite cells for skeletal muscle regeneration. Science 309(5743): 2064–2067. https://doi.org/10.1126/science.1114758
4. Arpke RW, Darabi R, Mader TL et al (2013) A new immuno-, dystrophin-deficient model, the NSG-mdx(4Cv) mouse, provides evidence for functional improvement following allogeneic satellite cell transplantation. Stem Cells 31(8): 1611–1620. https://doi.org/10.1002/stem.1402

5. Chan SS, Shi X, Toyama A et al (2013) Mesp1 patterns mesoderm into cardiac, hematopoietic, or skeletal myogenic progenitors in a context-dependent manner. Cell Stem Cell 12(5):587–601. https://doi.org/10.1016/j.stem.2013.03.004
6. Sacco A, Doyonnas R, Kraft P et al (2008) Self-renewal and expansion of single transplanted muscle stem cells. Nature 456(7221):502–506. https://doi.org/10.1038/nature07384
7. Chal J, Pourquie O (2017) Making muscle: skeletal myogenesis in vivo and in vitro. Development 144(12):2104–2122. https://doi.org/10.1242/dev.151035
8. Kodaka Y, Rabu G, Asakura A (2017) Skeletal muscle cell induction from pluripotent stem cells. Stem Cells Int 2017:1376151. https://doi.org/10.1155/2017/1376151
9. Murry CE, Keller G (2008) Differentiation of embryonic stem cells to clinically relevant populations: lessons from embryonic development. Cell 132(4):661–680. https://doi.org/10.1016/j.cell.2008.02.008
10. Penaloza JS, Pappas MP, Hagen HR et al (2019) Single-cell RNA-seq analysis of Mesp1-induced skeletal myogenic development. Biochem Biophys Res Commun 520(2):284–290. https://doi.org/10.1016/j.bbrc.2019.09.140
11. Buckingham M, Relaix F (2015) PAX3 and PAX7 as upstream regulators of myogenesis. Semin Cell Dev Biol 44:115–125. https://doi.org/10.1016/j.semcdb.2015.09.017
12. Buckingham M, Rigby PW (2014) Gene regulatory networks and transcriptional mechanisms that control myogenesis. Dev Cell 28(3):225–238. https://doi.org/10.1016/j.devcel.2013.12.020
13. Darabi R, Arpke RW, Irion S et al (2012) Human ES- and iPS-derived myogenic progenitors restore DYSTROPHIN and improve contractility upon transplantation in dystrophic mice. Cell Stem Cell 10(5):610–619. https://doi.org/10.1016/j.stem.2012.02.015
14. Filareto A, Parker S, Darabi R et al (2013) An ex vivo gene therapy approach to treat muscular dystrophy using inducible pluripotent stem cells. Nat Commun 4:1549. https://doi.org/10.1038/ncomms2550
15. Jiwlawat N, Lynch E, Jeffrey J et al (2018) Current progress and challenges for skeletal muscle differentiation from human pluripotent stem cells using transgene-free approaches. Stem Cells Int 2018:6241681. https://doi.org/10.1155/2018/6241681
16. Borchin B, Chen J, Barberi T (2013) Derivation and FACS-mediated purification of PAX3+/PAX7+ skeletal muscle precursors from human pluripotent stem cells. Stem Cell Rep 1(6):620–631. https://doi.org/10.1016/j.stemcr.2013.10.007
17. Xu C, Tabebordbar M, Iovino S et al (2013) A zebrafish embryo culture system defines factors that promote vertebrate myogenesis across species. Cell 155(4):909–921. https://doi.org/10.1016/j.cell.2013.10.023
18. Chal J, Oginuma M, Al Tanoury Z et al (2015) Differentiation of pluripotent stem cells to muscle fiber to model Duchenne muscular dystrophy. Nat Biotechnol 33(9):962–969. https://doi.org/10.1038/nbt.3297
19. Shelton M, Metz J, Liu J et al (2014) Derivation and expansion of PAX7-positive muscle progenitors from human and mouse embryonic stem cells. Stem Cell Rep 3(3):516–529. https://doi.org/10.1016/j.stemcr.2014.07.001
20. Chan SS, Arpke RW, Filareto A et al (2018) Skeletal muscle stem cells from PSC-derived teratomas have functional regenerative capacity. Cell Stem Cell 23(1):74-85.e76. https://doi.org/10.1016/j.stem.2018.06.010
21. Xie N, Chu SN, Azzag K et al (2021) In vitro expanded skeletal myogenic progenitors from pluripotent stem cell-derived teratomas have high engraftment capacity. Stem Cell Rep 16(12):2900–2912. https://doi.org/10.1016/j.stemcr.2021.10.014
22. Pappas MP, Xie N, Penaloza JS (2022) Defining the skeletal myogenic lineage in human pluripotent stem cell-derived teratomas. Cells 11(9):1589. https://doi.org/10.3390/cells11091589
23. Arpke RW, Kyba M (2016) Flow cytometry and transplantation-based quantitative assays for satellite cell self-renewal and differentiation. Methods Mol Biol 1460:163–179. https://doi.org/10.1007/978-1-4939-3810-0_12

Part II

Animal Models for Muscle Stem Cells & Regeneration

Chapter 14

Techniques for Injury, Cell Transplantation, and Histological Analysis in Skeletal Muscle

Norio Motohashi, Katsura Minegishi, Michihiro Imamura, and Yoshitsugu Aoki

Abstract

Skeletal muscle can adjust to changes in physiological and pathological environments by regenerating using myogenic progenitor cells or adapting muscle fiber sizes and types, metabolism, and contraction ability. To study these changes, muscle samples should be appropriately prepared. Therefore, reliable techniques to accurately analyze and evaluate skeletal muscle phenotypes are required. However, although technical approaches to genetically investigating skeletal muscle are improving, the fundamental strategies for capturing muscle pathology are the same over the decades. Hematoxylin and eosin (H&E) staining or antibodies are the simplest and standard methodologies for assessing skeletal muscle phenotypes. In this chapter, we describe fundamental techniques and protocols for inducing skeletal muscle regeneration by using chemicals and cell transplantation, in addition to methods of preparing and evaluating skeletal muscle samples.

Key words Muscle regeneration, Myogenic cells, Cell transplantation, Dystrophin, *mdx*

1 Introduction

Skeletal muscle possesses a high capacity to repair following severe injury caused by exercise or disease. Myogenic progenitor cells and satellite cells (SCs) play a major role in muscle regeneration by proliferating and differentiating into myofibers or by self-renewal for SC pool maintenance [1–3]. In aging [4, 5] and muscular diseases, such as Duchenne muscular dystrophy (DMD) [6], the number of SCs significantly declines because of repeated expansions and defects in the self-renewal mechanism [4, 7, 8], impairing muscle regeneration. However, the mechanism underlying SC number maintenance is still unclear.

Several studies using genetically modified mice or cells have reported various genes that control SC function in skeletal muscle [9]. Recent technological advances have further enabled the modification of individual gene expression in a tissue-specific manner.

Atsushi Asakura (ed.), *Skeletal Muscle Stem Cells: Methods and Protocols*, Methods in Molecular Biology, vol. 2640, https://doi.org/10.1007/978-1-0716-3036-5_14,

The generation of Pax7-*CreER* mice has enabled the modulation of targeted gene expression, especially in Pax7-expressing cells, clarifying gene function in SCs [10–13].

Induction muscle injury in transgenic mice is one of the most reliable and easiest methods of evaluating the effects of individual genes on skeletal muscle. Different muscular injury models have been developed, such as myotoxin (cardiotoxin, notexin), chemical agents (barium chloride), and physical trauma (freezing or crushing) in order to study mechanisms underlying muscle regeneration and SC maintenance. Cell transplantation experiments are also used to assess the effects of transgenes on SCs by evaluating the contribution of donor cells to myofiber or SC pool reconstitution [14]. In case of difficulty in generating transgenic mice, exogenous gene-edited cell transplantation can be used to assess specific functions. Cell transplantation is currently believed to be a potential therapeutic approach for DMD patients [15].

In addition to its regenerative potential, skeletal muscle also has the unique ability to adapt to various physiological conditions or diseases by altering muscle volume, fiber type, and metabolic or contraction status. For example, exercise, aging, calorie restriction, cancer cachexia, or immobilization cause muscular hypertrophy or atrophy because of a synthesis–degradation imbalance [16–18]. These pathological changes are further associated with changes in muscle fiber type and metabolism, providing clues for diagnosing muscle diseases [17, 18].

To accurately and satisfactorily study these pathological changes, it is essential to establish a methodology for appropriately collecting and analyzing skeletal muscle samples. Pathological analysis including hematoxylin and eosin (H&E), nicotinamide adenine dinucleotide hydride (NADH), or cytochrome C oxidase (COX) staining combined with immunohistology using antibodies provides us with detailed information about muscles and helps us evaluate muscle phenotypes to make pathological diagnoses of diseases. In this chapter, we describe the fundamental techniques and protocols used in our laboratory for inducing muscle regeneration via chemicals, conducting cell transplantation, and preparing and evaluating muscle samples.

2 Materials

2.1 Intramuscular Injection of Chemical Solutions for Inducing Muscle Regeneration

1. Eight-week-old normal standard laboratory strain mice including C57/BL/6 J.
2. Isoflurane vaporizer.
3. Hair removal cream and a shaving razor or a shaver.
4. Sterile insulin syringes 29G × 1/2 needles.

5. Barium chloride solution ($BaCl_2$): Barium chloride is dissolved in sterile demineralized water at the concentration of 1.2% and stored at −80 °C. Draw 50 μL of $BaCl_2$ solution into a 0.5 mL insulin syringe (*see* **Note 1**).

2.2 Intramuscular Transplantation of Cultured Myoblasts to Immunodeficient Mice

1. Eight-week-old recipient mice including NOD/*scid* (NOD.CB17-*Prkdc*^{scid}/J), NSG (NOD.Cg-*Prkdc*^{scid}*Il2rg*^{tm1Wjl}/SzJ), or NOG (NOD/Shi-scid, IL-2Rγ^{null}) immunodeficient mice.
2. Isoflurane vaporizer.
3. Hair removal cream and a shaving razor or a shaver.
4. Sterile insulin syringes with 29G × 1/2 needles.
5. Cultured myoblasts.
6. 1.2% $BaCl_2$ solution in sterile demineralized water.

2.3 Isolation and Freezing of Muscle Samples

1. Regenerating or myoblast-transplanted murine muscles.
2. Isoflurane or CO_2 for euthanizing mice.
3. Scissors, forceps, and tweezers.
4. Tragacanth gum: Mix equal volumes of tragacanth gum and water until the gum becomes soft and sticky. Stuff the gum into 10 mL syringes and store them at 4 °C or −20 °C.
5. Cork disks (diameter 22 mm).
6. Liquid nitrogen.
7. Isopentane (2-methylbutane).
8. Dry ice.
9. Glass vials.

2.4 Sectioning and Staining of Muscle Samples

1. Cryostat.
2. Disposable microtome blades.
3. Poly-l-lysine- or silane-coated slides.
4. Cover glasses.
5. Moisture chamber.
6. Hydrophobic barrier pen.
7. Hematoxylin.
8. Eosin.
9. Ethanol: Ethanol is dissolved in sterile demineralized water at the concentration of 70%, 90%, and 100%, stored at −80 °C.
10. Xylene.
11. Mounting media.
12. Cold acetone (−20 °C).
13. (If required) 4% paraformaldehyde (PFA) solution: PFA is dissolved in phosphate-buffered saline at the concentration of 4% and stored at 4 °C.

14. Phosphate-buffered saline (PBS).
15. Goat serum.
16. Primary and secondary antibodies:
    - Anti-developmental myosin heavy chain (mouse monoclonal, clone: RNMY2/9D2, Leica Biosystems, Wetzlar, Germany).
    - Anti-dystrophin rod domain antibody (mouse monoclonal, polyclonal, clone: Dy4/6D3; Leica Biosystems)
    - Anti-laminin-α2 antibody (rat monoclonal, clone: 4A8; Sigma-Aldrich, St. Louis, MO, USA).
    - Alexa 488 goat anti-mouse immunoglobulin G (IgG) (H + L) highly cross-adsorbed (Thermo Fisher Scientific, Waltham, MA, USA).
    - Alexa 594 goat anti-rat IgG (H + L) highly cross-adsorbed (Thermo Fisher Scientific).
    - (If required) Anti-Green Fluorescent Protein (GFP: rabbit polyclonal, EMD Millipore Corporation, Burlington, MA, USA)
    - (If required) Anti-Pax7 (mouse monoclonal, clone: PAX7, R&D systems, Minneapolis, MN, USA)
17. Vectashield mounting medium with 4′,6-diamidino-2-phenylindole (DAPI; Vector Laboratories, Burlingame, CA, USA).
18. Clear nail polish.
19. Fluorescence microscope.

3 Methods

3.1 Intramuscular Injection of Chemical Solutions for the Induction of Muscle Regeneration

Typically used muscle regeneration models are developed by injecting myotoxic agents and chemicals or by inducing physical injury (freezing, irradiation, or crushing). Myotoxins include notexin (NTX; *Notechis scutatus* venom) or cardiotoxin (CTX; *Naja pallida* venom), and the commonly used chemical agent is $BaCl_2$. To induce muscle regeneration, the tibialis anterior (TA) muscle is generally used since it is easy to uniformly inject the solution into this muscle using a syringe.

All investigators should wear gloves and lab coats, following the regulations of their respective institutes. Syringes should be handled carefully and disposed of in a chemical hazard sharps container after procedures. The steps to induce synchronous muscle regeneration are as follows:

1. Anesthetize the mice using isoflurane.
2. Shave the hair around the TA muscle.

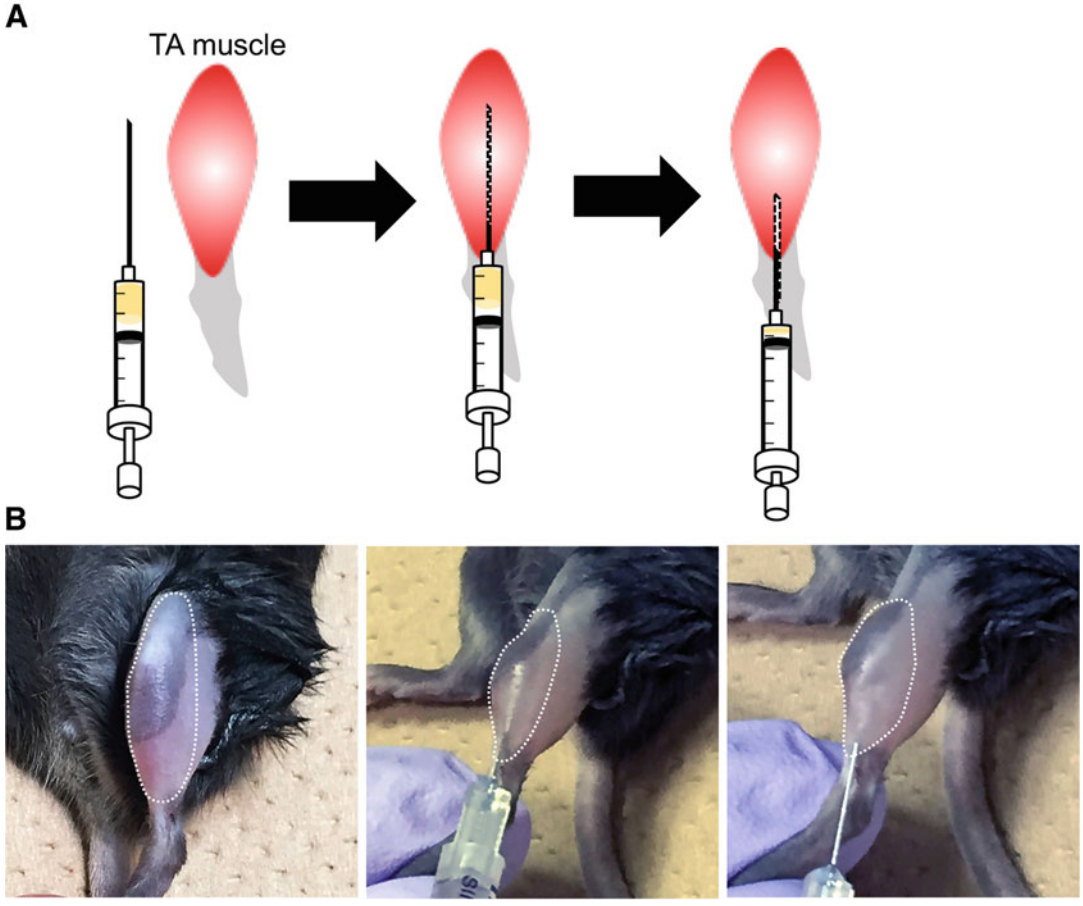

Fig. 1 Intramuscular injection of $BaCl_2$ solution in the TA muscle to induce muscle regeneration. (**a**) Schematic images of the injection. The needle tip is inserted from the distal side of the TA muscle and pushed further to the center to the proximal side of the TA muscle. The $BaCl_2$ solution is injected while slowly drawing back the needle so that the solution spreads throughout the muscle. (**b**) $BaCl_2$ (50 μL) is injected into a shaved TA muscle

3. Inject the $BaCl_2$ solution into the TA muscle (Fig. 1) using a 29G insulin syringe. Insert the needle tip from the distal side of the TA muscle and go further to the center, reaching the proximal side of the TA muscle. Inject the solution while slowly pulling back the needle to let the solution spread throughout the muscle (*see* **Note 2**).
4. Replace the mice in the cage.

3.2 Intramuscular Transplantation of Cultured Myoblasts into TA Muscle of mdx *Mice*

For high cell engraftment efficacy, donor myoblasts are transplanted into regenerating muscles. When donor myoblasts are injected into *mdx* dystrophin-deficient mice with degeneration and regeneration, there is no need to induce muscle injury before myoblast transplantation. To avoid immune rejection against injected myoblasts in the recipient's muscles, immunosuppressant drugs, such as FK506, or immunodeficient mice are used.

The steps to perform intramuscular transplantation are as follows:

One day prior to myoblast transplantation.

1. Anesthetize the mice using isoflurane.
2. Shave the hair around the TA muscle.
3. Twenty-four hours before myoblast transplantation, inject 50 μL of $BaCl_2$ into the TA muscle using a 29G insulin syringe to induce muscle regeneration (*see* **Note 3**).
4. Replace the mice in the cage.

On the day of myoblast transplantation.

5. Prepare donor myoblasts.

   Briefly, dissociate cultured myoblasts with 0.25% trypsin solution and centrifuge them at 400 × *g* for 5 min. Aspirate and discard the supernatant and resuspend the pellet in PBS (density 1×10^6 cells/30 μL of PBS). Transfer the suspended myoblasts into a 29G insulin syringe (*see* **Note 4**).

6. Anesthetize the mice using isoflurane.
7. Transplant the donor myoblasts into the TA muscle.

   Briefly, insert the needle tip from the distal side of the TA muscle and go further to the center, reaching the proximal side of the TA muscle. Inject 30 μL of the myoblast suspension while slowly pulling back the needle to let the solution spread throughout the muscle. Post-injection, hold the needle tip in the muscle for ~30 s to prevent myoblast suspension leakage.

8. Replace the mice in the cage.
9. One or two weeks post-transplantation, euthanize the recipient mice following the regulations of your respective institutes and dissect the necessary muscle tissue.

3.3 Isolation and Freezing of the Muscle Samples

The steps to dissect and freeze muscle samples are as follows:

1. At specified time points following muscle injury or myoblast transplantation, euthanize the mice following the regulations of your respective institutes.
2. Dissect the required muscle tissue and place the samples in dishes covered with moistened Kimwipe (Fig. 2) to prevent drying (*see* **Note 5**).
3. Mix equal volumes of tragacanth gum and water until the gum becomes soft and sticky (Fig. 3a). Stuff the gum into 10 mL syringes and store them at 4 °C or − 20 °C.

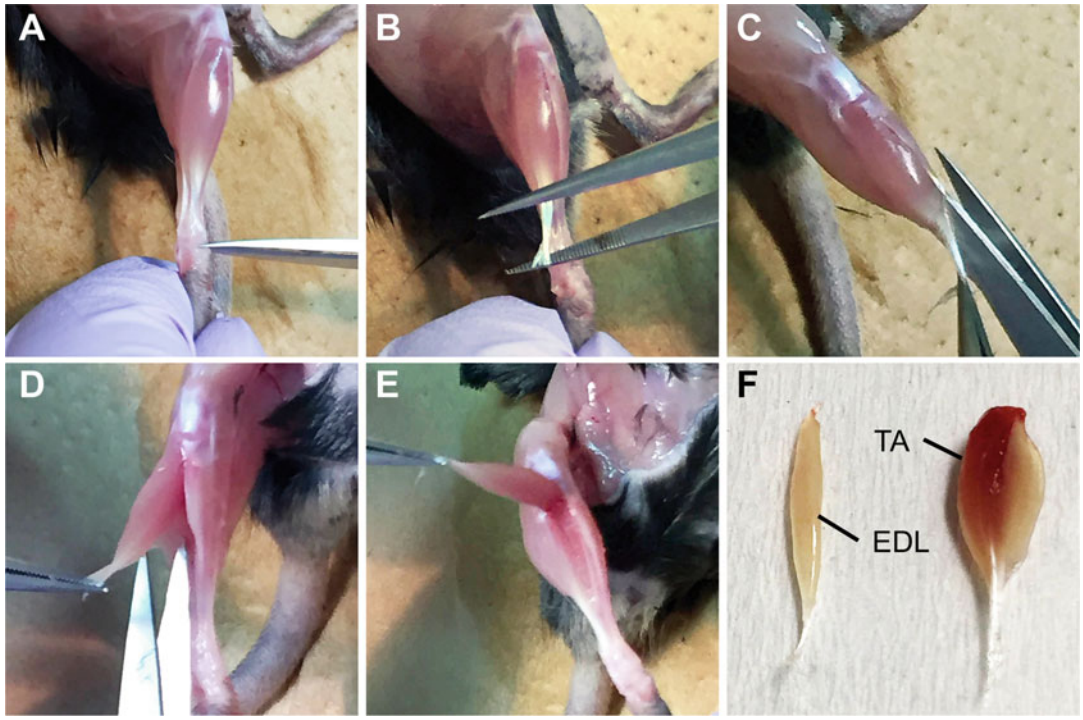

Fig. 2 Dissection of the TA and extensor digitorum longus (EDL) muscle. (**a**) The distal side of the TA tendon is cut around the instep. (**b**) The TA tendon is pulled out with tweezers. (**c**) The distal TA tendon is gripped with tweezers, and an edge of the TA muscle is carefully cut along the tibia with scissors. (**d**) The opposite edge of the hold of the TA muscle is carefully cut. (**e**) The TA muscle is held vertical to the tibia, cut close to the knee joint, and removed. (**f**) The TA and EDL muscles are separated

4. Place ~1 cm of tragacanth gum on a cork disc.
5. Embed the dissected samples in tragacanth gum. To prepare transverse sections, place samples perpendicular to the cork. To prepare longitudinal sections, mount samples horizontally to the cork (Fig. 3b).
6. Pour isopentane into a glass beaker and dip the beaker in liquid nitrogen. Wait until a frozen layer of isoflurane appears on the wall of the beaker (Fig. 3c).
7. Using tweezers, place each cork in cold isopentane for freezing. Move the samples constantly until they are completely frozen (for 1 min) and then keep them on dry ice for 30 min (Fig. 3c).
8. Put the samples in appropriately sized containers and store them at −80 °C.

3.4 Cryosectioning and Staining of Muscle Samples

Before cryosectioning, refer to the cryostat manufacturer's instructions. The following protocol has been optimized for staining dystrophin and laminin-α2 in *mdx* muscles, where muscle-derived myoblasts obtained from wild-type (WT) mice are injected. Before

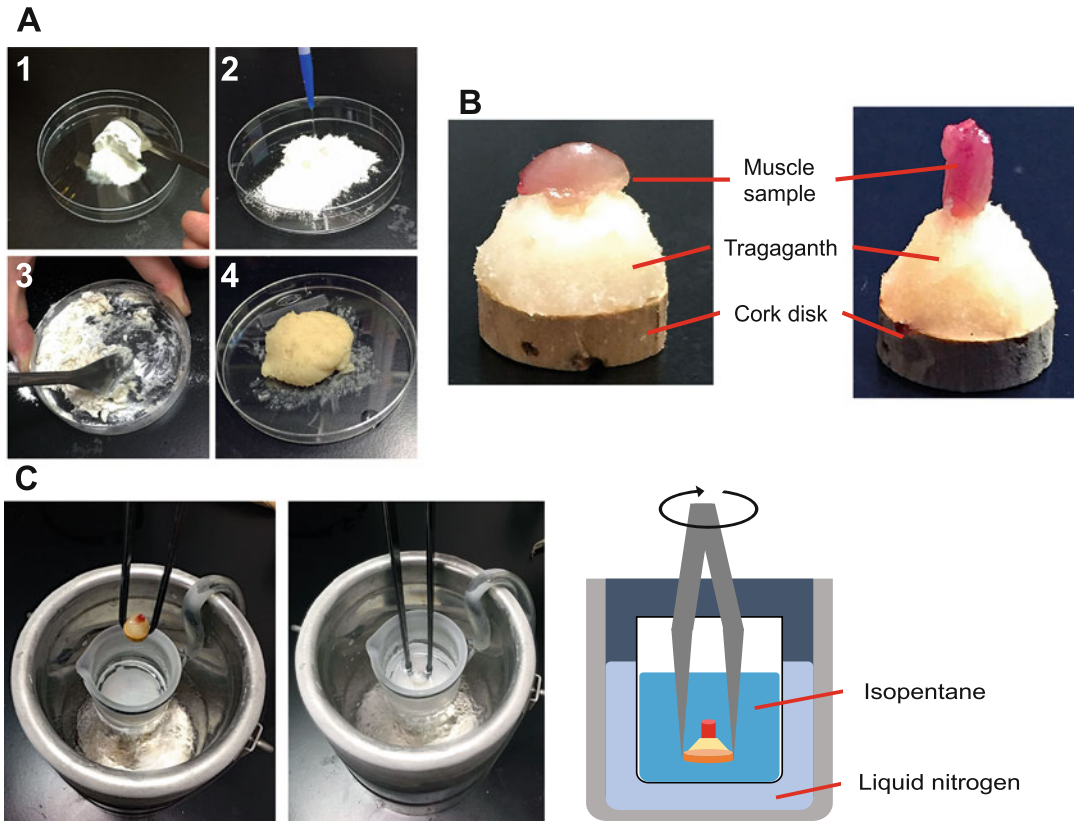

Fig. 3 Preparation of muscle sample freezing. (**a**) Preparation of tragacanth gum. Equal volumes of tragacanth gum and water are mixed. (**b**) The dissected TA muscle is embedded into tragacanth gum. The muscle samples are placed horizontally (left) or vertically (right) on the cork for longitudinal or transverse sections, respectively. (**c**) Each sample is placed in cold isopentane for freezing. The samples are shaken continuously until they are completely frozen

cryosectioning, make sure to set the cryostat chamber temperature at −25 °C. After temperature stabilization, place the cryostat chuck, frozen muscle samples, and disposable microtome blades inside the cryostat chamber for equilibration.

3.4.1 Cryosectioning

1. Drop water or an optimal cutting temperature (OCT) compound onto the cold cryostat chuck and place muscle samples on it. Wait for the water or OCT to freeze in order to secure the muscle samples (Fig. 4a).
2. Attach the cryostat chuck to the objective holder.
3. Place a microtome blade in the knife holder.
4. Trim the muscle samples to obtain flat sections.
5. Cut and place the sections onto glass slides. Ensure the section thickness is 6–8 μm for immunohistochemistry and 10 μm for H&E staining.

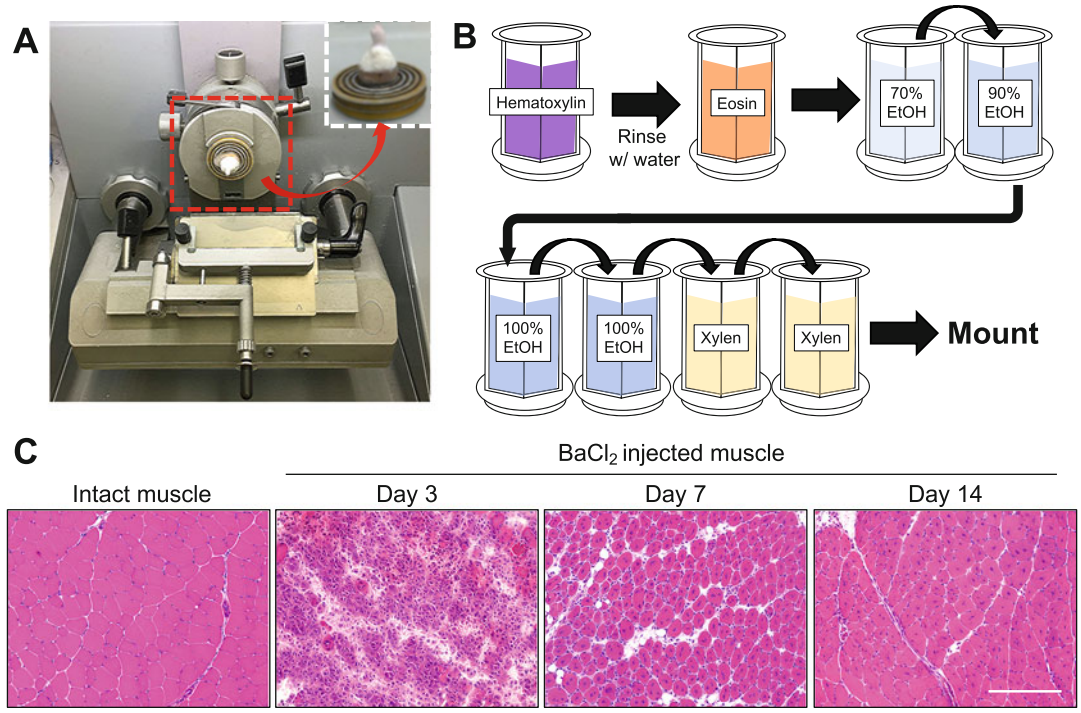

Fig. 4 H&E staining in regenerating muscle samples. (**a**) Preparation for sectioning. A muscle sample is placed on a cold cryostat chuck, which is attached to the objective holder. (**b**) H&E staining. (**c**) Representative images of intact and regenerating TA muscles (3, 7, and 14 days after $BaCl_2$ injection). Scale bar = 200 μm

6. Air-dry the glass slides at room temperature (RT).
7. If not processed immediately, store the glass slides with the sections in a box at −80 °C.

3.4.2 *H&E Staining*

Prior to H&E staining, equilibrate the stored glass slides at RT and dry them for 30 min. Prepare each H&E staining solution and ethanol in staining jars (Fig. 4b).

1. Soak the sections in hematoxylin solution for 5 min.
2. Rinse them with tap water for 5 min.
3. Soak the sections in eosin solution for 30 s.
4. Dehydrate the sections with ethanol as follows (Fig. 4b): 70%, 10 s → 90%, 10 s → 100%, 10 s → 100%, 10 s.
5. Rinse the sections twice with xylene for 10 s each time.
6. Mount the glass slides with a mounting medium.
7. Observe the stained sections under a microscope (Fig. 4c).

3.4.3 *Immunohistochemistry for dMyHC and Dystrophin*

The following protocol has been optimized for staining the developmental myosin heavy chain (dMyHC), dystrophin, and laminin-α2 in mice muscles. We do not recommend using formaldehyde-fixed samples, because these antibodies would not work enough to

obtain a satisfying signal in 4% paraformaldehyde (PFA)-fixed samples (*see* **Note 6**). Prior to staining, dry the prepared sections for 30 min.

1. Fix the sections in cold acetone for 15 min at −20 °C.
2. Dry the glass slides at RT.
3. Circle around the samples using a hydrophobic barrier pen and dry the glass slides again at RT.
4. Prepare a blocking solution containing 5% goat serum in 2% bovine serum albumin (BSA)/PBS.
5. Incubate the sections with the blocking solution in a moisture chamber for 15 min at RT.
6. Wash the sections with PBS for 5 min (three times).
7. Incubate the samples with primary antibodies diluted in the blocking solution in the moisture chamber overnight at 4 °C or 1 h at RT. For antibody dilution, refer to the manufacturers' datasheets (dMyHC: 1/200; dystrophin: 1/200; laminin-α2: 1/200).
8. After incubation, wash the samples with PBS for 5 min (three times).
9. Incubate the samples with secondary antibodies diluted with the blocking solution in the moisture chamber protected from light with foil for 30–60 min at RT.
10. Wash the samples with PBS for 5 min (three times).
11. Mount the glass slides with Vectashield antifade mounting medium with DAPI. Seal the glass slides using clear nail polish.
12. Count the maximum number of dMyHC- or dystrophin-positive fibers in all sections on one glass slide under a fluorescence microscope to evaluate the regeneration ability or efficiency of myoblast transplantation (Fig. 5).

4 Notes

1. The $BaCl_2$ injection volume is 50–100 μL per TA muscle of adult mice (>8 weeks old). This volume depends on the age or body weight of the mice analyzed. When inducing muscle regeneration in the gastrocnemius (GAS) or quadriceps femoris (QF) muscle of adult mice, the estimated injection volume is 150 L for GAS and 100 L for QF.
2. Injection does not require an incision of the skin to expose the TA muscle; shaving hair is enough.
3. GAS and QF muscles can also be used for myoblast transplantation.

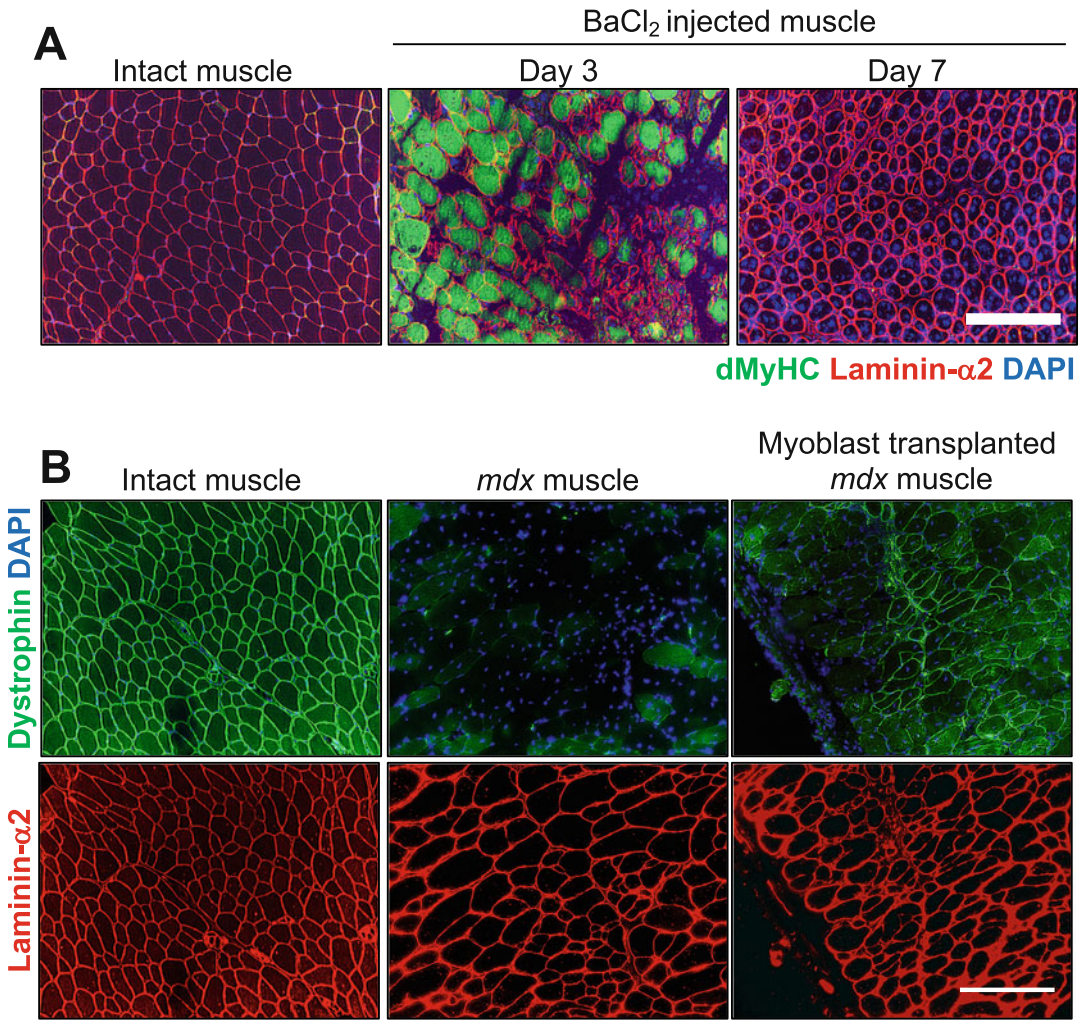

Fig. 5 Immunofluorescent staining in regenerating and myoblast-transplanted muscle samples. (**a**) Cross sections of regenerating TA muscles (3 and 7 days after $BaCl_2$ injection) were stained with dMyHC (green), laminin-α2 (red), and DAPI (blue). The dMyHC staining was temporally expressed in the early phase of regeneration, while it diminished by 7 days after $BaCl_2$ injection. Scale bar = 200 μm. (**b**) Representative images of dystrophin (green), laminin-α2 (red), and DAPI (blue) staining in intact WT, *mdx*, and myoblast-engrafted TA muscle of *mdx* mice (14 days post-transplantation). Myoblast transplantation from WT mice could restore dystrophin expression in the *mdx* TA muscle. Scale bar = 200 μm

4. The cell suspension concentration varies depending on the experiment. We recommend investigators prepare a cell suspension with high concentration and inject a small amount to avoid leakage.
5. If the dissected muscles contain fluorescent proteins, such as green fluorescent protein (GFP) or red fluorescent protein, they should be fixed in 4% PFA on ice for 30 min immediately

after dissection in order to avoid quenching fluorescence. After fixation, the samples should be soaked in 10% sucrose in PBS for 6 h at 4 °C and then soaked in 20% sucrose in PBS for 12 h at 4 °C. Then the samples can be embedded in tragacanth gum and frozen in cooled isopentane.

6. To stain GFP or Pax7, sections should be fixed with 4% PFA for 15 min at RT.

Acknowledgments

We would like to thank all members of the Department of Molecular Therapy, NCNP, for technical assistance, especially Reiko Terada. This work was supported by the Japan Society for the Promotion of Science Grant-in-Aid for Scientific Research (C) [grant number 18 K11067 to N.M].

References

1. Mauro A (1961) Satellite cell of skeletal muscle fibers. J Biophys Biochem Cytol 9:493–495
2. Charge SB, Rudnicki MA (2004) Cellular and molecular regulation of muscle regeneration. Physiol Rev 84:209–238
3. Collins CA, Olsen I, Zammit PS (2005) Stem cell function, self-renewal, and behavioral heterogeneity of cells from the adult muscle satellite cell niche. Cell 122:289–301
4. Day K, Shefer G, Shearer A et al (2010) The depletion of skeletal muscle satellite cells with age is concomitant with reduced capacity of single progenitors to produce reserve progeny. Dev Biol 340:330–343
5. Verdijk LB, Snijders T, Drost M et al (2013) Satellite cells in human skeletal muscle; from birth to old age. Age (Dordr) 36:545–547
6. Webster C, Blau HM (1990) Accelerated age-related decline in replicative life-span of Duchenne muscular dystrophy myoblasts: implications for cell and gene therapy. Somat Cell Mol Genet 16:557–565
7. Bernet JD, Doles JD, Hall J et al (2014) p38 MAPK signaling underlies a cell-autonomous loss of stem cell self-renewal in skeletal muscle of aged mice. Nat Med 20:265–271
8. Cosgrove BD, Gilbert PM, Porpiglia E et al (2014) Rejuvenation of the muscle stem cell population restores strength to injured aged muscles. Nat Med 20:255–264
9. Motohashi N, Asakura A (2014) Muscle satellite cell heterogeneity and self-renewal. Front Cell Dev Biol 2:1
10. Nishijo K, Hosoyama T, Bjornson CR et al (2009) Biomarker system for studying muscle, stem cells, and cancer in vivo. FASEB J 23: 2681–2690
11. Lepper C, Conway SJ, Fan CM (2009) Adult satellite cells and embryonic muscle progenitors have distinct genetic requirements. Nature 460:627–631
12. Murphy MM, Lawson JA, Mathew SJ et al (2011) Satellite cells, connective tissue fibroblasts and their interactions are crucial for muscle regeneration. Development 138:3625–3637
13. Mourikis P, Sambasivan R, Castel D et al (2012) A critical requirement for notch signaling in maintenance of the quiescent skeletal muscle stem cell state. Stem Cells 30:243–252
14. Motohashi N, Uezumi A, Asakura A et al (2018) Tbx1 regulates inherited metabolic and myogenic abilities of progenitor cells derived from slow- and fast-type muscle. Cell Death Differ 26:1024–1036

15. Motohashi N, Shimizu-Motohashi Y, Roberts TC et al (2019) Potential therapies using myogenic stem cells combined with bio-engineering approaches for treatment of muscular dystrophies. Cell 8:1066
16. Cohen S, Nathan JA, Goldberg AL (2015) Muscle wasting in disease: molecular mechanisms and promising therapies. Nat Rev Drug Discov 14:58–74
17. Ciciliot S, Rossi AC, Dyar KA et al (2013) Muscle type and fiber type specificity in muscle wasting. Int J Biochem Cell Biol 45:2191–2199
18. Talbot J, Maves L (2016) Skeletal muscle fiber type: using insights from muscle developmental biology to dissect targets for susceptibility and resistance to muscle disease. Wiley Interdiscip Rev Dev Biol 5:518–534

Chapter 15

Murine Models of Tenotomy-Induced Mechanical Overloading and Tail-Suspension-Induced Mechanical Unloading

Shin Fujimaki and Yusuke Ono

Abstract

Skeletal muscle is a highly plastic tissue that can alter its mass and strength in response to mechanical stimulation, such as overloading and unloading, which lead to muscle hypertrophy and atrophy, respectively. Mechanical loading in the muscle influences muscle stem cell dynamics, including activation, proliferation, and differentiation. Although experimental models of mechanical overloading and unloading have been widely used for the investigation of the molecular mechanisms regulating muscle plasticity and stem cell function, few studies have described the methods in detail. Here, we describe the appropriate procedures for tenotomy-induced mechanical overloading and tail-suspension-induced mechanical unloading, which are the most common and simple methods to induce muscle hypertrophy and atrophy in mouse models.

Key words Muscle plasticity, Muscle hypertrophy, Muscle atrophy, Mechanical loading, Tenotomy, Tail suspension

1 Introduction

Skeletal muscle accounts for a large proportion of the total body mass, making up approximately 30% of the total body weight in women and 38% in men [1]. It has indispensable roles in locomotion, whole-body metabolism, and reserving proteins [2]. Skeletal muscle has remarkable plasticity, and its mass and strength are flexibly altered to adapt to nutrition, changes in the environment, and physical activity [3].

Muscle hypertrophy and atrophy are physiological events that occur during the maintenance of biological homeostasis. Accumulating evidence has revealed that muscle mass and strength are controlled by mechanical stimulation [4–7]. Mechanical stimulations can also influence the dynamics of muscle stem cells termed "satellite cells." In adult muscle tissues, satellite cells are mitotically

Atsushi Asakura (ed.), *Skeletal Muscle Stem Cells: Methods and Protocols*, Methods in Molecular Biology, vol. 2640, https://doi.org/10.1007/978-1-0716-3036-5_15,

quiescent under steady conditions, but are rapidly activated in response to muscle injury; satellite cells then become myoblasts, which proliferate extensively and then undergo myogenic differentiation, fusing to the damaged myofibers and/or generating new myofibers [8]. Physical exercise or mechanical overloading in the muscle leads to an increase in muscle mass by activating satellite cells and inducing their proliferation, and differentiation [9–12]. The fusion of satellite cells with existing myofibers is thought to be controlled by paracrine signals derived from myofibers in the overloaded muscle [13]. In contrast, mechanical unloading, which results in a decrease in muscle mass, reduces satellite cell content and proliferative ability [14–17]. This indicates that satellite cells sense mechanical stimulations and subsequently alter their dynamics, a process dependent on myofiber size.

Muscle hypertrophy and atrophy are induced by mechanical overloading and unloading, respectively, in the muscles of rodent models [18–24]. Two methods are used to induce muscle hypertrophy: synergist ablation (SA), the partial excision of the gastrocnemius and soleus muscles, and tenotomy, where the tendons of those muscles alone are ablated. In both models, the plantaris muscle is overloaded, resulting in compensatory hypertrophy. However, there is a difference in the efficiency of hypertrophic responses between SA and tenotomy. A vast number of regenerating myofibers are observed in the non-irradiated muscle, but not in the irradiated (satellite cell–depleted) muscle following SA [18], suggesting that SA produces an overload model with extremely high intensity, stimulating satellite cells to form new myofibers. Meanwhile, tenotomy produces a mild overload model that does not induce such a robust increase in the number of regenerating myofibers. Indeed, the increase in muscle mass of the plantaris reaches a plateau 2–3 weeks after tenotomy surgery [19], while it continues to grow for a longer period after SA surgery [20, 21].

Tail suspension and hindlimb immobilization are widely used to produce animal models of muscle atrophy, caused by a decrease in mechanical loading. In both models, reduced muscle mass and cross-sectional area of myofibers are observed in the hindlimb muscles, especially the slow-fiber-rich soleus muscle [22, 23]. The reduction in muscle mass in fast-fiber-rich muscles such as the gastrocnemius and plantaris can be affected by the angle of the fixed ankle in rodents, especially in the hindlimb immobilization model [24].

It is important to choose appropriate overloading and unloading models and precisely perform the operations. In this chapter, we describe the detailed methods for operating tenotomy and tail suspension, which are the most common and simple models to induce muscle hypertrophy and atrophy, respectively.

2 Materials

2.1 Tenotomy Model

1. Surgical blade No.11 (FEATHER).
2. Fine forceps.
3. Pointed-tip scissors.
4. Suture with needle (No. 5-0).
5. Hair remover (depilatory cream).
6. Cotton swab.
7. Three types of mixed anesthetic were used (*see* **Note 1**).
8. Atipamezole hydrochloride (medetomidine antagonist).
9. Syringe with 26G needle.

2.2 Tail Suspension Model

1. Animal cages (CL-0106-2, CLEA Japan, Inc.) (*see* **Note 2**).
2. Cage lid (made to order) (Fig. 2a) (*see* **Note 3**).
3. Water bottle with dispenser.
4. Kite string.
5. Sponge tape.
6. Key rings.
7. Swivel.
8. Plastic tape.
9. Normal mice chow.

3 Methods

3.1 Surgical Operation for Tenotomy

1. C57BL/6 mice are anesthetized by intraperitoneal injection with three types of mixed anesthetics (10 μL/g body weight).
2. Remove the hair on the posterior hindlimbs with a depilatory cream and wipe the area with the cotton swab (Fig.1a).
3. Carefully make an incision along the midline of the calf (Fig.1b) (*see* **Note 4**).
4. Gently roll the skin toward the tibia in order to reveal the tendons belonging to the gastrocnemius, soleus, and plantaris (Fig. 1c).
5. To easily find the boundary between the tendon of the plantaris and those of the gastrocnemius and soleus, insert fine forceps into the boundary (Fig. 1d).
6. Cut the tendons of the gastrocnemius and soleus using pointed-tip scissors (Fig. 1e).

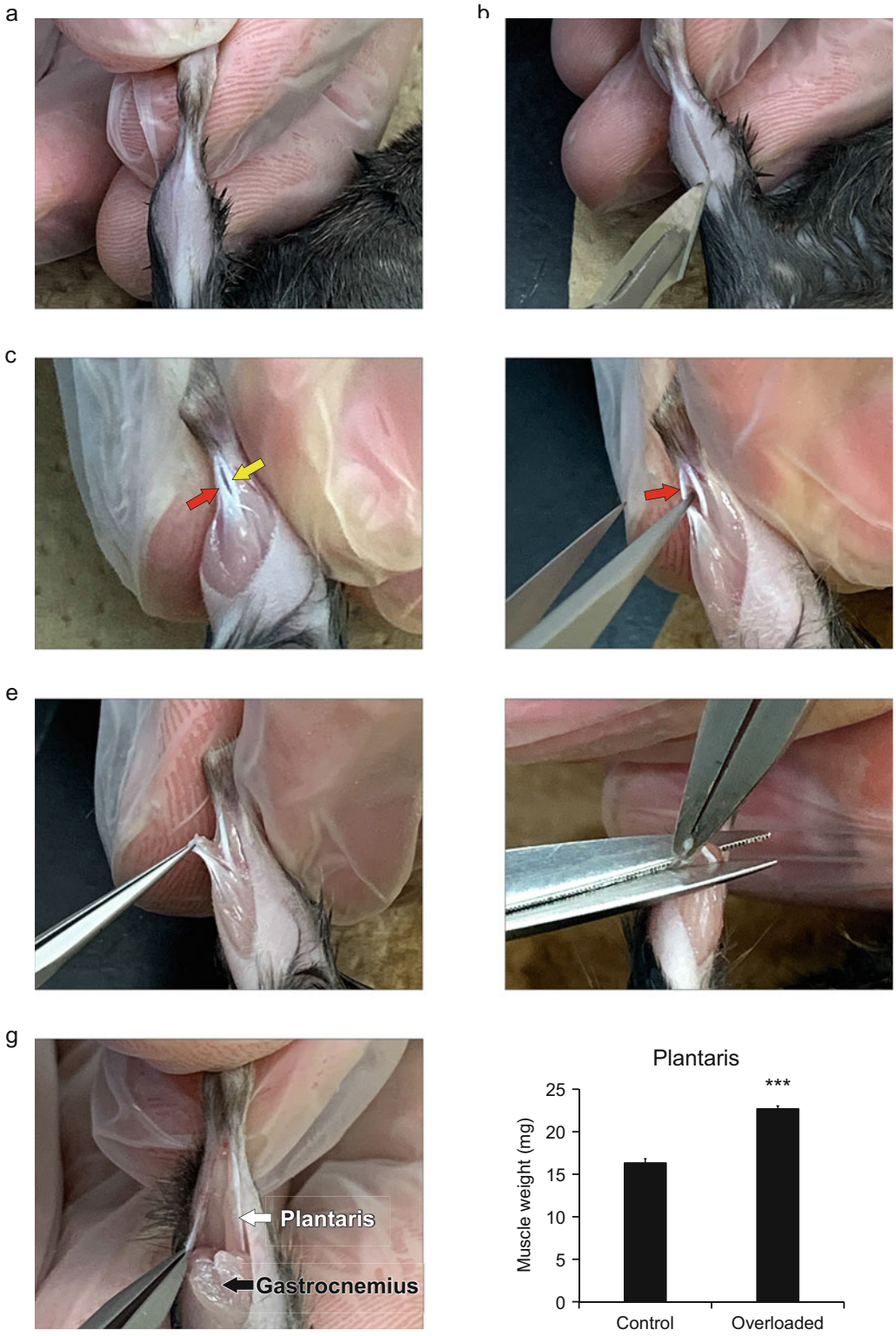

Fig. 1 Tenotomy model operation. (**a**) Exposed skin of hindlimb after hair removal. (**b**) The incision is made in the middle of the calf with a surgical blade. (**c**) The boundary between the tendon belonging to the plantaris (indicated by a yellow arrow) and the gastrocnemius and soleus (indicated by a red arrow). (**d**) The boundary is

7. To prevent the reconnection of the tendons to the calcaneus bone, excise the tendons completely, including the tips of muscles (Fig. 1f, g) (*see* **Note 5**).
8. Close the incision with three or four stitches (*see* **Note 6**).
9. Repeat the procedure for another leg (*see* **Note 7**).
10. Administer 0.75 mg/kg of atipamezole hydrochloride through intraperitoneal injection for the reversal of the sedative and analgesic effects of medetomidine.
11. Collect the plantaris at an optional timepoint after the surgery (Fig. 1h) (*see* **Note 8**).

3.2 Tail Suspension Method

1. Supply lab animal bedding and chow in the animal cage and ensure water is accessible to the animals.
2. Prepare the following materials (Fig. 2b): two 2-cm long pieces of sponge tape (1); 15 cm of kite string, tied into a ring with a knot (2); a swivel with key rings on both ends (3).
3. Sandwich the root of the tail of the C57BL/6 mouse and the ring of kite string between two pieces of sponge tape. The loop end of the string is located on the side of the tail tip and the knot is located outside of the sponge tape (Fig. 2c) (*see* **Note 9**). To reinforce the adhesion of the sponge tape, put plastic tape on top of the sponge tape (Fig. 2d).
4. Hang the key ring from the middle horizontal bar of the cage lid (Fig. 2e). The angle between the line of the mouse's body and that of the cage bottom was adjusted to approximately 45° (Fig. 2e) (*see* **Note 10**).
5. Make the rail stoppers using plastic tape on the cage lid in order to prevent the mouse from climbing up the water bottle or walls of the cage (Fig. 2f) (*see* **Note 11**).
6. Ensure that the mouse is able to drink from the water bottle the day after the operation.
7. Collect muscle tissues at an optional timepoint after the operation (Fig. 2g) (*see* **Note 12**).

Fig. 1 (continued) enlarged with forceps for easier access to cut the tendons belonging to gastrocnemius and soleus (indicated by a red arrow). (**e**) The root of the tendons belonging to the gastrocnemius and soleus are cut with pointed-tip scissors. (**f**) Dissection of the tendons, including the tip of the muscle tissues, prevents the reconnection of tendons to the calcaneus bone. (**g**) Dissected gastrocnemius (indicated by a black arrow) and intact plantaris (indicated by a white arrow). (**h**) A representative bar graph depicting weights of the plantaris muscles in control and overloaded mice. Plantaris weights are significantly increased by overloading for two weeks. Values are represented as averages +SE ($n = 6$). *** indicates a significant difference compared to control ($P < 0.001$)

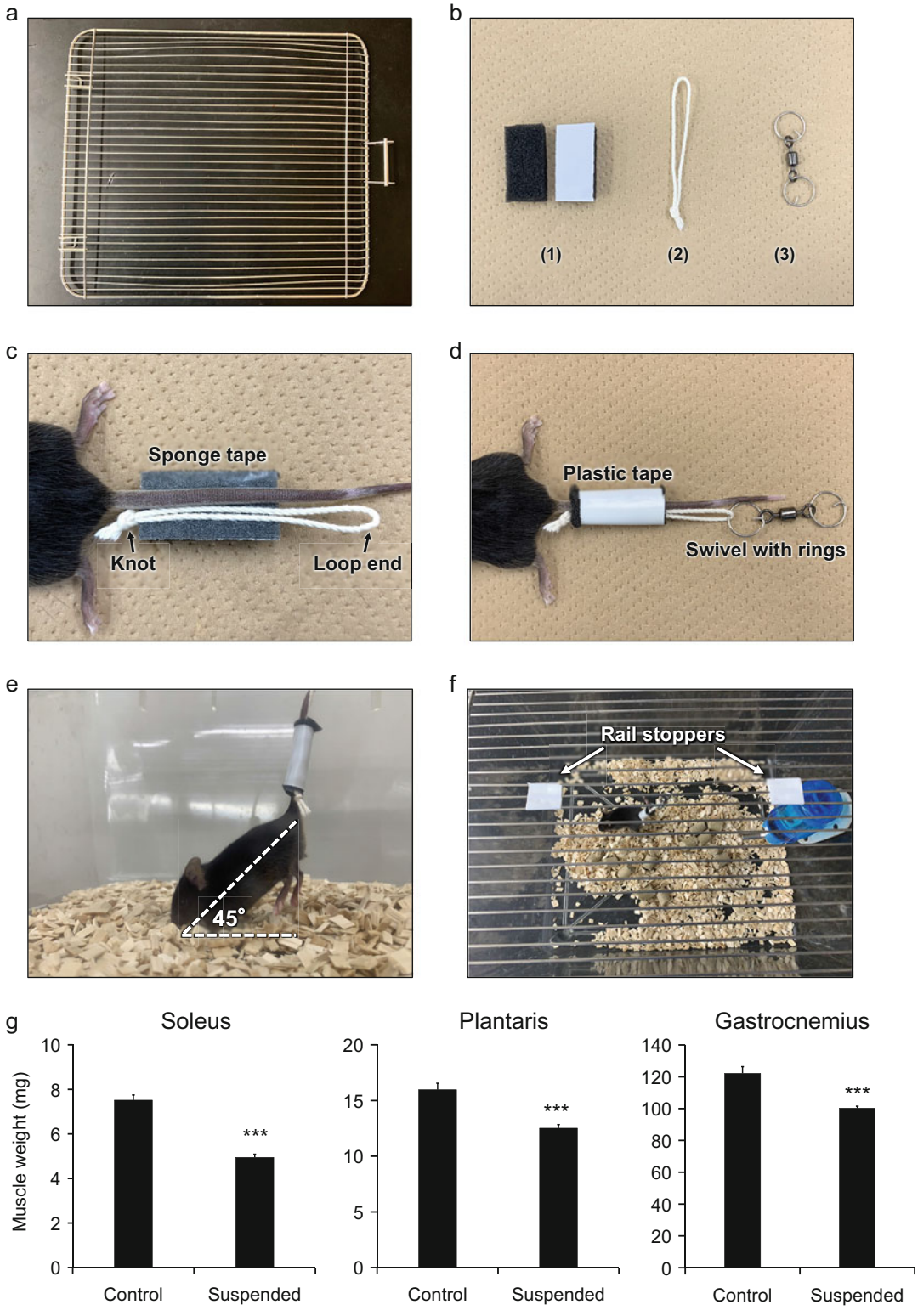

Fig. 2 Tail suspension method. (**a**) A customized cage lid without vertical bars in the middle of the lid is required in order to use the horizontal bars as rails for the ring (**b**) Prepared materials for suspending mice:

4 Notes

1. The combination of anesthetics is prepared with medetomidine (0.75 mg/kg body weight), midazolam (4 mg/kg body weight), and butorphanol (5 mg/kg body weight).
2. Prepare the animal cages with a height of over 15 cm.
3. Cage lids need to be customized. Vertical bars in the middle of the lids are removed in order to use the horizontal bars as rails for the rings, which are used to suspend the mouse. This allows the mouse to move freely to some degree and reduce its stress.
4. Ensure not to deviate from the midline of the calf to avoid breaking the blood vessels around the tendons.
5. The tendons must be completely removed; in particular, a piece of the tendon in the soleus muscle often remains uncut.
6. Do not suture the tendon of the plantaris with the skin.
7. If another leg is used as a control, this process is skipped. Operations on both legs are recommended because the hypertrophic responses are higher than when the operation is performed on only one leg.
8. If the plantaris muscles are collected 2 weeks or longer after surgery, the remaining gastrocnemius and soleus muscles may become attached to the plantaris muscles. To obtain precise data for muscle weight, adherent muscle tissues should be carefully removed using forceps and a surgical blade.
9. The loop end of the string should be placed at approximately 1.5 cm under the tail tip of the mouse.
10. Over-hanging causes severe difficulties in mouse excretion. Adjust the length of the hanging materials using additional rings.
11. Ensure that the mouse has access to drinking water.

Fig. 2 (continued) (1) Two pieces of sponge tape (2 cm in length), (2) kite string, folded and knotted, and (3) swivel with two key rings. (**c**) Mouse tail and kite string are attached to the adhesive surface of the sponge tape. The loop end of the string is located on the side of the tail tip. The knot is located outside of the sponge tape. (**d**) Fixed mouse tail and string with sponge tape and plastic tape for reinforcement. The swivel is connected to the loop end of the string with a key ring. (**e**) The mouse is suspended from the cage lid using the swivel with the key rings. The angle between the line of the mouse body and that of the cage bottom should be adjusted to approximately 45°. (**f**) Rail stoppers made of plastic tape are used to prevent the mouse from climbing up the water bottle and the walls of the cage. (**g**) Representative bar graphs depicting the muscle weights in the control and suspended mice. Decreased muscle weights are observed in the soleus (left), plantaris (middle), and gastrocnemius (right) following hindlimb unloading for 1 week. Values are represented as averages +SE ($n = 6$). *** indicates a significant difference compared to control ($P < 0.001$)

12. Unloading for 1 week is sufficient to induce muscle atrophy in the posterior lower legs, including the gastrocnemius, plantaris, and soleus (Fig. 2g) but not in the anterior lower legs, for example, the tibialis anterior (TA) and extensor digitorum longus [25]. However, decreased muscle weight in the TA is observed after 2 weeks of unloading [23].

Acknowledgments

This work was supported by the Japan Agency for Medical Research and Development (AMED, JP18ek0109383 and JP19bm0704036), the FOREST program of the Japan Science and Technology Agency (JST, JPMJFR205C) the Grant-in-Aid for Scientific Research KAKENHI (18H03193, 20K21763, 20K19641, 22K18414 and 22H00505) from the Japan Society for the Promotion of Science (JSPS), the Uehara Memorial Foundation, and the Takeda Science Foundation.

References

1. Janssen I, Heymsfield SB, Wang ZM et al (2000) Skeletal muscle mass and distribution in 468 men and women aged 18-88 yr. J Appl Physiol 89(1):81–88
2. Baskin KK, Winders BR, Olson EN (2015) Muscle as a "mediator" of systemic metabolism. Cell Metab 21:237–248
3. Miyazaki M, Esser KA (2009) Cellular mechanisms regulating protein synthesis and skeletal muscle hypertrophy in animals. J Appl Physiol 106(4):1367–1373
4. Young A, Stokes M, Round JM et al (1983) The effect of high-resistance training on the strength and cross-sectional area of the human quadriceps. Eur J Clin Investig 13(5): 411–417
5. Kandarian SC, Young JC, Gomez EE (1992) Adaptation in synergistic muscles to soleus and plantaris muscle removal in the rat hindlimb. Life Sci 51(21):1691–1698
6. LeBlanc A, Gogia P, Schneider V et al (1988) Calf muscle area and strength changes after five weeks of horizontal bed rest. Am J Sports Med 16(6):624–629
7. Cadena SM, Zhang Y, Fang J et al (2019) Skeletal muscle in MuRF1 null mice is not spared in low-gravity conditions, indicating atrophy proceeds by unique mechanisms in space. Sci Rep 9(1):9397
8. Zammit PS, Golding JP, Nagata Y et al (2004) Muscle satellite cells adopt divergent fates: a mechanism for self-renewal? J Cell Biol 166(3):347–357
9. Fujimaki S, Hidaka R, Asashima M et al (2014) Wnt protein-mediated satellite cell conversion in adult and aged mice following voluntary wheel running. J Biol Chem 289(11): 7399–7412
10. Fujimaki S, Wakabayashi T, Asashima M et al (2016) Treadmill running induces satellite cell activation in diabetic mice. Biochem Biophys Rep 8:6–13
11. Fujimaki S, Machida M, Wakabayashi T et al (2016) Functional overload enhances satellite cell properties in skeletal muscle. Stem Cells Int 2016:7619418
12. Fukuda S, Kaneshige A, Kaji T et al (2019) Sustained expression of HeyL is critical for the proliferation of muscle stem cells in overloaded muscle. elife 8:e48284
13. Guerci A, Lahoute C, Hébrard S et al (2012) Srf-dependent paracrine signals produced by myofibers control satellite cell-mediated skeletal muscle hypertrophy. Cell Metab 15(1): 25–37
14. Guo BS, Cheung KK, Yeung SS et al (2012) Electrical stimulation influences satellite cell proliferation and apoptosis in unloading-induced muscle atrophy in mice. PLoS One 7(1):e30348
15. Arentson-Lantz EJ, English KL, Paddon-Jones D et al (2016) Fourteen days of bed rest induces a decline in satellite cell content and

robust atrophy of skeletal muscle fibers in middle-aged adults. J Appl Physiol 120(8): 965–975

16. Guitart M, Lloreta J, Mañas-Garcia L et al (2018) Muscle regeneration potential and satellite cell activation profile during recovery following hindlimb immobilization in mice. J Cell Physiol 233(5):4360–4372
17. Brooks MJ, Hajira A, Mohamed JS et al (2018) Voluntary wheel running increases satellite cell abundance and improves recovery from disuse in gastrocnemius muscles from mice. J Appl Physiol 124(6):1616–1628
18. Phelan JN, Gonyea WJ (1997) Effect of radiation on satellite cell activity and protein expression in overloaded mammalian skeletal muscle. Anat Rec 247(2):179–188
19. Fukada SI, Akimoto T, Sotiropoulos A (2020) Role of damage and management in muscle hypertrophy: different behaviors of muscle stem cells in regeneration and hypertrophy. Biochim Biophys Acta, Mol Cell Res 1867(9): 118742
20. Hubbard RW, Ianuzzo CD, Mathew WT et al (1975) Compensatory adaptations of skeletal muscle composition to a long-term functional overload. Growth 39(1):85–93
21. Fry CS, Lee JD, Jackson JR et al (2014) Regulation of the muscle fiber microenvironment by activated satellite cells during hypertrophy. FASEB J 28(4):1654–1665
22. Hanson ED, Betik AC, Timpani CA et al (2020) Testosterone suppression does not exacerbate disuse atrophy and impairs muscle recovery that is not rescued by high protein. J Appl Physiol 129(1):5–16
23. Brocca L, Toniolo L, Reggiani C et al (2017) FoxO-dependent atrogenes vary among catabolic conditions and play a key role in muscle atrophy induced by hindlimb suspension. J Physiol 595(4):1143–1158
24. Booth FW (1978) Regrowth of atrophied skeletal muscle in adult rats after ending immobilization. J Appl Physiol Respir Environ Exerc Physiol 44(2):225–230
25. Fujimaki S, Matsumoto T, Muramatsu M et al (2022) The endothelial Dll4–muscular Notch2 axis regulates skeletal muscle mass. Nat Metab 4(2):180–189

Chapter 16

Skeletal Muscle Denervation: Sciatic and Tibial Nerve Transection Technique

Katsumasa Goto and Kazuya Ohashi

Abstract

The nerve transection model is an established and validated experimental model of skeletal muscle atrophy prepared by denervating the skeletal muscle in rodents. While a number of denervation techniques are available in rats, the development of various transgenic and knockout mice has also led to the wide use of mouse models of nerve transection. Skeletal muscle denervation experiments expand our knowledge of the physiological role of nerval activity and/or neurotrophic factors in the plasticity of skeletal muscle. The denervation of the sciatic or tibial nerve is a common experimental procedure in mice and rats, as these nerves can be resected without great difficulty. An increasing number of reports have recently been published on experiments using a tibial nerve transection technique in mice. In this chapter, we demonstrate and explain the procedures used to transect the sciatic and tibial nerves in mice.

Key words Denervation, Transection, Sciatic nerve, Tibial nerve, Skeletal muscle, Atrophy

1 Introduction

Skeletal muscle exhibits high plasticity in its responses to various extracellular and intracellular stimuli. Motor neuron activity also has impacts on the functional and morphological properties of skeletal muscle cells. Denervation by nerve transection has been widely used as an experimental research model to evaluate the physiological role of nerve activity and/or neurotrophic factors in skeletal muscle plasticity [1–7]. Denervation of the sciatic and tibial nerves is a common surgical technique in rodent experiments [7, 8], as both of these nerves can be easily identified.

Skeletal muscle denervation can result from a traumatic injury to a central or peripheral nerve, or from any of various nerve diseases. Once denervated, the skeletal muscle atrophies. Denervation-associated muscle atrophy [1, 4, 7, 9], a process attributed to the elimination of both motor nerve activity and neurotrophic factors, is characterized by muscle fiber atrophy and degeneration, the decline of the number of myonuclei per muscle

Atsushi Asakura (ed.), *Skeletal Muscle Stem Cells: Methods and Protocols*, Methods in Molecular Biology, vol. 2640,
https://doi.org/10.1007/978-1-0716-3036-5_16,

fiber, the loss of mitochondria, intra- and inter-myofibrillar lipid accumulation [10–13], etc. On the other hand, the peripheral nerves of rodents are likely to reinnervate muscles after they are transected. As such, special treatments on the distal or proximal terminal of the axon are essential to prevent the regrowth of a transacted nerve. If, on the contrary, the axon terminal is left untreated, the denervation model can be used as a regeneration model after peripheral nerve injury [13]. Some alterations of neuromuscular junctions, such as poly-innervation and endplate fragmentation, are observed when reinnervation occurs.

In this chapter, we demonstrate and explain the procedures used to transect the sciatic and tibial nerves of mice. The sciatic nerve originates from the lumbar spinal nerves (L3–L5 in mice, L4–L6 in rats) and divides into three peripheral nerves (the tibial, sural, and common peroneal nerves) at the popliteal fossa. The sciatic nerve has a larger axon diameter than the tibial nerve, which makes it easier to transect. While skilled techniques are essential for the transection of any of the peripheral nerves, the tibial nerve transection requires more experience, training, and skill than the sciatic nerve transection. The tibial nerve transection is generally recognized to have a smaller and more limited impact on the hindlimb muscles. Further, the sciatic and tibial nerves both consist of motor- and sensory-nerve axons. Hence, the transection of these nerves also ablates afferent signals.

2 Materials

All of the procedures described are carried out in accordance with the Guide for the Care and Use of Laboratory Animals as adopted and promulgated by the National Institutes of Health (Bethesda, MD, USA), and have been approved by the Animal Use Committee of Toyohashi SOZO University (A2020006).

2.1 Tools and Equipment

The following equipment and instruments are required for the mouse denervation experiments described:

1. Dissection board.
2. Fine forceps (Fig. 1a).
3. Hemostatic forceps (Fig. 1b).
4. Micro scissors (Fig. 1c).
5. Needle holder with suture scissors (Fig. 1d).
6. Scalpel blade (Fig. 1e).
7. Micro spatula (Fig. 1f).
8. Hair removal foam (Fig. 1g).

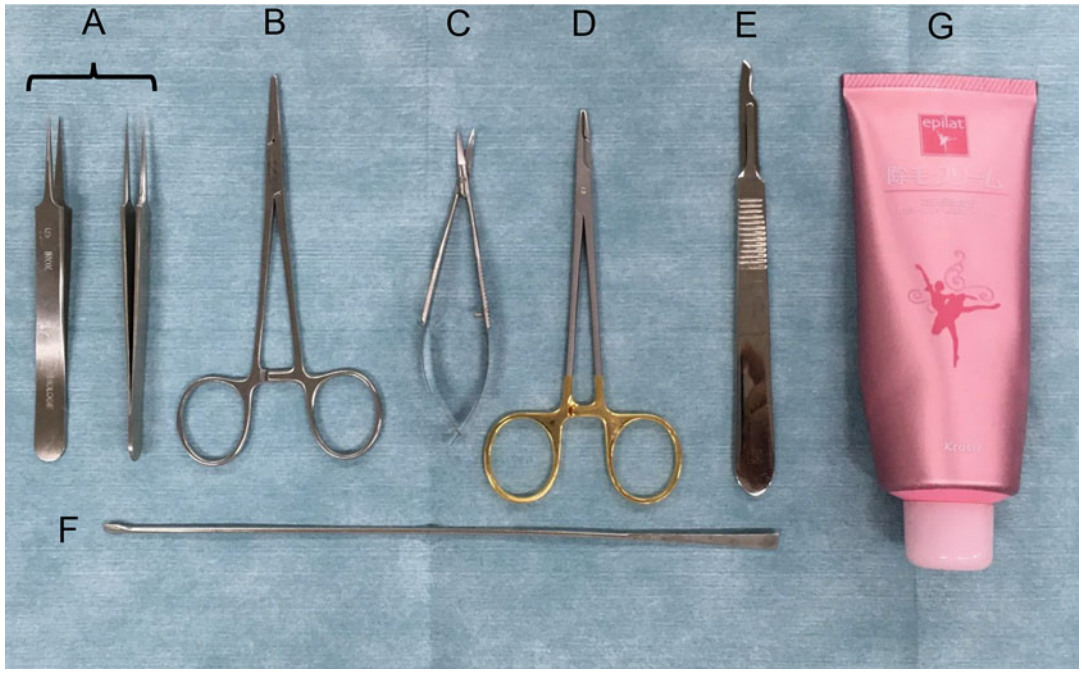

Fig. 1 Instruments and equipment for the sciatic and tibial nerve transection. (**a**) fine forceps, (**b**) hemostatic forceps, (**c**) micro scissors, (**d**) needle holder with suture scissors, (**e**) scalpel blade, (**f**) micro spatula, and (**g**) hair removal foam. A dissection board, needle and suture thread, and disposable gloves should also be prepared. A stereomicroscope or binocular magnifying glasses may be used if needed

9. Needle and suture thread: 4-0 braided silk (USP, 4/0 silk suture; needle length, 15 mm, 1/2 circle; AR15-40 braided silk; Natsume Seisakusho, Yushima, Tokyo, Fig. 3g, h).
10. Disposable gloves.
11. Stereomicroscope or binocular magnifying glasses (if needed).

2.2 Animals

Male, 6- to 8-month-old C57BL/6J mice are used for the experiments. The animals are deeply anesthetized with inhaled isoflurane (1.5%), hair is removed from the left hindlimb (Fig. 2a–c), and the sciatic or tibial nerve is transected.

3 Methods

3.1 Sciatic Nerve Transection

The sciatic nerve is the largest nerve in the body. The sciatic nerve innervates hamstring muscles (the biceps femoris, semimembranosus, and semitendinosus muscles) and adductor magnus muscle, as well as the skeletal muscles of the leg and foot, via the common peroneal and tibial nerves.

1. An incision (~1 cm) is introduced in the skin of the outer thigh, and the hamstring muscle is pushed aside (Figs. 2a–f and 3a, b).

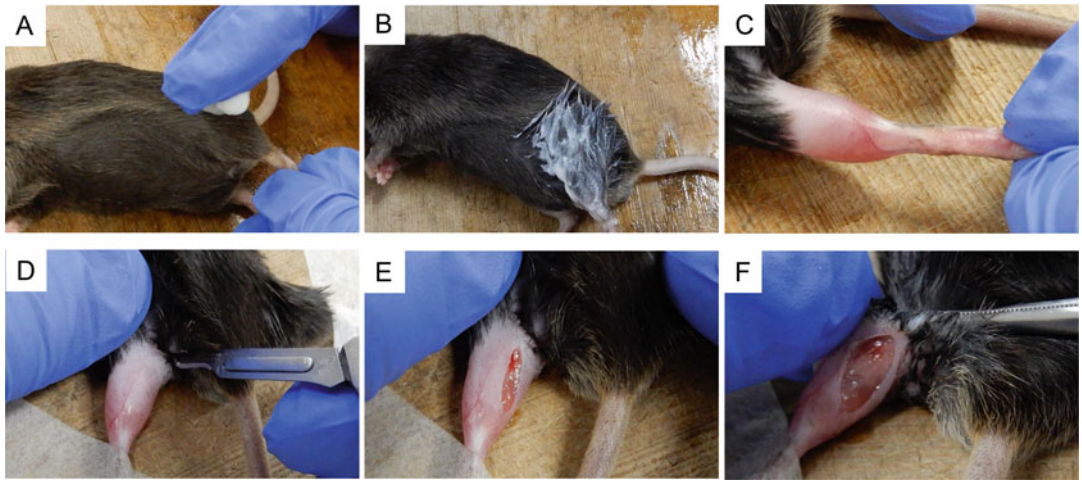

Fig. 2 Preparation of the mouse left hindlimb. Hair is removed using a commercially available hair removal foam (a–c). An incision (~1 cm) of the skin is then introduced using a scalpel blade (d–f)

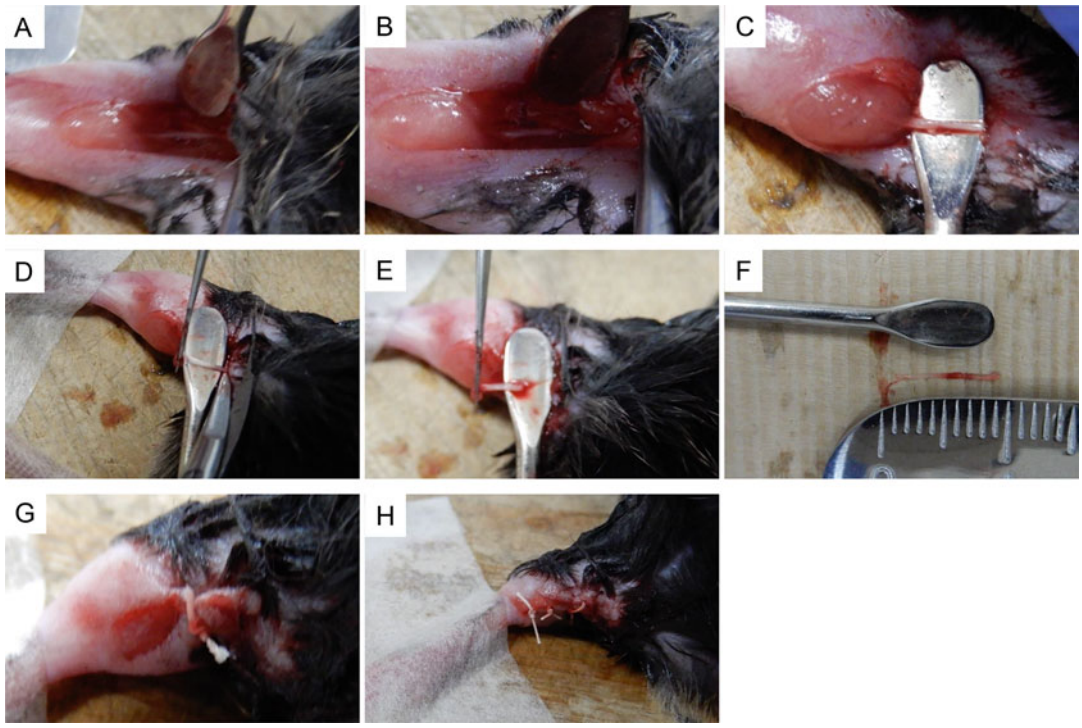

Fig. 3 Procedure for the sciatic nerve transection in the mouse left hindlimb. An incision (~1 cm) is introduced in the skin of the outside of the thigh, and the hamstring muscle is pushed aside using a micro spatula (**a**, **b**). Once the sciatic nerve is identified, it is cut by micro scissors as distally as possible (**c**–**e**). The sciatic nerve can be protected from damage by holding it gently with the micro spatula (**c**, **d**). To prevent reinnervation, an approximately 10 mm segment of the axon of the sciatic nerve is cut at the proximal portion of the distal cutting point (**f**). The muscle and skin incisions are sutured closed with 4-0 braided silk (**g**, **h**)

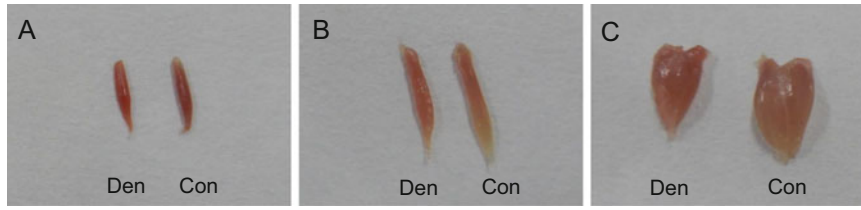

Fig. 4 Denervation-induced skeletal muscle atrophy. (**a**) soleus muscle, (**b**) plantaris muscle, (**c**) gastrocnemius muscle; Den, denervated; Con; contralateral control

2. After the sciatic nerve is identified, the axon of the nerve is cut with micro scissors as distally as possible (Fig. 3c–e). The sciatic nerve can be protected from damage by holding it gently with the micro spatula (Fig. 3c, d).
3. An approximately 10 mm segment of the axon of the sciatic nerve is cut at the proximal portion of the distal cutting point (Fig. 3f) to prevent reinnervation, as the peripheral nerve can regrow after nerve resection and reinnervate target skeletal muscle(s). Alternatively, the proximal end of the sciatic nerve can be sutured to the back of the skin (*see Figs. 5f and g in* "2.4 *Tibial nerve transection*").
4. The muscle and skin incision are sutured closed using 4-0 braided silk (Fig. 3g, h).
5. Povidone-iodine is applied to disinfect the sutured incision wound.
6. The mice are monitored for recovery from anesthesia and then returned to their cages.
7. At 1 week after surgery, the soleus (Fig. 4a), plantaris (Fig. 4b), and gastrocnemius muscles (Fig. 4c) are dissected from the denervated hindlimbs and the contralateral-innervated hindlimb controls.
8. Muscle atrophy of the hindlimb is confirmed (*see* Subheading 4.1).
9. Reinnervation of the hindlimb is confirmed (*see* Subheading 4.2).
10. Control experiment is used in the contralateral hindlimb muscle (*see* Subheading 4.3).
11. The above procedures can be applied to the mouse muscle (*see* Subheading 4.4).
12. Partial denervation is also useful as a mild model (*see* Subheading 4.5).
13. Hindlimb unloading can be combined with denervation experiments (*see* Subheading 4.6).

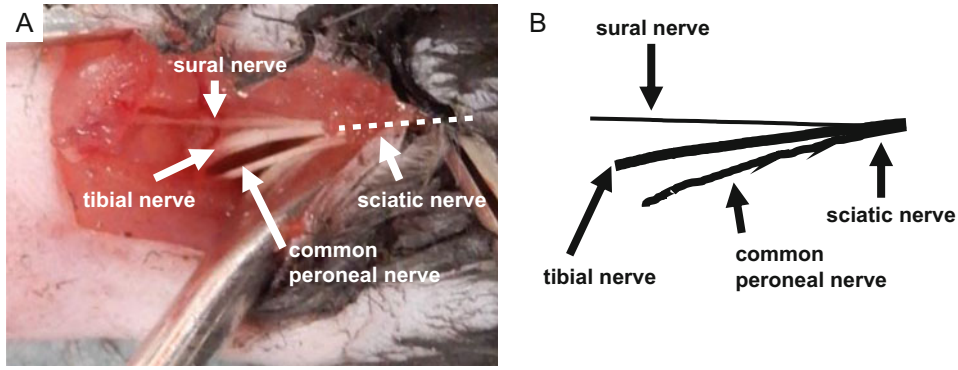

Fig. 5 The tibial nerve. (**a**) photo image, (**b**) illustrated image. The tibial nerve is the larger terminal branch of the two main muscle branches of the sciatic nerve

3.2 Tibial Nerve Transection

The tibial nerve is the larger branch of the two main muscle branches of the sciatic nerve and arises at the apex of the popliteal fossa (Figs. 5 and 6a, b). The tibial nerve innervates the gastrocnemius, soleus, plantaris tibialis posterior, flexor digitorum longus, popliteus, and flexor hallucis longus muscles. The nerve consists of both motor and sensory axons.

1. The mice are anesthetized using isoflurane.
2. The tibial nerve axon is carefully isolated from the common peroneal nerve using fine forceps (Fig. 6c, d). If needed, the use of a stereomicroscope or magnifying glasses can facilitate this procedure. The tibial nerve axon should be isolated with great care, as several arterioles are located nearby the tibial and common peroneal nerves.
3. The tibial nerve axon is held with fine forceps as distally as possible, and the axon is cut with micro scissors at the point peripheral to the portion being held.
4. The proximal end of the tibial nerve is sutured to the back of the skin to prevent reinnervation (Fig. 6f, g).

4 Advanced Protocols

4.1 Muscle Atrophy

1. Skeletal muscle atrophy in the hindlimb is observed following the transection of the sciatic or tibial nerve.
2. Abnormality in the locomotion of the denervated hindlimb is also normally encountered.
3. Muscle atrophy associated with denervation is generally severe than muscle atrophy associated with unloading. Therefore, neural factors, including nerve activity, may play an important role in maintaining the morphological properties of skeletal muscle.

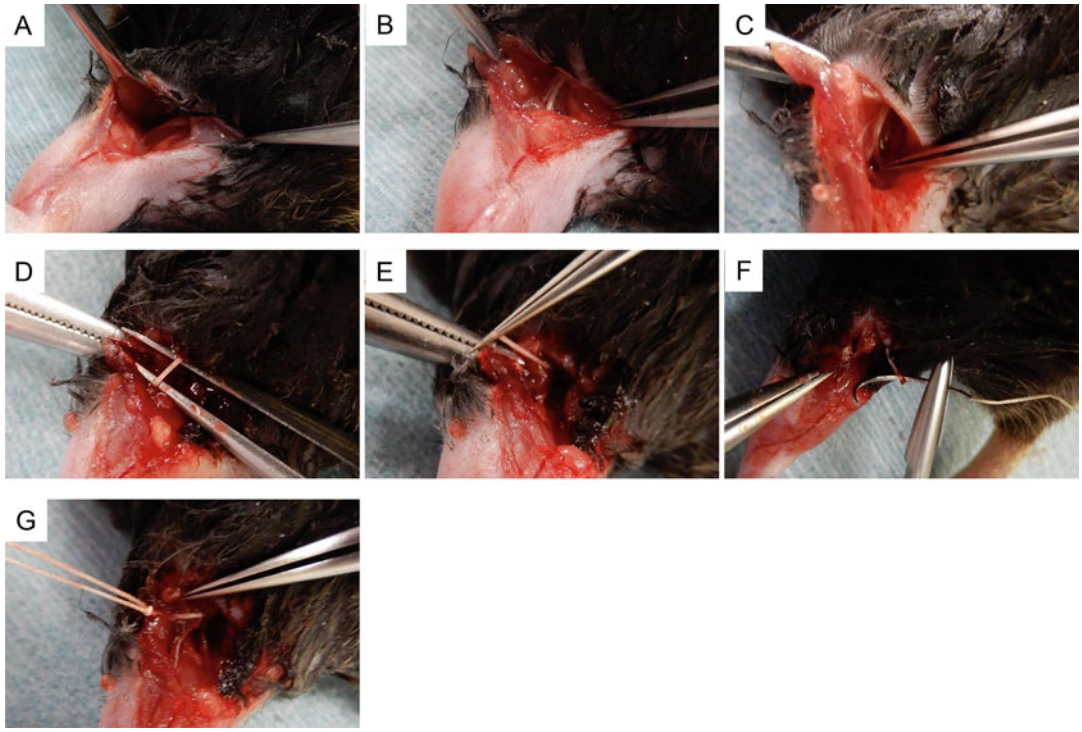

Fig. 6 Procedure for the tibial nerve transection in the mouse left hindlimb. Once the tibial nerve is identified (**a**, **b**), the tibial nerve axon is carefully isolated from the common peroneal nerve using fine forceps (**c**, **d**). The distal portion of the tibial nerve axon is held with fine forceps as distally as possible, and the axon is cut with micro scissors at the point peripheral to the held portion (**e**). The proximal end of the tibial nerve is then sutured to the back of the skin to prevent reinnervation (**f**, **g**)

4.2 Reinnervation

1. As mentioned earlier, the peripheral nerves of mice or rats will often regrow and reinnervate the muscle after a simple cutting of a nerve axon. Several treatments to avoid reinnervation are therefore available.
2. For a sciatic nerve transection, a long dissection (>10 mm) of the axon can be easily performed.
3. A long dissection of the axon is unduly difficult, however, for a transection of the tibial nerve.
4. Suture the proximal cut terminal of the tibial nerve to the back of the skin or the superficial surface of the biceps femoris muscle to prevent reinnervation.
5. Another potentially useful approach is to crush the distal and proximal axons with fine forceps or freeze the nerve with dry ice.
6. If a nerve injury and regeneration model is needed, a simple cut on the nerve axon with micro scissors should be sufficient. After the axon is cut, sutures between the distal and proximal terminals are also possible.

4.3 Experimental Control of Denervation Study

1. In general, the hindlimb muscles are denervated unilaterally in denervation studies on mouse hindlimb muscles.
2. The contralateral hindlimb muscle is used as an experimental control in most studies, though in some cases a separate control group is assigned.
3. The locomotive activity of the contralateral muscles is generally not used as an experimental control, as the activity of the denervated hindlimb is suppressed. As such, the selection of the experimental control in a denervation study should be carefully considered [3] or validated by a pilot study.
4. A sham operation without transection of the nerve axon is usually applied on the contralateral hindlimb muscles.

4.4 Advanced Denervation Study

While the above procedures are performed on rat muscle, they could also be applied to the mouse muscle.

4.5 Partial Denervation

1. A partial denervation of the rat soleus muscle could be performed under a stereomicroscope.
2. The soleus muscle is innervated by the three branches of the tibial nerve.
3. One or two of the branches can be cut under a stereomicroscope.
4. Once the tibial nerve is partially denervated, grouping atrophy of muscle fibers is observed in the operated soleus muscle.

4.6 Hindlimb Unloading with Denervation

1. Hindlimb unloading also causes atrophy of the skeletal muscle, especially the antigravitational soleus muscle.
2. Mouse and rat hindlimb suspension models are widely used for experimental research in space and sports medicine.
3. Denervation can be applied immediately before the suspension.

Acknowledgments

This work was supported by KAKENHI (JP18H03160, K.G.; JP19K22825, K.G.; JP19KK0245, K.G.; 22H03474, K.G.; 22K19722, K.G.; 22H03319, K.G.; 22K18413, K.G.) from the Japan Society for the Promotion of Science; the Science Research Promotion Fund from the Promotion and Mutual Aid Corporation for Private Schools of Japan; Toyohashi SOZO University (K.G.); and Graduate School of Health Sciences, Toyohashi SOZO University (K.G.).

References

1. Ehmsen JT, Kawaguchi R, Mi R et al (2019) Longitudinal RNA-seq analysis of acute and chronic neurogenic skeletal muscle atrophy. Sci Data 6:179
2. Liu H, Ferrington DA, Baumann CW et al (2016) Denervation-induced activation of the standard proteasome and immunoproteasome. PLoS One 11:e0166831
3. Liu H, Thompson LV (2019) Skeletal muscle denervation investigations: selecting and experimental control wisely. Am J Physiol Cell Physiol 316:C456–C461. https://doi.org/10.1152/ajpcell.00441.2018
4. Nagpal P, Plant PJ, Correa J et al (2012) The ubiquitin ligase Nedd4-1 participates in denervation-induced skeletal muscle atrophy in mice. PLoS One 7:e46427. https://doi.org/10.1371/journal.pone.0046427. Epub 2012 Oct 26
5. Komiya Y, Kobayashi C, Uchida N et al (2019) Effect of dietary fish oil intake on ubiquitin ligase expression during muscle atrophy induced by sciatic nerve denervation in mice. Anim Sci 90:1018–1025. https://doi.org/10.1111/asj.13224
6. Graham ZA, Harlow L, Bauman WA et al (2018) Alterations in mitochondrial fission, fusion, and mitophagic protein expression in the gastrocnemius of mice after a sciatic nerve transection. Muscle Nerve 58:592–599. https://doi.org/10.1002/mus.26197
7. Lang F, Aravamudhan S, Nolte H et al (2017) Dynamic changes in the mouse skeletal muscle proteome during denervation-induced atrophy. Dis Model Mech 10:881–896. https://doi.org/10.1242/dmm.028910
8. Batt JA, Bain JR (2013) Tibial nerve transection – a standardized model for denervation-induced skeletal muscle atrophy in mice. J Vis Exp 81:e50657. https://doi.org/10.3791/50657
9. Lala-Tabbert N, Lejmi-Mrad R, Timusk K et al (2019) Targeted ablation of the cellular inhibitor of apoptosis 1 (clAP1) attenuates denervation-induced skeletal muscle atrophy. Skelet Muscle 9:13. https://doi.org/10.1186/s13395-019-0201-6
10. Madalo L, Passafaro M, Sala D et al (2018) Denervation-activated STAT3-IL-6 signalling in fibro-adipogenic progenitors promotes myofibres atrophy and fibrosis. Nat Cell Biol 20:917–927. https://doi.org/10.1038/s41556-018-0151-y
11. Tryon LD, Crilly MJ, Hood DA (2015) Effects of denervation on the regulation of mitochondrial transcription factor A expression in skeletal muscle. Am J Physiol Cell Physiol 309:C228–C238. https://doi.org/10.1152/ajpcell.00266.2014
12. Viguie CA, Lu D-X, Huang DS-K et al (1997) Quantitative study of the effects of long-term denervation on the extensor digitorum longus muscle of the rat. Anat Rec 248:346–354. https://doi.org/10.1002/(SICI)1097-0185(199707)248:3<346::AID-AR7>3.0.CO;2-N
13. Vannucci B, Santosa KB, Keane AM et al (2019) What is normal? Neromuscular junction reinnervation after nerve injury. Muscle Nerve 60:604–612. https://doi.org/10.1002/mus.26654

Chapter 17

Skeletal Muscle Regeneration in Zebrafish

Tapan G. Pipalia, Sami H. A. Sultan, Jana Koth, Robert D. Knight, and Simon M. Hughes

Abstract

Muscle regeneration models have revealed mechanisms of inflammation, wound clearance, and stem cell–directed repair of damage, thereby informing therapy. Whereas studies of muscle repair are most advanced in rodents, the zebrafish is emerging as an additional model organism with genetic and optical advantages. Various muscle wounding protocols (both chemical and physical) have been published. Here we describe simple, cheap, precise, adaptable, and effective wounding protocols and analysis methods for two stages of a larval zebrafish skeletal muscle regeneration model. We show examples of how muscle damage, ingression of muscle stem cells, immune cells, and regeneration of fibers can be monitored over an extended time-course in individual larvae. Such analyses have the potential to greatly enhance understanding, by reducing the need to average regeneration responses across individuals subjected to an unavoidably variable wound stimulus.

Key words Muscle wounding, Needlestick injury, Laser injury, Zebrafish muscle, Muscle precursor cells, Satellite cell, Pax7, Confocal live imaging, Spinning disk imaging, Second harmonic generation, Multiphoton microscopy, Muscle regeneration

1 Introduction

Wound repair is essential in maintaining tissue and organ function and is thus linked to survival. In skeletal muscle, wounds, surgery, degenerative diseases, and even high-force exercise trigger damage that is repaired by satellite cells, resident muscle stem cells (MuSCs) that lie beneath the basal lamina of healthy muscle fibers [1, 2]. During repair, these MuSCs activate to form proliferative myoblasts some of whose progeny regenerate fibers by cell cycle exit, terminal differentiation, and fusion. Other, undifferentiated, progeny return to quiescence in their stem cell niche for potential future recruitment. Molecular mechanisms involved in MuSC-dependent muscle repair are increasingly understood, mainly through studies in rodents (in vivo) and in tissue culture cells [3]. For example, studies

Atsushi Asakura (ed.), *Skeletal Muscle Stem Cells: Methods and Protocols*, Methods in Molecular Biology, vol. 2640, https://doi.org/10.1007/978-1-0716-3036-5_17,

have highlighted the importance of the transcription factor Pax7 as a marker of satellite cells and a key regulator of the skeletal muscle regeneration process [4, 5].

The difficulty of imaging the muscle repair process in the live animal has hampered efforts to analyze muscle stem cell contributions to repair. But in zebrafish embryos and larvae, optical clarity permits cell lineage tracing and monitoring of individual identified cells in vivo over long periods. Moreover, by combining multiple fluorescent transgenes marking different cell types, cell interactions during muscle regeneration can be observed [6]. The zebrafish also permits the use of genetically inducible systems, screens of small molecules/drugs, and high throughput "omics" approaches to reveal specific genes and molecules regulating muscle repair. Zebrafish have been shown to efficiently repair muscle wounds [6–10], and some behaviors of Pax7-expressing cells in wounds have been described [6, 9, 11, 12]. These studies generally utilized a needlestick or laser injury to trigger muscle repair. Zebrafish models of several muscle-degenerative diseases have also been developed [13–17] and their abnormal regeneration analyzed [11]. Chemical treatments have been used to induce muscle damage, but the lack of targeted injury makes it harder to eliminate potential side effects in other tissues [18]. Genetic manipulation has also been deployed to induce more targeted tissue- or cell-type-specific damage and has also allowed conditional ablation of muscle cells [6, 19]. Using a needlestick protocol, we have been able to reliably injure single muscle fibers, or larger cell groups in single or multiple somites at various developmental stages. With our recent development of a zebrafish adult MuSC isolation and cell culture protocol [20–22], Ganassi et al., Chap. 3, this volume, tools are now available to study muscle regeneration across the zebrafish life course.

Here we describe our customizable myotome needlestick and laser injury protocols for larval zebrafish and their use as an in vivo model to study skeletal muscle wound repair. The protocols can be used to study the regeneration process at single-cell resolution over extended periods in individual animals.

2 Materials

1. Tricaine methanesulfonate 160 mg/L solution in sterile water, Tris–HCl buffered to pH 7, stored in aliquots at −20 °C and used fresh.
2. Pair of No. 5.SA watchmaker forceps (Ideal-tek).
3. 1 mL microfine, 1 mL and 3 mL plastic pipettes (Starlab, #E1414-1100, #E1414-0100, #E1414-0300).
4. 60 mm petri dishes.

5. 100 mm petri dishes.
6. 6/12/24 well plates.
7. 60 mg/mL 1-phenyl-2-thiourea in sterile water, stored at 4 °C.
8. E3 embryo medium (see Ref. [23]).
9. Phosphate buffered saline (PBS).
10. 4% paraformaldehyde in PBS stored at −20 °C and used freshly thawed.
11. Agarose (1% in E3 medium).
12. Low melt agarose (LMA) (0.8–1.5% in E3 medium).
13. Penicillin/Streptomycin.
14. 37 °C and 65 °C heat blocks.
15. 28.5 °C Incubator.
16. Glass capillaries/needles (World precision instruments, #1B100-6).
17. Needle puller (P-97 Flaming Brown, Sutter Instruments).
18. Tungsten wire, sharpened by electrolysis in 5 M KOH.
19. Fluorescent dissecting microscope Leica MZ-16F and/or Zeiss Stemi SV11.
20. Micromanipulator (Narishige M153) mounted next to dissecting scope stage.
21. Upright confocal and/or epifluorescence microscope with suitable dipping objectives. In the current report, we used a long working-distance Zeiss 20×/1.0 DIC (UV) VIS-IR W objective (#421452-9900) on an upright Zeiss Exciter LSM (laser scanning microscope) with a Materials stand with bright-field condenser and motorized stage to provide sufficient working distance, and an inverted Zeiss Observer spinning disk microscope (with Yokogawa disk and dual camera Axiocam and Deltavision) or a Zeiss 7MP microscope with a W Plan-Apochromat 20×/1.0 DIC VIS-IR M27 WD = 75 mm objective.
22. Image Analysis software used for our studies was ZEN 2012 and above, FIJI 1.53f, Volocity 6.3, and IMARIS 8.2.

3 Methods

3.1 Preparation

1. Collect embryos from appropriate crosses and rear in 100 mm petri dishes in fish facility water with methylene blue, or, if subsequently dechorionated, in E3 medium [23]. Clean out debris/waste from dishes and maintain embryos in a 28.5 °C incubator.

2. Track their developmental progress, remove unfertilized eggs around 2 h post-fertilization (hpf), and split the embryos into clutches of 50–70 embryos per petri dish to ensure their optimal development and cleanliness.
3. To aid subsequent imaging, pigmentation in melanophores can be inhibited by treating the embryos to 0.2 mM final concentration of 1-phenyl-2-Thiourea (PTU) post gastrulation, from 10 hpf onwards. Note that PTU-treated embryos do not develop normally in later larval life. Therefore, its use should be avoided if possible.
4. Assemble materials and tools that will be needed for mounting embryos/larvae, as shown in Fig. 1a. Take glass capillaries and use a needle puller to prepare a batch of needles (*see* **Note 1**). Store pulled needles in a 150 mm petri dish on a Blutack support strip. Some needles may be blunted for use to orient larvae during mounting by flaming the tip with a Bunsen burner for 1–3 s and rounding off by pressing the tip against a flat surface. Store further unbroken needles, which will be used to injure somites.
5. Make a 1% agarose solution in E3 medium and, before it sets, add 5 mL to each 60 mm petri dish. Gently swirl so that each plate is evenly covered. Allow to cool on the bench (10–15 mins) before moving the plates. A plate which is set will appear as shown in Fig. 1b. Extra plates can be returned to their packing sleeve, taped, and stored in 4 °C for up to a month.
6. Prepare desired LMA solution in E3 medium and before it sets aliquots into 2 mL Eppendorf tubes. Allow to set for 10–15 mins (Fig. 1c). Store at 4 °C for up to 3 months.

3.2 Mounting Zebrafish Embryos/Larvae

1. If using agarose plates from stock in fridge, allow them to equilibrate to room temperature before use (around 15 min) (*see* **Note 2**).
2. Take LMA aliquots from fridge and place them on 65 °C heat block for 5–10 min. Check that LMA has melted completely by inverting the tube. If it has, it should appear clear and no differences in refractive index should be seen when the tube is viewed against a light source. Thereafter, keep the LMA aliquot in 37 °C heat block (Fig. 1c, d).
3. Sort required embryos or larvae at suitable developmental stage (e.g., transgenic reporter line visible in desired structure). Discard any sick or malformed larvae.
4. Dechorionate manually all 2.5–3.5 dpf larvae, if necessary, using watchmaker forceps.
5. Anesthetize larvae in tricaine prepared according to [23].

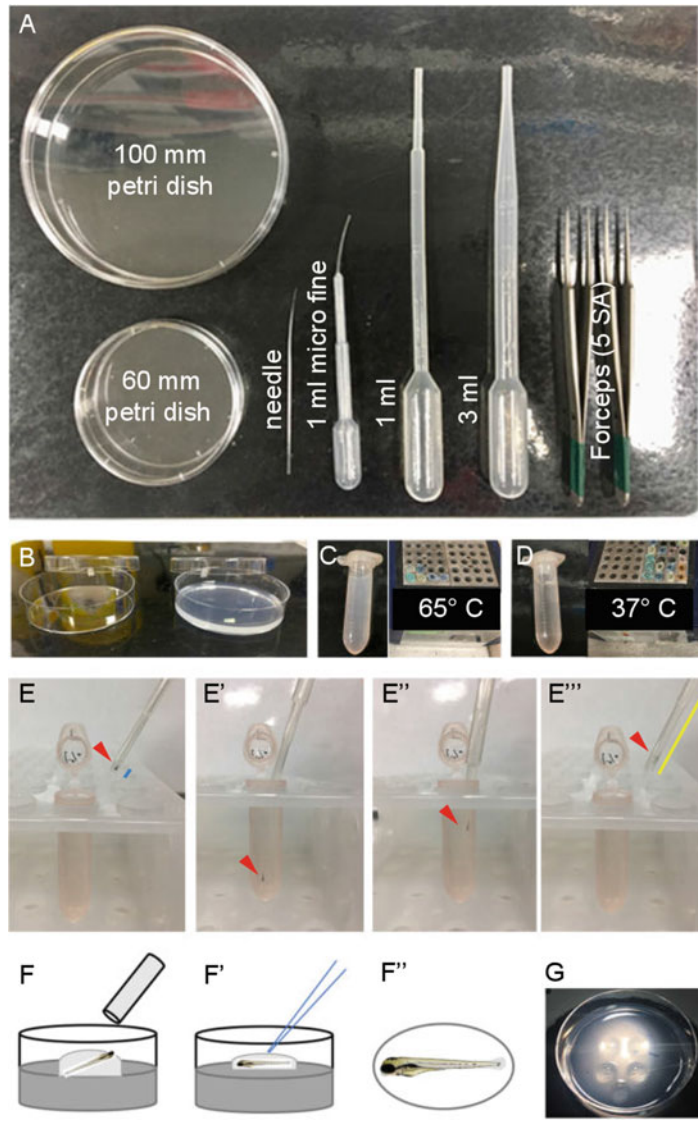

Fig. 1 Mounting zebrafish embryos/larvae for wounding and confocal imaging. (**a**) Materials and tools needed for mounting zebrafish larvae. Starting from top left corner, 100 mm petri dish, 60 mm petri dish, pulled needle (s), 1 mL microfine plastic Pasteur pipette, 1 mL plastic Pasteur pipette and 3 mL plastic Pasteur pipette, and watchmaker No. 5 SA forceps laid upon a clean laminated sheet. (**b**) Pouring agar plates for wounding. On the left side an empty 60 mm petri dish and on the right side a plate with fully set 1% agarose. (**c**) 2 mL Eppendorf tube containing 1.5 mL set LMA (left) ready to melt on a 65 °C heat block filled with distilled water (right). (**d**) The melted LMA aliquot (left) is thereafter allowed to stabilize at 37 °C in a second heat block. (**e**–**e**‴) Images showing steps of handling embryo/larva in LMA. A melted 2 mL LMA aliquot recently removed from 37 °C heat block, 1 mL Pasteur pipette, and pigmented larva (red arrow) is present in each image. An anesthetized larva is picked up using 1 mL pipette along with a minimal amount of water indicated by the blue line (**e**). Larva is gently expelled into the LMA aliquot and allowed to sink (**e**′). Larva is then collected using 1 mL pipette (**e**″) and, as pipette is withdrawn, excess LMA is expelled to leave larva near the tip of the pipette along with some LMA, indicated by the yellow line (**e**‴). (**f**–**f**″) Schematic showing mounting of embryo on agar plate. Larva and LMA (from **e**‴) are expelled onto the agarose plate with larva initially in a random orientation (**f**). Using a fine-pulled needle, larva is then bought at the center of the LMA drop, the drop is flattened by spreading the LMA using the needle and then oriented with the head on the left and left side of the body facing the operator (**f**″). (**g**) A 60 mm agarose plate containing evenly spaced spread LMA drops each holding one oriented larva

6. Use 1 mL plastic Pasteur pipette to carefully suck up a single larva with as little water as possible and without bending the fish and decant the larva into the LMA aliquot, which has been kept at 37 °C (Fig. 1e, e′). Before adding the larva, the LMA aliquot should be removed from the heat block and opened with one hand and viewed against a light source, while the pipette is operated with the other hand. This aids in tracking the larva within the pipette/tube (*see* **Note 3**).
7. Allow the larva to sink deeper into tube away from the pipetted liquid. If necessary, gently but rapidly pipette the LMA (without sucking up the fish again) in the tube to ensure the larva is surrounded by full-strength LMA solution. Quickly recollect the larva in a drop's worth of LMA and expel onto a 60 mm agarose plate placed under a dissecting microscope (Fig. 1e, f). With practice, one should perform steps 6 and 7 in 15–30 s) (*see* **Note 4**).
8. Initially the larva will be oriented randomly in LMA drop. Using a blunt needle or closed forceps, spread the LMA around with circular movements to flatten the LMA drop leaving a thin covering over the larva. Move rapidly to complete Step 9 before the LMA sets.
9. Orient the larva as desired, usually in a lateral view. We usually place the head to the left, with the left side of the body facing up before the agarose solidifies (perform steps 8 and 9 in 15–30 s) (Fig. 1f). Setting is noticeable as a change in the refractive index of LMA and higher viscosity when maneuvered by the needle.
10. Avoid any sudden movement and keep an eye on the larva for any drifting from the desired orientation. If the LMA is far from setting, it may be necessary to re-orient the larva until setting commences. Allow the LMA to set for 5–10 min.
11. Once fully set, the mounted larva can thereafter be covered with E3 medium containing a suitable amount of tricaine. Allow the larva and LMA to stabilize for at least 10–15 min (*see* **Note 5**).
12. Equally, multiple larvae can be mounted in a single 60 mm agarose dish. Up to six larvae can be easily mounted side by side within the central part of the dish (Fig. 1g). With some practice, larger numbers of larvae can be arranged in larger dishes in such a manner for high throughput studies too. If high magnification imaging is desired, check the location of the larvae to ensure that the animals are at the center and the side edge of the dish does not touch the objective.
13. After embedding and at ages beyond 4 dpf, tricaine may be reduced to half or less of the normal concentration to minimize cardiac blockade and lethality [24, 25]. High concentration

LMA (1.5%) can hold fish in position even without anesthesia, although 3D stack LSM scans will contain twitch movement artifacts. Note that higher LMA concentration reduces high-resolution image quality.

3.3 Needlestick Muscle Injury

1. Place mounted larvae covered with fish water containing anesthetic under the upright confocal or epifluorescence microscope. Count the somites through the eye piece and select the region for injury. In 2–3 dpf larvae, we focus on the region above the yolk extension (somites 15–17). Acquire high-resolution confocal z-stacks of mounted larvae, as desired. This will record the pre-wound (pre-w) state of individuals of a genetic strain and lay under study.
2. Once larvae are scanned, place the agarose plate under the binocular dissecting microscope with a graticule scale bar eyepiece and a Narishige micromanipulator set up alongside (Fig. 2a). Ensure the microscope is correctly focused for both eyes of the individual operator, to yield optimal binocular vision and depth perception.
3. Load an unbroken pulled needle into the needle holder of the micromanipulator.
4. Using watchmaker No. 5 SA forceps, break the needle tip under the microscope until the tip diameter is 15–30 μm. Calibrate the size of the tip using a graticule scale bar in the eyepiece of the microscope. Depending on the extent of injury desired and the stage of the larvae/muscle fiber size, different needle tip sizes can be created (*see* **Note 6**).
5. Position the needle at about a 45° angle to the anteroposterior body axis, pointing at one or more epaxial somites at the end of the yolk extension using the micromanipulator (Fig. 2b). The needle should enter the myotome parallel to the vertical myosepta or body axis and point downward between 30° and 45°.
6. Advance the needle with the micromanipulator to pierce the LMA with the needle, aligning the needle tip close to the surface of the embryo/larva and parallel to the vertical somite borders (Fig. 2c). Shallow LMA makes this procedure easier. If necessary, withdraw the needle, adjust the angle, and readvance. Select a high magnification such as 15×.
7. Carefully but rapidly pierce through the skin and then into the muscle, while judging the depth of the needle using the focus. By advancing the needle while viewing at high magnification, damage to tissues such as notochord and neural tube can be avoided (Fig. 2c). Withdraw and reinsert the needle 1–3 times at the same spot for effective fiber injury (*see* **Note 7**).

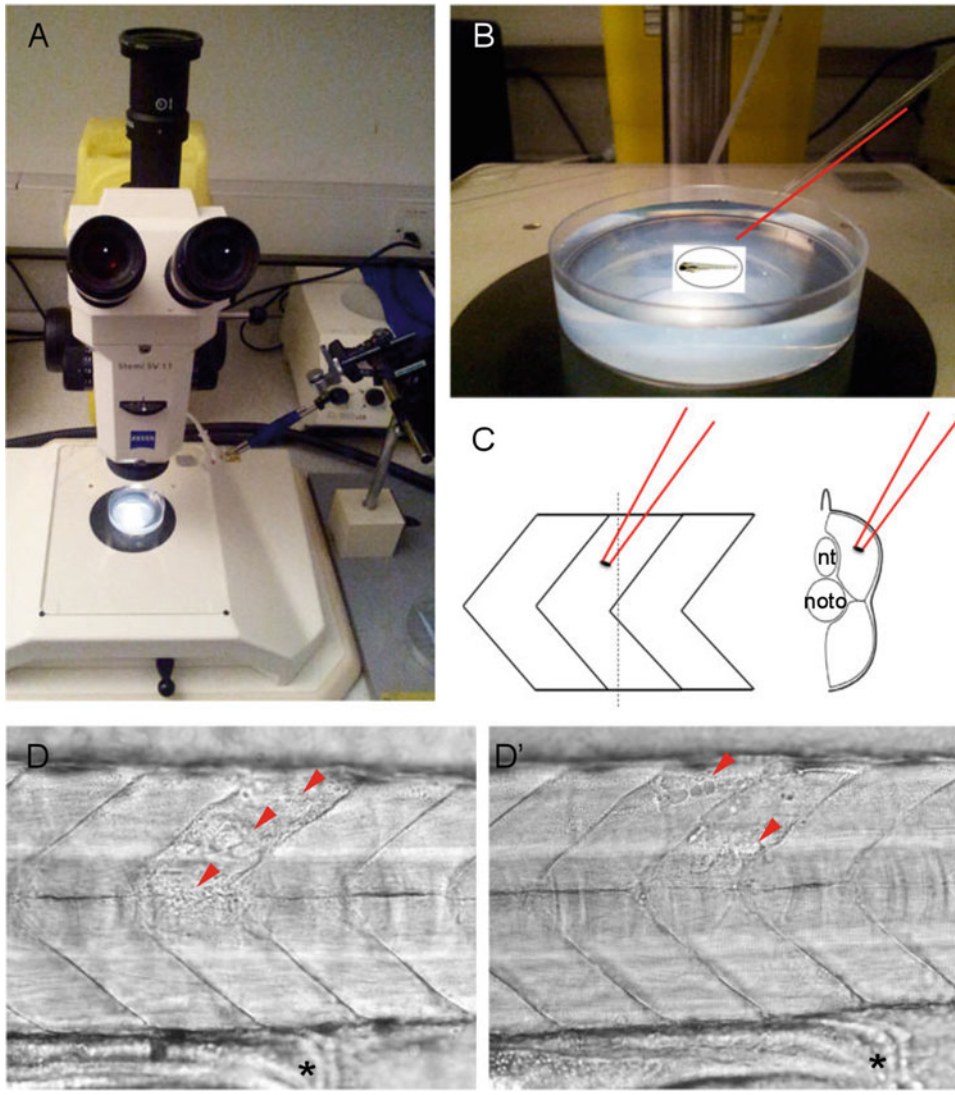

Fig. 2 Wounding skeletal muscle of zebrafish embryos. (**a**) Zeiss Stemi SV11 dissecting microscope and Narishige microinjector set up to perform the wounding procedure. (**b**) Embryo mounted in LMA on agarose plate filled with medium is placed on the microscope. The injector is positioned such that the needle (highlighted by the red line) is pointing at the mounted embryo at around 40° angle. Fish drawing inserted by way of illustration. (**c**) Schematic showing the ideal alignment of the needle relative to somite from lateral (left) and transverse (right) views. The needle is inserted through the LMA covering the embryo and positioned parallel to the vertical somite border (myoseptum) with the sharp needle tip pointing at the center of the myotome. The schematic on the right shows the transverse view from a position of a dotted line on the left. It highlights the depth at which the needle can be inserted without danger of damage to adjacent tissues. However, to go deeper into the myotome, careful maneuvering while judging the depth by adjustment of the focus is required. (**d**–**d**′) Two examples of injured somites about 1 h after wounding. Brightfield images taken with a 20× dipping objective of the injured somites above the anal vent (asterisks). Red arrows indicate positions where the needle was inserted into the myotome of 3 dpf larvae

8. Record the time, location, and extent of the wound for each fish immediately after injury (Fig. 2d, d′ show two examples). If a camera is available on the dissecting microscope, record an image.
9. After wounding, the fish can be returned to the confocal for immediate further scanning. However, it is recommended that, if the experimental protocol allows, each fish is released from the perturbed LMA and remounted as described. This is because the needle disrupts the LMA near the injury, leading to optical aberrations due to uneven mounting, which are not ideal for high-resolution confocal imaging. After remounting post-wounding, which may alternatively be performed in a glass-bottomed dish for imaging on inverted microscopes (*see* **Note 8**), high-resolution *Z*-stacks can again be acquired.
10. Larvae can be removed from LMA at the end of scanning post-wounding and kept separately in 6/12/24 well plates and daily re-embedded for imaging.
11. Penicillin (50 Units/mL) and streptomycin (50 μg/mL) and 0.2 mM PTU were added to E3 medium to reduce infection and enhance imaging. We have not observed the side effects of antibiotics on development or wound repair. With no antibiotics present in the media, mold and wound infection can occur, impairing larval recovery and reducing survival.
12. The wounded somite and adjacent control unwounded somites can thus be tracked over time with careful mounting and unmounting at each stage (see Subheading 3.5). It is not recommended to leave larvae embedded for over 12 h as this constrains morphogenesis and anesthetic both affects muscle development [26] and can facilitate pathogenic attack. Larvae may be left embedded for longer periods if the anesthetic is removed, but twitches will be observed and gradually weaken the LMA mount. Transient re-exposure to anesthetic can facilitate time-lapse imaging.

3.4 Laser-Induced Muscle Injury

We have employed several methods to induce damage to the myofibers in later stage zebrafish, including needlestick [9]. Below, we describe how to perform an injury using a high-powered ultraviolet laser. A similar approach can be used to cause injuries with a 2-photon microscope.

1. Anesthetize larvae and mount larvae in a glass-bottom (*see* **Note 8**) dish as per Subheading 3.2.
2. Place mounted embryos covered with fish water containing anesthetic on the stage of a microscope with a high-powered ultraviolet laser (we use a Zeiss PALM Microbeam system equipped with a solid state 355 nm laser). Count the somites through the eye piece and select the region for injury. In 7 dpf larvae, an optically advantageous region is in ventral/hypaxial

myotome 13, counting from anterior, a location chosen to minimize collateral damage to other organs.

3. Select a high magnification objective with high NA if possible (however, we use a Zeiss 40× LD Plan-NeoFluar NA 0.6 Corr objective). Focus the transmitted light onto the region of interest and ensure the condenser is centered and focused.
4. In the microscope control software select a region of interest for ablation. To cut myofibers it is best to select a narrow region of interest with dimensions X ~ 5 μm and Y ~ 20 μm that extends across several myofibers (Fig. 3). Having selected the

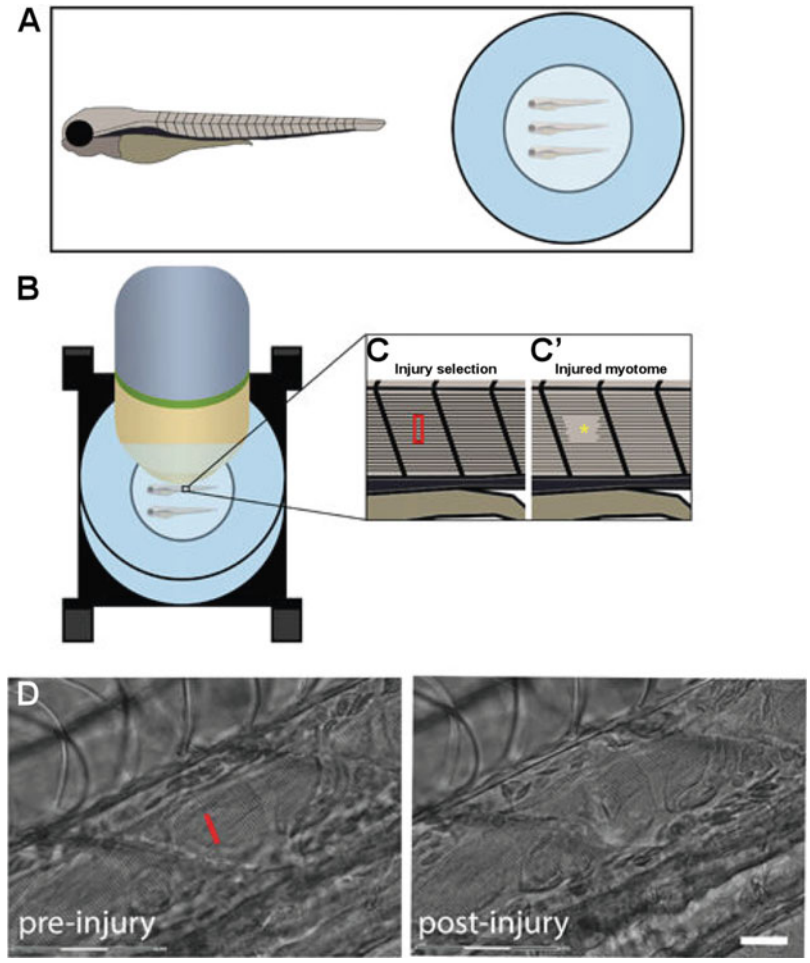

Fig. 3 Laser-induced muscle injury. (**a**) Zebrafish larvae are mounted laterally in 1.5% LMA in a glass-bottom dish and submerged in fish water. (**b**) The region of interest is identified and focused on an upright microscope. (**c**–**c′**) Schematic representation of the 13th left ventral myotome laser injury. (**c**) The injured region is selected (red box) to span multiple myofibers using the microscope control software. (**c′**) Following laser injury, the selected myofibers deform and break. Asterisk indicates the injured region. (**d**) Brightfield images of the ventral region of an anesthetized 7 dpf larva under muscle immediately before and shortly after laser-induced injury in myotome 13. Red line indicates the laser target region. Note the contraction of severed myofiber ends and partial occlusion of the tissue in the post-injury image. Bar = 75 mm

region, use the software to magnify the image until the selected region almost fills the field of view.

5. Adjust the 355 nm laser power settings to an appropriate value (we use 30%) and set acquisition parameters to capture transmitted light. Set the number of scanning iterations to n = 3 with the region of interest selected for scanning. Then start scanning and observe the tissue to determine whether the power is sufficient to cut the myofibers. This should be seen by changes to myofiber morphology and super-contraction of myofibers. If the power is insufficient to cut the myofibers, repeat the scan. Depending on the power of the laser and the alignment of the optics it may be necessary to adjust the power. Care must be taken that sufficient power is used for cutting the tissue, but not so much as to cause overheating. Overheating causes "holes" to appear in the tissue at the region of interest, presumably through gas production.
6. After confirmation of injury, remove larvae as per protocol in Subheading 3.3. Of note, we have observed that later stage larvae (>7 dpf) show increased mortality in response to repeated anesthesia and remounting when reimaging, so it is best to minimize such steps when possible and gradually reduce anesthesia concentration with age [25].

3.5 Tracking Zebrafish Skeletal Muscle Regeneration

The protocols described in Subheadings 3.1, 3.2, 3.3 and 3.4 can be used to prepare wild type or genetically altered embryos or larvae with somitic muscle lesions and then follow them to understand the regeneration process (Figs. 4 and 5). After a needlestick, the initial lesion in the surface cells of the enveloping layer, the larval "skin," closes within about 1 h through a "purse string"-like epithelial sealing process [6]. Subsequent muscle repair takes up to 8 days, depending on the size of the lesion [6]. Such preparations may be treated with drugs or other experimental manipulations, either before lesion or during the repair process, in order to gain insight into the control of regeneration.

The use of transgenic fish in which either slow or fast muscle fibers are labeled with fluorescent reporters permits the analysis of the extent of muscle lesion and its time course of repair (Fig. 4). For example, *Tg(9.7 kb smyhc1:gfp)*^{i104} fish are marked with GFP in slow muscle fibers [27], which form a single layer of lateral (superficial) mononucleate fibers that are oriented parallel to the anteroposterior body axis on the surface of each myotome [28, 29]. When such fish are lesioned by needlestick at 3 dpf, a clear localized loss of slow fibers is apparent 1 day post-wound (1 dpw) (Fig. 4b). Repeated imaging of the same larva over ensuing days reveals that such small lesions begin to form new *Tg(9.7 kb smyhc1:gfp)*^{i104}-expressing slow fibers by 6 dpf (3 dpw; Fig. 4b), a time course reminiscent of that observed in adult mouse muscle

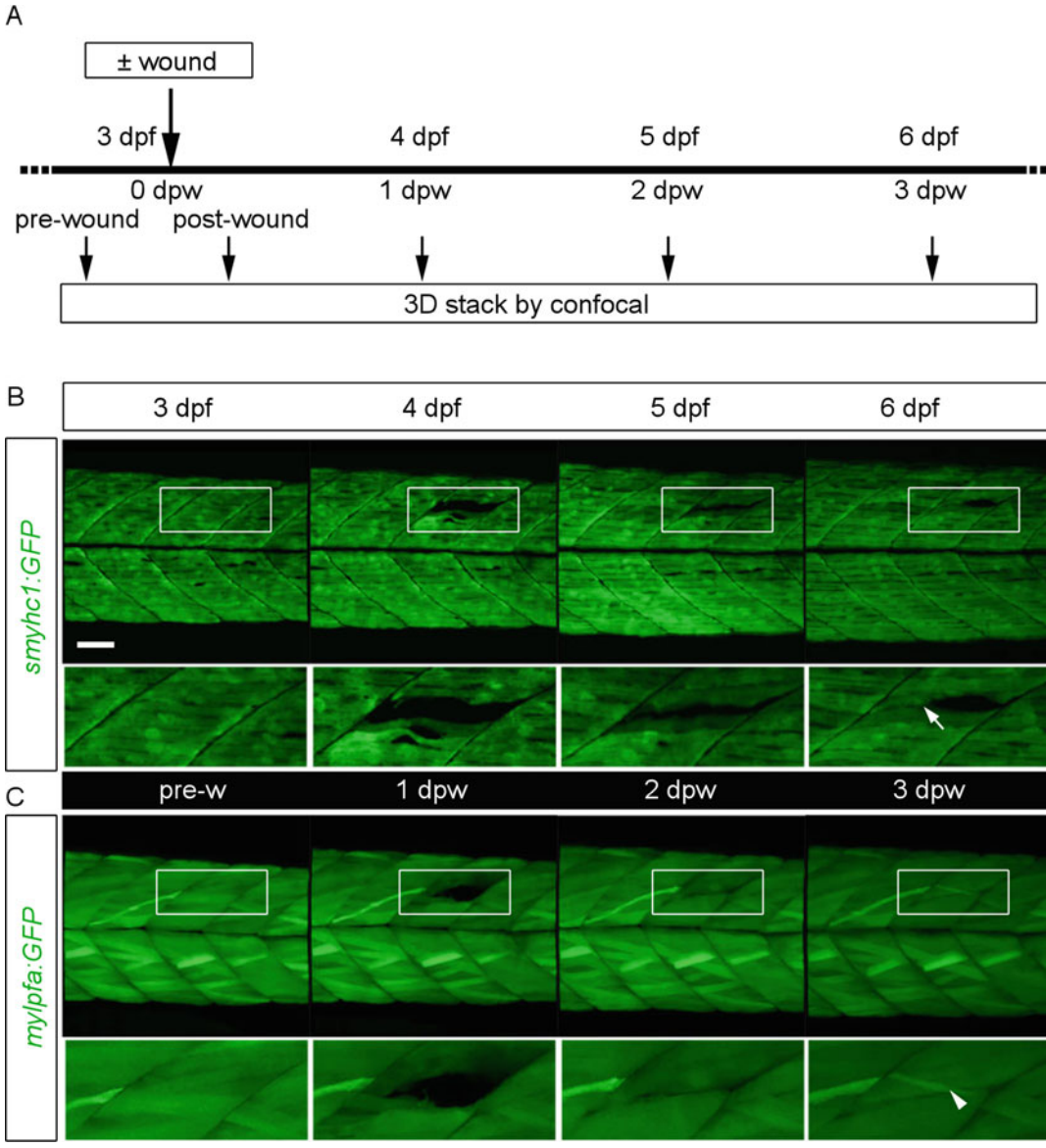

Fig. 4 Tracking lesions and their repair in slow and fast muscle. (**a**) Schematic showing the timeline of a typical wounding experiment. Wounding was performed at 3 dpf/0 dpw and regeneration tracked until 6 dpf/3 dpw using 4D confocal imaging. (**b**, **c**) Repair of needlestick lesions of epaxial somite 17 were tracked for 3 days. Images show maximum intensity projections of confocal stacks through the entire left side of the larva at each stage. Boxed regions are magnified two-fold beneath. Bar = 50 mm. *Tg(9.7 kb smyhc1:GFP)*^{i104} (**b**) and *Tg (mylpfa:GFP)*^{i135} (**c**) were imaged (left, pre-wound) and then lesioned at 3 dpf. Re-embedding and imaging of the same fish at 1, 2, and 3 dpw show the efficient regeneration of the lesioned region. Arrow in B indicates an elongating regenerated slow fiber. Arrowhead in C indicates a misoriented nascent fiber within the lesion region. Note that, although the lesioned region is filled with GFP, three-dimensional scanning reveals that the muscle is not yet fully regenerated

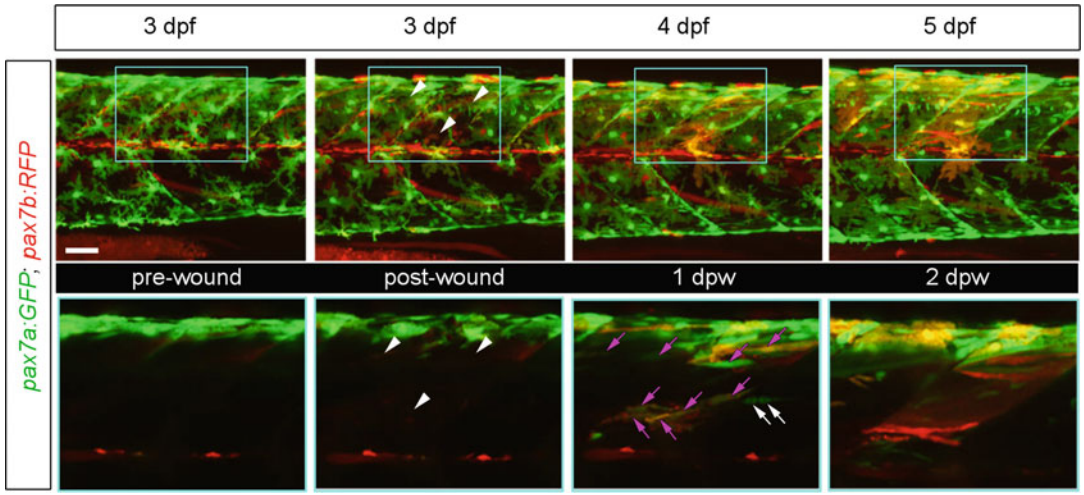

Fig. 5 Tracking MuSC response in skeletal muscle regeneration. *Tg(BAC pax7a:GFP); pax7b:gal4; Tg(5XUAS:RFP)* embryo injured at 3 dpf and muscle regeneration tracked until 5 dpf. Fish was generated by crossing *TgBAC (pax7a:EGFP)*^{t32239Tg} [31] to *pax7b:Gal4FFD*^{nkgsaizGFFD164AGt}*;Tg(5xUAS:RFP)*^{nkuasrfp1aTg} [33]. Upper panels are maximal intensity projections of somite 15–17 of the left side of the larva at each stage. Note the spreading superficial xanthophores and deep labeling in the spinal cord visible in the post-wound panels. Most RFP-labeled MuSCs are present near the horizontal myoseptum, whereas GFP-labeled MuSCs are more widespread within the somite. Lower panels show short stack maximal intensity projections taken within the cyan box and magnified beneath to track the wounded region (white arrowheads). Note the absence of xanthophores and spinal cord labeling due to the *Z*-level within the image stack. At 1 dpw, MuSC-derived cells have entered the lesion region (purple arrows), and some appear to have divided (white arrows). New brightly reporter-labeled regenerated fibers are present at 2 dpw

regeneration (Ciciliot and Schiaffino, 2010). Interestingly, on occasion, such fibers are observed extending posteriorly from the anterior vertical myoseptum, gradually filling the lesioned muscle region (Fig. 3b).

Deeper wounds also damage fast muscle, which is composed of multinucleate fibers arrayed in a complex pattern dependent on their precise position within the somite. Fast fibers are specifically marked with GFP in *Tg(−2.2mylpfa:gfp)*^{i135} transgenic fish [30], which allows us to analyze the extent of the wound and the process of regeneration. For example, a small fast muscle wound regenerated extensively within 3 dpw with regenerated fibers rapidly extending to span the entire length of the somite between the anterior and posterior vertical myosepta (Fig. 4C). However, we note that regeneration is sometimes imperfect, as shown by the small misoriented fiber within the regenerating region (Fig. 4c). We previously used such transgenic lines to characterize muscle repair in larger lesions spanning several somites [6].

Imaging possibilities are, of course, not limited to muscle fibers. The response of MuSCs, immune cells, and neurons to a lesion can also be examined in suitable reporter lines. For example,

we have used this method to analyze distinct populations of MuSCs located in specific regions of the somite labeled by reporters to the two zebrafish Pax7 genes, *pax7a* and *pax7b* (Fig. 5; [6]). Upon lesioning at 3 dpf, few MuSCs are present within the myotome but, after muscle fiber damage, both *pax7a*- and *pax7b*-expressing cells accumulate in the wounded region(s) within 1 dpw, where some already begin to elongate (Fig. 5). By 2 dpw, nascent fibers are visible within the wounds, labeled by perdurance of the fluorescent label from the MuSCs (Fig. 5). We used this approach to demonstrate that MuSC-derived cells fuse with each other and with adjacent large pre-existing fibers during wound repair in vivo [6].

Time lapse imaging using a spinning disk confocal microscope allows analysis of the behavior of cells in the wound site at higher time resolution. *pax7a:GFP;pax7b:Gal4FF;UAS:RFP* also labels xanthophores and neural tube cells, along with MuSCs [6, 31]. For example, time lapse imaging between 14 and 32 hpw in a 3 dpf larva revealed several striking phenomena. Firstly, damaged xanthophores often underwent process-retraction and then complete loss of GFP signal between two scans 5 min apart (Fig. 6a–p). RFP signal was completely retained, but the cell remnant contracted (Fig. 6c, d and k, l). Subsequently, additional such remnants coalesced and then rapidly migrated away from the wound site (Fig. 6n–p). We interpret these changes as the engulfment of damaged xanthophores by professional phagocytes, to clear debris from the wound. The striking loss of GFP signal, but retention of RFP, suggests these two proteins are differentially sensitive to the intracellular conditions encountered inside phagocytes following engulfment. Based on their high subsequent migration speed and eventual accumulation on the yolk extensions (data not shown), the engulfing cells are most likely macrophages/leucocytes. A similar phenomenon is also observed with three other xanthophores within the wound region (Fig. 6n–p).

A second phenomenon that we observed was an association of MuSC-derived muscle precursor cells (mpcs) with the clusters of engulfed xanthophores (Fig. 6n–t). Individual mpcs extended into the wound site, underwent mitosis, and divided. After division, one daughter cell frequently remained associated with the vertical myoseptum, whereas the other daughter migrated into the myotome center (Fig. 6q–t).

1. Mount and lesion muscle in larvae of choice as described in Subheadings 3.1, 3.2, 3.3 and 3.4.
2. Immediately before and after lesioning, low magnification fluorescence imaging of live transgenic embryos/larvae can readily be obtained using a digital camera attached to any basic microscope (we use Leica MZ-16F with BF/GFP filter set and supporting software).

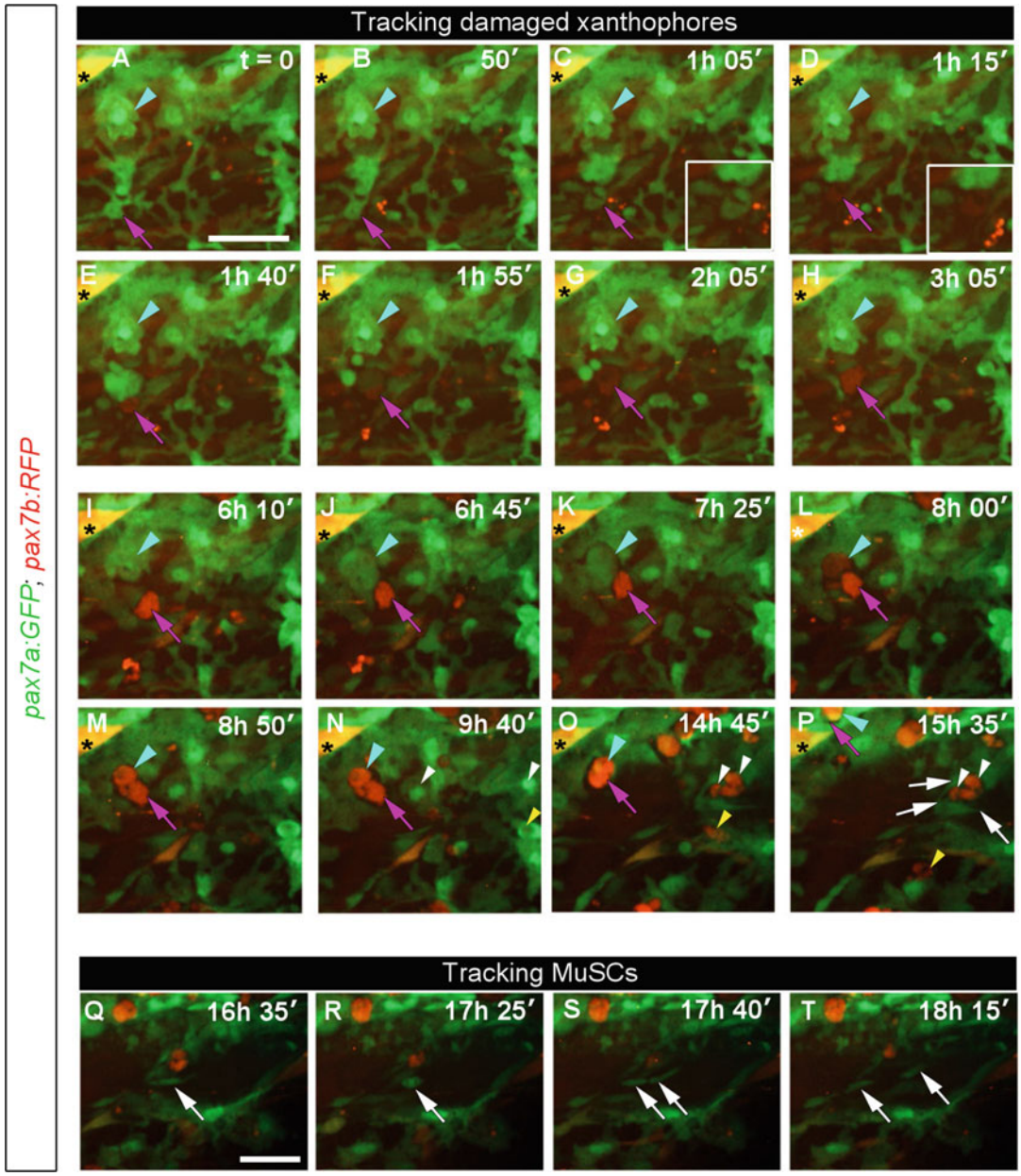

Fig. 6 Tracking cellular behavior during inflammation and MuSC invasion of the wounded area by time lapse 3D microscopy. A *TgBAC(pax7a:GFP);pax7b:GalFFD4;Tg(5XUAS:RFP)* larva injured at 2.5 dpf and the wound imaged every 5 min between 14 and 32 hpw (t = 0–18 h) on a spinning disk confocal (as a *Z*-stack, with ~3.5 min rest between each scan). Images shown are maximum intensity projections of som 15 (**a**–**p**) and som 16 (**q**–**t**) regions of the wounded on the left side of the larva. Anterior to left, dorsal up. Note that step changes in the brightness of the red channel reflect the adjustment of the microscope scan parameters between panels **g**, **h**, and **i**. Bar = 50 mm. **a**–**p**. Tracking the fate of xanthophores in the wound region over 16 h post-wound. A GFP- and RFP-marked xanthophore (purple arrows) with stellate morphology on the surface of myotome (**a**, **b**) loses processes (**c**), GFP is lost between two timepoints, while RFP remains unaltered and signal becomes more compact (compare magnified insets in **c** and **d**). The RFP-marked cell then moves dorsally within the wound (**d**–**h**), approaching a second xanthophore (cyan arrowhead), which

3. Dishes with transgenic anaesthetized embryos/larvae (e.g., expressing GFP in slow and fast muscle cells; Fig. 3) may then be transferred for live imaging to a suitable upright microscope for time-lapse or regular 3D scanning. A motorized stage permits repeated scanning of multiple samples in each dish, which can be beneficial to increase data collection rate and prevent excess phototoxicity in each fish. Such imaging can be achieved at different financial and labor costs, ranging from manual imaging for each fish on basic microscopes to more sophisticated programmable software solutions for multiple positions/wells on conventional or laser scanning microscopes or dedicated confocal multi-well plate scanners with automated tracking software.
4. Initial image processing was done using the Zen confocal software (2009 + 2012) or Zen lite (2012) followed by Volocity 6.3/IMARIS 8.2 to select and export short stacks or tiff images of specific slices, cross-sectional views, and maximum intensity projections from wholemount confocal stacks (*see* **Note 9**). In the event of imperfect orientation of the larva in the LMA, rotation of the entire confocal stack and digital re-slicing using Volocity is advantageous for analysis, preparation of comparable images, and subsequent quantification (*see* **Note 10**).
5. Fish may be released from agarose by flooding the dish with an anesthetic-free medium and under a high magnification dissecting microscope, using No. 5 SA forceps, a fine scalpel, or glass needles to cut away the LMA around the larva. Cuts should be directed, as far as possible, away from the larva and extra care should be taken with the head, yolk, and pectoral fins. As the fish awakens, its efforts to swim can often help free it. Store larvae in individual labeled wells in a 24 well plate in a 28.5 °C incubator ensuring enough medium to avoid drying out (*see* **Note 11**).
6. For subsequent imaging, embryos/larvae can be re-embedded as in Subheading 3.2. Providing suitable feeding and light/

Fig. 6 (continued) simultaneously assumes a rounded morphology (**i**, **j**). Rapid loss of GFP but retention of RFP now occurs in the second xanthophore (**k**, **l**). The remains of the two xanthophores coalesce (**m**–**o**) and then rapidly move dorsally into the adjacent somite, leaving the wounded area (**p**). Note the RFP-marked superficial muscle fiber (asterisk) in uninjured somite 14. Similar loss of GFP, retention of RFP, coalescence, and rapid migration occur to other xanthophores in the wound in somite 16 (white arrowheads, **n**–**p**). GFP-labeled MuSCs (white arrows, **p**) accumulate in association with the clustered xanthophore remnants. An additional xanthophore also losses GFP and rapidly translocates ventrally, eventually leaving the somite (yellow arrowhead, **n**–**p**). **q**–**t**. Tracking a GFP-labeled MuSC (white arrows). After the phase of xanthophore elimination within the wound region, one GFP-labeled MuSC (white arrow, **q**) enters mitosis (**r**) and the two daughter cells separate within the wound myotome (**s**). One daughter (to left) remains attached to the vertical myoseptum and the other daughter (to right) migrates away (**t**)

dark cycle can be achieved, imaging can be continued for many days or weeks, if care is taken to avoid excessive loss of mucilage.

7. When live imaging is complete, larvae may be freed from agarose and allowed to swim to ensure they are free from small pieces of agarose. They can then be fixed for further analysis or processed for genotyping.
8. Wholemount larvae can be processed for immunohistochemistry and imaged either mounted under a suitable coverslip or after embedding, using 10×/0.3 air EC Plan-NEOFLUAR or 40×/1.1 W LD C-APOCHROMAT Corr UV-VIS-IR objectives on a confocal LSM. Note that very long antibody incubation times, perhaps accompanied by proteinase treatment, may be required to stain deep within older larvae.

An alternative method for imaging of damaged myofibers is to use label-free imaging on a multiphoton microscope (Fig. 7). Here we take advantage of the phenomenon of second harmonic generation (SHG) that occurs in highly ordered polarized structures [32]. The high myofibril content of myofibers with polarized alignment of myosin heads emit light at half the excitation frequency of a 2-photon excitation laser as a consequence of sum frequency generation. Using a Zeiss 7MP Multiphoton microscope equipped with a Vision II Titanium Sapphire laser and MPX optical

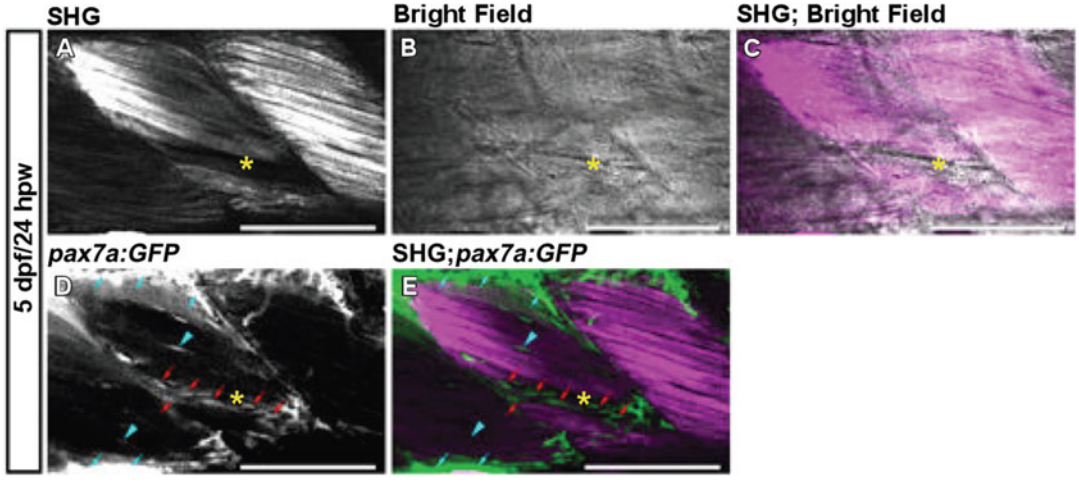

Fig. 7 Tracking recovery from laser injury with Second Harmonic Generation and Confocal Laser Scanning Microscopy. *Tg(BAC pax7a:GFP)* larva subjected to laser-injury in myotome 13 at 4 dpf was re-embedded and imaged at 5 dpf by brightfield (**b**), second harmonic generation microscopy (SHG; **a**, **c**, **e**), and confocal laser scanning microscopy for GFP (**d**, **e**). Asterisk indicates the site of injury. Note the absence of SHG signal at the injury site, which is filled with GFP-marked MuSCs aligning between fibers at 24 h post-injury (hpi; red arrows). Additional MuSCs are present in dermomyotome (cyan arrows) and between uninjured fibers (cyan arrowheads). Bar = 100 mm

parametric oscillator (OPO), we have developed a protocol for visualizing and quantifying muscle injury in larvae in a label-free manner. This can also be combined with animals expressing fluorophores such as GFP and mCherry although it is important to ensure the filters used allow separation of emitted light from the fluorophore and any SHG signal.

A protocol for visualizing the SHG and GFP in *pax7a:GFP* transgenic larvae after injury (by needlestick or by laser) is as follows:

1. For inverted microscopes, larvae are mounted in a glass-bottomed dish (size = 0 coverslip, used for gaining maximum working distance/sample depth, not optimal for imaging, if possible size 1.5 should be used to match the objective unless correction collar objectives are used) as per Subheading 3.2 with the modification that the larva is embedded in LMA with the wound facing the lower glass surface. The dish is mounted on a sample holder in a 2-photon or multiphoton microscope. We use an inverted Zeiss 7MP microscope for visualizing a muscle injury by SHG with a 20× water dipping objective (W Plan-Apochromat 20×/1.0 DIC VIS-IR M27 WD = 75 mm).
2. The Vision II laser is tuned to 860 nm and MPX is tuned to 1100 nm. Filters for Non-Descanned Detectors are configured to capture transmitted light below 485 nm using a short pass filter (SP485) and reflected light between 500 and 550 nm using a bandpass filter (BP 500–550).
3. The injured myotome is centered in the field of view and the focus is adjusted to visualize myofibers with transmitted light. It is important to ensure striated myofibers are visible as these are expected to produce an SHG signal and so can act as a control for the generation of the SHG signal.
4. The Vision II laser is set to 20% power and MPX is set to 40% power initially. Fast scanning of the sample enables the observer to determine whether there is any signal from the GFP (in the reflected direction) and SHG (in the transmitted direction). The scan speed can be slowed down if a signal is observed to enable a higher definition scan. If no signal is observed the power of each laser may be increased. In our experience, SHG generally requires ~50% laser power when using two tandemly arrayed lasers as in the 7MP.
5. After identifying a suitable power, scan speed and the average number of scans per slice must be adjusted so that animals may be imaged over time. Both the power used and the frequency of imaging dictate the effect of imaging on the animal's health. It is beneficial to ensure there is at least 10 mL of medium in the 60 mm dish.

An important technical note for imaging larvae by multiphoton microscopy is to ensure larvae do not have black pigmented cells, either by use of PTU or by using animals carrying mutations that inhibit the development of melanophores. This is because these cells effectively absorb infrared radiation from the lasers used in multiphoton microscopes leading to rapid overheating of the animal and tissue damage.

It is worth mentioning that all the imaging methods described here can permit simultaneous analysis of apparently normal development of muscle and associated tissues in distant unwounded somites within the same fish, in parallel with analysis of regeneration in wounded somites. Clearly, however, the development of unlesioned somites in an injured fish cannot be assumed to be entirely wild type.

4 Notes

1. Optimal settings of the needle puller to get short needle tips suitable for muscle injury are heat – 620, pull – 150, velocity – 150, and time – 150 (for P-97 Flaming Brown, Sutter Instruments). Settings may vary depending on the precise positioning of the heating coil, which should not be adjusted by novices.
2. If using the 1% agarose plates stored in the fridge, ensure they equilibrate to room temperature. If the plate remains cold, it will trigger rapid LMA setting during mounting preventing optimal larva positioning.
3. Once the LMA aliquot is removed from the 37 °C heat block, keep in mind the room temperature. It is essential to ensure the LMA does not start to form lumps that will result in sub-optimal imaging. The LMA should be fully melted when applied to the plate and during orienting of the larva.
4. Alternatively, the larva can be placed on the 1% agarose surface, excess liquid removed with a fine pipette, and a drop of LMA solution applied to embed the larva.
5. LMA and agarose swell somewhat when immersed in E3 medium. To prevent drift during scanning, it is best to allow agarose to swell before scanning. The higher the concentration of LMA, the more time is needed to permit swelling. For 0.8% LMA, the dish should be allowed to rest after adding E3 medium for at least 15 min.
6. Alternatively, a tungsten wire, sharpened by electrolysis in 5 M KOH, may be employed.
7. Damage to the neural tube/notochord should be avoided. If the neural tube/notochord is damaged, take note and prioritize scanning other larvae. The chances of survival of such a

damaged larva are low the next day, thus such animals should be excluded from experiments and terminated by the legally required route (e.g., anesthesia overdose). Even if the larva survives, development is generally significantly affected, and therefore it is not advisable to use such injured animals for the experiment.

8. Glass-bottomed dishes can be made by cutting a hole in a 60 mm petri plastic dish and gluing a No. 0 glass coverslip over the hole with superglue. Commercially bought and self-made dishes can also be washed, then rinsed with 80% ethanol, and carefully dried and reused.
9. Care must be taken to export from Zeiss Zen software and subsequent import into Volocity or other image analysis programs correctly to avoid image distortion in the *Z* plane. Voxel and image dimensions should always be noted and kept constant for the experiments.
10. While misorientation in LMA is undesirable and should be avoided, in situations where it is essential to process a large number of fish rapidly to find a small fraction with a required characteristic (such as a rare genotype in a complex genetic cross that can only be genotyped after imaging), such software-based re-orientation after scanning can be very helpful.
11. An alternative method to remove larvae is to use No. 5 SA forceps. Keeping the tips of the forceps together, first break up the LMA around the head, and then at regular intervals around the larva, always using the blunt outer side of the forceps for any fish contact. Then use forceps under the head from the dorsal side to scoop out the larva.

Acknowledgments

We thank members of the Hughes lab for advice and R.K. Patient for enabling J.K. to work in Oxford and access the Wolfson Imaging facility WIMM. We are grateful to Bruno Correia da Silva and his staff for fish care. S.M.H is a Medical Research Council Scientist with MRC Programme Grant (G1001029 and MR/N021231/1) support.

References!

1. Katz B (1961) The terminations of the afferent nerve fibre in the muscle spindle of the frog. Phil Trans Royal Soc B 243:221–240
2. Mauro A (1961) Satellite cell of skeletal muscle fibers. J Biophys Biochem Cytol 9:493–495
3. Ciciliot S, Schiaffino S (2010) Regeneration of mammalian skeletal muscle. Basic mechanisms and clinical implications. Curr Pharm Des 16: 906–914

4. Gunther S, Kim J, Kostin S et al (2013) Myf5-positive satellite cells contribute to Pax7-dependent long-term maintenance of adult muscle stem cells. Cell Stem Cell 13:590–601
5. Seale P, Sabourin LA, Girgis-Gabardo A et al (2000) Pax7 is required for the specification of myogenic satellite cells. Cell 102:777–786
6. Pipalia TG, Koth J, Roy SD et al (2016) Cellular dynamics of regeneration reveals role of two distinct Pax7 stem cell populations in larval zebrafish muscle repair. Dis Model Mech 9: 671–684
7. Berberoglu MA, Gallagher TL, Morrow ZT et al (2017) Satellite-like cells contribute to pax7-dependent skeletal muscle repair in adult zebrafish. Dev Biol 424:162–180
8. Gurevich DB, Nguyen PD, Siegel AL et al (2016) Asymmetric division of clonal muscle stem cells coordinates muscle regeneration in vivo. Science 353: aad9969
9. Knappe S, Zammit PS, Knight RD (2015) A population of Pax7-expressing muscle progenitor cells show differential responses to muscle injury dependent on developmental stage and injury extent. Front Aging Neurosci 7:61
10. Nguyen PD, Gurevich DB, Sonntag C et al (2017) Muscle stem cells undergo extensive clonal drift during tissue growth via Meox1-mediated induction of G2 cell-cycle arrest. Cell Stem Cell 21:107–119.e106
11. Seger C, Hargrave M, Wang X et al (2011) Analysis of Pax7 expressing myogenic cells in zebrafish muscle development, injury, and models of disease. Dev Dyn 240:2440–2451
12. Sharma P, Ruel TD, Kocha KM et al (2019) Single cell dynamics of embryonic muscle progenitor cells in zebrafish. Development 146: dev178400
13. Bassett DI, Bryson-Richardson RJ, Daggett DF et al (2003) Dystrophin is required for the formation of stable muscle attachments in the zebrafish embryo. Development 130: 5851–5860
14. Gupta V, Kawahara G, Gundry SR et al (2011) The zebrafish dag1 mutant: a novel genetic model for dystroglycanopathies. Hum Mol Genet 20:1712–1725
15. Gupta VA, Kawahara G, Myers JA et al (2012) A splice site mutation in laminin-alpha2 results in a severe muscular dystrophy and growth abnormalities in zebrafish. PLoS One 7: e43794
16. Ruparelia AA, Zhao M, Currie PD et al (2012) Characterization and investigation of zebrafish models of filamin-related myofibrillar myopathy. Hum Mol Genet 21:4073–4083
17. Sztal TE, Sonntag C, Hall TE et al (2012) Epistatic dissection of laminin-receptor interactions in dystrophic zebrafish muscle. Hum Mol Genet 21:4718–4731
18. Coffey EC, Pasquarella ME, Goody MF et al (2018) Ethanol exposure causes muscle degeneration in zebrafish. J Dev Biol 6:7
19. Pourghadamyari H, Rezaei M, Ipakchi-Azimi A et al (2019) Establishing a new animal model for muscle regeneration studies. Mol Biol Res Commun 8:171–179
20. Ganassi M, Badodi S, Ortuste Quiroga HP et al (2018) Myogenin promotes myocyte fusion to balance fibre number and size. Nat Commun 9: 4232
21. Ganassi M, Badodi S, Wanders K et al (2020) Myogenin is an essential regulator of adult myofibre growth and muscle stem cell homeostasis. Elife 9:e60445
22. Ganassi M, Zammit PS, Hughes SM (2021) Isolation of myofibres and culture of muscle stem cells from adult zebrafish. Bio-protocol 11(17):e4149. https://doi.org/10.21769/BioProtoc.4149
23. Westerfield M (2000) The zebrafish book – a guide for the laboratory use of zebrafish (Danio rerio). University of Oregon Press, Corvallis
24. Denvir MA, Tucker CS, Mullins JJ (2008) Systolic and diastolic ventricular function in zebrafish embryos: influence of norepenephrine, MS-222 and temperature. BMC Biotechnol 8: 21
25. Rombough PJ (2007) Ontogenetic changes in the toxicity and efficacy of the anaesthetic MS222 (tricaine methanesulfonate) in zebrafish (Danio rerio) larvae. Comp Biochem Physiol A Mol Integr Physiol 148:463–469
26. Yogev O, Williams VC, Hinits Y et al (2013) eIF4EBP3L acts as a gatekeeper of TORC1 in activity-dependent muscle growth by specifically regulating Mef2ca translational initiation. PLoS Biol 11:e1001679
27. Elworthy S, Hargrave M, Knight R et al (2008) Expression of multiple slow myosin heavy chain genes reveals a diversity of zebrafish slow twitch muscle fibres with differing requirements for hedgehog and Prdm1 activity. Development 135:2115–2126
28. Devoto SH, Melancon E, Eisen JS et al (1996) Identification of separate slow and fast muscle precursor cells in vivo, prior to somite formation. Development 122:3371–3380
29. Roy S, Wolff C, Ingham PW (2001) The u-boot mutation identifies a hedgehog-regulated myogenic switch for fiber-type

diversification in the zebrafish embryo. Genes Dev 15:1563–1576

30. von Hofsten J, Elworthy S, Gilchrist MJ et al (2008) Prdm1- and Sox6-mediated transcriptional repression specifies muscle fibre type in the zebrafish embryo. EMBO Rep 9:683–689
31. Mahalwar P, Walderich B, Singh AP et al (2014) Local reorganization of xanthophores fine-tunes and colors the striped pattern of zebrafish. Science 345:1362–1364
32. Plotnikov SV, Millard AC, Campagnola PJ et al (2006) Characterization of the myosin-based source for second-harmonic generation from muscle sarcomeres. Biophys J 90:693–703
33. Asakawa K, Suster ML, Mizusawa K et al (2008) Genetic dissection of neural circuits by Tol2 transposon-mediated Gal4 gene and enhancer trapping in zebrafish. Proc Natl Acad Sci U S A 105:1255–1260

Chapter 18

Methods to Monitor Circadian Clock Function in Skeletal Muscle

Xuekai Xiong and Ke Ma

Abstract

The circadian clock exerts temporal regulation in physiology and behavior. The skeletal muscle possesses cell-autonomous clock circuits that play key roles in diverse tissue growth, remodeling, and metabolic processes. Recent advances reveal the intrinsic properties, molecular regulations, and physiological functions of the molecular clock oscillators in progenitor and mature myocytes in muscle. While various approaches have been applied to examine clock functions in tissue explants or cell culture systems, defining the tissue-intrinsic circadian clock in muscle requires sensitive real-time monitoring using a Period2 promoter-driven luciferase reporter knock-in mouse model. This chapter describes the gold standard of applying the *Per2::Luc* reporter line to assess clock properties in skeletal muscle. This technique is suitable for the analysis of clock function in ex vivo muscle preps using intact muscle groups, dissected muscle strips, and cell culture systems using primary myoblasts or myotubes.

Key words Circadian clock, Per2-luciferase reporter, Skeletal muscle explant, Primary myoblast, Amplitude

1 Introduction

The circadian clock oscillators in mammals are composed of a hierarchical system consisting of the central clock pacemaker residing in the suprachiasmatic nuclei in the hypothalamus and the peripheral clocks in nearly all cells in the body [1]. This evolutionarily conserved temporal control mechanism to anticipate environmental cues is driven by a molecular circuit of transcriptional/translational feedback loop that generates ~24-h oscillations in behavioral, physiological, and metabolic processes. In normal physiology, the behavioral rhythm is controlled by the central clock, while peripheral clocks respond to neural or humoral output generated by the central clock, systemic metabolic signals, or tissue-specific cues [2]. Skeletal muscle possesses a tissue-intrinsic molecular clock network for temporal coordination of locomotor activity, tissue growth, and metabolism [3, 4]. This temporal

Atsushi Asakura (ed.), *Skeletal Muscle Stem Cells: Methods and Protocols*, Methods in Molecular Biology, vol. 2640,
https://doi.org/10.1007/978-1-0716-3036-5_18,

regulatory element is intimately involved in muscle mass regulations through sarcomeric structural organization, myogenic progenitor behavior, and metabolic control [5–8]. Timed exercise has been shown to phase-shift the muscle clock [9, 10], and the clock resetting effects of exercise are proposed to prevent sarcopenia in susceptible populations [11].

Various methods for measuring molecular clock activity have been developed. Historically, the use of four-hour samplings for gene expression analysis over a 24-h time-point sampling in mice or synchronized cells is a common approach for circadian studies [7]. However, the poor time-scale resolution renders it mostly suitable only for high-amplitude oscillations of certain clock outputs. Current guideline for genomic analyses requires sample collection of a minimum of every 2-h intervals over two independent circadian cycles [12]. Although this improves time resolution, the requirement for a very large cohort renders it cumbersome. Additionally, analyses based on core clock or clock output gene transcript or protein levels may not accurately reflect real-time clock activity. To date, the gold standard for quantitative monitoring of circadian clock properties utilizes various core clock gene-driven luciferase reporter cell lines [13, 14]. Luciferase reporters that faithfully reflect clock activity, made possible by clock gene promoter-driven luciferase expression, offer accurate and sensitive readouts through bioluminescence detection that allows quantitative measurements of key clock properties, including phase angle, period length, cycling amplitude, and robustness of the oscillation [14]. Commonly adopted luciferase reporter cell lines include Per2-driven or Bmal1-driven U2OS and immortalized Per2-driven mouse fibroblasts [15, 16]. More recently, the generation of a Period2::luciferase (Per2::Luc) knock-in mouse provided the field with a versatile tool to reliably monitor clock oscillations in vivo and ex vivo [17]. This knock-in mice line harboring the Per2-luciferase reporter in the 3' UTR of the endogenous Period2 gene recapitulates its gene transcription, established by the Takahashi lab, and becomes a critical tool for in vivo and ex vivo clock functional analysis. Various tissue explants and primary or immortalized cell types derived from the Per2::luciferase reporter mouse have been applied to real-time measurement of clock properties [17]. Adopting similar analyses using ex vivo muscle explants or primary myoblasts obtained from Per2-luciferase reporter mice offers the most sensitive and reliable approach for evaluating clock function in skeletal muscle. However, using muscle explants presents specific challenges due to the low tissue permeability to allow luciferin access by myocytes. Various protocols in current literature using Per2-luc tissue explant culture for clock activity assessment lack descriptions of the precise precautions taken to reduce variability and obtain reproducible results.

In this chapter, we describe the detailed method for optimizing luciferase signal by ensuring uniform luciferin permeability into isolated muscle explants from Per2-Luc reporter mice for clock monitoring. Our protocol specifically controls the weight and quality of the muscle strips for reproducibility. To minimize the variability of results, maintaining intact myofiber structure and selecting uniform size of the explants are critical. In addition, we report a newly established method of using isolated primary myoblasts for assessing cell-autonomous clock rhythms in culture [18]. We report synchronization by dexamethasone as a key approach to elicit robust clock rhythm in primary myoblasts, a valuable tool to assess muscle cell-autonomous clock properties.

2 Materials

2.1 Reagents

2.1.1 Mice

Per2-luciferase mice (C57BL/6 background, Jackson Laboratory B6.129S6-Per2tm1Jt/J Stock No: 006852).

2.1.2 Luciferase Explant Media

1. DMEM, powder, high glucose, pyruvate (10 × 1 L).
2. HEPES (1 M) 100 mL.
3. Sodium Bicarbonate (7.5%) 100 mL.
4. PSG (100X) 100 mL.
5. FBS 500 mL.
6. XenoLight D-Luciferin – Monopotassium Salt Bioluminescent Substrate (1 × 1 g), PerkinElmer, Catalog No: 122799.
7. Sodium Hydroxide (NaOH) 500 g.

2.1.3 2xDMEM Buffer Stock

Reagent	*Volume*
DMEM powder (1 L medium)	
Sterile MilliQ water	485 mL
pH 7 1 M HEPES	10 mL
7.5% Sodium Bicarbonate	5 mL
Total volume	500 ml

2.1.4 1X Fresh Explant Medium

Reagent	*Final Concentration*	*Volume*
2X DMEM buffer stock	1X	5 mL
(100X) PSG	1X	100 µL
Luciferin (100 mM)	1 mM	100 µL
100% FBS	10%	1 mL

(continued)

NaOH (100 mM)	100 μM	10 μL
Sterile MilliQ water		3.79 mL
Total volume		10 mL

2.2 Supplies and Equipment

1. Mouse surgical dissection tools.
2. Adhesive PCR Plate Seals.
3. VisiPlate-24 Black, black clear bottom tissue culture-treated microplate for bioluminescence recording, Perkin Elmer, Catalog No. 1450-605.
4. Laxco MZS1 Series Stereo Zoom Binocular Microscope, Fisher Scientific, Catalog No. MZS122.
5. Fisherbrand Isotemp Microbiological Incubator, Fisher Scientific, Catalog No. 15-103-0513.
6. LumiCycle 96-Channel Luminometer, Actimetrics, Wilmette, IL.
7. LuniCycle Analysis Program, Actimetrics, Wilmette, IL.

3 Methods

3.1 Preparation of Per2::Luc Muscle Explants for Bioluminescence Activity Recording

1. Euthanize 16- to 20-week-old Per2-luciferase mice. This line of mice, mPER2::LUC-SV40 knock-in, was originally generated by the Takahashi group at Northwestern University. Mice are bred as homozygotes and maintained in regular LD 12:12 light cycles (12 hr. light, 12 hr. dark) until used for experiments. All procedures are conducted according to the IACUC protocol approved by the investigator's institution.
2. Carefully dissect the specific muscle groups tendon-to-tendon without damaging the myofiber. Remove all connective tissue capsules covering the muscle bundle to allow efficient luciferin diffusing into the myofiber (*see* **Note 1–3**).
3. Intact soleus or extensor digitorum longus (EDL) is used as a single muscle explant, after clearing connective tissue covering the muscle (Fig. 1a).

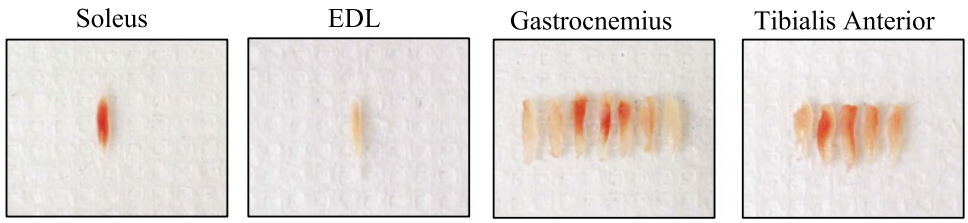

Fig. 1 Dissected intact muscle groups (soleus, EDL) and muscle strips of (Gas, TA) for bioluminescence recording

4. Larger muscle groups commonly used, such as tibialis anterior (TA) and gastrocnemius (Gas), are trimmed free of fat and connective tissue. Individual muscles are divided into uniform strips to ensure consistent surface area and adequate diffusion of luciferin into myofiber. Each muscle strip is obtained along the longitudinal orientation of the myofiber at ~5 mm in diameter, 15–20 mg of wet tissue weight, as shown in Fig. 1.
5. Muscle strips are kept on the plastic petri dish containing ice-cold PBS prior to transferring into black 24-well black clear bottom tissue culture microplates containing luciferase explant media for bioluminescence recording (*see* **Note 4**).
6. Explant luciferase media contains DMEM supplemented with 10% FBS, 1% penicillin/streptomycin, 10 mM of HEPES, and 4 mM of $NaHCO_3$ made fresh from 2x stock with the addition of 100 μM NaOH and 1 mM luciferin.

3.2 Preparation of Per2::Luc Primary Myoblasts for Bioluminescence Recording

1. Isolate primary myoblast from 4-week-old Per2-Luc mice using established protocol as described[1]. The purity of the culture is determined by differentiating efficiency of >98%.
2. Primary myoblasts are maintained in primary myoblast growth media containing 20% FBS with 2 mg/L bFGF and expanded. Prior to bioluminescence recording, cells are seeded at 1.5×10^6/well in 24-well culture plates.
3. For bioluminescence recording of myotube culture, primary myoblasts at >90% confluency are induced to differentiate in media containing 2% horse serum for 1 day prior to switching to luciferase explant media with 2% serum.
4. For bioluminescence monitoring of primary myoblast or myotubes, 0.1 μM dexmethasone can be added to luciferase explant media to synchronize the culture, which will augment the robustness of the rhythm to sustain for 5–6 days (*see* **Note 6**). Cells were washed with PBS and then switched to luciferase explant media with dexamethasone for 6 days.

3.3 LumiCycle 96 Bioluminescence Recording of Per2::Luc Muscle Explant or Myoblasts

1. Set up a light-tight bacterial incubator at 36 °C to accommodate LumiCycle 96 luminometer. The incubator has an enclosable opening in the back to allow cable connection with the sensor box placed on top.
2. LumiCycle 96 luminometer is maintained in a 36 °C incubator with room air for continuous real-time bioluminescence recording. Photomultiplier tubes positioned at ≈1 cm above corresponding wells of the culture dish capture continuous bioluminescence light emission from cultured muscle explant or cells. Photon count sampling frequency was set at 10-min intervals.

3. Transfer the dissected muscle strip into 24 well dishes containing explant media. For myoblasts or myotube cultures, cells are washed once in PBS and switched to explant media with or without dexamethasone synchronization.
4. Twenty-four-well black clear bottom cell culture plates containing muscle explant or cells were vacuum-sealed with an adhesive optical plastic sealing film and immediately placed into LumiCycle 96 for continuous bioluminescence recording without interruption for 6 days.
5. The LumiCycle software was used to collect raw bioluminescence data from muscle explant cultures in 1.2-min bins at 10-min intervals and recorded as photon counts/second. The raw data collected as counts/s is plotted in real-time and stored continuously during the recording.

3.4 Bioluminescence Data Analysis of Muscle Explant and Myoblast

1. The raw data obtained from muscle explants or myoblasts over 7 days were analyzed using the LumiCycle Analysis Program to determine clock properties. The raw data was smoothed by adjacent-averaging method with 0.5-h running means, and subsequently fitted to a linear baseline is subtracted and becomes a baseline-subtracted curve. Due to frequent changes in baseline recordings for the first few days during explant culture, baselines are adjusted for each sample individually.
2. The first day's data was trimmed from analysis due to fluctuations induced by media change and temperature equilibration during this period of recording.
3. Baseline-subtracted, trimmed data were then fitted to a dampened sine wave curve and used to calculate the phase, period length, amplitude, and robustness of the *Per2::Luc* bioluminescence rhythms of the cultured muscle explant or myoblasts (Figs. 2a and 3). The goodness-of-fit of the curve is determined to assess the quality of the curve fit and a cutoff of 80% is applied. Results below the cutoff are considered technically invalid.

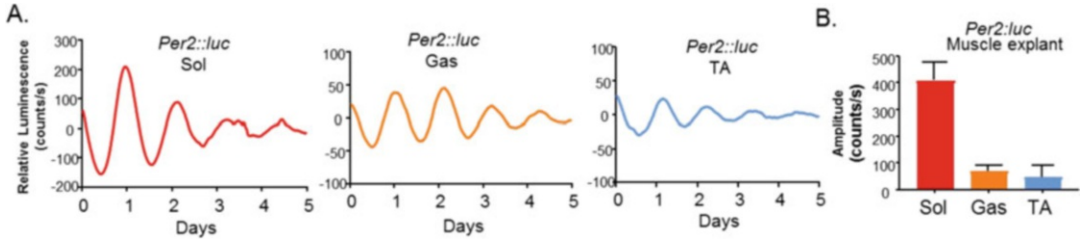

Fig. 2 Bioluminescence recordings of *Per2::Luc* reporter muscle explant by LumiCycle 96. (**a**) Baseline-subtracted data from soleus, gastrocnemius, and TA over 7 days of culture in explant media. (**b**) Quantitative analysis of *Per2::Luc* muscle explant clock oscillation amplitude

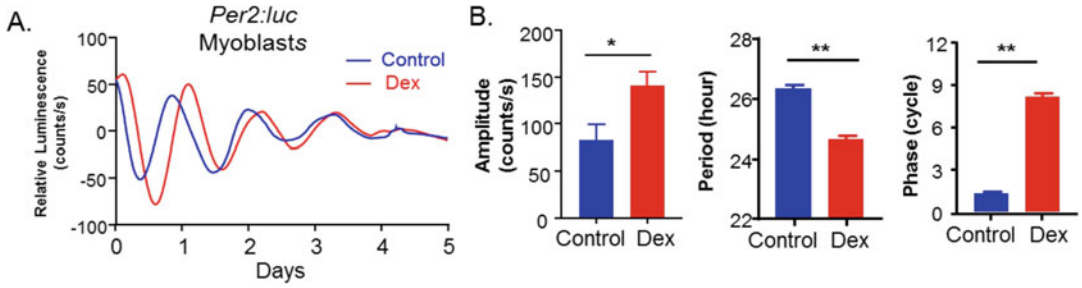

Fig. 3 Bioluminescence recordings of *Per2:: Luc* primary myoblasts by LumiCycle 96. (**a**) Baseline-subtracted bioluminescence of untreated controls in explant media or synchronization by dexamethasone (Dex, 0.1 μM). (**b**) Quantitative analysis of clock oscillation amplitude, period length, and phase angle in control or dexamethasone-synchronized primary myoblasts

4. The clock phase is measured as the time of the first peak of the *Per2::Luc* bioluminescence rhythm after 24 h in culture. Data from day 2 to day 5 are used to determine the clock rhythm period length and oscillating amplitude (Fig. 2b).
5. For muscle explant culture, each muscle strip from one muscle group is a technical repeat for a given animal. The average is plotted as the representative curve. A minimum of three biological replicates are required for the quantitative analysis.

4 Notes

1. Dissecting large muscle groups, such as tibialis anterior or gastrocnemius, into uniform 15–20 mg muscle strips allows better diffusion of luciferin into myofibers to reduce variability.
2. Preservation of full-length myofibers for individual muscle strips are critical to obtain high luciferase luminescence signals. Avoid cutting across myofibers during dissection and separation of muscle strips to minimize the loss of activity.
3. Dividing muscle strips could be done under a dissection microscope, which minimizes damage to myofiber, especially when initially testing out the method. Do not use muscle bundles or strips that are too thick or damaged to ensure consistent luciferase activity of the myofibers.
4. We observed that soleus muscle exhibits the highest cycling amplitude as compared to TA, Gas, or EDL. We thus prefer using soleus as the representative muscle explant for Per2-Luc bioluminescence.
5. Rhythms of muscle strip explants persist longer than isolated myoblasts. Most muscle strip rhythms last 6–7 days while myoblasts typically sustain 5–6 days. The change to explant media at the start of bioluminescence recording synchronizes tissue explant or cells.

6. The aggregate clock rhythm of cells dampens due to the dispersion of stochastic phase of their individual clock oscillations over time [15]. Dexamethasone is applied to synchronize cells in culture [19]. The addition of dexamethasone synchronizes myoblast or myotube cultures to elicit robust clock cycling properties. Cycling amplitude are weaker and the rhythm dampens over 4–5 days without dexamethasone synchronization (Fig. 3).
7. pH of explant media can be adjusted to account for the metabolic rate of the muscle explant or myoblasts. Due to the high metabolic rate of the differentiated myotubes, increasing PH accordingly will prolong cell viability and luciferase activity in culture. Early-stage differentiated myotubes are more suitable for lumicycle due to the culture condition in explant media.
8. Certain tissue explants such as SCN slices require insert to secure tissue explants [17]. This practice is not required for muscle strips we have tested.
9. The robustness of the explant oscillations in culture may vary, particularly near the later days of the recording. For low amplitude oscillations that deteriorate in later days of the recording with severely dampened amplitude, the data may be trimmed to 4 days for analysis of period parameters to avoid variable signals.

References

1. Takahashi JS (2017) Transcriptional architecture of the mammalian circadian clock. Nature reviews. Genetics 18:164–179
2. Dibner C, Schibler U, Albrecht U (2010) The mammalian circadian timing system: organization and coordination of central and peripheral clocks. Annu Rev Physiol 72:517–549
3. Chatterjee S, Ma K (2016) Circadian clock regulation of skeletal muscle growth and repair. F1000Research 5:1549
4. Harfmann BD, Schroder EA, Esser KA (2015) Circadian rhythms, the molecular clock, and skeletal muscle. J Biol Rhythm 30:84–94
5. Andrews JL, Zhang X, McCarthy JJ et al (2010) CLOCK and BMAL1 regulate MyoD and are necessary for maintenance of skeletal muscle phenotype and function. Proc Natl Acad Sci U S A 107:19090–19095
6. Guo B, Chatterjee S, Li L et al (2012) The clock gene, brain and muscle Arnt-like 1, regulates adipogenesis via Wnt signaling pathway. FASEB J 26:3453–3463
7. Chatterjee S, Nam D, Guo B et al (2013) Brain and muscle Arnt-like 1 is a key regulator of myogenesis. J Cell Sci 126:2213–2224
8. Nam D, Chatterjee S, Yin H et al (2015) Novel function of rev-erbalpha in promoting brown adipogenesis. Sci Rep 5:11239
9. Wolff G, Esser KA (2012) Scheduled exercise phase shifts the circadian clock in skeletal muscle. Med Sci Sports Exerc 44:1663–1670
10. Eastman CI, Hoese EK, Youngstedt SD et al (1995) Phase-shifting human circadian rhythms with exercise during the night shift. Physiol Behav 58:1287–1291
11. Choi Y, Cho J, No MH et al (2020) Re-setting the circadian clock using exercise against sarcopenia. Int J Mol Sci 21(9):3106
12. Hughes ME, Abruzzi KC, Allada R et al (2017) Guidelines for genome-scale analysis of biological rhythms. J Biol Rhythm 32:380–393
13. Brandes C, Plautz JD, Stanewsky R et al (1996) Novel features of drosophila period transcription revealed by real-time luciferase reporting. Neuron 16:687–692
14. Yu W, Hardin PE (2007) Use of firefly luciferase activity assays to monitor circadian molecular rhythms in vivo and in vitro. Methods Mol Biol 362:465–480

15. Welsh DK, Yoo SH, Liu AC et al (2004) Bioluminescence imaging of individual fibroblasts reveals persistent, independently phased circadian rhythms of clock gene expression. Curr Biol 14:2289–2295
16. Liu AC, Tran HG, Zhang EE et al (2008) Redundant function of REV-ERBalpha and beta and non-essential role for Bmal1 cycling in transcriptional regulation of intracellular circadian rhythms. PLoS Genet 4:e1000023
17. Yoo SH, Yamazaki S, Lowrey PL et al (2004) PERIOD2::LUCIFERASE real-time reporting of circadian dynamics reveals persistent circadian oscillations in mouse peripheral tissues. Proc Natl Acad Sci U S A 101:5339–5346
18. Kemler D, Wolff CA, Esser KA (2020) Time-of-day dependent effects of contractile activity on the phase of the skeletal muscle clock. J Physiol 598:3631–3644
19. Balsalobre A, Brown SA, Marcacci L et al (2000) Resetting of circadian time in peripheral tissues by glucocorticoid signaling. Science 289:2344–2347

Chapter 19

Visualizing MyoD Oscillations in Muscle Stem Cells

Ines Lahmann and Carmen Birchmeier

Abstract

The bHLH transcription factor MyoD is a master regulator of myogenic differentiation, and its sustained expression in fibroblasts suffices to differentiate them into muscle cells. MyoD expression oscillates in activated muscle stem cells of developing, postnatal and adult muscle under various conditions: when the stem cells are dispersed in culture, when they remain associated with single muscle fibers, or when they reside in muscle biopsies. The oscillatory period is around 3 h and thus much shorter than the cell cycle or circadian rhythm. Unstable MyoD oscillations and long periods of sustained MyoD expression are observed when stem cells undergo myogenic differentiation. The oscillatory expression of MyoD is driven by the oscillatory expression of the bHLH transcription factor Hes1 that periodically represses MyoD. Ablation of the Hes1 oscillator interferes with stable MyoD oscillations and leads to prolonged periods of sustained MyoD expression. This interferes with the maintenance of activated muscle stem cells and impairs muscle growth and repair. Thus, oscillations of MyoD and Hes1 control the balance between the proliferation and differentiation of muscle stem cells. Here, we describe time-lapse imaging methods using luciferase reporters, which can monitor dynamic MyoD gene expression in myogenic cells.

Key words Muscle stem cell, MyoD, Oscillation, Time-lapse imaging, Bioluminescence, Dynamic gene expression

1 Introduction

Skeletal muscle grows during development and the postnatal period, and it can even regenerate in the adult. This is due to a small cell population, the Pax7+ stem cells of the skeletal muscle tissue [1–6]. The transition from a single muscle stem cell to a mature and multinucleated myofiber is coordinated by the timed expression of transcription factors of the basic helix-loop-helix (bHLH) family like MyoD and MyoG [7, 8]. In the adult, muscle stem cells are quiescent but in response to a stimulus, for example, a muscle injury, Pax7+ stem cells begin to proliferate and start to express proteins like MyoD [9–11]. During development and regeneration, such activated muscle stem cells can either

Atsushi Asakura (ed.), *Skeletal Muscle Stem Cells: Methods and Protocols*, Methods in Molecular Biology, vol. 2640,
https://doi.org/10.1007/978-1-0716-3036-5_19,

self-renew or progress toward terminal differentiation by expressing Myogenin (MyoG) and finally fusion into multinucleated myofibers [12, 13].

Notch signaling is important for muscle stem cells: Without Notch signals, muscle stem cells are quickly depleted because they differentiate and do not self-renew [14–19]. Conversely, Notch signals repress the differentiation of myogenic cells [20–26]. The binding of a ligand to the Notch receptor releases the Notch intracellular domain (NICD), which translocates to the nucleus where it binds the transcription factor RBP-J and induces expression of members of the Hes/Hey family like Hes1. Hes1, a transcriptional repressor, binds directly to its own promoter and represses its own expression [27, 28]. When the Hes1 promoter is repressed, both Hes1 mRNA and Hes1 protein disappear rapidly, because they are very unstable. This then leads to a new round of Hes1 expression. Because of the negative feedback and the instability of the protein and mRNA, Hes1 mRNA and protein expression oscillate with a periodicity of around 3 h in mouse cells [27].

Notch signaling represses myogenic differentiation using various mechanisms [18, 29–33]. For instance, Hes1 directly represses the myogenic transcription factor MyoD [34]. Therefore, the oscillation of Hes1 periodically represses MyoD. Due to the instability of MyoD mRNA and protein, MyoD disappears rapidly when Hes1 is present and reappears when Hes1 is absent. This results in MyoD oscillations with a periodicity that is similar to the one of Hes1 [34]. When Hes1 is mutated, oscillatory MyoD expression in proliferating muscle stem cells is disrupted. This is accompanied by an early differentiation of the cells and their inability to self-renew, which interferes with muscle growth and regeneration. Thus, oscillatory Hes1 and MyoD expression regulate the balance between muscle cell growth and differentiation [34]. It should be noted that oscillations of components of the Notch signaling pathway and its target genes are observed not only in the skeletal muscle but also in presomitic mesoderm, neuronal progenitor cells, in endothelia, or in the pancreas [35–38].

Methods such as in situ hybridization and immunostaining only provide a snapshot of the dynamic expression of transcripts and protein; therefore, their use for the analysis of oscillations is limited. Time-lapse recordings of reporter expression make it possible to visualize the dynamics of gene expression. Because of the short period of MyoD oscillations, the reporter gene expression must be rapidly induced, and the reporter mRNA and protein must also be unstable. We use luciferase as a reporter instead of fluorescent proteins like GFP because luciferase immediately generates luminescence in the presence of ATP and its substrate luciferin. In contrast, most fluorescent proteins take a few hours to fold properly and emit fluorescence. Additionally, luciferase provides higher sensitivity and a wider dynamic range than fluorescent proteins, and

the lack of auto luminescence in mammalian tissue makes the bioluminescence reporter ideal for live imaging [39, 40]. Furthermore, this luminescence does not require light excitation, which prevents photodamage to the cells during time-lapse imaging [41, 42]. The detection of luciferase activity in individual cells requires highly sensitive equipment and particularly a sensitive camera. In this chapter, we describe detailed methods to monitor oscillatory MyoD expression in muscle stem cells that are dispersed, associated with the muscle fiber, or located in a muscle tissue biopsy.

2 Materials

2.1 MyoD-Luciferase Knock-In Reporter Mouse

The MyoD-Luc2 allele was generated using CRISPR/Cas9-initiated homologous recombination. A targeting vector was generated in which Luciferase cDNA was fused in frame to MyoD coding sequences (Fig. 1a). The targeting vector together with guide RNA was injected into fertilized eggs, which leads to frequent insertion of the targeting vector by homologous recombination [43]. Animals that carried the MyoD-Luc2 allele were then identified by Southern blotting and verified by sequencing (Fig. 1b).

2.2 Bioluminescence Imaging System, Image Processing, and Analysis

2.2.1 Image Acquisition

- Inverted microscope IX83-ZDC (Olympus #IX83P22F).
- Objectives: 10× UPLSAPO super apochromat (Olympus #N2249100), 20× UPLSAPO super apochromat (Olympus #N2178900), and 40× semi apochromat UPLFL (Olympus #N1478700).
- Incubator system cellVivo-2 (Olympus #E0439867 and PeCon #800492).
- Heating system (PeCon #840-800078).
- CO_2 controller (Vivo-CB1G, Olympus #E0438505).

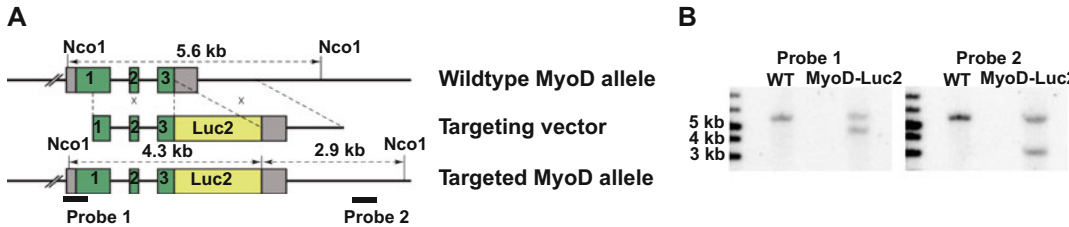

Fig. 1 Generation of the MyoD-Luc2 allele. (**a**) Schematic drawing of the MyoD wildtype allele, the targeting vector, and the MyoD-Luc2 allele. Luciferase cDNA (yellow) was inserted into the MyoD coding region (green) to generate the MyoD-Luciferase fusion gene. Shown are also the NcoI sites and the location of probes used for Southern blot analysis to confirm correct insertion. (**b**) Wildtype and MyoD-Luc2 mice were analyzed by Southern blotting

- Temperature controller (Vivo-CBT, Olympus #E0438504).
- Water-cooled electron multiplying (EM) charged-coupled device (CCD) camera (EM-X2, Hamamatsu #C9100-23B).
- Refrigerated circulator CORIO CD-200F (Julabo #9012701.03).
- Uninterruptible power supply (UPS) (AEG, Protect C. 3000).

2.2.2 Computer and Monitor

- Software cellSense Dimension (Olympus #N5184200) and cellVivo (PeCon).
- Image deconvolution and processing.
- Fiji/ImageJ [44] and optionally the following plug-ins: spike-noise filter [45] and semi-automatic cell tracker [34].

2.2.3 Image Analysis

- Microsoft Excel (Microsoft Cooperation, Redmond, USA).
- Origin Pro software (Origin Lab, Northampton, USA).

2.3 Other Materials

- Bacterial shaker at 37 °C.

2.3.1 General Equipment and Solutions

- Stereomicroscope.
- 15 mL and 50 mL conical tubes, 2 mL reaction tubes.
- Cell strainer 100 μm, 70 μm, and 40 μm.
- 5 mL polystyrene round-bottom tubes with cell-strainer cap.
- Dissection tools.
- Labeling tape.
- MatTek 35 mm dish, No. 1.5 coverslip (MatTek: #P35G-1.5-14-C).
- Silicone inserts (ibidi #80209; ibidi #80409).
- 10× Dulbecco's phosphate buffer saline (DPBS).
- Albumin fraction V (BSA).
- Fetal calf serum.
- D-luciferine Na-salt: Dissolve 100 mg in 3.3 mL 1× DPBS. Store in aliquots at −20 °C. Use 1:100.
- BD Matrigel™ basement membrane matrix (BD #356234): Dilute to 3 mg/mL in ice-cold DMEM. Store aliquots at −20 °C. Use 1 mg/mL for coating. Place the ibidi silicon insert on the glass coverslip of the 35 mm dish (MatTek #P35G-1.5-14-C) and add 20 μL of Matrigel™ solution. Remove Matrigel™ solution and incubate dish for 30 min at 37 °C in a cell culture incubator.

2.3.2 Media and Reagents for Isolation of Single Muscle Stem Cells

- Muscle dissection medium: DMEM containing 4.5 g/L glucose and GlutaMAX™ (Gibco™ #31966–021), 25 mM HEPES, 1:100 gentamycin.

- Dispase™ II (Roche, #04942078001): Dissolve to 100 units/mL in 50 mM HEPES/KOH, 150 mM NaCl, pH 7.4. Store in aliquots at −20 °C.
- NB4 Collagenase proved grade (Nordmark, #S1746502): Dissolve 6 mg/mL in 1× HBSS. Store in aliquots at −20 °C.
- FACS staining buffer: Hanks' balanced salt solution (HBSS), 25 mM HEPES, 1:100 gentamycin, 2 mM EDTA pH 8.0.
- Antibodies: Phycoerythrin (PE) rat anti-mouse CD31 (BD Bioscience #553373), PE rat anti-mouse CD45 (BD Bioscience #553081), goat anti-mouse VCAM-1 (R&D #AF643), Alexa647 donkey anti-goat (ThermoFisher #A32849), propidium iodide (Sigma #P4864).
- Primary muscle cell growth medium: DMEM/F12, 20% fetal calf serum, 10% donor horse serum, 1% penicillin/streptomycin, 1% GlutaMAX™ supplement (Gibco™ #35050061), 2.5 ng/mL basic fibroblast growth factor bFGF (Sigma #F3133), 1:1000 Leukemia inhibitory factor (LIF) (ESGRO™ Sigma #ESG1106).

2.3.3 Media and Solutions for Single Myofiber and Muscle Biopsies

- 5% BSA in 1× DPBS: Heat-inactivate for 20 min at 65 °C, pass through a 0.2 μm filter.
- Muscle fiber isolation medium: DMEM containing 4.5 g/L glucose and GlutaMAX™ (Gibco™ #31966–021), 1% penicillin/streptomycin, 2% GlutaMAX™ supplement (Gibco™ #35050061).
- Collagenase type I (Sigma, #C0130): Immediately before dissection, prepare 2–3 mL per muscle of 0.2% collagenase solution. Dissolve 12 mg collagenase in 6 mL DMEM, 4.5 g/L glucose, GlutaMax™ (Gibco™ #31966–021) and pass through a 0.2 μm filter.
- Collagen solution for coating [46].
- Muscle fiber cultivation medium (used for myofibers and muscle biopsies): DMEM/F12, 10% donor horse serum, 1% penicillin/streptomycin, 2% GlutaMAX™ supplement (Gibco™ #35050061), 0.5% chicken embryo extract solution (Biotrend #MD004-D-UK).

3 Methods

3.1 Bioluminescence Imaging

To image bioluminescence in muscle stem cells derived from MyoD-Luc2 mice, a dark room is required without any ambient light, with a constant temperature of 21 °C, low humidity, and a CO_2 supply chain.

We use an inverted microscope (IX83-ZDC, Olympus), equipped with a cellVivo incubator chamber (cellVivo-2, Olympus), and a highly sensitive water-cooled EM CCD camera (EM-X2, Olympus) connected to a computer. An uninterruptable power supply (UPS, AEG) is used for the microscope, camera, cooling device, and computer. This power supply will protect from fluctuations in the power supply system that can cause a shut-off of the imaging process. In order to exclude ambient light in the imaging chamber (e.g., from light-emitting diodes on the computer or cooling devices), cover the sides of the incubator chamber using tape or use aluminum foil to cover light-emitting diodes. The CO_2 concentration and temperature inside the incubator chamber have to be monitored during imaging (cellVivo software, PeCon).

Imaging of MyoD-Luc2 expressing muscle cells isolated as described in Subheadings 3.3, 3.4 and 3.5.

1. One hour before the start of the imaging, start the microscope and set the water-cooling system of the camera to 10 °C and the temperature controller of the incubator chamber to 37 °C. Fill the incubator chamber with 5% CO_2. Thus, temperature as well as CO_2 levels can stabilize before imaging starts.
2. Switch on the camera when the final cooling temperature (10 °C) is reached. Start circulating the cooled water.
3. Switch on the computer. Start the software required to record live images and the CO_2 and temperature surveillance programs.
4. Open the incubator chamber, place the specimens onto the microscope stage, and close the chamber.
5. Focus on the specimen using bright-field illumination.
6. Record time-lapse images, alternating between bioluminescence and brightfield illumination. Exposure time for the bioluminescence signal depends on the Luciferase expression level; we use between 2 and 10 minutes (min) for single muscle cells in culture, 5–15 min for muscle cells associated with the myofiber, and 5–20 min for ex vivo muscle biopsies. We recommend testing the time settings by starting a short time-lapse movie.
7. Before starting longer imaging experiments, make sure that the CO_2 level in the chamber is stable at 5% and the temperature at 37 °C.
8. Confirm that the camera's cooling system is working by touching it.
9. Start recording the time-lapse movie and switch off the monitor.

3.2 Image Processing and Quantification

The bioluminescence signal of MyoD-Luc2 expressing cells can be tracked and analyzed frame by frame in Fiji/ImageJ, or semi-automatically using a tracking software described previously [34]. In principle, a region of interest (ROI) of a defined diameter that roughly corresponds to the size of a muscle stem cell is marked in each frame. The mean gray value of the ROI is determined, which corresponds to the intensity of the signal. To subtract the background, the mean gray value of an identical area outside the ROI (e.g., the myofiber) is subtracted. The expression of the MyoD-Luc2 bioluminescence over time is visualized by plotting mean gray values of the ROI in different frames using Microsoft Excel (Fig. 2a–c). The curves can be smoothed by polynomial fitting, applying the Savitzky-Golay filter [47] (Fig. 2e). The time between maximum or minimum values of such a curve corresponds to the period of oscillation.

To differentiate between stable oscillations and random fluctuations, the mean gray values that reflect MyoD-Luc2 expression levels over time are analyzed by Fast Fourier Transformation (Origin software, FFT function) (Fig. 3a). To allow robust FFT transformation, muscle cells that have been followed for at least 10 h should be analyzed. By plotting the resulting amplitude over time, a curve with a sharp peak will be visible when MyoD-Luc2 oscillates in a stable manner (Fig. 3b, c). In some cases, the oscillations are interrupted before a long stable oscillation period follows. Such interruptions lead to additional peaks in the FFT plot. We determine the area under such peaks (in a time window between 1.5 and 3 h) to quantify the stability of the oscillations. This can also be used to compare the stability of the oscillations in different cell types, for example, MyoD-Luc2 expression dynamics in control and Hes1 mutant cells.

3.3 Preparation of Dissociated Muscle Stem Cells for Bioluminescence Imaging

Muscle stem cells are isolated from adult MyoD-Luc2 mice using a modification of a previously established protocol [17, 48]. It usually takes around 3–4 h to isolate muscle stem cells from the tissue. Prepare a 10 cm dish with 1× DPBS, the dissection medium, thaw NB4 collagenase and Dispase™ II solutions on ice, and preheat the shaker to 37 °C.

1. Sacrifice the mouse by cervical dislocation and take a tail biopsy for genotyping.
2. Soak hindlimbs with 70% ethanol.
3. Make small cuts in the skin on the ankle and pull the skin up.
4. Cut the hindlimb close to the hip joint.
5. Transfer hindlimbs to a petri dish containing 1× DPBS to wash away the blood.
6. Prepare a 3.5 cm petri dish with 1 mL of dissection medium.

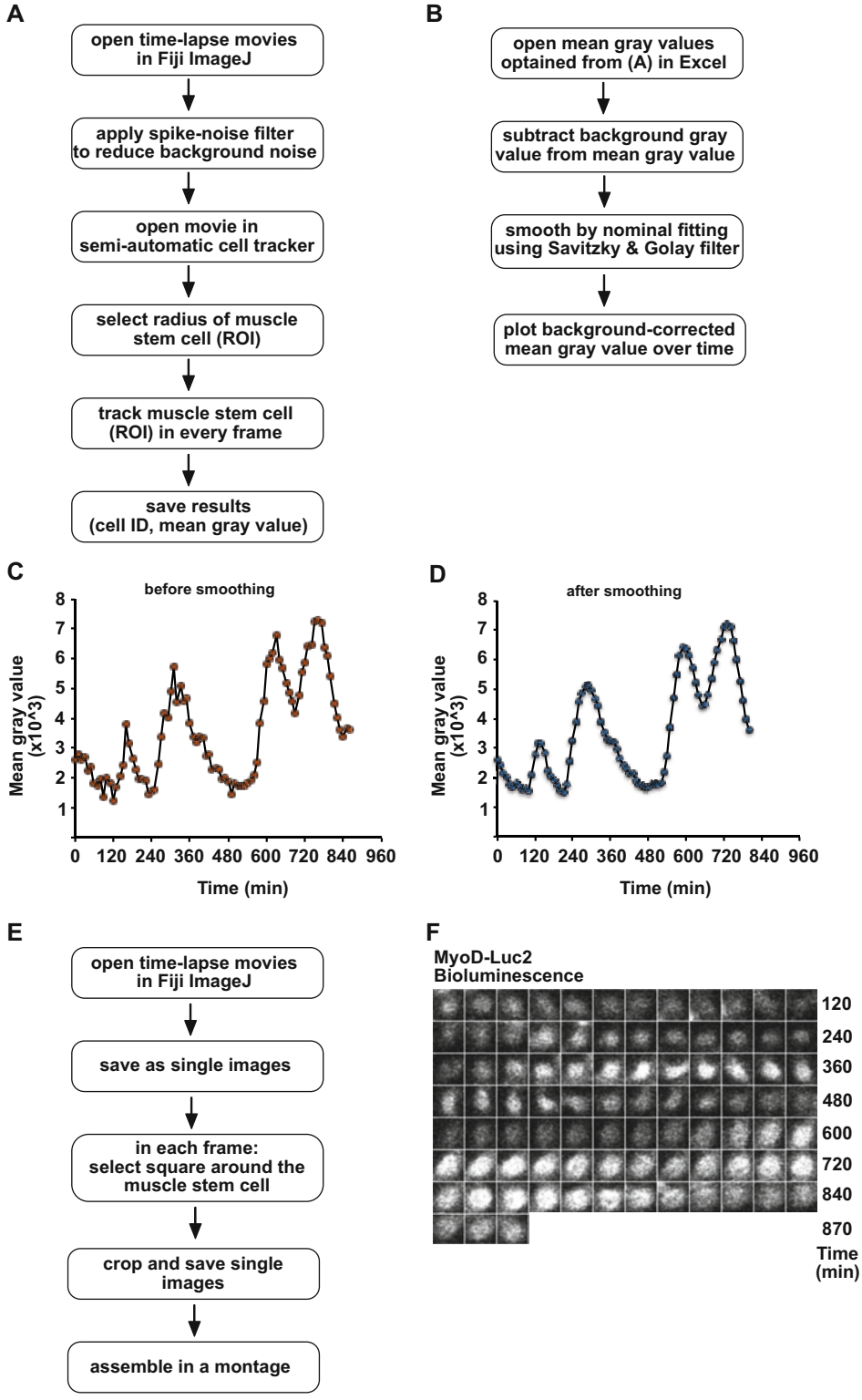

Fig. 2 Analysis of time-lapse videos of MyoD-Luc2 bioluminescence. (**a**) Flow chart of steps used to obtain MyoD-Luc2 expression values using Fiji/ImageJ. (**b**) Flow chart of steps used to plot MyoD-Luc2 expression levels over time. (**c, d**) MyoD-Luc2 expression values over time of a single muscle cell before (**c**) and after (**d**) applying the Savitzky-Golay filter. (**e**) Flow chart of steps used to assemble montages displaying images of MyoD-Luc2 expression in a single cell. (**f**) Montage of a MyoD-Luc2 expressing muscle cell over 910 min

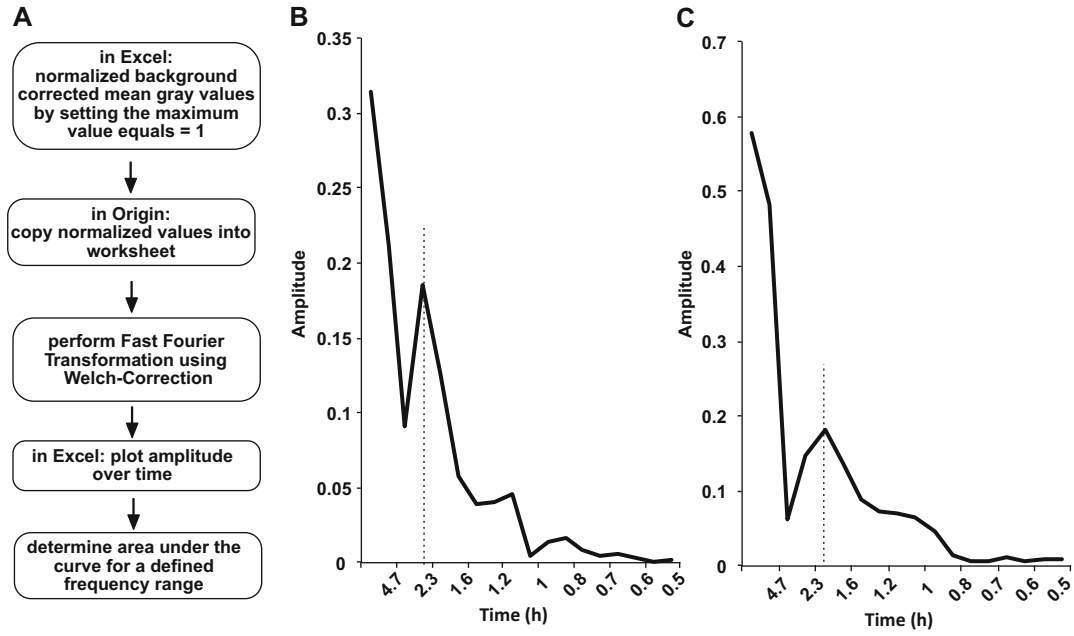

Fig. 3 Fast Fourier transformation (FFT) analysis of oscillatory MyoD-Luc2 expression. (**a**) Flow chart of steps used for an FFT analysis of oscillatory MyoD-Luc2 expression. (**b, c**) Examples of FFT. The dotted line marks the peak, and the time value corresponds to the period of oscillation

7. Place a hindlimb on the lid of the petri dish positioned under the stereomicroscope and remove the muscle with tweezers and scissors. Transfer muscle pieces to a 3.5 cm dish containing 1 mL of dissection medium (*see* **Note 1**).
8. When all hindlimb muscles are isolated, use curved iris scissors to cut the tissue into small pieces.
9. Transfer the suspension to a 15 mL reaction tube, using a 1 mL filter tip that was cut off at the end to enlarge the opening. Add 500 µL NB4 collagenase and 250 µL Dispase™ II and fill up to 10 mL with the dissection medium (*see* **Note 2**).
10. Remove fat that floats on top of the solution.
11. Cap the reaction tubes with Parafilm™ and incubate them lying flat in a shaking incubator at 37 °C and 110 rpm for 25 min.
12. Use a 10 mL disposable pipette to triturate the tissue ten times (*see* **Note 3**).
13. Place the reaction tube back into the shaker and incubate for 20 min at 110 rpm and 37 °C. Repeat trituration and incubation three more times. The mixture should be a homogeneous slurry after the last trituration.

14. Prepare five 50 mL reaction tubes for the tissue from each 15 mL tube. Each 50 mL reaction tube contains a filter; prepare one with a mesh filter, one each with 100 μm and 70 μm filters, and two with 40 μm filters. Prepare the stop medium and moisten all filters with 5 mL of stop medium (*see* **Note 4**).
15. Transfer the slurry through the mesh filter and wash the reaction tube and mesh with the dissection medium. Discard the filter and fill the tube with the dissection medium.
16. Centrifuge for 5 min at 500 rpm and discard the pellet. Pass the supernatant through the 100 μm filter.
17. Centrifuge for 5 min at 500 rpm and discard the pellet. Pass the supernatant through the 70 μm filter (*see* **Note 5**).
18. Pass the cell solution through the 40 μm filter.
19. Pellet the muscle stem cells at 1500 rpm for 15 min at room temperature and dissolve the pellet in 20 mL staining buffer (*see* **Note 6**).
20. Centrifuge for 15 min at 1500 rpm and resuspend the pellet in 1 mL ice-cold staining buffer containing 10 μL of goat anti-mouse VCAM-1 antibody, 5 μL PE rat anti-mouse CD31, 5 μL PE rat anti-mouse CD45, and 5 μL PE rat anti-mouse Ly6A/E (Sca1) (*see* **Note 7**).
21. Wrap the reaction tube in aluminum foil and incubate for 15 min at 4 °C on a rotating wheel.
22. Centrifuge the stained muscle cells for 5 min at 1500 rpm and 4 °C and resuspend the pellet in 1 mL ice-cold staining buffer. Repeat centrifugation and washing two more times.
23. Resuspend the pellet in 1 mL ice-cold staining buffer containing 2 μL of Alexa647 donkey anti-goat antibody.
24. Wrap the reaction tube in aluminum foil and incubate for 15 min at 4 °C on a rotating wheel.
25. Centrifuge the staining solution containing muscle cells for 5 min at 1500 rpm and 4 °C and resuspend the pellet in 1 mL ice-cold staining buffer.
26. Wash the cells twice more using centrifugation and resuspension in 1 mL ice-cold staining buffer.
27. After the last centrifugation, resuspend the pellet in 300–500 μL ice-cold staining buffer; the cells are now ready for sorting.
28. To mark dead cells, add 0.5 μL of propidium iodide to the solution; pass the solution through a cell-strainer cap of a 5 mL polystyrene round-bottom tube and start sorting.

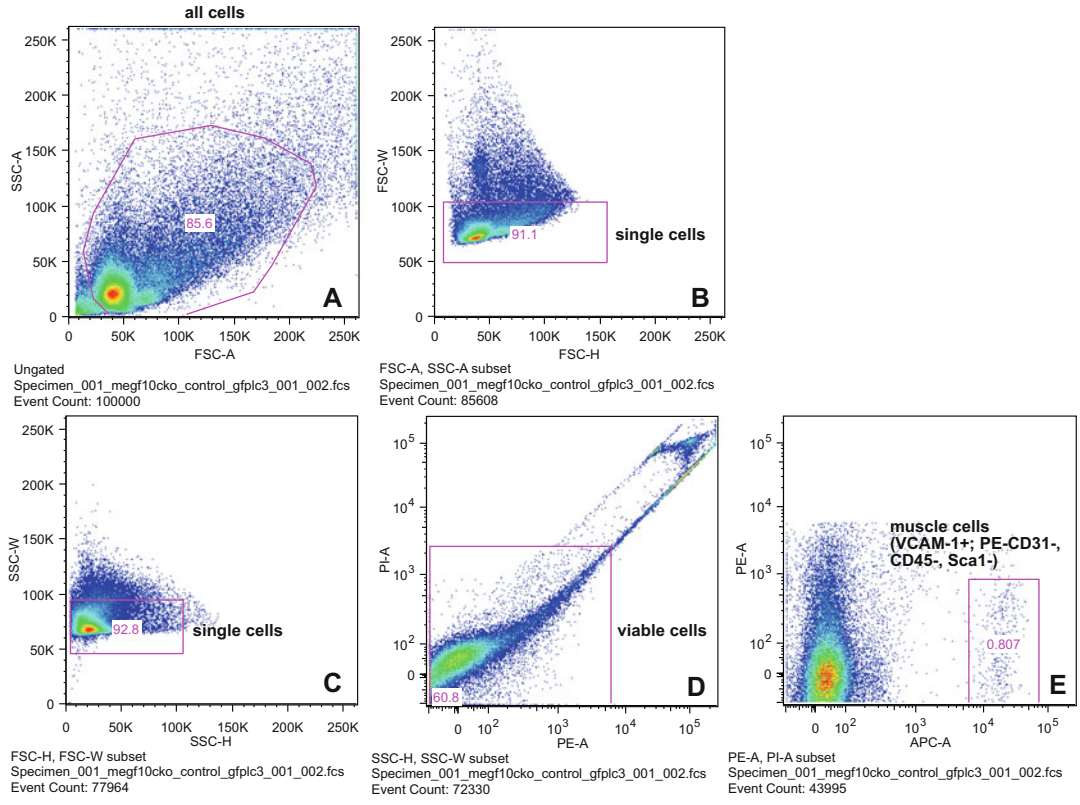

Fig. 4 FACS gating strategy to isolate muscle stem cells. (**a**) Side scatter area (SSC-A) versus forward scatter area (FCS-A) pseudo color density plot. Each dot on the plot represents an individual particle that has passed the laser. A gate (red outline) is applied to a population of interest. (**b, c**) Single cells are then identified by plotting forward scatter width (FSC-W) versus forward scatter height (FSC-H) (shown in B) and side scatter width (SSC-W) versus side scatter height (SSC-H) (shown in **c**). (**d**) Dead cells are eliminated by gating on propidium iodide (PI) negative cells. (**e**) Muscle stem cells are then separated by expression of VCAM-1/Alexa647 and exclusion of hematopoietic cells (phycoerythrin PE-CD45+), endothelial cells (PE-CD31+), and bone marrow stem cells (PE-Sca1+). APC: allophycocyanin

29. Sort viable, single cells that are PE-CD31/45/Sca1-negative, VCAM-647 positive into 1 mL primary muscle growth medium (see Fig. 4 for a FACS gating strategy) (*see* **Note 8**).
30. After sorting, incubate cells for 10 min at room temperature to allow the cells to recover from the FACS procedure.
31. Centrifuge for 5 min at 1500 rpm at room temperature and resuspend the pelleted cells in primary muscle growth medium at a concentration of 50,000 FACS events per 10 μL.
32. Pipette 10 μL per well into the Matrigel-coated ibibi silicon insert (#80409) on a glass bottom culture dish (*see* Subheading 2.3.1). Incubate for 30–50 min at 37 °C (*see* **Note 9**).
33. Carefully add 150 μL growth medium to the ibidi silicon insert, and 150 μL to the glass dish (*see* **Note 10**).

34. Incubate the cells overnight. Switch medium to growth medium plus D-luciferin 1 h prior to imaging.
35. Place the dish on the microscope stage. Focus on the cells using a 20× objective and brightfield illumination and start acquisition of bioluminescence signals and brightfield pictures (*see* Subheading 3.1).

3.4 Preparation of Myofiber-Associated Muscle Stem Cells for Bioluminescence Imaging

In this chapter, we describe the isolation of fibers from MyoD-Luc2 mice for imaging of muscle stem cells associated with myofibers using an adapted protocol previously described [49]. This allows monitoring of MyoD-luciferase expression in muscle stem cells during the transition from quiescence to an activated state, as well as imaging of activated single cells or small cell colonies that are formed after fiber culture. Individual myofibers are isolated from the extensor digitorum longus muscle (EDL) of adult MyoD-Luc2 mice. Isolation of the individual myofibers takes about 2 h. Prepare fiber isolation medium, BSA-coating solution, and fiber cultivation medium before the isolation (*see* Subheading 2.3.3).

1. Sacrifice the mouse by cervical dislocation and take the tail biopsy for genotyping.
2. Soak hindlimbs with 70% ethanol and make a small incision into the skin at the ankle.
3. Holding the skin and foot, pull the skin off.
4. Pin the foot on a polystyrene plate, exposing the lower hindlimb muscles (Fig. 5a, b).
5. Hold the tendons by the ankle with tweezers (Fig. 5c, d) and carefully remove the facia of the tibialis anterior (TA)/EDL muscles.
6. Lift the tendons at the foot, cut them, and lift the TA/EDL muscles to separate it from the tibia below (Fig. 5e).
7. Cut into the knee with sharp iris scissors. The tendon of the EDL is now visible (Fig. 5e).
8. Grasp the tendon of the EDL with forceps without touching the muscle and separate the EDL from the TA (Fig. 5f, g). Do not overstretch the EDL, as this damages myofibers (*see* **Note 11**).
9. Transfer the EDL muscle to a 2 mL reaction tube containing a fiber isolation medium with proteases; isolate the second EDL.
10. Transfer the tube containing both EDLs to a 37 °C incubator and incubate for 90 min. Gently invert the tube every 20 min (*see* **Notes 12** and **13**).
11. After 90 min, remove the fiber isolation medium.
12. Transfer the EDL muscles to the first well of a 6-well dish and triturate the EDL muscles 10–15 times using a wide-mouth BSA-coated glass pipette (*see* **Note 14**).

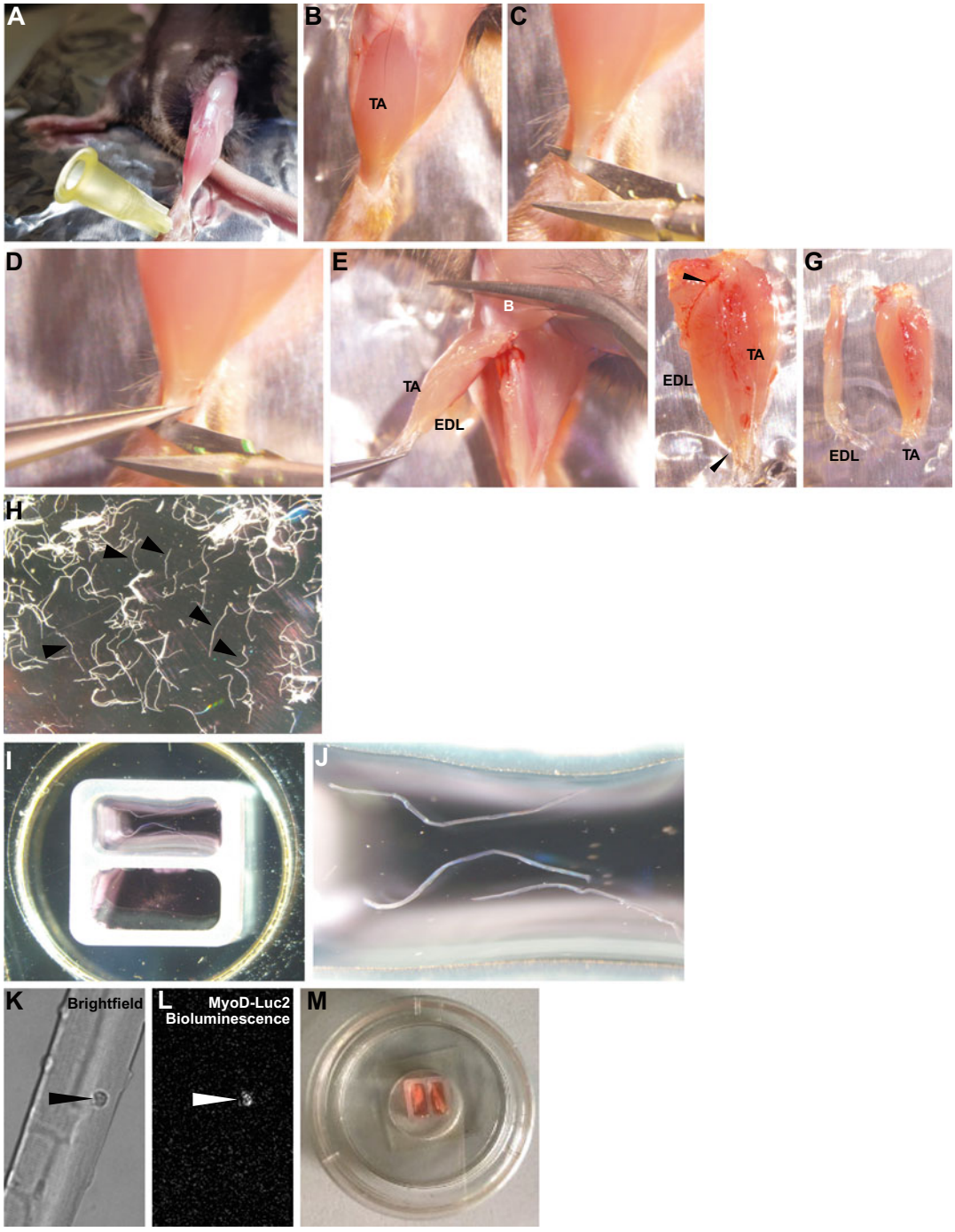

Fig. 5 Preparation of single myofibers and muscle biopsies. (**a-f**) Preparation of EDL and TA muscles from an adult mouse. The hindlimb was pinned to expose EDL and TA muscles (**a, b**). The distal tendons were exposed by a scissor (**c**) and cut (**d**). By pulling the muscle up and cutting through the knee (**e**), the EDL/TA muscle was dissected (**f**). Careful pulling at the tendons (shown by arrowheads in **f**) separates the EDL and TA (**g**). (**h**) Single myofiber (arrowheads) and larger bundles of myofibers can be observed during the trituration of the collagenase-digested EDL muscles. (**i, j**) Single muscle fibers in the upper chamber of the silicon insert before imaging. (**k, l**) A fiber-associated muscle stem cell imaged in brightfield (**k**, arrowhead) and the MyoD-Luc2 signal (**l**, arrowhead). (**m**) Muscle biopsies placed in a silicon insert before imaging

13. Under a stereomicroscope, transfer the remaining muscle pieces to the second well and leave already separated myofibers behind. Repeat the trituration 10–15 times and change to a smaller pipette tip when muscle pieces become small (*see* **Note 15**).
14. If larger pieces of muscle remain after the second trituration, transfer these to a third well and continue trituration 10–15 times.
15. Incubate the myofibers for 10 min at 37 °C, 5% CO_2 (Fig. 5h; *see* **Note 16**).
16. Transfer undamaged myofibers with a BSA-coated 200 μL pipette tip into a second BSA-coated 6-well dish containing fiber cultivation medium.
17. Incubate muscle fibers at 37 °C and 5% CO_2 until imaging.
18. Prepare culture dish for imaging: a. Place the ibidi silicon insert (#80209) in the middle of a glass-bottomed culture dish. b. For coating, add 150 μL collagen solution to the chambers of the insert, incubate briefly at room temperature, and remove the solution. c. Add 50 μL myofiber cultivation medium containing D-luciferin.
19. To monitor MyoD-Luc2 expression in muscle stem cells during exit from quiescence, collect 20 fibers immediately after isolation and transfer them to the BSA-coated 6-well dish containing fiber cultivation medium and D-luciferin.
    (a) Incubate for 10 min; transfer 2–5 fibers to a chamber of an ibidi silicon insert (#80209) in the glass-bottom dish (Fig. 5i, j). The small size of the chamber prevents myofibers from moving during time-lapse imaging.
    (b) Fill the chamber with fiber cultivation medium and D-luciferin and transfer the glass bottom dish to the microscope stage.
    (c) Use bright field illumination to identify myofiber-associated muscle stem cells. Muscle stem cells can be identified by their round shape and their location on the myofiber (*see* Fig. 5k, l).
    (d) Start the acquisition of the bioluminescence signal and brightfield pictures as described in Subheading 3.1.
20. To image MyoD-Luc2 expression after activation of the stem cells, image the isolated muscle fibers after incubation for 16–20 h at 37 °C, 5% CO_2. In order to record the MyoD-Luc2 expression in small colonies associated with the myofiber, start imaging 48 h after isolation.

3.5 Preparation of Muscle Biopsies for Bioluminescence Imaging

To follow the expression of MyoD-Luc2 in muscle stem cells that are exposed to their native environment, we established an ex vivo approach using muscle biopsies for live imaging. Muscle biopsies are isolated from the TA muscle of adult MyoD-Luc2 mice. Before starting, prepare isolation and cultivation medium (*see* Subheading 2.3.3).

1. Follow the instruction in Subheading 3.3, **step 1–13** for the isolation of the TA muscle.
2. Transfer the isolated TA muscle to an empty new dish.
3. To isolate fiber bundles, grasp the distal tendon of the TA with two tweezers and pull the muscle in a longitudinal direction to split it. Repeat this step until myofiber bundles have a size of 3–5 mm (*see* **Note 17**).
4. Transfer muscle pieces into a chamber of an ibidi silicon insert (#80209) placed in a glass bottom dish and coated with collagen (*see* Subheading 3.3; **step 18**). Fill the chamber with D-luciferin containing cultivation medium (Fig. 5m).
5. Place the glass bottom dish on the microscope stage. Use a 10× objective and brightfield settings to focus on the muscle fiber bundles. Start acquisition of the bioluminescence signal and brightfield images as described in Subheading 3.1.

4 Notes

1. Use forceps and scissors to remove muscle from the bones. Avoid broken bones as this will lead to the release of bone marrow stem cells that would have to be removed during sorting, which would increase sorting time.
2. If the volume of the muscle tissue exceeds 5 mL, divide the slurry into two 15 cm tubes to ensure efficient enzymatic digestion.
3. Trituration can be difficult in the beginning. Remove clogged material (e.g., parts of tendons) from the pipette tip with tweezers and discard.
4. All the following steps are performed at room temperature to reduce collagenase activity.
5. The centrifugation steps at 500 rpm remove debris.
6. The EDTA in the staining buffer blocks Dispase™ II and collagenase activities.
7. CD31 marks endothelial, CD45 hematopoietic, and Ly6A/E (Sca1) bone marrow stem cells.

8. The settings for the isolation of muscle stem cells by FACS must be set up with the help of experienced staff. Controls needed are unstained cells, cells only stained with PE-antibodies, and cells only stained with goat anti-mouse VCAM-1/Alexa647 donkey anti-goat.
9. Viable cells attach during this period. Test after 30 min whether they are spreading. If not, wait for another 10–20 min.
10. The presence of the medium in the glass dish prevents the evaporation of the medium from the insert.
11. Do not overstretch the EDL, as this damages myofibers.
12. After 60 min, the EDL muscles are swollen indicating successful digestion.
13. Prepare two 5% BSA-coated 6-well culture dishes under sterile conditions.
    (a) Rinse wells with 2 mL of 5% BSA in 1× DPBS solution per well.
    (b) Add 2 mL of fiber dissection medium without collagenase to three wells of the first 6-well culture dish.
    (c) Add 2 mL of fiber cultivation medium to three wells of the second 6-well dish.
    (d) Incubate the culture dishes at 37 °C and 5% CO_2.
14. After a few trituration steps, individual, long myofibers and larger muscle pieces become visible under the stereomicroscope (Fig. 5h).
15. Continuing the trituration in a second well prevents damage to already released fibers.
16. After incubation, undamaged fibers are elongated and can be distinguished from short-damaged fibers.
17. Avoid cutting the TA with scissors, which results in fiber damage and contraction of the damaged fibers.

Acknowledgments

I.L. and C.B. thank all members of the laboratory who contributed know-how to these protocols, especially Elena Vasyutina, Dominique Bröhl, Tatiana Zyrianova, Joscha Griger, and Yao Zhang. We thank Thomas Müller for helpful discussions of the timelapse image analysis and a critical reading of the manuscript. Grants: Helmholtz society, Deutsche Forschungsgemeinschaft (DFG, FOR 2841 and ANR/DFG), and the French Muscular Dystrophy Association (AFM-Téléthon).

References

1. Mauro A (1961) Satellite cell of skeletal muscle fibers. J Biophys Biochem Cytol 9:493–495
2. Seale P, Sabourin LA, Girgis-Gabardo A et al (2000) Pax7 is required for the specification of myogenic satellite cells. Cell 102:777–786
3. Relaix F, Rocancourt D, Mansouri A et al (2005) A Pax3/Pax7-dependent population of skeletal muscle progenitor cells. Nature 435:948–953
4. Lepper C, Partridge TA, Fan CM (2011) An absolute requirement for Pax7-positive satellite cells in acute injury-induced skeletal muscle regeneration. Development 138:3639–3646
5. Murphy MM, Lawson JA, Mathew SJ et al (2011) Satellite cells, connective tissue fibroblasts and their interactions are crucial for muscle regeneration. Development 138:3625–3637
6. Sambasivan R, Yao R, Kissenpfennig A et al (2011) Pax7-expressing satellite cells are indispensable for adult skeletal muscle regeneration. Development 138:3647–3656
7. Bentzinger CF, Wang YX, Rudnicki MA (2012) Building muscle: molecular regulation of myogenesis, vol 4. Cold Spring Harb Perspect Biol, p a008342
8. Zammit PS (2017) Function of the myogenic regulatory factors Myf5, MyoD, Myogenin and MRF4 in skeletal muscle, satellite cells and regenerative myogenesis. Semin Cell Dev Biol 72:19–32
9. Smith CK, Janney MJ, Allen RE (1994) Temporal expression of myogenic regulatory genes during activation, proliferation, and differentiation of rat skeletal-muscle satellite cells. J Cell Physiol 159:379–385
10. Cooper RN, Tajbakhsh S, Mouly V et al (1999) In vivo satellite cell activation via Myf5 and MyoD in regenerating mouse skeletal muscle. J Cell Sci 112:2895–2901
11. Dhawan J, Rando TA (2005) Stem cells in postnatal myogenesis: molecular mechanisms of satellite cell quiescence, activation and replenishment. Trends Cell Biol 15:666–673
12. Zammit PS, Golding JP, Nagata Y (2004) Muscle satellite cells adopt divergent fates: a mechanism for self-renewal? J Cell Biol 166:347–357
13. Collins CA, Olsen I, Zammit PS et al (2005) Stem cell function, self-renewal, and behavioral heterogeneity of cells from the adult muscle satellite cell niche. Cell 122:289–301
14. Schuster-Gossler K, Cordes R, Gossler A (2007) Premature myogenic differentiation and depletion of progenitor cells cause severe muscle hypotrophy in Delta1 mutants. Proc Natl Acad Sci U S A 104:537–542
15. Vasyutina E, Lenhard DC, Wende H (2007) RBP-J (Rbpsuh) is essential to maintain muscle progenitor cells and to generate satellite cells. Proc Natl Acad Sci U S A 104:4443–4448
16. Bjornson CR, Cheung TH, Liu L et al (2012) Notch signaling is necessary to maintain quiescence in adult muscle stem cells. Stem Cells 30:232–242
17. Bröhl D, Vasyutina E, Czajkowski MT et al (2012) Colonization of the satellite cell niche by skeletal muscle progenitor cells depends on Notch signals. Dev Cell 23:469–481
18. Mourikis P, Gopalakrishnan S, Sambasivan R et al (2012a) Cell-autonomous Notch activity maintains the temporal specification potential of skeletal muscle stem cells. Development 139:4536–4548
19. Czajkowski MT, Rassek C, Lenhard DC et al (2014) Divergent and conserved roles of Dll1 signaling in development of craniofacial and trunk muscle. Dev Biol 395:307–316
20. Kopan R, Nye JS, Weintraub H (1994) The intracellular domain of mouse Notch: a constitutively activated repressor of myogenesis directed at the basic helix-loop-helix region of MyoD. Development 120:2385–2396
21. Shawber C, Nofziger D, Hsieh JJ et al (1996) Notch signaling inhibits muscle cell differentiation through a CBF1-independent pathway. Development 122:3765–3773
22. Kuroda K, Tani S, Tamura K et al (1999) Delta-induced Notch signaling mediated by RBP-J inhibits MyoD expression and myogenesis. J Biol Chem 274:7238–7244
23. Delfini MC, Hirsinger E, Pourquie O et al (2000) Delta 1-activated notch inhibits muscle differentiation without affecting Myf5 and Pax3 expression in chick limb myogenesis. Development 127:5213–5224
24. Hirsinger E, Malapert P, Dubrulle J (2001) Notch signalling acts in postmitotic avian myogenic cells to control MyoD activation. Development 128:107–116
25. Conboy IM, Rando TA (2002) The regulation of Notch signaling controls satellite cell activation and cell fate determination in postnatal myogenesis. Dev Cell 3:397–409

26. Mourikis P, Sambasivan R, Castel D et al (2012b) A critical requirement for notch signaling in maintenance of the quiescent skeletal muscle stem cell state. Stem Cells 30:243–252
27. Hirata H, Yoshiura S, Ohtsuka T (2002) Oscillatory expression of the bHLH factor Hes1 regulated by a negative feedback loop. Science 298:840–843
28. Jensen MH, Sneppen K, Tiana G (2003) Sustained oscillations and time delays in gene expression of protein Hes1. FEBS Lett 541: 176–177
29. Umbhauer M, Boucaut JC, Shi DL (2001) Repression of XMyoD expression and myogenesis by Xhairy-1 in Xenopus early embryo. Mech Dev 109:61–68
30. Shen H, McElhinny AS, Cao Y (2006) The Notch coactivator, MAML1, functions as a novel coactivator for MEF2C-mediated transcription and is required for normal myogenesis. Genes Dev 20:675–688
31. Kondoh K, Sunadome K, Nishida E (2007) Notch signaling suppresses p38 MAPK activity via induction of MKP-1 in myogenesis. J Biol Chem 282:3058–3065
32. Buas MF, Kadesch T (2010) Regulation of skeletal myogenesis by Notch. Exp Cell Res 316:3028–3033
33. Fukada S, Yamaguchi M, Kokubo H et al (2011) Hesr1 and Hesr3 are essential to generate undifferentiated quiescent satellite cells and to maintain satellite cell numbers. Development 138:4609–4619
34. Lahmann I, Bröhl D, Zyrianova T, Isomura A et al (2019) Oscillations of MyoD and Hes1 proteins regulate the maintenance of activated muscle stem cells. Genes Dev 33(9–10): 524–535
35. Palmeirim I, Henrique D, Ish-Horowicz D et al (1997) Avian hairy gene expression identifies a molecular clock linked to vertebrate segmentation and somitogenesis. Cell 91: 639–648
36. Shimojo H, Ohtsuka T, Kageyama R (2008) Oscillations in notch signaling regulate maintenance of neural progenitors. Neuron 58:52–64
37. Ubezio B, Blanco RA, Geudens I (2016) Synchronization of endothelial Dll4-Notch dynamics switch blood vessels from branching to expansion. elife 5:e12167
38. Seymour PA, Collin CA, Egeskov-Madsen AR et al (2020) Jag1 modulates an oscillatory Dll1-notch-Hes1 signaling module to coordinate growth and fate of pancreatic progenitors. Dev Cell 52:731–747 e738
39. Adams ST Jr, Miller SC (2014) Beyond D-luciferin: expanding the scope of bioluminescence imaging in vivo. Curr Opin Chem Biol 21:112–120
40. Kaskova ZM, Tsarkova AS, Yampolsky IV (2016) 1001 lights: luciferins, luciferases, their mechanisms of action and applications in chemical analysis, biology and medicine. Chem Soc Rev 45:6048–6077
41. Carlton PM, Boulanger J, Kervrann C et al (2010) Fast live simultaneous multiwavelength four-dimensional optical microscopy. Proc Natl Acad Sci U S A 107:16016–16022
42. Magidson V, Khodjakov A (2013) Circumventing photodamage in live-cell microscopy. Methods Cell Biol 114:545–560
43. Wefers B, Bashir S, Rossius J et al (2017) Gene editing in mouse zygotes using the CRISPR/Cas9 system. Methods 121–122:55–67
44. Schindelin J, Arganda-Carreras I, Frise E et al (2012) Fiji: an open-source platform for biological-image analysis. Nat Methods 9: 676–682
45. Imayoshi I, Isomura A, Harima Y (2013) Oscillatory control of factors determining multipotency and fate in mouse neural progenitors. Science 342:1203–1208
46. Springer ML, Rando TA, Blau HM (2002) Gene delivery to muscle. Curr Protoc Hum Genet Chapter 13:Unit13.4
47. Savitzsky A, Golay MJE (1964) Smoothing and differentiation of data by simplified least squares procedures. Anal Chem 36:1627–1639
48. Kuang S, Kuroda K, Le Grand F et al (2007) Asymmetric self-renewal and commitment of satellite stem cells in muscle. Cell 129:999–1010
49. Collins CA, Zammit PS (2009) Isolation and grafting of single muscle fibres. Methods Mol Biol (Clifton, NJ) 482:319–330

Chapter 20

In Vivo Modeling of Skeletal Muscle Diseases Using the CRISPR/Cas9 System in Rats

Katsuyuki Nakamura, Takao Tanaka, and Keitaro Yamanouchi

Abstract

The CRISPR/Cas9 system is a powerful gene editing tool that can be used to modify a target gene in almost all species. It unlocks the possibility of generating knockout or knock-in genes in laboratory animals other than mice. The Dystrophin gene is implicated in human Duchenne muscular dystrophy; however, Dystrophin gene mutant mice do not show severe muscle degenerating phenotypes when compared to humans. On the other hand, Dystrophin gene mutant rats made with the CRISPR/Cas9 system show more severe phenotypes than those seen in mice. The phenotypes seen in dystrophin mutant rats are more representative of the features of human DMD. This implies that rats are better models of human skeletal muscle diseases than mice. In this chapter, we present a detailed protocol for the generation of gene-modified rats by microinjection into embryos using the CRISPR/Cas9 system.

Key words CRISPR/Cas9, Genome editing, Gene-modified rats, Duchenne muscular dystrophy

1 Introduction

For a long time, genetic manipulation in laboratory animals has served as a powerful tool for understanding the molecular mechanism of human diseases and developing therapeutic options for these diseases. Mice have been widely used for this purpose because of the relative ease in manipulating their genome. However, mice models of human diseases are sometimes limited in their ability to mimic the severity of human diseases. An example is seen in the case of Duchenne muscular dystrophy (DMD), a severe muscle degeneration disease caused by a mutation in the *Dmd* gene [1]. Its model mice, called mdx mice, have the same mutation of the dystrophin gene in humans [2]; however, the phenotypes of mdx mice are much milder than those of human patients. Since mdx mice do not show progressive myofiber degeneration, severe fibrosis, and adipose infiltration, preclinical data from mdx mice is limited in its application to human clinical studies aimed at developing therapeutic options for DMD.

Atsushi Asakura (ed.), *Skeletal Muscle Stem Cells: Methods and Protocols*, Methods in Molecular Biology, vol. 2640,
https://doi.org/10.1007/978-1-0716-3036-5_20,

The CRISPR/Cas9 system was developed as a method to edit target gene/genes [3, 4]. This system takes advantage of our ability to manipulate the immune system of bacteria. This breakthrough theoretically allows us to manipulate the genome of all known species, including humans.

Previously, we showed that using the CRISPR/Cas9 system to knock out the *Dmd* gene in rats mimicked the pathology of DMD better than *Dmd* KO mice. In addition, *Dmd* KO rats exhibit severe phenotypes like constitutive degeneration, fibrosis, and fat accumulation in muscle [5]. Another group generated *Dmd* mutant rats using a gene editing technology called TALEN; the severity of their phenotypes was comparable to those seen in our previous results [6]. This indicates the usefulness of rats as a suitable background for modeling human skeletal muscle diseases.

Here, we highlighted a method of generating gene-modified rats using the CRISPR/Cas9 system. Obtaining gene-modified rats with this technique is quick and highly efficient. Gene-modified rats serve as a powerful tool for deepening our understanding of disease mechanisms in severe pathological conditions. Gene-modified rats also hasten the process of developing therapeutic options for human muscle diseases.

2 Materials

2.1 CRISPR/Cas9 Reagents

1. Source of Cas9: Cas9 mRNA (e.g., CAS9MRA, Sigma, or house-made) or Cas9 protein (Fasmac, Japan).
2. Source of Cas9: Single guide (sg) RNA (Fasmac, Japan).
3. In vitro transcription: Cas9 vector (48,625, Addgene).
4. In vitro transcription: mMESSAGE mMACHINE™ T3 Transcription Kit (AM13148, Thermo Fisher Scientific).
5. In vitro transcription: UltraPure™ DNase/RNase-Free Distilled Water (10,977,015, Thermo Fisher scientific).
6. In vitro transcription: HiFi DNA assembly kit (NEB).
7. In vitro transcription: Gibson assembly kit (NEB).

2.2 Embryo Collection

1. Sexually matured (over 8-week-old) or immature (4- to 5-week-old) female rats (Wistar-Imamichi, the Institute for Animal Production, Japan).
2. Pregnant mare serum gonadotropin (PMSG).
3. Human chorionic gonadotropin (hCG).
4. Glass capillary (G-100, Narishige, Japan).
5. Hyaluronidase.

6. Polyvinylpyrrolidone.
7. Saline.
8. M2 medium.
9. M16 medium.
10. 27 G needle.
11. Hotplate.
12. 3.5 cm dish.
13. Paraffin liquid (cell culture grade).

2.3 Injection of Cas9/sgRNA into Embryos

1. VacuTip I, holding capillary (Eppendorf) or house-made holding capillary.
2. Microscope (IX-70, Olympus, Japan).
3. Puller (Narishige or Sutter).
4. Injection capillary (prepared with puller).
5. Micromanipulator (MO-202 U, Narishige, Japan).
6. Microinjector (IM-11-2, Narishige, Japan).
7. Microforge (MF-900, Narishige, Japan).
8. Anti-vibration table (SBP-2, Narishige, Japan).
9. 6 cm dish.
10. Microloader™ Tip (930,001,007, Eppendorf, Germany).
11. Microscope (IX-70, Olympus, Japan).

2.4 Transfer of Embryos to Pseudo-Pregnant Rats

1. Pseudo-pregnant rats (Wistar-Imamichi, the Institute for Animal Production, Japan).
2. Microscissors.
3. Glass capillary.
4. Anesthesia (Isoflurane or the mixture of Xylazine, Diazepam, and butorphanol).
5. Forceps.
6. Small clamps (e. Cat: 18051–35, F.S.T).

2.5 Genotype PCR

1. 50 mM NaOH.
2. 1 M Tris-HCl pH 8.0.
3. KOD FX or KOD FX neo (Toyobo, Japan).
4. Oligo DNA Primers (Fasmac, Japan).
5. Microchip Electrophoresis System for DNA/RNA Analysis (MultiNA, Shimadzu, Japan).

3 Methods

3.1 Tips for Designing sgRNAs and Homologous Recombination Vector

1. There are many useful tools for designing sgRNAs on the web (e.g., ATUM sgRNA designer: https://www.atum.bio/eCommerce/cas9/input). If there is a preference for a specific target location, the target region of sgRNAs can be manually selected by searching for the "G(N)20GG" sequence in the target gene locus.
2. The homologous recombination vector is designed by using the NEBuilder Assembly Tool (http://nebuilder.neb.com/#!/). For the following vector construction, PCRs are conducted with the PrimeSTAR MAX, and purified PCR products are assembled with the NEB HiFi DNA assembly kit or the Gibson assembly kit according to the manufacturer's protocol.
3. All the sgRNAs, HR vector, and Cas9 mRNA and/or protein are dissolved in ultra-pure water. The concentration range of each component is as follows:

   sgRNAs: 10–50 ng/μL.

   Cas9 mRNA 10–50 ng/μL.

   Cas9 protein 50–100 ng/μL.

   HR vector: 10 ng/μL.

3.2 Preparation of the Embryos from Female Rats

1. Sexually immature female rats (4- to 5-week-old) are intraperitoneally injected with 25 IU PMSG. Forty-eight hours after PMSG injection, rats are injected with hCG and then housed for mating with a male rat of proven fertility. Sexually mature female rats can also be used for the collection of embryos. The estrous cycle is monitored by vaginal smear, and female rats at the pro-estrous stage are cohabitated with male rats of proven fertility (*see* **Note 1**).
2. Prepare a 3.5 cm dish by applying a drop of saline containing 0.1% PVP and 0.1% hyaluronidase and several drops of M2 medium. Cover the drops with enough paraffin liquid to avoid evaporation of these drops.
3. The day after mating, sacrifice female rats and transfer their oviducts to the 3.5 cm dish. Remove fat and uterine tissues surrounding the oviducts rapidly but carefully so as not to disturb the ampulla of the uterine tube. Using the 27 G needle, puncture the ampulla of the uterine tube and lead its contents, embryos and cumulus cells, into the hyaluronidase-containing drop.
4. Incubate on a hot plate at 37 °C for 5 min, then wash the hyaluronidase and the cumulus cells surrounding the embryos by transferring the embryos to fresh M2 medium via a glass capillary, repeat at least two to three times (*see* **Note 2**).
5. Wash the embryos with M16 medium and incubate them in a CO_2 incubator for approximately 1 h before using in the following injection step.

3.3 Microinjection of Cas9 and sgRNAs into the Embryos

1. Prepare a 6 cm dish by applying several drops of 30–50 μL M2 medium and cover these drops with paraffin liquid.
2. Load Cas9/sgRNA mixture into the injection capillary using a Microloader™ tip and set the injection and holding capillaries to the manipulator.
3. After washing the embryos with an M2 medium, transfer the embryos to the M16 medium in the 6 cm dish. Remove unfertilized embryos before using them for the injection.
4. Under a microscope, inject Cas9/sgRNA mixture into the embryos with a micromanipulator (*see* **Note 3**, Fig. 1).
5. After injection, wash the embryos with the M16 medium several times and incubate them in the M16 medium in a CO_2 incubator for approximately 1 h to recover them.

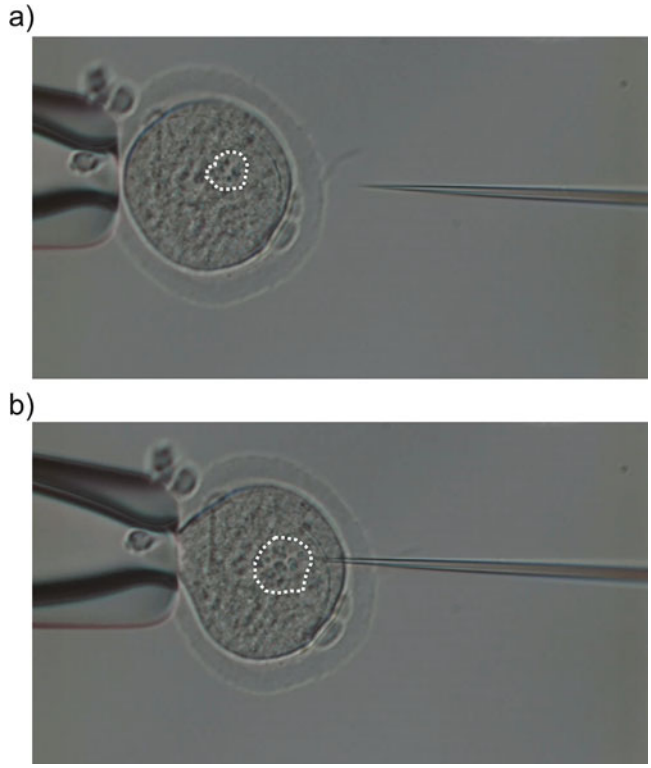

Fig. 1 Pronuclear microinjection of Cas9, gRNA, and plasmid mixture into rat embryo. (**a**) Before injecting the mixture into the pronucleus of the rat embryo, it is necessary to clearly visualize the pronucleus. This can be achieved by maneuvering the location of the holding pipette. The dotted line indicates the pronucleus of the rat embryo. (**b**) After pronuclear microinjection of the RNA and DNA mixture. The pronucleus was expanded and made transparent as indicated by a broken line in the photo

3.4 Transfer of Embryos into Pseudo-Pregnant Rats

1. Anesthetize the pseudo-pregnant rats, antisepticize, and make an incision at the abdominal part just above an ovary.
2. Take an ovary out of the body and fix the location of the ovary by using a small clamp to clamp the fat tissue surrounding the ovary. Under the microscope, adjust the angle of the oviducts by changing the location of the ovary (Fig. 2a).
3. Load embryos into glass capillary with minimum M2 medium. Put an air bubble before and after the M2 medium containing the embryos. Air bubbles can be used for checking whether embryo transfer from the glass capillary was successful.

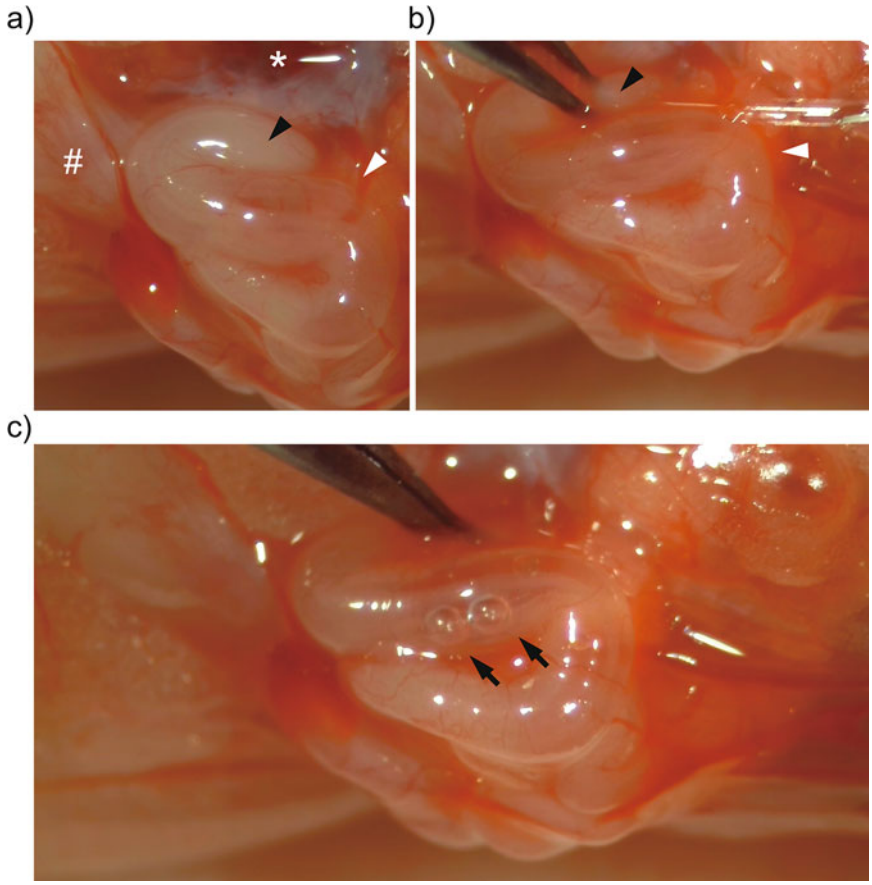

Fig. 2 Transfer of the microinjected embryos into the rat ampulla of the uterine tube. (**a**) A photo of the rat oviduct after adjusting the angle of the oviduct. The black arrowhead indicates the position on the oviduct at which the incision should be made for embryo transfer. The white arrowhead indicates the ampulla of the uterine tube. The position labeled * is the ovary while the position labeled # is uterine. (**b**) A photo of the rat oviduct during embryo transfer. The black arrowhead indicates the position where a glass pipette is being inserted into the oviduct. (**c**) A photo of the rat oviduct after embryo transfer. Black arrowheads indicate air bubbles in the oviduct after a successful embryo transfer

a)

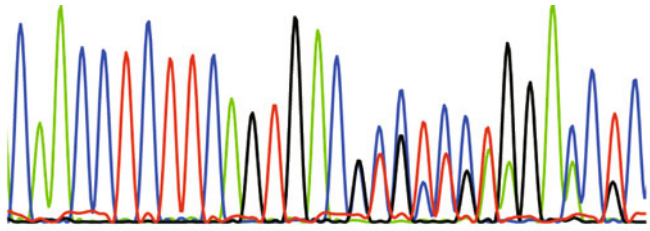

b)

```
CAACCTCTTTCAGTGACCTGCCCTGGACCTC
                GCCTTGAAGAACGC
```

c)

```
CAACCTCTTTCAGTGACCTGCAGGATGGGAA Reference
CAACCTCTTTCAGTGACCTGCCCTGGACCTC
          GCCTTGAAGAACGC

WT      CAACCTCTTCAGTGACCTGCAGGATGGGAAACGCCTCCTGGACCTC
```

d)

```
Refference ATGGGAAACGCCTCCTGGACCTC
CAACCTCTTTCAGTGACCTGCCCTGGACCTC
          GCCTTGAAGAACGC
```

e)

```
WT      CAACCTCTTCAGTGACCTGCAGGATGGGAAACGCCTCCTGGACCTC
#1      CAACCTCTTCAGTGAC----------------GCCTCCTGGACCTC -16 bp
#2      CAACCTCTTCAGTGACCTGC----TGAAGAACGCCTCCTGGACCTC -4 bp (3bp mutation)
```

f)

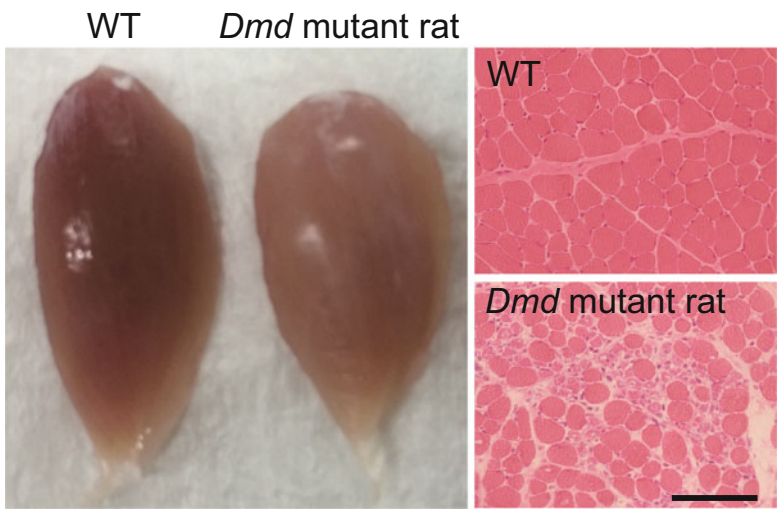

Fig. 3 Manual analysis of the sequencing data. (**a**) Overlapping of two different spectrums of rat *Dmd* gene locus targeted by CRISPR/Cas9. (**b**) Sequence from the spectrum data. The black bar indicates the initiation site of overlap. When there are two different spectrums in a locus, record two different bases as written in the figure. When there is only one spectrum even after overlap, record the same two bases. (**c**) Comparison of the sequence before the start of overlap with the reference sequence. Bases underscored with black lines are the same in the reference sequence. Once you find the same bases referenced in your data, circle the bases not

4. Under the microscope, make an incision right after the ampulla of the uterine tube with microscissors. Insert the glass pipette and transfer the embryos into the oviducts through the incision (*see* **Note 4**, Fig. 2b). If you can see air bubbles in the oviducts, the embryos sandwiched between them should be in there (Fig. 2c).
5. Suture the abdominal wound after putting antibiotics (e.g., Penicillin) into the scar. Repeat **steps 4–5** to the other side.

3.5 Genotyping and Confirmation of Mutation Pattern in F0 Pups

1. After spontaneous delivery, collect tissues from F0 pups into a 1.5 mL tube for genotype PCR.
2. Add 180 μL of 50 mM NaOH into each sample and incubate at 95 °C for at least 10 min.
3. Add 20 μL of 1 M Tris-HCl pH 8.0 to neutralize the samples for PCR.
4. Use 1 μL of these samples for genotype PCR.
5. After PCR, load PCR samples to the Microchip Electrophoresis System for DNA/RNA Analysis to see the different sizes of PCR products shifted by mutation; or purify the samples and confirm their mutation pattern through Sanger sequencing. The overlapped spectrum obtained from Sanger sequencing can be analyzed through CRISP-ID [7] or manually (Fig. 3).

4 Notes

1. The ratio of male to female rats can significantly affect the success rate of mating. For optimal results, one male rat should be mated with one or two female rats.
2. Depending on the strain of the rats used for the collection of the embryos, the cumulus cells may be difficult to wash out (e.g., Wistar rats). The embryos from Wistar-Imamichi rats are easy to wash in this step.

Fig. 3 (continued) found in the reference. In this figure, "GCCT" was not found in the reference. Then try to find these "GCCT" in the reference sequence. (**d**) If you can find the same sequence as "GCCT" in the reference, check the sequence of the reference after "GCCT" to see whether the following sequence is included in the overlapped sequence. Bases underscored with red lines are the set of one of the mutation alleles. The remaining bases are another allele and are underscored with black lines as well as in Fig. 3c. (**e**) Alignment results of mutation alleles analyzed through the steps above. The WT allele is used as the reference. (**f**) Typical images of tibialis anterior muscle (TA) in *Dmd* mutant rats. Left panel: TA of WT and male *Dmd* mutant rat. Right panel: Hematoxylin and eosin staining of TA in WT and *Dmd* mutant rat. Scale bar = 100 μm. This figure is made from the figures of ref. 5 with some modifications [5]

3. For the generation of KO rats, inject Cas9 and sgRNA mixture into the cytosol of embryos. For KI rats, inject them into the pronucleus to avoid the cell toxicity of plasmids in the cytosol.
4. We usually transfer about ten embryos into each oviduct. For a knock-in experiment, increase this number to 15–20 per oviduct to increase the number of the pups since DNA injection into the embryos is toxic and can decrease the number of the pups.

Acknowledgments

We would like to thank Priscilla Ajilore, Georgetown University, School of Medicine, for her advice in preparing this manuscript.

References

1. Hoffman EP, Brown RH Jr, Kunkel LM (1987) Dystrophin: the protein product of the Duchenne muscular dystrophy locus. Cell 51:919–928
2. Partridge TA (2013) The mdx mouse model as a surrogate for Duchenne muscular dystrophy. FEBS J 280:4177–4186
3. Mali P, Yang L, Esvelt KM et al (2013) RNA-guided human genome engineering via Cas9. Science 339:823–826
4. Cong L, Ran FA, Cox D et al (2013) Multiplex genome engineering using CRISPR/Cas systems. Science 339:819–823
5. Nakamura K, Fujii W, Tsuboi M et al (2014) Generation of muscular dystrophy model rats with a CRISPR/Cas system. Sci Rep 6:28973
6. Larcher T, Lafoux A, Tesson L et al (2014) Characterization of dystrophin deficient rats: a new model for Duchenne muscular dystrophy. PLoS One 9(10):e110371
7. Dehairs J, Talebi A, Cherifi Y et al (2016) CRISP-ID: decoding CRISPR mediated indels by Sanger sequencing. Sci Rep 4:5635–5656

Chapter 21

In Vivo Investigation of Gene Function in Muscle Stem Cells by CRISPR/Cas9-Mediated Genome Editing

Liangqiang He, Zhiming He, Yuying Li, Hao Sun, and Huating Wang

Abstract

Skeletal muscle satellite cells (SCs) are adult stem cells responsible for muscle development and injury-induced muscle regeneration. Functional elucidation of intrinsic regulatory factors governing SC activity is constrained partially by the technological limitations in editing SCs in vivo. Although the power of CRISPR/Cas9 in genome manipulation has been widely documented, its application in endogenous SCs remains largely untested. Our recent study generates a muscle-specific genome editing system leveraging the Cre-dependent Cas9 knockin mice and AAV9-mediated sgRNAs delivery, which allows gene disruption in SCs in vivo. Here, we illustrate the step-by-step procedure for achieving efficient editing using the above system.

Key words CRISPR/Cas9, Adeno-associated virus, sgRNA, Muscle satellite cell, Genome editing

1 Introduction

Skeletal muscle is built up by numerous multinucleated myofibers and presents excellent regenerative potential after damage, which is executed by adult muscle stem cells also called satellite cells (SCs) [1]. Juvenile SCs characterized by paired-box gene 7 (Pax7) expression emerge about 2 days before birth in mice and undergo myogenesis to form muscle components in the postnatal stage [2]. In adult muscles, SCs are in a dormant stage beneath the basal lamina. Upon injury, the quiescent SCs (QSCs) are rapidly activated and re-enter the cycle to generate the proliferating myoblasts, a large portion of which further differentiate to form new muscle fibers and fuse to repair the damage [1]. Meanwhile, a subset of activated SCs return to the quiescent stage to replenish the stem cell pool [2]. It is important to illuminate key factors regulating each phase of the SC lineage progression. The late stages of SC proliferation

Supplementary Information The online version contains supplementary material available at https://doi.org/10.1007/978-1-0716-3036-5_21.

Atsushi Asakura (ed.), *Skeletal Muscle Stem Cells: Methods and Protocols*, Methods in Molecular Biology, vol. 2640, https://doi.org/10.1007/978-1-0716-3036-5_21,

and differentiation are relatively well studied; however, investigation of the early phases of quiescence and early activation has been hindered by the lack of efficient tools to manipulate SCs in their quiescent niche in vivo. It is time- and labor-consuming to generate the traditional genetically manipulated mice that rely on transgenesis or gene targeting in embryonic stem cells [3]. And this shortcoming would be exacerbated when simultaneous disruption of multiple genes is required. Therefore, a facile platform that allows rapid gene inactivation in endogenous SCs is needed.

The clustered regularly interspaced short palindromic repeats (CRISPR)/CRISPR-associated 9 (Cas9) is a widely used tool for genome editing [4]. By directing of a single guide RNA (sgRNA), Cas9 cuts DNA at a specific site to produce a double-strand break (DSB). Based on whether a template is provided, the DSB can be repaired in two ways: the homology-directed repair (HDR) pathway, which is precise, and the error-prone non-homologous end joining (NHEJ) pathway [4, 5]. The NHEJ-mediated DSB repair results in random deletion or insertion (indel) at the cleavage site, which is leveraged to deplete target gene expression if the indel occurs in the coding region.

In vivo application of CRISPR/Cas9 is emerging to generate mouse models and correct genetic diseases by viral or non-viral-based Cas9/sgRNA delivery. In skeletal muscle tissue, recently it has been applied to treat Duchenne muscular dystrophy (DMD) [6–8], an X-chromosome-linked neuromuscular disorder caused by the mutation of the dystrophin gene, by employing adeno-associated virus (AAV) mediated Cas9/sgRNA delivery to delete the mutated exon generating a truncated dystrophin protein which demonstrates partial function in the mdx mouse model of DMD. Normally co-transduction of multiple AAV vectors is required to deliver the Cas9 and sgRNAs separately due to the restricted packaging capacity of the AAV virus (~4.7 kb) [6, 7], which however limits the modification efficiency since successful editing only occurs in nuclei simultaneously receiving all the components. To solve this problem, our recently generated CRISPR/Cas9/AAV9-sgRNA platform is designed to disrupt target gene expression in endogenous SCs by leveraging a muscle-specific Cas9 knockin mouse line and AAV9-mediated sgRNAs delivery [9]. We have demonstrated the high efficiency of this system to introduce mutagenesis at the target locus in juvenile SCs at the postnatal stage and applied it to investigate the regulators coordinating SC functions, including protein-coding genes [9] and lincRNA [10]. It allows the manipulation of SC genomes in situ without requiring cell isolation or culture, thereby making it possible to study the impact on SC quiescence, homeostasis in their native niche, and early activation upon damage. Indeed, we recently applied to screen for functional transcription factor (TF) regulators modulating SC early activation and successfully demonstrated that Myc plays a key role in

promoting SC early activation [9]. The entire procedure from sgRNA selection to phenotypic dissection only takes several weeks, which will accelerate the pace at which gene function and pathways can be interrogated in endogenous SCs.

Here, we introduce the step-by-step procedure of how to edit protein-coding genes in endogenous SCs at postnatal stage by applying dual-sgRNA strategy, which can also be applied to manipulate non-coding regions. Four main sections are included: sgRNA selection; construction and in vitro validation of AAV9-dual sgRNA vector; AAV9 virus production, purification, and titration; and in vivo AAV9 virus administration and SC isolation.

2 Materials

2.1 Plasmid Construction

1. PCR-grade water.
2. Oligonucleotides for sgRNAs and necessary primers (BGI).
3. pSpCas9(BB)-2A-GFP (pX458, Addgene, 48,138).
4. AAV: ITR-U6-sgRNA (backbone)-pCBh-Cre-WPRE-hGHpA-ITR (Addgene, 60,229).
5. Bbs I.
6. Age I.
7. EcoR I.
8. Sap I.
9. Xba I.
10. Kpn I.
11. T4 polynucleotide kinase.
12. T4 Ligase.
13. Phusion High-Fidelity PCR Master Mix (New England BioLabs, M0531S).
14. Agarose.
15. DH5α *E. coli*.
16. Ampicillin sodium salt.
17. LB Broth (Miller).
18. LB Broth with agar (Miller).
19. NucleoSpin Plasmid kit (Macherey-Nagel, 740588.250).
20. NucleoSpin Gel and PCR Clean-up kit (Macherey-Nagel, 740609.250).
21. 14 mL Polystyrene round-bottom tube.
22. 1.5 mL microcentrifuge tube.
23. 200 μL PCR tube.

24. Thermocycler (Bio-Rad, C1000).
25. Nanodrop 2000 (Thermo Scientific).
26. Microcentrifuge.
27. ALLIANCETM Q9-ADVANCED™ (Uvitec, 154,112,001).
28. Mini dry incubator.
29. Shaker incubator.
30. Gel electrophoresis system: PowerPac basic power supply (Bio-Rad, 1,645,050); Sub-Cell GT System gel tray (Bio-Rad, 1,704,401).

2.2 Testing Editing Efficiency Using SURVEYOR Nuclease Assay

1. C2C12 cell line (ATCC, CRL-1772).
2. DMEM.
3. Penicillin-Streptomycin.
4. FBS.
5. DMEM growth medium: DMEM with 10% FBS, 100 units/mL Penicillin-Streptomycin.
6. Lipofectamine 3000 Transfection Reagent (Invitrogen, L3000–015).
7. Trypsin-EDTA.
8. PBS.
9. QuickExtract DNA Extraction Solution (Epicentre, QE09050).
10. 10 × Taq PCR buffer.
11. SURVEYOR Mutation Detection Kits (Integrated DNA Technologies, 706,020).
12. 6 well plate.
13. FACSAria Fusion Cell Sorter (BD).

2.3 AAV9 Virus Production, Purification, and Titration

1. HEK293FT cell line (Life Technologies, R700–07).
2. pHelper (Addgene, 112,867).
3. AAV9 serotype plasmid (Addgene, 112,865).
4. Polyethylenimine.
5. $MgCl_2$.
6. Benzonase.
7. Chloroform.
8. Dnase I, Amplification Grade.
9. SYBR Green PCR Master Mix (New England BioLabs, M3003E).
10. Proteinase K.
11. AAV lysis buffer: 50 mM Tris-HCl, pH 8.0; 150 mM NaCl.

12. 5× PEG/NaCl solution: 40% PEG 8000 (w/v); 2.5 M NaCl.
13. Hard-Shell 384-Well PCR Plate (Bio-Rad, HSR4801).
14. 15 mL tube.
15. 50 mL tube.
16. T75 flask.
17. 0.45 μm sterile filter.
18. 0.22 μm sterile filter.
19. Amicon Ultra centrifugal filter unit (Sigma, Z648043-24EA).
20. LightCycler 480 Instrument II (Roche, 05015243001).
21. High-Speed Centrifuge (Eppendorf, 5810R).
22. Water bath.
23. 4 °C cold room.
24. Liquid nitrogen.

2.4 AAV9 Virus Administration

1. Saline.
2. $Pax7^{Cre}$ mice (The Jackson Laboratory, 010530).
3. B6;129-Gt(ROSA)26Sor$^{tm1(CAG-cas9*-EGFP)Fezh/J}$ mice (The Jackson Laboratory, 024857).
4. BD Insulin Syringe with the BD Ultra-Fine™ Needle 0.5 mL (BD, 320312).

3 Methods

3.1 sgRNA Selection

3.1.1 sgRNA Design

Selection of sgRNA with high efficiency is essential for the successful editing of endogenous SCs. To achieve high editing efficiency, we harness dual-sgRNA strategy which would induce indels and deletions simultaneously [11]. Several online tools are available to predict site-specific sgRNAs. Here, we recommend the web tool Crispor (http://crispor.tefor.net/) [12] following the general standards listed below:

1. To minimize off-target effects, only sgRNAs with a score higher than 5 should be selected since higher scores are correlated with lower off-target probability. Similarly, if other online tools are used, higher scores are preferred.
2. Ideally, the cutting sites of the two sgRNAs should locate upstream of the CDS region of the target gene, and the expected deletion fragment by the two sgRNAs should be larger than 100 bp. From our experience, short distance tends to decrease the editing efficiency possibly because of the spatial hindrance that limits Cas9/sgRNA function. We recommend a distance of 200 ~ 300 bp between the two sgRNA sites.

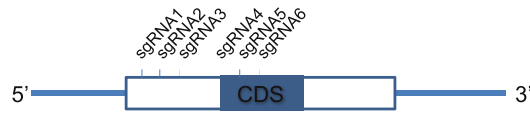

Fig. 1 Schematic illustration of the design of dual sgRNAs targeting the coding region of a target gene. Three upstream sgRNAs (sgRNA 1–3) and three downstream ones (sgRNA 4–6) are designed

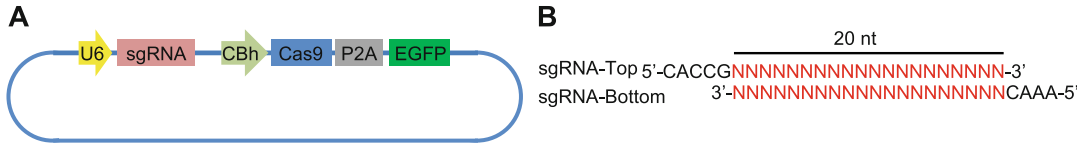

Fig. 2 Construction of the pX458-sgRNA vector. (**a**) Schematic illustration of the pX458-EGFP vector. (**b**) Illustration of the sgRNA oligonucleotides containing overhangs for Bbs I enzyme

Table 1
Digestion of pX458-GFP plasmid

Components	Amount (μL)
pX458 (4 ug)	X
Bbs I	1
10 × NEB buffer	4
ddH_2O	to 40 μL
Total	40

3. Usually six sgRNAs should be designed for each gene (three for upstream and three for downstream). As shown in Fig. 1, one sgRNA from the upstream (sgRNA1-sgRNA3) and one sgRNA from the downstream (sgRNA4-sgRNA6) will be selected.

3.1.2 Testing the Editing Efficiency Using SURVEYOR Nuclease Assay

For sgRNA selection, the editing efficiency of each sgRNA should be tested in vitro first in C2C12 myoblasts using a Cas9-EGFP expressing vector (pX458, Fig. 2a) using an adopted protocol [13].

1. *sgRNA oligonucleotides ordering.* Order the predicted sgRNA oligonucleotides from above with overhangs (Fig. 2b) for ligation into the pX458 vector digested by Bbs I.
2. *Digestion of pX458-GFP plasmid using Bbs I.*
   1) Prepare the reaction mix in a 200 μL PCR tube as follows (Table 1):
   2) Incubate in a thermocycler at 37 °C overnight.

Table 2
Phosphorylating of the sgRNA oligonucleotides

Components	Amount (μL)
sgRNA top	1
sgRNA bottom	1
10 × T4 ligation buffer	1
T4 PNK	1
ddH_2O	6
Total	10

Table 3
Ligation reaction for the pX458-sgRNA vector

Components	Amount (μL)
pX458 (20 ng, digested by BbsI)	X
sgRNA duplex	2
T4 ligase	1
10 × T4 ligation buffer	1
ddH_2O	to 10 μL
Total	10

3) Run the mixture on a 1% (wt/vol) agarose gel and extract the digested products by using the NucleoSpin Gel and PCR Clean-up kit.
4) Calculate the concentration of the extracted DNA.

3. *Phosphorylating and annealing of the sgRNA oligonucleotides.*
   1) Dissolve the top and bottom strands of oligonucleotides for each sgRNA to a final concentration of 100 μM.
   2) Prepare the reaction mix as follows (Table 2; *see* **Note 1**):
   3) Incubate in a thermocycler by using the following parameters: 37 °C for 30 min; 95 °C for 5 min; ramp down to 25 °C at 5 °C/min.
4. *Construction of the pX458-sgRNA vector.*
   1) Dilute the phosphorylated and annealed oligos at a ratio of 1:200 by adding 1 μL of oligo to 199 μL of ddH2O.
   2) Prepare the ligation mix as follows (Table 3):
   3) Incubate in a thermocycler at 16 °C overnight.

4) Transform the ligation product to a competent *E. coli* strain such as DH5α.

5) Plate the transformed competent cells onto an LB plate containing 100 μg/mL ampicillin and incubate overnight at 37 °C.

6) Pick 2–3 clones and inoculate them in 3 mL of LB-ampicillin broth.

7) Culture the clones at 37 °C overnight and isolate the plasmid DNA using the NucleoSpin Plasmid kit.

8) Sanger sequence the plasmid DNA using human U6 as the sequencing primer to confirm the correct insertion of sgRNA.

5. *Transfection of the pX458-sgRNA plasmid into C2C12 myoblasts.*

1) Plate the well-dissociated C2C12 myoblasts onto 6-well plates in DMEM growth medium 16–24 h before transfection until the cells reach 50–60% confluence (*see* **Note 2**).

2) Transiently transfect 2 ug of the seven pX458-sgRNA plasmids (three for upstream, three for downstream, and an empty pX458 vector without any sgRNA insertion as control) into the C2C12 cells using Lipofectamine 3000 according to the manufacturers' instructions (*see* **Note 3**).

3) Sort out GFP-positive cells using FACS 24 h after transfection (*see* **Note 4**).

4) Seed the above isolated cells onto 6-well plates and culture them in DMEM growth medium for another 2 days (*see* **Note 5**).

5) Harvest the cells using trypsin-EDTA and wash them one time using PBS.

6) Extract genomic DNAs from the harvested cells using QuickExtract solution according to the manufacturers' instructions.

6. *Evaluate the editing efficiency using SURVEYOR nuclease assay.*

The indel formation induced by CRISPR/Cas9 can be evaluated by the SURVEYOR nuclease assay. Specific primers need to be designed to amplify the region of interest from genomic DNAs. The primers can be designed manually or by an online tool like Crispor.

1) Set up the SURVEYOR PCR system as described below (Table 4; *see* **Note 6**):

2) Run the reaction in a thermocycler with no more than 30 cycles.

Table 4
SURVEYOR PCR reaction

Components	Amount (μL)
2 × Phusion buffer	25
Surveyor-F primer (10 μM)	1
Surveyor-R primer (10 μM)	1
DNA template (~100 ng)	X
ddH_2O	To 50 μL
Total	50

Table 5
Annealing reaction

Components	Amount (μL)
10 × Taq PCR buffer	2
PCR products (20 ng/μL)	18
Total	20

3) Run 2–5 μL of the PCR products on a 1% (wt/vol) agarose gel to confirm the specificity of the PCR products.
4) Purify the PCR products with the NucleoSpin Gel and PCR Clean-up kit and normalize the eluted product to 20 ng/μL.
5) Set up the annealing reaction as follows (Table 5; *see* **Note 7**):
6) Anneal the reaction in a thermocycler by using the following conditions:

Cycle number	Condition
1	95 °C, 10 min
2	95–85 °C, −2 °C/s
3	85 °C, 1 min
4	85–75 °C, −0.3 °C/s
5	75 °C, 1 min
6	75–65 °C, −0.3 °C/s
7	65 °C, 1 min
8	65–55 °C, −0.3 °C/s
9	55 °C, 1 min

(continued)

Cycle number	Condition
10	55–45 °C, −0.3 °C/s
11	45 °C, 1 min
12	45–35 °C, −0.3 °C/s
13	35 °C, 1 min
14	35–25 °C, −0.3 °C/s
15	25 °C, 1 min
16	25–4 °C, −0.3 °C/s
17	4 °C, hold

Table 6
SURVEYOR nuclease assay

Components	Amount (μL)
Annealed heteroduplex	20
$MgcCl_2$ stock solution from the kit (0.15 M)	2.5
ddH_2O	0.5
SURVEYOR nuclease S	1
SURVEYOR enhancer S	1
Total	25

7) Add the following components from the SURVEYOR kit on ice (Table 6):
8) Mix the reaction thoroughly and incubate in a thermocycler at 42 °C for 30 min.
9) Visualize the SURVEYOR product by running a 2% (wt/vol) agarose gel.
10) Image the gel by using a quantitative imaging system without overexposing the bands. We use high-end imaging software provided by the ALLIANCETM Q9-ADVANCED Imager.
11) Quantify the total intensity of the undigested and cleaved PCR bands by gel quantification software. We use Image J for the quantification.
12) Calculate the percentage of the cleavage rate of the PCR product (f_{cut}) by using the following formula [13]: $f_{\mathrm{cut}} = (b+c)/(a+b+c)$, where a is the integrated intensity of the undigested PCR products and b and c are the integrated intensity of each cleavage product.

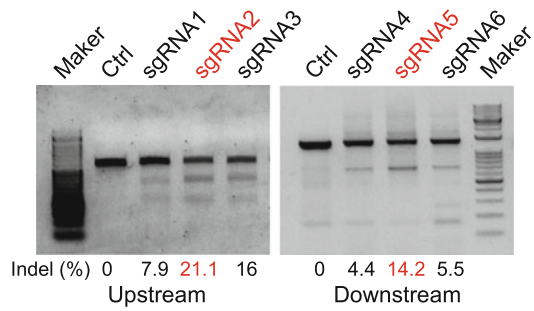

Fig. 3 Agarose gel image showing the result of SURVEYOR nuclease assay on *Sugt1* locus. The percentage of indel formation is shown at the bottom. SgRNAs with the highest indel frequency are highlighted in red

13) Estimate the indel occurrence for each sgRNA using the following formula:

$$\text{indel}\ (\%) = 100 \times \left(1 - \sqrt{(1 - f_{\text{cut}})}\right)$$

14) Compare the indel occurrence for each sgRNA and select the one with the highest editing efficiency for up and downstream, respectively (*see* **Note 8**). For example, in a study where we tested sgRNAs targeting Sugt1, suppressor of the G2 allele of SKP1 (*S. cerevisiae*) [14] gene, the cleavage efficiency of each of the six sgRNAs was examined by SURVEYOR assay as described above. SgRNA2 (21.1%) and sgRNA5 (14.2%) demonstrated the highest editing efficiency upstream and downstream, respectively, and were thus chosen for further application (Fig. 3).

3.2 Construction and in Vitro Validation of AAV9-Dual sgRNA Vector

After selection, the next step is cloning the selected sgRNAs to the AAV9 transfer vector. Since previous study indicates that expressing two sgRNAs from a single vector displays higher cleavage potential compared to sgRNAs from two separate vectors [15], we choose AAV9-dual sgRNA vector for packaging of sgRNA expressing virus (Fig. 4). This AAV9 vector also carries a fluorescent DsRed gene controlled by a CBh promoter to facilitate the evaluation of transduction efficiency (*see* **Note 9**).

3.2.1 Construction of AAV9-Dual sgRNA Backbone

1. *Generation of the AAV9-sgRNA vector.*

   The AAV: ITR-U6-sgRNA (backbone)-pCBh-Cre-WPRE-hGHpA-ITR (AAV-Cre) is used as donor plasmid. Coding sequencing for DsRed is PCR-amplified from a DsRed-containing plasmid and cloned into the donor plasmid by replacing the sequence encoding Cre using Age I and EcoR I sites. The sequences of PCR primers to amplify DsRed is shown in Table S1.

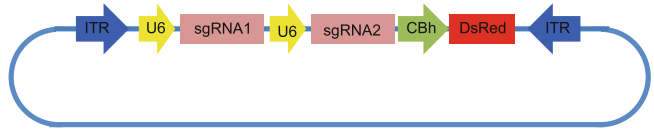

Fig. 4 Schematic illustration of the pAAV9-sgRNA vector used for dual sgRNAs expression

Table 7
Amplification of DsRed by PCR

Components	Amount (μL)
2 × Phusion buffer	25
DsRed-F primer (10 μM)	1
DsRed-R primer (10 μM)	1
DsRed containing vector (100 ng)	X
ddH_2O	to 50 μL
Total	50

1) Set up the PCR system as follows (Table 7):
2) Perform the RCR with the following conditions:

Cycle step	Temperature	Time	Cycle
Initial denaturation	98 °C	3 min	1
Denaturation Annealing Extension	98 °C 60 °C 72 °C	30 s 30 s 30 s	35
Final extension	72 °C	5 min	1
Holding	4 °C	∞	

3) Purify the PCR products with the NucleoSpin Gel and PCR Clean-up kit.
4) Digest the DsRed DNA and AAV-Cre vector by Age I/EcoR I as follows (Table 8):
5) Incubate the reaction in a thermocycler at 37 °C overnight.
6) Run the mixture on a 1% (wt/vol) agarose gel and extract the digested products by using the NucleoSpin Gel and PCR Clean-up kit.
7) Calculate the concentration of the extracted DNA.
8) Prepare the ligation mix as follows (Table 9):

Table 8
Digestion of the DsRed DNA and AAV-Cre vector

Components	Amount (ul)
DsRed DNA (200 ng) or AAV-cre vector (1 μg)	X
Age I	1
EcoR I	1
10 × NEB buffer	4
ddH_2O	to 40 μL
Total	40

Table 9
Ligation reaction of the AAV-Cre vector and DsRed

Components	Amount (ul)
Digested AAV-Cre vector	X (50 ng)
Digest DsRed DNA	Y (1:3 vector to insert molar ratio)
T4 ligase	1
10 × T4 ligation buffer	1
ddH_2O	to 10 μL
Total	10

9) Incubate in a thermocycler at 16 °C overnight.
10) Transform the ligation product to a competent *E. coli* strain such as DH5α.
11) Plate the transformed competent cells onto an LB plate containing 100 μg/mL ampicillin and incubate it overnight at 37 °C.
12) Pick 2–3 clones and inoculate them in 3 mL of LB-ampicillin broth.
13) Culture the clones at 37 °C overnight and isolate the plasmid DNA using the NucleoSpin Plasmid kit.
14) Validate the insertion of DsRed by Sanger sequencing using WRPE-R as the sequencing primer.

2. *Generation of the AAV9-single sgRNA transfer vector.*
The first selected sgRNA from the upstream is cloned into the AAV9-sgRNA vector using the Sap I site.

1) Order single-stranded sgRNA oligonucleotides with overhangs as shown in Fig. 5.

Fig. 5 Illustration of the sgRNA oligonucleotides containing overhangs for Sap I enzyme

Table 10
Phosphorylating of the sgRNA oligonucleotides

Components	Amount (ul)
sgRNA top	1
sgRNA bottom	1
10 × T4 ligation buffer	1
T4 PNK	1
ddH_2O	6
Total	10

Table 11
Digestion of the AAV-sgRNA vector

Components	Amount (μL)
AAV-sgRNA (4 ug)	X
Sap I	1
10 × NEB buffer	4
ddH_2O	to 40 μL
Total	40

2) Dissolve the top and bottom strands of the upstream sgRNA to a final concentration of 100 μM.
3) Prepare the annealing reaction mix as follows (Table 10):
4) Incubate in a thermocycler by using the following parameters: 37 °C for 30 min; 95 °C for 5 min; ramp down to 25 °C at 5 °C/min.
5) Dilute the phosphorylated and annealed oligos at a ratio of 1:200 by adding 1 μL of oligo to 199 μL of ddH_2O.
6) Digest the AAV-sgRNA vector by Sap I as follows (Table 11):
7) Incubate in a thermocycler at 37 °C overnight.

Table 12
Ligation reaction for the AAV9-single sgRNA transfer vector

Components	Amount (μL)
AAV-sgRNA (20 ng, digested by Sap I)	X
sgRNA duplex	2
T4 ligase	1
10 × T4 ligation buffer	1
ddH_2O	To 10 μL
Total	10

8) Run the mixture on a 1% (wt/vol) agarose gel and extract the digested products by using the NucleoSpin Gel and PCR Clean-up kit.
9) Calculate the concentration of the extracted DNA.
10) Prepare the ligation mix as follows (Table 12):
11) Incubate in a thermocycler at 16 °C overnight.
12) Transform the ligation product to a competent *E. coli* strain such as DH5α.
13) Plate the transformed competent cells onto an LB plate containing 100 μg/mL ampicillin and incubate it overnight at 37 °C.
14) Pick 2–3 clones and inoculate them in 3 mL of LB-ampicillin broth.
15) Culture the clones at 37 °C overnight and isolate the plasmid DNA using the NucleoSpin Plasmid kit.
16) Send the plasmid DNA for Sanger sequencing using human U6 as the sequencing primer to confirm the correct insertion of sgRNA.

3. *Generation of the AAV9-dual sgRNA transfer vector.*
To generate the AAV-dual sgRNA transfer vector, the second sgRNA selected from the downstream is constructed into the AAV9-single sgRNA vector together with the gRNA cassette and U6 promoter using Xba I and Kpn I sites. The pX458-sgRNA vector containing the second sgRNA is then used as a template to PCR amplify the U6-sgRNA. For the control vector, we normally use the AAV-dual sgRNA backbone without any sgRNA insertion and its construction process is the same as described below. The PCR primer sequence to amplify the U6-sgRNA is shown in Table S1.
1) Set up the PCR system as follows (Table 13):

Table 13
PCR reaction for U6-sgRNA

Components	Amount (μL)
2 × Phusion buffer	25
U6-sgRNA-F primer (10 μM)	1
U6-sgRNA-R primer (10 μM)	1
pX458-sgRNA (containing the second sgRNA, 100 ng)	X
ddH_2O	to 50 μL
Total	50

2) Perform the RCR with the following conditions:

Cycle step	Temperature	Time	Cycle
Initial denaturation	98 °C	3 min	1
Denaturation Annealing Extension	98 °C 60 °C 72 °C	30 s 30 s 30 s	35
Final extension	72 °C	5 min	1
Holding	4 °C	∞	

3) Purify the PCR products with the NucleoSpin Gel and PCR Clean-up kit.
4) Digest the U6-sgRNA DNA and AAV-single sgRNA vector by Xba I/Kpn I as follows (Table 14):
5) Incubate the reaction in a thermocycler at 37 °C overnight.
6) Run the mixture on a 1% (wt/vol) agarose gel and extract the digested products by using the NucleoSpin Gel and PCR Clean-up kit.
7) Calculate the concentration of the extracted DNA.
8) Prepare the ligation mix as follows (Table 15):
9) Incubate in a thermocycler at 16 °C overnight.
10) Transform the ligation product to a competent *E. coli* strain such as DH5α.
11) Plate the transformed competent cells onto an LB plate containing 100 μg/mL ampicillin and incubate it overnight at 37 °C.
12) Pick 2–3 clones and inoculate them in 3 mL of LB-ampicillin broth.

Table 14
Digestion of the U6-sgRNA DNA and AAV-single sgRNA vector

Components	Amount (μL)
U6-sgRNA DNA (200 ng) or AAV-single sgRNA vector (1 μg)	X
Xba I	1
Kpn I	1
10 × NEB buffer	4
ddH_2O	to 40 μL
Total	40

Table 15
Ligation reaction of the AAV-single sgRNA vector and U6-sgRNA DNA

Components	Amount (μL)
Digested AAV-single sgRNA vector	X (50 ng)
Digest U6-sgRNA DNA	Y (1:3 vector to insert molar ratio)
T4 ligase	1
10 × T4 ligation buffer	1
ddH_2O	to 10 μL
Total	10

13) Culture the clones at 37 °C overnight and isolate the plasmid DNA using the NucleoSpin Plasmid kit.
14) Validate the insertion of U6-sgRNA by Xba I/Kpn I double-digestion as follows (Table 16):
15) Incubate the reaction in a thermocycler at 37 °C for 2 h.
16) Run the mixture on a 1% (wt/vol) agarose gel. Plasmid with successful insertion should release a digested band.

3.2.2 In Vitro Validation of the AAV9-Dual sgRNA Vector

Before AAV9 packaging, it is necessary to test the deletion efficiency of the AAV9-dual sgRNA vector in C2C12 cells. Since the vector does not express Cas9, a Cas9-expressing vector (pX458) needs to be co-transfected. For the control group, the AAV9-dual sgRNA backbone without any sgRNA insertion is used.

1. Plate the well-dissociated C2C12 myoblasts onto 6-well plates in DMEM growth medium 16–24 h before transfection until the cells reach 50–60% confluence.
2. Transiently transfect AAV9-dual sgRNA and pX458 (1:1) plasmids into C2C12 cells using Lipofectamine 3000.

Table 16
Validation of Xba I/Kpn I double-digestion for AAV-dual sgRNA vector

Components	Amount (μL)
AAV-dual sgRNA vector (1 ug)	X
Xba I	1
Kpn I	1
10 × NEB buffer	2
ddH_2O	to 20 μL

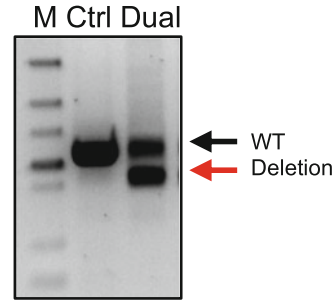

Fig. 6 Agarose gel image showing the PCR validation of the deletion efficiency of the AAV-dual sgRNA vector. The WT and deleted PCR products are indicated by blank and red arrowheads, respectively

3. Sort out GFP and DsRed double positive cells using FACS 24 h after transfection.
4. Seed the isolated cells onto 6-well plates and culture them in DMEM growth medium for another 2 days.
5. Harvest the cells using trypsin-EDTA and wash them one time using PBS.
6. Extract genomic DNA from the harvest cells using QuickExtract solution according to the manufacturers' instructions.
7. Use PCR to validate the editing efficiency with primers, which cover the cutting region of the two sgRNAs. Efficient editing will cause the appearance of a smaller PCR band (Fig. 6).

3.3 AAV9 Virus Production, Purification, and Titration

AAV9 virus is produced in HEK293FT cells by the triple transfection method [16, 17]. Polyethylenimine (PEI) is used as the transfection reagent.

3.3.1 AAV9 Virus Production and Purification

1. Seed HEK293FT cells onto T75 flask in DMEM growth medium and do transfection when the confluence reaches 80–90%. Normally we transfect cells on 4 × T75 flasks to produce enough AAV9-dual sgRNA virus.

Table 17
Transfection for the AAV9 virus production

Components	Amount
pHelper	10 ug
AAV9 serotype plasmid	5 ug
AAV9-dual sgRNA vector	5 ug
Serum-free DMEM medium	1 mL
PEI (1 mg/mL)	80 μL

2. Change the medium to 9 mL antibiotic-free medium (DMEM with 10% FBS) before transfection.
3. Set up the transfection mix in a 1.5 mL microcentrifuge tube as follows (Table 17):
4. Mix the mixture briefly and sit at room temperature for 20 min.
5. Add the transfection mix to the T75 flask of 293FT cells and briefly swirl the flask to distribute throughout the medium.
6. Twenty-four hours after transfection, change the medium to a normal DMEM growth medium (20 mL for each flask).
7. After another 48 h, harvest the cells by using trypsin-EDTA. Pellet the cells by centrifugation at 2000 rpm for 10 min at 4 °C (*see* **Note 10**).
8. Discard the supernatant and wash the cell pellet with sterile PBS one time. Pellet the cells by centrifugation at 2000 rpm for 10 min at 4 °C.
9. Re-suspend the cell pellet with AAV lysis buffer (1 mL for 1 × T75 flask).
10. Freeze-thaw cell pellets three times in liquid nitrogen and 37 °C water bath to release the virus into the supernatant. Vortex the cell pellets between the freeze-thaw cycles.
11. Add $MgCl_2$ (final concertation is 1.6 mmol/l, add 6.4 μL 1 M $MgCl_2$ for 4 mL AAV lysis buffer) to the mixture together with Benzonase (final concertation is 50 U/mL).
12. Mix the mixture thoroughly and incubate at 37 °C water bath for 0.5 ~ 1 h to digest the DNA contaminants.
13. Centrifuge the mixture at 3000 g, 4 °C for 10 min.
14. Filter the supernatant with a 0.45 μm sterile filter and transfer it to a new 15 mL tube.
15. Measure the volume of the supernatant and add 1/4 volume of 5× PEG/NaCl solution.

16. Mix the mixture thoroughly and incubate at 4 °C overnight.
17. Spin the mixture at 4000 g, 4 °C, for 30–45 min.
18. Discard the supernatant and re-suspend the pellet with l mL PBS for every T75 flask.
19. Centrifuge the mixture at 3000 g, 4 °C for 10 min.
20. Transfer the supernatant to a new 15 mL tube and add another l mL PBS for every T75 flask to re-suspend the pellet one more time.
21. Centrifuge the mixture at 3000 g, 4 °C for 10 min and combine the supernatant.
22. Measure the volume of the total supernatant and add an equal volume of chloroform.
23. Vigorously vortex the mixture for 2 min and centrifuge at 1000 g for 5 min at room temperature.
24. Transfer the top layer (AAV-containing supernatant) to a new tube and discard the bottom layer (chloroform).
25. Place the supernatant at room temperature for 30 min to evaporate the remaining chloroform.
26. Filter the supernatant with a 0.22 μm sterile filter and transfer it to a 100 kDa Amicon Ultra centrifugal filter unit.
27. Centrifuge at 3000 g, 4 °C until the volume is <1.5 mL.
28. Add another 4 mL PBS to the 100 kDa Amicon Ultra centrifugal filter unit and re-suspend the virus.
29. Centrifuge again and repeat the wash process three times. Leave about 500 μL liquid for the last wash.
30. Re-suspend the solution inside a 100 kDa Amicon Ultra centrifugal filter unit and transfer the solution to a new 1.5 mL tube.
31. Wash the Amicon Ultra centrifugal filter unit with another 200 μL PBS and mix the virus.
32. Split the virus to about 300 μL for each 1.5 mL tube (*see* **Note 11**).
33. Use 10 μL of the virus to a 200 μL PCR tube for concentration qualification.
34. Store the AAV9 virus at −80 °C.

3.3.2 AAV9 Virus Titration

The titer of the AAV9 virus is determined by quantitative PCR using primers targeting the CBh promoter.

1. Add 50 U of DNase I to the 10 μL of the AAV9 virus solution and incubate in a thermocycler at 37 °C for 1 h to remove residual plasmid DNA.
2. Inactivate the DNase I at 65 °C for 10 min.

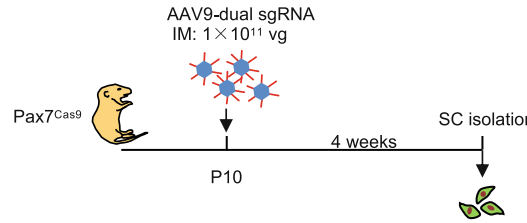

Fig. 7 Schematic illustration of the design for in vivo editing of SCs using Cas9/AAV9-sgRNA system

3. Add proteinase K (0.4 U) to the mixture and incubate at 50 °C for 1 h to release vector DNA from the AAV9 virus.
4. Inactivate the proteinase K at 95 °C for 20 min and the final mixture can be used for concentration qualification.
5. Quantify the viral DNA by qRT-PCR targeting the CBh promoter region (*see* **Note 12**).

3.4 AAV9 Virus Administration and Satellite Cell (SC) Isolation

To inactivate target gene expression endogenously in SCs, the muscle-specific Cas9 knockin line ($Pax7^{Cas9}$) is used [9] following the scheme shown in Fig. 7.

1. Generate the $Pax7^{Cas9}$ mouse by crossing homozygous $Pax7^{Cre}$ mouse with the Cre-dependent $Rosa26^{Cas9\text{-}EGFP}$ knockin (B6;129-Gt (ROSA)$26Sor^{tm1(CAG\text{-}cas9*\text{-}EGFP)Fezh/J}$) mouse (*see* **Note 13**).
2. Dilute the AAV9-dual sgRNA virus in saline and intramuscularly (IM) inject 50–100 μL of the virus (1×10^{11} vg/mouse) (*see* **Note 14**) into the skeletal muscles of $Pax7^{Cas9}$ at postnatal day 10 (P10) (*see* **Note 15**) using an Ultra-Fine needle (0.5 mL, 29G). For the control group, the same dose and volume of AAV-dual sgRNA virus without any sgRNA insertion is injected.
3. Isolate SCs according to published protocol [18] by FACS based on GFP expression 4 weeks after injection (*see* **Note 16**).
4. Collect 50,000 freshly isolated SCs and extract the genomic DNAs using QuickExtract solution according to the manufacturers' instructions.
5. Use PCR to validate the editing efficiency with primers encompassing the cutting region of the two sgRNAs. A smaller PCR band together with a smear is usually an indicator of efficient editing (*see* **Note 17**) (Fig. 8). To confirm the cutting, other methods including Western blot or qRT-PCR (*see* **Note 18**) to validate the loss of the target protein or mRNA can be used; alternatively, deep sequencing of the target locus can be applied to further confirm the editing efficiency (*see* **Note 19**).

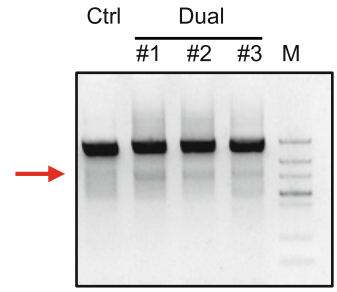

Fig. 8 Agarose gel image showing the PCR validation of the deletion efficiency of the AAV-dual sgRNA virus targeting the *Sugt1* locus. The arrow indicates the edited PCR product

4 Notes

1. The buffer used here is the T4 ligation buffer, not the T4 PNK buffer.
2. Transfections should be performed at the recommended cell confluence. A high density may induce spontaneous myoblast differentiation, which may confound the result.
3. Other transfection reagents such as Lipofectamine 2000 can also be used for transient transfection. But from our experience Lipofectamine 3000 will yield the best result.
4. To achieve optimal results, it is necessary to sort out cells with high GFP signal; The gating parameter used for each sample should be identical.
5. Prolonged culture time is not recommended, and DNAs should be extracted within 3 days after transfection. This is because the editing of some genes may alter cell proliferation rate, prolonged culture time may thus lead to enrichment or loss of the edited alleles, which will bias the result of SURVEYOR nuclear assay.
6. SURVEYOR nuclear assay relies on the detection of single-base mismatches; therefore, it is crucial to use a high-fidelity polymerase. Because SURVEYOR can detect naturally occurring single-nucleotide polymorphisms [13], it is important to run negative control using genomic DNAs extracted from C2C12 cells transfected with pX458 vector without any sgRNA insertion. SURVEYOR primers should be designed to amplify 200–400 bp on either side of the Cas9 target (for an amplicon of 400–800 bp long) to allow clear visualization of cleavage bands by gel electrophoresis. It is necessary to ensure each pair of candidate primers produces a single PCR product.
7. Other 10× PCR buffer can also be used.

8. It has been reported that the CRISPR/Cas9-mediated deletion via dual-sgRNAs tends to be precise ligation of the two predicted cutting sites [19], thereby, the predicted deletion should cause frameshift within the target gene.
9. From our experience, excessive DsRed expression may also influence SC homeostasis, it is thus essential to ensure the identical dosage of control and AAV9-dual sgRNA virus is administrated.
10. Since the AAV9-dual sgRNA vector expresses DsRed, the red color of the cell pellet can be used as an indicator of successful transfection.
11. Normally one freeze-thaw cycle causes a 10% loss of the AAV virus, therefore, aliquoting the virus right after the production is highly recommended for long-term storage.
12. Normally, the dual AAV9-sgRNA backbone containing no sgRNA is used as the standard. From our calculation, 0.695 ug plasmid contains 1×10^{11} copies. Use ddH_2O to dilute the plasmid and usually eight dilutions are needed (10^{10}–10^4). As the plasmid contains two strands and AAV9 only contains one DNA strand, a correction factor of 2 is used for the calculation of the AAV9 concentration. Other regions like ITR or DsRed can also be used for titration.
13. The heterozygous offspring is used for in vivo genome editing. Our recent findings show that Cas9 expression in the heterozygous $Pax7^{Cas9}$ mice has no obvious defect on muscle development and SC function [9] while homozygous Cas9 expression results in a significant decrease in SC number. Moreover, in some homozygous mice, Cas9 was found to be expressed in multiple tissues possibly because Pax7 was expressed in a rare subpopulation of spermatogonia of the mouse [20] thus induced Cas9 expression as early as in the zygote.
14. From our experience, AAV9 dosage to achieve efficient editing may depend on the locus. Normally, we use 1×10^{11} vg/mouse for the initial try. Injection of this dosage of AAV9-dual sgRNA virus results in a complete disruption of the MyoD expression but 5×10^{11} vg/mouse is needed for *Myc* locus [9].
15. P10 is chosen mainly because the skeletal muscles at this stage are large enough for IM injection. An early injection can be considered, which may lead to even higher editing efficiency.
16. From our experience, during the isolation of SCs from $Pax7^{Cas9}$ mice injected with AAV-dual sgRNA virus, differential expression of DsRed in SCs is not observed [9], which indicates 100% infection of all SCs. Thus, we normally isolate the GFP-positive population for the following analyses.

17. Since dual sgRNAs can cause deletions and indels at the same time, it is possible to observe a shifted deletion band and a smear around the WT band on gel. In this case, the editing efficiency is usually high enough to disrupt target gene expression even when the intensity of the deletion band is not high.
18. Sometimes, we observe a loss of protein level without alteration of mRNA level. It is known that CRISPR/Cas9-induced mRNA degradation is mediated by nonsense-mediated decay (NMD) of mRNA [21], thus weak efficiency of NMD in SCs may cause the discrepancy.
19. Deep sequencing is the most precise way to evaluate the editing efficiency as it will allow for sensitive detection and accurate quantification of the editing patterns mediated by dual sgRNAs including deletions and indels formed at both sites.

References

1. Dumont NA, Wang YX, Rudnicki MA (2015) Intrinsic and extrinsic mechanisms regulating satellite cell function. Development 142:1572–1581
2. Tajbakhsh S (2009) Skeletal muscle stem cells in developmental versus regenerative myogenesis. J Intern Med 266:372–389
3. Goldstein JM, Tabebordbar M, Zhu K et al (2019) In situ modification of tissue stem and progenitor cell genomes. Cell Rep 27:1254–1264 e7
4. Hsu PD, Lander ES, Zhang F (2014) Development and applications of CRISPR-Cas9 for genome engineering. Cell 157:1262–1278
5. Komor AC, Badran AH, Liu DR (2017) CRISPR-based technologies for the manipulation of eukaryotic genomes. Cell 168:20–36
6. Long C, Amoasii L, Mireault AA et al (2016) Postnatal genome editing partially restores dystrophin expression in a mouse model of muscular dystrophy. Science 351:400–403
7. Nelson CE, Hakim CH, Ousterout DG et al (2016) In vivo genome editing improves muscle function in a mouse model of Duchenne muscular dystrophy. Science 351:403–407
8. Nance ME, Shi R, Hakim CH et al (2019) AAV9 edits muscle stem cells in normal and dystrophic adult mice. Mol Ther 27:1568–1585
9. He L, Ding Y, Zhao Y et al (2021) CRISPR/Cas9/AAV9-mediated in vivo editing identifies MYC regulation of 3D genome in skeletal muscle stem cell. Stem Cell Reports 16:2442–2458
10. Zhao Y, Zhou J, He L et al (2019) MyoD induced enhancer RNA interacts with hnRNPL to activate target gene transcription during myogenic differentiation. Nat Commun 10:5787
11. Guo Y, VanDusen NJ, Zhang L et al (2017) Analysis of cardiac myocyte maturation using CASAAV, a platform for rapid dissection of cardiac myocyte gene function in vivo. Circ Res 120:1874–1888
12. Haeussler M, Schönig K, Eckert H (2016) Evaluation of off-target and on-target scoring algorithms and integration into the guide RNA selection tool CRISPOR. Genome Biol 17:148
13. Ran FA, Hsu PD, Wright J (2013) Genome engineering using the CRISPR-Cas9 system. Nat Protoc 8:2281–2308
14. Li Y, Yuan J, Chen F et al (2020) Long noncoding RNA SAM promotes myoblast proliferation through stabilizing Sugt1 and facilitating kinetochore assembly. Nat Commun 11:1–16
15. Zhu S, Li W, Liu J et al (2016) Genome-scale deletion screening of human long non-coding RNAs using a paired-guide RNA CRISPR–Cas9 library. Nat Biotechnol 34:1279–1286
16. Grieger JC, Choi VW, Samulski RJ (2006) Production and characterization of adeno-associated viral vectors. Nat Protoc 1:1412–1428
17. Kimura T, Ferran B, Tsukahara Y et al (2019) Production of adeno-associated virus vectors for in vitro and in vivo applications. Sci Rep 9:1–13
18. Liu L, Cheung TH, Charville G et al (2015) Isolation of skeletal muscle stem cells by fluorescence-activated cell sorting. Nat Protoc 10:1612–1624

19. Guo T, Feng YL, Xiao JJ et al (2018) Harnessing accurate non-homologous end joining for efficient precise deletion in CRISPR/Cas9-mediated genome editing. Genome Biol 19: 170
20. Aloisio GM, Nakada Y, Saatcioglu HD et al (2014) PAX7 expression defines germline stem cells in the adult testis. J Clin Invest 124:3929–3944
21. Smits AH, Ziebell F, Joberty G et al (2019) Biological plasticity rescues target activity in CRISPR knock outs. Nat Methods 16:1087–1093

Chapter 22

Exons 45–55 Skipping Using Antisense Oligonucleotides in Immortalized Human DMD Muscle Cells

Merry He and Toshifumi Yokota

Abstract

Antisense oligonucleotides (AOs) have demonstrated high potential as a therapy for treating genetic diseases like Duchene muscular dystrophy (DMD). As a synthetic nucleic acid, AOs can bind to a targeted messenger RNA (mRNA) and regulate splicing. AO-mediated exon skipping transforms out-of-frame mutations as seen in DMD into in-frame transcripts. This exon skipping approach results in the production of a shortened but still functional protein product as seen in the milder counterpart, Becker muscular dystrophy (BMD). Many potential AO drugs have advanced from laboratory experimentation to clinical trials with an increasing interest in this area. An accurate and efficient method for testing AO drug candidates in vitro, before implementation in clinical trials, is crucial to ensure proper assessment of efficacy. The type of cell model used to examine AO drugs in vitro establishes the foundation of the screening process and can significantly impact the results. Previous cell models used to screen for potential AO drug candidates, such as primary muscle cell lines, have limited proliferative and differentiation capacity, and express insufficient amounts of dystrophin. Recently developed immortalized DMD muscle cell lines effectively addressed this challenge allowing for the accurate measurement of exon-skipping efficacy and dystrophin protein production. This chapter presents a procedure used to assess DMD exons 45–55 skipping efficiency and dystrophin protein production in immortalized DMD patient-derived muscle cells. Exons 45–55 skipping in the DMD gene is potentially applicable to 47% of patients. In addition, naturally occurring exons 45–55 in-frame deletion mutation is associated with an asymptomatic or remarkably mild phenotype as compared to shorter in-frame deletions within this region. As such, exons 45–55 skipping is a promising therapeutic approach to treat a wider group of DMD patients. The method presented here allows for improved examination of potential AO drugs before implementation in clinical trials for DMD.

Key words Duchenne muscular dystrophy, Becker muscular dystrophy, Exon skipping, Antisense oligonucleotides, Primary muscle cells, Immortalized DMD patient-derived muscle cells, Cell models, Viltolarsen, Eteplirsen, Morpholinos

1 Introduction

Duchene muscular dystrophy (DMD) is an X-linked recessive genetic disorder caused by a mutation in the DMD gene [1]. As one of the most common and lethal inherited genetic disorders found in children, DMD affects around 1 in 3500–5000 newborn

Atsushi Asakura (ed.), *Skeletal Muscle Stem Cells: Methods and Protocols*, Methods in Molecular Biology, vol. 2640, https://doi.org/10.1007/978-1-0716-3036-5_22,

males. Muscle weakness is typically first observed at the age of 3–5, and progressive muscle degeneration results in most patients being confined to a wheelchair by the age of 11. Cardiac and respiratory complications as a result of muscle deterioration significantly reduces the average lifespan of patients to 30–40 years of age [2]. The DMD gene is the largest in the human genome and is composed of 79 exons that encode the dystrophin protein [3]. Dystrophin plays a critical role in connecting the internal muscle fiber cytoskeleton to the extracellular matrix through the muscle cell membrane. This linkage prevents membrane damage of muscle cells and is essential for proper muscle function. Without dystrophin, muscle fibers are easily injured under mechanical stress as seen during muscle contraction, which can lead to chronic muscle damage and fiber necrosis [4]. As a result, muscle fibers are replaced by fat and fibrotic tissue [5].

Mutations in the DMD gene lead to two different types of muscular dystrophies: DMD and BMD (Becker muscular dystrophy) [3]. In DMD patients, mutations in the DMD gene cause a shift in the open reading frame (ORF) of the messenger RNA (mRNA) resulting in no dystrophin expression and a severe phenotype [6]. Although several types of mutations in the DMD gene can cause DMD, nonsense and frameshift mutations typically result in DMD [7]. Within the mutational spectrum of DMD, out-of-frame deletion mutations involving one or more exons represent the majority of mutational events [8]. The less severe form, BMD, produces partially functional dystrophin that is reduced in size [3]. Unlike DMD, many BMD patients have slower disease progression and retain ambulation for a longer period of time [9]. Whether a mutation in the DMD gene will manifest into the DMD or BMD phenotype typically depends on modifications to the reading frame [10]. The milder BMD phenotype arises from a mutational event where exons retain the ORF of the spliced mRNA due to in-frame mutations and results in the expression of a shortened but semi-functional dystrophin protein product [6].

The emergence of antisense oligonucleotides (AOs) to induce exon skipping has drastically changed the field of nucleic acid therapy and provides a promising approach for treating DMD [11, 12]. AOs are synthetic single-stranded nucleic acids that can bind to a targeted region of the pre-messenger ribonucleic acid (pre-mRNA). Depending on the targeted disease and type of modification, AOs can be used to alter RNA function through different mechanisms including the reduction of certain toxic proteins to be expressed, modifying mutant proteins, or restoring the reading frame to rescue protein expression [12]. The exon skipping approach using AOs to restore the disrupted reading frame is particularly applicable to DMD patients [13]. As one of the most promising methods to treat DMD, exon skipping aims to alter the reading frame of dystrophin transcripts from out-of-frame to

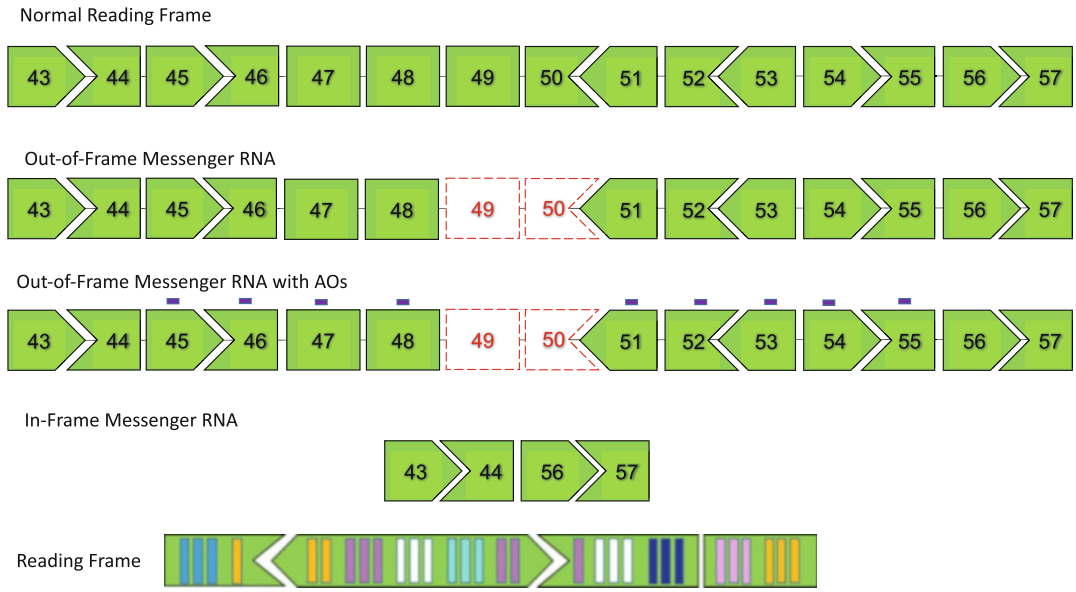

Fig. 1 Messenger RNA (mRNA) reading frame restoration by exon 45–55 skipping. The deletion of exons 49 and 50 (red dashed line boxes) results in an out-of-frame shift of the mRNA. Skipping exons 45–55 through the use of antisense oligonucleotides (AO, short purple lines) restores the reading frame

in-frame. This induces specifically mutated or frame-shifting exon (s) to be skipped and allows restoration of the reading frame (Fig. 1). In many cell and animal models of DMD, AO-mediated exon skipping efficiently corrected deletion, duplication, nonsense, and splice-site mutations [14–17]. In September 2016, the United States Food and Drug Administration (FDA) approved eteplirsen, an AO that induces exon 51 skipping to treat DMD [18]. However, a major drawback to single skipping of exon 51 is that it would be applicable to only ~13% of patients [19]. By contrast, multi-exon skipping of exons 45–55 could rescue up to ~63% of DMD patients that have deletion mutations [20]. Furthermore, it has been observed that a naturally occurring deletion mutation of exons 45–55 is associated with a milder to almost asymptomatic phenotype compared to shorter in-frame deletions within this mutational hotspot. Due to the applicability and promising outcomes demonstrated in preclinical studies, exon 45–55 skipping has gained great interest as a potential approach for treating a wider group of DMD patients [20–22].

Although the search for more efficacious AO drugs is currently being studied, a critical aspect during the selection process is the requirement for an effective procedure to ensure proper screening before entry into clinical trials [23]. In vitro studies to assess AO drug candidates are commonly conducted before examination in vivo. A fundamental aspect of AO drug screening in vitro is the need for a robust cell model that is capable of achieving both

consistent and reproducible results. In particular, evaluating AO drug candidates for DMD can be accomplished through quantifying exon skipping efficiency at the RNA level and dystrophin rescue at the protein level. However, past in vitro models, including primary muscle cells, have critical limitations such as limited proliferative capacity and produce insufficient amounts of dystrophin to be quantified [23, 24]. Previous studies in primary muscle cells typically use an additional step of polymerase chain reaction (PCR) to detect the exon-skipped products (nested PCR) [23]. However, this approach is not quantitative, likely overestimates exon skipping levels, and the results are often not reproducible. Also, difficulties with dystrophin quantification at the protein level due to insufficient differentiation capability limit the potential to effectively screen for AOs in this model. More recent studies have constructed cell models where a plasmid carrying the human DMD gene was transduced [25]. These artificial models are easy to maintain; however, due to the large size of the DMD gene, only selected exons were incorporated into the plasmid. In addition, most sequences of the introns are removed to minimize the size of the plasmid and as a result, exon skipping efficacy examined in vitro may not reflect the efficacy in vivo [23, 25]. Furthermore, dystrophin protein rescue cannot be examined in these models [23]. As an alternative approach, the MyoD-transduced fibroblast cell model was employed to overcome these challenges. In this transdifferentiated cell model, fibroblasts were converted to myotubes using a virus vector [26]. Although dystrophin protein expression was detected after 1 week of differentiation in canine cells, human cells required 2 weeks or more. While this model was demonstrated to be appropriate to study exon skipping efficacy and dystrophin protein restoration by Western blotting, it requires viral vector-mediated transdifferentiation, a labor-intensive and time-consuming process [23].

Here, we present a method to efficiently evaluate the effects of cocktail AO-mediated exons 45–55 skipping in DMD patient-derived immortalized cell lines. These cell lines, immortalized by transducing the murine cyclin-dependent kinase (cdk)-4 and human telomerase reverse transcriptase (hTERT), efficiently proliferate and differentiate into mature myotubes, which express a large amount of dystrophin after AO treatment [24]. Dystrophin protein production can be easily detected using Western blotting as compared to other DMD cell models [23]. The method presented here allows for a highly efficient and quantitative examination of potential AO drugs for DMD.

2 Materials

2.1 Immortalized Muscle Cell Culture

1. Immortalized DMD patient-derived muscle cells: Cells with different types of mutations can be available from the MRC Centre for Neuromuscular Diseases Biobank upon request.
2. Immortalized healthy muscle cells.
3. Growth medium: DMEM/F-12 basal medium (with L-glutamine and 15 mM HEPES) containing 50 U penicillin, 50 μg/mL streptomycin, 20% fetal bovine serum, and supplement mix for skeletal muscle cell growth medium (Promocell).
4. Differentiation medium: DMEM/F-12 basal medium (with L-glutamine and 15 mM HEPES) containing 50 U penicillin, 50 μg/mL streptomycin, 2% horse serum, and 1x ITS (Sigma).

2.2 Transfecting AOs

1. Endo-porter transfection reagent (Gene Tools).
2. 1 mM phosphorodiamidate morpholino oligomer (PMO) AOs stocks to be tested according to the outline published previously [27] (Gene Tools):

   Exon 45 PMO (Ex45_Ac9_30mer): GACAACAGTTTGCCG CTGCCCAATGCCATC.

   Exon 46 PMO (Ex46_Ac93_30mer): AGTTGCTGCTCTTT TCCAGGTTCAAGTGGG.

   Exon 47 PMO (Ex47_Ac13_30mer): GTTTGAGAATTCCC TGGCGCAGGGGCAACT.

   Exon 48 PMO (Ex48_Ac7_30mer): CAATTTCTCCTTGTT TCTCAGGTAAAGCTC.

   Exon 48 PMO (Ex48_Ac78_30mer): CAGATGATTTAACT GCTCTTCAAGGTCTTC.

   Exon 49 PMO (Ex49_Ac17_30mer): ATCTCTTCCACATC CGGTTGTTTAGCTTGA.

   Exon 50 PMO (Ex50_Ac19_30mer): GTAAACGGTTTACC GCCTTCCACTCAGAGC.

   Exon 51 PMO (Ex51_Ac0_30mer): GTGTCACCAGAGTAA CAGTCTGAGTAGGAG.

   Exon 52 PMO (Ex52_Ac24_30mer): GGTAATGAGTTCTT CCAACTGGGGACGCCT.

   Exon 53 PMO (Ex53_Ac26_30mer): CCTCCGGTTCTGAA GGTGTTCTTGTACTTC.

   Exon 54 PMO (Ex54_Ac42_30mer): GAGAAGTTTCAGGG CCAAGTCATTTGCCAC.

   Exon 55 PMO (Ex55_Ac0_30mer): TCTTCCAAAGCAGCC TCTCGCTCACTCACC

3. Type I-coated collagen well plates.

2.3 RT-PCR and Exon Skipping Analysis

1. Trizol reagent (Invitrogen).
2. Chloroform.
3. 100% isopropanol.
4. 20 mg/mL stock of RNA-grade glycogen (Invitrogen).
5. 75% ethanol.
6. RNase-free water.
7. SuperScript™ III One-Step RT-PCR system with Platinum™ *Taq* (Invitrogen).
8. DMD forward primer (Ex43/44_167-12_hDMD_F) [27]: GACAAGGGCGATTTGACAG.
9. DMD reverse primer (Ex56_135-154_hDMD_R): TCCGAAGTTCACTCCACTTG.
10. GAPDH forward primer (hGAPDH_662-81_Fwd1): TCCCTGAGCTGAACGGGAAG.
11. GAPDH reverse primer (hGAPDH_860-79_Rv1): GGAGGAGTGGGTGTCGCTGT.
12. 1–2% agarose gel
13. SYBR Safe DNA gel stain (Invitrogen).
14. Cooled centrifuge.
15. PCR thermocycler.
16. Gel electrophoresis machine.
17. UV transilluminator.
18. ImageJ software (NIH).

2.4 Protein Extraction

1. Lysis and extraction buffer: RIPA buffer (Thermo Scientific) containing cOmplete, Mini, EDTA-free protease inhibitor cocktail (Roche).
2. Cell scraper.
3. 21G needles.
4. 1 mL syringes.
5. Coomassie (Bradford) Protein Assay kit (Thermo Scientific).

2.5 Western Blotting and Dystrophin Expression Quantification

1. Loading buffer: 0.004% w/v bromophenol blue, 5 mM EDTA, 20% glycerol, 70 mM Tris-HCl at pH 6.8, 10% SDS, and 5% b-mercaptoethanol.
2. NuPAGE™ Novex™ 3–8% Tris-Acetate Midi gel (Invitrogen).
3. NuPAGE™ Tris-Acetate SDS running buffer, 20× stock (Invitrogen).
4. NuPAGE™ Antioxidant (Invitrogen).
5. HiMark™ Pre-stained protein standard (Thermo Fisher) ladders.

6. Extra thick (2.5 mm) filter paper sheets, 8.0 × 13.5 cm (Thermo Fisher).
7. Methanol.
8. Concentrated anode buffer: 0.3 M Tris-HCl, 20% methanol.
9. Anode buffer: 0.03 M Tris-HCl, 20% methanol.
10. Cathode buffer: 25 mM Tris-HCl, 40 mM 6-amino-n-hexanoic acid, 20% methanol, 0.01% SDS.
11. Immobilon polyvinylidene difluoride (PVDF) membrane, 0.45 μm pore size (Millipore).
12. Phosphate-buffered saline with 0.05% Tween 20 (PBST).
13. PageBlue Protein Staining Solution (Thermo Scientific).
14. Amersham™ ECL Prime Blocking Agent (GE Healthcare).
15. Anti-dystrophin antibodies: Use rabbit polyclonal antibody (ab15277, Abcam) against the C-terminal domain of dystrophin or use DYS1 antibody against the rod domain of dystrophin (Leica Biosystems).
16. Amersham™ ECL Select Western Blotting Detection Reagent (GE Healthcare).
17. 70 °C water bath or heat block.
18. XCell4 SureLock™ Midi-Cell SDS-PAGE tank (Thermo Fisher).
19. Novex™ Semi-Dry Blotter (Life Technologies).
20. Power supply.
21. Imaging system.
22. ImageJ software (NIH).

3 Methods

3.1 Immortalized Muscle Cell Culture

1. Obtain an adequate number of immortalized DMD patient-derived muscle cells for seeding by growing them in sterile culture flasks containing the growth medium. Incubate at 37 °C with 5% CO_2.
2. As a control, immortalized healthy muscle cells can also be grown for quantifying dystrophin expression. AO transfection is not necessary for these cells. Incubate at 37 °C with 5% CO_2.
3. In a 12- or 24-well collagen type I-coated plate, seed the muscle cells at a density of ~$1.7 \times 10^4/cm^2$ per well and grow to 80–90% confluence (*see* **Note 1**).
4. Remove the growth medium and replace it with the differentiation medium.

5. Using 6 μM of the endo-porter transfection reagent, transfect muscle cells with appropriate PMO/s (e.g., 10 μM total) to be tested at the desired dosage level 3 days after differentiation. Before transfection, ensure to pre-heat the PMO stocks at 65 °C for 10 min. This allows for complete disaggregation.
6. After the desired number of days post-transfection, collect and isolate muscle cells from the culture for RNA or protein (*see* **Note 2**).
7. Two days after incubation, replace the differentiation medium containing AOs with the regular differentiation medium. To prevent cell death, ensure to replace the differentiation medium as needed.

3.2 RT-PCR and Exon Skipping Analysis

1. Using a pipette, aspirate as much medium as possible out of the well and then add 1 mL ice-cold Trizol to the cells. To ensure cells are lysed, pipette up and down. Add the resulting suspension of cells into sterile tubes.
2. Vortex for 15 s to allow the cell suspensions to further homogenize (*see* **Note 3**).
3. To the tubes, add 200 μL of chloroform and vigorously shake for 30 s to allow the formation of the aqueous and organic layers after centrifugation later on. Incubate at room temperature for 5 min.
4. Centrifuge samples for 15 min at 12000 × g and 4 °C.
5. To fresh tubes, transfer as much of the top aqueous layer as possible and add 1 μL of RNA-grade glycogen along with 500 μL of 100% isopropanol.
6. To mix the samples, vortex and then incubate at room temperature for 10 min.
7. Centrifuge samples for 10 min at 12000 × g and 4 °C.
8. Ensuring not to disturb the now visible white pellet in the tubes, carefully remove as much supernatant as possible. To this, add 1 mL of 75% ethanol and then vortex just until the pellet floats.
9. Centrifuge samples for 5 min at 7500 × g and 4 °C.
10. Ensure to carefully remove as much supernatant as possible from the tubes and then at room temperature, air-dry samples for a minimum of 5 min (*see* **Note 4**).
11. Use 20–40 μL RNase-free water to resuspend the RNA pellet once samples are dried and incubate the RNA at 60 °C.

12. Using UV-Vis spectrophotometry at 260 nm, measure the absorbance of the sample to quantify the isolated RNA. To allow for later use, dilute the RNA samples to the chosen concentration using RNase-free water and then place on ice until use or store at −80 °C for later use.
13. Assemble the one-step RT-PCR reaction. For each 25 μL reaction, mix ~200 ng of the extracted total RNA with 12.5 μL of the 2× reaction mix. Add 1 μL of each forward and reverse primers (at a final concentration of 0.2 μM), 1 μL of the SuperScript™ III RT/Platinum™ *Taq* mix, and fill to volume using RNase-free water.
14. Carry out the following PCR program (*see* **Note 5**):
    (a) 50 °C, 5 min
    (b) 94 °C, 2 min
    (c) 94 °C, 15 s
    (d) 60 °C, 30 s
    (e) 68 °C, 35 s
    (f) Repeat steps c–e 34 times.
    (g) 68 °C, 5 min
    (h) 4 °C, hold.
15. Using a 1–2% agarose gel, run the PCR products and add SYBR Safe DNA for 30 min to post-stain with shaking. Visualize the resulting bands by using a UV transilluminator or a similar visualizing system (*see* **Note 6**).
16. Capture an image of the gel and then measure the intensities of non-skipped and skipped bands by using ImageJ.
17. Using the following formula, determine the exon skipping efficiencies for the tested PMOs: [(intensity of exons 45–55 skipped band)/(intensity of non-skipped + skipped bands)] * 100 (%).

3.3 Protein Extraction

1. Using a pipette, aspirate as much medium as possible out of the well. To this, add 100 μL of ice-cold lysis buffer and use a cell scraper to thoroughly homogenize.
2. Add the resulting lysates to fresh tubes and pass through a 21G needle ten times to allow for further homogenization (*see* **Note 7**). Incubate on ice for 30 min.
3. For a minimum of 15 min, centrifuge samples at the max speed and at 4 °C. Without disturbing the visible white pellet, carefully transfer the protein-containing supernatant into fresh tubes.
4. Use the Coomassie protein assay kit to quantify the concentration of protein contained within the obtained extracts (*see* **Note 8**). Samples can be diluted using the lysis buffer and either kept on ice until use or stored at −80 °C.

3.4 Western Blotting and Dystrophin Rescue Quantification

1. Add the sample loading buffer to the extracted protein samples in a 1:1 ratio for SDS-PAGE. Heat the mixture at 70 °C for 10 min.
2. Assemble the SDS-PAGE tank by preparing a pre-cast 3–8% Tris-Acetate Midi gel in the apparatus while samples heat. Add 1x Tris-Acetate SDS running buffer to the indicated level in the outer buffer chamber. For the inner buffer chamber, fill using the same buffer with the antioxidant added until the gel wells are immersed in the solution. Before loading, ensure to flush wells with the running buffer.
3. In the corresponding wells, load at least 12 μg of protein. The quantity of added protein can be adjusted as desired. As a standard for the calibration curve to quantify dystrophin expression later on, ensure to also load the extracted protein from immortalized healthy muscle cells at various dilutions. To determine protein size, load the designated protein ladder and run the gel for 75 min at 150 V.
4. Prepare the PVDF membrane by briefly wetting it in methanol and then before the transfer, ensure to incubate the membrane in the anode buffer for a minimum of 10 min. On the top of the semi-dry blotting system anode surface, set up the following stack for the transfer process: bottom/anode surface, filter paper pre-soaked in concentrated anode buffer, filter paper pre-soaked in anode buffer, SDS-PAGE gel, prepared PVDF membrane, filter paper pre-soaked in cathode buffer, and cathode surface/top cover (*see* **Note 9**). Evenly and securely place the cover on top to ensure an even transfer of protein across the membrane.
5. Transfer for 70 min at 20 V.
6. Remove the membrane and rinse with PBST for 5 min at room temperature while shaking.
7. Use PageBlue staining solution to stain the gel for a minimum of 1 h at room temperature while shaking, and afterward, destain with distilled water overnight at room temperature while shaking. Visualization of the myosin-heavy chain, which serves as a loading control, can be achieved.
8. To block the membrane, use 2% ECL Prime blocking agent in PBST overnight at 4 °C while shaking.
9. In the chosen anti-dystrophin antibody, incubate the membrane for 1 h at room temperature while shaking. Using the blocking agent which serves as the diluent, carry out a dilution of 1:2500 for the C-terminal rabbit polyclonal antibody or a dilution of 1:400 for DYS1.
10. Using PBST, rinse the resulting membrane three times for 10 min each at room temperature with shaking.

11. Using the ECL Select Western blotting detection kit, proceed to prepare for dystrophin detection by combining solutions A (luminol) and B (peroxide) in a 1:1 ratio. A total volume of 3 mL per midi-sized gel should be enough. Incubate the membrane in this solution for 5 min.
12. Visualize the blot under a chemiluminescent imaging system.
13. To quantify dystrophin expression for each sample, use ImageJ to measure the observed band intensities.
14. Using the measured band intensities for the proteins of the immortalized healthy muscle cells as a standard protein control, create a calibration curve and apply the equation obtained from the curve to quantify the amount of dystrophin rescued from the AO treatment samples as compared to the control.

4 Notes

1. This may take ~2 days as demonstrated in previous experiences.
2. As early as 2 days after transfection in harvested muscle cells, differences in the ability of tested AOs to efficiently skip exons can be detected at the RNA level. It will take longer to detect dystrophin protein.
3. The samples can now be stored at −80 °C and extraction can be completed later on.
4. Before resuspending the RNA pellet, ensure that all the ethanol has been removed from the tubes as this can affect later steps in the protocol.
5. Based on the type of primers used and the region to be amplified, additional optimization may be required.
6. Exon skipping patterns can be confirmed by cutting out the skipped bands, obtaining the pure DNA, and then sent to be sequenced.
7. Ensure to avoid bubble formation as this can cause the protein to degrade.
8. Initially, quantifying samples in a 1:100 dilution is suggested, and then modify the dilution as appropriate.
9. Before transfer, place filter papers in the buffers to soak for a minimum of 30 min. We recommend removing the stacking gel section of the SDS-PAGE gel and then incubating it for 5 min in the cathode buffer prior to transfer. To allow even transfer, ensure bubbles are not present within any layers of the stack.

References

1. Hoffman EP, Brown RH Jr, Kunkel LM (1987) Dystrophin: the protein product of the Duchenne muscular dystrophy locus. Cell 51(6):919–928. https://doi.org/10.1016/0092-8674(87)90579-4
2. Walter MC, Reilich P (2017) Recent developments in Duchenne muscular dystrophy: facts and numbers. J Cachexia Sarcopenia Muscle 8(5):681–685. https://doi.org/10.1002/jcsm.12245
3. Beggs AH, Hoffman EP, Snyder JR et al (1991) Exploring the molecular basis for variability among patients with Becker muscular dystrophy: dystrophin gene and protein studies. Am J Hum Genet 49(1):54–67
4. Deconinck N, Dan B (2007) Pathophysiology of Duchenne muscular dystrophy: current hypotheses. Pediatr Neurol 36(1):1–7. https://doi.org/10.1016/j.pediatrneurol.2006.09.016
5. Klingler W, Jurkat-Rott K, Lehmann-Horn F et al (2013) The role of fibrosis in Duchenne muscular dystrophy. Acta Myol 31(3):184–195
6. Monaco AP, Bertelson CJ, Liechti-Gallati S et al (1988) An explanation for the phenotypic differences between patients bearing partial deletions of the DMD locus. Genomics 2(1):90–95. https://doi.org/10.1016/0888-7543(88)90113-9
7. Muntoni F, Torelli S, Ferlini A (2003) Dystrophin and mutations: one gene, several proteins, multiple phenotypes. Lancet Neurol 2(12):731–740. https://doi.org/10.1016/s1474-4422(03)00585-4
8. Flanigan KM, Dunn DM, von Niederhausern A et al (2009) Mutational spectrum of DMD mutations in dystrophinopathy patients: application of modern diagnostic techniques to a large cohort. Hum Mutat 30(12):1657–1666. https://doi.org/10.1002/humu.21114
9. Yazaki M, Yoshida K, Nakamura A et al (1999) Clinical characteristics of aged Becker muscular dystrophy patients with onset after 30 years. Eur Neurol 42(3):145–149. https://doi.org/10.1159/000008089
10. Le Rumeur E (2015) Dystrophin and the two related genetic diseases, Duchenne and Becker muscular dystrophies. Bosn J Basic Med Sci 15(3):14–20. https://doi.org/10.17305/bjbms.2015.636
11. Rinaldi C, Wood MJA (2018) Antisense oligonucleotides: the next frontier for treatment of neurological disorders. Nat Rev Neurol 14(1):9–21. https://doi.org/10.1038/nrneurol.2017.148
12. Evers MM, Toonen LJ, van Roon-Mom WM (2015) Antisense oligonucleotides in therapy for neurodegenerative disorders. Adv Drug Deliv Rev 87:90–103. https://doi.org/10.1016/j.addr.2015.03.008
13. Niks EH, Aartsma-Rus A (2017) Exon skipping: a first in class strategy for Duchenne muscular dystrophy. Expert Opin Biol Ther 17(2):225–236. https://doi.org/10.1080/14712598.2017.1271872
14. Yokota T, Duddy W, Echigoya Y et al (2012) Exon skipping for nonsense mutations in Duchenne muscular dystrophy: too many mutations, too few patients? Expert Opin Biol Ther 12(9):1141–1152. https://doi.org/10.1517/14712598.2012.693469
15. Aoki Y, Nakamura A, Yokota T et al (2010) In-frame dystrophin following exon 51-skipping improves muscle pathology and function in the exon 52-deficient mdx mouse. Mol Ther 18(11):1995–2005. https://doi.org/10.1038/mt.2010.186
16. Wein N, Vulin A, Findlay AR et al (2017) Efficient skipping of single exon duplications in DMD patient-derived cell lines using an antisense oligonucleotide approach. J Neuromuscul Dis 4(3):199–207. https://doi.org/10.3233/JND-170233
17. Maruyama R, Echigoya Y, Caluseriu O et al (2017) Systemic delivery of Morpholinos to skip multiple exons in a dog model of Duchenne muscular dystrophy. Methods Mol Biol 1565:201–213. https://doi.org/10.1007/978-1-4939-6817-6_17
18. Wurster CD, Ludolph AC (2018) Antisense oligonucleotides in neurological disorders. Ther Adv Neurol Disord 11:1–19. https://doi.org/10.1177/1756286418776932
19. Aartsma-Rus A, Fokkema I, Verschuuren J et al (2009) Theoretic applicability of antisense-mediated exon skipping for Duchenne muscular dystrophy mutations. Hum Mutat 30(3):293–299. https://doi.org/10.1002/humu.20918
20. Béroud C, Tuffery-Giraud S, Matsuo M et al (2007) Multiexon skipping leading to an artificial DMD protein lacking amino acids from exons 45 through 55 could rescue up to 63% of patients with Duchenne muscular dystrophy. Hum Mutat 28(2):196–202. https://doi.org/10.1002/humu.20428
21. Aoki Y, Yokota T, Nagata T et al (2012) Bodywide skipping of exons 45-55 in dystrophic

mdx52 mice by systemic antisense delivery. Proc Natl Acad Sci U S A 109(34): 13763–13768. https://doi.org/10.1073/pnas.1204638109

22. Dzierlega K, Yokota T (2020) Optimization of antisense-mediated exon skipping for Duchenne muscular dystrophy. Gene Ther. https://doi.org/10.1038/s41434-020-0156-6
23. Nguyen Q, Yokota T (2017) Immortalized muscle cell model to test the exon skipping efficacy for Duchenne muscular dystrophy. J Pers Med 7(4):13. https://doi.org/10.3390/jpm7040013
24. Mamchaoui K, Trollet C, Bigot A et al (2011) Immortalized pathological human myoblasts: towards a universal tool for the study of neuromuscular disorders. Skelet Muscle 1:34. https://doi.org/10.1186/2044-5040-1-34
25. Shimo T, Tachibana K, Saito K et al (2014) Design and evaluation of locked nucleic acid-based splice-switching oligonucleotides in vitro. Nucleic Acids Res 42(12): 8174–8187. https://doi.org/10.1093/nar/gku512
26. Saito T, Nakamura A, Aoki Y et al (2010) Antisense PMO found in dystrophic dog model was effective in cells from exon 7-deleted DMD patient. PLoS One 5(8):e12239. https://doi.org/10.1371/journal.pone.0012239
27. Echigoya Y, Lim KRQ, Melo D et al (2019) Exons 45-55 skipping using mutation-tailored cocktails of antisense Morpholinos in the DMD gene. Mol Ther 27(11):2005–2017. https://doi.org/10.1016/j.ymthe.2019.07.012

Chapter 23

In Vivo Evaluation of Exon 51 Skipping in *hDMD/Dmd*-null Mice

Narin Sheri and Toshifumi Yokota

Abstract

Duchenne muscular dystrophy (DMD) is a fatal X-linked condition that affects 1 in 3500–6000 newborn boys a year. An out-of-frame mutation in the DMD gene typically causes the condition. Exon skipping therapy is an emerging approach that uses antisense oligonucleotides (ASOs), short synthetic DNA-like molecules that can splice out mutated or frame-disrupting mRNA fragments, to restore the reading frame. The restored reading frame will be in-frame and will produce a truncated, yet functional protein. ASOs called phosphorodiamidate morpholino oligomers (PMO), including eteplirsen, golodirsen, and viltolarsen, have recently been approved by the US Food and Drug Administration as the first ASO-based drugs for DMD. ASO-facilitated exon skipping has been extensively studied in animal models. An issue that arises with these models is that the DMD sequence differs from the human DMD sequence. A solution to this issue is to use double mutant *hDMD/Dmd*-null mice, which only carry the human DMD sequence and are null for the mouse Dmd sequence. Here, we describe intramuscular and intravenous injections of an ASO to skip exon 51 in *hDMD/Dmd*-null mice, and the evaluation of its efficacy in vivo.

Key words Phosphorodiamidate morpholino oligomer, Antisense oligonucleotide, *hDMD/Dmd*-null, Duchenne muscular dystrophy, Becker muscular dystrophy, Eteplirsen (Exondys 51), Golodirsen (Vyondys 53), Viltolarsen (Viltepso), Exon skipping, Dystrophin

1 Introduction

Duchenne muscular dystrophy (DMD) is a fatal X-linked recessive disorder that is characterized by progressive muscle weakness [1]. DMD is caused by a frameshift mutation, typically a large deletion, in the *DMD* gene which produces the dystrophin protein. The mutation can lead to the degradation of mRNA and causes no protein to be formed [2]. Dystrophin plays an important role in muscle membrane integrity, and without a functional protein, there is severe muscle degradation that occurs [3]. While DMD is typically caused by out-of-frame mutations [4], Becker muscular dystrophy (BMD) is a milder form of the disorder that consists of an in-frame mutation in the *DMD* gene [5].

Atsushi Asakura (ed.), *Skeletal Muscle Stem Cells: Methods and Protocols*, Methods in Molecular Biology, vol. 2640, https://doi.org/10.1007/978-1-0716-3036-5_23,

Antisense oligonucleotides (ASOs), short synthetic DNA-like molecules that bind to mRNA fragments, are a promising therapeutic option for DMD [6]. ASOs can mediate exon skipping in pre-mRNA splicing which causes out-of-frame mutations to be converted to in-frame transcripts [7]. This is achieved through the skipping of one or multiple exons to produce an in-frame, functional transcript that is truncated. In pre-clinical studies with animals and cell models, exon skipping has been able to correct deletions, duplications, nonsense, and splice-site mutations [8–12]. In 2016, the US Food and Drug Administration (FDA) approved the first phosphorodiamidate morpholino oligomer (PMO) treatment for DMD, eteplirsen (brand name Exondys 51) [13]. The drug skips exon 51 during splicing, thereby restoring the translational reading frame of the *DMD* gene and producing a truncated but functional dystrophin protein [14]. The restoration of the translational reading frame causes the mutation to be in-frame, rather than out-of-frame, representing a phenotype more similar to BMD than DMD [14]. Golodirsen (brand name Vyondys 53) is another PMO treatment for DMD that was accepted for accelerated approval by the FDA in December 2019 [15]. Golodirsen works similarly to eteplirsen, except that it is designed to induce exon 53 skipping rather than exon 51. Viltolarsen (brand name Viltepso) is another exon 53 skipping PMO which has been approved in Japan in March 2020 and by the FDA in August 2020 [16, 17]. Viltolarsen differs from golodirsen in that it is a 21-mer oligonucleotide while golodirsen is a 25-mer oligonucleotide [18].

Many animal models have been used to test the efficacy of ASOs and treatment of DMD, including *mdx* mice, CXMD (Canine X-linked Muscular Dystrophy) dogs, and *GRMD* (Golden Retriever model of Duchenne) dogs [19, 20]; however, the main challenge of all these conventional DMD animal models is that their sequences are different from humans. Recently, a new mouse model has been produced carrying the full human *DMD* gene, the transgenic *hDMD* mouse [21]. Unlike the *mdx* mouse model, the *hDMD* mouse is more applicable to human studies of DMD treatment as ASOs are sequence-specific. By examining the efficacy of ASOs using the *hDMD* mouse model, we will gain better insights into how ASOs effectively target the human DMD gene in vivo. We cross-bred the *hDMD* mice with mice lacking the murine *Dmd* gene, to create an *hDMD/Dmd*-null mouse [22]. This double mutant was created to avoid cross-reaction between ASOs targeting the human *DMD* sequence and the mouse *Dmd* sequence [22]. It is possible for human-targeting ASOs to react with the mouse sequences and can, therefore, create false results; however, this is not an issue with the double mutant model as there is no mouse *Dmd* sequence. Although the benefit of using an *hDMD* mouse model for ASO testing is evident, it is worth noting that, unlike the

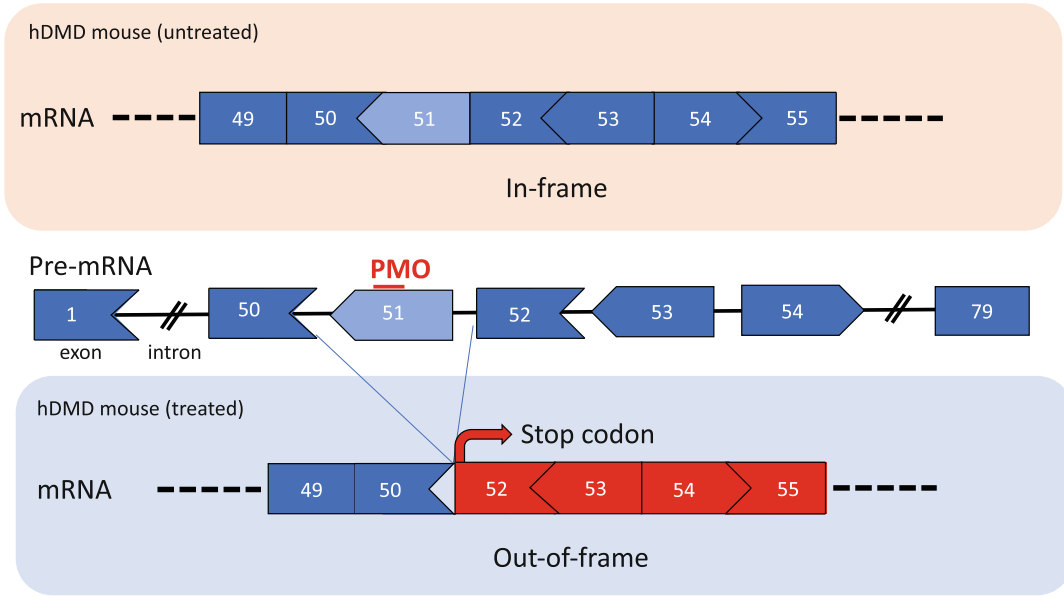

Fig. 1 The exon 51 skipping strategy for *hDMD/Dmd*-null mice using a PMO. Exon 51 skipping using an appropriate PMO, as indicated by the red line, can disrupt the reading frame of dystrophin in *hDMD/Dmd*-null mice. As *hDMD/Dmd*-null mice do not carry a mutation, the exon-skipping strategy will cause an out-of-frame mutation in the mRNA

mdx mouse, the *hDMD* mouse used here does not harbor any *DMD* gene mutations. There are some humanized DMD mouse models that harbor *DMD* deletions, including those with deletions of exon 45 (hDMD del45) and exon 52 (del52hDMD/*mdx*), which can be useful in exon skipping experiments [23–25].

The use of *hDMD* mice to test ASOs exon skipping is beneficial to the future treatment of DMD in boys, as it will indicate the in vivo effects of ASOs that directly target the human *DMD* gene. In this chapter, we summarize the method and protocol of intravenous and intramuscular injections of an ASO to skip exon 51 in the *hDMD* mouse (Fig. 1) and the evaluation of the efficacy using reverse transcription polymerase chain reaction (RT-PCR) in vivo.

2 Materials

All protocols listed below are in accordance with the animal care guidelines set forth by the University of Alberta.

Prepare all solutions using ultrapure water (prepared by purifying deionized water, to attain a sensitivity of 18 MΩ cm at 25 °C) and special-grade reagents. Prepare and store all reagents at room temperature (unless indicated otherwise).

2.1 Design of Antisense Morpholinos

1. The website of the UCSC Genome Browser to identify the *Dmd* mRNA sequence (https://genome.ucsc.edu/index.html).
2. A website to identify splicing motifs, for example, ESE finder (http://krainer01.cshl.edu/cgi-bin/tools/ESE3/esefinder.cgi?process=home) and Human Splicing Finder (http://www.umd.be/HSF3/HSF.shtml).

2.2 Intramuscular and Intravenous Injection of Antisense Morpholinos in Mice

1. 8-week-old male *hDMD/Dmd*-null mice.
2. 1 mL syringe.
3. Needles (27G).
4. Saline (0.9% sodium chloride solution).
5. Isoflurane.
6. Sterile insulin syringes with needle 29G × 1/2.
7. Antisense morpholino (Gene-tools, Philomath, OR, USA). The PMO cocktail will target the 5′ splice site (hEx51_Ac0G TGTCACCAGAGTAACAGTCTGAGTAGGAG) of *DMD* mRNA.
8. Depilatory cream.
9. Incandescent lamp.
10. Univentor 400 Anesthesia unit.

2.3 Muscle Sampling

1. Tragacanth gum.
2. Cork disks (diameter 12 mm, thickness 4 mm).
3. Liquid nitrogen.
4. Isopentane (2-Methylbutane).
5. Dumont Tweezers #5, 0.1 × 0.06 mm, Dumoxel (World Precision Instruments, Sarasota, FL, USA).
6. Dry ice.
7. Surgical instruments (forceps and scissors).
8. A 25 ml syringe.
9. Glass vials.

2.4 RT-PCR and Direct Sequencing of PCR Product

1. Trizol (Thermo Fisher, Waltham, MA, USA).
2. Chloroform.
3. Isopropanol.
4. Ethanol.
5. High Capacity cDNA Reverse Transcription Kit (Thermo Fisher).
6. TaKaRa Ex Taq® Hot Start Version (Takara Bio, Shiga, Japan).

7. Primers [22] (forward primer in exon 49/50: 5′-CAGCCAGT GAAGAGGAAGTTAG-3′ and reverse primer in exon 52: 5′-GATTGTTCTAGCCTCTTGATTGC-3′).
8. QIAquick gel extraction kit (Qiagen, Hilden, Germany).
9. Agarose.
10. Tris Acetate-EDTA (TAE) buffer.
11. Microwave oven.
12. GelRed® Nucleic Acid Stain (Biotium, Fremont, CA, USA).
13. Casting tray.
14. RNase-free water.
15. Heat block set.

3 Methods

3.1 Design of Antisense Morpholinos

1. Identify the *DMD* pre-mRNA target sequence from the website of the UCSC Genome Browser.
2. Copy and paste the target exon sequence from the full pre-mRNA sequence into the sequence information window on the page of ESEfinder 3.0 and Human Splicing Finder to identify the exonic splicing enhancer (ESE) site.
3. Design 21–30 mer PMOs that are antisense sequences of the targeted sites. Potential targets may include ESE or exon/intron boundaries. Design several sequences because their efficacy is highly unpredictable. The GC content of each sequence should be 40–65%, but approximately 60% is ideal. Avoid four consecutive "G"s, self-complementary sequences, and self-dimers. When PMOs are injected as a cocktail, it is also important to avoid heterodimers. Check the abovementioned specificities of sequences using IDT OligoAnalyzer (https://sg.idtdna.com/calc/analyzer) and NCBI Blast.

3.2 Intramuscular Injection of Antisense Morpholinos in Mice

1. Use 2.5–3% isoflurane to anesthetize the mouse via inhalation to maintain general anesthesia. Check breathing to assess the depth of anesthesia.
2. Using depilatory cream, remove the fur from the area of the tibialis anterior (TA) to better visualize the muscle.
3. Load sterile insulin syringes with needles with 10 μg of the oligonucleotides diluted in 30–40 μL saline (*see* **Note 1**).
4. Insert the needle into the *hDMD* mouse's TA muscle and inject half of the solution. Ensure the needle is inserted 2/3 into the muscle.

5. Pull back the needle to the 1/2 point of the TA muscle and inject the remaining half of the solution (*see* **Note 2**).
6. Wait for 10 s before pulling the needle out of the muscle to avoid leaking fluid.
7. Collect the muscle after 2 weeks.

3.3 Intravenous Injection of Antisense Morpholinos in Mice

1. Use 2.5–3% isoflurane to anesthetize the mouse via inhalation to maintain general anesthesia. Check breathing to assess the depth of anesthesia.
2. Use an incandescent lamp to irradiate the tail for a few minutes to dilate the tail vein. This will make visualization easier.
3. Select several doses of PMOs to be injected for a dose-escalation study to examine the dose-dependent effects of the screened PMOs. As an example, load sterile insulin syringes with needles with 80 mg/kg, 160 mg/kg, or 320 mg/kg PMOs in 100 μL saline (*see* **Notes 1** and **3**).
4. Insert the needle along the tail vein, superficially just under the skin. There will be backward blood flow into the syringe if the needle is placed correctly in the vein (*see* **Note 4**).
5. Inject the solution slowly. Once all of the solution is injected, keep the syringe in the muscle for 10 s to avoid leaking fluid after the removal of the needle.
6. Collect the muscle after 2 weeks [26].

3.4 Muscle Sampling

1. Mix equal volumes of tragacanth gum and water until the gum becomes soft and sticky. Load into 25 mL syringes. The gum in syringes can be stored in a refrigerator for later use.
2. Label the cork discs with the appropriate muscles. On the opposite side of the cork disc, place approximately 0.5–1 cm tragacanth gum.
3. Euthanize mice by cervical dislocation under general anesthesia.
4. Dissect the following samples as necessary: TA, extensor digitorum longus, gastrocnemius, soleus, quadriceps, diaphragm, heart, kidney, and liver.
5. Place the dissected muscles in the tragacanth gum. The longitudinal axis of each muscle should be perpendicular to the cork. To ensure proper placement, place some gum around the bottom of each muscle (*see* **Note 5**).
6. Place a container of isopentane in liquid nitrogen until it is cold enough to see some frozen portions.
7. Using tweezers, place each muscle/cork in cold isopentane to freeze the sample. Move the muscles constantly for 1 min or until completely frozen, and then keep them on dry ice temporarily.

8. Place the samples in glass vials and store them at −80 °C.
9. Set up the cryostat for sectioning with a working temperature of −25 °C. The section thickness should be 6–8 μm for immunohistochemistry, 10–12 μm for hematoxylin and eosin (HE) staining, and 10–20 μm for RT-PCR.
10. Mount each sample block and trim one-fourth of the muscle to obtain flat sections.
11. For RT-PCR, put 20–40 sections in a 1.5 mL tube and store at −80 °C.

3.5 RT-PCR and Direct Sequencing of PCR Product

1. Add 1 mL cold Trizol per 50–100 mg of tissue sample and vortex for 30 s. Incubate for 10 min at 20–25 °C.
2. Add 200 μL chloroform and vortex. Incubate for 2 min at 20–25 °C.
3. Centrifuge the sample at 12,000× *g* for 15 min at 4 °C.
4. Carefully collect only the aqueous phase in the top layer and transfer it to a new tube (*see* **Note 6**). Add 500 μL isopropanol. Incubate for 10 min at 20–25 °C.
5. Centrifuge at 12,000× *g* for 10 min at 4 °C.
6. Remove all supernatant, leaving only the RNA pellet. Add 1 mL of cold 75% ethanol.
7. Centrifuge at 7500× *g* for 5 min at 4 °C.
8. Remove as much ethanol as possible and dry the RNA pellet for 5–10 min by opening the tube and keeping it upside down (*see* **Note 7**).
9. Add 20–50 μL RNase-free water. Incubate in a water bath or heat block set at 55–60 °C for 10 min to denature. Quantify total RNA concentration by a UV-Vis spectrophotometer at 260 nm.
10. Set up cDNA synthesis reaction. For 1 reaction, mix 2 μL 10× RT Random Primers, 0.8 μL 25× dNTP Mix, 2 μL 10× RT Buffer, and 1 μL Reverse Transcriptase from the cDNA Reverse Transcription Kit with 200 ng total RNA. Add RNase-free water to bring the final volume to 20 μL.
11. Set the conditions of the thermal cycler as follows: 25 °C for 10 min, 37 °C for 120 min, and 85 °C for 5 min. Store the cDNA at 4 °C or −20 °C.
12. Set up the RT-PCR reaction. For 1 reaction, mix 14.3 μL water, 0.5 μL 10 μM forward primer, 0.5 μL 10 μM reverse primer, 1.6 μL dNTPs, 2 μL 10× Ex Taq Buffer, and 0.1 μL Ex Taq HS from the Ex Taq Hot Start Version kit with 1 μL cDNA template.

13. Set the conditions of the thermal cycler as follows: 1 cycle of 95 °C for 4 min; 35 cycles of 94 °C for 30 s, 61 °C for 30 s, and 72 °C for 30 s; and 1 cycle of 72 °C for 7 min. Store the PCR products at 4 °C or −20 °C.
14. Dissolve 1–2% agarose completely in TAE buffer using a microwave oven and after cooling down for 5 min, add GelRed® Nucleic Acid Stain in the diluted agarose at 1:10,000 and pour the solution into the casting tray. Then, insert a comb with the proper number of wells. Leave the assembly for over 30 min to prepare the gel.
15. Run 5–10 μL of each PCR product on the agarose gel and observe the targeted bands under UV radiation (*see* **Note 8**).
16. Cut the band of interest and collect it in a 1.5 mL tube (*see* **Note 9**). Use the Qiagen Gel Extraction Kit to purify the PCR product.
17. Sequence the purified PCR product using the same primer used for RT-PCR.

4 Notes

1. PMOs should be incubated at 65 °C for 10 min just before use.
2. **Steps 5** and **6** are crucial in inducing exon skipping in the broader area of the target muscles.
3. The experimental design will determine the amount of PMOs used and the frequency of injections used. The injection(s) can also be repeated weekly for the desired number of weeks.
4. If the needle is in the proper location in the vein, there should be almost no resistance to needle advancement. Upon injection, the fluid will flow easily into the vein, and the vein will become clear (changing from dark to light) as the fluid temporarily replaces blood.
5. When mounting the diaphragm onto the tragacanth gum for cross-sectioning, fold the isolated muscle and place the bottom of the cone-shaped folded muscle pointed downward. This will allow for the best cross-sectioning sample.
6. Do not include any middle or bottom layers, only the clear aqueous layer. If any of the middle or bottom layers are included, it will cause contamination of protein and DNA.
7. Do not dry the RNA pellet completely, or it will lose its solubility.
8. The intensity of each PCR band can be analyzed using ImageJ software (http://rsbweb.nih.gov/ij/). The skipping efficiency can be calculated using the following formula: [(the intensity of the skipped band)/(the intensity of the skipped band + the

intensity of the unskipped band)]. For the detection of PCR bands, you can alternatively use a microchip electrophoresis system such as MultiNA (SHIMADZU, Kyoto, Japan). This system can detect bands at a higher sensitivity and resolution compared to standard agarose gel staining and calculate the size (bp) and area (mV/μm) or concentration (ng/μL) of each band automatically with electropherograms.

9. The estimated size of the skipped exon 51 band is 226 bp with the given primer pair.

Acknowledgments

This research was funded by Alberta Innovates Summer Research Studentship Program, the Friends of Garrett Cumming Research Chair Fund, HM Toupin Neurological Science Research Chair Fund, Muscular Dystrophy Canada, Canadian Institutes of Health Research (CIHR) FDN 143251, the University of Alberta Faculty of Medicine and Dentistry, Alberta Innovates, and the Women and Children's Health Research Institute (WCHRI) IG 2874.

References

1. Moser H (1984) Duchenne muscular dystrophy: pathogenetic aspects and genetic prevention. Hum Genet 66:17–40. https://doi.org/10.1007/BF00275183
2. Hoffman EP, Brown RH, Kunkel LM (1987) Dystrophin: the protein product of the Duchenne muscular dystrophy locus. Cell 51:919–928. https://doi.org/10.1016/0092-8674(87)90579-4
3. Cox GA, Cole NM, Matsumura K et al (1993) Overexpression of dystrophin in transgenic mdx mice eliminates dystrophic symptoms without toxicity. Nature 364:725–729. https://doi.org/10.1038/364725a0
4. Koenig M, Beggs AH, Moyer M et al (1989) The molecular basis for Duchenne versus Becker muscular dystrophy: correlation of severity with type of deletion. Am J Hum Genet 45:498–506
5. Monaco AP, Bertelson CJ, Liechti-Gallati S et al (1988) An explanation for the phenotypic differences between patients bearing partial deletions of the DMD locus. Genomics 2:90–95. https://doi.org/10.1016/0888-7543(88)90113-9
6. Di Fusco D, Dinallo V, Marafini I et al (2019) Antisense oligonucleotide: basic concepts and therapeutic application in inflammatory bowel disease. Front Pharmacol 10. https://doi.org/10.3389/fphar.2019.00305
7. Brolin C, Shiraishi T (2011) Antisense mediated exon skipping therapy for Duchenne muscular dystrophy (DMD). Artif DNA PNA XNA 2:6–15. https://doi.org/10.4161/adna.2.1.15425
8. Yokota T, Duddy W, Echigoya Y et al (2012) Exon skipping for nonsense mutations in Duchenne muscular dystrophy: too many mutations, too few patients? Expert Opin Biol Ther 12:1141–1152. https://doi.org/10.1517/14712598.2012.693469
9. Lu QL, Rabinowitz A, Chen YC et al (2005) Systemic delivery of antisense oligoribonucleotide restores dystrophin expression in body-wide skeletal muscles. Proc Natl Acad Sci 102:198–203. https://doi.org/10.1073/pnas.0406700102
10. Aoki Y, Nakamura A, Yokota T et al (2010) In-frame dystrophin following exon 51-skipping improves muscle pathology and function in the exon 52–deficient mdx mouse. Mol Ther 18:1995–2005. https://doi.org/10.1038/mt.2010.186
11. Wein N, Vulin A, Findlay AR et al (2017) Efficient skipping of single exon duplications in DMD patient-derived cell lines using an antisense oligonucleotide approach. J Neuromuscular Dis 4:199–207. https://doi.org/10.3233/JND-170233

12. Maruyama R, Echigoya Y, Caluseriu O et al (2017) Systemic delivery of morpholinos to skip multiple exons in a dog model of Duchenne muscular dystrophy. Methods Mol Biol 1565:201–213
13. Dowling JJ (2016) Eteplirsen therapy for Duchenne muscular dystrophy: skipping to the front of the line. Nat Rev Neurol 12:675–676. https://doi.org/10.1038/nrneurol.2016.180
14. Lim KR, Maruyama R, Yokota T (2017) Eteplirsen in the treatment of Duchenne muscular dystrophy. Drug Design Dev Ther 11:533–545. https://doi.org/10.2147/DDDT.S97635
15. Heo Y-A (2020) Golodirsen: first approval. Drugs 80:329–333. https://doi.org/10.1007/s40265-020-01267-2
16. Dhillon S (2020) Viltolarsen: first approval. Drugs 80:1027–1031. https://doi.org/10.1007/s40265-020-01339-3
17. U.S. Food and Drug Administration FDA Approves Targeted Treatment for Rare Duchenne Muscular Dystrophy Mutation. https://www.fda.gov/news-events/press-announcements/fda-approves-targeted-treatment-rare-duchenne-muscular-dystrophy-mutation. Accessed 24 Aug 2020
18. Aartsma-Rus A, Corey DR (2020) The 10th oligonucleotide therapy approved: Golodirsen for Duchenne muscular dystrophy. Nucleic Acid Ther 30:67–70. https://doi.org/10.1089/nat.2020.0845
19. Nakamura A, Takeda S (2011) Mammalian models of Duchenne muscular dystrophy: pathological characteristics and therapeutic applications. J Biomed Biotechnol 2011:1–8. https://doi.org/10.1155/2011/184393
20. McGreevy JW, Hakim CH, McIntosh MA et al (2015) Animal models of Duchenne muscular dystrophy: from basic mechanisms to gene therapy. Dis Model Mech 8:195–213. https://doi.org/10.1242/dmm.018424
21. Bremmer-Bout M, Aartsma-Rus A, de Meijer EJ et al (2004) Targeted exon skipping in transgenic hDMD mice: a model for direct preclinical screening of human-specific antisense oligonucleotides. Mol Ther 10:232–240. https://doi.org/10.1016/j.ymthe.2004.05.031
22. Echigoya Y, Lim KRQ, Trieu N et al (2017) Quantitative antisense screening and optimization for exon 51 skipping in Duchenne muscular dystrophy. Mol Ther 25:2561–2572. https://doi.org/10.1016/j.ymthe.2017.07.014
23. Young CS, Mokhonova E, Quinonez M et al (2017) Creation of a novel humanized dystrophic mouse model of Duchenne muscular dystrophy and application of a CRISPR/Cas9 gene editing therapy. J Neuromuscular Dis 4:139–145. https://doi.org/10.3233/JND-170218
24. Veltrop M, van Vliet L, Hulsker M et al (2018) A dystrophic Duchenne mouse model for testing human antisense oligonucleotides. PLoS One 13:e0193289. https://doi.org/10.1371/journal.pone.0193289
25. Lim KRQ, Nguyen Q, Dzierlega K et al (2020) CRISPR-generated animal models of duchenne muscular dystrophy. Genes (Basel) 11:342. https://doi.org/10.3390/genes11030342
26. Aartsma-Rus A, Straub V, Hemmings R et al (2017) Development of exon skipping therapies for duchenne muscular dystrophy: a critical review and a perspective on the outstanding issues. Nucleic Acid Ther 27:251–259. https://doi.org/10.1089/nat.2017.0682

Part III

Bioinformatics & Imaging Analysis for Muscle Stem Cells

Chapter 24

Functional Analysis of MicroRNAs in Skeletal Muscle

Satoshi Oikawa and Takayuki Akimoto

Abstract

MicroRNAs (miRNAs) are small non-coding RNAs that are highly conserved in vertebrates and play important roles in diverse biological processes. miRNAs function to fine-tune gene expression by accelerating the degradation of mRNA and/or by inhibiting protein translation. Identification of muscle-specific miRNAs has extended our knowledge of the molecular network in skeletal muscle. Here we describe methods that are commonly used to analyze the function of miRNAs in skeletal muscle.

Key words Mature microRNAs, Precursor microRNAs, Primary microRNAs, Real-time PCR, Reporter assay, Skeletal muscle

1 Introduction

MicroRNAs (miRNAs) are a class of small non-coding RNAs that control gene expression by inducing decay and/or translational inhibition of their target mRNAs [1]. MiRNAs have emerged as critical regulators in diverse biological events, including development, tissue homeostasis, and disease [2]. In the nucleus, primary miRNAs (pri-miRNAs) are transcribed by RNA polymerase II and then cleaved by a nuclear ribonuclease III Drosha and a cofactor DGCR8 into ~65 nucleotides (nt) precursor miRNAs (pre-miRNAs). The pre-miRNAs are exported from the nucleus to the cytoplasm by the importin β-like nuclear export receptor Exportin 5 and subsequently processed by a cytoplasmic ribonuclease III Dicer into ~22-nt double-stranded miRNAs. Finally, one strand (called "guide strand") of the miRNA duplex is loaded into an Argonaute protein to form an RNA-induced silencing complex (RISC). RISC complex binds to 3′-untranslated regions (3′-UTRs) of target mRNAs through base-pairing of seed sequence (miRNA nucleotides 2–7) and inhibits the gene expressions [3, 4].

Skeletal muscle is a highly plastic tissue and its development, mass, metabolic, and contractile properties are coordinately controlled by molecular networks of several transcription factors

Atsushi Asakura (ed.), *Skeletal Muscle Stem Cells: Methods and Protocols*, Methods in Molecular Biology, vol. 2640, https://doi.org/10.1007/978-1-0716-3036-5_24,

[5–8]. Myogenic regulatory factors (MRFs), which include myogenic factor 5 (Myf5), myogenic differentiation 1 (MyoD), myogenin, and MRF4, play key roles in determining myogenic cell fate and terminal differentiation [9–12]. On the other hand, contractile and metabolic properties of skeletal muscle are coordinated by another set of key molecules, including peroxisome proliferator-activated receptor-γ coactivator-1α (PGC-1α), myocyte enhancer factor-2 (MEF2), and calcineurin [13–15].

Recent studies have shown that several muscle-enriched miRNAs controlled muscle development, growth, and differentiation through interaction with the key molecules [16]. These findings have extended our understanding of the molecular network in skeletal muscle. The expression of muscle-enriched miRNAs, miR-1, miR-133, and miR-206, are regulated by the myogenic transcription factors, including MyoD, myogenin, and MEF2, and these miRNAs modulate myoblasts proliferation and differentiation [17–20]. Besides, several studies revealed that the redundant roles of two intronic miRNAs, miR-208b and miR-499, are encoded by slow myosin genes, Myh7 and Myh7b, respectively, in determining energy metabolism and muscle fiber types [21–23].

In this chapter, we describe protocols that are commonly used to analyze the function of miRNAs in skeletal muscle. Using these protocols, we are able to detect a miRNA that is specifically expressed in skeletal muscle and test its interaction with putative target mRNAs. Moreover, manipulation of the miRNA expression enables an analysis of their functions in myoblasts as well as in an adult skeletal muscle.

2 Materials

2.1 Measurement of Mature miRNAs by PCR

1. ISOGEN II (Wako Chemicals).
2. TaqMan MicroRNA Reverse Transcription Kit (Thermo Fisher Scientific).
3. TaqMan MicroRNA Assay (RT primer, TaqMan probe, and PCR primer sets, Thermo Fisher Scientific).
4. TaqMan Universal PCR Master Mix, no AmpErase UNG (Thermo Fisher Scientific).
5. Primers for Rnu6 (a small non-coding RNA, commonly used as an internal control for miRNA measurement): Forward, 5′- C GCTTCGGCAGCACATATAC -3′; Reverse, 5′- TGCGTGT CATCCTTGCGCAG-3′.
6. THUNDERBIRD SYBR qPCR Mix (TOYOBO).
7. StepOnePlus Real-Time PCR system (Thermo Fisher Scientific).

2.2 Measurement of Pri-miRNAs and Pre-miRNAs

1. Specific primers for pri-miRNAs, pre-miRNAs, and GAPDH.
2. SuperScript III Reverse Transcriptase (Thermo Fisher Scientific).
3. RNase Inhibitor, Recombinant (TOYOBO).
4. TaKaRa Ex Taq Hot Start Version (TaKaRa).
5. 2% Agarose gels.
6. 100 bp DNA ladder.
7. Thermal cycler.

2.3 miRNA-Target mRNA Interaction

1. cDNA.
2. Primers with EcoRI and XbaI sites for 3′UTR of a target mRNA.
3. Primers for mutagenesis.
4. pLuc2EXN vector (firefly) [24].
5. pRL-TK vector (Renilla).
6. QuikChange Lightning site-directed mutagenesis kit (Stratagene).
7. HeLa cell (the other cell lines can also be used for reporter assay).
8. pCXbG plasmid vector with a specific miRNA.
9. Dual-Luciferase Reporter Assay System (Promega).
10. SpectraMax L Luminometer (Molecular Devices).

2.4 Manipulation of miRNA Expression: Overexpression of miRNAs

1. miRNA expression vector: pCXbG plasmid vector.
2. Genomic DNA.
3. miRNA-specific primers with restriction sites.
4. Restriction enzymes (EcoRV and XhoI).
5. QIAEX II Gel Extraction Kit (Qiagen).
6. LB Agar plates containing ampicillin.
7. T4 DNA Ligase (TaKaRa).
8. ECOS Competent *E. coli* DH-α (Wako Chemicals).
9. Orientation-specific primers for colony PCR.
10. QIAGEN Plasmid Kits (Qiagen).
11. C2C12 myoblasts.
12. Lipofectamine 2000 (Thermo Fisher Scientific).

2.5 Manipulation of miRNA Expression: Knockdown of miRNAs

1. LNA-based antisense oligonucleotides.
2. Lipofectamine RNAiMAX (Thermo Fisher Scientific).
3. C2C12 myoblasts.

3 Methods

3.1 Quantification of Mature miRNAs by Real-Time PCR

Carry out all procedures at room temperature unless otherwise specified.

1. Extract total RNA from cells or muscle tissues using ISOGEN II according to the manufacturer's protocol.
2. The concentration of total RNA should be adjusted to 5 ng/μL.
3. Prepare the Reverse Transcription (RT) Reaction Mixture into a 0.2 mL tube on ice. The mixture contains 2.58 μL of Nuclease-free water, 0.75 μL of 10× Reverse Transcription Buffer, 0.075 μL of 100 mM dNTPs, 0.095 μL of RNase inhibitor, 0.5 μL of MultiScribe Reverse Transcriptase, 2 μL of diluted RNA sample (10 ng), and 1.5 μL of a miRNA-specific RT primer or 1.5 μL of Rnu6 reverse primer (*see* **Note 1**).
4. Incubate the RT reaction mixture for 30 min at 16 °C, 30 min at 42 °C, 5 min at 85 °C, and then place it on ice (cDNA synthesis).
5. The synthesized cDNAs can be used for real-time PCR reactions or stored at −20 °C.
6. Prepare a PCR reaction mixture for miRNA quantification. The mixture contains 3.835 μL of Nuclease-free water, 5 μL of TaqMan Universal PCR Master Mix, no AmpErase UNG, 0.5 μL of TaqMan Probe, and 1 μL of cDNA.
7. Prepare a PCR reaction mixture for Rnu6 quantification. The mixture contains 3.8 μL of Nuclease-free water, 5 μL of THUNDERBIRD SYBR qPCR Mix, 0.2 μL of 50× ROX reference dye, 0.2 μL of Rnu6 F/R primer, and 1 μL of cDNA.
8. Perform PCR reactions on a real-time PCR system in a 96-well plate at 95 °C for 10 min followed by 40 cycles of 95 °C for 15 s and 60 °C for 1 min.
9. Analyze the relative expression of miRNAs using the ΔΔCt method.

3.2 Quantification of Pri- and Pre-miRNAs by Semi-quantitative RT-PCR

Carry out all procedures at room temperature unless otherwise specified.

1. The Reverse primer is commonly used for both pri- and pre-miRNA measurements. The Forward primer should be designed for the pri- and pre-miRNA measurements, respectively (Fig. 1).
2. Prepare the RT reaction mixture into a 0.2 mL tube on ice. The mixture contains 1 μL of pri−/pre-miRNA common reverse primer (10 μM), 1 μL of 10 mM dNTP Mix, 500 ng total RNA, and Nuclease-free water up to 13 μL.

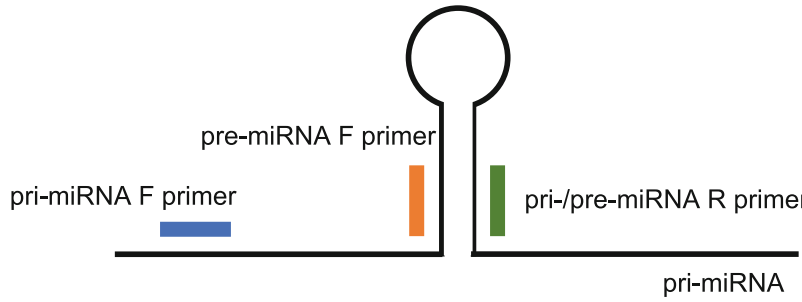

Fig. 1 The primers targeting pri- and pre-miRNAs

3. Incubate the mixture at 65 °C for 5 min and place it on ice for at least 1 min (*see* **Note 2**).
4. Add the following components of the Master reaction mixture including 4 μL of 5× First-Strand Buffer, 1 μL of 0.1 M DTT, 1 μL of RNase inhibitor, and 1 μL of SuperScript III Reverse Transcriptase.
5. Incubate the master reaction mixture at 55 °C for 60 min and 70 °C for 15 min (cDNA synthesis).
6. The cDNA can be used as PCR templates or stored at −20 °C.
7. For quantification of pri- and pre-miRNAs, the cDNAs are amplified by standard PCR protocol using Ex Taq Hot Start Version.
8. PCR products are electrophoresed on 2% agarose gels containing ethidium bromide for 30 min, and images are acquired by a gel imager such as LAS 3000 (Densitometry).

3.3 miRNA-Target mRNA Interaction: Target Prediction Using the Online Database

1. Access the website of miRBase (http://www.mirbase.org/) and enter the name of the miRNA of your interest.
2. Confirm the number of "reads" in the deep sequencing to identify which strand (3p or 5p) is a guide miRNA that is preferentially loaded into the Argonaute proteins of RISC.
3. Search putative target genes of the miRNA by accessing the TargetScan website or other miRNA target prediction tools (Table 1) via the link of miRBase or directly (http://www.targetscan.org/).

3.4 miRNA-Target mRNA Interaction: Reporter Assay

Carry out all procedures at room temperature unless otherwise specified.

1. To generate a reporter vector, amplify about 300-bp of 3′-UTR of the predicted gene, including putative miRNA binding sites, from cDNA by standard PCR (50 μL volume) with primers containing EcoRI and XbaI sites.
2. Digest the PCR products with EcoRI and XbaI at 37 °C for several hours to overnight.

Table 1
miRNA target prediction tools

miRNA sequence databases	
miRBase	http://www.mirbase.org/
miROrtho	http://cegg.unige.ch/mirortho
miRNA target prediction tools	
TargetScan	http://www.targetscan.org/
PicTar	https://pictar.mdc-berlin.de/
miRDB	http://mirdb.org/
miR-TarBase	http://mirtarbase.mbc.nctu.edu.tw/
DIANA-TarBase	http://www.microrna.gr/tarbase
miRWalk 2.0	http://zmf.umm.uni-heidelberg.de/mirwalk2

3. Digest 5 μg pLuc2EXN vector with EcoRI and XbaI at 37C° overnight.
4. Electrophorese the digested products and purify them using QIAEX II Gel Extraction Kit according to the manufacturer's protocol.
5. Prepare the ligation mixture containing 1 μL of 10× ligation buffer, 50 ng of digested pLuc2EXN vector, an appropriate volume of the digested PCR products, 0.5 μL of T4 DNA Ligase, and add sterile distilled water up to 10 μL.
6. Incubate the mixture at 16 °C overnight.
7. Mix 1 μL of ligated pLuc2EXN vector and 10 μL of ECOS Competent cells in a 1.5 mL tube. Vortex the mixture for 1 s.
8. Incubate the vector/competent cell mixture on ice for 5 min and heat shock the mixture at 42 °C for 45 s.
9. Plate the transformed competent cells onto a 10 cm LB agar plate containing ampicillin.
10. Incubate the plate at 37 °C overnight.
11. A part of the colony can be used as a template for colony PCR.
12. Culture positive clones in an LB medium containing ampicillin at 37 °C overnight in a shaking incubator.
13. Purify the vectors from the bacterial culture using QIAGEN Plasmid Mini Kit.
14. Confirm the sequence of the cloned vector (pLuc2EXN-target gene 3′-UTR).
15. Culture a sequence-confirmed clone in an LB medium containing ampicillin at 37 °C overnight in a shaking incubator.
16. Purify the vectors from the bacterial culture using QIAGEN Plasmid Midi Kit.

17. Synthesize two complementary oligonucleotides primers containing the desired mutations on the targeted sequence of the 3′-UTR of target mRNA to generate a mutant version of the vector (pLuc2EXN-target gene 3′-UTRΔ) (*see* **Note 3**). pLuc2EXN-target gene 3′-UTR vector is used as a template for the PCR-based site-directed mutagenesis with the QuickCharge Lightning site-directed mutagenesis kit.
18. Prepare the reaction mixture into a 0.2 mL tube on ice. The mixture contains 5 μL of 10× reaction buffer, 100 ng of pLuc2EXN-target gene 3′-UTR vector, 125 ng of forward primer, 125 ng of reverse primer, 1 μL of dNTP Mix, 1.5 μL of QuickSolution reagent, and Nuclease-free water to a final volume of 50 μL. Then add 1 μL of QuickChange Lightning Enzyme into the mixture.
19. Perform PCR reactions on a thermal cycler at 95 °C for 2 min followed by 18 cycles of 95 °C for 20 s, 60 °C for 10 s, and 68 °C for 30 s/kb of plasmid length and incubate at 68C° for 5 min.
20. Add 2 μL of the DpnI restriction enzyme directly to each amplification product in the 0.2 mL tube.
21. Incubate the mixture at 37C° for 5 min to digest nonmutated template vectors.
22. Mix 1 μL of the mixture containing pLuc2EXN-target gene 3′-UTRΔ and 10 μL of ECOS Competent cells in a 1.5 mL tube. Vortex the mixture for 1 s.
23. Incubate the vector/competent cell mixture on ice for 5 min and heat shock the mixture at 42 °C for 45 s.
24. Plate the transformed competent cells onto a 10 cm LB agar plate containing ampicillin.
25. Incubate the plates at 37 °C overnight.
26. A part of the colony can be used as a template for colony PCR.
27. Culture several positive clones in an LB medium containing ampicillin at 37 °C overnight in a shaking incubator.
28. Purify the vectors from the bacterial culture using QIAGEN Plasmid Mini Kit.
29. Sequence the vectors to validate the sequence.
30. Culture a sequence-confirmed clone in an LB medium containing ampicillin at 37 °C overnight in a shaking incubator and purify the vector using QIAGEN Plasmid Midi Kits.
31. Transfect 0.1 μg of pLuc2EXN-target gene 3′-UTR or pLuc2EXN-target gene 3′-UTRΔ (mutant), 0.05 μg of pRL-TK, and 0.05 μg of pCXbG-miRNA into HeLa cells using Lipofectamine 2000.

32. Wash and lyse the cells with Passive Lysis Buffer 24 h after transfection.
33. Prepare Luciferase Assay Reagent II (LAR II) by resuspending the provided lyophilized Luciferase Assay Substrate in the supplied Luciferase Assay Buffer II.
34. Prepare Stop & Glo Reagent by adding 1 volume of 50× Stop & Glo Substrate to 50 volumes of Stop & Glo Buffer in a 1.5 mL tube.
35. Predispense 100 μL of LAR II into the appropriate number of wells in a 96-well luminometry plate.
36. Transfer up to 20 μL of cell lysates into the 96-well luminometry plate containing LAR II and mix by pipetting two or three times and initiate reading of the firefly luciferase activity in a luminometer.
37. Take the 96-well plate out from the luminometer and add 100 μL of Stop & Glo Reagent into each well and shake the plate to mix.
38. Replace the 96-well plate in the luminometer and initiate reading of the *Renilla* luciferase activity.
39. The firefly luciferase activity is normalized to *Renilla* luciferase activity.

3.5 Manipulation of miRNA Expression: Overexpression of miRNAs

Carry out all procedures at room temperature unless otherwise specified.

1. To generate an expression vector for a certain miRNA, amplify about 300–400 bp of the pre-miRNA from genomic DNA by standard PCR (50 μL volume) with primers containing SalI and EcoRV sites.
2. Digest the amplified fragments with SalI and EcoRV at 37 °C for several hours to overnight.
3. Digest 5 μg pCXbG-sΔ with XhoI and EcoRV at 37 °C overnight.
4. Electrophorese the digested products and purify them using QIAEX II Gel Extraction Kit according to the manufacturer's protocol.
5. Prepare the ligation mixture containing 1 μL of 10× ligation buffer, 50 ng of digested pCXbG vector, an appropriate volume of digested PCR products, 0.5 μL of T4 DNA Ligase, and add sterile distilled water up to 10 μL.
6. Incubate the mixture at 16 °C overnight.
7. Mix 1 μL of ligated pCXbG vector and 10 μL of ECOS Competent cells in a 1.5 mL tube. Vortex the mixture for 1 s.
8. Incubate the vector/competent cell mixture on ice for 5 min and heat shock the mixture at 42 °C for 45 s.

9. Plate the transformed competent cells onto a 10 cm LB agar plate containing ampicillin.
10. Incubate the plate at 37 °C overnight.
11. A part of the colony can be used as a template for colony PCR.
12. Culture positive clones in an LB medium containing ampicillin at 37 °C overnight in a shaking incubator.
13. Purify the vectors from the bacterial culture using QIAGEN Plasmid Mini Kit.
14. Confirm the sequence of the cloned vectors (pCXbG-miRNA).
15. Culture a sequence-confirmed clone in an LB medium containing ampicillin at 37 °C overnight in a shaking incubator.
16. Purify the vectors from the bacterial culture using QIAGEN Plasmid Midi Kit.
17. Transfect 5 μg of pCXbG-sΔ (Control) and pCXbG-miRNA into C2C12 myoblasts using Lipofectamine 2000 according to the manufacturer's protocol.
18. About 24–48 h after transfection, check for an increase in the miRNA expression by real-time PCR.

3.6 Manipulation of miRNA Expression: Knockdown of miRNAs

Carry out all procedures at room temperature unless otherwise specified.

1. Synthesize an antisense DNA/LNA oligomer to a miRNA as well as a random LNA oligomer for control (*see* **Note 4**). These LNA-based antisense oligonucleotides contain 5 bases of LNA on their 3′ and 5′ sides (Fig. 2).
2. Transfect the random LNA (control) or the anti-miRNA LNA (final concentration: 10 nM) into C2C12 myoblasts using Lipofectamine RNAiMAX according to the manufacturer's protocol.
3. About 24–48 h after transfection, confirm a decrease in the miRNA expression by real-time PCR.

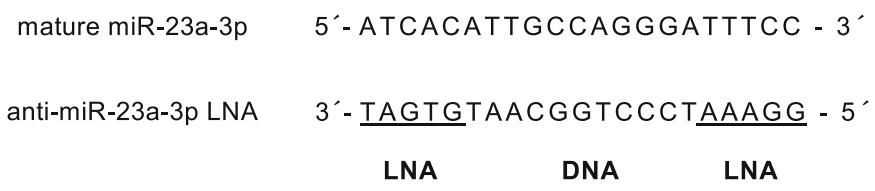

Fig. 2 Design of LNA-based antisense oligonucleotides (LNA; underlined)

4 Notes

1. The reverse transcription of mature miRNAs and Rnu6 can be performed simultaneously in the same reaction tube (the amount of nuclease-free water needs to be reduced from 2.58 μL to 1.08 μL). In this case, it does not affect their relative expression levels, although the Ct values of both the miRNA and Rnu6 would be lower.
2. The cDNA synthesis of pri-miRNAs and pre-miRNAs should be performed at higher temperatures with specific primers because the secondary structure of these RNAs, including short hairpin, may interfere with reverse transcription reaction [25].
3. The introduction of the mutations into the sequence of a 3′-UTR of the predicted target gene may give rise to a new miRNA target sequence. It is necessary to confirm that the mutated sequence in the reporter vector does not contain another target sequence of different miRNAs.
4. Random LNA may target other transcripts. If any adverse actions of the random LNA on the cells are observed, other control LNAs (anti-GFP or anti-Luciferase LNA which are not expressed in mammalian cells) can also be used as a control LNA.

Acknowledgments

This study was supported in part by Grant-in-Aid for JSPS fellows (19F19408 to T.A.) and Grant-in-Aid for Research activity start-up (19K24293 to S.O) from the Japan Society for the Promotion of Science and Grant-in-Aid from the Uehara memorial foundation.

References

1. Bartel DP (2004) MicroRNAs genomics, biogenesis, mechanism, and function. Cell 116: 281–297. https://doi.org/10.1016/s0092-8674(04)00045-5
2. Bartel DP (2018) Metazoan MicroRNAs. Cell 173:20–51. https://doi.org/10.1016/j.cell.2018.03.006
3. Ha M, Kim VN (2014) Regulation of microRNA biogenesis. Nat Rev Mol Cell Biol 15: 509–524. https://doi.org/10.1038/nrm3838
4. Treiber T, Treiber N, Meister G (2018) Regulation of microRNA biogenesis and its crosstalk with other cellular pathways. Nat Rev Mol Cell Biol 20:1. https://doi.org/10.1038/s41580-018-0059-1
5. Baskin KK, Winders BR, Olson EN (2015) Muscle as a "mediator" of systemic metabolism. Cell Metab 21:237–248. https://doi.org/10.1016/j.cmet.2014.12.021
6. Rudnicki MA, Jaenisch R (1995) The MyoD family of transcription factors and skeletal myogenesis. BioEssays 17:203–209. https://doi.org/10.1002/bies.950170306
7. Bassel-Duby R, Olson EN (2006) Signaling pathways in skeletal muscle remodeling. Annu Rev Biochem 75:19–37. https://doi.org/10.1146/annurev.biochem.75.103004.142622

8. Schiaffino S, Reggiani C (2011) Fiber types in mammalian skeletal muscles. Physiol Rev 91: 1447–1531. https://doi.org/10.1152/physrev.00031.2010
9. Hasty P, Bradley A, Morris JH et al (1993) Muscle deficiency and neonatal death in mice with a targeted mutation in the myogenin gene. Nature 364:364501a0. https://doi.org/10.1038/364501a0
10. Rudnicki MA, Schnegelsberg PNJ, Stead RH et al (1993) MyoD or Myf-5 is required for the formation of skeletal muscle. Cell 75:1351–1359. https://doi.org/10.1016/0092-8674(93)90621-v
11. Nabeshima Y, Hanaoka K, Hayasaka M et al (1993) Myogenin gene disruption results in perinatal lethality because of severe muscle defect. Nature 364:532–535. https://doi.org/10.1038/364532a0
12. Millay DP, O'Rourke JR, Sutherland LB et al (2013) Myomaker is a membrane activator of myoblast fusion and muscle formation. Nature 499:301–305. https://doi.org/10.1038/nature12343
13. Wu H, Rothermel B, Kanatous S et al (2001) Activation of MEF2 by muscle activity is mediated through a calcineurin-dependent pathway. EMBO J 20:6414–6423. https://doi.org/10.1093/emboj/20.22.6414
14. Potthoff MJ, Wu H, Arnold MA et al (2007) Histone deacetylase degradation and MEF2 activation promote the formation of slow-twitch myofibers. J Clin Invest 117:2459–2467. https://doi.org/10.1172/jci31960
15. Lin J, Wu H, Tarr PT et al (2002) Transcriptional co-activator PGC-1 alpha drives the formation of slow-twitch muscle fibres. Nature 418:797–801. https://doi.org/10.1038/nature00904
16. Williams AH, Liu N, van Rooij E, Olson EN (2009) MicroRNA control of muscle development and disease. Curr Opin Cell Biol 21:461–469. https://doi.org/10.1016/j.ceb.2009.01.029
17. Liu N, Williams AH, Kim Y et al (2007) An intragenic MEF2-dependent enhancer directs muscle-specific expression of microRNAs 1 and 133. Proc Natl Acad Sci U S A 104: 20844–20849. https://doi.org/10.1073/pnas.0710558105
18. Rao PK, Kumar RM, Farkhondeh M et al (2006) Myogenic factors that regulate expression of muscle-specific microRNAs. Proc Natl Acad Sci U S A 103:8721–8726. https://doi.org/10.1073/pnas.0602831103
19. Chen J-F, Mandel EM, Thomson JM et al (2005) The role of microRNA-1 and microRNA-133 in skeletal muscle proliferation and differentiation. Nat Genet 38:228–233. https://doi.org/10.1038/ng1725
20. Kim HK, Lee YS, Sivaprasad U et al (2006) Muscle-specific microRNA miR-206 promotes muscle differentiation. J Cell Biol 174:677–687. https://doi.org/10.1083/jcb.200603008
21. van Rooij E, Quiat D, Johnson BA et al (2009) A family of microRNAs encoded by myosin genes governs myosin expression and muscle performance. Dev Cell 17:662–673. https://doi.org/10.1016/j.devcel.2009.10.013
22. Liu J, Liang X, Zhou D et al (2016) Coupling of mitochondrial function and skeletal muscle fiber type by a miR-499/Fnip1/AMPK circuit. EMBO Mol Med 8:1212–1228. https://doi.org/10.15252/emmm.201606372
23. Gan Z, Rumsey J, Hazen BC et al (2013) Nuclear receptor/microRNA circuitry links muscle fiber type to energy metabolism. J Clin Invest 123:2564–2575. https://doi.org/10.1172/jci67652
24. Wada S, Kato Y, Okutsu M et al (2011) Translational suppression of atrophic regulators by MicroRNA-23a integrates resistance to skeletal muscle atrophy. J Biol Chem 286:38456–38465. https://doi.org/10.1074/jbc.m111.271270
25. Schmittgen TD (2004) A high-throughput method to monitor the expression of microRNA precursors. Nucleic Acids Res 32:43e 43. https://doi.org/10.1093/nar/gnh040

Chapter 25

Targeted Lipidomics Analysis of Adipose and Skeletal Muscle Tissues by Multiple Reaction Monitoring Profiling

Xiyue Chen, Christina R. Ferreira, and Shihuan Kuang

Abstract

Lipid homeostasis is critical for maintaining normal cellular functions including membrane structural integrity, cell metabolism, and signal transduction. Adipose tissue and skeletal muscle are two major tissues involved in lipid metabolism. Adipose tissue can store excessive lipids in the form of triacylglyceride (TG), which can be hydrolyzed to release free fatty acids (FFAs) under insufficient nutrition states. In the highly energy-demanding skeletal muscle, lipids serve as oxidative substrates for energy production but can cause muscle dysfunction when overloaded. Lipids undergo fascinating cycles of biogenesis and degradation depending on physiological demands, while dysregulation of lipid metabolism has been increasingly recognized as a hallmark of diseases such as obesity and insulin resistance. Thus, it is important to understand the diversity and dynamics of lipid composition in adipose tissue and skeletal muscle. Here, we describe the use of multiple reaction monitoring profiling, based on lipid class and fatty acyl chain specific fragmentation, to explore various classes of lipids in skeletal muscle and adipose tissues. We provide a detailed method for exploratory analysis of acylcarnitine (AC), ceramide (Cer), cholesteryl ester (CE), diacylglyceride (DG), FFA, phosphatidylcholine (PC), phosphatidylethanolamine (PE), phosphatidylglycerol (PG), phosphatidylinositol (PI), phosphatidylserine (PS), sphingomyelin (SM), and TG. Characterization of lipid composition within adipose tissue and skeletal muscle under different physiological situations will provide biomarkers and therapeutic targets for obesity-related diseases.

Key words Fatty acid, Triacylglyceride/Triacylglycerol/triglyceride, Metabolism, Obesity, Lipidome, Multiple reaction monitoring profiling, Mass spectrometry

1 Introduction

Lipids are essential for human physiology, functioning as structural components of membranes, a medium for energy storage, and signaling molecules in modulating protein activity. Lipid metabolic network is highly dynamic and comprises thousands of molecular lipid species that participate in the regulation of cellular processes and systemic circulation during physiological adaptations [1] (Fig. 1). Adipose tissue is the main site for lipid storage and mobilization. In fed states, adipocytes can uptake, esterificate, and store lipids in the form of triacylglyceride (TG). The stored lipids can

Atsushi Asakura (ed.), *Skeletal Muscle Stem Cells: Methods and Protocols*, Methods in Molecular Biology, vol. 2640, https://doi.org/10.1007/978-1-0716-3036-5_25,

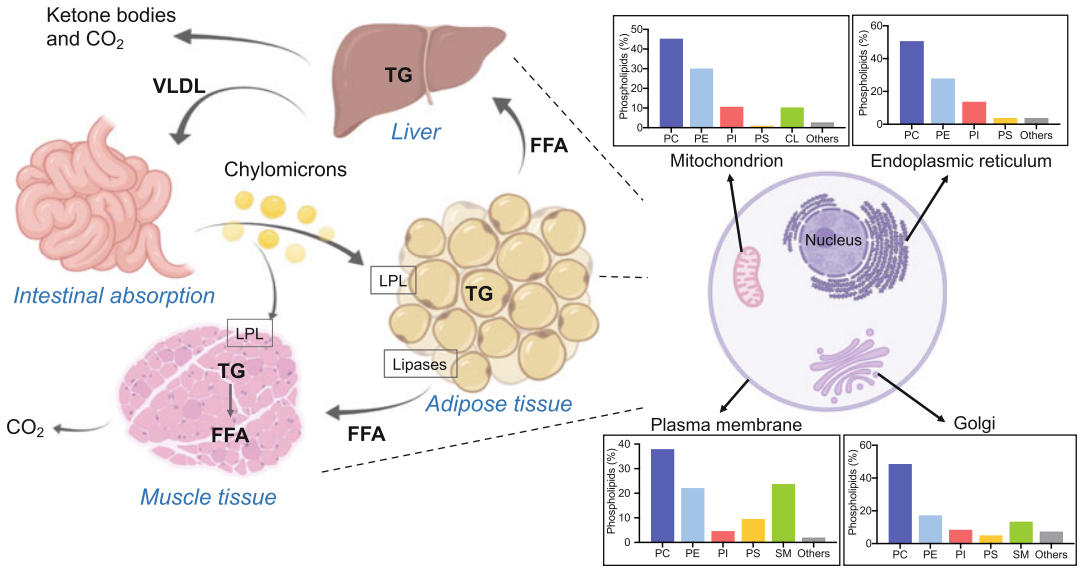

Fig. 1 Lipid metabolic network and lipid composition of different membranes vary throughout the cell. The left panel shows the general lipid metabolic process in mammals. Chylomicrons from the small intestine enter the blood circulation and deliver TG to tissues expressing lipoprotein lipase (LPL) such as adipose and muscle tissue. Adipose tissues can hydrolyze stored TG and release FFA into the plasma. The liver takes up FFAs and liberates very-low-density lipoprotein (VLDL) particles. Muscles are primary metabolic tissues, consuming FFA for oxidation. In mammal cells, lipid compositions of different membranes are shown in the right panel. The lipid compositional data expressed as a percentage of the total phospholipid (PL) in mammals are adapted from Ref. [7]. Major PLs assembled are PC and PE for most organelles including some small portion of PI, PS, and cardiolipin (CL). (Created with Biorender.com)

undergo lipolysis to facilitate free fatty acid (FFA) flux in the circulation when nutrition is limited. Skeletal muscle is responsible for a large proportion of lipid mobilization in the whole body. Lipids delivered to muscle serve as substrates for oxidation, during which FFA from extracellular and intracellular sources are utilized to generate energy to support muscle contraction. As bioactive metabolites and energy suppliers, lipids are also important for muscle development and regeneration. Lipid composition is dynamic during muscle development, indicated by different lipidomes between skeletal muscle in vivo and primary myotubes cultured in vitro from human samples [2] (Fig. 2). After cardiotoxin (CTX)-induced injury in muscle, lipid remodeling is correlated with muscle satellite cells activation, inflammatory responses, and membrane reconstruction in the mouse model [3–5] (Fig. 2). Ectopic lipid deposition in muscle results from either a limited capacity of adipose tissue to accumulate lipid or impaired cellular regulation of lipid storage and utilization, and appears to trigger not only insulin resistance but also muscle functional decline and degeneration. Thus, understanding the dynamics of lipid accumulation and mobilization in adipose and skeletal muscle tissue is

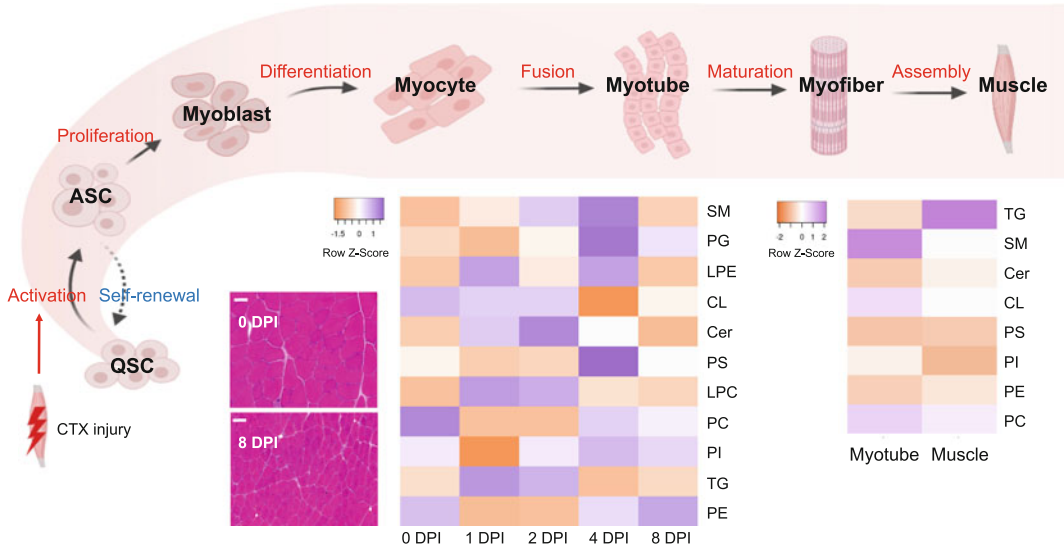

Fig. 2 Dynamic lipid composition during muscle development and regeneration. During normal muscle growth and in response to injury, quiescent satellite cells (QSCs) are activated, becoming satellite cells (ASCs). Some ASCs undergo self-renewal to re-enter a quiescent status for further myogenesis. ASC can also proliferate and differentiate, ultimately giving rise to myofibers and mature muscle tissue. Lipid compositions in skeletal muscle tissues and primary myotubes of human subjects shown in the lower-right panel are adapted from Ref. [2]. The lower-left panel shows morphology and lipid profiles of the tibialis anterior (TA) muscle after selected time points after CTX-induced injury adapted from Ref. [3]. (Created with Biorender.com)

crucial for developing potential targets and biomarkers for disease therapeutics.

As the central component of cellular membranes, the lipid bilayer provides a functional barrier between subcellular compartments and between the cell and its environment. Variance in lipid composition affects membrane physical properties and protein functions [6]. For example, polyunsaturated fatty acids (PUFAs) in glycerophospholipids reduce membrane rigidity. The high diversity of lipids among different cell types, organelles, membranes, and membrane subdomains highlights its importance in cellular functions [7, 8] (Fig. 1). Most membrane lipids are glycerol-based phospholipids, including PS, PE, PG, PC, and PI. Differences in sidechains and head structure diversify their distribution and biological function. PGs are synthesized in and confined to mitochondria, while PCs and PEs are essential for the functional embedding of membrane proteins and membrane fusion and fission [9]. In addition, sphingolipids and sterols are enriched in the plasma membrane and endosomes, where they play a key role in membrane structure and signaling. Therefore, it is important to understand how membranal lipid compositions change in response to cellular adaptation under different situations.

Technological developments, especially in mass spectrometry (MS) and bioinformatics, have led to new insights into global lipid

diversity. Lipidomics is a lipid-targeted metabolomics approach for the comprehensive analysis of lipid profiles [10]. Since each lipid class has its own patterns of fragmentation and specific ionization efficiency, a major bottleneck in lipidomics is the lack of a standardized method to detect all lipid classes due to the chemical diversity of the lipidome. Even though combining the separation power of high-performance liquid chromatography (HPLC) adds retention time as a layer of selectivity to increase specificity for lipid identification, this LC-MS method has polarity selection and requires specialized software and user expertise to visualize and interpret the complicated quantitation of each spectrum [11]. Identification of lipids via tandem mass spectrometry depends on the structural differences in both class-specific head groups and fatty acyl chains. In order to establish a lipidomics approach that interrogates lipids based on their structural features, we applied multiple reaction monitoring (MRM) profiling to explore the lipid composition of lipid extracts from adipose and skeletal muscle tissues. This is a method of direct injection, and the methodological details have recently been reviewed in detail [12]. The detection of lipid functional groups by precursor (Prec) and neutral loss (NL) scans is based on the predicted ionized product ions or neutral losses diagnostic of the lipid class or of a lipid structural component, such as the fatty acyl chains. Information obtained by Prec and NL scans is converted into MRM lists for sample screening, and the relative abundancies of the MRMs are considered as the chemical profile for each sample. Since the use of internal standards (IS) are acceptable for some lipid classes, lipidomics can be semi-quantitative and performed without the need for chromatographic separation [13]. Compared with other exploratory lipidomics approaches, MRM profiling does not include full mass or product ion scans to obtain the lipid profile. These scans modes can be used in a further step for structural confirmation. The method neither uses high mass resolution measurements nor liquid chromatography (LC) separation. These features confer to the MRM profiling the ability to profile compounds by their class or chemical functionalities in a fast (no LC separation) and sensitive (by MRM scans) way.

Here, by using MRM profiling, we describe an exploratory workflow for target lipidomics focused on a collection of 1591 MRMs related to 12 lipid classes. These MRMs were established by combining expected precursor ions listed at the Lipid Maps LIPID MAPS® Structure Database (LMSD) and product ions or neutral losses diagnostic of the lipid class of the fatty acyl compositions. The data generated by MRM profiling are bidimensional (MRMs and ion intensities), conferring less complexity in data manipulation and streamlining data interpretation and planning of further research and analytical efforts.

2 Materials and Instrumentation

Organic solvents should be at least of analytical grade (ideally HPLC grade). Chemical and biohazard waste disposal regulations should be followed.

2.1 Samples

Fresh or flash-frozen adipose and skeletal muscle samples can be used. Tissue weight should be recorded before homogenization. Ideally, similar amounts of tissue should be used in lipid profiling. Samples containing fixatives (e.g., formaldehyde), detergents, or embedded in paraffin are not recommended due to the loss of lipid content and the introduction of contaminants in MS analysis [14].

2.2 Materials

1. Dilution solvent: methanol:chloroform {3:1 (v/v)}.
2. Injection solvent: 300 mM acetonitrile:methanol:ammonium acetate {3:6.65:0.35 (v/v)}.
3. Lipidomix quantitative mass sepc internal standard (IS) (Avanti Lipids EquiSPLASH, #330731) (*see* **Note 1**).
4. CK14 soft tissue homogenizing kit, tubes with screw cap and skirt (Precellys CK 14, Bertin Corp, part # P000912-LYSK0A).
5. Screw Thread Glass Vials with ID Patch, Flat Bottom (2 mL).
6. Polypropylene plastic, screw-top vial, 300 uL, with L/N cap and bonded pre-slit PTFE/Silicone septa (#186002639, Waters Corp).
7. PEEK Coated Fused Silica Capillaries (Agilent G1375-87324).

2.3 Equipment

1. Precellys tissue homogenizer (Bertin Corp, Rockville, MD, USA).
2. Swing-bucket centrifuge (Thermo Scientific, model: CL2).
3. Speedvac centrifuge (Savant Speedvac, Thermo Scientific Inc., San Jose, CA, USA).
4. Micro-autosampler (G1377A).
5. Agilent 6410 triple quadrupole mass spectrometer (Agilent Technologies, Santa Clara, CA, USA).

2.4 Software

1. MetaboAnalyst 5.0 software (https://www.metaboanalyst.ca) statistical analysis tool. There are MetaboAnalyst tutorials explaining the workflow of the statistical analysis included in this freeware [15, 16]. We have used a data format from test data that can be downloaded from the software's test data. The test data files available for MS peak intensities (LC-MS peak intensity table for 12 mice spinal cord samples [17]. Group 1-wild-type; group 2 – knock-out) are a good resource for the types of file formatting necessary to be followed for an upload.
2. Graphpad Prism Software Version 8.0.1.

3 Methods

Carry out all procedures on ice unless otherwise specified.

3.1 Lipid Extraction

1. Lipid extraction is performed according to the Bligh & Dyer extraction method [18] (*see* the workflow in Fig. 3).
2. The used amount of adipose tissue is 50 mg and skeletal muscle is 10 mg for each profiling, but lower amounts (10–100X) can be used.
3. Transfer the sample to a 2 mL tissue homogenizing tube (Precellys CK 14; other tissue homogenizer kits can be used).
4. Add 500 μL of ultrapure water to homogenize the sample using the Precellys tissue homogenizer at three cycles of 6200 rpm for 20 s (*see* **Note 2**).
5. Transfer 200 μL of homogenized tissue to a new microtube (*see* **Note 2**) and mix with 250 μL of chloroform and 450 μL of methanol (one-phase solution) (*see* **Note 3**).

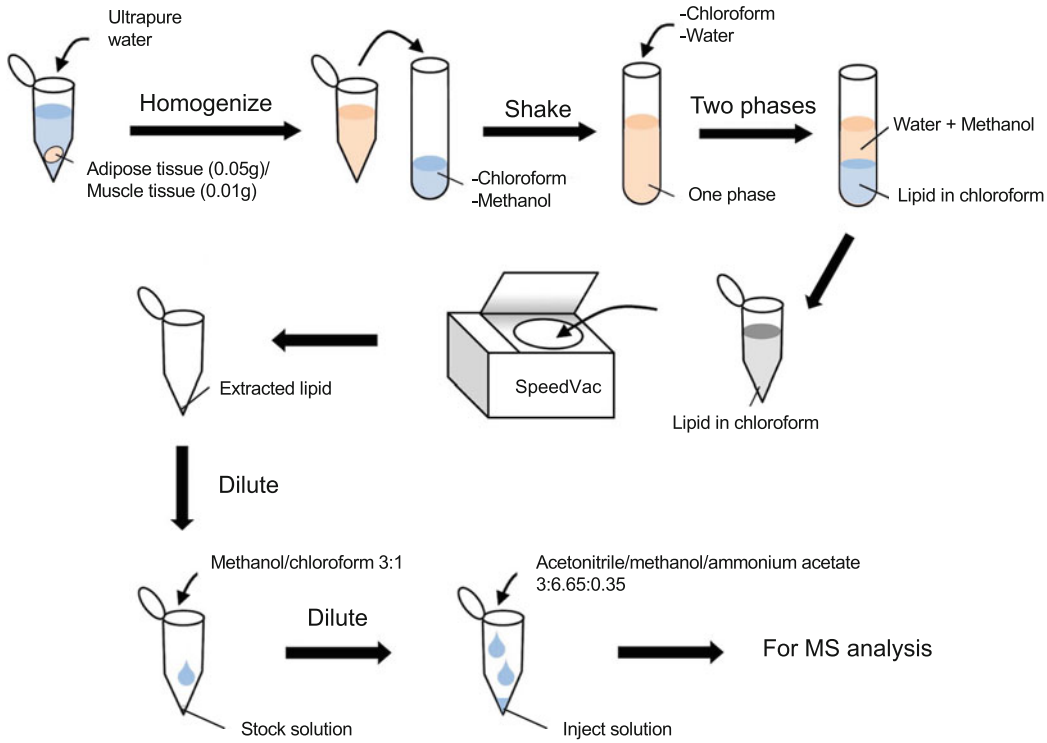

Fig. 3 Workflow for lipid extraction by the Bligh and Dyer method. Samples are homogenized and exposed to organic solvents (chloroform and methanol). Different ratios of water/chloroform and methanol are used to create a one- or two-phase solution. In the latter one, the chloroform forms the bottom phase and concentrates the lipids. After separation by centrifugation, the bottom phase is transferred to a new vial and the lipid extract is dried using a vacuum concentrator

6. Incubate for 15 min at 4 °C with gentle shaking for two times.
7. Add 250 μL of chloroform and 250 μL of ultrapure water. Incubate for 5 min at room temperature.
8. Centrifuge the sample for 10 min at 16,000× *g*. A 2-phase solution is generated, and the bottom phase is an organic phase containing the lipids (*see* **Notes 4** and **5**).
9. Transfer the organic phase to a new tube and dry it using a vacuum concentrator (*see* **Note 6**).
10. Dilute the dried lipid extracts in 500 μL of dilution solvent as stock solution.

3.2 Targeted Lipid Exploratory Analysis by MRM Profiling Methods

1. Targeted lipid profiling of adipose and muscle tissue samples is performed using the discovery MRM profiling methods as previously reported [19] (*see* **Note 7**). Detailed workflow for constructing MRM lists using MRM profiling methods is explained in the *video* (https://youtu.be/XkbDiWE_vbA). These methods have been run in an Agilent 6410 mass spectrometer. Other details of the instrumentation settings have been described [19]. Method settings should be specifically optimized for the mass spectrometer.
2. Constitutional isomers are combined into one single entry in which only the lipid class, number of total fatty acyl residues, and unsaturation number are listed.
3. Twelve classes of lipids are included in this protocol. For each lipid class, one sample injection was performed. The lipids classes screened included AC, Cer, CE, DG, FFA, PC, PE, PG, PI, PS, SM, and TG. The IS are available for nine of them (TG, DG, CE, PC, SM, PE, PS, PI, and PG) in the EquiSPLASH lipidomix.
4. TG and DG lipids are profiled based on the NL of the esterified fatty acyl residues [14]. FFAs are profiled by monitoring the precursor ions. CE, ceramides, and phospholipids are profiled in Table 1 (*see* **Notes 8** and **9**).

3.3 Instrument and Pump Settings

1. Autosampler.
2. A capillary pump is connected to the autosampler and operated at a flow rate of 7 μL/min and pressure of 150 bar with the use of restrictive capillary, since there is no column to provide back pressure to the pump. The capillary voltage on the instrument is 3.5–5 kV and the gas flow 5.1 L/min at 300 °C.
3. MS electrospray ion source parameters: gas temperature 300 °C, gas flow 11 L/min, Nebulizer 15 psi, and capillary voltage 4 Kv both for positive and negative ion modes.

Table 1
Typical productions and neutral losses of selected lipid classes and fatty acyl chains used as the basis of the MRM profiling methods used in this research

Lipid class	Precursor ion	Typical fragment	References
Phophatidylcholine (PC) and sphingomyelin (SM)	[M + H]+	*m/z* 184.1 (phosphoryl choline)	[20]
Phosphatidylethanolamine (PE)	[M + H]+	Neutral loss of 141 Th (phosphorylethanolamine)	[20]
Cholesteryl esters (Chol esters)	[M + H]+	*m/z* 369.2	[21]
Phosphatidylinositol (PI)	[M + NH_4]+	Neutral loss of 277 Th (phosphoryl inositol + NH_4)	[20]
Phosphatidylserine (PS)	[M + H]+	Neutral loss of 185.1 Th (phosphorylserine)	[20]
Phosphatidylglycerol (PG)	[M + NH_4]+	Neutral loss of 189 Th (phosphoryl glycerol + NH_4)	[20]
Ceramides (d18:1; sphingosines) and cerebrosides	[M + H]+	*m/z* 264.2	[22, 23]
Ceramides (d18:0; sphingosines)	[M + H]+	*m/z* 266.2	[22, 23]
Ceramides (d20:1)	[M + H]+	*m/z* 292.2	[22, 23]
Ceramides (t18: 0 4-hydroxysphinganines)	[M + H]+	*m/z* 282.2	[22, 23]
Glycerolipids containing dodecanoic acid acyl chain	[M+H]+ and [M+NH_4]+	Neutral loss of 217 Th (phosphoryl glycerol + NH_4)	[24]
Glycerolipids containing myristic acid acyl chain	[M+H]+ and [M+NH_4]+	Neutral loss of 245 Th (phosphoryl glycerol + NH_4)	[24]
Glycerolipids containing myristoleic acid acyl chain	[M+H]+ and [M+NH_4]+	Neutral loss of 257 Th (phosphoryl glycerol + NH_4)	[24]
Glycerolipids containing palmitoleic/ sapienic acid acyl chain	[M+H]+ and [M+NH_4]+	Neutral loss of 271 Th (phosphoryl glycerol + NH_4)	[24]
Glycerolipids containing palmitic acid acyl chain	[M+H]+ and [M+NH_4]+	Neutral loss of 273 Th (phosphoryl glycerol + NH_4)	[24]
Glycerolipids containing -Gama-linolenic acid acyl chain	[M+H]+ and [M+NH_4]+	Neutral loss of 295 Th (phosphoryl glycerol + NH_4)	[24]
Glycerolipids containing linoleic/ linoelaidic acid acyl chain	[M+H]+ and [M+NH_4]+	Neutral loss of 297 Th (phosphoryl glycerol + NH_4)	[24]
Glycerolipids containing oleic/ elaidic/vaccenic acyl chain	[M+H]+ and [M+NH_4]+	Neutral loss of 299 Th (phosphoryl glycerol + NH_4)	[24]
Glycerolipids containing stearic acid acyl chain	[M+H]+ and [M+NH_4]+	Neutral loss of 301 Th (phosphoryl glycerol + NH_4)	[24]
Glycerolipids containing eicosapentaenoic acid acyl chain	[M+H]+ and [M+NH_4]+	Neutral loss of 319 Th (phosphoryl glycerol + NH_4)	[24]
Glycerolipids containing arachidonic acid acyl chain	[M+H]+ and [M+NH_4]+	Neutral loss of 321 Th (phosphoryl glycerol + NH_4)	[24]

(continued)

Table 1
(continued)

Lipid class	Precursor ion	Typical fragment	References
Glycerolipids containing eicosatrienoic acyl chain	[M+H]+ and [M+NH_4]+	Neutral loss of 323 Th (phosphoryl glycerol + NH_4)	[24]
Glycerolipids containing eicosadienoic acyl chain	[M+H]+ and [M+NH_4]+	Neutral loss of 325 Th (phosphoryl glycerol + NH_4)	[24]
Glycerolipids containing gondoic acid acyl chain	[M+H]+ and [M+NH_4]+	Neutral loss of 327 Th (phosphoryl glycerol + NH_4)	[24]
Glycerolipids containing arachidic acid acyl chain	[M+H]+ and [M+NH_4]+	Neutral loss of 329 Th (phosphoryl glycerol + NH_4)	[24]
Glycerolipids containing docosahexaenoic DHA acyl chain	[M+H]+ and [M+NH_4]+	Neutral loss of 345 Th (phosphoryl glycerol + NH_4)	[24]
Glycerolipids containing eicosapentaenoic acid EPA acyl chain	[M+H]+ and [M+NH_4]+	Neutral loss of 347 Th (phosphoryl glycerol + NH_4)	[24]
Glycerolipids containing docosatetraenoic acid acyl chain	[M+H]+ and [M+NH_4]+	Neutral loss of 349 Th (phosphoryl glycerol + NH_4)	[24]
Glycerolipids containing docosadienoic acyl chain	[M+H]+ and [M+NH_4]+	Neutral loss of 353 Th (phosphoryl glycerol + NH_4)	[24]
Glycerolipids containing erucic acid acyl chain	[M+H]+ and [M+NH_4]+	Neutral loss of 355 Th (phosphoryl glycerol + NH_4)	[24]
Glycerolipids containing behenic acid acyl chain	[M+H]+ and [M+NH_4]+	Neutral loss of 357 Th (phosphoryl glycerol + NH_4)	[24]
Glycerolipids containing lignoceric acid acyl chain	[M+H]+ and [M+NH_4]+	Neutral loss of 385 Th (phosphoryl glycerol + NH_4)	[24]

3.4 Quality Control (QC) and Blank Samples

1. As sample blank we use injection solvent. The use of blank extracts is also recommended.
2. Quality control samples should be used throughout the acquisition to monitor instrument performance. These samples should present similar chromatograms (Fig. 4) and can be delivered every 10–15 injections. Any method and any sample can be used as QC. We recommend using a method for monitoring the different isotopically labeled lipid classes present in the Avanti Equisplash mix.

3.5 Data Acquisition

1. The lipid stock solution is further diluted in injection solvent.
2. The dilution factor of the lipid extracts is determined by the amount of signal obtained for the most abundant lipid class. Different amounts of lipid classes occur in adipose tissue (the most abundant lipid class is TG lipids) compared to skeletal muscle (the most abundant lipid class is PCs; Fig. 5). This step is important for establishing the appropriate dilution factor for

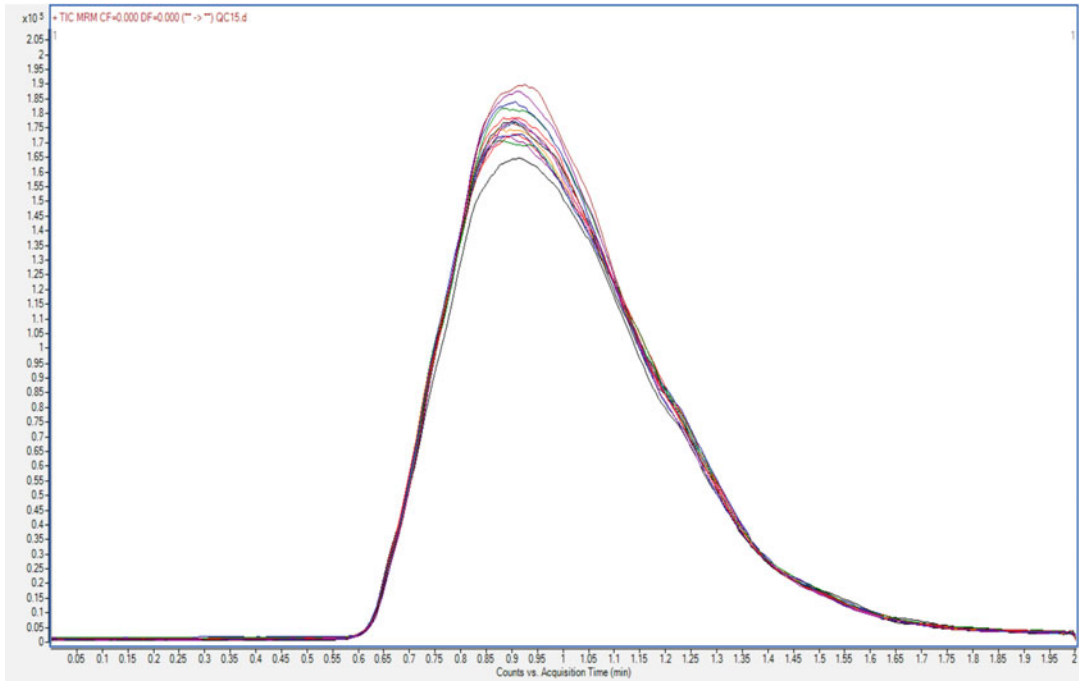

Fig. 4 Overlay of the total ion chromatograms for 16 quality control (QC) samples run for the profiling of muscle and adipose tissues. These QC samples are simply the Avanti Equiplash mix diluted in injection solvent at the concentration of 0.4 ng/injection and the method used to monitor the QC sample has the MRMs for 13 isotopically labeled lipids of this lipid standard mixture

each sample type to avoid over-diluting and obtaining a low signal, or over-concentrating and causing signal saturation and instrument contamination issues (Fig. 6). For the Agilent 6410 mass spectrometer used, we have observed sample total ion chromatograms (TIC) with the ideal peak between $5e^5$ and $2e^6$ ion counts at the peak of the chromatogram. Therefore, different dilutions are tested in order to reach appropriate ion count intensities, and this can vary according to the instrument. For the amounts recommended at the extraction procedure, we have diluted the lipid extracts by a factor of 500 for samples of adipose tissues and 100 for samples of muscle tissue, and each injection corresponded to approximately 16 μg of tissue.

3. After the sample dilution factor is determined, the sample is diluted with injection solvent having a final concentration of 0.1 ng/uL of IS mix.
4. 8 μL of the sample (total amount of 0.8 ng of IS mix) is delivered to the mass spectrometer electrospray ion source using the micro-autosampler.
5. One sample injection is performed for each lipid class and data is acquired over two minutes (*see* **Note 10**).

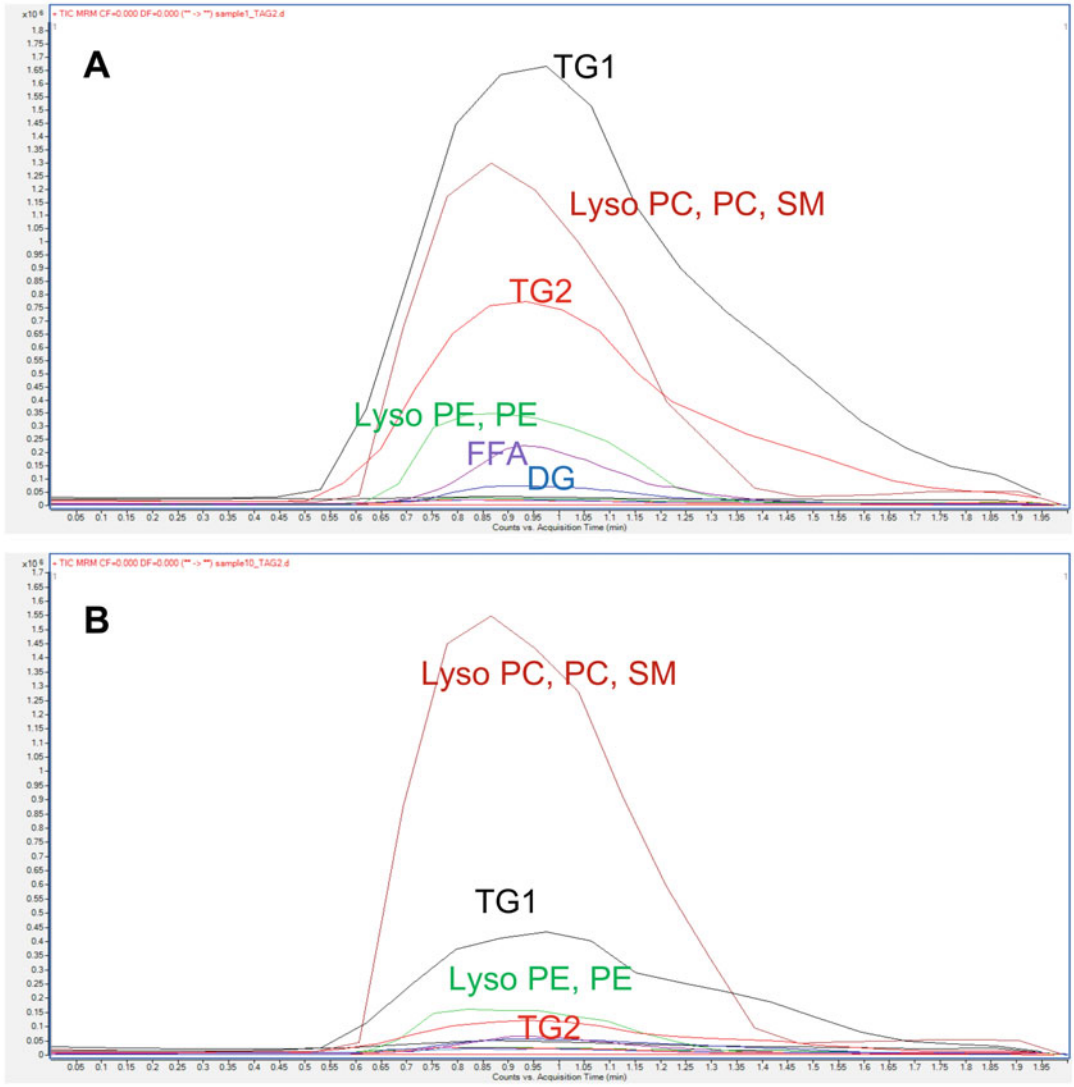

Fig. 5 Overlay of the total ion chromatograms obtained in two minutes of data acquisition by direct sample injection for the different lipid classes monitored by the MRM profiling methods in (**a**) one adipose and (**b**) one muscle sample tissue lipid extract. The lipid classes presenting the highest ion signals are labeled (lysopohosphatidylcholine – Lyso PC, PC, SM, Lyso phosphatidylethanolamine – Lyso PE, TG, 2 lists of MRMs, *see* **Note 9**). In the adipose tissue the TG 1 list (TGs containing C16:0, C16:1, C18:0, and C18:1) generates the most abundant total ion signal, while in muscle Lyso PC, PC and SM lipids are the most abundant

3.6 Data Analysis

1. Raw MS data are processed for each lipid class using an in-house script and lists containing MRM transitions. By doing that, the MRMs and respective ion intensity values are exported to Microsoft Excel.
2. Usually in a profiling experiment all ions with ion intensities higher than those of the blank samples are used. Here, to avoid carrying the background noise of MRMs to the statistical

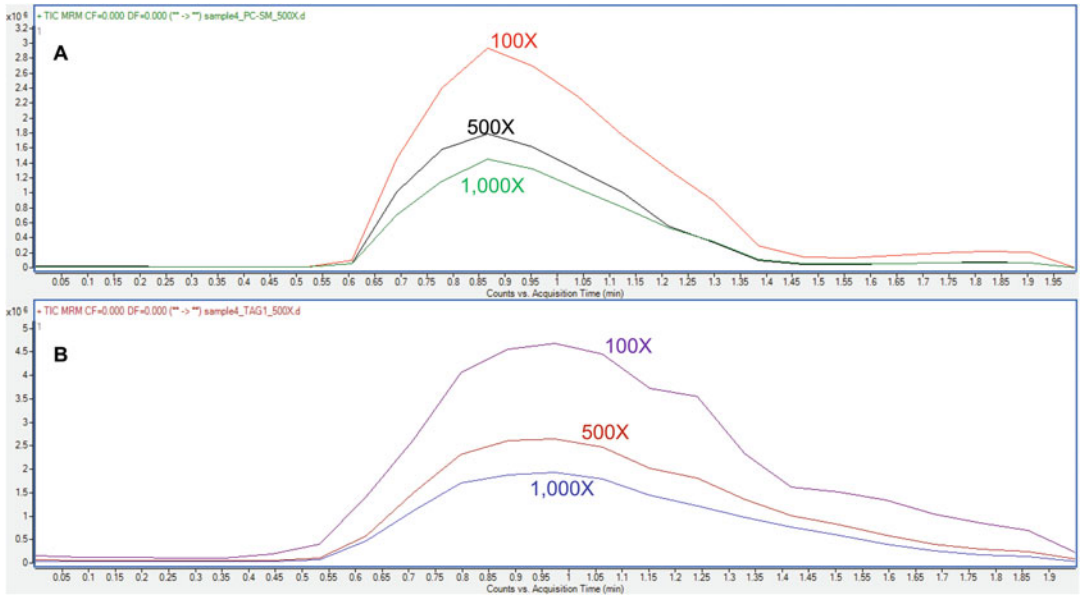

Fig. 6 Total ion chromatograms for different dilutions (100×, 500×, and 1000×) of the resuspended lipid extracts (stock solutions) in injection solvent for a sample of adipose tissue. In (**a**) total ion intensities for the profiling of PC and SM lipids are shown. In (**b**) the total ion intensities for the TG1 method are shown and higher than for the PC and SM due to the nature of this sample. Dilutions of 100×, for this specific sample, provide a higher ion signal, but it lasts too long, increasing the chances of sample carryover and instrument contamination. Therefore, a dilution factor of 500× or preferentially 1000 should be recommended for this sample

analysis, we apply an ion count threshold. Only MRMs that yielded a signal equal to or above 1.3-fold of the level seen in blank samples were selected for analysis.

3. When analyzing the relative amount of lipids, each method is considered an experiment, and therefore, the statistical analysis is performed class by class. Values of ion intensities for each of the MRMs monitored are normalized by the total ion intensity of all MRMs in the method for a given sample (*see* **Note 11**).
4. When analyzing the relative quantity of lipids, response ratios are calculated by dividing the values of ion intensities for each of the MRMs monitored by the ion intensity of the IS and multiplied by 0.8 ng (or by the amount of IS added). If different amounts of tissue are used among the samples, normalization of the total amounts (ng) by tissue weight should be performed.
5. Univariate and multivariate statistical analyses are then performed using MetaboAnalyst 5.0 software [15, 16]. Uploaded data (relative ion amounts or quantification data) should be auto-scaled and processed. Volcano plots (Fold change threshold 2, *P* value threshold 0.05) are used to compare the absolute value of change among groups. Principal component analysis (PCA) score plots are used to observe if the lipid profiles

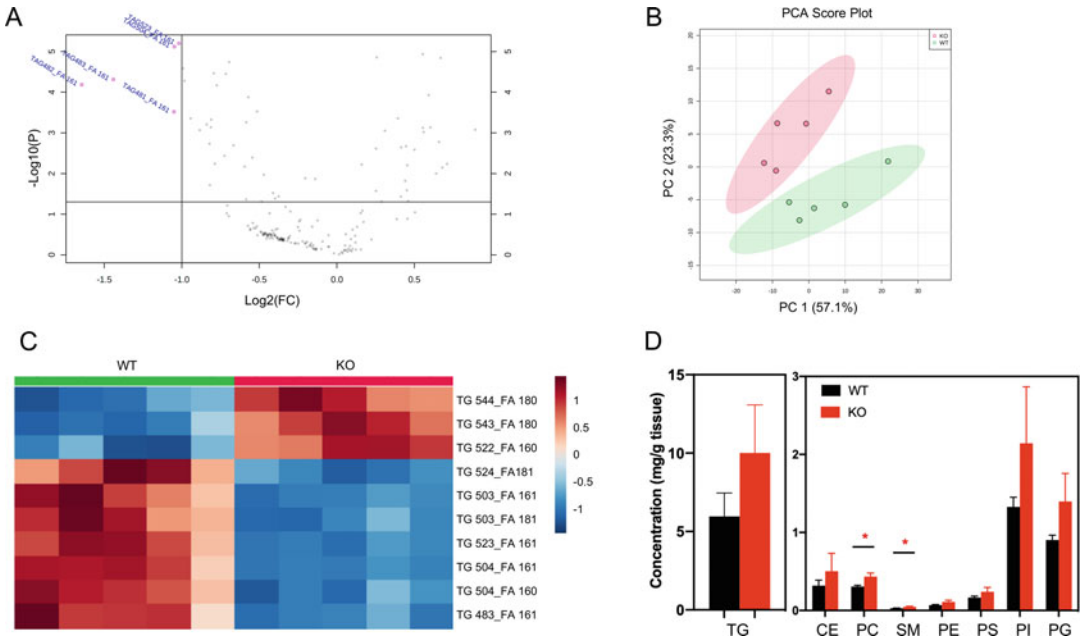

Fig. 7 Typical lipid profile results adapted from Ref. [25]. (**a**) Volcano plot of TG lipids with *P* values < 0.05 and fold change threshold of 2 between the two groups. (**b**) Principal component analysis (PCA) of TG lipids between two groups. (**c**) Heatmap of top ten significant TG lipids between two groups. (**d**) Relative quantification of TG, CE, PC, SM, PE, PI, PG, and PS

changed according to the treatment, and loading plots are used to identify lipids up- or down-regulated according to the experimental group in a non-supervised strategy. Heatmaps are plotted with distance measured by Euclidean and algorithm clustered by Ward to visualize different lipid compositions. Typical results adapted from Ref [25] are shown in Fig. 7.

6. Fold change is calculated by dividing values of ion intensities for each of the MRMs measured in each sample by the ion intensity of the corresponding MRM in the blank. Average fold change is graphed for significantly different lipid species using Graphpad 8.0.1 Prism Software.
7. Changes between groups are analyzed by Student's t-test. *P* values < 0.05 are considered significant.

3.7 Comments on Biological Interpretation of MRM Lipid Profiling

The MRM profiling strategy allows lipid profiling in a quick and reliable manner for major lipid components. However, this method has a limitation in detecting unexpected lipid species and is particularly susceptible for overlapping isobaric compounds.

An example of the MRM profile has been presented recently and differences in both relative abundance and quantality have been found in several classes like TG, FFA, PC, and SM [25] (Fig. 7). When conducting biological interpretation for lipid remodeling, it is important to consider the main biological function of each class.

For instance, dysregulated TG and FFA suggest alternation in lipid metabolism, while PC and SM determine membrane bilayer structures and signaling transport. As an illustrative example, the presence of an increased ratio of FFA C18:1/C16:0 shown in our previous result indicates defective de novo lipid synthesis [25].

Another important tip to keep in mind is that the lipid profile represents the end products of metabolism or regulation, which depend on metabolic upstream events including gene expression and protein activity, as well as lipid utilization. Thus, it is important to do sampling at the right time, especially for muscle regeneration studies using the injury model. For instance, almost all of the lipid classes in muscle tissue showed increase at 14 days post-glycerol-induced injury [26], while another study showed fluctuations for several lipid classes (TG: reduced first and rose again, PG and PC: increase fist and then drop) in the CTX-injured model [3]. Possible explanations for the variation are either the different responses toward glycerol and CTX-induced injury model, or certain lipid responses in a short window can only be identified at certain time points. For example, signaling and structural lipids like PC and PI may be committed for muscle satellite cells activation and proliferation at an early stage and lose their importance during muscle maturation. So, timing should be decided based on specific aims and pilot experiments.

4 Notes

1. The IS can be spiked before or after the sample extraction. It is recommended that they are added before sample extraction. Nonetheless, that may require testing of the amounts to be added. Therefore, for the lipid exploratory profiling, injection solvent can be spiked with the IS mixture after defining the ideal concentration of the lipid extract to be used, as described in Subheading 3.3.
2. If the sample amounts are different, add water for homogenezing according to the sample weight, such as 20 μL/mg of tissue. The 300 μL homogenized tissue left can be stored at −80 °C as a backup sample or only 300 μL can be added in total if there is less tissue amount available for the research.
3. Adding chloroform and methanol to the mixture should form an one-phase solution. If more than one phase is formed, add more methanol until there is only one phase. If you add methanol to one sample, do the same for all others in the experiment. The amount of 0.01% of the antioxidant butylated hydroxytoluene (BHT) can be added to chloroform to better preserve the lipids after extraction and also to avoid the formation of carbony chloride over time in the solvent.

4. The use of methanol and chloroform promotes protein precipitation and forms another layer between the organic and non-organic layer. Both the non-organic and protein layer should be removed carefully to avoid contaminating the lipid extract.
5. The upper phase can be used for metabolite screening or quantification experiments.
6. The dried lipid extracts should be stored at −80 °C until dilution. We don't recommend using lipid extracts beyond two months of storage as lipid profiles change beyond 2 months of storage, as indicated by the MRM profiling data of mouse tissue extracts [27].
7. The list of MRMs is generated by combining the *m/z* for the molecular ion based on the form LipidMAPS online database (http://www.lipidmaps.org/) with selected production resulting from the Prec or NL scan for each class. Only even-chain lipids are included in the experiments reported but the methods are flexible. It is noticeable that lists downloaded from the Lipid MAPS structure database (LMSD) have monoisotopic masses instead of average mass.
8. TGs and DGs are based on ammonium adducts of parent ions and neutral losses only for the fatty acyl chains that are most common in mammalian cells, which are palmitic, palmitoleic, stearic, oleic, and linoleic. TGs are also screened for arachidonic acid fatty acyl chain presence. Because of the diverse fatty acyl chains monitored, the MRMs for the TGs have been split into two methods (TG1 and TG2). The abbreviation of TGs and DGs is given by the class abbreviation (TG or DG) followed by the fatty acyl chain targeted with the MRM product ion, and underline ("_") and the number of carbon and unsaturation remaining in the fatty acyl chain(s), for example, DG 18:1_18:1 or TG 16:0_32:3. ACs include five or six MRMs for each one. The MRM containing the product ion of *m/z* 85.1 is expected to be the most abundant one and it is used for statistical analysis. The other MRMs can be evaluated if necessary, as an extra set of information supporting the presence of the specific acyl-carnitine. The precursor ion scan for the Cers is based on Merrill [28]. All MRM profiling methods including the MRMs related to deuterated IS for phospholipids, DG, TG, and CE included 1,591 MRMs, but these methods are easily expandable and should be updated as the Lipid Maps database continuously expands.
9. The number of MRMs recommended for each sample injection depends on the duration of the ion signal obtained for the sample. If lower flow rates or higher volumes of samples are injected, the duration of the ion signal will be longer. In our conditions, we observed that 7–10 μL/min solvent flow rates

and 8 μL of diluted lipid extract proportionate around 45–60 s of ion signal. Since the scan rate is 25 ms, by adding up to 200 MRMs in each method it is possible to sum around 10 scans/MRM. Since for the TGs we monitored six fatty acyl residues (C16:0, C16:1, C18:0, C18:1, C18:2, and C20:4), the total number of MRMs is 335. We therefore split these MRMs into two different lists (TG1 and TG2) and two sample injections are performed to screen for TG.

10. One sample injection is performed for the screening of each lipid class, and this is referred to as the discovery phase. For experiments with a large number of samples or when microscopic samples are analyzed, selected MRMs related to lipids from different classes (profiled by NL and Prec scans or directly by MRM targeted methods) can be monitored in the same sample injection (screening phase) [12, 19, 24, 29–35].
11. In this protocol we use one sample injection for each lipid class. Sample ion signal with direct sample injection under the conditions reported here is short (around 45 s). Therefore, the MRM lists should not be very extensive. It is possible to combine diverse lipid classes in the same sample injection, but this is usually done after experiments establishing which MRMs are detectable or of interest in a small set of samples. When a pool or few samples are screened for a large amount of MRMs, and only the MRMs presenting higher ion signals in actual samples than the blank sample are selected for the screening of a larger number of samples, these steps are named "discovery" and "screening", respectively.

Acknowledgments

This work is partially supported by the National Institute of Health (NIH) to S. K. (R01DK132819, R01AR079235, R01AR078695, R01CA212609).

References

1. Frayn KN, Arner P, Yki-Järvinen H (2006) Fatty acid metabolism in adipose tissue, muscle and liver in health and disease. Essays Biochem 42:89–103
2. Loizides-Mangold U, Perrin L, Vandereycken B et al (2017) Lipidomics reveals diurnal lipid oscillations in human skeletal muscle persisting in cellular myotubes cultured in vitro. Proc Natl Acad Sci U S A 114:E8565–E8574
3. Giannakis N, Sansbury BE, Patsalos A et al (2019) Dynamic changes to lipid mediators support transitions among macrophage subtypes during muscle regeneration. Nat Immunol 20:626–636
4. Forcina L, Cosentino M, Musarò A (2020) Mechanisms regulating muscle regeneration: insights into the interrelated and time-dependent phases of tissue healing. Cells 9:1297
5. Oprescu SN, Yue F, Qiu J et al (2020) Temporal dynamics and heterogeneity of cell populations during skeletal muscle regeneration. iScience 23:100993

6. Harayama T, Riezman H (2018) Understanding the diversity of membrane lipid composition. Nat Rev Mol Cell Biol 19:281–296
7. Meer GV, Voelker DR, Feigenson GW (2008) Membrane lipids: where they are and how they behave. Nat Rev Mol Cell Biol 9:112–124
8. Paolo GD, Camilli PD (2006) Phosphoinositides in cell regulation and membrane dynamics. Nature 443:651–657
9. Meer GV, Kroon AIPMD (2011) Lipid map of the mammalian cell. J Cell Sci 124:5–8
10. Han X, Gross RW (2003) Global analyses of cellular lipidomes directly from crude extracts of biological samples by ESI mass spectrometry: a bridge to lipidomics. J Lipid Res 44: 1071–1079
11. Köfeler HC, Fauland A, Rechberger GN et al (2012) Mass spectrometry based lipidomics: an overview of technological platforms. Metabolites 2:19–38
12. Xie Z, Ferreira CR, Virequ AA, Cooks RG (2021) Multiple reaction monitoring profiling (MRM profiling): Small molecule exploratory analysis guided by chemical functionality. Chem Phys Lipids 235:105048
13. Brügger B, Erben G, Sandhoff R et al (1997) Quantitative analysis of biological membrane lipids at the low picomole level by nano-electrospray ionization tandem mass spectrometry. Proc Natl Acad Sci U S A 94:2339–2344
14. Keller BO, Sui J, Young AB et al (2008) Interferences and contaminants encountered in modern mass spectrometry. Anal Chim Acta 627:71–81
15. Chong J, Wishart DS, Xia J (2019) Using MetaboAnalyst 4.0 for comprehensive and integrative metabolomics data analysis. Curr Protoc Bioinformatics 68:1–128
16. Xia J, Sinelnikov IV, Han B et al (2015) MetaboAnalyst 3.0-making metabolomics more meaningful. Nucleic Acids Res 43:W251–W257
17. Saghatelian A, Trauger SA, Want EJ et al (2004) Assignment of endogenous substrates to enzymes by global metabolite profiling. Biochemistry 43:14332–14339
18. Bligh EG, Dyer WJ (1959) Canadian Journal of Biochemistry and Physiology. Can J Biochem Physiol 37
19. Lima CBD, Ferreira CR, Milazzotto MP et al (2018) Comprehensive lipid profiling of early stage oocytes and embryos by MRM profiling. J Mass Spectrom 53:1247–1252
20. Onjiko RM, Portero EP, Moody SA et al (2017) In situ microprobe single-cell capillary electrophoresis mass spectrometry: metabolic reorganization in single differentiating cells in the live vertebrate (*Xenopus laevis*) embryo. Anal Chem 89:7069–7076
21. Ferreira CR, Yannell KE, Mollenhauer B et al (2016) Chemical profiling of cerebrospinal fluid by multiple reaction monitoring mass spectrometry. Analyst 141:5252–5255
22. Taguchi R, Houjou T, Nakanishi H et al (2005) Focused lipidomics by tandem mass spectrometry. J Chromatogr B Anal Technol Biomed Life Sci 823:26–36
23. Liebisch G, Binder M, Schifferer R et al (2006) High throughput quantification of cholesterol and cholesteryl ester by electrospray ionization tandem mass spectrometry (ESI-MS/MS). Biochim Biophys Acta Mol Cell Biol Lipids 1761:121–128
24. Li M, Butka E, Wang X (2014) Comprehensive quantification of triacylglycerols in soybean seeds by electrospray ionization mass spectrometry with multiple neutral loss scans. Sci Rep 4:1–11
25. Jia Z, Yue F, Chen X et al (2020) Protein arginine methyltransferase PRMT5 regulates fatty acid metabolism and lipid droplet biogenesis in white adipose tissues. Adv Sci 2002602: 1–18
26. Xu Z, You W, Chen W et al (2020) Single-cell RNA sequencing and lipidomics reveal cell and lipid dynamics of fat infiltration in skeletal muscle. J Cachexia Sarcopenia Muscle
27. Kobos L, Ferreira CR, Sobreira TJP, Rajwa B, Shannahan J (2021) A novel experimental workflow to determine the impact of storage parameters on the mass spectrometric profiling and assessment of representative phosphatidylethanolamine lipids in mouse tissues. Anal Bioanal Chem 413(7):1837–1849. https://doi.org/10.1007/s00216-020-03151-0. Epub 2021 Jan 18. PMID: 33462657; PMCID: PMC7933124
28. Merrill AH, Sullards MC, Allegood JC et al (2005) Sphingolipidomics: High-throughput, structure-specific, and quantitative analysis of sphingolipids by liquid chromatography tandem mass spectrometry. Methods 36:207–224
29. Dhillon J, Ferreira CR, Sobreira TJP et al (2017) Multiple reaction monitoring profiling to assess compliance with an almond consumption intervention. Curr Dev Nutr 1:1–8
30. Cordeiro FB, Ferreira CR, Sobreira TJP et al (2017) Multiple reaction monitoring (MRM)-profiling for biomarker discovery applied to human polycystic ovarian syndrome. Rapid Commun Mass Spectrom 31:1462–1470
31. Franco J, Ferreira C, Paschoal Sobreira TJ et al (2018) Profiling of epidermal lipids in a mouse

model of dermatitis: identification of potential biomarkers. PLoS One 13:1–21

32. Yannell KE, Ferreira CR, Tichy SE et al (2018) Multiple reaction monitoring (MRM)-profiling with biomarker identification by LC-QTOF to characterize coronary artery disease. Analyst 143:5014–5022
33. Harlow KL, Ferreira CR, Sobreira TJP et al (2019) Lipidome profiles of postnatal day 2 vaginal swabs reflect fat composition of gilt's postnatal diet. PLoS One 14:1–16
34. Kobos LM, Alqatani S, Ferreira CR et al (2019) An integrative proteomic/lipidomic analysis of the gold nanoparticle biocorona in healthy and obese conditions. Appl Vitr Toxicol 5:150–166
35. Franco J, Rajwa B, Ferreira CR et al (2020) Lipidomic profiling of the epidermis in a mouse model of dermatitis reveals sexual dimorphism and changes in lipid composition before the onset of clinical disease. Metabolites 10:1–18

Chapter 26

Single-Cell Transcriptomic Analysis of Mononuclear Cell Populations in Skeletal Muscle

Gary J. He, Johanna Galvis, Tom H. Cheung, and Fabien Le Grand

Abstract

Skeletal muscle possesses a remarkable regenerative capacity, mainly relying on a population of undifferentiated and unipotent muscle progenitors, called muscle stem cells (MuSCs) or satellite cells, and their interplay with various cell types within the niche. Investigating the cellular composition of skeletal muscle tissues and the heterogeneity among various cell populations is crucial to the unbiased understanding of how cellular networks work in harmony at the population level in the context of skeletal muscle homeostasis, regeneration, aging, and diseases. As opposed to probing the average profile in a cell population, single-cell RNA-seq has unlocked access to the transcriptomic landscape characterization of individual cells in a highly parallel manner. This chapter describes the workflow for single-cell transcriptomic analysis of mononuclear cells in skeletal muscle by taking advantage of the droplet-based single-cell RNA-seq platform, Chromium Single Cell 3′ solution from 10x Genomics®. Using this protocol, we can reveal insights into muscle-resident cell-type identities, which can be exploited to study the muscle stem cell niche further.

Key words Skeletal muscle, Mononuclear cells, Droplet-based, Single-cell RNA-seq, Chromium single cell 3′ solution

1 Introduction

Skeletal muscle is one of the three types of muscle in the body, providing locomotive ability, skeletal support and protection, as well as metabolic and endocrine regulation. It possesses remarkable regenerative capacity that relies on a population of undifferentiated, unipotent muscle progenitors, called muscle stem cells (MuSCs), or satellite cells. MuSCs reside between the basal lamina and plasma membrane of muscle fibers. Upon injury, MuSCs are activated, subsequently proliferate, and differentiate to form new muscle fibers or fuse to existing injured fibers. In parallel, the muscle stem cell pool is maintained via self-renewal. Within the muscle interstitium, auxiliary muscle-resident cells also contribute to homeostasis and regeneration, such as fibro/adipogenic progenitors (FAPs) [1], macrophages [2], endothelial cells [3], Twist2-

Atsushi Asakura (ed.), *Skeletal Muscle Stem Cells: Methods and Protocols*, Methods in Molecular Biology, vol. 2640,
https://doi.org/10.1007/978-1-0716-3036-5_26,

dependent progenitor cells [4], pericytes [5], and smooth muscle cells [6]. These diverse cell types within the microenvironment or niche exert influence on each other in a highly orchestrated manner. However, the harmonic cellular networks are compromised due to aging and diseases to various extents.

Conventional genome-wide transcriptomic analysis of various distinct cell types is done by bulk RNA-seq in association with fluorescence-activated cell sorting (FACS). Unfortunately, the cellular heterogeneity is masked in these population-averaged measurements. Single-cell RNA-seq enables the transcriptional profiling of complex tissues at an unprecedented level of resolution. It provides insights into the gene expression dynamics of individual cells and underlying regulatory mechanisms. To date, ultra-high-throughput single-cell RNA-seq systems have enabled massively parallel profiling of tens of thousands of cells, such as the state-of-the-art Chromium Single Cell 3′ solution [7] from 10x Genomics®, which outperforms other popular methods [8] like Drop-seq [9], inDrop [10], and sci-RNA-seq [11] in terms of sensitivity, reproducibility, and accuracy.

Despite previous studies investigating the regulatory networks in skeletal muscle at the population-level, the protocol in this chapter delineates a step-by-step single-cell RNA-seq workflow for mononuclear cells in skeletal muscle from sample preparation to data analysis. Cell preparation is critical for downstream single-cell RNA-seq library quality to ensure meaningful analysis and conclusions. In particular, the tissue dissociation strategy described here is a "best practice" through heuristic optimization of a previously described protocol [12]. The single-cell RNA-seq library preparation protocol refers specifically to the downloadable user guides CG000204_ChromiumNextGEMSingleCell3'v3.1_RevD and CG000315_ChromiumNextGEMSingleCell3-_GeneExpression_v3.1(DualIndex)_RevE from the 10x Genomics official website (https://www.10xgenomics.com). The referred guides will be revised for updated kits. We also introduce a general data analysis scheme which includes data preprocessing using Cell Ranger and cell identity classification with differential gene expression (DGE) analysis using Seurat [13].

2 Materials

2.1 Cell Preparation Reagents

1. HyClone Ham's F-10 Nutrient Mixture with 1 mM l-glutamine (GE Life Sciences, cat. no. SH30025.01).
2. Gibco Horse serum (Thermo Fisher Scientific, cat. no. 16050-122).
3. PS-20: Penicillin-streptomycin mixture 100× (Omega Scientific, cat. no. PS-20).

4. Collagenase II (Worthington Biochemical Corporation, cat. no. LS004176).
5. Dispase II, powder (Thermo Fisher Scientific, cat. no. 17105-041).
6. Invitrogen Propidium iodide – 1.0 mg/mL Solution, (Invitrogen, Thermo Fisher Scientific, cat. no. P3566).
7. PBS, 1×, pH 7.4, (Gibco, Life Technologies, cat. no. 10010-023).
8. DMEM 1×, (Corning, cat. no. 10-013-CV).
9. Bovine Serum Albumin (BSA), (Sigma-Aldrich, cat. no. A9418).

2.2 Cell Preparation Reagent Setup

1. Wash medium (WM): Ham's F-10 supplemented with 10% (v/v) horse serum and 1× penicillin-streptomycin, stored at 4 °C for up to 1 month (*see* **Note 1**).
2. Muscle dissociation buffer (MDB): 800–1000 U/mL Collagenase II solution prepared in WM. Freshly prepare each time before use (*see* **Note 1**).
3. Stock collagenase II solution: 3000 U/mL Collagenase II prepared in 1× PBS. Thaw before use.
4. Stock Dispase solution: 33 U/mL Dispase prepared in 1× PBS. Thaw and spin briefly before use. Use only the supernatant fraction for digestion.
5. 1× PBS with 0.04% BSA: 1× PBS with 0.04% BSA (v/v), sterilize by filtration (0.45 μm) before use.

2.3 Cell Preparation Equipment

1. Dumont forceps with straight tips.
2. Dissection scissors.
3. Sterile surgical blades size 11 (Aspen, Fisher Scientific, cat. no. 08-915-13 or equivalent).
4. Petri dishes with Clear Lid, 10 cm (Fisherbrand, Fisher Scientific, cat. no. FB0875713 or equivalent).
5. Conical centrifuge tubes, 50 mL (Corning, Fisher Scientific, cat. no. 14-432-22 or equivalent).
6. Parafilm™ M Wrapping Film (Bemis).
7. Shaking water bath, 37 °C (Fisher Scientific, cat. no. 15-453-205 or equivalent).
8. Syringes, 10 mL, point style: Luer-Lok (BD, Fisher Scientific, cat. no. 14-823-2A or equivalent).
9. Kimwipes (Kimtech Science).
10. Hypodermic 20-gauge 1-inch needles (BD, Fisher Scientific, cat. no. 14-826D or equivalent).

11. Falcon cell strainer, 40 μm, (Fisher Scientific, cat. no. 08-771-1 or equivalent).
12. Microcentrifuge tube, Seal-Rite, round-bottom, 2 mL (USA Scientific, cat. no. 1620-2700 or equivalent).
13. Refrigerated centrifuge with swing rotor (Sorvall Legend XTR or equivalent).
14. Refrigerated microcentrifuge (Eppendorf 5418 or equivalent).
15. Falcon round-bottom test tubes with a strainer Snap cap, 5 mL (Corning, Fisher Scientific, cat. no. 08-771-23 or equivalent).
16. Falcon 5 ml round-bottom polystyrene test tubes (Falcon, Fisher Scientific, cat. no. 14-959-2A or equivalent).
17. Sterile hood for cell culture.
18. BD cell sorter (BD Biosciences).
19. Pipettes: ranges 0.1–10, 2–20, 20–200, 100–1000 μL and matching tips.
20. Sterile 5 and 10 mL serological pipettes and a pipettor.

2.4 Library Preparation Reagents

1. Chromium Next GEM Single Cell 3′ GEM, Library & Gel Bead Kit v3.1 (10x Genomics, PN-1000121/PN-1000128) or Chromium Next GEM Single Cell 3′ Kit v3.1 (10x Genomics, PN-1000268/PN-1000269).
2. Chromium Next GEM Chip G Single Cell Kit (10x Genomics, PN-1000120/PN-1000127).
3. Single Index Kit T Set A (10x Genomics, PN-1000213) or Dual Index Kit TT Set A (10x Genomics, PN-1000215).
4. UltraPure™ DNase/RNase-Free Distilled Water (Invitrogen, Thermo Fisher Scientific, cat. no. 10977-015 or equivalent).
5. TE Buffer (Invitrogen, Thermo Fisher Scientific, cat. no. 12090-015 or equivalent).
6. Ethyl alcohol, Pure (200 proof, for molecular biology) (Millipore Sigma-Aldrich, cat. no. E7023 or equivalent).
7. SPRIselect Reagent Kit (Beckman Coulter Life Sciences, cat. no. B23318).
8. Tween® 20 (Sigma-Aldrich, cat. no. P1379 or equivalent).
9. Glycerol, for molecular biology (Sigma-Aldrich, cat. no. G5516 or equivalent).
10. Qiagen Buffer EB (Qiagen, cat. no. 19086).
11. Qubit™ dsDNA HS Assay Kit (Invitrogen, Thermo Fisher Scientific, cat. no. Q32854).
12. High Sensitivity NGS Fragment Analysis Kit (Advanced Analytical, cat. no. DNF-474) (*see* **Note 2**).

2.5 Library Preparation Reagent Setup

1. 10% Tween® 20: 10% (v/v) Tween® 20 in Nuclease-free water.
2. 50% Glycerol: 50% (v/v) Glycerol in Nuclease-free water.
3. Template Switch Oligo (10x Genomics, PN-3000228): Centrifuge briefly, reconstitute in 80 μL TE Buffer. Store at −80 °C.

2.6 Library Preparation Equipment

1. 10x Vortex Adapter (10x Genomics, PN-330002).
2. 10x Magnetic Separator (10x Genomics, PN-230003).
3. Chromium Next GEM Secondary Holder (10x Genomics, PN-3000332).
4. ProFlex PCR System (Applied Biosystems or equivalent).
5. PCR Tubes 0.2 mL 8-tube strips (Eppendorf, cat. no. 951010022 or equivalent) (*see* **Note 3**).
6. DNA LoBind Tubes, 1.5 mL (Eppendorf, cat. no. 022431021 or equivalent).
7. DNA LoBind Tubes, 2.0 mL (Eppendorf, cat. no. 022431048 or equivalent).
8. Pipet-Lite Multi Pipette: L8-10XLS+, 20XLS+, 50XLS+, 200XLS+ (Rainin).
9. Pipet-Lite LTS Pipette: L-2XLS+, L-10XLS+, L-20XLS+, L-100XLS+, L-200XLS+, L-1000XLS+ (Rainin).
10. Tips LTS 200UL Filter: RT-L10FLR, RT-L200FLR, RT-L1000FLR (Rainin).
11. Vortex Mixer (VWR, cat. no. 10153-838 or equivalent).
12. MYFUGE 12 Mini Centrifuge (Thermo Fisher Scientific, cat. no. C1012 or equivalent).
13. Eppendorf ThermoMixer C (Eppendorf, cat. no. 5382000023 or equivalent).
14. Eppendorf SmartBlock 1.5 mL, Thermoblock for 24 reaction vessel (Eppendorf, cat. no. 5360000038 or equivalent).
15. Qubit 4.0 Fluorometer (Thermo Fisher Scientific, cat. no. Q33226).
16. Fragment Analyzer Automated CE System (Advanced Analytical) (*see* **Note 2**).

2.7 Software for Data Analysis

1. Cell Ranger 3.0 or greater.
2. R version 4.0 or greater.
3. Seurat v3 or greater.
4. clusterProfiler v3 or greater.
5. Any of SingleCellSignalR/CellChat/NicheNet.
6. Velocyto and/or scVelo.

3 Methods

3.1 Cell Preparation

1. Prepare 10 mL of Muscle Dissection Buffer (MDB) for each mouse.
2. Sacrifice the mice according to the institutionally approved protocol.
3. Dissect the muscles of interest. Trim away any visible fat (*see* **Note 4**).
4. Wash muscle tissues in Wash Medium (WM) in a petri dish.
5. Mince muscle in sufficient amounts of MDB in a clean petri dish quickly with dissection scissors.
6. Using a blade, further mince muscles until they are approximately 1 mm in diameter.
7. Transfer the slurry of minced muscle from each mouse to an individual sterile 50 mL tube with a spatula.
8. Rinse any remaining residue, with remaining MDB from the petri dish, and transfer into the corresponding 50 mL tube.
9. Seal the conical tube(s) with Parafilm.
10. Incubate the conical tube(s) at 37 °C with agitation (water bath shaker set to 65–70 rpm) for 90 min. The conical tubes should be horizontally positioned along the shaking path axis and fully submerged into the water (use weights to keep them submerged).
11. After 90 min, adjust the volume of each tube to 50 mL with WM. Gently mix by inverting a few times. To maximize yield, spilt cell suspension equally into two tubes (volumes of both tubes should be filled to 50 mL with WM).
12. Centrifuge the tubes at 500 g at 4 °C for 10 min, ensure the centrifuge is balanced.
13. Carefully remove the supernatant from each tube until only 10–12.5 mL remains. Combine both tubes using a 25 mL pipette into a single conical tube.
14. Add 1 mL Stock Dispase (use supernatant fraction only) and 1 mL Stock Collagenase II to the tube.
15. Adjust the tube volume to 30 mL with WM.
16. Using a 25 mL pipette, triturate the cells suspension up and down 10–15 times against the tube wall until the pipette stops clogging.
17. Seal the conical tube(s) well with Parafilm and incubate at 37 °C with agitation for a further 30 min with the same settings in **step 10**.

18. Use a 30 mL syringe with a 20-gauge needle to syringe the suspension for ten times. Avoid generating bubbles by ejecting the suspension against the wall of the tube.
19. Blot away any blockage in the syringe tip (undigested muscle chunks, bones, tendons, or collagen) with Kimwipes.
20. Filter the cell suspension through a cell strainer (40 μm Nylon). Adjust the filtered suspension volume to 50 mL with WM and mix the suspension well by gentle inversion.
21. Centrifuge at 500 g at 4 °C for 10 min.
22. Carefully remove all the supernatant immediately after centrifugation, as the cell pellet will gradually dislodge from the bottom of the tube.
23. Resuspend the cell pellet in 300 μL of WM.
24. Transfer 10 μL of the cell suspension to a 5 mL FACS tube, fill up to 200 μL with WM, and leave on ice. This is the unstained control.
25. Make up the remaining cell suspension to 1mL with Propidium Iodide to a final concentration of 0.3 μg/mL, mix well with the P200 pipette. Pass the suspension through the cell strainer cap before loading on cell sorter.

3.2 Cell Sorting

1. Set up the cell sorter according to the manufacturer's specification with the 70 μm nozzle.
2. Run the unstained control at a relatively low flow rate to ensure appropriate voltage settings, particularly ensure the cell population is correctly positioned on the FSC and SSC plots.
3. Create a gate on the FSC-A and SSC plot that excludes debris.
4. Create gates on the FSC and SSC A&W plots hierarchically that exclude cell doublets, multiplets, or clumps.
5. Run the PI stained sample, create a gate, and collect the PI negative singlet population into 1 mL of WM in a 5 mL round-bottom tube pre-rinsed with WM.

3.3 Processing of Sorted Cells

1. Centrifuge the cells at 300 g at 4 °C for 10 min.
2. Remove the supernatant carefully without disturbing the cell pellet.
3. Resuspend the cell pellet gently with 1 mL 1× PBS with 0.04% BSA and then centrifuge the cells at 300 g at 4 °C for 10 min. Carefully remove the supernatant. Use wide-pore pipette tips for cell resuspension before cell loading to minimize cell damage and lysis.
4. Estimate the volume for resuspension by the sorted cell count reported on the cell sorter. Resuspend the cell pellet gently by adding an appropriate volume of 1× PBS with 0.04% BSA to achieve the target cell concentration.

5. Filter the cell suspension through a 35 μm cell strainer to remove any cell debris and clumps.
6. Determine the cell concentration using a hemocytometer. Adjust the volume to achieve the target cell concentration if necessary.
7. Place the cells on ice and proceed to GEM generation.

3.4 GEM Generation and Barcoding

1. Prepare Master Mix on ice as follows (adding reagents in the order listed):

Component	Volume (μL)
RT Reagent B	18.8
Template Switch Oligo	2.4
Reducing Agent B	2.0
RT Enzyme C	8.7
Total	31.8

   If processing multiple samples per experiment, prepare a master mix with 10% excess. Prepare Master Mix directly into a well of an 8-tube strip on ice if processing only one sample.
2. Assemble the Chromium Next GEM Chip G and holder according to manufacturer's instructions. Cover the chip when not in use to prevent dusts and contaminants.
3. Dispense 50% glycerol solution into each unused chip well if processing fewer than eight samples. Add 70 μL to unused wells in the row labeled 1, 50 μL in the row labeled 2, and 45 μL in the row labeled 3.
4. Prepare the pre-thawed Gel Beads by vortexing for 30 s with a 10x Vortex Adapter. Briefly spin down and confirm there are no bubbles at the bottom of the tubes and the liquid levels are even.
5. Transfer 31.8 μL Master Mix into each well of an 8-tube strip. Add the appropriate volume of cell suspension (up to 43.2 μL with nuclease-free water) by targeted cell recovery (typically no more than 10,000 as recommended) to the Master Mix to a total volume of 75 μL. Gently mix the cell suspension using wide-pore pipette tips before adding to the well.

$$\text{Targeted Cell Recovery (Cells)} \approx \text{Cell Stock Conc.(Cells/}\mu\text{L)} \times \text{Vol.of Cell Suspension (}\mu\text{L)} \times 0.61$$

$$\text{Multiplet Rate (\%)} \approx \text{Targeted Cell Recovery (Cells)} \div 500 \times 0.38\%$$

6. Gently mix the Master Mix and Cell Suspension and carefully dispense 70 μL into the bottom center of each well in the row labeled 1 using the same pipette tip. Avoid introducing any bubbles.
7. Puncture the foil seal of the Gel Beads tubes using a clean pipette tip. Gently transfer 50 μL Gel Beads into the wells in the row labeled 2 without introducing bubbles. Wait for 30 s.
8. Slowly dispense 45 μL Partitioning Oil into the wells in the row labeled 3.
9. Carefully attach the 10x Gasket immediately after loading the Partitioning Oil. Ensure the notch is aligned with the top left corner, and the gasket holes are aligned with the wells.
10. Run the assembled chip in the Chromium Controller immediately according to the manufacturer's instructions. It takes approximately 18 min to complete the run. Cell lysis begins immediately after cell encapsulation into droplets.
11. Harvest the chip from the Controller once the run is completed.
12. Carefully remove the gasket, open the chip holder, and expose the wells at 45° by folding the lid back until it clicks.
13. Check the volume in rows labeled 1–2. Abnormally high volumes indicate clogs.
14. Slowly aspirate 100 μL GEMs from the lowest points (without creating a seal) of the recovery wells in the row labeled 3. GEMs should be uniformly opaque without excess clear Partition Oil in the pipette tips.
15. Carefully and swiftly dispense GEMs into the tube strip on ice, with the pipette tips against the sidewalls of the tubes.
16. Immediately incubate the GEMs in a thermocycler that can accommodate at least 100 μL volume and run the following protocol:

    Hot lid 53 °C, reaction volume 100 μL.

53 °C	45
85 °C	5 min
4 °C	Hold

17. At this point, samples can be stored at 4 °C for up to 72 h or at −20 °C for up to a week.

3.5 Post GEM–RT Cleanup and cDNA Amplification

1. Add 125 μL Recovery Agent to each sample dropwise at room temperature. Do not disturb the biphasic mixture. Wait for 2 min. There will be two layers: the Recovery Agent/Partitioning Oil (pink) and an aqueous phase (clear). No persisting emulsion (opaque) is expected. Any clog during GEM generation leads to a smaller aqueous phase volume.

2. Slowly remove and discard 125 μL Recovery Agent/Partitioning Oil (pink) from the bottom of the tube without aspirating the aqueous phase.
3. Thaw Cleanup Buffer for 10 min at 65 °C on a thermomixer at maximum speed. There should be no visible crystals. Cool down to room temperature.
4. Fully resuspend Dynabeads MyOne SILANE by vortexing.
5. Prepare Dynabeads Cleanup Mix as follows (adding reagents in the order listed):

Component	Volume (μL)
Cleanup Buffer	182
Dynabeads MyOne SILANE	8
Reducing Agent B	5
Nuclease-free water	5
Total	200

The volumes above are for one sample. If processing multiple samples per experiment, scale up Dynabeads Cleanup Mix with 10% excess. Mix well before use.

6. Add 200 μL Dynabeads Cleanup Mix to each sample, mix well by pipetting.
7. Incubate at room temperature for 10 min. Avoid clumps of settled beads by pipetting over the course of incubation.
8. Prepare Elution Solution I, as shown in the table below (adding reagents in the order listed). Mix well and spin down briefly.

Component	Volume (μL)
Buffer EB	98
10% Tween 20	1
Reducing Agent B	1
Total	100

9. Place the tube strip on a 10x Magnetic Separator (set in the High position) until the solution is clear.
10. Remove the supernatant without disturbing the beads.
11. Add 300 μL 80% freshly prepared ethanol (20 mL is needed for 8 reactions) to the tube while it is on the magnet. Incubate at room temperature for 30 s and discard the supernatant.

12. Repeat the washing with 200 μL 80% freshly prepared ethanol and discard the supernatant after 30 s of incubation at room temperature.
13. Spin down briefly and place the tube strip on the magnet (set in the Low position).
14. Remove residual ethanol and air dry for 1 min.
15. Remove the tube from the magnet and elute the cDNA from the beads with 35.5 μL Elution Solution I. Mix well and incubate at room temperature for 2 min.
16. Place the tube strip on the magnet (set in the Low position) to separate the beads from the supernatant until the solution is clear (approximately 2 min), transfer 35 μL sample to a new tube strip.
17. Prepare cDNA Amplification Mix on ice as directed in the table below (adding reagents in the order listed). Mix well and spin down briefly.

Component	Volume (μL)
Amp Mix	50
cDNA Primers	15
Total	65

The volumes given are for a single sample. If processing multiple samples per experiment, scale up the cDNA Amplification Mix with 10% excess. Mix well before use.

18. Add 65 μL cDNA Amplification Reaction Mix to 35 μL sample, mix well using a pipette, and centrifuge briefly.
19. Place the tube strip in the thermocycler and perform the following procedure:

Hot lid 105 °C, reaction volume 100 μL

98 °C	3 min		
98 °C 63 °C	15 s 20 s	]	n cycles (see the table below)
72 °C	1 min		
72 °C	1 min		
4 °C	Hold		

Targeted cell recovery	n cycles	n cycles (low RNA content)
<500	13	15
500–6000	12	13–14
>6000	11	12

20. Samples can be stored at 4 °C for up to 72 h or at −20 °C for up to a week. Alternatively, proceed to the next step for cDNA cleanup.
21. Fully resuspend the SPRIselect reagent by vortexing.
22. Add 60 μL SPRIselect reagent (0.6×) to each sample, mix well by pipetting.
23. Incubate at room temperature for 5 min.
24. Place the tube strip on the 10x Magnetic Separator (set in the High position) until the solution is clear.
25. Remove the supernatant without disturbing the beads.
26. Add 200 μL 80% freshly prepared ethanol to the tube while it is on the magnet. Incubate at room temperature for 30 s and then discard the supernatant.
27. Repeat **step 26** once more.
28. Spin down briefly and place the tube strip on the magnet (set in the Low position).
29. Remove residual ethanol and air dry for no more than 2 min. Exceeding 2 min will decrease elution efficiency.
30. Remove the tube from the magnet and elute the cDNA from the beads with 40.5 μL Buffer EB. Mix well and incubate at room temperature for 2 min.
31. Place the tube strip on the magnet (set in the High position) to separate the beads from the supernatant. After the solution is clear (approximately 2 min), transfer 40 μL of the sample to a new tube strip.
32. Quantify cDNA concentration using Qubit Fluorometer and Qubit dsDNA HS Assay Kit.
33. Run the sample on a Fragment Analyzer with DNF-474 kit for the quality control of cDNA.
34. The remaining sample can be stored at 4 °C for up to 72 h or at −20 °C for up to one month.

3.6 3′ Gene Expression Library Construction

1. Set up a thermocycler with the following procedure:

   Hot lid 65 °C, reaction volume 50 μL

4 °C	Hold
32 °C	5 min
65 °C	30 min
4 °C	Hold

2. Thaw and fully resuspend the Fragmentation Buffer by vortexing.
3. Prepare Fragmentation Mix on ice as follows (adding the reagents in the order listed):

Component	Volume (μL)
Fragmentation Buffer	5
Fragmentation Enzyme	10
Total	15

Mix well and spin down briefly. The volumes given above are for a single sample. If processing multiple samples per experiment, scale up the Fragmentation Mix with 10% excess. Mix well before use.

4. Transfer 10 μL purified cDNA sample into a new tube strip. Add 25 μL Buffer EB and 15 μL Fragmentation Mix to each cDNA sample. Mix well by pipetting and centrifuge briefly.
5. Place the tube strip in the thermocycler and skip the 4 °C pre-cooling to initiate the incubation procedure.
6. Fully resuspend the SPRIselect reagent by vortexing.
7. Add 30 μL SPRIselect reagent (0.6×) to each sample, mix well by pipetting.
8. Incubate the tube strip at room temperature for 5 min.
9. Place the tube strip on the 10x Magnetic Separator (set in the High position) until the solution is clear.
10. Transfer 75 μL supernatant without disturbing the beads to a new tube strip.
11. Vortex to resuspend the SPRIselect reagent. Add 10 μL SPRI-select reagent (0.8×) to each sample, mix well by pipetting.
12. Incubate at room temperature for 5 min.
13. Place the tube strip on the magnet (set in the High position) until the solution is clear.
14. Remove 80 μL supernatant without disturbing the beads.

15. Add 125 μL 80% ethanol to the tube while it is on the magnet. Incubate at room temperature for 30 s and discard the supernatant.
16. Repeat **step 15** once more.
17. Spin the tube strip down briefly and place the tube strip on the magnet (set in the Low position) until the solution is clear.
18. Remove residual ethanol and air dry for no more than 2 min. Exceeding 2 min will decrease elution efficiency.
19. Remove the tube from the magnet and elute the DNA from the beads in 50.5 μL Buffer EB. Mix well by pipetting up and down. Incubate at room temperature for 2 min.
20. Place the tube strip on the magnet (set in the High position) to separate beads from the supernatant until the solution is clear (approximately 2 min), transfer 50 μL sample to a new tube strip.
21. Prepare Adaptor Ligation Mix on ice as follows (adding the reagents in the order listed):

Component	Volume (μL)
Ligation Buffer	20
DNA Ligase	10
Adaptor Oligos	20
Total	50

Mix well and spin down briefly. The volumes given above are for a single reaction. If processing multiple samples per experiment, scale up the Adaptor Ligation Mix with 10% excess. Mix well before use.

22. Add 50 μL Adaptor Ligation Mix to 50 μL sample, mix well by pipetting and centrifuge briefly.
23. Place the tube strip in the thermocycler and perform the following procedure:

    Hot lid 30 °C, reaction volume 100 μL

20 °C	15 min
4 °C	Hold

24. Fully resuspend the SPRIselect reagent by vortexing.
25. Add 80 μL SPRIselect reagent (0.8×) to each sample, mix well by pipetting.
26. Incubate at room temperature for 5 min.

27. Place the tube strip on the 10x Magnetic Separator (set in the High position) until the solution is cleared.
28. Remove the supernatant without disturbing the beads.
29. Add 200 μL 80% freshly prepared ethanol to the tube while on the magnet. Incubate at room temperature for 30 s and discard the supernatant.
30. Repeat **step 29** once more.
31. Spin down briefly and place the tube strip on the magnet (set in the Low position).
32. Remove residual ethanol and air dry for no more than 2 min. Exceeding 2 min will decrease elution efficiency.
33. Remove the tube from the magnet and elute the DNA from the beads in 30.5 μL Buffer EB. Mix well by pipetting and incubate at room temperature for 2 min.
34. Place the tube strip on the magnet (set in the Low position) to separate the beads from the supernatant until the solution is clear (approximately 2 min), transfer 30 μL sample to a new tube strip.
35. Choose the appropriate sample index for each sample and record which 10x Sample Index name is used. Ensure no sample indices overlap in a multiplexed sequencing run.
36. When using Single Index Kit T Set A, prepare Sample Index PCR Mix on ice as directed in the following table (adding the reagents in the order listed):

Component	Volume (μL)
Amp Mix	50
SI Primer	10
Total	60

Mix well and spin down briefly. The volumes given above are for a single sample. If processing multiple samples per experiment, scale up the Sample Index PCR Mix accordingly with 10% excess. Mix well before use. Skip this step when using Dual Index Kit TT Set A.

37. When using Single Index Kit T Set A, add 60 μL Sample Index PCR Mix and 10 μL of an individual Single Index to 30 μL sample, mix well, and centrifuge briefly. When using Dual Index Kit TT Set A, add 50 μL Amp Mix and 20 μL of an individual Dual Index TT A to 30 μL sample, mix well, and centrifuge briefly. Record the well ID used.
38. Place the tube strip in the thermocycler and perform the following protocol:

Hot lid 105 °C, reaction volume 100 μL

98 °C	45 s	
98 °C 54 °C	20 s 30 s	n cycles (see the table below)
72 °C	20 s	
72 °C	1 min	
4 °C	Hold	

cDNA input (ng)	n cycles
<25	14–16
25–150	12–14
150–500	10–12
500–1,000	8–10
1000–1500	6–8
>1500	5

39. Samples can be stored at 4 °C for up to 72 h or at −20 °C for up to a week. For Post Sample Index PCR Double Sided Size Selection, proceed further.
40. Fully resuspend the SPRIselect reagent by vortexing.
41. Add 60 μL SPRIselect reagent (0.6×) to each sample, mix well by pipetting.
42. Incubate at room temperature for 5 min.
43. Place the tube strip on the magnet (set in the High position) until the solution is clear.
44. Transfer 150 μL supernatant to a new tube strip without disturbing the beads.
45. Vortex to resuspend the SPRIselect regent. Add 20 μL SPRIselect reagent (0.8×) to each sample, mix well by pipetting.
46. Incubate at room temperature for 5 min.
47. Place the tube strip on the magnet (set in the High position) until the solution is clear.
48. Remove the supernatant without disturbing the beads.
49. Add 200 μL 80% freshly prepared ethanol to the tube while it is on the magnet. Incubate at room temperature for 30 s and then discard the supernatant.
50. Repeat **step 49** once more.

51. Spin down briefly and place the tube strip on the magnet (set in the Low position).
52. Remove residual ethanol and air dry for no more than 2 min.
53. Remove the tube from the magnet and elute the DNA from the beads with 35.5 μL Buffer EB. Mix well by pipetting and incubate at room temperature for 2 min.
54. Place the tube strip on the magnet (set in the Low position) to separate beads from the supernatant. After the solution is clear (about 2 min), transfer 35 μL supernatant (containing the cDNA sample) to a new tube strip.
55. Quantify the cDNA concentration using Qubit Fluorometer and Qubit dsDNA HS Assay Kit.
56. Run the sample on the Fragment Analyzer with the DNF-474 kit to perform quality control of cDNA.
57. Samples can be stored at 4 °C for up to 72 h or at −20 °C for long-term storage.

3.7 Sequencing

1. Calculate the molarity of each sample based on the Fragment Analyzer result and sample concentration determined by Qubit assay.
2. The quantified and normalized libraries should be denatured and diluted as recommended for Illumina sequencing platforms before loading onto the sequencer. Ensure the sample indices of different samples are well-balanced with high nucleotide diversity (the relative proportion of nucleotides A, C, G and T present in every cycle of the index sequencing) in a multiplexed sequencing run.
3. Sequencing run parameters for Chromium Single Cell 3' Gene Expression Libraries are shown below:

Sequencing read	Number of cycles	
Read 1	28	16 bp 10× Barcodes and 12 bp UMI
i7 Index	8 or 10	8 bp Sample Index for Single Index Kit T Set A or 10 bp Sample Index for Dual Index Kit TT Set A
i5 Index	0 or 10	10 bp Sample Index for Dual Index Kit TT Set A only
Read 2	100	100 bp cDNA Insert

4. The technical performance of Chromium Single Cell 3′ Gene Expression libraries is driven by sequencing depth per cell. 80,000–100,000 raw reads per cell for uninjured muscle samples are recommended. For injured conditions, sequencing depth should be increased accordingly (*see* **Note 5**).

3.8 Basic Data Analysis

1. The raw data generated by the Illumina sequencer are in the base call (BCL) format. Preprocessing of raw data is performed by the cellranger mkfastq pipeline implemented in Cell Ranger. The BCL files are converted and demultiplexed into FASTQ files of an individual library. Alternatively, the FASTQ files can be generated by Illumina bcl2fastq2. These FASTQ files can be directly used for data analysis.
2. The resulting FASTQ files are subjected to the cellranger count pipeline with a corresponding transcriptome reference for read alignment, filtering, cell barcode counting, and UMI counting. Briefly, the FASTQ files are mapped with STAR aligner which performs splicing-aware read alignments with a transcript annotation file (GTF format) to a reference genome. For each read, STAR calculates a mapping quality score (MAPQ) representing the confidence to alignments between reads to a reference. The exonic reads are aligned to annotated transcripts (intronic reads can also be included in the analysis to maximize sensitivity). If the read is compatible with a single gene annotation, it is considered a uniquely mapped read. Only the uniquely mapped reads are considered for UMI counting.

   Finally, each observed barcode, UMI, gene combination, is recorded as a UMI count in the unfiltered feature-barcode matrix. Feature information is also recorded. One folder is created containing three files: barcodes, features, and matrix information.
3. After completing the pipeline successfully, web_summary.html in the result files contains the summary metrics for quality control. Potential issues can be identified from metrics with abnormal values and alerts automatically generated by Cell Ranger.
4. For downstream analysis, we use an R toolkit designed for single-cell genomics: Seurat. Install R, Seurat, and other dependent packages according to the corresponding installation instructions.
5. The Read10X function in Seurat loads barcodes, features, and matrix information and generates a unique R object as a count matrix.
6. Use the CreateSeuratObject function to create a Seurat object from the count matrix. The object produced is a container for data (e.g., the count matrix), metadata, and future analysis (e.g., dimensional reduction and clustering results) for a single-cell dataset.
7. Calculate the percentage of reads mapping to the mitochondrial genome with the PercentageFeatureSet function. A string pattern starting by "MT" or "mt" should be used as parameter.
8. Filter cells based on UMI counts, unique genes detected, and mitochondrial reads percentages (*see* **Note 6**).

9. The filtered data is normalized by the NormalizeData function, in which a global-scaling LogNormalize method is used. For each cell, it normalizes the gene expression values by the total expression. The resulting values are multiplied by a scale factor (10,000 by default) and then log-transformed (*see* **Note 7**).
10. Use the FindVariableFeatures function to calculate the highly variably expressed genes in the dataset. This subset of transcripts helps highlight the biological variables in the downstream analysis. By default, the top 2000 genes are selected.
11. Use the ScaleData function for a linear transformation that shifts and scales the expression of each gene to have a mean expression of 0 and a variance of 1 across cells, respectively. We can also use the ScaleData function to remove unwanted variation (e.g., mitochondrial gene percentage) by including the vars.to.regress parameter.
12. OPTIONAL: For multi-sample analysis, it is highly recommended to use the anchor-based data integration method implemented in Seurat (*see* **Note 8**). We first identify anchors shared by multiple datasets using the FindIntegrationAnchors function and then integrate these datasets with the IntegrateData function. A competitive option for data integration is Harmony. Indeed, the Harmony algorithm scales to large datasets and outperforms in fine-grained subpopulation identification. Moreover, Harmony efficiently corrects technical and other undesired batch effects by a strategy in which a soft clustering is applied iteratively. A mixture model-based linear batch correction is computed subsequently [14].
13. Perform PCA for linear dimensional reduction on the scaled data with the RunPCA function. By default, only the selected highly variably expressed genes are used as input.
14. Determine the number of top principal components (PCs) by the JackStraw procedure which is a statistical test based on a random null model. Run JackStraw, ScoreJackStraw, and JackStrawPlot functions in order and select "significant" PCs with a strong enrichment of low p-value features (solid curve above the dashed line in JackStrawPlot) for downstream clustering. Alternatively, run the ElbowPlot function which calculates the percentage of variance explained by each principal component, and choose the top-ranking PCs that capture the majority of biological variability for subsequent analysis.
15. Seurat v3 (or greater) implements a graph-based clustering approach for cell clustering (*see* **Note 9**). Run the FindNeighbors function with the previously defined significant PCs of the dataset, and then run the FindClusters function with optimal resolution parameters for clustering.

16. Visualize and explore the data by running nonlinear dimensional reduction approaches, for example, UMAP (the RunUMAP function) and t-SNE (the RunTSNE function) (*see* **Note 10**).
17. For visualizing gene expression, the VlnPlot (shows single-cell gene expression level distribution across clusters) and FeaturePlot functions (visualizes feature expression on a dimensional reduction plot) are commonly used. Manually assign cell population identity based on cell-type-specific canonical markers.
18. Find differentially expressed genes or marker genes for each cluster by running the FindMarkers function for a single cluster and FindAllMarkers function for all clusters. These approaches can identify both positive and negative markers. Assign novel cell type identity based on their putative markers along with corresponding prior knowledge from the literature. Moreover, gene ontology enrichment analysis or gene set enrichment analysis (GSEA) can be used to test the putative marker genes of the unknown novel cell type and see if they significantly overlap with any gene ontology term or gene set, such that the new cell type can be characterized by its function and similarities to other cells (*see* **Note 11**).
19. As toolkits and packages for Gene Ontology enrichment analysis do not offer yet specific versions designed for scRNA-seq data, the user can choose those applied to bulk RNA-seq, such as clusterProfiler [15]. This Bioconductor R package offers three methods: groupGO, enrichGO, and enrichKEGG for gene classification and enrichment analysis. It supports DAVID, KEGG pathways, and many other annotations. Notably, clusterProfiler considers the ranks of log-fold changes of our differentially expressed genes to refine the reporting of associated GO terms.

3.9 Ligand-Receptor Pairs

Predicting ligand-target links in scRNA-seq may play a role in functional analysis design. Softwares designed for this aim assume that differentially expressed genes across the observed subpopulations reflect cell-to-cell communication. Most of the packages rely on curated ligand-receptor databases for detection, scoring, and reporting of potentially relevant interactions, as implemented in SingleCellSignalR [16], CellChat [17], NicheNet [18], among others. More complex approaches integrate probabilistic modeling [19, 20] or find triadic relationships (hypergraphs) [21].

As an example, the R toolkit NicheNet [18] provides a means to obtain interacting sender-receiver cell populations based on the observed gene expression and the weighted support of identified interaction (quantified with a series of parameters that includes the level of evidence). The algorithm calculates a regulatory potential score between all pairs of ligands and target genes, for all genes in a

chosen species (*M. musculus* or *H. sapiens*). It then applies network propagation methods to propagate the signal from a ligand over receptors, signaling proteins, transcriptional regulators and, finally, to target genes. Highly expressed ligands in cell populations of interest are used to define possible active ligands (in the "sender" population(s)). Similarly, it is possible to proceed with possible active targets/receptors (in the "acceptor" population(s)). Of note, the number of selected genes must be much smaller than the background. This gene set is expected to consist of genes regulated by the extracellular microenvironment. A one-sided Fisher's exact test is performed to assess whether genes belonging to the gene set of interest are more likely to be part of the top predicted targets than background genes. Results are presented as heatmaps and "circos" plots that can be customized to highlight the most relevant predicted interactions.

3.10 RNA Velocity

RNA velocity is a concept referring to the transition from non-spliced to spliced RNA molecules in a given cell type. BAM files and a genome annotation file are required to obtain the two output count matrices, called spliced counts and unspliced counts, which serve as input to the velocyto package [22]. Velocyto estimates the rate of increase of mature mRNA abundance by applying a mathematical model (a differential equation) expressed in terms of capturing transcription (α), splicing (β), and degradation (γ) rates involved in the production of unspliced (u) and spliced (s) mRNA products. Solving this equation for each gene results in a vector termed the velocity. Its direction and magnitude represent a "progression" from one state to another, as it occurs in cell type differentiation processes. The result is a graphical representation of each cell plotted on a bidimensional projection (PCA, t-SNE or UMAP) and associated with a vector. All vectors reflect the dynamics of the maturation of RNA molecules along with the related cell types. This can be assimilated to pseudotemporal trajectories; however, inferred trajectories do not necessarily represent biological processes as these denote transcriptional similarity in the first instance [23].

The more recently developed Python toolkit scVelo [24] is inspired by velocyto, but instead of using fixed assumptions, it implements a stochastic and dynamical model that makes the tool more suited to the study of non-stationary populations. It extends the ordinary differential equations by computation of transition probabilities, which are aggregated into a transition matrix describing the Markov chain of the differentiation process. Using this stochastic model, scVelo can infer a "universal gene-shared latent time," which is a more faithful reconstruction of cell fate "decisions" timings than the diffusion pseudotime.

4 Notes

1. All medium and buffer should be sterilized by filtration (0.45 μm) before use and kept on ice until needed. Stock solutions should be sterilized by filtration (0.45 μm) and stored in 1 mL aliquots at −20 °C for up to 3 months.
2. For library quality control, alternative platforms such as the 2100 Bioanalyzer, 4200 TapeStation with corresponding reagents can be used.
3. It is highly recommended to use emulsion-safe plasticware validated by 10x Genomics. Otherwise, it may adversely affect system performance. Alternative items that may be used are listed below:

   TempAssure PCR 8-tube strip (USA Scientific, cat. no. 1402-4700)

   MicroAmp 8-Tube Strip, 0.2 mL (Thermo Fisher Scientific, cat. no. N8010580)

   MicroAmp 8-Cap Strip, clear (Thermo Fisher Scientific, cat. no. N8010535)
4. Avoid damaging blood vessels and lymph nodes whenever possible. The presence of excessive blood-driven cells and lymphocytes will increase the proportion of such cells in the sample. The sequencing budget may increase for equivalent sequencing depth for muscle-resident cells.
5. Typically, we aim for 0.1 M reads/cell or follow the allocation of approximately one read per cell per gene [25], meaning for a single gene is to have ~1 UMI per cell on average. Given the estimated transcript capture efficiency for the 10x technology (approximately 6.7–8.1% for v1, 14–15% for v2, or 30–32% for v3), there should be at least $1/0.32 \approx 3$ transcripts in the cell for a gene to achieve one read per cell when using v3 chemistry. For a typical mammalian cell that contains 200,000 transcripts [26], a sequencing depth of at least $200{,}000/0.32 = 625{,}000$ reads is recommended. However, the recommended sequencing depth should be scaled proportionally for cells with different sizes and growth rates.
6. "Cells" with very few expressed genes are often low-quality cells or empty droplets. On the other hand, cell doublets or multiplets usually have an aberrantly high number of expressed genes and can be inferred in silico. Similarly, the total number of UMI counts within a cell is highly correlated with the number of unique transcripts detected. The threshold should be determined based on the distribution of the total number of UMI counts and transcripts detected among all cells within a

dataset. Empirically, the lower boundary for both the total number of UMI counts and expressed genes is 300–500.

Dying cells often exhibit increased ratios of reads mapping to mitochondrial genes and remaining endogenous genes. An overrepresentation of mitochondrial genes is due to the mitochondrial RNA retained in the cells while remaining cytoplasmic RNA is lost through the leaky membrane. Usually the ratio is in a range of 5–20%.

7. Alternatively, we can use the SCTransform function for data normalization. The single command replaces three functions, including NormalizeData, ScaleData, and FindVariableFeatures. Unwanted variations (e.g., cell-cycle state, mitochondrial gene percentage) can also be removed by including the vars.to.regress parameter. SCTransform normalizes the data and stabilizes variance by taking advantage of regularized negative binomial modeling framework [27] that effectively removes the technical noise while maintaining biological variability. For multi-sample analysis, running the SelectIntegrationFeatures and PrepSCTIntegration functions in order are needed before data integration.
8. In single-cell analysis, data integration is a higher-level batch effect correction method, which is often done by nonlinear approaches, particularly for datasets with cell-type-specific batch effects or when there is a shift in the percentage of cell types across experiments [13]. Moreover, data integration focuses on batch effects and biological differences between cell types or states that are not shared among datasets. However, due to the increased degrees of freedom of nonlinear data integration techniques, over-correction may occur and mask the heterogeneity among cells to some extent. On the other hand, unwanted variances that are not corrected will also introduce artifacts in the data outcome. The only way to fully eliminate "batch effects" is to apply experimental methods like "cell tagging" [28–30].
9. If the transitional states of cells (e.g., muscle stem cell activation) are the biological question of interest, approaches for inferring dynamic biological trajectory are needed. Dimensional reduction methods like t-SNE and UMAP are not recommended for such trajectory analysis. The clustered structure of the dataset generated by t-SNE or UMAP has no real meaning on the cluster positions so that the cluster proximity does not indicate biological similarity. The trajectory inference tools computationally order the cells along a pseudotime in a trajectory of different types. Different trajectory inference methods are suited for different topological structures [31], among which PAGA [32], Slingshot [33], and SCORPIUS [34] are highly recommended. Monocle [11] is also a well-known package for trajectory analysis. It should be noted that

for many of the current trajectory methods, prior knowledge of marker genes or starting cells originating in the trajectory is required.

10. An interesting option among cluster visualization algorithms is FIt-SNE [35], which uses Fourier Transform to capture each cluster signal and consequently distribute the cells in a bidimensional space. As in UMAP, the "perplexity" parameter can be tuned in FIt-SNE to refine the visual representation [36]. Both algorithms perform similarly in terms of computational resources and runtime. Moreover, some developers have highlighted that t-SNE is superior when resolving the case of "containment," that is, smaller clusters embedded into bigger ones (https://pair-code.github.io/understanding-umap/), which also stands true for FIt-SNE. FIt-SNE is available for MacOS, Windows, and Linux systems, with wrappers for both R and Python implementations.

11. Advanced Preprocessing of the count matrix (Recommended): The barcodes, features, and matrix information obtained at **step 2** (*see* Subheading 3.6) should be subjected to strict quality control (QC) even though the upstream steps were correctly performed. Biological interpretation derived from any bioinformatic analysis depends on the capacity of minimizing artifactual findings, such as *multiplets* or outliers that may escape standard filtering. The detailed analysis centered on specific cellular populations (e.g., computing pseudotemporal trajectories) is especially sensitive to this kind of misinformation.

    Library size may vary from one experiment to another depending on the sampled cell populations and tested conditions. Therefore, employing statistically supported thresholds rather than rigid/arbitrary cutoffs is highly recommended (e.g., defining UMI counts and detected Features by barcode reflecting viable good quality cells).

    Packages "scran" and "scater" are recommended for this purpose [23], using complementary functions from "DropletUtils." This QC must be done separately on each single experimental batch, in the form of SingleCellExperiment objects. *At minima*, the following functions should be included:

    (A) "nexprs," "perCellQCMetrics," and "addPerFeatureQC" yield expressed features, counts sum (i.e., the library size), number of detected features, and mean counts per features. If the subset is specified, a nested DataFrame of a subset (e.g., when available in our count matrix, a sub-matrix of non-genomic features per barcode). A threshold for the number of detected features (detection. limit) can be tuned. The default is 0.

(B) "IsOutlier" determines the inferior (and/or superior) outliers for a sample of cells according to the number of features detected. By default, the three median absolute deviations (MADs) below or above the median log-library size are marked as outliers. It is possible to choose one or both tails by specifying the "type" option.

(C) "barcodeRanks" computes the total UMI counts for each barcode and the rank of each barcode, such that barcodes with the same total count receive the same average rank to avoid issues with discrete runs on the same total. Thus, the plotted sigmoidal curve "Ranks vs. UMI counts" (known as a knee plot) can be seen as a function where the computed inflection point determines a threshold to distinguish between real cells and empty drops/barcodes. This information can be stored as a boolean variable.

(D) "doubletCells" on the log-transformed matrix first simulates thousands of doublets in the proximity of each cell and then calculates the densities of both simulated and neighboring original cells. Finally, the computed ratio is stored as a score. Therefore, this CANNOT be done on combined batches, as impossible multiplets will be reported. To add robustness, several other simulation methods can be applied to each experimental batch. For instance, installing and running "DoubletFinder" on separated Seurat objects (always one by experimental batch): the resulting metadata will be used to filter out barcodes found in the intersection (or in the union, depending on your data and objectives) of the called "doublets" by the different implemented methods.

As doublets scoring is different from one method to another, classify by the percentile, for instance, the upper 5%, in coherence with the multiplet formation rate reported by the scRNA-seq technology protocol.

(E) Final QC results within a SingleCellExperiment object are stored in a dataframe (a table in R) with barcodes as row names, which can be then integrated using R syntax to the analogous Seurat object metadata immediately after the creation of the main Seurat object. Column names corresponding to the advanced QC results serve as exclusion/inclusion criteria for the Seurat object, adding coherently logical conditions to the options inside a Seurat "subset" function.

(F) We recommend developing a customized pipeline instead of using generic ones. For instance, stem cells are transcriptionally less active than their differentiated counterparts, thus investigating satellite cells or fibro-adipogenic

progenitors requires extra care in terms of exclusion criteria. Contamination with contaminant RNA/DNA must be checked out both in the alignment phase and after UMI counting. An example of an extended-version QC pipeline is available at https://github.com/LeGrand-Lab/QC_single_cell. Alternatively, modular steps are available at https://github.com/LeGrand-Lab/INMG_SingleCell. Note that computational methods explained in this note remain approximative, and the only way to eliminate multiplets/outliers and "batch effects" as much as possible is to apply experimental methods like "cell tagging" [28–30].

Acknowledgments

The authors wish to thank Erin Tse for helpful comments on this manuscript. Work in T.H.C. lab was supported by research grants from the Hong Kong Research Grant Council (A-HKUST604/14, C6018-19GF, C6027-19GF, AoE/M-604/16, T13-607/12R), the National Key R&D Program of China (2018YFE0203600), the Guangdong Provincial Key S&T Program (2018B030336001), Lee Hysan Foundation (LHF17SC01), Hong Kong Epigenome Project (Lo Ka Chung Charitable Foundation), and the Croucher Innovation Award (CIA14SC04) from Croucher Foundation. This study was supported in part by the Innovation and Technology Commission (ITCPD/17-9). T.H.C. is the S.H. Ho Associate Professor of Life Science at HKUST. Work in F.L.G lab was supported by funding from the Institut National pour la Santé et la Recherche Médicale (INSERM), the Centre National pour la Recherche Scientifique (CNRS), the Agence National pour la Recherche (ANR-19-CE14-0008, ANR-19-CE13-0016), and the European Joint Program on Rare Disease (EJPRD JTC 2019, MYOCITY).

References

1. Joe AW, Yi L, Natarajan A et al (2010) Muscle injury activates resident fibro/adipogenic progenitors that facilitate myogenesis. Nat Cell Biol 12:153–163
2. Arnold L, Henry A, Poron F et al (2007) Inflammatory monocytes recruited after skeletal muscle injury switch into antiinflammatory macrophages to support myogenesis. J Exp Med 204:1057–1069
3. Latroche C, Weiss-Gayet M, Muller L et al (2017) Coupling between myogenesis and angiogenesis during skeletal muscle regeneration is stimulated by restorative macrophages. Stem Cell Rep 9:2018–2033
4. Liu N, Garry GA, Li S et al (2017) A Twist2-dependent progenitor cell contributes to adult skeletal muscle. Nat Cell Biol 19:202–213
5. Dellavalle A, Maroli G, Covarello D et al (2011) Pericytes resident in postnatal skeletal muscle differentiate into muscle fibres and generate satellite cells. Nat Commun 2:499
6. Giordani L, He GJ, Negroni E et al (2019) High-dimensional single-cell cartography reveals novel skeletal muscle-resident cell populations. Mol Cell 74:609–621 e606
7. Zheng GX, Terry JM, Belgrader P et al (2017) Massively parallel digital transcriptional profiling of single cells. Nat Commun 8:14049

8. Ding J, Adiconis X, Simmons SK et al (2020) Systematic comparison of single-cell and single-nucleus RNA-sequencing methods. Nat Biotechnol 38:737–746
9. Macosko EZ, Basu A, Satija R et al (2015) Highly parallel genome-wide expression profiling of individual cells using nanoliter droplets. Cell 161:1202–1214
10. Klein AM, Mazutis L, Akartuna I et al (2015) Droplet barcoding for single-cell transcriptomics applied to embryonic stem cells. Cell 161:1187–1201
11. Cao J, Spielmann M, Qiu X et al (2019) The single-cell transcriptional landscape of mammalian organogenesis. Nature 566:496–502
12. Liu L, Cheung TH, Charville GW et al (2015) Isolation of skeletal muscle stem cells by fluorescence-activated cell sorting. Nat Protoc 10:1612–1624
13. Stuart T, Butler A, Hoffman P et al (2019) Comprehensive integration of single-cell data. Cell 177:1888–1902.e1821
14. Korsunsky I, Millard N, Fan J et al (2019) Fast, sensitive and accurate integration of single-cell data with Harmony. Nat Methods 16:1289–1296
15. Yu G, Wang L-G, Han Y et al (2012) clusterProfiler: an R Package for comparing biological themes among gene clusters. OMICS 16:284–287
16. Cabello-Aguilar S, Alame M, Kon-Sun-Tack F et al (2020) SingleCellSignalR: inference of intercellular networks from single-cell transcriptomics. Nucleic Acids Res 48:e55
17. Jin S, Guerrero-Juarez CF, Zhang L et al (2021) Inference and analysis of cell-cell communication using CellChat. Nat Commun 12:1088
18. Browaeys R, Saelens W, Saeys Y (2020) NicheNet: modeling intercellular communication by linking ligands to target genes. Nat Methods 17:159–162
19. Wang S, Karikomi M, Maclean AL et al (2019) Cell lineage and communication network inference via optimization for single-cell transcriptomics. Nucleic Acids Res 47:e66
20. Efremova M, Vento-Tormo M, Teichmann SA et al (2020) CellPhoneDB: inferring cell–cell communication from combined expression of multi-subunit ligand–receptor complexes. Nat Protoc 15:1484–1506
21. Tsuyuzaki K, Ishii M, Nikaido I (2019) Uncovering hypergraphs of cell-cell interaction from single cell RNA-sequencing data. bioRxiv:566182
22. La Manno G, Soldatov R, Zeisel A et al (2018) RNA velocity of single cells. Nature 560:494–498
23. Luecken MD, Theis FJ (2019) Current best practices in single-cell RNA-seq analysis: a tutorial. Mol Syst Biol 15:e8746
24. Bergen V, Lange M, Peidli S et al (2020) Generalizing RNA velocity to transient cell states through dynamical modeling. Nat Biotechnol 38:1408–1414
25. Zhang MJ, Ntranos V, Tse D (2020) Determining sequencing depth in a single-cell RNA-seq experiment. Nat Commun 11:774
26. Shapiro E, Biezuner T, Linnarsson S (2013) Single-cell sequencing-based technologies will revolutionize whole-organism science. Nat Rev Genet 14:618–630
27. Hafemeister C, Satija R (2019) Normalization and variance stabilization of single-cell RNA--seq data using regularized negative binomial regression. Genome Biol 20:296
28. Stoeckius M, Zheng S, Houck-Loomis B et al (2018) Cell Hashing with barcoded antibodies enables multiplexing and doublet detection for single cell genomics. Genome Biol 19:224
29. Gehring J, Hwee Park J, Chen S et al (2020) Highly multiplexed single-cell RNA-seq by DNA oligonucleotide tagging of cellular proteins. Nat Biotechnol 38:35–38
30. Mcginnis CS, Patterson DM, Winkler J et al (2019) MULTI-seq: sample multiplexing for single-cell RNA sequencing using lipid-tagged indices. Nat Methods 16:619–626
31. Saelens W, Cannoodt R, Todorov H et al (2019) A comparison of single-cell trajectory inference methods. Nat Biotechnol 37:547–554
32. Wolf FA, Hamey FK, Plass M et al (2019) PAGA: graph abstraction reconciles clustering with trajectory inference through a topology preserving map of single cells. Genome Biol 20:59
33. Street K, Risso D, Fletcher RB et al (2018) Slingshot: cell lineage and pseudotime inference for single-cell transcriptomics. BMC Genomics 19:477
34. Cannoodt R, Saelens W, Sichien D et al (2016) SCORPIUS improves trajectory inference and identifies novel modules in dendritic cell development. bioRxiv:079509
35. Linderman GC, Rachh M, Hoskins JG et al (2019) Fast interpolation-based t-SNE for improved visualization of single-cell RNA-seq data. Nat Methods 16:243–245
36. Kobak D, Berens P (2019) The art of using t-SNE for single-cell transcriptomics. Nat Commun 10:5416

Chapter 27

Assay for Transposase-Accessible Chromatin Using Sequencing of Freshly Isolated Muscle Stem Cells

Michail Yekelchyk, Stefan Guenther, and Thomas Braun

Abstract

Actively transcribed genes harbor cis-regulatory modules with comparatively low nucleosome occupancy and few high-order structures (="open chromatin"), whereas non-transcribed genes are characterized by high nucleosome density and extensive interactions between nucleosomes (="closed chromatin"), preventing transcription factor binding. Knowledge about chromatin accessibility is crucial to understand gene regulatory networks determining cellular decisions. Several techniques are available to map chromatin accessibility, among which the **A**ssay for **T**ransposase-**A**ccessible **C**hromatin using **seq**uencing (ATAC-seq) is one of the most popular. ATAC-seq is based on a straightforward and robust protocol but requires adjustments for different cell types. Here, we describe an optimized protocol for ATAC-seq of freshly isolated murine muscle stem cells. We provide details for the isolation of MuSC, tagmentation, library amplification, double-sided SPRI bead cleanup, and library quality assessment and give recommendations for sequencing parameters and downstream analysis. The protocol should facilitate generation of high-quality data sets of chromatin accessibility in MuSCs, even for newcomers to the field.

Key words Muscle stem cells, Satellite cells, ATAC-seq, Transposase, Sequencing, Chromatin accessibility, NGS

1 Introduction

Genomic DNA is wrapped around a set of eight histone proteins, thereby constituting nucleosomes. Nucleosomes are folded into more complex structures eventually forming chromosomes. Depending on the degree of condensation, "closed" heterochromatin, containing mostly inactive regions of the genome, can be distinguished from "open" euchromatin, which harbors the majority of actively transcribed genes. The position of nucleosomes on the genomic DNA is not fixed. Chromatin remodeling complexes can shift nucleosomes along the DNA, thereby allowing changes in the accessibility of gene regulatory regions. In addition, a special class of transcription factors, called pioneer transcription factors, facilitate chromatin remodeling and allow binding of secondary

Atsushi Asakura (ed.), *Skeletal Muscle Stem Cells: Methods and Protocols*, Methods in Molecular Biology, vol. 2640, https://doi.org/10.1007/978-1-0716-3036-5_27,

transcription factors, which are unable to penetrate chromatin and break the nucleosome barrier on their own [1]. The regulation of chromatin accessibility by pioneer transcription factors and chromatin remodelers is a highly complex and dynamic process, eventually allowing formation of the RNA Polymerase II-containing transcriptional initiation complex at specific sites [2]. Different cell types have distinct chromatin accessibility signatures, reflecting their specific gene expression profiles [3]. Promoters and/or enhancers of actively transcribed genes are kept open and accessible. However, many open chromatin regions are not yet transcribed, but maintained in a poised "primed" state, enabling fast transcriptional responses upon receiving specific external or internal signals.

Numerous cellular processes, including cellular linage specification and pathological responses, are orchestrated by changes in chromatin accessibility. For example, Jia and Preussner showed that accessibility of the *Nkx2–5* and *Isl1* promoter regions (and their subsequent expressions) determine the fate of cardiac progenitor cells in developing murine hearts [4]. Accessibility and expression of the *Isl1* transcription factor, which also acts as a pioneer factor, restricts cardiac progenitor cells within the cardiomyocyte, smooth muscle, and endothelial cells linages, while accessibility and expression of *Nkx2-5* irreversibly prime cells toward a cardiomyocyte fate. Similarly, chromatin accessibility regulates human erythropoiesis [5], oligodendroglia [6], and forebrain development [7]. Chromatin accessibility is often pathologically altered in cancer [8, 9] and upon formation of metastases [10, 11], in schizophrenia [12], and in osteoarthritis [13].

Hence, it is not very surprising that changes in chromatin accessibility also play an important role in the regulation of muscle stem cells (MuSCs, also called "Satellite cells"), which are essential for skeletal muscle regeneration [14]. Under basal conditions, MuSCs remain mostly in a quiescent state [15]. Upon muscle damage, MuSCs become activated, extensively proliferate, and eventually differentiate and fuse together into mature muscle fibers. A fraction of activated MuSCs (approx. 10%) is set aside and does not contribute to myofiber formation but replenishes the stem cell pool and returns to quiescence [16]. Activation, proliferation, and differentiation cause dramatic changes in chromatin accessibility. Several histone-modifying enzymes and histone-remodeling complexes but also transcription factors have been described to regulate chromatin organization in MuSCs [17, 18]. For example, *Pax7*, a transcription factor that specifically labels MuSCs but is also instrumental for their maintenance, is also involved in chromatin remodeling [19]. Furthermore, alterations of the chromatin in MuSCs are associated with various pathologies [20] and aging [21].

In order to assess the chromatin accessibility, the ATAC-seq method was introduced in 2013 by Jason Buenrosto [22]. The assay relies on a hyperactive Tn5 transposase, which is able to

reach open regions of chromatin, where it cuts double-stranded DNA. In addition, Tn5 attaches primers to the ends of DNA fragments [3]. This process was dubbed "Tagmentation." Notably, the nucleus stays intact during Tagmentation and fragments stay inside the nucleus. Since tagmented nuclei can be either FAC-sorted [23] or used for droplet-based protocols [24], an excellent resolution can be achieved, down to the single-cell level. For the more classical bulk ATAC-seq approach, digested DNA fragments are released and purified via a DNA purification column. Here we describe an ATAC-seq protocol, which is based on the protocols of Jason Buenrosto [3] and Xi Chen [23], but was optimized for MuSCs. We provide several *know-how* tips, allowing rapid establishment of the procedure.

2 Materials

See Table 1 for the list of used or suggested equipment and Table 2 for the list of used chemicals, reagents, and enzymes.

Table 1
Laboratory equipment

Equipment	Manufacturer
Tissue Chopper	McllWain, USA
Centrifuge (for 50 mL falcons, 15 mL falcons, and 1.5 mL tubes)	No preference
50 mL and 15 mL falcons, 1.5 mL tubes, and 0.2 mL tubes	No preference
Water bath or thermal block (37 °C)	No preference
Fluorescent-activated cell sorting (FACS) machine or Magnetic-activated cell sorting (MACS) device (depends on MuSCs isolation strategy)	No preference
Thermo-shaker (for 1.5 mL tubes, 37 °C)	No preference
Polymerase Chain Reaction (PCR) thermocycler	No preference
Quantitative PCR (qPCR) thermocycler	No preference
Magnetic separator for SPRI bead cleanup	No preference
Qubit measurement device	Thermo, USA
Capillary electrophoresis machine	Agilent, USA or PerkinElmer, USA
Next generation sequencer	Illumina, USA

Table 2
Chemicals and enzymes

Chemicals and enzymes	Manufacturer
Dulbecco's Modified Eagle Medium (DMEM)	Sigma, Germany
Penicillin and streptomycin	No preference
Dispase	354,235, Corning, USA
Collagenase type II	Worthington, USA
Fetal Calf Serum (FCS)	No preference
Percoll	P1644, sigma, Germany
Phosphate Buffered Saline (PBS) 10X and 1X	No preference
4′,6-diamidino-2-phenylindole (DAPI)	No preference
Tris-acetate, pH 7.8	No preference
Potassium acetate	95,843-100ML-F, Sigma, Germany
Magnesium acetate	63,052-100ML, Sigma, Germany
Dimethylformamide (DMF)	D4551-250ML, Sigma, Germany
Nuclease-free water	No preference
Digitonin	G9441, Promega, USA
TDE1 Tn5 transposase	20,034,197, Illumina, USA
MinElute PCR Purification Kit	28,004, Qiagen, Netherlands
Elution Buffer (EB)	Qiagen, Netherlands
Nextera index kit	FC-121-1011 (1012), Illumina, USA
NEB Next High-Fidelity PCR Master Mix (2X)	M0541S, NEB, USA
SYBR-Green Mastermix (2X)	4,309,155, Thermo, USA
Solid Phase Reversible Immobilization (SPRI) magnetic beads	AC-60050, MagBio, Switzerland
Ethanol 100%	No preference
High-75 NextSeq500 cartridge	20,024,906, Illumina, USA

3 Methods

3.1 Brief Description of the MuSC Isolation

The following protocol describes the isolation of quiescent MuSCs from *Pax7*^{zsGreen} mice. *Pax7* is a unique marker of MuSCs and the *Pax7*^{zsGreen} mouse strain expresses a transgene *zsGreen* fluorescent tag under the control of the *Pax7* promoter [25]. Therefore, only MuSCs show a green fluorescence signal in skeletal muscles (*see* **Note 1**).

1. Sacrifice *Pax7*^{zsGreen} mice and collect all the resectable skeletal muscles (lower limb muscles, upper limb muscles, breast muscles, and back muscles). Place the muscles in 50 mL falcon tubes with isolation media (DMEM +2% penicillin-streptomycin).
2. Chop the muscles into a fine slurry using a tissue chopper.
3. Add 18 mL of isolation media and 2 mL of Dispase solution to the muscle slurry in 50 mL falcons. Falcons should be incubated in a water bath (37 °C) for 30 min with regular shaking (every 10 min). Afterward, thoroughly disrupt the tissue mixture by passing through a 20 or 24 mL syringe several times without an attached needle.
4. Add 2 mL of 0.5% Collagenase type II to the 50 mL falcons. Falcons should be incubated in a water bath (37 °C) for 30 min with regular shaking (every 10 min). Afterward passage again through a 20 or 24 mL syringe (without needle) for homogenization of cell suspension.
5. Fill every tube up to 50 mL volume with FCS-containing media (DMEM +1% penicillin-streptomycin +10% FCS) to inactivate the enzymes.
6. Filter the cell mixtures consecutively through 100 μm, 70 μm, and 40 μm cell strainers (*see* **Note 2**).
7. Centrifuge the filtered cell suspension at 1200 g for 10 min.
8. In the meantime, prepare Percoll sugar gradient tubes. Prepare 90% Percoll (9 parts of Percoll and 1 part of 10X PBS). Dilute 90% Percoll with 1X PBS to make 70% Percoll, and with FCS-containing media to make 30% Percoll. Slowly inject 3 mL of 70% Percoll with a long syringe needle under the 5 mL of 30% Percoll in a 15 mL falcon tube (*see* **Note 3**).
9. Resuspend the cell pellet in 5 mL of cell-sorting buffer (PBS + 1% FCS + 10 mM EDTA) and slowly load the mixture on top of the Percoll gradient. Centrifuge the Percoll tubes with samples for 20 min at 1200 g with the lowest settings of acceleration and deceleration to avoid any mixture of liquid phases (*see* **Note 4**).
10. Collect 1–2 mL of media from the 30%/70% interface with a 1 mL pipette and filter through a 40 μm cell strainer.
11. Stain the collected samples with DAPI to identify viable (DAPI-neg) and dead (DAPI-pos) cells. This final mixture is used for the FACS.
12. The gating strategy should include thresholds on the forward and side scatters (the cells should be smaller than 20–30 μm in diameter and round), and sorted cells should be DAPI-negative and *zsGreen*-positive (*see* **Note 5**).

3.2 Tagmentation

The ATAC-seq protocol is tolerant to a wide range of input of cell numbers. The recommended amount is 50 k cells, but we have good experience with numbers ranging from 5 k to 100 k cells (*see* **Note 6**).

1. Prepare 1 mL of 4X THS buffer (*can be stored at − 20 °C for 2 months*):

   123 μL Tris-acetate, pH 7.8.

   52.8 μL Potassium acetate.

   40 μL Magnesium acetate.

   640 μL Dimethylformamide (DMF).

   135.2 μL Nuclease-free water.

   ———————————

   Total: 1 mL
2. Prepare fresh Lysis/Tagmentation Mastermix (per sample):

   12.5 μL 4X THS buffer.

   5 μL 0.1% Digitonin (1:20 dilution of 2% Digitonin stock in water).

   30 μL Nuclease-free water.

   2.5 μL TDE1 (Tn5 Transposase).

   ———————————

   Total: 50 μL
3. Aliquot the desired number of cells in a 1.5 mL tube (50 k cells by default). Centrifuge the cells for 5 min at 1200 g and discard the supernatant (*see* **Note 7**).
4. Add fresh Lysis/Tagmentation Mastermix to the cell pellet. Pipette well to resuspend the pellet in Mastermix. Incubate for 30 min in a thermoshaker (37 °C, 800 rpm).
5. Immediately following transposition, purify the mixture using Qiagen MinElute PCR Purification Kit (add 250 μL of binding buffer, then follow the manufacturer's protocol). Elute transposed DNA in 10 μL of the EB buffer.
6. Store purified DNA at −20 °C if necessary (safe stopping point; up to 6 months) (*see* **Note 8**).

3.3 First PCR Amplification

The digested DNA fragments contain Illumina-compatible adapters on 3′ and 5′ ends. The indexed primers (from the Nextera indexing kit or custom; *see* Table 3) are designed for demultiplexing of libraries upon massive parallel sequencing.

1. To amplify the transposed DNA fragments, combine the following (per sample):

   10 μL transposed DNA.

   13 μL nuclease-free H_2O.

Table 3
ATAC-seq oligo primers for PCR designed by Buenrosto et al. (index sequences are provided next to primer names; their reverse-complement parts of oligos are marked in bold italics) [22]

Index	Sequence
Fw_universal	AATGATACGGCGACCACCGAGATCTACACTCGTCGGCAG CGTCAGATGTG
Rev_1 (TAAGGCGA)	CAAGCAGAAGACGGCATACGAGAT***TCGCCTTA***GTCTCGTGGGC TCGGAGATGT
Rev_2 (CGTACTAG)	CAAGCAGAAGACGGCATACGAGAT***CTAGTACG***GTCTCGTGGGC TCGGAGATGT
Rev_3 (AGGCAGAA)	CAAGCAGAAGACGGCATACGAGAT***TTCTGCCT***GTCTCGTGGGC TCGGAGATGT
Rev_4 (TCCTGAGC)	CAAGCAGAAGACGGCATACGAGAT***GCTCAGGA***GTCTCGTGGGC TCGGAGATGT
Rev_5 (GGACTCCT)	CAAGCAGAAGACGGCATACGAGAT***AGGAGTCC***GTCTCGTGGGC TCGGAGATGT
Rev_6 (TAGGCATG)	CAAGCAGAAGACGGCATACGAGAT***CATGCCTA***GTCTCGTGGGC TCGGAGATGT
Rev_7 (CTCTCTAC)	CAAGCAGAAGACGGCATACGAGAT***GTAGAGAG***GTCTCGTGGGC TCGGAGATGT
Rev_8 (CAGAGAGG)	CAAGCAGAAGACGGCATACGAGAT***CCTCTCTG***GTCTCGTGGGC TCGGAGATGT
Rev_9 (GCTACGCT)	CAAGCAGAAGACGGCATACGAGAT***AGCGTAGC***GTCTCGTGGGC TCGGAGATGT
Rev_10 (CGAGGCTG)	CAAGCAGAAGACGGCATACGAGAT***CAGCCTCG***GTCTCGTGGGC TCGGAGATGT
Rev_11 (AAGAGGCA)	CAAGCAGAAGACGGCATACGAGAT***TGCCTCTT***GTCTCGTGGGC TCGGAGATGT
Rev_12 (GTAGAGGA)	CAAGCAGAAGACGGCATACGAGAT***TCCTCTAC***GTCTCGTGGGC TCGGAGATGT
Rev_13 (GTCGTGAT)	CAAGCAGAAGACGGCATACGAGAT***ATCACGAC***GTCTCGTGGGC TCGGAGATGT
Rev_14 (ACCACTGT)	CAAGCAGAAGACGGCATACGAGAT***ACAGTGGT***GTCTCGTGGGC TCGGAGATGT
Rev_15 (TGGATCTG)	CAAGCAGAAGACGGCATACGAGAT**CAGATCCA**GTCTCGT GGGCTCGGAGATGT
Rev_16 (CCGTTTGT)	CAAGCAGAAGACGGCATACGAGAT***ACAAACGG***GTCTCGTGGGC TCGGAGATGT
Rev_17 (TGCTGGGT)	CAAGCAGAAGACGGCATACGAGAT***ACCCAGCA***GTCTCGTGGGC TCGGAGATGT
Rev_18 (GAGGGGTT)	CAAGCAGAAGACGGCATACGAGAT***AACCCCTC***GTCTCGTGGGC TCGGAGATGT

(continued)

Table 3
(continued)

Index	Sequence
Rev_19 (AGGTTGGG)	CAAGCAGAAGACGGCATACGAGAT***CCCAACCT***GTCTCGTGGGC TCGGAGATGT
Rev_20 (GTGTGGTG)	CAAGCAGAAGACGGCATACGAGAT***CACCACAC***GTCTCGTGGGC TCGGAGATGT
Rev_21 (TGGGTTTC)	CAAGCAGAAGACGGCATACGAGAT***GAAACCCA***GTCTCGTGGGC TCGGAGATGT
Rev_22 (TGGTCACA)	CAAGCAGAAGACGGCATACGAGAT***TGTGACCA***GTCTCGTGGGC TCGGAGATGT
Rev_23 (TTGACCCT)	CAAGCAGAAGACGGCATACGAGAT***AGGGTCAA***GTCTCGTGGGC TCGGAGATGT
Rev_24 (CCACTCCT)	CAAGCAGAAGACGGCATACGAGAT***AGGAGTGG***GTCTCGTGGGC TCGGAGATGT

1 μL Nextera Index1 + 1 μL Nextera Index2.

25 μL NEB Next High-Fidelity PCR Master Mix (2X).

Total: 50 μL

2. Thermal cycle as follows:

1 cycle:	5 min 72 °C 30 s 98 °C
5 cycles:	10 s 98 °C 30 s 63 °C 1 min 72 °C
Hold	4 °C

3.4 Side qPCR Reaction

The initial concentration of digested DNA fragments is very low. Thus, it is not possible to directly measure DNA content and estimate the exact number of PCR cycles that are required for sufficient amplification, while avoiding overamplification. Side qPCR is utilized to determine the required number of additional PCR cycles.

1. Prepare the side qPCR reaction Mastermix (per sample):

   5 μL of initial PCR reaction.

   2.5 μL Nuclease-free water.

   7.5 μL SYBR-Green Mastermix (2X).

   Total: 15 μL

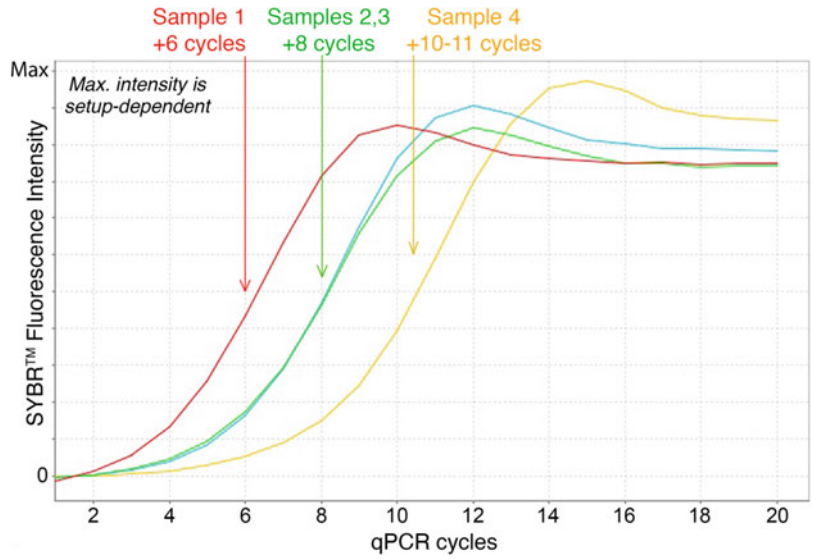

Fig. 1 qPCR-estimation of additional PCR cycles for ATAC-seq libraries. Final library amplification is monitored by SYBR-green incorporation in a side reaction for additional 20 cycles. Typically, the exponential phase is reached after 5–12 cycles, depending on cell numbers and chromatin composition, followed by the plateau phase with a decrease in amplification. The goal is to identify the number of cycles required to reach the early phase of exponential amplification. For limited amounts of starting material, the cutoff may be set to the end of the exponential phase to increase the obtained amount of library after cleanup and size selection

2. Thermal cycle as follows on the qPCR instrument:

1 cycle:	30 s 98 °C
20 cycles:	10 s 98 °C 30 s 63 °C 1 min 72 °C

3. Evaluate the additional number of cycles needed (N): plot linear ΔRn versus cycle and determine the cycle number that corresponds to the half of the maximum fluorescent intensity (Fig. 1).

3.5 Second PCR Amplification

1. Run the remaining 45 μL of PCR reaction with the cycle number determined by qPCR:

1 cycle:	30 s 98 °C
N cycles:	10 s 98 °C 30 s 63 °C 1 min 72 °C
Hold:	4 °C

3.6 Double-Sided SPRI Bead Clean-up

An amplified library still contains small-sized primer leftovers (50–60 bp) and large fragments (>1 kb) that cannot be sequenced. The double-sided SPRI bead cleanup is necessary to purify and size-select the sequencing library.

1. Perform 1.2X bead cleanup:

   Add 54 μL of SPRI beads to 45 μL of the PCR reaction and mix well. Incubate for 5 min at room temperature (RT). Place the tube on a magnet and wait until the solution clears. Discard the supernatant. Wash the bead pellet twice with freshly prepared 80% ethanol. Discard the ethanol and air-dry the beads for 2 min at RT. Add 10 μL of EB buffer to the beads and thoroughly pipette to resuspend the bead pellet. Incubate for 2 min at RT. Place the tube on the magnet and transfer 9 μL to a new tube.

2. Perform 0.5X inversed bead cleanup:

   Add 4.5 μL of SPRI beads to 9 μL of library and mix well. Incubate for 5 min at RT. Place the tube on a magnet and wait until the solution clears. Transfer 12.5 μL of supernatant to a new tube.

3. Perform 0.6X bead cleanup:

   Add 5.4 μL of SPRI beads to 12.5 μL of supernatant. Incubate for 5 min at RT. Place the tube on a magnet and wait until the solution clears. Discard the supernatant. Wash the bead pellet twice with freshly prepared 80% ethanol. Discard the ethanol and air-dry the beads for 2 min at RT. Add 12.5 μL of EB buffer to the beads and thoroughly pipette to resuspend the bead pellet. Incubate for 2 min at RT. Place a tube on the magnet and transfer 12 μL of the final library to the new tube (Safe stopping point; store the libraries at −20 °C for the short-term (1–2 months) and at −80 °C for long-term storage (years)) (*see* **Note 9**) (Fig. 2).

3.7 Quality Assessment

To evaluate the quantity and the quality of the final ATAC-seq libraries, the concentrations and size distributions should be measured. We suggest to use the Qubit HS DNA kit for concentration measurements. Normally, library concentrations range between 1 and 50 ng/μL. To estimate the size distribution of libraries, capillary electrophoresis might be done (Agilent Bioanalyzer, Agilent Fragment-Analyzer, PerkinElmer Lab-Chip, etc.). Avoid standard agarose gel electrophoresis since resolution and sensitivity are not sufficient for NGS libraries. A useful ATAC-seq library often has a "wavy structure," which reflects the nucleosome pattern (Fig. 3). Although a "wavy structure" is a good sign, it is not mandatory and highly dependent on the cell type and state of chromatin (*see* **Note 10**).

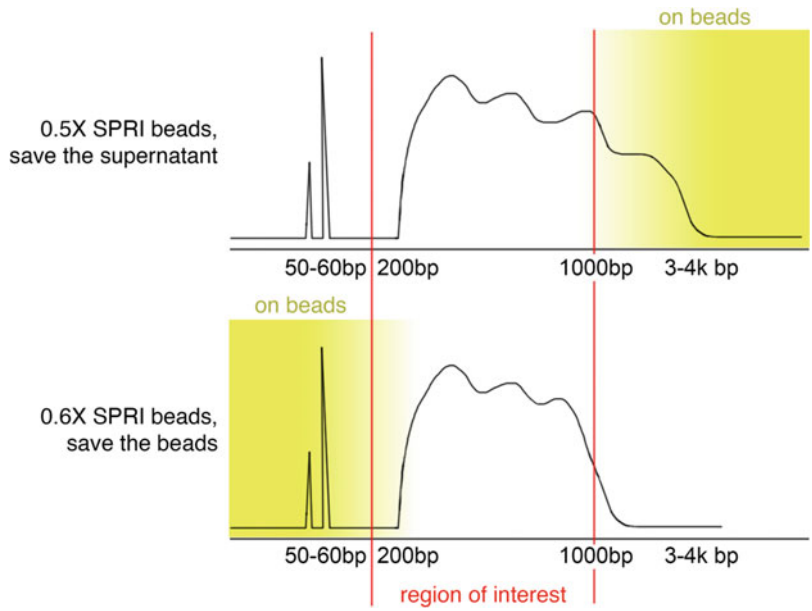

Fig. 2 Concept of double-sided SPRI bead cleanup. Addition of different ratios of SPRI beads to the samples allows preferential binding of small or large fragments. The double-sided cleanup consists of two steps, the left-sided cleanup with a lower ratio of beads to exclude fragments too big for the sequencing reaction (upper panel – yellow), followed by right-sided bead cleanup to eliminate smaller fragments such as remaining primers and adapter-dimer (lower panel – yellow). The cutoff sizes may be adjusted by changing bead ratios. The described ratios were optimal in our hands for ATAC libraries

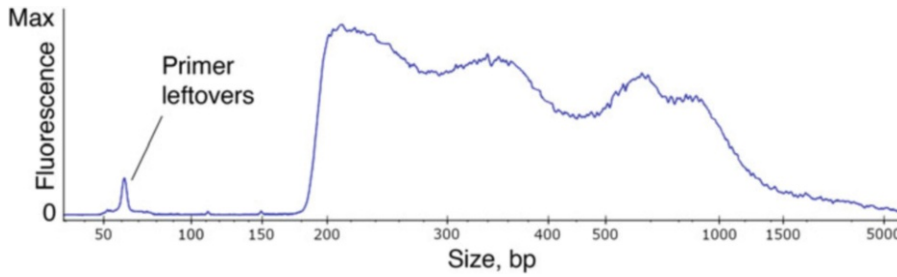

Fig. 3 Wavy structure of the ATAC-seq library. Typical example of MuSCs ATAC library after size selection. Only minimal leftovers of primer and fragments with insert sizes (> 1kb) are visible. Since freshly isolated MuSCs mostly carry dense heterochromatin, a clear enrichment for nucleosome fragments is visible (several peaks with distance of ~150 bp from maxima to maxima), resulting in a wave-like distribution of the library size

3.8 Sequencing

Sequencing should be performed on the Illumina platform. We usually use Illumina NextSeq500 and "High-75" cartridges, which allow to obtain 400–500 M of sequencing reads, comfortably accommodating 12–14 ATAC-seq libraries (30–40 M of reads per library).

The following setup should be used (paired-end sequencing; bp) (*see* **Note 11**):

Read 1–38 *(may be more, but not less than 30)*;
Read 2–38 *(may be more, but not less than 30)*;
Index 1–8 *(fixed length)*;
Index 2–8 *(fixed length)*.

3.9 Brief Description of the Bioinformatical Analysis

The sequencing reads should be demultiplexed into separate samples (with *bcl2fastq* function, supplied by Illumina). The reads should be trimmed and filtered (using the *trimmomatic* pipeline, for example) [26]. Next, the reads should be mapped to the reference genome (with *STAR*, for example) [27] (Fig. 4). The mapped reads should be counted and annotated to the nearest genes.

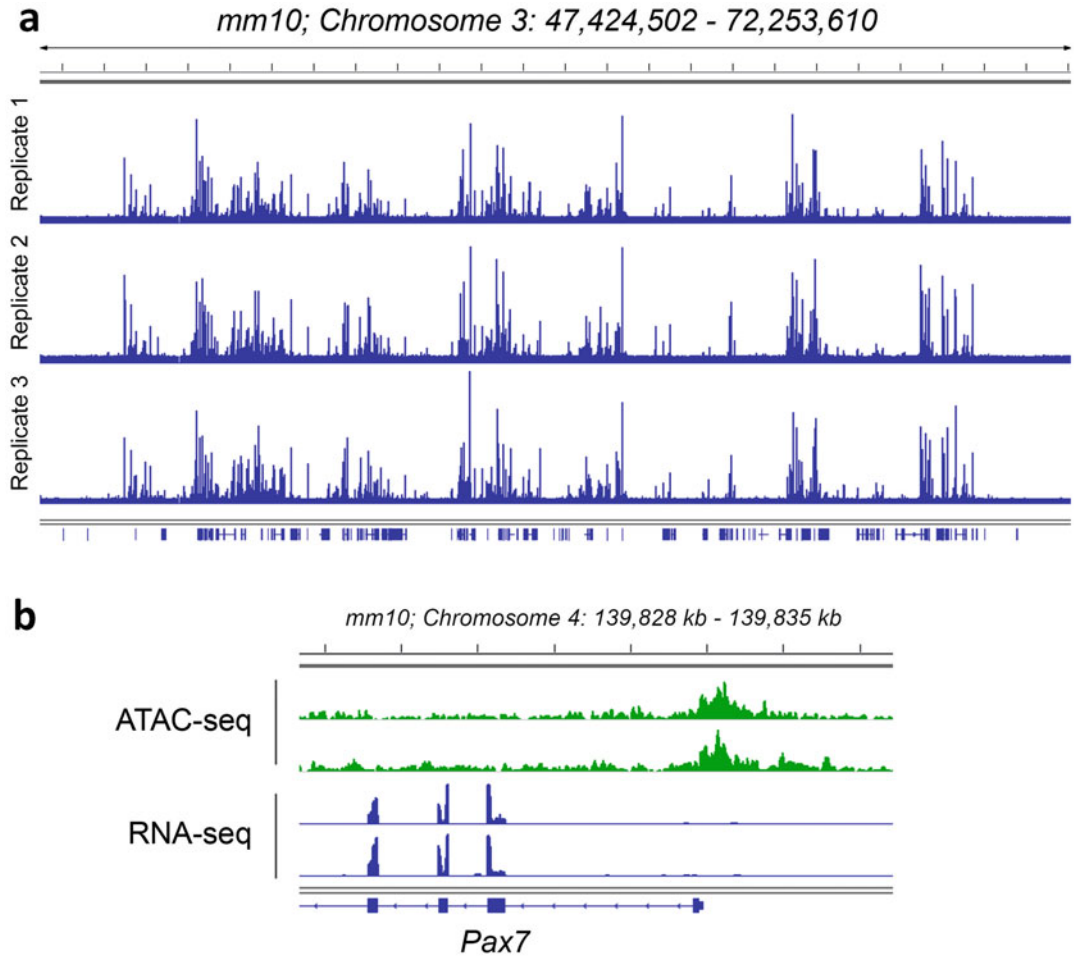

Fig. 4 (**a**) A screenshot from an IGV browser, illustrating the distribution of accessibility peaks across the genome at low magnification. (**b**) A screenshot from the IGV browser at the accessible *Pax7* promoter. The data from the ATAC-seq analysis (green) are compared to RNA-seq results (blue) as an example of the correlation between promoter accessibility and gene expression

Commonly, a read is associated with a gene, if it is located within 5 kb from the transcription starting site (TSS) or overlaps with the gene body. Conflicting reads should be excluded from the analysis (*see* **Note 12**).

Resulting count tables should be normalized (by the library size, for example). A differential accessibility analysis can be performed between the conditions. Furthermore, it is possible to perform a motif analysis, which searches for enriched Transcription Factor binding motifs, and a Footprint analysis, which evaluates the probability of transcription factor binding at selected promoters (using TOBIAS, for example) [28].

4 Notes

1. Antibody-based isolation methods are also compatible with the ATAC-seq protocol [29]. The current isolation procedure is recommended, but might be replaced by other isolation protocols, depending on personal preferences or experimental demands. The crucial result is to acquire a pure suspension of viable and intact MuSCs.
2. The debris might clog the filter, short centrifugation (30 s, 500 g) will pellet all debris at the bottom of the falcon and ease filtration.
3. Due to the different colors of Percoll solutions, the border between 30% and 70% Percoll gradients will be clearly visible.
4. After centrifugation, a cloud of cells, enriched for MuSCs, will be visible at the border between 30% and 70% Percoll. Aspirate and discard the upper aqueous phase.
5. Isolation of quiescent MuSCs from one *Pax7*^{zsGreen} mouse usually generated 100–150 k cells. The isolated cells should be immediately used for ATAC-seq library preparation.
6. It is important to have an equal number of cells in each sample, which makes the lowest concentrated sample the limiting factor.
7. A 50 k cell pellet might be faintly visible at the bottom of the tube. You will not see a pellet which contains less than ~20 k cells. In this case, carefully and slowly aspirate the supernatant, avoiding to touch the tube walls. It is allowed to leave few microliters of liquid at the bottom of the tube.
8. The original protocol from Jason Buenrosto suggests to use 0.1% IGEPAL for the lysis of cellular membrane [3]. In contrast, we use Digitonin to lyse cells and release nuclei. The advantage of Digitonin is that it only lyses the membranes, which are cholesterol-rich [23]. Therefore, membranes of mitochondria (which are cholesterol-low) [30] are not lysed

together with cellular membrane, avoiding contamination of the libraries with mitochondrial DNA.

9. Resulting samples should contain sequencing libraries in the target diapason (200–1000 bp). 0.5X inversed cleanup removes large DNA fragments that cannot be sequenced, while 0.6X cleanup removes small primer leftovers, as well as possible primer dimers (Fig. 2).
10. If your libraries do not look "wavy," we recommend to sequence one-two of them with low sequencing depth (5–10 M reads) as a test. Since all libraries have unique indexes, you can add test runs to the "normal" sequencing run together with other (not necessarily ATAC-seq) samples. Evaluate the peak distribution and decide if you want to sequence the rest of the samples.
11. It is allowed to alter the length of the first and second reads. The higher numbers may improve the mapping rate of reads to the genome. In addition, we do not recommend decreasing the numbers below 30bp to avoid random mapping.
12. Therefore, pay attention to the reads, allocated to repetitive elements. If you are interested in those reads, you should allow multi-mapping in the analysis pipeline.

Acknowledgments

This work was supported by the Excellence Initiative "Cardiopulmonary Institute" (CPI), the DFG collaborative research center SFB1213, the DFG Transregional Collaborative Research Centre 81, the DFG Clinical Research Unit FKO 309, and the European Research Area Network on Cardiovascular Diseases project CLARIFY.

References

1. Mayran A, Drouin J (2018) Pioneer transcription factors shape the epigenetic landscape. J Biol Chem 293(36):13795–13804. https://doi.org/10.1074/jbc.R117.001232
2. Klemm SL, Shipony Z, Greenleaf WJ (2019) Chromatin accessibility and the regulatory epigenome. Nat Rev Genet 20(4):207–220. https://doi.org/10.1038/s41576-018-0089-8
3. Buenrostro JD, Wu B, Chang HY et al (2015) ATAC-seq: a method for assaying chromatin accessibility genome-wide. Curr Protoc Mol Biol 109:21 29 21-21 29 29. https://doi.org/10.1002/0471142727.mb2129s109
4. Jia G, Preussner J, Chen X et al (2018) Single cell RNA-seq and ATAC-seq analysis of cardiac progenitor cell transition states and lineage settlement. Nat Commun 9(1):4877. https://doi.org/10.1038/s41467-018-07307-6
5. Ludwig LS, Lareau CA, Bao EL et al (2019) Transcriptional states and chromatin accessibility underlying human erythropoiesis. Cell Rep 27(11):3228–3240 e3227. https://doi.org/10.1016/j.celrep.2019.05.046
6. Huang N, Niu J, Feng Y et al (2015) Oligodendroglial development: new roles for chromatin accessibility. Neuroscientist 21(6):579–588. https://doi.org/10.1177/1073858414565467

7. Trevino AE, Sinnott-Armstrong N, Andersen J et al (2020) Chromatin accessibility dynamics in a model of human forebrain development. Science 367(6476):eaay1645. https://doi.org/10.1126/science.aay1645
8. Corces MR, Granja JM, Shams S et al (2018) The chromatin accessibility landscape of primary human cancers. Science 362(6413):eaav1898. https://doi.org/10.1126/science.aav1898
9. Deutschmeyer V, Breuer J, Walesch SK et al (2019) Epigenetic therapy of novel tumour suppressor ZAR1 and its cancer biomarker function. Clin Epigenetics 11(1):182. https://doi.org/10.1186/s13148-019-0774-2
10. Zhou ZH, Wang QL, Mao LH et al (2019) Chromatin accessibility changes are associated with enhanced growth and liver metastasis capacity of acid-adapted colorectal cancer cells. Cell Cycle 18(4):511–522. https://doi.org/10.1080/15384101.2019.1578145
11. Jia Y, Vong JS, Asafova A et al (2019) Lamin B1 loss promotes lung cancer development and metastasis by epigenetic derepression of RET. J Exp Med 216(6):1377–1395. https://doi.org/10.1084/jem.20181394
12. Bryois J, Garrett ME, Song L et al (2018) Evaluation of chromatin accessibility in prefrontal cortex of individuals with schizophrenia. Nat Commun 9(1):3121. https://doi.org/10.1038/s41467-018-05379-y
13. Liu Y, Chang JC, Hon CC et al (2018) Chromatin accessibility landscape of articular knee cartilage reveals aberrant enhancer regulation in osteoarthritis. Sci Rep 8(1):15499. https://doi.org/10.1038/s41598-018-33779-z
14. Gunther S, Kim J, Kostin S et al (2013) Myf5-positive satellite cells contribute to Pax7-dependent long-term maintenance of adult muscle stem cells. Cell Stem Cell 13(5):590–601. https://doi.org/10.1016/j.stem.2013.07.016
15. Evano B, Tajbakhsh S (2018) Skeletal muscle stem cells in comfort and stress. NPJ Regen Med 3:24. https://doi.org/10.1038/s41536-018-0062-3
16. Kuang S, Kuroda K, Le Grand F et al (2007) Asymmetric self-renewal and commitment of satellite stem cells in muscle. Cell 129(5):999–1010. https://doi.org/10.1016/j.cell.2007.03.044
17. Sreenivasan K, Ianni A, Kunne C et al (2020) Attenuated epigenetic suppression of muscle stem cell necroptosis is required for efficient regeneration of dystrophic muscles. Cell Rep 31(7):107652. https://doi.org/10.1016/j.celrep.2020.107652
18. Boonsanay V, Zhang T, Georgieva A et al (2016) Regulation of skeletal muscle stem cell quiescence by Suv4-20h1-dependent facultative heterochromatin formation. Cell Stem Cell 18(2):229–242. https://doi.org/10.1016/j.stem.2015.11.002
19. Lilja KC, Zhang N, Magli A et al (2017) Pax7 remodels the chromatin landscape in skeletal muscle stem cells. PLoS One 12(4):e0176190. https://doi.org/10.1371/journal.pone.0176190
20. Zhou J, So KK, Li Y et al (2019) Elevated H3K27ac in aged skeletal muscle leads to increase in extracellular matrix and fibrogenic conversion of muscle satellite cells. Aging Cell 18(5):e12996. https://doi.org/10.1111/acel.12996
21. Garcia-Prat L, Munoz-Canoves P (2017) Aging, metabolism and stem cells: spotlight on muscle stem cells. Mol Cell Endocrinol 445:109–117. https://doi.org/10.1016/j.mce.2016.08.021
22. Buenrostro JD, Giresi PG, Zaba LC et al (2013) Transposition of native chromatin for fast and sensitive epigenomic profiling of open chromatin, DNA-binding proteins and nucleosome position. Nat Methods 10(12):1213–1218. https://doi.org/10.1038/nmeth.2688
23. Chen X, Miragaia RJ, Natarajan KN et al (2018) A rapid and robust method for single cell chromatin accessibility profiling. Nat Commun 9(1):5345. https://doi.org/10.1038/s41467-018-07771-0
24. Scott RW, Arostegui M, Schweitzer R et al (2019) Hic1 defines quiescent mesenchymal progenitor subpopulations with distinct functions and fates in skeletal muscle regeneration. Cell Stem Cell 25(6):797–813 e799. https://doi.org/10.1016/j.stem.2019.11.004
25. Preussner J, Zhong J, Sreenivasan K et al (2018) Oncogenic amplification of zygotic dux factors in regenerating p53-deficient muscle stem cells defines a molecular cancer subtype. Cell Stem Cell 23(6):794–805 e794. https://doi.org/10.1016/j.stem.2018.10.011
26. Bolger AM, Lohse M, Usadel B (2014) Trimmomatic: a flexible trimmer for Illumina sequence data. Bioinformatics 30(15):2114–2120. https://doi.org/10.1093/bioinformatics/btu170
27. Dobin A, Davis CA, Schlesinger F et al (2013) STAR: ultrafast universal RNA-seq

aligner. Bioinformatics 29(1):15–21. https://doi.org/10.1093/bioinformatics/bts635

28. Bentsen M, Goymann P, Schultheis H et al (2020) ATAC-seq footprinting unravels kinetics of transcription factor binding during zygotic genome activation. Nat Commun 11(1):4267. https://doi.org/10.1038/s41467-020-18035-1
29. Liu L, Cheung TH, Charville GW et al (2015) Isolation of skeletal muscle stem cells by fluorescence-activated cell sorting. Nat Protoc 10(10):1612–1624. https://doi.org/10.1038/nprot.2015.110
30. Elustondo P, Martin LA, Karten B (2017) Mitochondrial cholesterol import. Biochim Biophys Acta Mol Cell Biol Lipids 1862(1):90–101. https://doi.org/10.1016/j.bbalip.2016.08.012

Chapter 28

Efficient Genome-Wide Chromatin Profiling by CUT&RUN with Low Numbers of Muscle Stem Cells

Dong Ding and Thomas Braun

Abstract

Adult muscle stem cells (MuSCs), also called satellite cells, are situated under the basal lamina of myofibers in skeletal muscles. MuSCs are instrumental for postnatal muscle growth and regeneration of skeletal muscles. Under physiological conditions, the majority of MuSCs is actively maintained in a quiescent state but becomes rapidly activated during muscle regeneration, which is accompanied with massive changes in the epigenome. Moreover, aging, but also pathological conditions, such as in muscle dystrophy, results in profound changes of the epigenome, which can be monitored with different approaches. However, a better understanding of the role of chromatin dynamics in MuSCs and its function for skeletal muscle physiology and disease has been hampered by technical limitations, mostly due to the relatively low number of MuSCs but also due to the strongly condensed chromatin state of quiescent MuSCs. Traditional chromatin immunoprecipitation (ChIP) usually requires large amounts of cells and has several other shortcomings. Cleavage Under Targets and Release Using Nuclease (CUT&RUN) is a simple alternative to ChIP for chromatin profiling, providing higher efficiency and better resolution at lower costs. CUT&RUN maps genome-wide chromatin features, including genome-wide localization of transcription factor binding in small numbers of freshly isolated MuSCs, facilitating analysis of different subpopulations of MuSCs. Here we describe an optimized protocol to profile global chromatin in freshly isolated MuSCs using CUT&RUN.

Key words Muscle stem cells, Quiescence, Chromatin, Transcription factor, Epigenome, CUT&RUN

1 Introduction

Adult muscle stem cells (MuSCs) account for approximately 5% of all myonuclei under the basal lamina and are therefore relatively rare compared to myonuclei in myofibers. Despite their low numbers, MuSCs are extremely efficient to regenerate skeletal muscles after injury and maintain long-term muscle homeostasis over a lifetime [1]. Within a matter of weeks, a damaged muscle containing no viable myofibers can be completely rebuilt, if the architecture of a skeletal muscle is not destroyed. MuSCs are mostly locked in a quiescent state in resting muscles, which is associated with a

Atsushi Asakura (ed.), *Skeletal Muscle Stem Cells: Methods and Protocols*, Methods in Molecular Biology, vol. 2640,
https://doi.org/10.1007/978-1-0716-3036-5_28,

high content of heterochromatin, required to prevent precocious activation, differentiation, and reduction of the stem cell pool [2]. Upon muscle damage, several cellular signaling pathways converge on the chromatin to mediate a switch from hetero- to euchromatin, orchestrating transcriptional programs that control activation, proliferation, and differentiation, as well as self-renewal of MuSCs [3]. Remodeling of the chromatin landscape (e.g., changes of the binding of transcription factors and altered distribution of modified histones or variants) directs coordinated transcriptional changes during regeneration [4]. Muscular dystrophy and other skeletal muscle diseases, but also physiological aging are accompanied by epigenetic changes in MuSCs, suggesting a critical role in these processes [2, 5]. A deeper understanding of chromatin biology in MuSCs will be instrumental to design epigenetic therapies upholding MuSC functions in diseased and aged muscles.

The relative paucity of MuSCs in skeletal muscles poses a significant challenge for genome-wide chromatin profiling, since standard chromatin immunoprecipitation followed by sequencing (ChIP-Seq) requires a large number of cells. Traditional ChIP enriches antibody-bound cross-linked, sheared, and solubilized chromatin fragments before DNA extraction. Since the efficiency to recover chromatin fragments by ChIP is inherently low, large numbers of cells have to be processed. This problem becomes more severe when freshly isolated MuSCs are analyzed, which cannot be expanded in culture and which contain a high content of condensed chromatin, requiring several adaptions. Traditional ChIP has been modified to cope with low numbers but still requires millions of cells to profile transcription factors [6]. Hence, it is difficult to successfully apply such protocols to freshly isolated MuSCs. Moreover, cross-linking and sonication frequently introduce biases and artifacts [7, 8], and produce relatively large chromatin fragments that do not provide sufficient base-pair resolution when mapping transcription factors. The complexity of ChIP also requires a sophisticated spike-in strategy for quantitative analysis [9].

CUT&RUN (Cleavage Under Targets and Release Using Nuclease) is based on a different principle than ChIP, offering a novel and simple approach for efficient epigenomic profiling [10, 11]. In CUT&RUN, the controlled cleavage by antibody-tethered micrococcal nuclease releases targeted chromatin/DNA from nearly intact nuclei into the supernatant for isolation and high-throughput DNA sequencing (Fig. 1). Since only the targeted DNA fragments become soluble, while the vast majority of the genome remains in the nucleus, background levels in CUT&RUN are remarkably low, allowing reduced sequencing depth [11]. Low background levels enable CUT&RUN to profile transcription factors in 1000 [10] or even single cells [12]. Shorter fragments generated by micrococcal nuclease result in higher resolution in mapping protein binding [13]. Compared to ChIP or other

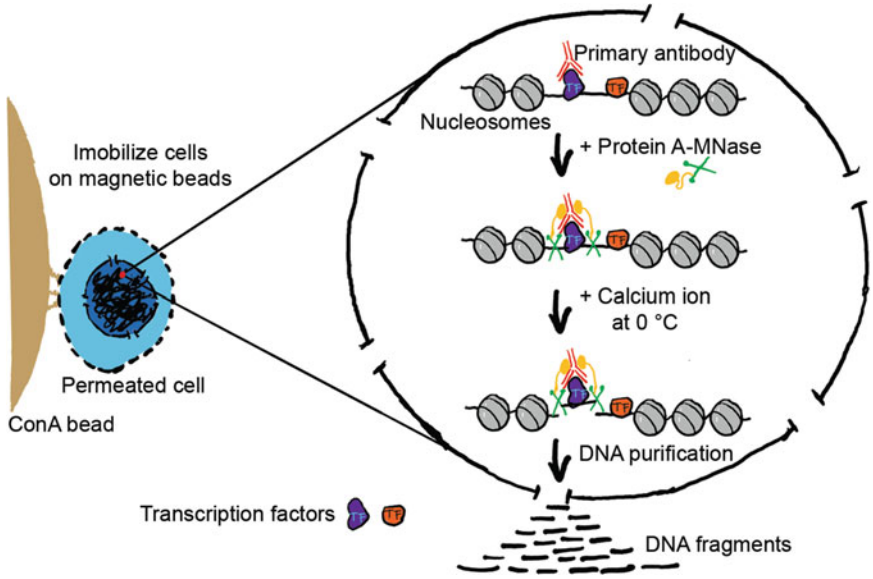

Fig. 1 The principle of CUT&RUN method. CUT&RUN is a genome-wide chromatin profiling technique performed in situ. For simplified handling, cells are bound to Concanavalin A-coated magnetic beads (ConA beads). Cytoplasmic membranes are permeated with digitonin for penetration of antibodies, which minimally affects nuclear envelopes and does not compromise nuclear integrity. Specific binding of the antibody to its epitope then recruits pA-MNase (Protein A-micrococcal nuclease fusion protein) for subsequent DNA cleavage of nearby chromatin. Digestion of DNA by micrococcal nuclease only begins by addition of Ca^{2+} at 0 °C. Chelation stops the reaction, and cleaved DNA fragments are released. Purified DNA fragments are suitable for downstream enrichment analysis by next-generation sequencing

immunoprecipitation-free epigenomic profiling methods with similar sensitivity [14], CUT&RUN is easier to perform and less time-consuming; target DNA fragments can be enriched and purified in 1 day starting from isolated cells. Only a few steps need to be optimized for each protein/target and cell type, facilitating adoption by different laboratories and for different cells [15]. The simplicity of CUT&RUN also comes with a straightforward calibration strategy for quantitative epigenomic analysis [15].

Similar to CUT&RUN, CUT&Tag (Cleavage Under Targets and Tagmentation) builds on the same principle of in situ tethering an enzyme to chromatin for the enrichment of specific fragments [16]. Instead of using a micrococcal nuclease, CUT&Tag utilizes a hyperactive Tn5 fused with protein A (pA-Tn5) to tagment DNA sequences bound by antibodies. Like CUT&RUN, CUT&Tag generates low-background chromatin profiles from low cell numbers and single cells. One unique advantage of CUT&Tag is that DNA fragments are ligated with adapters in situ, which considerably simplifies library preparation. However, CUT&RUN offers a higher resolution in mapping, especially for footprinting of transcription factors, and retains weak interactions to the chromatin due to mild washing steps. Both CUT&RUN and its cousin

CUT&Tag are attractive alternatives to ChIP-based techniques, especially when only small numbers of cells are available.

We have successfully applied CUT&RUN in profiling the chromatin of MuSCs. We have mapped the binding sites of transcription factors, the enrichment of chromatin-associated protein complexes, and the distribution of histone modifications, either from freshly isolated or cultured MuSCs. In contrast, ChIP-based protocols failed in our hands in such tasks. MuSCs isolated from one mouse were sufficient to profile multiple chromatin factors by CUT&RUN. Moreover, as reported for other cell types [11, 15], we found that CUT&RUN requires a reduced number of sequencing reads and its calibration based on carry-over *E. coli* DNA proved to be useful for detection of global chromatin changes. We reason that CUT&RUN is an ideal method for routine genome-wide chromatin profiling in the relatively small population of MuSCs.

In this chapter, we describe in detail our protocol for performing CUT&RUN with freshly isolated MuSCs. Since CUT&RUN and CUT&Tag are both based on the same principle, the CUT&RUN protocol can be easily adapted for CUT&Tag (which in some aspects is even simpler than CUT&RUN). We expect that this protocol will greatly facilitate the investigation of chromatin dynamics in MuSCs, which was hampered by the technical limitations of ChIP, thus helping to advance our knowledge about MuSC biology.

2 Materials

2.1 Reagents

1. Freshly isolated MuSCs in suspension.
2. Concanavalin A-coated magnetic beads (Abbr. ConA beads; Bangs Laboratories, Cat. No. BP531).
3. Antibody to an epitope of interest, for example, anti-CTCF rabbit polyclonal antibody (Millipore, Cat. No. 07-729), anti-H3K9ac rabbit polyclonal antibody (Abcam, Cat. No. ab10812).
4. Positive-control antibody to an abundant epitope, for example, anti-H3K27me3 rabbit monoclonal antibody (Cell Signaling Technology, Cat. No. 9733).
5. Negative-control antibody to an absent epitope (e.g., Rabbit IgG; Diagenode, Cat. No. C15410206).
6. A secondary antibody such as rabbit anti-mouse (e.g., Rabbit Anti-Mouse IgG H&L, Abcam, Cat. No. ab46540) (*see* **Note 1**).
7. Protein A-micrococcal nuclease (pA-MNase) fusion protein (The fusion protein was purified in house, now the improved

Protein A/G-micrococcal nuclease (pAG-MNase) fusion protein is commercially available) (*see* **Note 1**).

8. Ultrapure water.
9. HEPES.
10. 10 M Potassium hydroxide (KOH).
11. 1 M Potassium chloride (KCl).
12. 1 M Calcium chloride dihydrate ($CaCl_2 \cdot 2H_2O$).
13. 1 M Manganese (II) chloride dehydrate ($MnCl_2$).
14. 10 M Sodium hydroxide (NaOH).
15. 5 M Sodium chloride (NaCl).
16. 2 M Spermidine.
17. 10% Bovine serum albumin (BSA).
18. Roche cOmplete™ Protease Inhibitor (EDTA-free) tablets (Sigma-Aldrich, Cat. No. 5056489001).
19. Digitonin (EMD Millipore, Cat. No. 300410).
20. 0.5 M EDTA.
21. Dimethyl sulfoxide (DMSO).
22. 0.2 M EGTA.
23. RNase A, DNase and protease-free (10 mg/mL).
24. Glycogen.
25. 10% SDS.
26. Proteinase K (10 mg/mL).
27. Tris-buffered phenol/chloroform/isoamyl alcohol 25:24:1 (PCI).
28. Chloroform.
29. Ethanol.
30. TE Buffer.
31. Carboxylated magnetic beads (Mag-Bind® TotalPure NGS, Omega Bio-Tek, Cat. No. M1378).
32. Isopropanol.

2.2 Buffer Solutions

1. *Binding Buffer.*

   The *Binding Buffer* activates ConA beads for binding to cells.

   For 100 mL buffer, mix 2 mL of 1 M HEPES-KOH at pH 7.9, 1 mL of 1 M KCl, 100 µL of 1 M $CaCl_2$, 100 µL of 1 M $MnCl_2$, and 96.8 mL ultrapure water. Store the buffer at 4 °C for up to a year.

2. *Wash Buffer.*

   The *Wash Buffer* is used to rinse cells before binding to ConA beads. Spermidine in the *Wash Buffer* helps maintain chromatin properties, especially compensating for the removal of Mg^{2+} by chelation during antibody incubation and thereafter.

   For 50 mL *Wash Buffer*, mix 1 mL of 1 M HEPES-NaOH (pH 7.5), 1.5 mL of 5 M NaCl, 12.5 μL of 2 M spermidine, 500 μL of 10% BSA, and 46.45 mL ultrapure water and add one Roche cOmplete™ Protease Inhibitor (EDTA-free) tablet. Store the buffer at 4 °C for up to 1 week.

3. *Dig-Wash Buffer.*

   5% digitonin (wt/vol) stock solution is made by dissolving digitonin in DMSO and stored at −20 °C. The final concentration of digitonin in the buffer, in general, should be tested for each cell type and per batch of the non-ionic detergent. An ideal concentration is the lowest that effectively permeates all cells. Trypan blue exclusion assay is recommended for determining the concentration [10]. We found that 0.05% digitonin (wt/vol, final concentration) of two different batches worked well for MuSCs in CUT&RUN experiments.

   To make 0.05% *Dig-Wash Buffer* mix 450 μL of 5% digitonin with 45 mL *Wash Buffer*. Store the buffer at 4 °C for up to 1 day.

4. *Antibody Buffer.*

   This buffer is used to dilute the primary antibody for incubation with cells bound to beads. The addition of EDTA to *Dig-Wash Buffer* removes excess divalent cations used to activate ConA beads. Remnant Ca^{2+} from the beads will initiate DNA cleavage prematurely during incubation with pA-MNase. Chelating divalent cations also reduces endogenous DNase activity and chromatin changes during the procedure.

   To make 2 mL *Antibody Buffer*, mix 8 μL of 0.5 M EDTA and 2 mL of *Dig-Wash Buffer*. Prepare the buffer shortly before use and keep on ice.

5. *Low-Salt Buffer.*

   Rinse the cells with *Low-Salt Buffer* to ensure low-salt conditions during the following DNA cleavage step.

   To make 10 mL *Low-Salt Buffer*, mix 200 μL of 1 M HEPES-NaOH (pH 7.5), 2.5 μL of 2 M spermidine, 20 μL of 5% digitonin, and 9.78 mL ultrapure water. Store the buffer at 4 °C for up to 1 week.

6. *Incubation Buffer.*

   This buffer contains Ca^{2+} to activate MNase for DNA cleavage. The low-salt and high-divalent-cation (10 mM Ca^{2+}) conditions prevent premature release of chromatin-

MNase particles during incubation, thus reducing unwanted cleavage by otherwise mobilized MNase.

To make 2 mL *Incubation Buffer*, mix 7 μL of 1 M HEPES-NaOH (pH 7.5), 20 μL of 1 M $CaCl_2$, 4 μL of 5% digitonin, and 1969 μL ultrapure water. Store the buffer at 4 °C for up to 1 week.

7. *STOP Buffer*.

   The *STOP Buffer* chelates Ca^{2+} to terminate DNA digestion and allows diffusion of chromatin/DNA fragments out of the cells. The buffer can contain heterologous spike-in DNA (e.g., fragmented Drosophila genomic DNA) to calibrate the amounts of released DNA (*see* **Note 2**).

   For 2 mL *STOP Buffer*, mix 68 μL of 5 M NaCl, 200 μL of 0.2 M EGTA, 4 μL of 5% digitonin, 10 μL of 10 mg/mL RNase A, 2.5 μL of 20 mg/mL glycogen, and 1715.5 μL ultrapure water. Store the buffer at 4 °C for up to 1 week.

2.3 Equipment

1. Protein LoBind tubes, 1.5 mL (e.g., Eppendorf, Cat. No. 0030108116).
2. DNA LoBind tubes, 1.5 mL (e.g., Eppendorf, Cat. No. 0030108051).
3. Vortex mixer.
4. Centrifuge, refrigerated, with a fixed-angle rotor (e.g., Eppendorf, model No. 5415R).
5. Tube rotator (in a cold room or in a refrigerator).
6. Magnetic stand (e.g., Ambion, Cat. No. AM10055).
7. Heater block for 1.5 mL microcentrifuge tubes.
8. Phase-lock tubes (e.g., MaXtract phase-lock microcentrifuge tubes, Qiagen, Cat. No. 129046).
9. Capillary electrophoresis instrument (e.g., Perkin Elmer, LabChip Gx Touch 24).
10. Massively parallel DNA sequencer (e.g., Illumina, NextSeq 500).

2.4 Software

1. Bowtie 2, version 2.3.5 (http://bowtie-bio.sourceforge.net/bowtie2/index.shtml).
2. Picard, version 2.20.8 (https://broadinstitute.github.io/picard/).
3. Deeptools, version 3.3.1 (https://deeptools.readthedocs.io/en/develop/).
4. Integrative genomics viewer (IGV), version 2.4.16 (http://software.broadinstitute.org/software/igv/).

3 Methods

The CUT&RUN protocol is divided into nine sections. We provide a detailed description of each step, beginning with ConA beads preparation to extraction of cleaved DNA fragments, corresponding in order from Subheadings 3.1, 3.2, 3.3, 3.4, 3.5, 3.6 and 3.7. In Subheadings 3.8 and 3.9, we provide a guideline for the initial analysis of isolated DNA fragments, high-throughput sequencing, and bioinformatics analysis.

3.1 Preparation of ConA Beads

1. Resuspend ConA beads with gentle vortexing (vortex >30 s) or pipetting.
2. Transfer enough ConA beads slurry to a 1.5 mL microcentrifuge tube pre-loaded with 800 μL ice-cold *Binding Buffer*. For each final CUT&RUN reaction/sample, we use 10 μL of beads slurry, which usually is sufficient to bind up to one million cells.
3. Place the tube on a magnetic stand for ~2 min, until the solution is clear.
4. Once the solution is completely clear, carefully remove and discard the supernatant without disturbing the beads.
5. Remove the tube from the magnetic stand, add 800 μL ice-cold *Binding Buffer*, and mix by inversion.
6. Collect liquid from the cap and side by short and gentle centrifugation (e.g., 50–100 g for 2 s or a brief pulse on a microcentrifuge).
7. Place the tube on the magnetic stand, then remove and discard the supernatant after the solution turns clear.
8. Repeat wash **steps 5–7** one time.
9. Resuspend the beads in a volume of ice-cold *Binding Buffer* that equals the original volume of the slurry. Keep on ice until use.

3.2 Binding of MuSCs to Beads

1. Centrifuge freshly isolated MuSCs for 5 min at 1000× *g*, 4 °C, then carefully remove and discard the supernatant by pipetting.
2. Resuspend the cells in 1 mL ice-cold *Wash Buffer*.
3. Centrifuge for 5 min at 1000× *g*, 4 °C, and discard the supernatant by pipetting.
4. Wash the cells a second time by repeating wash **steps 2** and **3** one time.
5. Resuspend the cells in 1 mL ice-cold *Wash Buffer*.
6. Add fully resuspended ConA beads to the cell suspension while gently vortexing.
7. Rotate the tube of mixed cells and beads for 10 min at 4 °C.
8. Divide into aliquots in 1.5 mL Protein LoBind tubes, one for each final CUT&RUN reaction with different antibodies/conditions.

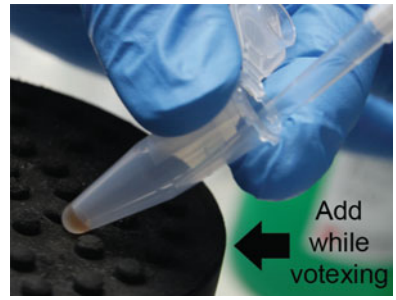

Fig. 2 Addition of reagents to the beads while ensuring proper mixing. Prompt and gentle mixing of cell-bound beads before and upon addition of reagents is critical for the CUT&RUN protocol. Vortexing too vigorously will damage cells/nuclei. However, pipetting when gentle mixing is crucial to distribute the antibody, pA-MNase, or Ca^{2+} immediately and uniformly to reduce artifacts from uneven spatial incorporation. Avoid holding the tube at the bottom to keep the sample cool

3.3 Primary Antibody Incubation

1. Place the tubes (with aliquots of the cell-bound beads) on the magnetic stand, then remove and discard the supernatant after the solution turns clear.
2. Place each tube at a low angle on the vortex mixer set to low speed (~1000 rpm) and pipette 50 µL of the *Antibody Buffer* (containing the antibody, *see* **Note 3**) per sample along the side where beads attach, to allow the solution to dislodge the beads (Fig. 2). If necessary, immediately tap with finger to dislodge the remaining beads into suspension after capping each tube.
3. Rotate the tubes on a rotator at RT or 4 °C for the required period. We routinely incubate the primary antibody overnight at 4 °C.
4. Collect liquid from the cap and side by rather short and gentle centrifugation (e.g., 50–100 g for 2 s or a brief pulse on a microcentrifuge). It helps to minimize the carryover of antibody and pA-MNase (in later steps), which may increase unwanted background cleavages.
5. Place the tubes on the magnetic stand, then remove and discard the supernatant after the solution turns clear.
6. Remove the tubes from the magnetic stand, add 1 mL ice-cold *Dig-Wash Buffer*, and mix by inversion. Collect liquid from the cap and side by rather short and gentle centrifugation.
7. Repeat wash **steps 5** and **6** one time.
8. If no secondary antibody is required, continue with Subheading 3.5; if binding of a secondary antibody is necessary, continue with Subheading 3.4 (*see* **Note 1**).

3.4 Secondary Antibody Incubation (Optional)

1. Dilute the secondary antibody in ice-cold *Dig-Wash Buffer*, 50 μL for each final reaction/sample. We usually use the secondary antibody in 1:100 dilution or follow the manufacturer's recommended dilution for immunofluorescence.
2. Place the tubes on the magnetic stand, then remove and discard the supernatant after the solution turns clear.
3. Place each tube at a low angle on the vortex mixer set to low speed (~1000 rpm) and pipette 50 μL of the diluted secondary antibody per sample along the side to allow the solution to dislodge the beads. If necessary, immediately tap with finger to dislodge the remaining beads into suspension after capping each tube.
4. Rotate the tubes at 4 °C for ~1 h.
5. Collect liquid from the cap and side by short and gentle centrifugation (e.g., 50–100 g for 2 s or a brief pulse on a microcentrifuge).
6. Place the tubes on the magnetic stand, then remove and discard the supernatant after the solution turns clear.
7. Remove the tubes from the magnetic stand, add 1 mL ice-cold *Dig-Wash Buffer*, and mix by inversion. Collect liquid from the cap and side by rather short and gentle centrifugation (e.g., 50–100 g for 2 s or a brief pulse on a microcentrifuge).
8. Repeat wash **steps 6** and **7** one time.

3.5 Binding of MNase Fusion Protein

1. Place the tubes on the magnetic stand, remove and discard the supernatant after the solution turns clear.
2. Remove the tubes from the stand, resuspend each in 50 μL ice-cold *Dig-Wash Buffer*, and keep the tubes on ice.
3. While gently vortexing the bead-bound cells, add 100 μL ice-cold *Dig-Wash Buffer* containing pA-MN (dilution according to the manufacturer's or supplier's instructions; we use a final concentration of ~300 ng/mL of home-made pA-MNase).
4. Rotate the tubes at 4 °C for ~1 h.
5. Collect liquid from the cap and side by short and gentle centrifugation (e.g., 50–100 g for 2 s or a brief pulse on a microcentrifuge).
6. Place the tube on the magnetic stand, remove and discard the supernatant after the solution turns clear.
7. Remove the tube from the magnetic stand, add 1 mL ice-cold *Dig-Wash Buffer*, and mix by inversion. Collect liquid from the cap and side by short and gentle centrifugation (e.g., 50–100 g for 2 s or a brief pulse on a microcentrifuge).
8. Repeat wash **steps 6** and **7** one time.

3.6 Targeted DNA Digestion and Chromatin Release

1. Place the tubes on the magnetic stand, remove and discard the supernatant after the solution turns clear.
2. Remove the tubes from the magnetic stand, add 1 mL ice-cold *Low-Salt Buffer*, and mix by inversion. Collect liquid from the cap and side by rather short and gentle centrifugation (e.g., 50–100 g for 2 s or a brief pulse on a microcentrifuge).
3. Prepare an ice-water bath with enough ice to prevent floating of tubes.
4. Place the tubes on the magnetic stand, then remove and discard the supernatant after the solution turns clear.
5. Place each tube at a low angle on the vortex mixer set to low speed (~1000 rpm) and pipette 200 μL of the ice-cold *Incubation Buffer* per sample along the side where the beads attach, to allow the solution to dislodge the beads. If necessary, immediately tap with a finger to dislodge the remaining beads into suspension after capping each tube. Do not hold the tubes at the lower part to avoid heating the sample, which will lead to hyperactivity of MNase causing high background.
6. Immediately incubate at 0 °C in the ice-water bath for 5–30 min. We routinely incubate for 25 min (*see* **Note 4**).
7. Place tubes on the chilled magnetic stand (buried in ice during the incubation), allow clearing for ≥10 s, and remove liquid. (Recommended) Store the removed supernatant in DNA LoBind tubes at −20 °C in case target DNA fragments leaked out during digestion incubation (*see* **Note 5**).
8. Add 200 μL *STOP Buffer* to the beads and mix by gentle vortexing.
9. Incubate 30 min at 37 °C to release DNA/chromatin fragments from the remaining insoluble nuclear chromatin.
10. Place the tubes on the magnet stand to clear. Carefully transfer the supernatant, containing digested DNA/chromatin, to a fresh 1.5 mL DNA LoBind tube.
11. (Recommended quality control step) Add 200 μL *STOP Buffer* to the beads and proceed until the next step in Subheading 3.7.

3.7 DNA Extraction

1. Add 2 μL of 10% SDS and 5 μL Proteinase K (10 mg/mL) to each sample (should be 200 μL; supernatant and beads, respectively). Mix by inversion and incubate 1 h at 50 °C (no vortexing). The appearance of the beads can be very informative if the experiment worked (Fig. 3). (Recommended) Store beads samples at −20 °C in case target DNA fragments were not released to the supernatant (*see* **Note 5**).
2. Add 200 μL of phenol/chloroform/isoamyl alcohol to each sample and mix by vigorous vortexing for ~2 s.

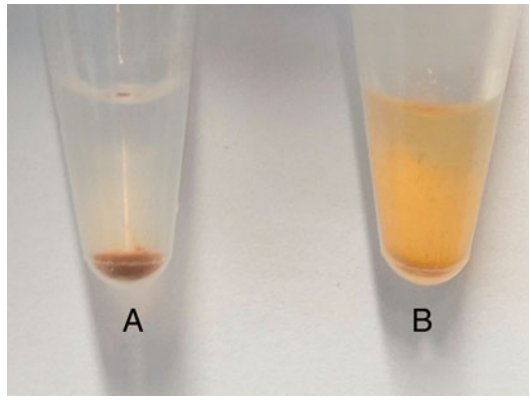

Fig. 3 A quick and straightforward readout of CUT&RUN experiments using recommended positive and negative controls. The picture shows typical appearances of beads shortly after moderate agitation following protease digestion. (**a**) is IgG, while (**b**) is anti-H3K27me3. In the IgG control, beads form a large clump during and after the incubation, since relatively intact genomic DNA has a high viscoelasticity and keeps the beads together. In contrast, massive DNA cleavage by MNase that was targeted to genome-wide abundant epitopes, for example, H3K27me3, cut the genome sufficiently so that clumping is significantly reduced, releasing the beads into a brownish suspension

3. Transfer to a phase-lock tube, mix by inverting a few times, and centrifuge 5 min at 16,000× *g*, room temperature.
4. Add 200 μL of chloroform, invert ~10 times to mix, and then centrifuge 5 min at 16,000× *g*, room temperature.
5. Pipette the top liquid phase to a fresh 1.5 mL tube (not DNA LoBind tubes for higher retention of the DNA pellet) that contains 2 μL of 2 mg/mL glycogen (diluted 1:10 in ultrapure water from 20 mg/mL glycogen stock).
6. Add 500 μL of 100% ethanol and mix by inverting 10 times.
7. Chill on ice for 2 min and centrifuge 10 min at 16,000× *g*, 4 °C. After centrifugation, a tiny whitish pellet should be visible in each tube regardless of the antibodies/conditions.
8. Pour off the liquid and place the opened tubes upside down on a clean paper towel to drain for ~30 s.
9. Rinse the pellet in 1 mL 100% ethanol, and then centrifuge 1 min at 16,000× *g*, 4 °C.
10. Carefully pour off the liquid, drain on a clean paper towel, and air dry.
11. Dissolve in 20–50 μL TE buffer when the pellet is dry, and transfer to a new 1.5 mL DNA Lo-Bind microcentrifuge tube.

3.8 Library Preparation and Sequencing

1. Perform capillary electrophoresis of extracted CUT&RUN DNA, following the manufacturer's instructions. A successful CUT&RUN reaction using antibodies against abundant

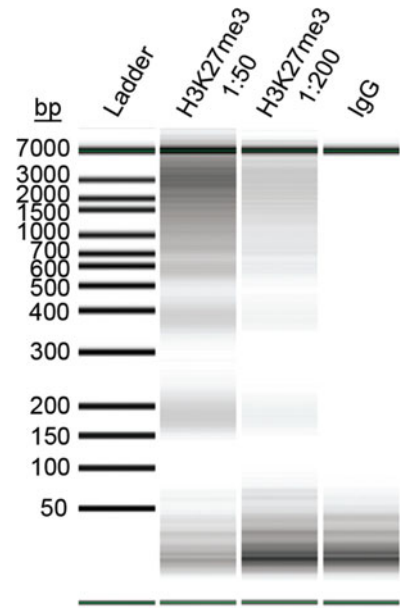

Fig. 4 CUT&RUN targeting abundant histone epitope as a positive control for pre-lib DNA analysis. Capillary electrophoretic analysis of pre-lib DNA from a CUT&RUN experiment using 100,000 cells is shown, comparing anti-H3K27me3 (recommended positive control) and IgG negative control. CUT&RUN targeting abundant histone epitope (e.g., H3K27me3) generates typical nucleosome ladder patterns, even using very low numbers of cells [10]

epitopes should result in a phased nucleosome pattern (Fig. 4). For less abundant epitopes (e.g., most transcription factors), it is more difficult to detect cleaved fragments [15]. Thus, we recommend analyzing DNA samples from a positive (e.g., H3K27me3) and IgG negative control at this step. Proceed with library preparation of other samples along with IgG control, if there is a good indication of success. It is not necessary to generate a sequencing library from the positive control.

2. Illumina sequencing libraries can be prepared using different commercial kits with modifications for optimized amplification of CUT&RUN DNA [10, 17]. We generate the sequencing library by using Takara's SMARTer ThruPLEX DNA-Seq Kit following the manufacturer's instructions. Before library preparation, we clean the DNA with 1.8× volumes of magnetic carboxylated beads and 5.4× volumes of 100% isopropanol, followed by two washes with 85% ethanol.
3. Determine the size distribution of libraries by capillary electrophoresis analysis, following the manufacturer's instructions. After library amplification, the enrichment patterns of even low abundant epitopes should be usually visible.

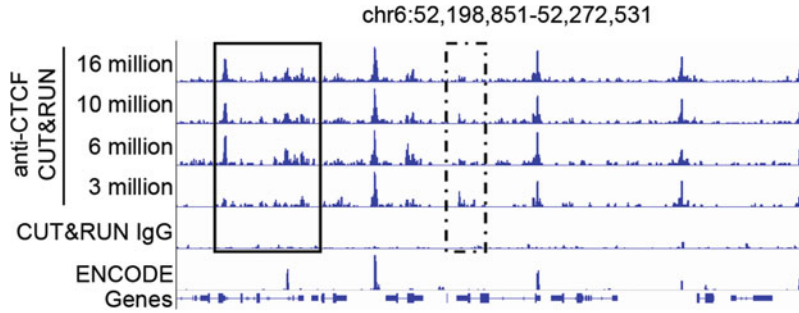

Fig. 5 CUT&RUN requires low sequencing depth. 16 million de-duplicated mapped reads (from 22 million raw reads) of anti-CTCF CUT&RUN performed using 70 k freshly isolated MuSCs were sub-sampled to 10, 6, and 3 million reads. Only when mapped reads reduced to three million, as seen in the example IGV screenshot, peaks or dense signal clusters (solid box) are lost and start to gain potential false-positive binding signals (dotted box). The ENCODE track is anti-CTCF ChIP-seq in C2C12 cells (accession ENCFF244USU)

4. Perform paired-end sequencing on barcoded libraries using an Illumina sequencer, following the manufacturer's instructions. Due to the low background levels, typically 5–10 million paired-end reads per sample are sufficient for nucleosome modifications and even for transcription factors (Fig. 5).

3.9 Data Processing and Analysis

1. Generate mouse and *E. coli* composite reference genome for simultaneous mapping of mouse target DNA, and *E. coli* carry-over DNA reads, to avoid counting of cross-mapping reads.
2. Align paired-end reads using Bowtie2 v2.3.5 with options: -local -very-sensitive-local -no-unal -dovetail -no-mixed -no-discordant -phred33 -I 10 -X 700.
3. (Optional) Use the Picard "MarkDuplicates" command to mark presumed PCR duplicates for removal from low-cell-number data (*see* **Note 6**).
4. (Recommended) Use the Picard "CollectInsertSizeMetrics" tool to make histograms of insert sizes of mapped paired-end reads. Assess the size distribution of insert DNA fragments to inspect specific enrichment profiles (Fig. 6).
5. (Optional) Calculate normalization factors according to the amounts of reads mapped to the *E. coli* genome and cross-correct the normalization factors between two or more conditions using corresponding IgG control reads. We use the deepTools "bamCoverage" with option –scaleFactor to generate scaled bigwig tracks for visualization. The carry-over *E. coli* DNA is valuable for comparing genome-wide systematic alternations of chromatin epitopes [15] (Fig. 7).

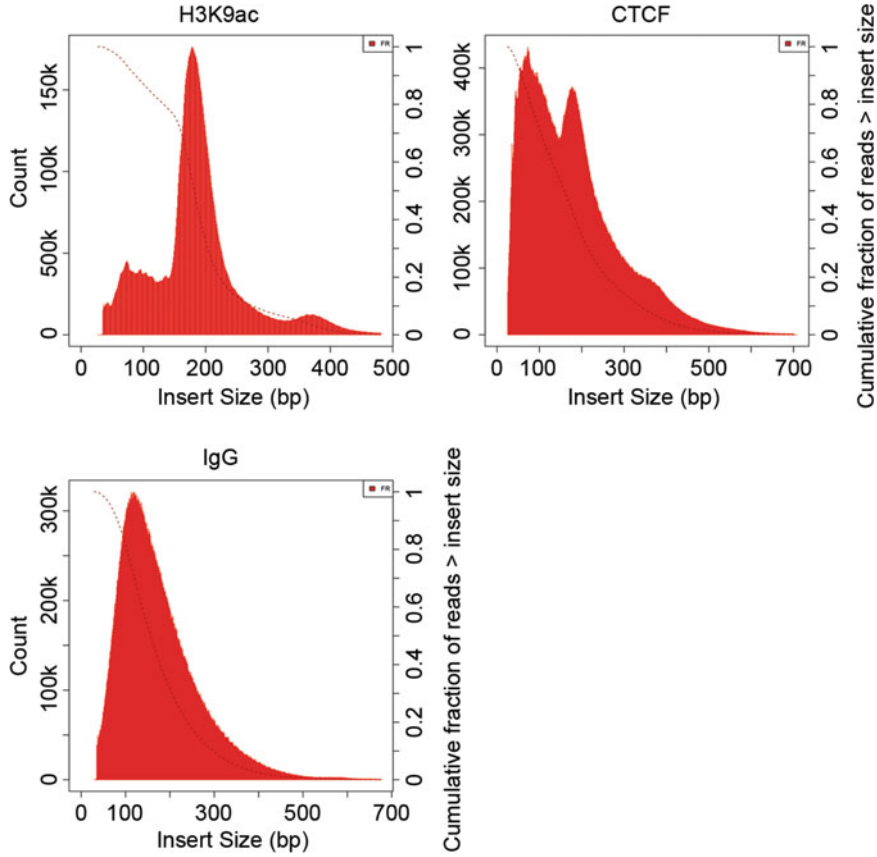

Fig. 6 Library insert size distributions distinguish different epitopes and indicate specificities. Insert sizes of the sequencing libraries correlate with released DNA fragments from CUT&RUN experiments. The library of H3K9ac from MuSCs shows a robust enrichment between 150 and 200 bp, corresponding to DNA fragments that were protected by nucleosomes and sometimes adjacent DNA binding proteins. Relative enrichment of the H3K9ac library at 350–400 bp and smaller than 150 bp reflects the cleavage of di-nucleosome DNA and accessible DNA near H9K9ac enriched sites, respectively. The CTCF library enriches mostly at smaller DNA fragments and secondary at fragments that are ~140 bp larger. The latter is probably due to the cleavage of DNA on the further side of nucleosomes close next to CTCF binding. In the negative control, where the random coating of IgG on the chromatin targets DNA cleavage, the library comprises of DNA fragments that were primarily protected by sparse nucleosomes from more accessible domains

4 Notes

1. Protein A binds poorly to mouse IgG. Therefore, a secondary antibody (e.g., rabbit anti-mouse) is required when using mouse antibodies to target pA-MN. The pAG-MNase comprises both Protein A and Protein G domains; thus, it binds strongly to most commercial antibodies [15]. A secondary antibody is generally not necessary for pAG-MNase. In some cases, however, a secondary antibody may still be required when using pAG-MNase.

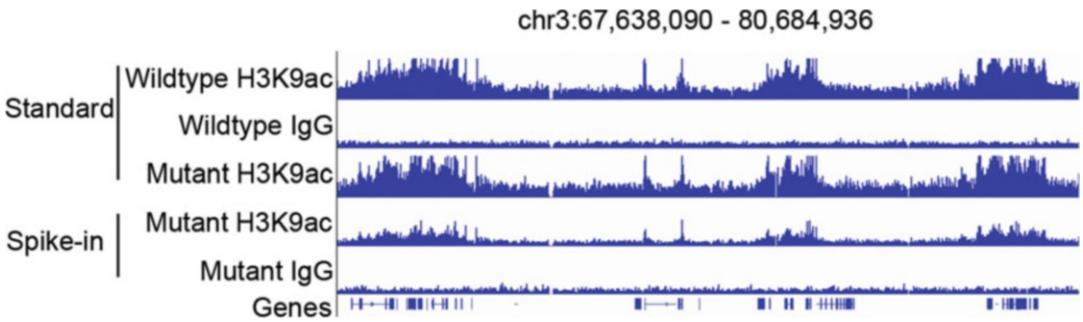

Fig. 7 *E. coli* carry-over DNA of pA-MNase for normalization. Indicated CUT&RUN sequencing dataset from MuSCs, in which mutant cells have reduced H3K9ac (40% reduction revealed by western blot, data not shown). Due to the global reduction, wildtype and mutant H3K9ac profiles show overall highly similar patterns when scaled to the numbers of total reads (the standard normalization, see the top three tracks). However, normalization based on the *E. coli* DNA (spike-in) reads suggests a ~ 50% reduction across the genome with few exceptions in the mutant, consistent with the western blot analysis. The figure shows a representative region

2. The very first CUT&RUN protocol included heterologous spike-in DNA to quantify chromatin profiles [11]. Later, the authors showed that counting the reads of carry-over E. coli DNA from the purified MNase fusion protein allows accurate quantification of relative abundance [15]. Hence, adding heterologous spike-in DNA in the STOP Buffer is not necessary. However, we recommend starting the CUT&RUN protocol with the addition of heterologous spike-in DNA. Because the amounts of *E. coli* carry-over DNA can vary among different preparations, and sometimes (depending on the abundance of the assayed epitope), the amount of *E. coli* reads may not be significantly higher than the environmental *E. coli* reads seen in other sequencing samples.

   Spike-in DNA should contain fragments of approximately 200 bp on average. We isolate DNA from sheared Drosophila chromatin and perform size selection to enrich DNA fragments corresponding to mono-nucleosomes. The amount of spike-in DNA should be adjusted based on the number of cells used per final CUT&RUN reaction: use 100 pg/mL for 10,000–-1 million cells and 2 pg/mL for 100–10,000 cells.

3. We usually use the primary antibody in 1:100 dilution or follow the manufacturer's recommended dilution for immunofluorescence. The suitability of an antibody for CUT&RUN is best tested by immunofluorescence. Ideally, the immunofluorescence protocol should be as similar as possible to the conditions of CUT&RUN (e.g., no fixation, permeation by digitonin, but without binding to ConA beads). CUT&RUN can work with fixed cells, yet, with reduced efficiency and resolution [11, 18]. For some chromatin factors, mild fixation might be

necessary for CUT&RUN, if the binding is not preserved during the washes while the antibody could specifically stain the target in immunofluorescence after fixation.

4. DNA-binding pA-MNase only cleaves in the presence of Ca^{2+}. Cleavage happens within seconds upon Ca^{2+} addition. Incubation at 0 °C (ice-water bath) minimizes background cleavages by significantly reducing the diffusion of pA-Mnase-bound particles after targeted DNA digestion. Thus, the cleavage pattern remains constant over time at this condition. Nonetheless, in the range from a few seconds until 30 min, longer digestion periods do yield more DNA fragments with little change in signal-to-noise ratio [10].
5. In rare cases, target DNA fragments may already leak out during the incubation of Mnase digestion. In addition, the majority of target DNA fragments may remain insoluble after *STOP Buffer* incubation and is still present in the bead suspension afterward. Thus, we recommend storing the supernatant and the beads suspension at −20 °C. If there is only limited yield following the above protocol, check if the target DNA fragments are present in these fractions.
6. Due to the precise digestion of DNA by targeted MNase, CUT&RUN has a much higher chance of producing duplicate DNA fragments that are not results of PCR amplification compared to ChIP of randomly sheared chromatin. We recommend to remove duplicated reads only when performing CUT&RUN with a few thousand cells or to compare results with and without removing duplicated reads to determine the best strategy.

Acknowledgments

We are grateful to Dr. Ulrich Laemmli for sharing the plasmid coding pA-MN (Addgene #86973) and to Dr. Steven Henikoff for sharing the plasmid of pA/G-MNase (Addgene #123461). We appreciate Dr. Karl Glastad for suggestions in library preparation using the Takara kit. We thank Xinyue Guo for isolating MuSCs, and Dr. Stefan Günther for performing library preparation and sequencing. We also thank other members from the laboratory of Dr. Thomas Braun for testing the CUT&RUN protocol with their targets of interest. This work was supported by the Excellence Initiative "Cardiopulmonary Institute" (CPI), the DFG collaborative research center SFB1213, the DFG Transregional Collaborative Research Centre 81, the DFG Clinical Research Unit FKO 309, and the European Research Area Network on Cardiovascular Diseases project CLARIFY.

References

1. Relaix F, Zammit PS (2012) Satellite cells are essential for skeletal muscle regeneration: the cell on the edge returns centre stage. Development 139(16):2845–2856. https://doi.org/10.1242/dev.069088
2. Boonsanay V, Zhang T, Georgieva A et al (2016) Regulation of skeletal muscle stem cell quiescence by Suv4-20h1-dependent facultative heterochromatin formation. Cell Stem Cell 18(2):229–242. https://doi.org/10.1016/j.stem.2015.11.002
3. Brancaccio A, Palacios D (2015) Chromatin signaling in muscle stem cells: interpreting the regenerative microenvironment. Front Aging Neurosci 7:36. https://doi.org/10.3389/fnagi.2015.00036
4. Ryall JG, Dell'Orso S, Derfoul A et al (2015) The NAD(+)-dependent SIRT1 deacetylase translates a metabolic switch into regulatory epigenetics in skeletal muscle stem cells. Cell Stem Cell 16(2):171–183. https://doi.org/10.1016/j.stem.2014.12.004
5. Liu L, Cheung TH, Charville GW et al (2013) Chromatin modifications as determinants of muscle stem cell quiescence and chronological aging. Cell Rep 4(1):189–204. https://doi.org/10.1016/j.celrep.2013.05.043
6. Hainer SJ, Fazzio TG (2019) High-resolution chromatin profiling using CUT&RUN. Curr Protoc Mol Biol 126(1):e85. https://doi.org/10.1002/cpmb.85
7. Meyer CA, Liu XS (2014) Identifying and mitigating bias in next-generation sequencing methods for chromatin biology. Nat Rev Genet 15(11):709–721. https://doi.org/10.1038/nrg3788
8. Baranello L, Kouzine F, Sanford S et al (2016) ChIP bias as a function of cross-linking time. Chromosom Res 24(2):175–181. https://doi.org/10.1007/s10577-015-9509-1
9. Egan B, Yuan CC, Craske ML et al (2016) An alternative approach to ChIP-Seq normalization enables detection of genome-wide changes in histone H3 lysine 27 Trimethylation upon EZH2 inhibition. PLoS One 11(11): e0166438. https://doi.org/10.1371/journal.pone.0166438
10. Skene PJ, Henikoff JG, Henikoff S (2018) Targeted in situ genome-wide profiling with high efficiency for low cell numbers. Nat Protoc 13(5):1006–1019. https://doi.org/10.1038/nprot.2018.015
11. Skene PJ, Henikoff S (2017) An efficient targeted nuclease strategy for high-resolution mapping of DNA binding sites. elife 6. https://doi.org/10.7554/eLife.21856
12. Hainer SJ, Boskovic A, McCannell KN et al (2019) Profiling of pluripotency factors in single cells and early embryos. Cell 177(5): 1319–1329.e11. https://doi.org/10.1016/j.cell.2019.03.014
13. Zhu Q, Liu N, Orkin SH et al (2019) CUT&RUNTools: a flexible pipeline for CUT&RUN processing and footprint analysis. Genome Biol 20(1):192. https://doi.org/10.1186/s13059-019-1802-4
14. Harada A, Maehara K, Handa T et al (2019) A chromatin integration labelling method enables epigenomic profiling with lower input. Nat Cell Biol 21(2):287–296. https://doi.org/10.1038/s41556-018-0248-3
15. Meers MP, Bryson TD, Henikoff JG et al (2019) Improved CUT&RUN chromatin profiling tools. elife 8. https://doi.org/10.7554/eLife.46314
16. Kaya-Okur HS, Wu SJ, Codomo CA et al (2019) CUT&Tag for efficient epigenomic profiling of small samples and single cells. Nat Commun 10(1):1930. https://doi.org/10.1038/s41467-019-09982-5
17. Liu N, Hargreaves VV, Zhu Q et al (2018) Direct promoter repression by BCL11A controls the fetal to adult hemoglobin switch. Cell 173(2):430–442 e417. https://doi.org/10.1016/j.cell.2018.03.016
18. Zheng XY, Gehring M (2019) Low-input chromatin profiling in Arabidopsis endosperm using CUT&RUN. Plant Reprod 32(1): 63–75. https://doi.org/10.1007/s00497-018-00358-1

Chapter 29

Epitranscriptome Mapping of N^6-Methyladenosine Using m^6A Immunoprecipitation with High Throughput Sequencing in Skeletal Muscle Stem Cells

Justin Law, Stefan Günther, and Shuichi Watanabe

Abstract

N^6-Methyladenosine (m^6A), one of the most abundant chemical modifications in mRNA (epitranscriptome), contributes to the regulation of biological processes by iterating gene expression post-transcriptionally. A number of publications on m^6A modification have escalated in the recent past, due to the advancements in profiling m^6A along the transcriptome using different approaches. The vast majority of studies primarily focused on m^6A modification on cell lines but not primary cells. We present in this chapter a protocol for m^6A immunoprecipitation with high throughput sequencing (MeRIP-Seq) that profiles m^6A on mRNA with merely 100 μg total RNA worth of muscle stem cells as starting material. With this MeRIP-Seq, we observed epitranscriptome landscape in muscle stem cells.

Key words m^6A, Mettl3/14, Epitranscriptome, Immunoprecipitation, RNA metabolism, YTH RNA binding proteins

1 Introduction

The breadth and importance of post-transcriptional modifications to RNA molecules have been characterized to play crucial roles in regulating gene expression and satellite cell activation [1–3]. Among all 150 different types of RNA modifications, N^6-Methyladenosine (m^6A) is one of the most abundant [4–7]. These m^6A marks can be observed in mRNA, tRNA, lncRNA, etc. On average there are 3–5 m^6A depositions on mRNA transcript [8, 9]. The addition of a methyl group to the N^6 position of adenosine does not alter Watson-Crick base pairing. However, m^6A methylation weakens RNA secondary and in turn tertiary structure [3]. Such an alteration has the power to both create and destroy binding site for m^6A reader proteins, that is, YTH RNA binding proteins, thereby regulating RNA metabolism, that is, mRNA splicing, export, degradation, and translation.

Atsushi Asakura (ed.), *Skeletal Muscle Stem Cells: Methods and Protocols*, Methods in Molecular Biology, vol. 2640, https://doi.org/10.1007/978-1-0716-3036-5_29,

Understanding the m^{6}A mapping patterns across the transcriptome landscape is pivotal for investigating its biological and physiological importance. A selection of high throughput sequencing methods have been published, with different degrees of resolution and starting material. MeRIP-Seq is the first published protocol commonly adapted among all peer-reviewed methods [5]. It is also extensively tested and optimized [10, 11] to allow the lowest possible starting material. MeRIP-Seq employs an m^{6}A-specific antibody approach to enrich m^{6}A-tagged RNA fragments at a resolution of 200–400 nucleotides. Better base-pair resolution approaches are also available; however, they involve complicated procedures and relatively low reproducible biochemistry assays [8, 10, 12–15].

Recent post-transcriptional gene regulation studies have focused on epitranscriptomics and rely on advances in high throughput sequencing techniques to map m^{6}A with varying assays, which have been developed to decipher the epitranscriptome landscape. These assays include MeRIP-Seq with or without motif calling (antibodies), m^{6}A -CLIP-Seq (prolonged biochemical procedures), ONT (oxford nanopore technology) direct-sequencing, DART-Seq (artificial RNA editing enzyme dependent approach), MAZTER-Seq (RNA-specific transposable element), etc. Since MeRIP-seq is not able to determine stoichiometry, it does not necessarily detect only m6A enriched in 3'UTR but also m6Am in 5'UTR. Despite these limitations, MeRIP-Seq remains particularly popular as the most commonly used method for mapping m6A. The strengths of this assay include a simple-to-follow protocol, less starting material, time-efficient method, higher coverage of more transcripts, and the ability in depicting de novo motif detection under m^{6}A peaks (motif identified as, e.g., GGACT or GGACA). Detailed procedures of the other assays are out of scope in this chapter and discussed in detail elsewhere [16].

Our laboratory has developed MeRIP-Seq optimized for primary cultured myoblasts, which profiles m^{6}A at a resolution of approximately 100 nucleotides with as little as 100 μg total RNA as starting material. Samples with lower starting material perform at similar enrichment of known m^{6}A targets in muscle cells than canonical MeRIP-Seq. Previous protocols regarding MeRIP-Seq have focused mainly on comparing reagents and materials, but a reproducible method conducting on both cell lines and primary cell cultures is urgently needed. This protocol will cover the five most important steps illustrated in the flowchart (Fig. 1). These include: (1) RNA Fragmentation, (2) Immunoprecipitation, (3) Washing, (4) Elution, and (5) Purification. These steps will allow researchers to profile m^{6}A mapping on muscle stem cells and to perform robust analysis on MeRIP-Seq data, to generate more biologically meaningful results.

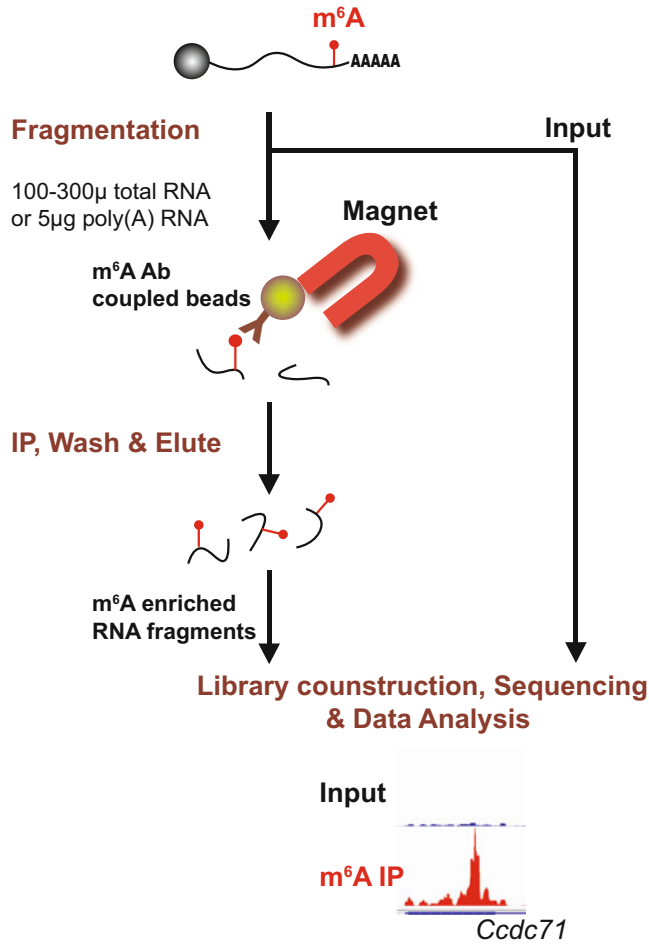

Fig. 1 Roadmap of MeRIP-seq (fragmentation, immunoprecipitation, and sequencing). An example of MeRIP seq results at *Ccdc71* locus is shown as IGV visualization in the bottom

2 Materials

2.1 RNA Fragmentation

- 1 M $ZnCl_2$.
- 10X RNA fragmentation buffer. 100 mM Tris-HCl, pH 7.0, 100 mM $ZnCl_2$ in RNase-free ultrapure water.
- 3 M NaOAC.

2.2 RNA Immunoprecipitation, Elution, and Purification

1. RNasin Ribonuclease Inhibitor (RNasin, Promega N2511).
2. Ribonucleoside vanadyl complexes VRC (Sigma-Aldrich 94740).

3. Igepal CA-63 (Sigma, I8896).
4. RNase-free Glycogen (5000 μg per mL).
5. RNase-free Bovine Serum Albumin (BSA).
6. 0.5 M EDTA, pH 8.0.
7. 20 mM N^6-Methyladenosine, 5′-monophosphate sodium salt (Sigma, M2780).
8. 5X IP buffer (5X IPB). 50 mM Tris-HCl, 750 mM NaCl, and 0.5% (v/v) Igepal CA-630. Prepare freshly.
9. 1x IP buffer (1X IPB). Dilute 5x IPB with RNase-free water.
10. Low salt buffer (LSB). 10 mM Tris HCl, pH 7.4, 50 mM NaCl, 0.1% Igepal, and 200 U per mL Rnasin. Prepare freshly.
11. High salt buffer (HSB). 10 mM Tris HCl, pH 7.4, 500 mM NaCl, 0.1% Igepal, and 200 U per mL Rnasin. Prepare freshly.
12. IP buffer with Rnase Inhibitor (IPBR). IP buffer (1X), Rnasin 200 U per mL, and RVC 10 mM. Prepare freshly.
13. IP buffer with BSA (0.5 mg per mL) (IPBB). IP buffer (1X) and Rnase-free BSA (0.5 mg per mL). Prepare freshly.
14. Elution buffer (EB). 200 U Rnasin, 1X IP buffer, and 6.7 mM m^6A. Prepare freshly.
15. High-strength Magnetic separation rack.
16. Magna ChIP™ Protein A+G Magnetic Beads (Millipore, 16–663).
17. Magnetic Separator (Magnetic separation stand for 1.5 mL tube).
18. m^6A-specific Ab stock solution, 1 mg per mL (Synaptic System, 202003).
19. Rabbit (DA1E) mAb IgG XP® Isotype Control (Cell Signaling).
20. Rneasy Mini kit, Rneasy MinElute spin column (Qiagen, 75142).

2.3 qPCR (Optional)

1. Thermal cycler.
2. Biozym Blue S'Green qPCR Kit (Biozym, 331416).
3. PCR primer set detecting *Hspa5* positive/negative region (*see* Table 2).

2.4 Others

1. Qubit RNA-HS assay (Thermo Fisher, Q32852) and Qubit machine.

3 Methods

Before Starting

- Ensure work area and materials are Rnase-free. If necessary, use Rnase-inactivating reagents (i.e., Rnase Zap, Applied Biosystems).
- Wear Personal Protective Equipment (PPE).
- Always mix fragmented RNAs by pipetting only, not vortex.

3.1 RNA Fragmentation (Approximately 3 Hours)

The quality of starting total RNA from cells or tissues of your interest is rather critical. We isolate RNA from primary cultured myoblasts with column-based purification (Rneasy Mini kit) and to check RNA integrity number (RIN). After that, another critical step for yielding valid m^{6}A peaks downstream is to perform a series of steps for optimizing chemical fragmentation with 100–200 base pair size distribution.

1. Dilute RNA to a concentration of ~1 μg per μL with RNase-free water. A starting material of the MeRIP sequence is generally ~100 μg total RNA from primary myoblasts (*see* **Note** 1).
2. Aliquot RNA 18 μL (18 μg) individually into 200 μL PCR tubes (total 6 wells 108 μg/sample).
3. Add 2 μL fragmentation buffer (10X) into individual RNA samples. Pipette to mix and spin down briefly (*see* **Note** 2).
4. Incubate tubes at 94 °C for 4–6 min with heated lid (*see* **Note** 3).
5. Add 2 μL 0.5 M EDTA to stop RNA fragmentation. Mix well and place the tube on ice while waiting to complete all batches.
6. Collect and combine all contents in a new RNase-free 1.5 mL microcentrifuge tube (*see* **Note** 4).
7. Assessment of RNA fragmentation (Fig. 2). Take 2 μL from samples for the analysis on 1.5% agarose gel.
8. Add 1/tenth volume of 3 M NaOAc, pH 5.2, glycogen (final concentration 100 μg per mL), and 4 volumes of 100% ice-cold ETOH.
9. Mix the contents well.
10. Place the mixture at −80 °C for 2 h or overnight (*see* **Note 5**).
11. To proceed, centrifuge tubes at >16,000× *g* for 30 min at 4 °C.
12. Discard the supernatant and do not disrupt the pellet.
13. Wash the pellet twice with 1 mL ice-cold 75% (v/v) ETOH.

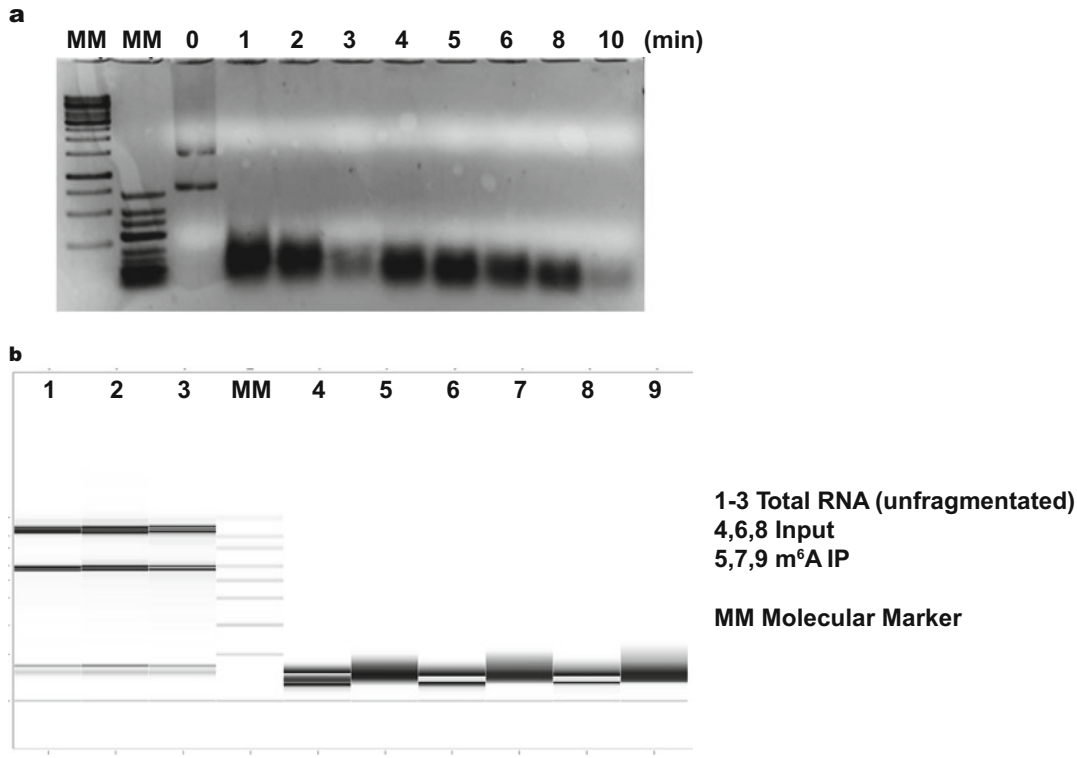

Fig. 2 Assessment of RNA fragmentation. (**a**) Gel image of fragmented RNA products. RNA was purified at individual time point indicated and loaded on 1.5% agarose gel (2 μg/lane). Note that fragmented RNA is visible near the bottom of gel after incubation on heat-block, whereas intact s18/s23 rRNA bands are visible before fragmentation (at 0 min). (**b**) Fragment analyzer results of total RNAs (Lanes 1–3); fragmented RNAs from input (Lanes 4, 6, and 8); and immunoprecipitated samples (Lanes 5, 7, and 9)

14. Spin at >16,000× *g* for 15 min at 4 °C.
15. Aspirate supernatant and air dry the pellet for 10 min.
16. Resuspend in 300 μL RNase-free water (*see* **Note 6**).
17. Measure RNA concentration (*see* **Note 7**).

3.2 Formulation of Immunocomplex Between Free Antibody and Fragmented RNAs (Approx. 3 Hours)

1. Label the appropriate number of 1.5 mL low-binding micro centrifuge tubes for the desired RIP reactions (one for 10% Input control, one for anti- m^6A IP, and another for negative control IgG).
2. Save aside the untreated fragmented RNA as "10% input control", 10% of original Input (*see* **Note 8**).
3. Aliquot the remaining fragmented RNA (~100 μg/sample) into another 1.5 mL low-binding microcentrifuge tube to prepare for "IP sample" and "IgG control" samples.

Table 1
Preparations of RNA samples for immunoprecipitation

Component	Volume (μL)	Final
Fragmented RNA	–	100 μg of total RNA
RNasin (40 U per ul)	10	200 U
RVC (200 mM)	10	2 mM
5X IPB	200	1x
m^{6}A antibody or IgG control	12.5	12.5 μg
Total volume	Up to 1000	

4. Mix the material for immunoprecipitation as described in Table 1.
5. Incubate samples with primary antibody for 2 h (or O/N) at 4 °C with head-over-tail rotation.

3.3 Preparation of Pre-Cleared Magnetic Beads for Immunoprecipitation (Approx. 3 Hours)

1. Aliquot Magna CHIP protein A/G magnetic beads (Maximally, 50 μL per sample) in each 1.5 mL low-binding centrifuge tube.
2. Add 1 mL IPB into beads to wash.
3. Place the magnetic beads on a magnetic separator. Once the solution becomes clear, remove the supernatant.
4. Repeat the washing step with IPBB twice.
5. Resuspend beads in 1 mL IPBB.
6. Incubate on the rotator for 1 h at room temperature.
7. After pre-clearing, wash twice in 1 mL IPB.
8. Resuspend in 200 μL IPBR per 50 μL beads.
9. Put bead-containing tubes immediately on ice, which are then ready for immunoprecipitation with fragmented RNA- m^{6}A complex.

3.4 Immunoprecipitation (Approx. 4 Hours)

1. Place the precleared magnetic beads on a magnetic separator.
2. After the solution becomes clear, remove the supernatant.
3. Transfer the reaction mixture, from Subheading 3.2, into the labeled bead-containing tube. Mix well.
4. Incubate all tubes for 3 h at 4 °C, head-over-tail rotation.
5. After incubation, spin down gently to collect liquid on the lid, and place on the magnetic separator (*see* **Note 9**).

3.5 Wash (Approx. 1 Hour)

1. Wash the magnetic beads with 0.5 mL ice-cold 1X IPBR. Mix well and spin gently.
2. Place tubes on magnetic separator and then remove the supernatant (*see* **Note 10**).

3. Repeat the wash procedure with ice-cold 1X IPBR once more.
4. Wash the beads with 0.5 mL ice-cold LSB. Mix well and spin gently.
5. Place tubes on magnetic separator and then discard the supernatant (*see* **Note 10**).
6. Repeat the wash procedure with ice-cold LSB once more.
7. Wash the beads with 0.5 mL ice-cold HSB. Mix well and spin gently.
8. Place the tubes on magnetic separator and then discard the supernatant (*see* **Note 10**).
9. Repeat the wash procedure with ice-cold HSB once more.
10. After six washes in total, it is important to remove any trace of final wash leaving only beads. The desired population of m^6A-enriched RNA fragments are on the beads.
11. Place tubes on ice and immediately proceed to the next step.

3.6 Elution (Approx. 2.5 Hours)

1. Add 100 μL EB to the sedimented beads of IP sample, and IgG control.
2. Mix well and incubate for 1 h at 4 °C with head-over-tail rotation.
3. Spin down beads gently and place them on magnetic separator.
4. Carefully transfer the supernatant to a fresh individually labeled RNase-free 1.5 mL tube (*see* **Note 11**).
5. Incubate beads with another 100 μL of EB and mix well.
6. Incubate on rotor for 10 min at RT.
7. Spin down and place on magnetic separator.
8. Collect and combine the elution of the same sample. The total elution volume is eventually 200 μL (*see* **Note 11**).
9. Immediately proceed to recovery and purification of RNA with RNeasy Mini kit.

3.7 Purification of Eluted m^6A Marked RNA Fragments (Approx. 1 Hour)

1. Transfer the 200 μL of eluates to a new 15 mL conical tube. Add 500 μL of Buffer RLT (from RNeasy Mini kit) and mix well.
2. Add 200 μL RLT buffer onto the beads to elute leftover.
3. Incubate for 2 min at RT.
4. Place beads on the magnetic rack and retrieve the RLT buffer.
5. Combine 700 μL RNA sample/RTL buffer mixture (prepared in **step 1**) and the 200 μL elution (prepared in **step 4**).
6. Add 1.4 mL of 100% ethanol to the sample and mix well.
7. Transfer 700 μL of the sample to an RNeasy MinElute spin column placed in a 2 mL collection tube.

8. Centrifuge for 15 s at ≥8000× *g*. Discard the flow-through. Repeat the process until all sample has loaded to the column.
9. Place the RNeasy MinElute spin column in a fresh 2 mL collection tube. Add 500 μL Buffer RPE to the spin column. Centrifuge for 15 s at ≥8000× *g*. Discard the flow-through.
10. Add 500 μL of 80% ethanol to the column. Centrifuge for 2 min at ≥8000× *g* to wash the spin column membrane. Discard the flow-through and collection tube.
11. Place the RNeasy MinElute spin column in a fresh 2 mL collection tube. Centrifuge at full speed for 5 min to dry the spin-column membrane. Discard the flow-through and collection tube.
12. Place the RNeasy MinElute spin column in a new labeled 1.5 mL collection tube.
13. Add 14 μL RNase-free water directly to the center of the spin-column membrane. Incubate for 3 min. Centrifuge for 2 min at full speed to elute the RNA.
14. Place on ice immediately. Proceed to the next steps or RNA can be stored at −80 °C for up to 1 year.

3.8 Sequence of m^{6}A IP RNA

The yield of MeRIP is generally low although a validation of m^{6}A MeRIP is possible by qPCR using specific primer for m^{6}A positive and negative locus specific primers. We generally utilize *Hspa5* m^{6}A Positive/Negative region specific primer sets for validation (Table 2). The qPCR is generally performed on samples: (1) 10% Input, (2) anti-m^{6}A IP, and (3) negative IgG control following instruction of qPCR master mix protocol (Biozym Blue S'Green qPCR Kit). The PCR using m^{6}A IP sample will be positive at m^{6}A Positive region but not at Negative region as shown in Fig. 3, if MeRIP is successfully performed.

3.8.1 m^{6}A MeRIP Validation by qPCR (Optional)

3.8.2 MeRIP-Seq (Library Preparation)

1. RNA and library preparation integrity were verified with LabChip Gx Touch 24 (Perkin Elmer). Approx. 10 ng of total RNA was used as input for SMARTer® Stranded Total RNA-Seq Kit – Pico Input Mammalian (Takara Clontech)

Table 2
Primer sequence for qPCR

Primer name	Sequence (5′ to 3′)
Hspa5 m6A positive	CCCAACTGGTGAAGAGGATACA
Hspa5 m6A positive	CAACGAAAGTTCCTGAGTCCAG
Hspa5 m6A negative	TCTGGTTGGTGGATCTACTCG
Hspa5 m6A negative	CTACAGCCTCATCGGGGTTTAT

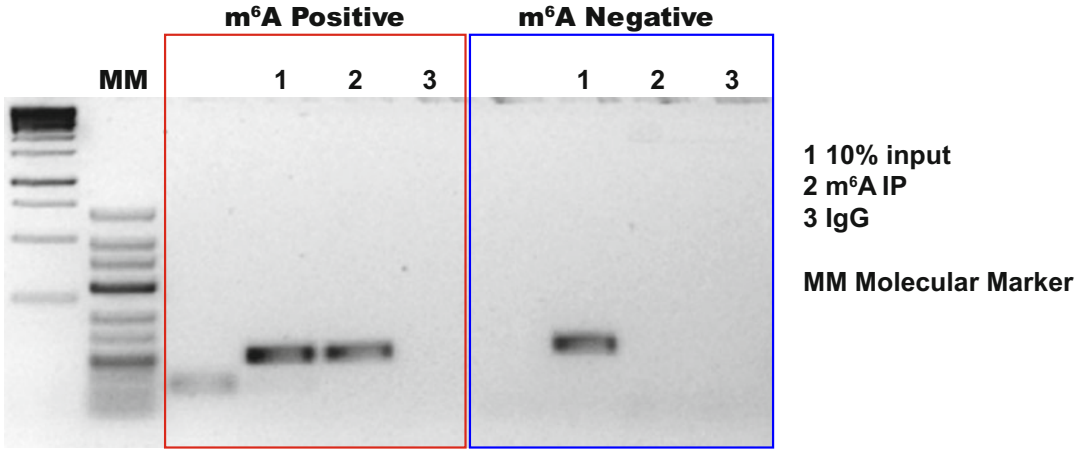

Fig. 3 Results of qPCR using 10% input (Lane 1), anti-m^{6}A IP (Lane 2), and IgG (Lane 3) samples. PCR reaction using anti-m^{6}A IP sample (Lane 2) detected only m^{6}A-positive region (red box) but not m^{6}A-negative region (blue box)

following the manufacturer protocol with 12 cycles of amplification and without initial fragmentation of RNA.

2. Sequencing was performed on the NextSeq500 instrument (Illumina) using v2 chemistry, resulting in average of 30 M reads per library with 1x 75 bp single-end setup. The resulting raw reads were assessed for quality, adapter content, and duplication rates with FastQC [17]. Trimmomatic version 0.39 was employed to trim reads after a quality drop below a mean of Q20 in a window of ten nucleotides [18].
3. The sequence data is ready to analyze using available bioinformatics methods. As an example, the IGV view at *Hspa5* of m^{6}A MeRIP-seq results using primary myoblasts is shown in Fig. 4.

4 Notes

1. Typically, one immunoprecipitation sample needs >100 μg of total RNA as starting material.
2. There are several parameters affecting peak distribution including the amount of RNA, incubation time and temperature of heat-block, and presence of residual EDTA or salts. Any scaling of the protocol may affect fragmentation efficiency and thus size distribution. For this purpose, we either fix RNA concentration at 1 μg per μL and incubation temperature at 94 °C or vary the concentration of RNA with constant time and temperature.

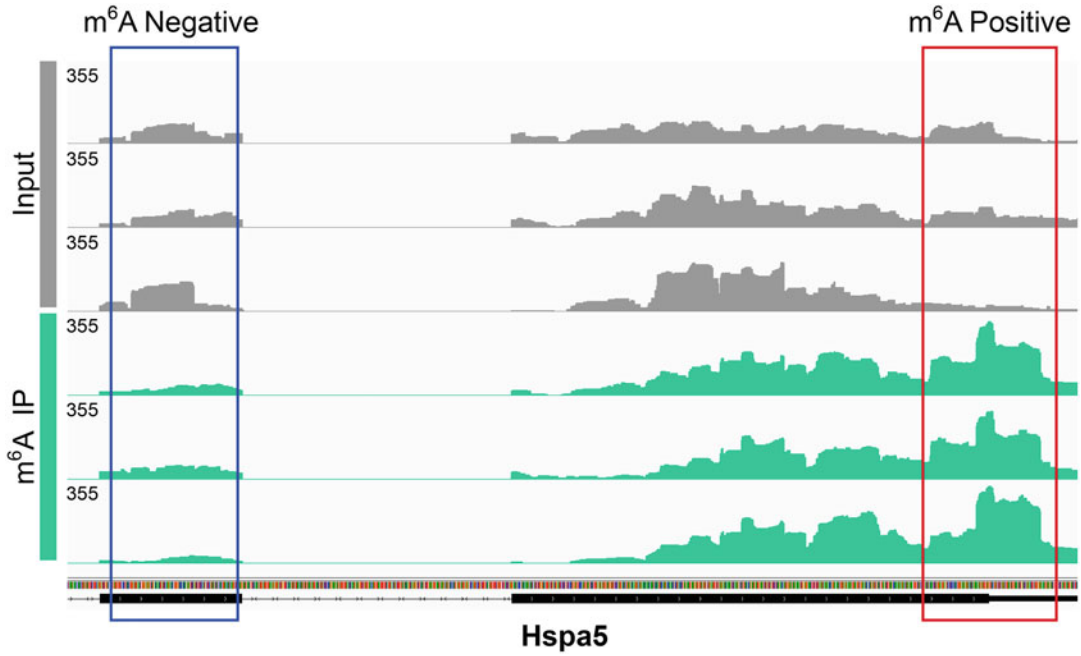

Fig. 4 IGV view of the MeRIP-seq results (The data range is 0–296). A peak at the m^{6}A-positive region of *Hspa5* locus (red box) is enriched in all anti-m^{6}A IP triplicates compared to input samples whereas no significant enrichment was identified at m^{6}A-negative region (blue box)

3. If necessary, validation of incubation time for RNA fragmentation can be performed as follows:

   Preheat the thermal cycler block to 94 °C. Adjust RNA concentration to ~1 μg per μL, that is, 18 μg RNA per 20 μL in thin-walled 200 μL PCR 8-strip tube. Add 2 μL 10x fragmentation buffer, mix well. Prepare 100 μL of 0.05 M EDTA. Incubate the tube in a heatblock for different minutes, for example, 1, 2, 3, 4, 5, 6, 8, and 10 min. Transfer 2 μl of the fragmented RNA per desired incubation minute into a new microcentrifuge tube, immediately add 2 μl of 0.05 M EDTA, mix by pipetting and store for analysis with the bioanalyzer. Analyze with Agilent 2100 Bioanalyzer with Agilent kit, or load 0.5 μg of fragmented RNA in 10 μL on 1–2% agarose gel, together with non-fragmented sample and genomic DNA controls. The optimal time for RNA fragmentation is between 4 and 6 min (Fig. 2).
4. Maximally, ~200 μg total RNA samples can be combined into one 1.5 mL tube.
5. RNA mixture is stable and possible to preserve at −80 °C for up to 1 year.
6. RNA can be stored at −80 °C at this stage until further use for up to 1 year.

7. Typically, more than 70% of total RNA will be recovered after RNA fragmentation.
8. This sample can be preserved at −80 °C up to a year and will be used to generate a standard curve or for comparison in RT-qPCR methods, or input control in sequencing.
9. Carefully transfer the supernatant into a freshly labeled 1.5 mL tube (as "IP QC" no m^6A enriched population).
10. It is appropriate to leave some suspension behind to avoid drying the sample.
11. Do not take or disturb the magnetic beads as it will increase background noise.

References

1. Farina NH, Hausburg M, Betta ND et al (2012) A role for RNA post-transcriptional regulation in satellite cell activation. Skelet Muscle 2(1):21. https://doi.org/10.1186/2044-5040-2-21
2. Hausburg MA, Doles JD, Clement SL et al (2015) Post-transcriptional regulation of satellite cell quiescence by TTP-mediated mRNA decay. elife 4:e03390. https://doi.org/10.7554/eLife.03390
3. Kierzek E, Kierzek R (2003) The thermodynamic stability of RNA duplexes and hairpins containing N6-alkyladenosines and 2-methylthio-N6-alkyladenosines. Nucleic Acids Res 31(15):4472–4480. https://doi.org/10.1093/nar/gkg633
4. Bohnsack MT, Sloan KE (2018) Modifications in small nuclear RNAs and their roles in spliceosome assembly and function. Biol Chem 399(11):1265–1276. https://doi.org/10.1515/hsz-2018-0205
5. Dominissini D, Moshitch-Moshkovitz S, Schwartz S et al (2012) Topology of the human and mouse m6A RNA methylomes revealed by m6A-seq. Nature 485(7397):201–206. https://doi.org/10.1038/nature11112
6. Fu Y, Dominissini D, Rechavi G et al (2014) Gene expression regulation mediated through reversible m(6)A RNA methylation. Nat Rev Genet 15(5):293–306. https://doi.org/10.1038/nrg3724
7. McIntyre ABR, Gokhale NS, Cerchietti L et al (2020) Limits in the detection of m(6)A changes using MeRIP/m(6)A-seq. Sci Rep 10(1):6590. https://doi.org/10.1038/s41598-020-63355-3
8. Meyer KD, Saletore Y, Zumbo P et al (2012) Comprehensive analysis of mRNA methylation reveals enrichment in 3′ UTRs and near stop codons. Cell 149(7):1635–1646. https://doi.org/10.1016/j.cell.2012.05.003
9. Molinie B, Wang J, Lim KS et al (2016) m(6)A-LAIC-seq reveals the census and complexity of the m(6)A epitranscriptome. Nat Methods 13(8):692–698. https://doi.org/10.1038/nmeth.3898
10. Dominissini D, Moshitch-Moshkovitz S, Salmon-Divon M et al (2013) Transcriptome-wide mapping of N(6)-methyladenosine by m(6)A-seq based on immunocapturing and massively parallel sequencing. Nat Protoc 8(1):176–189. https://doi.org/10.1038/nprot.2012.148
11. Wei CM, Gershowitz A, Moss B (1975) Methylated nucleotides block 5′ terminus of HeLa cell messenger RNA. Cell 4(4):379–386. https://doi.org/10.1016/0092-8674(75)90158-0
12. Hsu PJ, He C (2019) High-resolution mapping of N (6)-Methyladenosine using m(6)A crosslinking immunoprecipitation sequencing (m(6)A-CLIP-Seq). Methods Mol Biol 1870:69–79. https://doi.org/10.1007/978-1-4939-8808-2_5
13. Ke S, Alemu EA, Mertens C et al (2015) A majority of m6A residues are in the last exons, allowing the potential for 3′ UTR regulation. Genes Dev 29(19):2037–2053. https://doi.org/10.1101/gad.269415.115
14. Kudou K, Komatsu T, Nogami J et al (2017) The requirement of Mettl3-promoted MyoD mRNA maintenance in proliferative myoblasts for skeletal muscle differentiation. Open Biol 7(9). https://doi.org/10.1098/rsob.170119
15. Linder B, Grozhik AV, Olarerin-George AO et al (2015) Single-nucleotide-resolution mapping of m6A and m6Am throughout the

transcriptome. Nat Methods 12(8):767–772. https://doi.org/10.1038/nmeth.3453

16. Liu N, Dai Q, Zheng G et al (2015) N(6)-methyladenosine-dependent RNA structural switches regulate RNA-protein interactions. Nature 518(7540):560–564. https://doi.org/10.1038/nature14234
17. Andrews S (2010) FastQC: a quality control tool for high throughput sequence data. Available online at: https://www.bioinformatics.babraham.ac.uk/projects/fastqc/
18. Bolger AM, Lohse M, Usadel B (2014) Trimmomatic: a flexible trimmer for Illumina sequence data. Bioinformatics 30(15):2114–2120. https://doi.org/10.1093/bioinformatics/btu170

Chapter 30

Visualization of RNA Transcripts in Muscle Stem Cells Using Single-Molecule Fluorescence In Situ Hybridization

Lu Yue and Tom H. Cheung

Abstract

Uncovering the transcriptomic signatures of quiescent muscle stem cells elicits the regulatory networks on stem cell quiescence. However, the spatial clues of the transcripts are missing in the commonly used quantitative analysis such as qPCR and RNA-seq. Visualization of RNA transcripts using single-molecule in situ hybridization provides additional subcellular localization clues to understanding gene expression signatures. Here, we provide an optimized protocol of smFISH analysis on Fluorescence-Activated Cell Sorting isolated muscle stem cells to visualize low-abundance transcripts.

Key words Muscle stem cell, Satellite cell, Quiescence, RNA, FACS, In situ hybridization

1 Introduction

Adult stem cells are essential for tissue regeneration and homeostasis. Understanding the gene expression profiles allows us to elicit the genetic regulatory networks on adult stem cells. Skeletal muscle stem cells, also called satellite cells (SCs), reside in quiescence in resting muscles [1, 2]. Upon injury, quiescent satellite cells (QSCs) activate promptly for muscle regeneration. One of the standard practices to investigate QSCs is to isolate them from muscles using fluorescence-activated cell sorting (FACS) and perform further analysis. However, some QSCs have acquired activation signatures during the isolation process [3–6]. To preserve the quiescent signatures of QSCs as in vivo, we perform light fixative perfusion on the mouse to fix QSCs in situ before FACS isolation [4]. This optimized fixed SCs isolation technique allows us to uncover the in vivo features of QSCs.

Systematic quantification techniques such as RNA-seq allow us to understand the gene expression landscape of QSCs. However, spatial information is missing. The subcellular localization of target RNA transcripts helps understand its activities, functions, and potential protein outputs. In situ hybridization analysis allows us

Atsushi Asakura (ed.), *Skeletal Muscle Stem Cells: Methods and Protocols*, Methods in Molecular Biology, vol. 2640,
https://doi.org/10.1007/978-1-0716-3036-5_30,

to visualize the RNA transcripts inside the cell. Single-molecule fluorescence in situ hybridization (smFISH) provides a much higher signal-to-background ratio than conventional in situ hybridization [7]. Multiple small probes around 20 nucleotides annealing to one RNA transcript ensures high sensitivity and specificity. The uniform signals also allow for RNA quantification using computational approaches [8]. However, smFISH is heavily relying on imaging analysis. For the low abundant tissue-residing cells such as QSCs, it is time-consuming and labor-intensive to perform smFISH on tissue sections to obtain enough data of interested cells. With the optimized FACS to enrich low abundant tissue-residing cells and preserve their in vivo signatures, smFISH allows us to decipher the intracellular localizations of transcripts in quiescent muscle stem cells in vivo.

Using this technique, we have successfully observed the low-abundant intron-retained transcripts of MyoD accumulated in the nucleus of quiescent muscle stem cells (Fig. 1a) [9]. Upon activation, the mature mRNA transcripts of MyoD are enriched in the cytoplasm of activated muscle stem cells (Fig. 1b). The

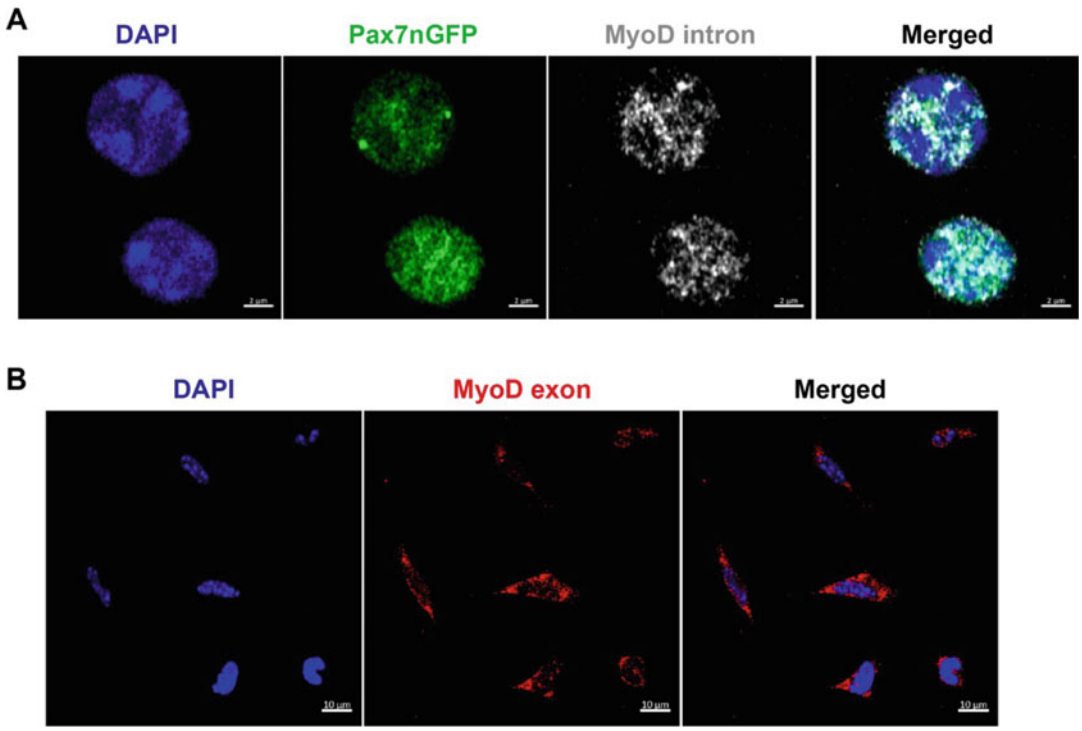

Fig. 1 Single-molecule in situ hybridization analysis of MyoD RNA transcripts on QSCs and activated satellite cells. (**a**) QSCs from PFA-perfused Pax7-nGFP mice were plated down for 1 h, fixed, and hybridized with probes targeting MyoD introns. Nuclei were stained with DAPI. Scale bar, 2 μm. (**b**) Freshly isolated SCs were cultured for 1 day for activation, then fixed and hybridized with probes targeting MyoD exons. Nuclei were stained with DAPI. Scale bar, 10 μm

intracellular localization of MyoD RNA transcripts ensures MyoD protein expression during QSC activation. This technique could lead to a better understanding of the spatial arrangement of low-abundant RNA transcripts.

2 Materials

1. DEPC-treated phosphate-buffered saline (PBS)/Nuclease-free PBS.
2. DEPC-treated H_2O/Nuclease-free H_2O.
3. 37% formaldehyde.
4. 1.1x Hybridization buffer.

Reagent	Weight/volume
Dextran sulfate	1 g
20x SSC	1 mL
DEPC-treated H_2O	8 mL
Total	9 mL

Note: Dextran sulfate is hard to dissolve. Wrap the tube with foil and shake overnight to dissolve dextran sulfate. Make small aliquots (i.e., 200 μL) and store aliquots at −20 °C.

Note: Before usage, add formamide freshly (i.e., add 10 μL formamide to 90 μL 1.1x hybridization buffer, so the final concentration of the formamide is 10%). Formamide should always be used with adequate ventilation, preferably in a fume hood. Eyes and skin exposure should be avoided. While handling formamide follow the safety data sheet. Warm formamide to room temperature before use.

5. Wash buffer.

Reagent	Volume
20x SSC	2 mL
Formamide	2 mL
DEPC-treated H_2O	16 mL
Total	20 mL

Freshly prepare wash buffer before usage. Wash buffer can be stored short-term for 1–2 days at 4 °C. Wrap the cap of the tube with parafilm and wrap the whole tube with foil for storage.

6. 2x SSC wash buffer.

Reagent	Volume
20x SSC	2 mL
DEPC-treated H_2O	18 mL
Total	20 mL

7. Mounting buffer.

Reagent	Volume
20x SSC	1 mL
Glycerol	1 mL
DEPC-treated H_2O	8 mL
Total	10 mL

8. Confocal dish (SPL Life Sciences, Catalog #: 1003500).
9. 16 mm round cover glasses (Paul Marienfeld, Catalog #: 0111560) or equivalent.
10. Transparent fingernail polish oil.
11. Poly-D-Lysine hydrobromide (Sigma-Aldrich, Catalog #: P6407-5MG).
12. Extra Cellular Matrix (ECM) gel, liquid, cell culture tested (Sigma-Aldrich, Catalog #: E1270-10ML).
13. Ham's F-10 (Sigma-Aldrich, Catalog #: N6635) or equivalent.
14. Hemocytometer (Gizmo Supply Co, Catalog # B-CNT-SLDE-V2) or equivalent.
15. Incubator (30 °C and 37 °C).

3 Methods

3.1 Preparation of the Confocal Dish (Day 1 and Day 2)

1. Day 1: Coat the well of the confocal dish with 200 μL 1x Poly-D-Lysine hydrobromide (PDL) and incubate overnight (~16 h) at 37 °C.
2. Day 2: Aspirate away the PDL and wash the confocal dish well using DEPC-treated H_2O three times.
3. Day 2: Dry the well in the tissue-culture hood for ~3 h.
4. Day 2: Before cell plating, coat the well with cold 200 μL ECM coating medium (1:100 ECM in cold Ham's F10 or equivalent) and incubate at room temperature (~22–25 °C) for 30–60 min.

3.2 QSC Isolation Using FACS (Day 2)

To isolate QSCs, fixative perfusion is used. As QSCs acquire an activation signature during FACS isolation, fixation prior to isolation allows the preservation of the quiescent signatures of QSCs in vivo. Perfusion provides an even fixation as the fixative goes through the systematic circulation from the left ventricle and exits from the right atrium of the heart. In addition, the light and timed fixation perfusion (0.5% paraformaldehyde for 5 min) strike a balance between the quality of the fixation and the yield of isolated cells. The detailed protocol of fixative perfusion and fixed satellite cell isolation using FACS is published in Yue and Cheung, 2020 [9]. Here, a brief protocol is described for these steps. The expected yield of unfixed QSCs from a Pax7nGFP mouse [10] is at least 600 K, while for the fixed QSCs it is ~100–300 K.

1. Anesthetize the mouse with 1.2% Avertin solution for a 20 g mouse (2,2,2-Tribromoethanol 250 mg/kg body weight of the mouse) through intraperitoneal injection. Alternative anesthetization methods can be used.
2. Perfuse the mouse with 30 mL cold PBS using a 10 mL syringe adapted with a 25 g needle.
3. Perfuse the mouse with 30 mL cold 0.5% PFA using a 10 mL syringe adapted with a 25 g needle. 0.5% PFA should be freshly prepared each time by diluting the 32% PFA with cold PBS. The perfusion should be finished in 5 min, so the total fixation is 5 min.
4. Perfuse the mouse with 30 mL cold 2 M glycine (in PBS) using a 10 mL syringe adapted with a 25 g needle.
5. Dissect the hindlimb muscles out. Mince and cut muscles into a slurry.
6. Digest muscles slurry in a 50 mL conical tube with 10 mL Collagenase II digestion medium at 37 °C for 90 min with agitation in a shaking water bath. 1000 U/mL Collagenase II (Worthington Biochemical, Catalog #: LS004177) is used for regular SC isolation. 2000 U/mL Collagenase II is used for fixed SC isolation.
7. Fill the tube with cold wash medium (F10, 10% HS, Pen/-Strep) till 50 mL.
8. Split the slurry into two, top-up each tube with cold wash medium (F10, 10% HS, Pen/Strep) till 50 mL.
9. Centrifuge at 500 *g*, 10 min, 4 °C using the centrifuge (Eppendorf 5408R).
10. Aspirate the solution till ~12.5 mL for each tube.

11. Combine the two tubes into one, add 1 mL 3000 U/mL Collagenase II and 1 mL 30 U/mL Dispase II (Thermo Fisher Scientific, Catalog #: 17105041) and mix well.
12. Fill the tube with cold wash medium (Ham's F10, 10% Horse Serum, 1 U/mL Penicillin Streptomycin) till 30 mL. Thus, the final working concentration of Collagenase II and Dispase II is 100 U/mL and 1 U/mL, respectively.
13. Incubate the tube at 37 °C for 30 min with agitation in a shaking water bath.
14. Mix the slurry with a 30 mL syringe adapted to a 20 g syringe for 10 times. Any muscle pieces that clog the needle should be discarded.
15. Filter the cell solution with a 40 μm filter adapted to a new 50 mL conical tube.
16. Fill the tube with a cold wash medium up to 50 mL.
17. Centrifuge at 500 *g*, 10 min, 4 °C using the centrifuge.
18. Carefully aspirate away the supernatant till ~3 mL without disturbing the cell pellet.
19. Filter the cell solution with a 40 μm filter adapted to a new 50 mL conical tube.
20. Transfer the cell solution to the loading tube.
21. Put ~100 μL wash medium into the collection tube for fixed SC collection.
22. Sort SCs into the collection tube using a cell sorter. For BD Influx cell sorter, the expected sort time is ~1 h for one mouse.

3.3 SC Plating, Fixation, and Permeabilization (Day 2)

FACS-isolated quiescent satellite cells can be plated down for the following smFISH analysis. The in situ hybridization allows visualization of RNA transcripts inside the cells, providing both the localization and the relative quantity of the target transcript. Here, the custom probes are purchased from LGC Biosearch Technologies. The smFISH protocol is adapted from the manufacturing instructions of the probes.

1. Count FACS-isolated cells using a hemocytometer.
2. Aspirate away the ECM coating medium of the confocal dish.
3. Plate down ~100 K FACS-isolated SCs (in ~100–200 μL collection medium) on the well of the confocal dish. The excess medium will result in poor plating of fixed SCs.
4. Incubate the confocal dish in the 37 °C incubator for 1 h for cells to sink to the bottom of the well.

5. Fix cells with 3.7% formaldehyde (diluted in 1x DEPC-treated PBS) for 10 min at room temperature.
6. Wash the well with DEPC-treated PBS twice.
7. Wash the well with freshly prepared 70% ethanol (diluted with DEPC-treated H_2O) twice.
8. Permeabilize cells with freshly prepared 70% ethanol for at least 16 h. Wrap the plate with parafilm.

3.4 Wash and Hybridization (Day 3)

1. Freshly prepare the wash buffer.
2. Freshly prepare the hybridization buffer. Add formamide to 1.1x hybridization buffer (i.e., add 10 μL formamide to 90 μL 1.1x hybridization buffer so the final concentration of the formamide is 10%).
3. Wash the well with the wash buffer twice.
4. Rehydrate the cells with the wash buffer for 5 min.
5. Prepare hybridization probes.

Reagent	Volume
Probes	1–2 μL
Hybridization buffer	100 μL
RNase inhibitor (20 U/mL)	1 μL
Total	~100 μL

6. Pipette away the wash buffer in the well.
7. Add hybridization probes to the well. Wrap the plate with parafilm. Incubate at 30 °C overnight in a humid and dark chamber.

3.5 Wash and Mounting (Day 4)

1. Wash the well with wash buffer twice.
2. Add wash buffer to the well, incubate at 30 °C for 30 min in a humid and dark chamber. Repeat this step twice so there is a total of three washing steps.
3. Add DAPI (1:10,000) to the wash buffer. Incubate at 30 °C for 30 min in a humid and dark chamber.
4. Wash the well with 2x SSC buffer at room temperature for 5 min twice.
5. Pipette away the 2x SSC buffer.
6. Add 150 μL mounting buffer to the well.
7. Cover the well with a coverslip.
8. Seal the edge of the coverslip with transparent fingernail polish oil (*see* **Note**).

4 Note

The plate is now ready for imaging and the signal would be sustained for a few days. It is recommended to finish imaging as soon as possible. Typically, we use a Zeiss LSM880 confocal microscope with Airyscan for imaging.

Acknowledgments

This work was supported by research grants from the Hong Kong Research Grant Council (GRF660313, GRF16102420, GRF16102021, GRF16100322, C6018-19GF, C6027-19GF, AoE/M-604/16, T13-607/12R), the National Key R&D Program of China (2018YFE0203600), the Guangdong Provincial Key S&T Program (2018B030336001), Lee Hysan Foundation (LHF17SC01), Hong Kong Epigenome Project (Lo Ka Chung Charitable Foundation), and the Croucher Innovation Award (CIA14SC04) from Croucher Foundation. This study was supported in part by the Innovation and Technology Commission (ITCPD/17-9). T.H.C. is the S.H. Ho Associate Professor of Life Science at HKUST.

References

1. Montarras D, L'honoré A, Buckingham M (2013) Lying low but ready for action: the quiescent muscle satellite cell. FEBS J 280: 4036–4050
2. Yin H, Price F, Rudnicki MA (2013) Satellite cells and the muscle stem cell niche. Physiol Rev 93:23–67
3. van den Brink SC, Sage F, Vértesy Á et al (2017) Single-cell sequencing reveals dissociation-induced gene expression in tissue subpopulations. Nat Methods 14:935–936
4. Yue L, Wan R, Luan S et al (2020) Dek modulates global intron retention during muscle stem cells quiescence exit. Dev Cell 53:661–676.e6
5. Machado L, de Lima JE, Fabre O et al (2018) In situ fixation redefines quiescence and early activation of skeletal muscle stem cells. Cell Rep 21:1982–1993
6. van Velthoven CTJ, de Morree A, Egner IM et al (2017) Transcriptional profiling of quiescent muscle stem cells in vivo. Cell Rep 21: 1994–2004
7. Raj A, van den Bogaard P, Rifkin SA et al (2008) Imaging individual mRNA molecules using multiple singly labeled probes. Nat Methods 5:877–879
8. Trcek T, Lionnet T, Shroff H et al (2017) mRNA quantification using single-molecule FISH in Drosophila embryos. Nat Protoc 12: 1326–1348
9. Yue L, Cheung TH (2020) Protocol for isolation and characterization of in situ fixed quiescent muscle stem cells. STAR Protoc 1:100128
10. Sambasivan R, Gayraud-Morel B, Dumas G et al (2009) Distinct regulatory cascades govern extraocular and pharyngeal arch muscle progenitor cell fates. Dev Cell 16:810–821

Chapter 31

Tissue Clearing and Confocal Microscopic Imaging for Skeletal Muscle

Smrithi Karthikeyan, Yoko Asakura, Mayank Verma, and Atsushi Asakura

Abstract

Skeletal muscle is a highly ordered tissue composed of a complex network of a diverse variety of cells. The dynamic spatial and temporal interaction between these cells during homeostasis and during times of injury gives the skeletal muscle its regenerative capacity. To properly understand the process of regeneration, a three-dimensional (3-D) imaging process must be conducted. With the advancement of imaging and computing technology, it has become powerful to analyze spatial data from confocal microscope images. In order to prepare whole tissue skeletal muscle samples for confocal imaging, the muscle must be subjected to tissue clearing. With the use of an ideal optical clearing protocol – one that minimizes light scattering via refractive index mismatching – a more accurate 3-D image of the muscle can be produced as it does not involve the physical sectioning of the muscle. While there have been several protocols relating to the study of 3-D biology in whole tissue, these protocols have primarily been focused on the nervous system. In this chapter, we present a new method for skeletal muscle tissue clearing. In addition, this protocol aims to outline the specific parameters required for taking 3-D images of immunofluorescence-stained skeletal muscle samples using a confocal microscope.

Key words Skeletal muscle, Myogenesis, Satellite cell, Muscle stem cell, Tissue clearing, 3D imaging, Muscle regeneration, Angiogenesis, Endothelial cell, Muscular dystrophy

1 Introduction

In the body, skeletal muscle performs several important functions, including voluntary movement, breathing, and posture maintenance. One key characteristic of skeletal muscle is its remarkable ability to regenerate, heal, and adapt to various physiological demands such as growth, exercise, and injury [1, 2]. Skeletal muscle is composed of a tight network of the following different types of cells: muscle stem cells (satellite cells), endothelial cells, pericytes, fibroadipogenic progenitors (FAPs), immune cells, and fibroblasts [3–5]. The various cross-cellular interactions and cellular organization present in this complicated cell network change from the basal state in times of development and regeneration [6, 7]. A deeper understanding of both the structure, function, and interactions of

Atsushi Asakura (ed.), *Skeletal Muscle Stem Cells: Methods and Protocols*, Methods in Molecular Biology, vol. 2640, https://doi.org/10.1007/978-1-0716-3036-5_31,

cells within the network would lead to a more complete understanding of the regeneration process and provide new insights into neuromuscular-degenerative diseases such as Duchenne muscular dystrophy (DMD).

Traditionally, this cellular network has been analyzed using longitudinal cross-sections of skeletal muscle, which are obtained from frozen tissue blocks. These cross-sections are typically then immunolabeled and examined under a light microscope [8]. This method's limitation is that it can only provide information on cells' respective orientations on a lateral plane. Information on the axial orientations of cells in the muscle section is completely lost, which leads to a misrepresentation of the actual 3-D muscle network [8]. Therefore, in order to get an accurate understanding of the dynamic interactions present in the cellular network, the skeletal muscle must be analyzed in all 3-D.

One method of creating a 3-D image of muscle tissue is by imaging a series of lateral sections and compiling all of the images manually/automatically to generate a 3-D representation. However, this method is time-intensive and error-prone due to artifacts present in the lateral sections. Instead, a more promising method of 3-D analysis is through optical sectioning using confocal microscopy. Optical sectioning uses software deconvolution and confocal microscopy to image the muscle tissue in 3-D without cutting through the sample. This approach has traditionally been limited due to the presence of light-scattering molecules such as lipids, proteins in the extracellular matrix, and endogenously fluorescent molecules such as myoglobin and NADH [2]. However, this problem can be addressed via a method known as optical tissue clearing protocols such as iDISCO [9], CUBIC [10], and CLARITY [11]. In tissue clearing, the skeletal muscle is subjected to various chemicals to turn the muscle transparent and ideal for optical sectioning. The ideal optical tissue clearing protocol for a muscle would reduce light scattering via refractive index mismatching, a signal from pigmented molecules, preserve fluorescence reporter molecules, and be amenable to immunolabeling [2]. In this chapter, we propose an ideal optical muscle tissue clearing protocol that achieves the above goals and prepares skeletal muscle samples ideal for confocal imaging.

2 Materials and Preparation

2.1 Tissue Dissection

1. *Pax7*^{tdTomato} mice: *B6.Cg-Pax7*$^{tm1(cre/ERT2)Gaka/J}$ mice (JAX stock# 017763) [12] were crossed with *B6.Cg-Gt(ROSA)*$^{26\text{-}Sortm9(CAG\text{-}tdTomato)Hze/J}$ mice (JAX stock # 007909) [13].
2. *Kdr*$^{tm2.1Jrt/J}$ (*Flk1*$^{+/GFP}$) mice were obtained from Masatsugu Ema [14].

3. *Pax7*^{tdTomato}:*Flk1*$^{+/GFP}$ mice: *Pax7*^{tdTomato} mice were crossed with *Flk1*$^{+/GFP}$ mice to generate *Pax7*^{tdTomato}:*Flk1*$^{+/GFP}$ mice [6].
4. Tamoxifen: Tamoxifen is dissolved in corn oil at a concentration of 20 mg/mL by shaking overnight at 37 °C, and the aliquots are stored in −80 °C freezer.
5. Fine forceps: Dumont #5, Inox.
6. Microdissection scissors.
7. A syringe pump (KDS single-syringe pump series 100, Z401358, MilliporeSigma).

2.2 Tissue Clearing

1. Fixation Buffer: 2% Paraformaldehyde (PFA) Buffer: 2 g Paraformaldehyde in 95 mL DI-H_2O: The solution is dissolved at 55–65 °C in an incubator by adding a few drops of 3 M NaOH. After the solution is clear, add 5 mL 20x PBS and adjust the pH to 6.9. Cool to 4 °C before use.
2. PBSTT: 500 mL PBS with 0.1% Triton X-100, 0.1% Tween-20, and 0.02% NaN_3 (Sodium Azide).
3. A4P0: 4% acrylamide and 0.25% VA-044 (LB-VA044-50GS, Fujifilm Wako Chemicals) in 50 mL PBS: Dissolve 2 g of acrylamide and 0.125 g of VA-044 in 50 mL PBS on ice. Aliquot in 15 mL tubes. The solution should be stored at −20 °C.
4. Clearing Solution 1 (CS1): 5% SDS in 20 mM Boric Acid Buffer. After dissolving, the solution should be approximately pH 8.0. The pH adjusts to 9.0–9.5 by adding a few drops of 3 M NaOH when starting out.
5. Clearing Solution 2 (CS2): 10% N, N, N′, N′-tetra-kis (2-Hydroxypropyl) ethylenediamine (122,262, MilliporeSigma-Aldrich), 10% Urea, 10% Triton X-100 in 20 mM Boric Acid: Warm up all reagents in a 50–60 °C incubator for 30 min to reduce the viscosity. This helps remove the SDS so that the muscle tissue can be kept at 4 °C. After dissolving, the solution should be approximately pH 10.8. The pH adjusts to 9.0–9.5 by adding a few drops of HCl when starting out.
6. PROTOS [10]: 23.5% (w/v) n-methyl-d-glucamine, 29.4% (w/v) diatrizoic acid, 32.4% (w/v) iodixanol (Histodenz or Omnipaque), and 0.01% NaN_3 (Sodium Azide) in H_2 O (*see* **Note 1**).

2.3 Embedding

1. PROTOS.
2. Grace Bio-Labs Press-To-Seal silicone isolator, No PSA (Round, 20 mm diameter, 1.6 mm depth or Rounded rectangle, 19 mm × 32 mm × 2.4 mm depth) (GBL664204 or GBL664303, MilliporeSigma).
3. Cover Glass Slides 24 mm × 60 mm.

2.4 Imaging

1. Nikon A1R Confocal Microscope (Nikon).
2. Objective lens: 20× water-immersion, NA: 0.95, working distance: 0.8 mm, Correction: PlanApo Lambda with correction color (Nikon).
3. Microscope Imaging Software: NIS Element Software (Nikon).
4. Image Analysis Software: FIJI ImageJ (NIH).

3 Methods

3.1 Perfusion Fixation and Muscle Dissection (Fig. 1)

1. For cre recombination-mediated satellite cell labeling, $Pax7^{tdTomato}:Flk1^{+/GFP}$ mice were used for subcutaneous injection of tamoxifen dosed as 75 mg/kg bodyweight × 3 times over 1 week at 2-months of age, inducing tdTomato expression in all satellite cells [6].
2. Sedate the tamoxifen-injected $Pax7^{tdTomato}:Flk1^{+/GFP}$ mice using a sedative of choice. Pin the mouse on a fixation chamber (*see* **Note 2**).
3. Open the chest cavity to expose the heart and pin the ribs up. Insert and secure the needle into the left ventricle of the heart.
4. Perfuse the mouse with 5.0 mL of ice-cold PBS with 5 mM of heparin (optional).
5. Perfuse with 50.0 mL of Fixation Buffer by a syringe pump with a 60 mL syringe: Perfusion is successful if the mouse's tail moves during this process (*see* **Note 3**).
6. Extensor digitorum longus (EDL) muscle is dissected as followed: The EDL tendon end, which is located next to the tibialis anterior (TA) muscle-tendon, was carefully lifted with the forceps and cut as close as possible to the foot. Free the EDL muscle from the other muscles till the upper tendon is visible, and then cut the upper tendon.
7. Post-fix the muscle tissue at 4 °C with rocking overnight.
8. Wash the muscle tissue with ice-cold PBS + 0.02% NaN_3 three times for 30 min at 4 °C with rocking.

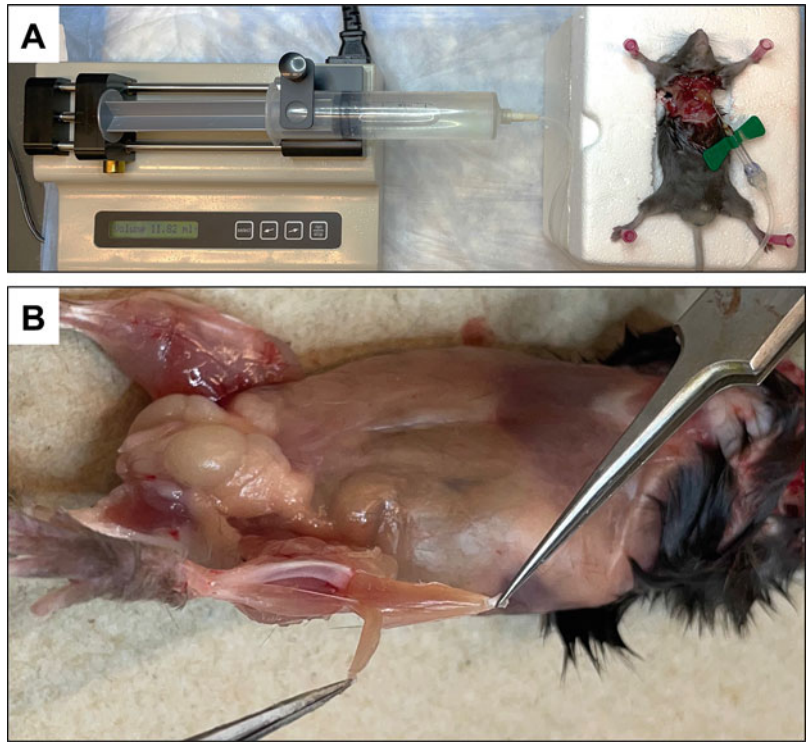

Fig. 1 EDL muscle dissection. The tamoxifen-injected *Pax7*^{tdTomato}:*Flk1*$^{+/GFP}$ mice were anesthetized and used for perfusion fixation by a syringe pump (**a**). EDL muscle was dissected from other muscle tissues (**b**)

3.2 Muscle Tissue Clearing

1. Thaw an A4P0 solution on ice. Make sure that the temperature of the solution does not increase by a significant amount.
2. Incubate the muscle tissue in the 1st cold A4P0 overnight at a 4 °C shaker.
3. Degas 2nd A4P0 solution.
   (a) Thaw and transfer 16 mL of AP40 into a 50 mL tube.
   (b) Bubble nitrogen gas into the liquid for 3 min.
   (c) Allow the solution to settle so that the bubbles in the solution are gone. This should occur in approximately 1 min.
4. Remove the 1st A4P0 solution from the muscle tissue and collect the waste for proper disposal.
5. Transfer the cold and degassed 2nd A4P0 solution into the 5 mL tube with the muscle tissue. Overfill and allow a meniscus to form above the tube. Avoid any air bubbles forming inside the tube.
   (a) Lightly cover the tube with 1 × 1 inch of plastic wrap.
   (b) Screw gently on the cap on the top of the tube while allowing the excess liquid to drip down into the waste.

6. Incubate the muscle tissue at 37 °C in a tube rotator to polymerize the acrylamide. If one is not available, one can use a bacterial shaker (60 rpm). Allow the polymerization to occur in a light-shielded tube (aluminum foil) for 3 h.
7. Remove the muscle tissue from the degassed A4P0 solution and discard the waste appropriately.
8. Wash the muscle tissue with PBSTT three times for 30 min at 37 °C.
9. Transfer the muscle tissue to the CS1 and rotate at 37 °C with a platform rocker shaker or a bacterial shaker. The bacterial shaker is more violent and clears faster (60 rpm). However, the muscle tissue must be fixed and polymerized well to prevent disintegration. EDL muscles are left overnight (*see* **Note 4**).
10. Wash the muscle tissue three times with PBSTT for 30 min at 37 °C with rocking.
11. Incubate the muscle tissue in CS2 for the same amount of time as CS1 (*see* **Note 4**). The muscle tissue should appear clear now.
12. Wash the muscle tissue three times with PBSTT with rocking at 37 °C.
13. Incubate in PROTOS for 30 min at 37 °C for EDL muscles three times with rocking. TA, gastrocnemius, and other thick muscle tissues may take 3 h twice and overnight.
14. Switch the PROTOS solution prior to imaging or use the embedding method below to perform Multiview imaging.
15. Store the muscle tissue in PROTOS after imaging at 4 °C.

3.3 Embedding (Fig. 2)

1. Press an approximately one-inch piece of tape on one side of the silicone isolator to remove any dust particles (*see* **Note 5**).
2. Attach the clean side of the isolator to one cover glass by pressing the isolator firmly to the center of the glass without air.
3. Using another one-inch piece of tape, remove any dust particles on the open side of the isolator.
4. Place a single tissue-cleared EDL muscle tissue from the PROTOS solution into the center of the isolator.
5. Fill the isolator with PROTOS with a pipette until the muscle tissue is completely submerged.
6. Attach the top cover glass on top of the submerged muscle tissue by pressing firmly onto the isolator without air bubbles. Pipette out/wipe using a Kimwipe any excess PROTOS solution on the slide.

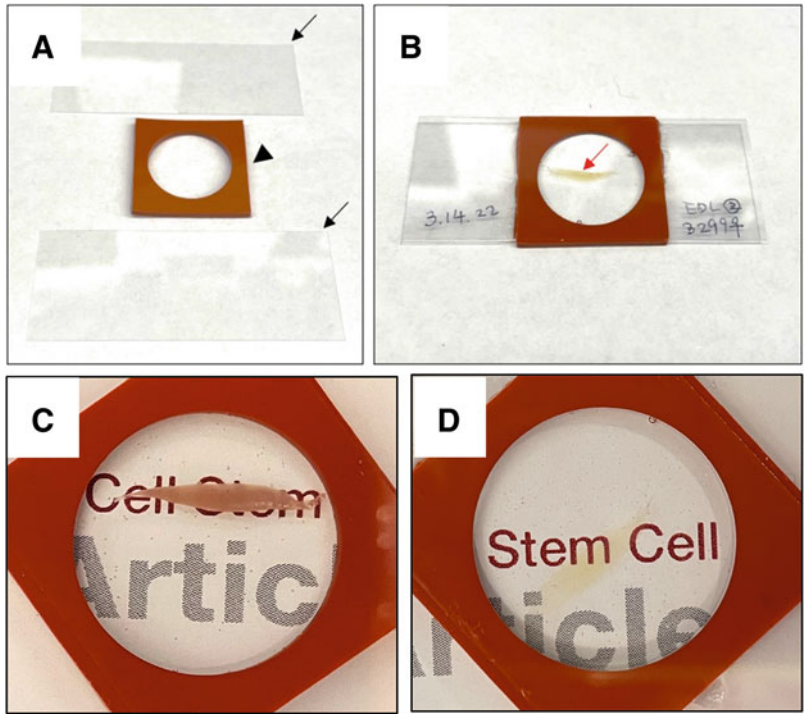

Fig. 2 Embedding step visual. A pair of cover glasses (arrows) and a silicon isolator (arrowhead) are shown (**a**). Tissue-cleared EDL muscle was embedded in the silicone isolator (**b**). EDL muscle before (**c**) and after (**d**) tissue clearing

3.4 Key Parameters for Image Acquisition

1. On the laser controller of the Nikon A1R Confocal Microscope, the 488 nm (GFP) and 561 nm (tdTomato) lasers must be switched on.
2. In the A1 Compact GUI window, adjust the pinhole diameter for the shortest wavelength laser (in this case, the 488 nm laser) to be 1.2 μm.
3. In the A1 Compact GUI window, select the image size of 1024 × 1024 pixels.
4. In the Scanning Window, select a Z range of 400 μm and Z slices at 1 μm steps (this should show up as total 401 steps).

3.5 General Protocol for Image Acquisition (Fig. 3)

1. Turn on the Nikon A1R Confocal Microscope based on facility instructions. On the laser controller, make sure the 488 nm and 561 nm lasers are turned on.
2. At the microscope, select the 20-x water-immersion objective lens. Place 2–3 drops of distilled water onto the lens.
3. Place the embedded muscle tissue slide onto the stage.
4. In the NIS Elements Software, select the "Eyepiece-EPI" tab. This will allow the user to find the muscle tissue using the

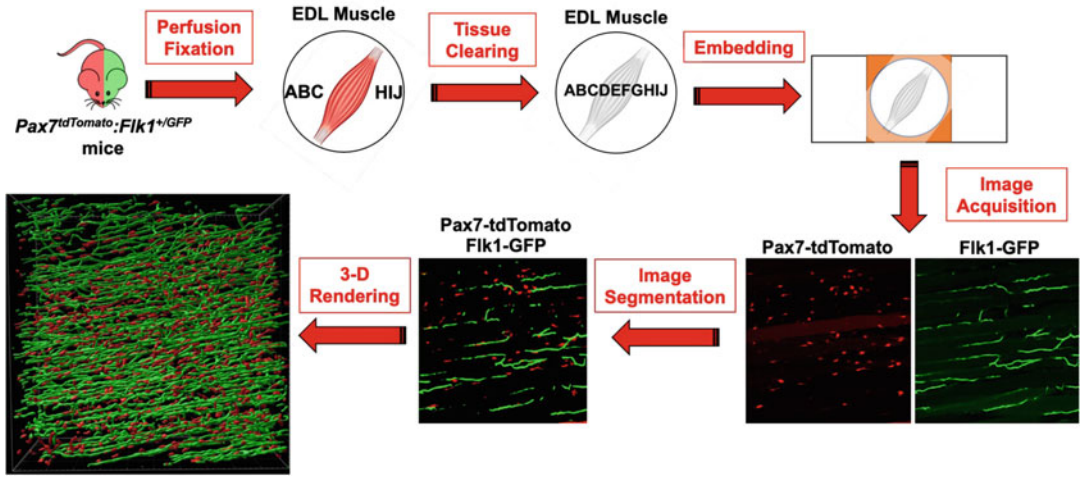

Fig. 3 Overall workflow from sample to 3-D-rendered imaging. EDL muscle from Pax7^{tdTomato}:Flk1$^{+/GFP}$ mice was used for tissue clearing. Embedded EDL muscle was used for confocal microscopic imaging acquisition, followed by image segmentation and 3-D rendering, generating precise 3-D imaging of Pax7-tdTomato(+) satellite cells (red) and Flk1-GFP(+) blood vessels (green)

eyepiece of the microscope. Select tdTomato or GFP in the menu to switch on the laser of the corresponding wavelength.

5. At the microscope, find a suitable area in a sample to image (one in which satellite cells are visible in tdTomato and blood vessels are visible in GFP).
6. Adjust the image brightness in both channels by moving the laser strength tab for each laser (tdTomato and GFP) in the A1 Compact GUI window. Adjust so that very few spots of the image are saturated.
7. As the sample is 3-D, the user must identify the top and the bottom of the sample for the microscope to take the image. Adjust the Z using the side knobs of the microscope until the top of the sample is reached.
8. When the top of the sample is reached, press "Top" in the Scanning Window. A corresponding bottom can then be manually entered to make sure the total depth of the image is 400 μm.
9. In the A1 Compact GUI window, select the desired image size of the 1024-pixel scan area.
10. Press "Run Now" in the Scanning Window to take the image. A new window should pop up displaying the image acquisition time.
11. After the images have been taken, press *File* > *Save As* to save the image in a desired location in the ND2 file format.

12. To convert the image file to a TIF/TIFF format for analysis, open the ND2 file in FIJI ImageJ. Once opened, select *File* > *Save As* > *Tiff*.

4 Notes

1. Wrap the bottle cap of PROTOS in Parafilm to avoid water loss. This solution is very volatile.
2. The animals were housed in an SPF environment and monitored by the Research Animal Resources (RAR) of the University of Minnesota. All protocols were approved by the Institutional Animal Care and Usage Committee (IACUC) of the University of Minnesota and complied with the NIH guidelines for the use of animals in research.
3. It is important that the heart is beating at the beginning of the perfusion process for the PBS to flow into the muscles properly.
4. This is good for muscle tissue but not for whole embryos or lungs. For CS1 and CS2 incubations, EDL and soleus muscles are left overnight; the diaphragm takes 6–12 h, the cremaster muscle takes 3 h, and the TA muscle and other thick muscle tissues may take a couple of days. Remember, the clearing time is not linearly scaled according to size.
5. It is important to remove any excess dust on the isolator as there is no glue holding the two cover glasses together.

Acknowledgments

We thank the Minnesota Supercomputing Institute, the University of Minnesota Imaging Center. We also thank Dr. Masatsugu Ema (Siga University of Medical Science) for providing *Flk1*$^{+/GFP}$ mice. This work was supported by NIHR01AR062142, NIH-R21AR070319, and Regenerative Medicine Minnesota (RMM) Grant to AA.

References

1. Wosczyna MN, Rando TA (2018) A muscle stem cell support group: coordinated cellular responses in muscle regeneration. Dev Cell 46(2):135–143
2. Schmidt M, Schüler SC, Hüttner SS (2019) Adult stem cells at work: regenerating skeletal muscle. Cell Mol Life Sci 76(13):2559–2570
3. Asakura A, Komaki M, Rudnicki M (2001) Muscle satellite cells are multipotential stem cells that exhibit myogenic, osteogenic, and adipogenic differentiation. Differentiation 68: 245–253
4. Asakura A, Seale P, Girgis-Gabardo A et al (2002) Myogenic specification of side population cells in skeletal muscle. J Cell Biol 159: 123–134
5. Mashinchian O, Pisconti A, Le Moal E et al (2018) The muscle stem cell niche in health and disease. Curr Top Dev Biol 126:23–65

6. Verma M, Asakura Y, Murakonda BSR et al (2018) Muscle satellite cell cross-talk with a vascular niche maintains quiescence via VEGF and notch signaling. Cell Stem Cell 23(4): 530–543.e9
7. Verma M et al (2019) Inhibition of FLT1 ameliorates muscular dystrophy phenotype by increased vasculature in a mouse model of Duchenne muscular dystrophy. PLoS Genet 15(12):e1008468
8. Verma M, Murkonda BS, Asakura Y et al (2016) Skeletal muscle tissue clearing for LacZ and fluorescent reporters, and immunofluorescence staining. Methods Mol Biol 1460: 129–140
9. Renier N, Wu Z, Simon DJ et al (2014) iDISCO: a simple, rapid method to immunolabel large tissue samples for volume imaging. Cell 159:896–910
10. Susaki EA, Tainaka K, Perrin D (2014) Whole-brain imaging with single-cell resolution using chemical cocktails and computational analysis. Cell 157:726–739
11. Chung K, Deisseroth K (2013) CLARITY for mapping the nervous system. Nat Methods 10(6):508–513
12. Murphy MM, Lawson JA, Mathew SJ et al (2011) Satellite cells, connective tissue fibroblasts and their interactions are crucial for muscle regeneration. Development 138(17): 3625–3637
13. Madisen L, Zwingman TA, Sunkin SM et al (2010) A robust and high-throughput Cre reporting and characterization system for the whole mouse brain. Nat Neurosci 13:133–140
14. Ema M, Takahashi S, Rossant J (2006) Deletion of the selection cassette, but not cis-acting elements, in targeted Flk1-lacZ allele reveals Flk1 expression in multipotent mesodermal progenitors. Blood 107:111–117

Chapter 32

Three-Dimensional Imaging Analysis for Skeletal Muscle

Smrithi Karthikeyan, Kyutae Kim, Yoko Asakura, Mayank Verma, and Atsushi Asakura

Abstract

Skeletal muscle is a highly ordered tissue composed of a complex network of a diverse variety of cells. The dynamic spatial and temporal interaction between these cells during homeostasis and during times of injury gives the skeletal muscle its regenerative capacity. In order to properly understand the process of regeneration, a three-dimensional (3-D) imaging process must be conducted. While there have been several protocols studying 3-D imaging, it has primarily been focused on the nervous system. This protocol aims to outline the workflow for rendering a 3-D image of the skeletal muscle using spatial data from confocal microscope images. This protocol uses the ImageJ, Ilastik, and Imaris software for 3-D rendering and computational image analysis as both are relatively easy to use and have powerful segmentation capabilities.

Key words Skeletal muscle, Myogenesis, Satellite cell, Muscle stem cell, Tissue clearing, 3D imaging, Muscle regeneration, Angiogenesis, Endothelial cell, Muscular dystrophy

1 Introduction

As the most abundant tissue type, skeletal muscle performs several of the body's vital functions, including voluntary locomotion, breathing, and posture maintenance [1]. Skeletal muscle is composed of a complex network between the following groups of cells: multi-nucleated muscle fibers, muscle satellite cells, endothelial cells, motor neurons, immune cells, and fibroblasts [1, 2]. The tight network and interplay between these cells from the basal state to times of injury or disease give the skeletal muscle its remarkable regenerative ability [3]. Satellite cells are a stem cell population responsible for postnatal skeletal muscle growth and regeneration. Satellite cells also possess the ability to differentiate into osteocytes and adipocytes following specific treatments or disease situations, indicating the multipotential differentiation ability of satellite cells [4]. Understanding the structure and function of cells within this network is essential for modeling/documenting the dynamic changes during muscle development and regeneration.

Atsushi Asakura (ed.), *Skeletal Muscle Stem Cells: Methods and Protocols*, Methods in Molecular Biology, vol. 2640, https://doi.org/10.1007/978-1-0716-3036-5_32,

A complete understanding of the regeneration process would lead to a better understanding of various neuromuscular-degenerative diseases such as Duchenne muscular dystrophy (DMD). Today, imaging has been proven to be one of the most powerful tools to examine the cellular network and the interplay between the different cell types. Typically, longitudinal cross-sections – obtained from frozen tissue blocks – are immunolabeled and examined underneath a microscope. Although this method provides valuable insight into the orientation of cells on the lateral plane, the axial orientation of cells is lost, leading to the underrepresentation of the actual data. Therefore, in order to get an accurate understanding of the skeletal muscle cellular network, one must gain information from all three dimensions (3-D) [5]. An example of the importance of 3-D imaging is documenting the interaction between muscle satellite cells and endothelial cells [6]. It has been shown that satellite cells are preferentially located near blood vessel endothelial cells via VEGF and Notch signaling [7]. This preference would be underestimated/misrepresented with 2-D imaging and therefore proves the value of analyzing cellular muscle interactions with 3-D. The imaging techniques outlined in this chapter would lead to a 3-D whole tissue quantification, which would allow for a better understanding of the spatial interactions between cell types during muscle homeostasis, injury, disease, and repair.

One method of generating a 3-D image of muscle tissue is by imaging a series of serial sections and combining all the images manually/automatically to create a 3-D representation. However, this process is labor-intensive and prone to error from unwanted artifacts in sections. Another more promising method of generating a 3-D image is through optical sectioning using confocal, 2-photon, or light-sheet microscopies as optical tissue clearing protocols such as iDISCO [8], CUBIC [9], and CLARITY [10]. With the use of an ideal optical clearing protocol – one that minimizes light scattering via refractive index mismatching – a more accurate 3-D image of the muscle can be produced as it does not involve the physical sectioning of the muscle [5].

With the advancement of imaging and computing technology, it is becoming increasingly powerful to analyze spatial data from confocal microscope images. This protocol aims to prepare confocal microscope images for computational analysis and 3-D rendering. The overall process involves segmenting the original microscope image using the software Ilastik, then creating a 3-D render with Imaris (Figs. 1 and 2) [7]. Segmentation is an imaging process that converts an image into a binary image. Segmentation is necessary for a computer to "see" the features of an image the researcher is interested in, such as cells, vessels, and nerves. Several different segmentation software have been developed, but this protocol uses Ilastik for its ease of use and robust segmentation algorithm.

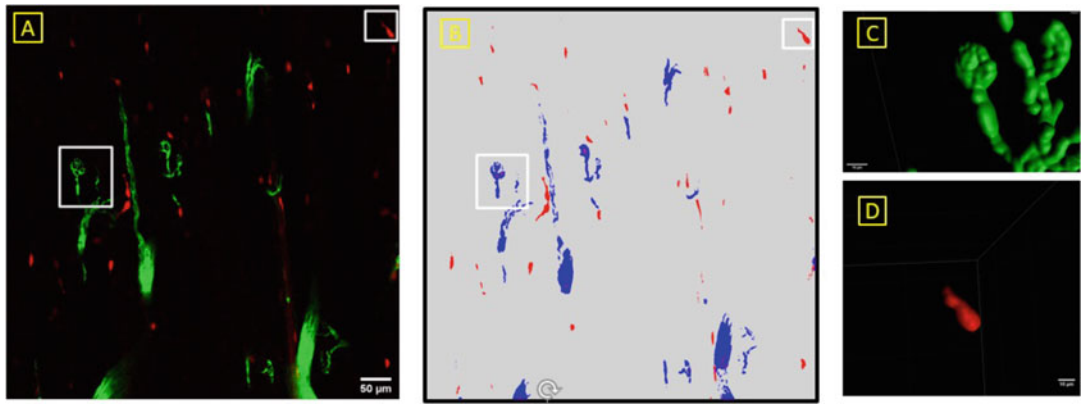

Fig. 1 (**a**) Workflow progression from acquiring the original image of satellite cells (red) and motor neurons (green) in EDL muscle of *Pax7*^{tdTomato}*:Thy1*^{YFP} mice. (**b**) Ilastik software is used to produce a segmented image, and (**c**, **d**) Imaris is used to create a 3-D rendering to show YFP(+) endplates of motor neurons (**c**) and tdTomato(+) satellite cells (**d**). Subset images show a magnified view. Bar in (**a**) denotes 50 μm. Bars in (**c**) and (**d**) denote 10 μm

2 Materials

2.1 Confocal Microscopic Imaging Files (e.g., Nikon A1R FLIM and FCS Confocal Microscope)

2.2 Image Analysis Software

1. FIJI (NIH) with the following plugins (*see* **Note 1** for plugin installation):
   (a) HDF5 plugin
   (b) Ilastik plugin
2. Ilastik Version 1.3.3 (European Molecular Biology Laboratory).
3. Imaris (Oxford Instruments).

3 Methods (Fig. 2)

3.1 Image Preparation

1. Import raw image file (TIF/TIFF file type) into FIJI [11, 12]. Fluorescent reporter mice such as *Pax7*^{tdTomato}*:Thy1*^{YFP} [13, 14] or *Pax7*^{tdTomato}*:Flk1*^{GFP} mice [13, 15] were used for extensor digitorum longus (EDL) muscle dissection after tamoxifen treatment and perfusion fixation [5, 7]. Raw image files are created after proper tissue-clearing and confocal

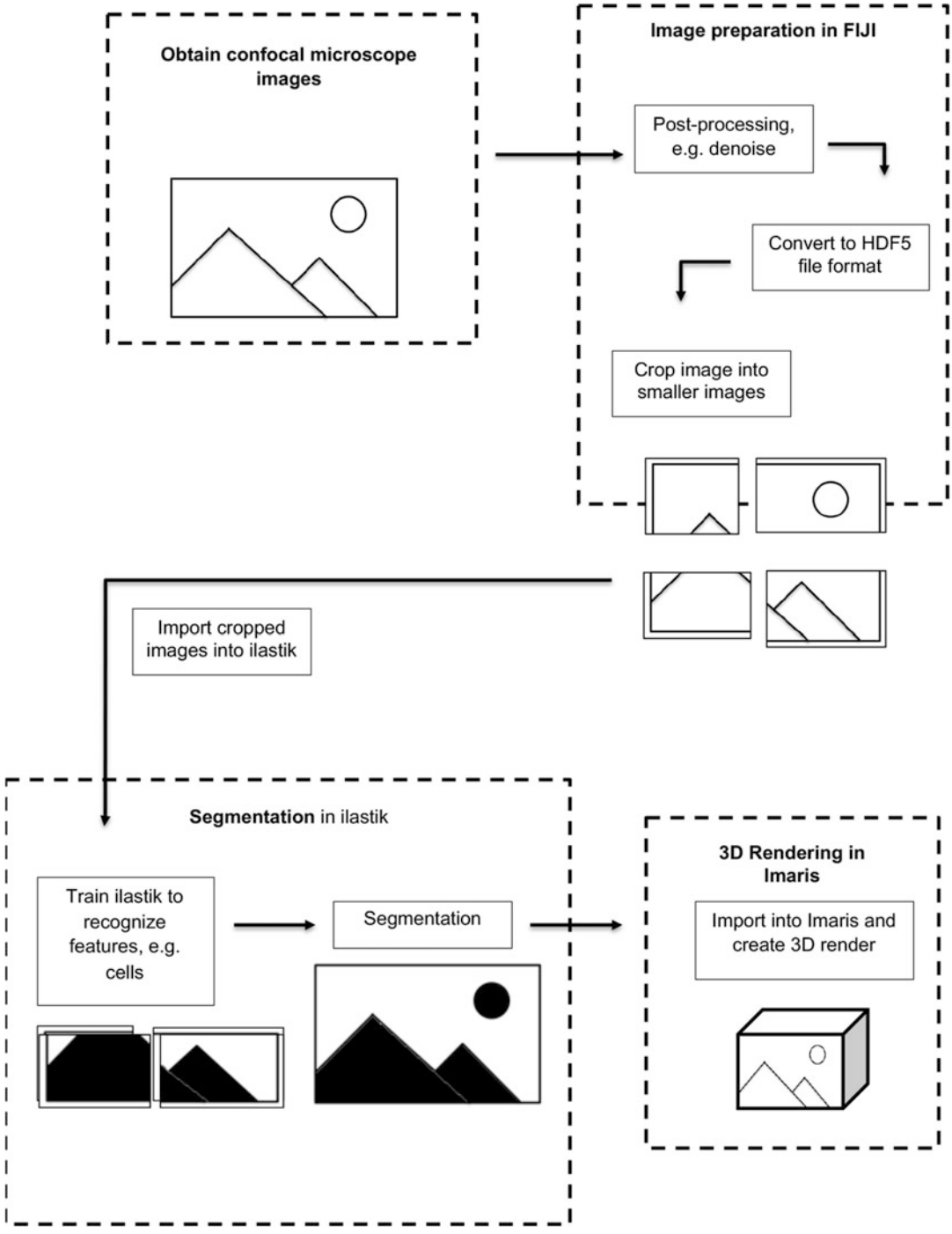

Fig. 2 Flowchart of the overview of the image processing protocol

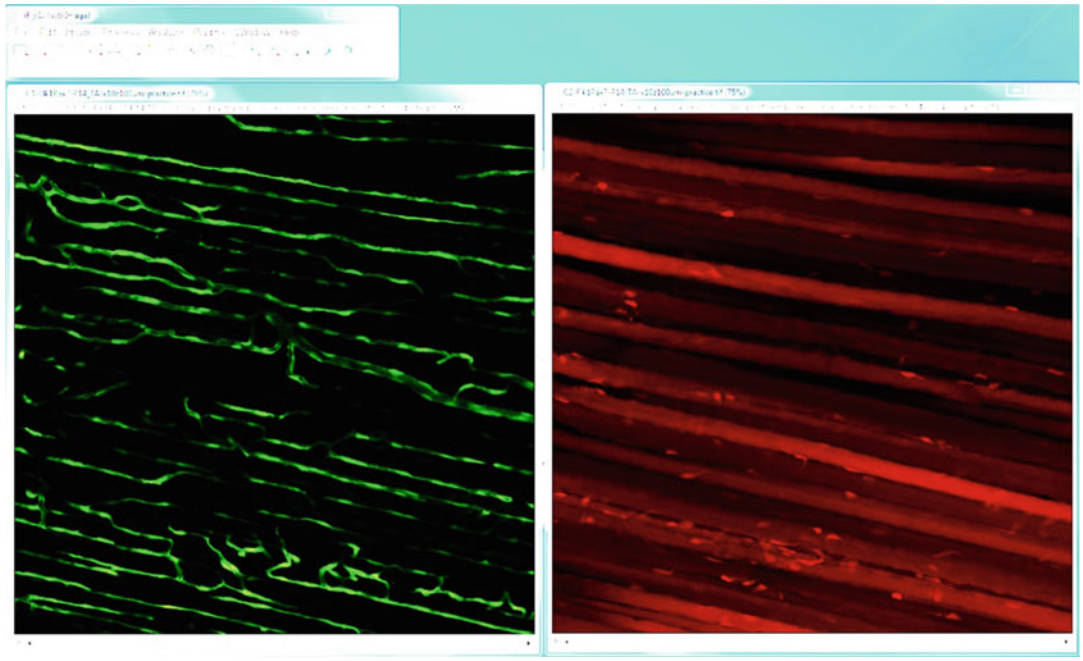

Fig. 3 Original full-sized image split into two channels (Subheading 3.3, **step 2**). EDL muscle of *Pax7*^{tdTomato}*:Flk1*^{GFP} mice was used for the confocal microscopic image. The green (left), in this case, represents GFP(+) blood vessels. The red (right) represents the tdTomato(+) satellite cells and muscle fibers

microscopic 3-D imaging (e.g., select the image size of 1024 × 1024 pixels, a Z range of 400 μm, and Z slices at 1 μm steps; this should show up as total 401 steps).

2. If using a multichannel image, split the image channels: *Image > Color > Split Channels* (*see* Figs. 3 and 5).
3. If post-processing is needed, such as denoising, it should be done at this point.
4. Use the HDF5 plugin to save the whole image in the HDF5 file format: *plugins > HDF5 > Save to HDF5 file (new or replace)* (*see* **Note 2** for multichannel images).

3.2 Cropping

1. For large image files, it will be helpful to crop the image into smaller images. This eases the computational workload of the computer during Segmentation training in Ilastik (*see* **step 2** and **3**, and **Note 3**) [16]. If the image file is small enough, segmentation will work smoothly in Ilastik, and this Cropping step can be skipped (*see* Fig. 4).
   (a) Cropping protocol on Fiji: *Image > Crop*. Ensure the rectangle item from the toolbar is selected before cropping the image.

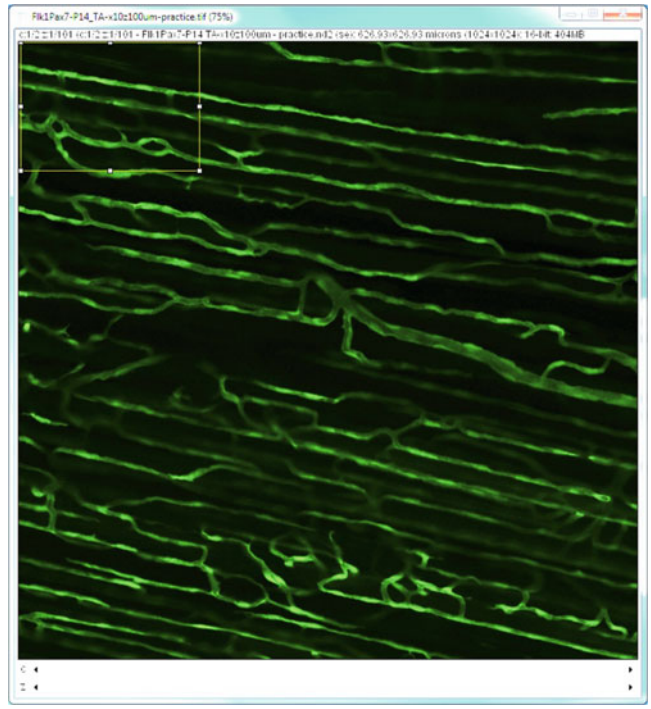

Fig. 4 Original image (with two channels) cropped to a smaller image. The yellow rectangle is the size the cropped image should be after cropping is complete (Subheading 3.3, **step 1**)

2. Crop the image into several 50 × 50 × 50 pixel images. Do this for each channel.
3. Save each cropped image to both a TIF and hdf5 file format (Fig. 5).

3.3 Segmentation Training in Ilastik

1. In this section, we will use the program Ilastik to "teach" the computer to recognize features, such as cells and blood vessels, in our images. This protocol is based on the documentation found on the Ilastik website. See **Note 4** for the website URL.
2. Start a new *Pixel Classification* project in Ilastik.
3. Import all your cropped image files (h5 file type) using the *Add New > Add separate Image(s)*.
4. Open the *Feature Selection* tab and then *Select Features*. Select all the available features by dragging the mouse to check the boxes (*see* Fig. 6).
5. Open the *Training* tab.
6. Select *Add Label* to create two labels.
7. Rename one of the Labels to "Background" by double-clicking the label name. The other label can be renamed to anything

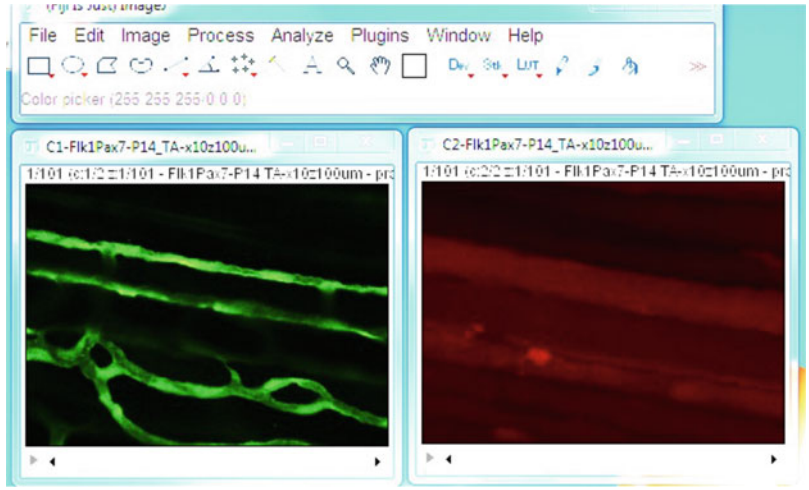

Fig. 5 Cropped image split into two channels (Subheading 3.3, **step 1**)

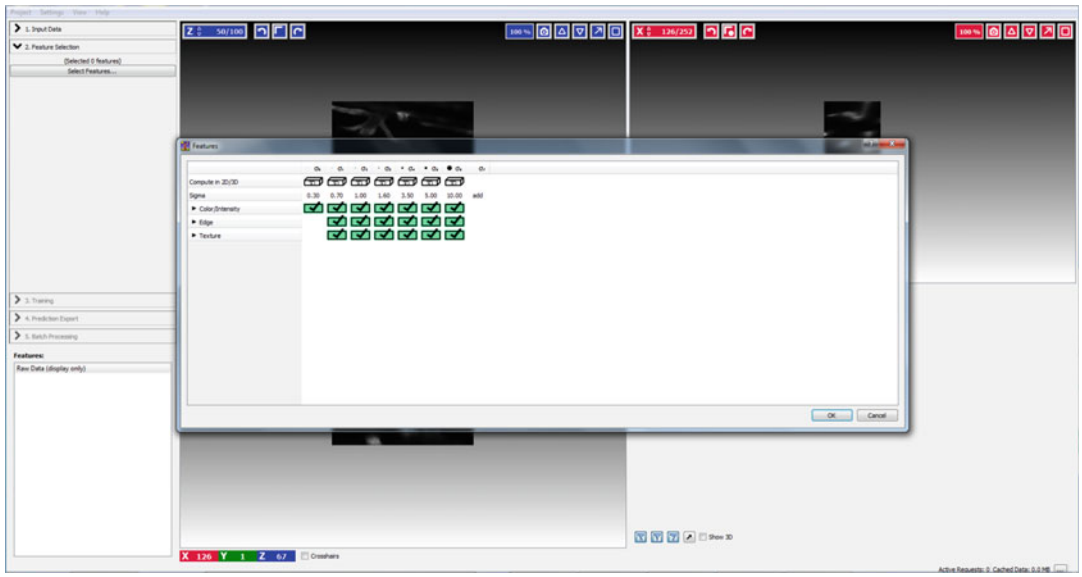

Fig. 6 Feature Selection window in Ilastik. Note how all of the features are checked (Subheading 3.3, **step 4**)

you would like, and this is the label we will use for the features of interest.

(a) If you wished to change the color of a label, click the color square beside the label. Change to the color of choice for both options in the pop-up window.

8. Select the Background label and select the Brush Cursor tool.
9. Click on the image in areas that are background. Ilastik will now learn that these areas are background.

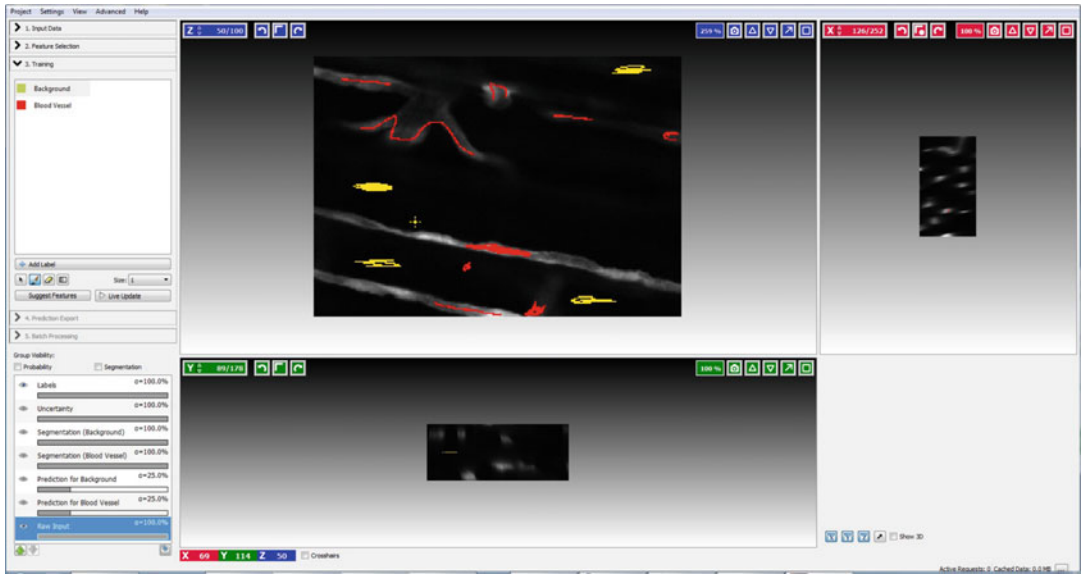

Fig. 7 Training window in Ilastik. The yellow marks are considered as the "Background," and the red marks are the "Blood Vessel" (Subheading 3.3, **step 10**)

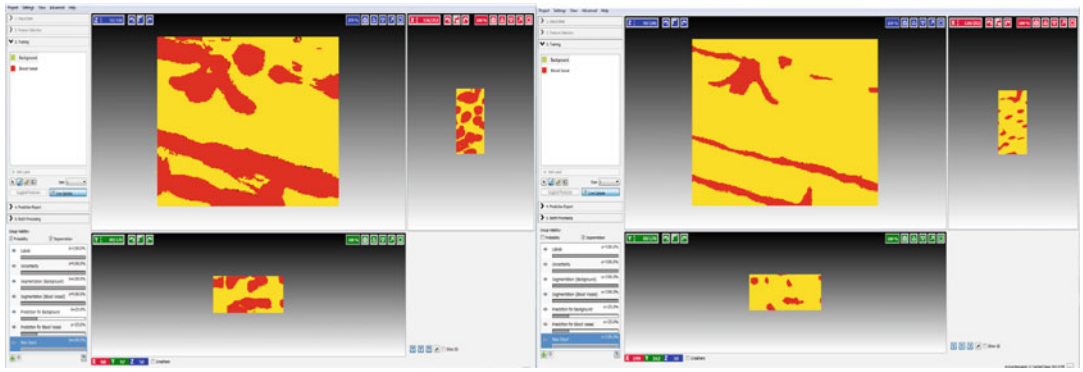

Fig. 8 Before (left) and after (right) refinement of segmentation (Subheading 3.3, **step 11**)

10. Select your other label and begin clicking on the features of interest in the image. Ilastik will now learn that these parts of the image are the features you are looking for (*see* Fig. 7).
11. Check your progress by selecting *Live Update* and checking *Segmentation* (Fig. 8).
    (a) Keyboard shortcuts: After selecting *Live Update*, press the "S" key to see/go between the original and finished image. Press the "U" key – if needed – to see the parts of the image (highlighted in blue) in which the computer is "unsure" of what color to assign.

12. Repeat until the segmentation is as accurate as you can achieve.
13. Repeat this process for each cropped image you imported.
14. Save and close Ilastik when you are finished.

3.4 Segmentation

1. Now that Ilastik is trained to recognize features from the background in your image, we will use Ilastik to segment your original image. This will be done by running Ilastik in "headless" mode. Additional details on running headless mode can be found on the Ilastik website (*see* **Note 5**).
2. Headless mode is initiated by entering the following code into the command prompt:
   (a) cd "\Program Files\ilastik-1.3.3"
   (b) .\ilastik.bat --headless --project="\file path\ilastik_project.ilp --export_source="Simple Segmentation" --export_dtype=uint8 --output_filename_format="\file path\desired_name_of_segmentated_image" --output-internal_path="\channel0" "\file path\original_image.h5\channel0"
   (c) For example:
   cd "\Program Files\ilastik-1.3.3"
   .\ilastik.bat --headless --project="/home/asakuaa/kimx3614/Documents/CTX_project.ilp" --export_source="Simple Segmentation" --export_dtype=uint8 --output_filename_format="/home/asakuaa/kimx3614/Documents/CTX_segmented_image" --output_internal_path="/channel0" "/home/asakuaa/kimx3614/Documents/CTX_original_image.h5/channel0"
3. Once completed, the segmented image can be viewed on FIJI (*see* **Note 6** and Fig. 9).
   (a) If the segmented image appears black, use the following protocol in Fiji: *Image>Adjust>Brightness/Contrast>Auto (or adjust the Maximum and Minimum to see the segmented image)*.
   (b) The segmented image on Fiji should not be a virtual stack. A virtual stack is symbolized by a (V) at the end of the image title header. If the image is a virtual stack, the image must be converted to a Tiff stack using FIJI via *File>Save As> Tiff*. All channels of the image saved as a tiff must be reopened again in Fiji to proceed.
4. For each channel, to convert the stack to binary, use the following procedure in FIJI: *Image>Adjust>Threshold>Auto>Apply>uncheck "Calculate threshold for each image"* (Fig. 10).

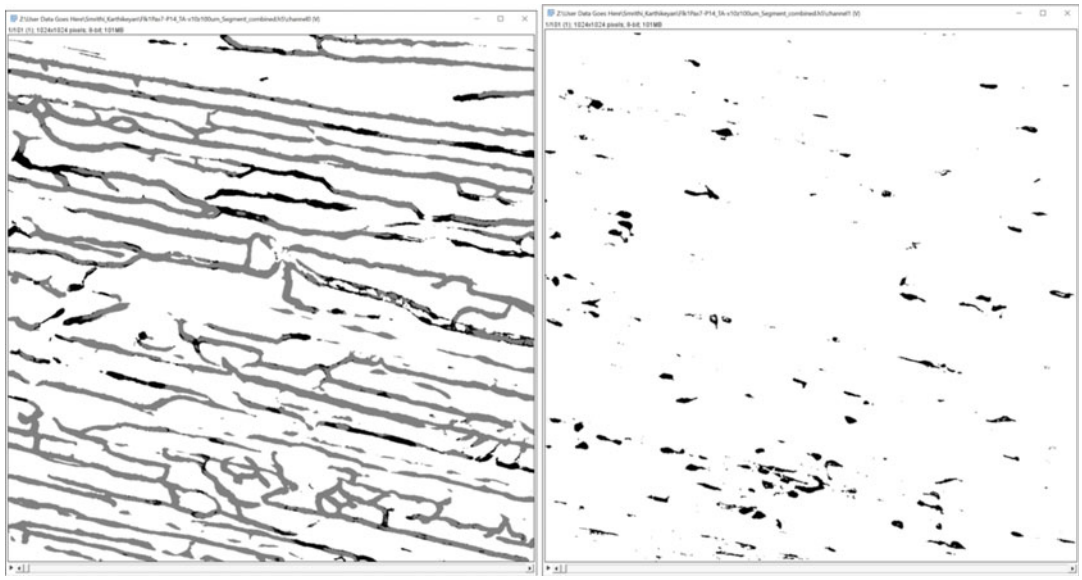

Fig. 9 Segmented h5 file opened in Fiji. Left image shows the segmented blood vessels. Right image shows the segmented stem cells (Subheading 3.4, **step 3**)

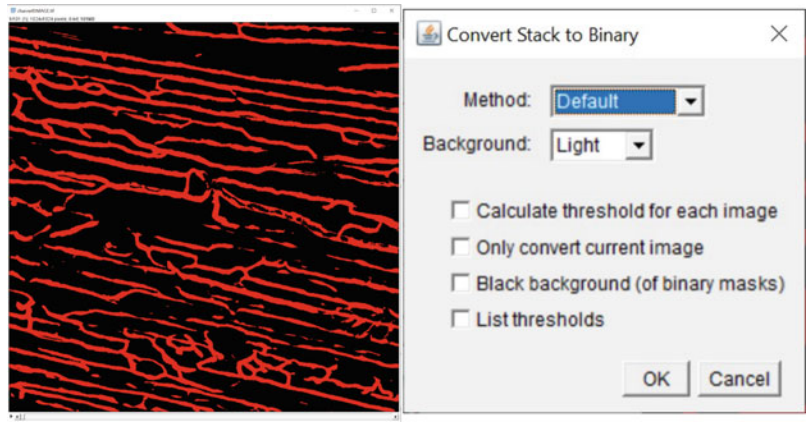

Fig. 10 Adjusting the threshold of each channel and converting the stack to a binary image (Subheading 3.4, **step 4**)

5. For multichannel images, the segmented images will need to be merged. This protocol separated the channels and segmented each as a separate project. These images can be merged again using FIJI via *Image>Color>Merge Channels* (Fig. 11).
   (a) After merging, click the Look-Up Table option (LUT) in Fiji's toolbar to assign each channel a color for labeling purposes. The merged image should now have a different color for each channel.
   (b) Save as a tiff file.

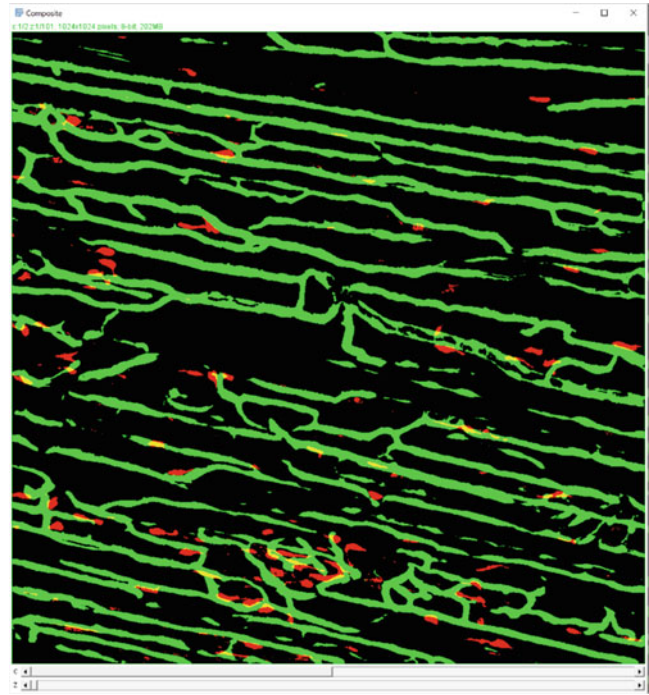

Fig. 11 The final segmented image with both channels merged (Subheading 3.4, **step 5**)

3.5 3-D Rendering on Imaris

1. Convert your segmented image (for multichannel images, the merged segmented image) into the Imaris file format using the Imaris file converter provided as part of the Imaris software package.
2. In Imaris, the following licenses must be checked: Imaris Cell, all of the Measurement Pros options, and Imaris XT (only if the computer has MATLAB installed). The Measurement Pros options will allow the computer to take measurements between the combined multichannel image objects of interest.
3. In the "Surpass" window, open the combined segmented image (now an Imaris file). Select the *Surfaces* tool and follow the software prompts. Ensure the "Object-Object Statistics" and "Background Subtraction" boxes are checked. Uncheck the "Classify Surfaces" box. This will create a 3D rendering of your segmented image. Do this for each channel for multichannel images (Figs. 12 and 13).
4. You can now use Imaris's suite of features to collect data and make movies with your 3D rendering.
5. To measure the shortest distance between two surfaces, do the following in Imaris: *click the "Statistics" tab (a grid with a red*

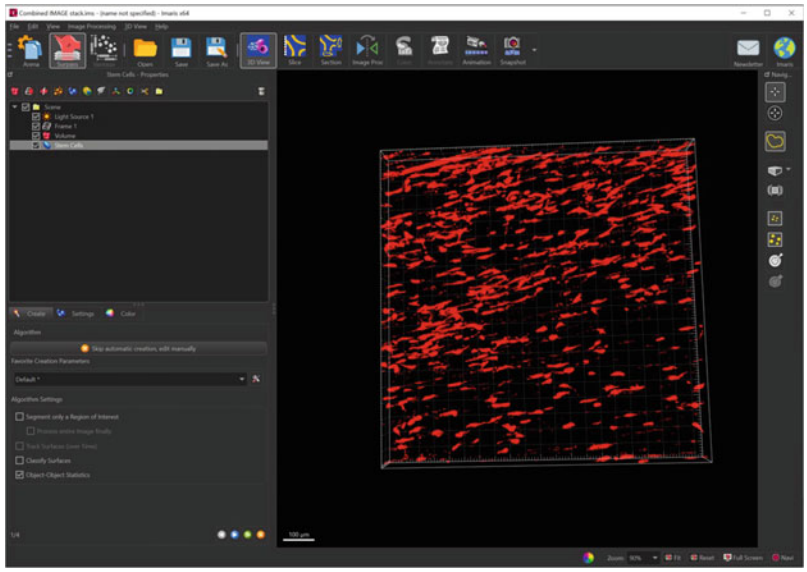

Fig. 12 Creating the stem cell surface from the imported segmented image (Subheading 3.5, **step 3**)

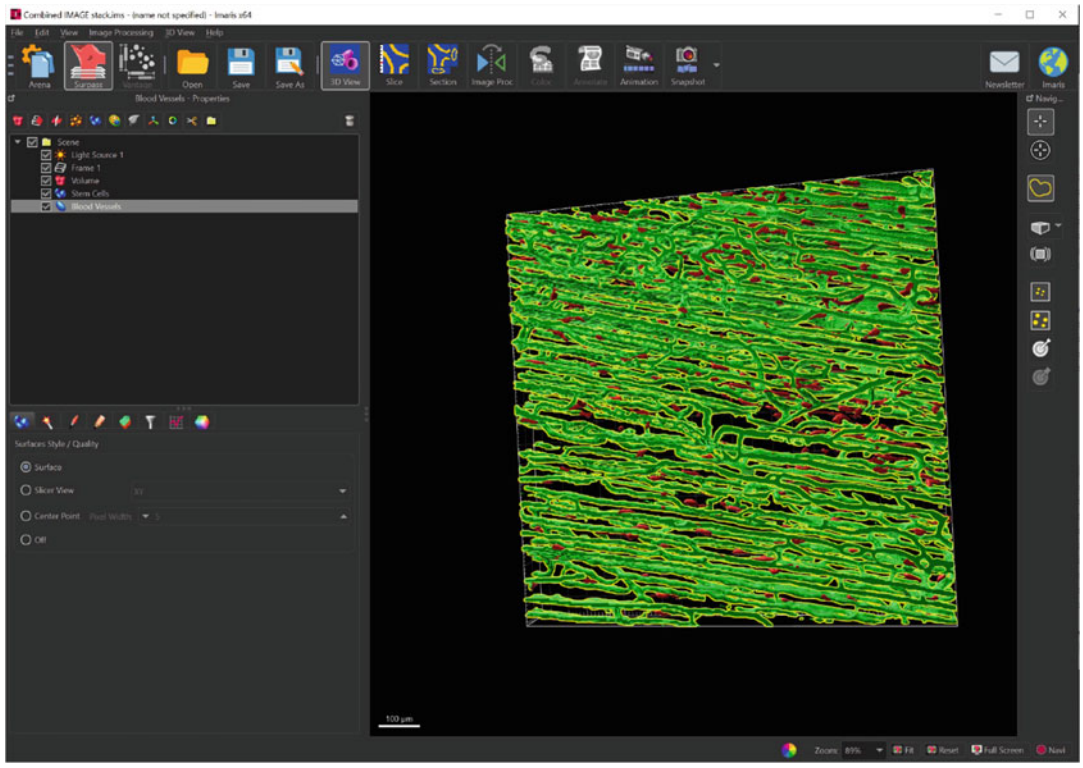

Fig. 13 The final 3D model of the muscle stem cells and the blood vessels (Subheading 3.5, **step 3**)

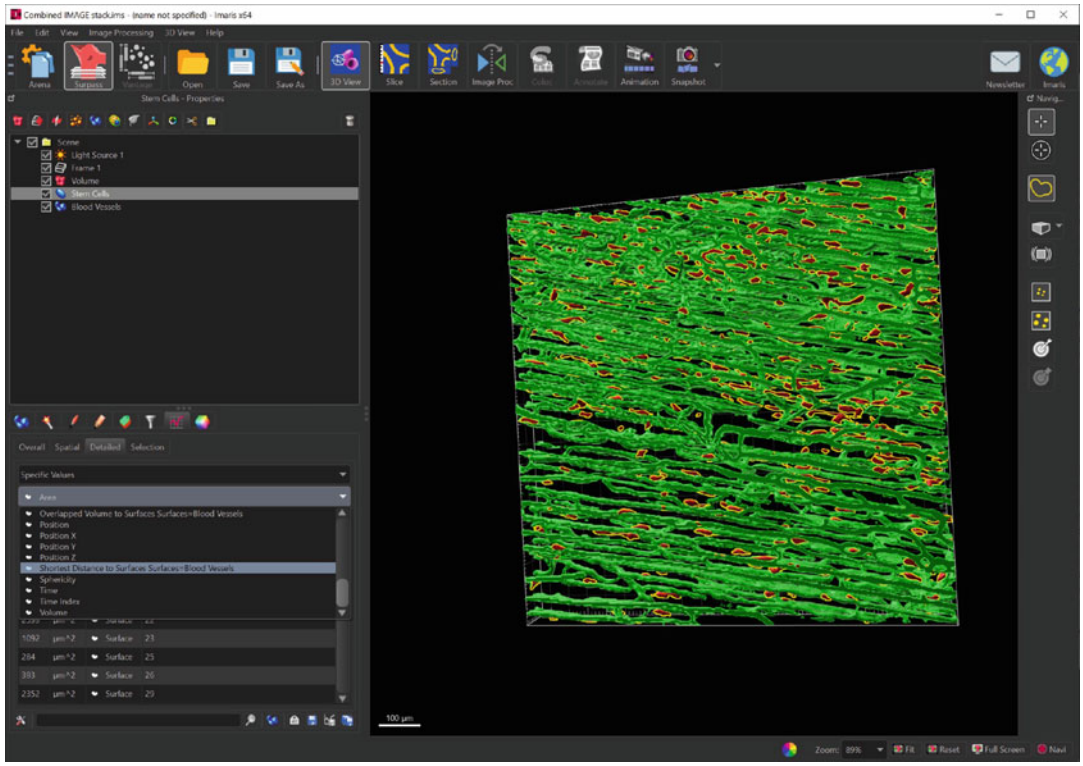

Fig. 14 Measurement of the distance between the two surfaces (Subheading 3.5, **step 5**)

line icon)> Detailed, Specific Values> Shortest distances to surfaces> Click the bottom to save measurements as a CSV file (*see* **Note 7** and Fig. 14).

4 Notes

1. Ilastik Import/Export plugin installation documentation can be found here: https://www.ilastik.org/documentation/fiji_export/plugin
2. After splitting the image to each channel, save each single-channel image to HDF5. Ensure that the internal file path keeps each channel separate, for example, the red channel should save to *channel{0}*, and the green channel should save to *channel{1}*.
3. The more images cropped and trained in Ilastik, the better the final result will be. The accuracy of segmentation can also be improved by cropping images that contain the features you want segmented. For example, if you are segmenting cells, try to crop images that contain cells. It would not be helpful to crop multiple images of a plain, dark background.

4. Ilastik Pixel Classification documentation can be found here: https://www.ilastik.org/documentation/pixelclassification/pixelclassification
5. Ilastik Headless operation documentation can be found here: https://www.ilastik.org/documentation/basics/headless
6. In order to view the segmented h5 files on Fiji, the "Ilastik" plugin must be installed. To add the plugin, use the following protocol in Fiji: *Help>Update>Manage Update Sites>Check the "Ilastik" box.*
7. In the measurement CSV file, 0 in the distance column means that the two surfaces are touching. A negative value means that the surface is partially inside the other surface.

Acknowledgments

We thank the Minnesota Supercomputing Institute, the University of Minnesota Imaging Center. We also thank Dr. Masatsugu Ema (Shiga University of Medical Science) for providing *Flk1*$^{+/GFP}$ mice. This work was supported by NIHR01AR062142, NIH-R21AR070319, and Regenerative Medicine Minnesota (RMM) Grant to AA.

References

1. Schmidt M, Schüler SC, Hüttner SS (2019) Adult stem cells at work: regenerating skeletal muscle. Cell Mol Life Sci 76(13):2559–2570
2. Asakura A, Seale P, Girgis-Gabardo A et al (2002) Myogenic specification of side population cells in skeletal muscle. J Cell Biol 159: 123–134
3. Asakura A (2003) Stem cells in adult skeletal muscle. Trends Cardiovasc Med 13(3): 123–128
4. Asakura A, Komaki M, Rudnicki M (2001) Muscle satellite cells are multipotential stem cells that exhibit myogenic, osteogenic, and adipogenic differentiation. Differentiation 68: 245–253
5. Verma M, Murkonda BS, Asakura Y et al (2016) Skeletal muscle tissue clearing for LacZ and fluorescent reporters, and immunofluorescence staining. Methods Mol Biol 1460: 129–140
6. Mashinchian O, Pisconti A, Le Moal E et al (2018) The muscle stem cell niche in health and disease. Curr Top Dev Biol 126:23–65
7. Verma M, Asakura Y, Murakonda BSR et al (2018) Muscle satellite cell cross-talk with a vascular niche maintains quiescence via VEGF and notch signaling. Cell Stem Cell 23(4): 530–543.e9
8. Renier N, Wu Z, Simon DJ et al (2014) iDISCO: a simple, rapid method to immunolabel large tissue samples for volume imaging. Cell 159:896–910
9. Susaki EA, Tainaka K, Perrin D (2014) Whole-brain imaging with single-cell resolution using chemical cocktails and computational analysis. Cell 157:726–739
10. Chung K, Deisseroth K (2013) CLARITY for mapping the nervous system. Nat Methods 10(6):508–513
11. Rueden CT, Schindelin J, Hiner MC et al (2017) ImageJ2: ImageJ for the next generation of scientific image data. BMC Bioinformatics 18:529
12. Schindelin J, Arganda-Carreras I, Frise E et al (2012) Fiji: an open-source platform for biological-image analysis. Nat Methods 9(7): 676–682

13. Murphy MM, Lawson JA, Mathew SJ et al (2011) Satellite cells, connective tissue fibroblasts and their interactions are crucial for muscle regeneration. Development 138(17): 3625–3637
14. Feng G, Mellor RH, Bernstein M et al (2000) Imaging neuronal subsets in transgenic mice expressing multiple spectral variants of GFP. Neuron 28(1):41–51
15. Ema M, Takahashi S, Rossant J (2006) Deletion of the selection cassette, but not cis-acting elements, in targeted Flk1-lacZ allele reveals Flk1 expression in multipotent mesodermal progenitors. Blood 107:111–117
16. Berg S, Kutra D, Kroeger T et al (2019) ilastik: interactive machine learning for (bio)image analysis. Nat Methods 16(12):1226–1232

INDEX

Atsushi Asakura (ed.), *Skeletal Muscle Stem Cells: Methods and Protocols*, Methods in Molecular Biology, vol. 2640, https://doi.org/10.1007/978-1-0716-3036-5, © Springer Science+Business Media, LLC, part of Springer Nature 2023

H

I

L

M

N

O

P

Q

R

S

T

V

Y

Z